

Statistical and simulation modelling for enhanced understanding of hospital pathogen and related health issues

Xing Ju Lee

BAppSc (Hons) (Maths)

under the supervision of

Principal Supervisor

Professor Anthony N. Pettitt

Associate Supervisors

Professor Adrian Barnett

Adjunct Professor Michael Whitby

School of Mathematical Sciences
Faculty of Science and Engineering
Queensland University of Technology

2017



SUBMITTED IN FULFILLMENT OF THE REQUIREMENTS OF THE DEGREE OF
DOCTOR OF PHILOSOPHY

Abstract

Methicillin-resistant *Staphylococcus aureus* (MRSA) is one of the most common multidrug resistant organisms causing infections in a hospital setting. Such healthcare associated infections are difficult to treat due to adaptability of the organism in developing resistance to commonly used antimicrobials. While the past decade has seen decreases in MRSA-related infections in developed countries due to large-scale initiatives on improving infection control and prevention (ICP) policies, MRSA still remains a substantial healthcare problem.

This thesis aims to investigate the transmission dynamics of MRSA in a hospital setting using statistical and mathematical modelling, and simulation. Improved understanding of the underlying MRSA transmission process within a hospital is key to improving ICP practices. Such improvements help reduce the spread of MRSA in hospitals and potentially prolong the efficacy of current treatment options for MRSA.

Analysis of transmission dynamics of MRSA in a hospital is challenging for three main reasons: (i) the transmission process is only partially observed, (ii) the variability associated with small population sizes (e.g. hospital wards) and (iii) the inherent dependence between MRSA cases detected close to one another.

As such, the methods used must be able to make inference with such imperfect information (typically by assuming a simplistic model form), or be able to impute missing data to facilitate inference, as well as be able to handle the inherent variability and dependence in the observations.

Proportional hazard survival models with time-varying covariates offer a simple but effective method to include the potential dependence between MRSA cases close in space and time, as well as appropriately account for the time ordering of events. Such models were used in two MRSA case studies presented here. In the first case study, these proportional hazard models quantified the differences in the temporal trend and effect of past MRSA cases within the same spatial structure on MRSA incidences detected in different wards of a single hospital. This case study provided a method to identify wards where additional interventions should be targeted. The second case study focused on data collected during an MRSA outbreak in a neonatal intensive care unit and showed that the daily proportion of MRSA-positive patients, or colonisation pressure, increased the hazard of a patient acquiring MRSA in the study period while patient bed movements did not. Additionally, it was also shown that patient length of stay was increased by MRSA acquisition, and colonisation pressure to a lesser extent.

A topic of particular interest in this thesis was the relative contribution of microbiological environmental contamination to the observed MRSA incidence in a

hospital ward. This was investigated using a non-homogeneous Poisson process (NHPP) where the instantaneous rate of event occurrence was governed by the prevalence of MRSA-positive patients, environmental contamination and a generic background source. The NHPP was fitted under a Bayesian framework which provided a straightforward means of imputing the unobserved MRSA acquisition times. These acquisition times were required to evaluate the NHPP model likelihood. This study quantified the relative contribution of environmental contamination based on observed environmental data.

The estimates obtained from the NHPP were subsequently used in a modelling study to investigate the impacts of common interventions and their various combinations on the MRSA incidence in a hypothetical hospital ward under different burden settings. This modelling study used the Mann–Whitney statistic to evaluate the distributional differences between the outcome measures under different intervention combinations given the inherent stochasticity of the system.

Model choice is an important aspect of statistical inference. For pathogen transmission models, including those for MRSA, model choice quantifies the support of the data for various potential transmission mechanisms, as represented by different candidate transmission models. A simulation-based method for performing model choice was developed and investigated as part of this thesis. The method was applied to a number of different pathogen transmission data sets for a variety of transmission models of differing complexities. The method developed was also applied to a spatial extremes example to highlight its general applicability to models for which data are readily simulated. The spatial extremes models considered are particularly suited for the simulation-based method developed as these models do not have closed form likelihood expressions. Such models are relevant to investigations attempting to associate extreme weather events with changes in population health, e.g. increased mortality, hospital admissions and disease incidence.

Key words

Approximate Bayesian computation; data-augmentation; environmental contamination; Hagelloch measles outbreak; Markov chain Monte Carlo; max-stable models; maximum temperature data; methicillin-resistant *Staphylococcus aureus*; model choice; non-homogeneous Poisson process; neonatal intensive care unit; proportional hazards model; Tristan da Cunha influenza outbreak; spatial extreme data.

List of acronyms

	Definition
ABC	approximate Bayesian computation
ABMC	approximate Bayesian model choice (algorithm)
AIC	Akaike information criterion
AMS	antimicrobial stewardship
ATP	adenosine triphosphate
BF	Bayes factor
BIC	Bayesian (Schwarz) information criterion
CI	confidence interval
CrI	credible interval
DA-MCMC	data-augmented Markov chain Monte Carlo
DIC	deviance information criterion
FP	Fearnhead and Prangle
FR	fractional risk
GEV	generalised extreme value (distribution)
HAI	healthcare associated infection
HQC	Hannan-Quinn information criterion
HCW	healthcare worker
HPP	homogeneous Poisson process
ICU	intensive care unit
IS	importance sampling
LOS	length of stay
LR	likelihood ratio
MCMC	Markov chain Monte Carlo
MDRO	multidrug resistant organisms
MH	Metropolis–Hastings
MRSA	methicillin-resistant <i>Staphylococcus aureus</i>
NICU	neonatal intensive care unit
NHPP	non-homogeneous Poisson process
ODE	ordinary differential equation
PCR	polymerase chain reaction
PH	proportional hazard
RJ-MCMC	reversible jump Markov chain Monte Carlo
RS	rejection sampling
SIR	Susceptible-Infectious-Recovered (model)
SMC	sequential Monte Carlo
TIC	Takeuchi information criterion
VRE	vancomycin-resistant enterococci
WAIC	widely applicable information criterion
WBIC	widely applicable Bayesian information criterion
WHO	World Health Organization

List of papers

Lee, X. J., Drovandi, C. C., and Pettitt, A. N. (2015). Model choice problems using approximate Bayesian computation with applications to pathogen transmission data sets. *Biometrics*, 71(1):198–207

Lee, X. J., McKeone, J.P., Drovandi, C. C., and Pettitt, A. N. (2016). ABC model selection for spatial max-stable models applied to South Australian maximum temperature data *Computational Statistics & Data Analysis*, under review.

Lee, X. J., Ruggeri, F. and Pettitt, A. N. (2016). Parametric survival analysis of hospital ward MRSA incidence allowing for carryover effects from previous cases *BMJ Open*, under review.

Lee, X. J., Pettitt, A. N. and Givney, R. (2016). Quantifying impact of an MRSA outbreak in a NICU, in preparation.

Lee, X. J., Pettitt, A. N., and Dancer, S.J. (2016). Quantifying the relative effect of environmental contamination on surgical ward MRSA incidence. *BMC Infectious Diseases*, under review.

Lee, X. J., Fulford, G.R., Pettitt, A. N., and Ruggeri, F. (2016). A stochastic model for MRSA transmission within a hospital ward incorporating environmental contamination *Epidemiology & Infection*, doi:10.1017/S0950268816002880s

Declaration

I hereby declare that this submission is my own work and to the best of my knowledge it contains no material previously published or written by another person, nor material which to a substantial extent has been accepted for the award of any other degree or diploma at QUT or any other educational institution, except where due acknowledgement is made in the thesis. Any contribution made to the research by colleagues, with whom I have worked at QUT or elsewhere, during my candidature, is fully acknowledged.

I also declare that the intellectual content of this thesis is the product of my own work, except to the extent that assistance from others in the project's design and conception or in style, presentation and linguistic expression is acknowledged.

QUT Verified Signature

Signature

Date

13/2/2017

Acknowledgements

Firstly, I would like to thank my principal supervisor, Professor Tony Pettitt, for his guidance, patience and supervision throughout my PhD candidature. It has been a thoroughly enjoyable experience working with Tony. His wit and wisdom have been greatly appreciated. I am also grateful for all the opportunities that Tony has provided me with throughout these years. I would like to acknowledge my associate supervisors for their valuable feedback throughout my PhD, as well as Dr. Glenn Fulford for his support particularly in the early stages of my PhD.

My sincere gratitude to each of my study collaborators for generously providing their time and expertise. I am especially grateful to clinical microbiologist, Dr. Stephanie Dancer, not only for her clinical expertise and providing the data set used in the environmental contamination modelling investigations, but also for her kind encouragements throughout our collaboration.

I would like to acknowledge the NHMRC-funded Centre of Research Excellence in Reducing Healthcare Associated Infections (CRE-RHAI) (NHMRC Grant 1030103) for the opportunity to pursue this particular PhD project. The centre hosted a large group of PhD candidates who have been a great, diverse bunch to have shared this experience with. In particular, our writing circles facilitated by Karyn Gonano and monthly meetings have been interesting learning experiences. A special thanks goes to the centre manager, Emily Bailey, for keeping us in line.

I am grateful to the funding sources which have allowed me to carry out the research presented here, namely Queensland University of Technology (QUT) for the QUT Postgraduate Research Award (QUTPRA) and the QUT Excellence Top Up scholarship, as well as the CRE-RHAI for an additional top up scholarship. I also acknowledge the travel funding provided by the School of Mathematical Sciences and Institute of Health and Biomedical Innovation which have allowed me to disseminate my work at various academic conferences.

I acknowledge the computational resources and support provided by the HPC and Research Support Group at QUT.

Finally, I would also like to thank my family and friends for their encouragement and support throughout this journey.

Contents

Abstract	i
Key words	iii
List of acronyms	v
List of papers	vii
Declaration	ix
Acknowledgements	xi
Chapter 1 Introduction	1
1.1 Thesis structure	2
Chapter 2 Literature review	5
2.1 Methicillin-resistant <i>Staphylococcus aureus</i>	5
2.1.1 MRSA transmission pathways	6
2.1.2 MRSA interventions	7
2.2 Modelling methods	10
2.2.1 Mathematical models for disease transmission	11
2.2.2 Mathematical models for hospital MRSA transmission	13
2.2.3 Poisson processes	16
2.2.4 Statistical models for extremes	18
2.2.5 Proportional hazard survival models	21
2.3 Inference methods	22
2.3.1 Markov chain Monte Carlo	23
2.3.2 Sequential Monte Carlo	27
2.3.3 Model selection	30
2.3.4 Approximate Bayesian Computation	32
Chapter 3 Model choice problems using approximate Bayesian computation with applications to pathogen transmission data	41
3.1 Introduction	43
3.2 Methodology	44
3.2.1 Overview of ABC algorithms	44
3.2.2 Approximate Bayesian Model Choice Algorithm	45
3.2.3 Validating Example	48
3.3 Application to Pathogen Transmission Data Sets	51
3.3.1 Pathogen Transmission in a Hospital Ward	51
3.3.2 Tristan da Cunha Cold Outbreak	53

3.3.3	Hagelloch Measles Outbreak 1861	55
3.4	Discussion	58
Chapter 4	ABC model selection for spatial max-stable models applied to South Australian maximum temperature data	61
4.1	Introduction	63
4.2	South Australian annual maximum temperature data	64
4.3	Max-stable models	65
4.4	Approximate Bayesian computation for model selection	68
4.5	Application	72
4.5.1	Implementation details	72
4.5.2	Results	73
4.6	Discussion	76
Chapter 5	Parametric survival analysis of hospital ward MRSA incidence allowing for carryover effects from previous cases	81
5.1	Introduction	83
5.2	Method	83
5.2.1	Data	83
5.2.2	Parametric survival models	84
5.3	Results	85
5.4	Discussion	87
Chapter 6	Quantifying the impact of an MRSA outbreak on patient outcomes in a NICU	91
6.1	Introduction	93
6.2	Data	93
6.3	Method	94
6.4	Results	96
6.4.1	MRSA acquisition	96
6.4.2	Length of stay	97
6.5	Discussion	98
Chapter 7	Quantifying the relative effect of environmental contamination on surgi- cal ward MRSA incidence	103
7.1	Introduction	105
7.2	Methods	105
7.2.1	Data	106
7.2.2	Non-homogeneous Poisson process formulation	107
7.2.3	Patient time imputation	109
7.2.4	Smoothing of environmental contamination data	110
7.2.5	Estimation procedure	110
7.3	Results	112
7.4	Discussion	117
7.5	Conclusions	119
Chapter 8	A stochastic model for MRSA transmission within a hospital ward in- corporating environmental contamination	121
8.1	Introduction	123
8.2	Methods	124
8.2.1	Model formulation	124
8.2.2	Parameter values	127

8.2.3	Interventions	128
8.3	Results	130
8.3.1	Normal burden setting	131
8.3.2	High burden setting	131
8.4	Discussion	132
Chapter 9	Conclusions	141
9.1	Summary	141
9.2	Future work	142
9.3	Concluding remarks	146
Appendix A	Supplementary Material for Chapter 3: ‘Model choice problems using approximate Bayesian computation with applications to pathogen transmission data’	149
A.1	Additional details for the validating example	149
A.1.1	Direct evaluation of the posterior model probabilities	149
A.1.2	Validating example with different sets of regression summary statistics	150
A.2	Additional details for the hospital MRSA example	152
A.2.1	Pseudo-equilibrium approximation	152
A.2.2	Priors used	154
A.2.3	Additional output from ABMC algorithm	154
A.3	Investigation of the use of bias-reduced logistic regression for the hospital MRSA example	155
A.4	Additional details for the Tristan da Cunha cold outbreak example	159
A.4.1	Priors used	161
A.4.2	Additional output from ABMC algorithm	161
A.5	Additional details for the Hagelloch measles example	163
A.5.1	Derivation of observed data set	163
A.5.2	Exposure and infectious periods distributions	165
A.5.3	Priors used	166
A.5.4	Additional output from ABMC algorithm	167
Appendix B	Supplementary Material for Chapter 4: ‘ABC model selection for spatial max-stable models applied to South Australian maximum temperature data’	171
B.1	Prior predictive checks	171
B.2	Posterior distributions	172
B.3	Simulation examples	181
B.4	Preliminary comparison of characteristics of exact and approximate simulation from max-stable processes	185
Appendix C	Supplementary Material for Chapter 5: ‘Parametric survival analysis of hospital ward MRSA incidence allowing for carryover effects from previous cases’	193
C.1	Model details	193
C.2	Data plots	195
C.3	Model comparison outputs	202
C.3.1	Output tables for Ward A 2-bed cubicles	203
C.3.2	Output tables for Ward A 4-bed cubicles	205
C.3.3	Output tables for Ward B	207
C.3.4	Output tables for Ward C 2-bed cubicles	209
C.3.5	Output tables for Ward C 4-bed cubicles	211

C.3.6	Output tables for Ward D 2-bed cubicles	213
C.3.7	Output tables for Ward D 4-bed cubicles	215
C.3.8	Output tables for Ward E 2-bed cubicles	217
C.3.9	Output tables for Ward E 4-bed cubicles	218
C.3.10	Output tables for Ward F 4-bed cubicles	220
C.3.11	Output tables for Ward G 2-bed cubicles	222
C.3.12	Output tables for Ward G 4-bed cubicles	223
Appendix D Supplementary Material for Chapter 6: ‘Quantifying the impact of an MRSA outbreak on patient outcome in a NICU’		225
D.1	MRSA outcome: Additional outputs	225
D.1.1	Simpler models for MRSA outcome	225
D.2	LOS outcome: Additional outputs	230
D.2.1	Simpler model for LOS outcome	231
Appendix E Supplementary material for Chapter 7: ‘Quantifying the relative effect of environmental contamination on surgical ward MRSA incidence’		235
E.1	MCMC specifications	235
E.1.1	Simulation method	238
E.2	Simulation study	239
E.3	Results without environmental contamination component	245
E.4	Ward B Results	249
Appendix F Supplementary Material for Chapter 8: ‘A stochastic model for MRSA transmission within a hospital ward incorporating environmental con- tamination’		253
F.1	Additional model details	253
F.1.1	Parameter estimation for fixed parameters	253
F.1.2	Parameter estimation for individual model’s force of infection . . .	254
F.1.3	Parameter estimation for time series component	255
F.1.4	Additional details on interventions	256
F.2	Parameter sensitivity analysis	258
F.2.1	Normal burden setting	258
F.2.2	High burden setting	260
F.3	Varying strength of single interventions	263
F.3.1	Normal burden setting	263
F.3.2	High burden setting	263
F.4	Additional results for normal burden setting	275
F.4.1	AR outcome	275
F.4.2	AC outcome	276
F.4.3	C_{xd} outcome	276
F.4.4	C_d outcome	277
F.4.5	I_{xd} outcome	278
F.4.6	I_d outcome	279
F.5	Additional results for high burden setting	293
F.5.1	AR outcome	293
F.5.2	AC outcome	294
F.5.3	C_{xd} outcome	294
F.5.4	C_d outcome	297
F.5.5	I_{xd} outcome	298
F.5.6	I_d outcome	298

1 Introduction

Healthcare associated infections (HAIs) are infections acquired during a person's stay in a hospital. Such infections are associated with increased mortality, morbidity and cost to both patients and hospitals. HAIs are endemic in most countries but affect developing countries more than developed countries. In a meta-analysis of the literature from 1995 to 2010, the pooled HAI prevalence from developed countries was estimated to be 7.6 (95% CI: [6.9, 8.5]) episodes per 100 patients while the corresponding estimate for developing countries was 10.1 (95% CI: [8.4, 12.2]) episodes per 100 patients (World Health Organization et al., 2011). HAIs more severely affect high risk patients such as those in intensive care units and neonates. Neonatal HAI rates in developing countries are estimated to be between three to 20 times the rates in developed countries (World Health Organization et al., 2011, Zaidi et al., 2005).

The issue of HAIs is further compounded by the rise in antimicrobial resistance worldwide. There exists a selective preference for antibiotic-resistant strains of microorganisms in hospitals where most patients receive antibiotic treatment to assist with their hospitalisation. As hospital pathogens become increasingly resistant to the commonly used antimicrobials, infections caused by these pathogens become harder and at times, impossible to control. As such, these multidrug resistant organisms (MDROs) represent a significant threat to hospital patients. It has been postulated that MDROs could potentially threaten achievements of modern medicine leading to a 'post-antibiotic' era where minor infections or injuries could become life-threatening due to the lack of treatment options (World Health Organization, 2014). Therefore, in addition to development of novel antimicrobial agents to target MDRO, it is also important to better prevent MDRO acquisition in hospitalised patients.

One research avenue, and the focus of this thesis, is to improve our understanding of the MDRO transmission dynamics through mathematical and statistical modelling. These models can assist in establishing effective infection control and prevention policies by providing insights into the transmission mechanisms of the pathogens, as well as comparisons of different interventions to better use limited hospital resources. Specifically, this thesis investigated the transmission of methicillin-resistant *Staphylococcus aureus* (MRSA), a common MDRO associated with a wide range of

infections such bacteraemia, sepsis, and skin and soft-tissue infections (Boucher et al., 2010), in a hospital setting. The contribution of microbiological environmental contamination to MRSA transmission is of particular interest.

However, statistical and mathematical modelling of MRSA in the healthcare setting is challenging for three main reasons: (i) the transmission process in a hospital ward is never fully observable, rather patients are only tested or screened for MRSA at intervals during their hospitalisation; (ii) there is an inherent dependence between MRSA cases detected close to one another; and (iii) there is substantial variability inherent with small population sizes typical of a hospital ward.

Additionally, heterogeneity in data collection and clinical practices across different hospitals affects the information contained in data sets, acknowledging that data collection is not the primary focus of healthcare workers particularly during an outbreak scenario. The data sets collected could thus be less than ideal for model inference, i.e. ‘scrappy’ data sets. As such, with the acquired MRSA data sets, it is important to identify research questions that could be answered, given the information available in the data set, as well as the methods that are best suited for statistical inference. The onus is on the statistician to analyse the data so that information extracted is optimised.

It is also often of interest to compare between two or more candidate models in such investigations, as well as in most modelling contexts. As such, a relatively general, simulation-based method for model selection is also investigated as part of this thesis.

1.1 Thesis structure

This thesis comprised of three parts to address the following six research aims:

1. To develop an approximate Bayesian computation (ABC) method to address model choice problems
2. To explore the use of the ABC method for model choice in infectious disease and spatial extremes applications
3. To investigate the temporal pattern of MRSA occurrences in hospital beds of different wards within a hospital
4. To investigate the relationship between length-of-stay (LOS), bed movements, colonisation pressure and MRSA acquisition within a neonatal ICU (NICU) during an outbreak scenario
5. To quantify the relative contribution of environmental contamination in MRSA transmission based on environmental contamination data
6. To propose a novel stochastic simulation model to represent transmission dynamics of MRSA between patients and the environment in a hospital ward

The first part involves the application of approximate Bayesian computation methods to address model choice problems. Model choice plays an important role in many

statistical applications. However, there are some models for which it can be difficult or computationally prohibitive to perform model choice. Approximate Bayesian computation is a relatively new and powerful method that could be used to address model choice for some of these models. A new approximate Bayesian computation algorithm for model choice problems, referred to as ABMC, is proposed in Chapter 3 and applied to a variety of infectious disease transmission models and data sets, including a data set on MRSA occurrences in an Australian intensive care unit (ICU).

In Chapter 4, the ABMC algorithm is applied to a model selection problem involving maximum temperature data and spatial max-stable models for describing spatial dependencies between extreme data. Max-stable models are a class of computationally demanding models due to the fact that the full model likelihood is not available in closed form except for low dimensional cases (specifically, only one or two-dimensional). As such, direct methods for model choice could not be used for these models and the ABMC algorithm proposed is ideally suited for such applications. The maximum temperature investigation was also motivated by the increased hospitalisation and mortality associated with extreme heat events (Hajat et al., 2010), and potential seasonality of *Staphylococcus aureus* infections with more cases occurring in warmer seasons (Leekha et al., 2012).

The second part comprises of two biostatistics case studies of MRSA. The first case study investigates the temporal heterogeneity of MRSA occurrences between wards in a hospital, extending the spatial heterogeneity finding from the same data set (Kong et al., 2012) (Chapter 5). The work aims to show how the MRSA occurrences differ between wards. The second case study in Chapter 6 investigates factors that contributed to an MRSA outbreak in a neonatal intensive care unit.

The third part focuses on the modelling of the contribution of environmental contamination on MRSA occurrence in a hospital ward. Chapter 7 provides the first quantification of the relative contribution of microbiological environmental contamination to MRSA occurrences in a hospital ward using microbiological environmental contamination data. This finding is used in the simulation model proposed in Chapter 8. The model couples the patient MRSA transmission dynamics in a hospital ward with a model describing the evolution of the ward's environmental contamination. The effects of various combinations of commonly proposed interventions were investigated using the proposed model.

A summary of the main findings from this thesis is in Chapter 9 as well as discussions on potential future research.

2 Literature review

This chapter provides the relevant background for the subsequent chapters. The transmission pathways and intervention strategies for MRSA in a hospital setting are elaborated in Section 2.1. Relevant mathematical and statistical models used in this thesis are detailed in Section 2.2, and the statistical inference methods for parameter estimation and model selection used are introduced in Section 2.3.

2.1 Methicillin-resistant *Staphylococcus aureus*

Staphylococcus aureus is a commensal, gram positive bacterium which approximately 30% of the general population carry asymptomatically in their nose. This asymptomatic carrier state is also frequently referred to as being ‘colonised’ with the organism, particularly when detected through screening tests in hospitals. *S. aureus* infections were primarily treated with penicillin when penicillin was first introduced in the early 1940s. However, penicillin-resistant staphylococci were reported as early as 1942 (Rammelkamp and Maxon, 1942). Methicillin was introduced into the clinical setting in 1959 in response to the rise in penicillin resistance, but resistance to methicillin was reported two years after its introduction (Jevons, 1961, Knox, 1961, Rolinson, 1961), giving rise to the emergence of methicillin-resistant *Staphylococcus aureus* (MRSA) as a significant healthcare associated pathogen (Peacock and Paterson, 2015). The term MRSA now refers to strains of *S. aureus* with resistance to virtually all β -lactam antibiotics. There have also been reports of MRSA being resistant to other antimicrobials including vancomycin (Saravolatz et al., 2012), considered one of the last treatment options for serious MRSA infections, and newer antimicrobial agents linezolid and daptomycin (Gould et al., 2012). As such, treatment for MRSA is becoming increasingly limited.

The rapid resistance development exhibited by MRSA underscores the importance of basic infection control and prevention practices in hospitals, rather than a reliance on treatments. A number of prevention initiatives and interventions were implemented in developed countries around the mid-2000s in order to reduce MDRO-related HAIs, in particular MRSA (see for example Duerden et al. (2015), Struelens and Monnet (2010)). Subsequent reports of reductions in MRSA-associated infections (Tong et al., 2015) have

been promising and highlight the importance of effective infection control and prevention practices. In addition, some countries, notably the Netherlands, have been able to maintain a low prevalence of MRSA due to their strict national infection control policy (Bode et al., 2011). Improving our understanding of the transmission mechanism of hospital pathogens should lead to further improvements in infection control.

2.1.1 MRSA transmission pathways

There are a number of potential transmission pathways for MRSA in a hospital setting. Perhaps the most obvious transmission pathway is through other MRSA-positive patients in the ward. These patients have been shown to ‘shed’ MRSA to their immediate environment, allowing for transmission to occur. The amount of shed material is very variable. There have been reported instances of ‘super shedders’ or ‘cloud adults’ in which the patients shed a very large amount of the microorganism which facilitates easier transmission of MRSA. The amount of shedding may also depend on the patient’s antibiotic treatment, and colonised body site (Dancer, 2008).

A patient could already be a dormant MRSA carrier, with the anterior nares of the nose being the most common carriage site for *S. aureus*. It is estimated that about 20% of the general population are persistent nasal carriers of *S. aureus* and 30% of the general population are intermittently colonised with the organism. However, these proportions vary considerably. *S. aureus* has also been found to colonise other body sites, such as the skin, perineum and pharynx (Wertheim et al., 2005). When a person is hospitalised, it is typical that their immune system is compromised, and the dormant *S. aureus* may develop into an infection. Given that the vast majority of hospitalised patients are administered with antimicrobials, this also creates a selective pressure for MRSA.

Healthcare workers (HCWs) and visitors could also transmit MRSA in hospital wards. They act as what is known as ‘vectors’ in the cross-transmission of MRSA between a colonised patient and susceptible patient. The vectors themselves could either only be transiently contaminated with MRSA, most likely from direct contact or close proximity to an MRSA-positive patient, or they could also be MRSA carriers themselves. There have also been reports of cloud adult HCWs (Sherertz et al., 2001).

There is also evidence to suggest that the effect of MRSA-positive patients on subsequent transmission lasts well beyond their hospitalisation. Prior bed occupancy by an MRSA-positive patient has been shown to increase the risk of a subsequent patient in the same bed acquiring the same strain of MRSA (Mitchell et al., 2014). Similar findings were also obtained for other MDROs (see the meta-analysis and review by Mitchell et al. (2015)). This highlights the difficulty in cleaning the fomite (mattress) and will be particularly exacerbated in busy wards.

The hospital bed is one example of near-patient sites which are frequently touched (Huslage et al., 2010) and commonly contaminated with hospital pathogen (Dancer,

2008). The presence of such environmental contamination is another potential transmission pathway for MRSA in hospital wards. Many MDRO organisms, including MRSA, have been shown to be very resilient on dry and inanimate surfaces for extended periods (Kramer et al., 2006). This increases the likelihood that a patient, healthcare worker or visitor could pick up the organism from the environment and transfer it to a susceptible hospitalised patient. There have been outbreak investigations which traced the origin of the outbreak to contaminated hospital equipment (Dancer, 2008), and studies which associated decreased environmental contamination with reduced incidence of MRSA infections (Dancer et al., 2009).

2.1.2 MRSA interventions

Interventions are actions implemented by hospitals to minimise the occurrence of preventable adverse events. While also referred to as control strategies, the term “interventions” will be used in this research. This section provides an overview of common interventions used to prevent MDRO HAIs.

The earliest literature on hospital interventions and how the interventions relate to the statistics of hospital adverse outcomes (e.g. disease acquisition and death) was by Florence Nightingale (Nightingale, 1863), which already advocated good hygiene practices, hospital cleaning, cohorting and contact precaution, in addition to good hospital data recording and statistic reporting practices.

Hand hygiene

Good hand hygiene practices and compliance have been the cornerstone of hospital infection control policies for HAI. Proper hand hygiene ensures that transfer of MDROs from a colonised person is minimised (World Health Organization, 2009). Hand hygiene interventions are the most studied intervention in reducing HAI. Inferences from such clinical studies have generally been positive with improved hand hygiene policies leading to a reduction in HAIs. However, hand hygiene interventions did not yield statistically significant differences due to the interventions in seven out of the 23 hand hygiene studies identified between 1977 to June 2008 in a WHO review assessment on hand hygiene interventions (Allegranzi and Pittet, 2009).

Barrier precaution

Barrier precaution aims at reducing contact of HCWs with potentially infectious body sites and subsequently the transfer of infectious agent to other patients facilitated by the HCWs. Proper use of gloves and gowns are the basis of barrier precaution against MDRO transmissions.

A 2006 review on barrier precautions and surveillance cultures interventions identified seven high quality studies where only four showed beneficial effects of such interventions

(Aboelela et al., 2006). More recently, a large 20-hospital study on universal glove and gown use failed to show statistically significant differences in their primary outcome of MRSA or VRE acquisition rate (Harris et al., 2013).

Cohorting and isolation

Cohorting limits the interaction of individuals to a small, specified cohort in order to control the potential spread of MDRO should any member of the cohort becomes colonised. Cohorting can be implemented on patients, HCWs and medical devices subject to space, staffing and resource constraints.

Isolation places a patient or small group of patients in isolation rooms where contacts with other individuals, including HCWs, are minimised. Isolation interventions are generally only actioned on high risk individuals or individuals detected with MDRO colonisation as isolation can adversely affect the patients' quality of care and hospitalisation experience (Morgan et al., 2009, Stelfox et al., 2003).

The impact of isolation on controlling the spread of MDRO has also been questioned with one review critiquing major methodological weaknesses of clinical studies which have evaluated isolation interventions (Cooper et al., 2004a). A prospective study investigating isolation and cohorting on the spread of MRSA showed no evidence of a difference between the study phases, with and without the intervention (Cepeda et al., 2005). However, isolation forms part of the hospital infection control policies in two hospitals where MRSA (van Trijp et al., 2007) and VRE (Christiansen et al., 2004) have been successfully controlled. The Dutch 'search-and-destroy' policy, which includes pre-emptive isolation of high risk patients in addition to isolation of MRSA-positive patients, has also been credited for the low MRSA prevalence in the Netherlands (Bode et al., 2011).

Improved screening and antimicrobial stewardship

As MDRO colonisations are asymptomatic, culture samples are taken from patients to be tested for the presence of particular MDROs. Not all patients are screened for MRDOs, particularly those with a short hospitalisation duration or thought to be of low risk of acquiring colonisation. There has been some success with active surveillance interventions where all patients are screened and isolated upon admission such as in the Netherlands. However, the substantial burden on hospital resources has limited the uptake of active surveillance. The uptake of more costly rapid diagnostic tests are being considered such as tests which use more advanced microbiological developments such as polymerase chain reaction (PCR) techniques to significantly reduce turnaround times.

Use of rapid diagnostics has been shown to significantly reduce MRSA acquisition in a hospital setting through simulation studies (Bootsma et al., 2006) though clinical

evidence on the impact of rapid diagnostics on patient outcomes is still limited (Geiger and Brown, 2013).

Rapid diagnostics can also form part of hospitals' antimicrobial stewardship (AMS) programmes. AMS programmes aim to increase appropriateness of antimicrobial prescription in order to minimise the unintended consequences of antimicrobial use, such as resistance development, and improve clinical outcomes. Clinical outcome improvements reported from AMS programmes include reductions in mortality, infection rates and length of stay. However, there are also studies evaluating such programmes which did not report such improvements (see recent reviews by Bauer et al. (2014) and Coulter et al. (2015)).

Hospital cleaning

MDRO reservoirs found in sterile hospital environments are another source of colonisation that should be accounted for since they can survive for several months (Kramer et al., 2006) and have been associated with patient colonisations. Effective cleaning protocols coupled with appropriate environmental surveillance can minimise the contribution of hospital environment on the risk of MDRO colonisation.

Environmental cleaning is an accepted part of core infection control and prevention hospital guidelines to reduce MDRO-related HAIs, however, the role of environmental contamination in transmission of MDROs is still not well defined. Studies of the environmental cleaning interventions have shown beneficial effects of improved cleaning in reducing specific HAI burdens (Hayden et al. (2006) for VRE and Dancer et al. (2009) for MRSA) while others did not (Wilson et al., 2011). This highlights the stochastic nature of MRSA occurrence in hospital wards, particularly for wards with relatively low rates of MRSA.

While all hospitals allocate a portion of their resources to cleaning activities, evaluation of cleaning activities is not well-established. Most hospitals rely on some form of visual inspection to assess the performance of cleaning activities (Cooper et al., 2007). However, such inspections will not be able to ascertain if microbiological environmental contamination has been removed through cleaning. More advanced forms of assessment require additional tools such as fluorescent markers, adenosine triphosphate (ATP) bioluminescence markers and microbiological samples provide more informative indicators as to the level of environmental contamination. These additional assessments require money and staff time to be performed and analysed. There is also a lack of standardised guidelines as to the appropriate levels of contamination to be considered as an alert to increase cleaning efforts for ATP and microbiological measurements. These factors all contribute to the lack of adoption of advanced environmental surveillance in hospitals (Carling, 2013).

Patient decolonisation

Patients detected to be colonised with MRSA can undergo a decolonisation treatment which typically involves administration of nasal mupirocin ointment, chlorhexidine baths (Climo et al., 2013), and oral antibiotics such as rifampin. Evaluations of the decolonisation strategies for MRSA have yielded positive, albeit heterogeneous, results and still require further investigation (Ammerlaan et al., 2009, Tacconelli and Johnson, 2011). There are also potential issues with resistance development (Hetem and Bonten, 2013, Horner et al., 2012, Poovelikunnel et al., 2015) which could lead to treatment failure for these decolonisation treatments (Rai et al., 2016).

2.2 Modelling methods

Evaluation of the interventions listed above is typically conducted through prospective studies which incur substantial cost and time on behalf of the hospital. There are also ethical issues in selecting only a subsection of the hospital patient population, and in randomising wards to evaluate the effects of an intervention. As a result, most clinical studies are conducted as observational studies or quasi-experimental studies which balance the investigation of an intervention with day-to-day patient care. However, such study designs have limitations in inferring causal relationships (Harris et al., 2004) and make it difficult to separate the effect of a single intervention among the multiple interventions generally in place in hospitals at any one time.

It can also be difficult to generalise the results of such studies beyond the hospital in which they were conducted due to the large variability in patients and practices between hospitals. This is a potential factor behind the differing findings for studies evaluating the same interventions.

Mathematical modelling is a useful tool to overcome the aforementioned difficulty in generalising results obtained from hospital-specific intervention studies by providing a general framework that could be fitted to different hospital-specific scenarios. In addition, other benefits of using mathematical models include:

- linking between preliminary hypotheses and execution of resource-heavy studies
- increased value from previous studies by incorporating observed data into mathematical models
- fewer, if any, ethical issues, as mathematical models can be used to simulate the patient data

As an example, consider the mathematical model investigation of interventions to reduce the level of MRSA burden in an ICU in McBryde et al. (2007b). The study investigated the impacts of modifying hand hygiene compliance, patients' expected length of stay, admission prevalence of colonised patients, HCW-to-patient ratio, use of a decolonisation treatment (enteral vancomycin) and changing ward size individually through the

proposed mathematical model. In contrast, clinical studies to evaluate the interventions trialled by the McBryde et al. (2007b) model would have been extremely costly.

The MRSA acquisition process, particularly in a small population setting such as in a hospital ward, is highly affected by the stochasticity of the process. As such, it is important to consider stochasticity when modelling patient MRSA acquisition in a hospital ward. In a review of the use of mathematical models in MDRO transmission, van Kleef et al. (2013) showed that the use of stochastic models has increased over time to provide more realistic representations of the transmission process in small population setting. The influential effect of stochasticity in modelling MRSA transmission in hospitals was shown in Cooper et al. (2004b). The authors showed that their model could exhibit high endemic levels of MRSA prevalence, low endemic levels and stochastic fadeout for different stochastic simulations of the model using the same parameter set.

van Kleef et al. (2013) provides a comprehensive review on the development of mathematical models in investigations of hospital MDRO transmissions and the effects of potential interventions. This section focuses instead on the relevant mathematical modelling literature to the research problems at hand. In particular, Section 2.2.1 provides a general overview of mathematical models to describe disease transmission, some of which are used in the analysis presented in Chapter 3. The mathematical models specific to MRSA transmission in hospitals are discussed in Section 2.2.2.

2.2.1 Mathematical models for disease transmission

Mathematical models describing infectious disease transmission assist in the understanding of the spread of the disease by providing a conceptual representation of the population dynamics during the disease spread. Infectious disease transmission models were first used to determine the effectiveness of smallpox inoculation (Bernoulli, 1766) and have since been applied to many different infectious diseases such as malaria (Smith et al., 2012), sexually transmitted diseases (Anderson and Garnett, 2000), pandemic influenza (Lee et al., 2009), and tuberculosis (Brooks-Pollock et al., 2014). More comprehensive accounts of applications are provided in Hethcote (2000) and Keeling and Rohani (2008).

These models categorise the population into discrete groups based on their disease status, typically as susceptible or disease-free (S), infectious (I), and recovered with acquired immunity to the disease (R). For large populations, the dynamics of these group can be represented by a system of ordinary differential equations (ODEs).

The Susceptible-Infectious-Recovered (SIR) model (Kermack and McKendrick, 1927) is perhaps the most well known mathematical model for describing disease transmission,

and can be represented diagrammatically as shown in Figure 2.1 as well as mathematically as

$$\begin{aligned}\frac{dS}{dt} &= -\beta SI \\ \frac{dI}{dt} &= \beta SI - \gamma I \\ \frac{dR}{dt} &= \gamma I.\end{aligned}$$

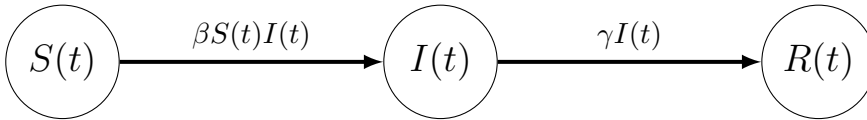


Figure 2.1: Compartment diagram for SIR model.

Of particular interest is the force of infection term $\kappa(t)$ which describes the rate that the susceptible population becomes infected, i.e. the transition rate from $S(t)$ to $I(t)$. For the basic SIR model in Figure 2.1, the force of infection $\kappa(t) = \beta S(t)I(t)$. This term dictates the spread of the disease in the model. As such, control or eradication of a particular disease is dependent on the the force of infection. A related quantity is the basic reproduction number R_0 defined as the number of new secondary infections arising from a single infectious individual in an entirely susceptible population. If $R_0 > 1$, the ODE system predicts that the disease will persist, at least for a short term, in the population whereas an R_0 value less than 1 implies that the disease will die out soon after its introduction. Disease control efforts are evaluated based on their impact on the R_0 value with the goal of reducing R_0 below 1.

For the basic SIR model, the R_0 value can be straightforwardly deduced from the model equations to be $\frac{\beta s_0}{\gamma}$ where s_0 is the initial population size of susceptible individuals, i.e. the product of the force of infection for one infectious individual in an entirely susceptible population of size s_0 (βs_0) multiplied by the average duration the individual remains infectious ($\frac{1}{\gamma}$). A more general method for determining R_0 is through the eigenvalue decomposition of the next-generation matrix (Diekmann et al., 2009, van den Driessche and Watmough, 2002).

Additional groups may be included in these mathematical models depending on the particular disease, e.g. a vaccinated group (V), or a latently infected group (E) where individuals are infected but are not yet infectious. For diseases with an associated vaccine, the corresponding R_0 of the model is used to determine the proportion of the population which have to be vaccinated in order to eradicate the diseases. This mechanism is called the herd immunity effect. These models can quickly grow in complexity by incorporating more details into the infection process. For example, it might be possible to separate the infected class into two (or more) groups of differing infectivity depending on broad risk factors (Britton et al., 2011), linking two or more

populations typically referred to as meta-population models (Riley, 2007, Rock et al., 2014), incorporating the effect of another potentially competing disease and incorporate external driving forces into the force of infection term (Breban et al., 2009, Eisenberg et al., 2013).

Cross-transmission models offer an alternative transmission pathway for disease spread and are perhaps more relevant to hospital acquired infections. Cross-transmissions models were originally proposed for investigation of malaria transmissions which were facilitated by mosquitoes acting as vectors for the disease. It is also frequently cited as the Ross-Macdonald model (see Smith et al. (2012) for a historical review on its development). A key difference between the cross-transmission models and the direct transmission models discussed above is that the disease transmissions occur between infective individuals and susceptible vectors, and susceptible individual and infective vectors (see compartment diagram in Figure 2.2) rather than directly from infective individuals to susceptible individuals.

The work in Chapter 3 presents a method for addressing model choice problems with such models using model simulations. These model simulations are generated using Gillespie’s algorithm (Gillespie, 1977, 2007) which treats the rate terms for the different transitions in the ODE system as competing, piecewise-constant non-homogeneous Poisson processes (Section 2.2.3) which are readily simulated from.

2.2.2 Mathematical models for hospital MRSA transmission

Use of mathematical modelling to describe the transmission of MDROs in hospitals began in the 1990s (Austin and Anderson, 1999, Austin et al., 1999, Massad et al., 1993, Sébille et al., 1997), and has been increasingly used since (van Kleef et al., 2013). The study settings for the majority of the pioneering work in this field were the intensive care units (ICUs) where patients are more susceptible to MDRO due to their weakened immune state. ICU patients also have limited mobility hence the transmission of MDRO from a colonised patient to a susceptible patient was postulated to be facilitated by a vector, a healthcare worker (HCW) in this setting. The HCW can either be colonised with the pathogen themselves, or transiently contaminated with the pathogen through contact with another patient who is colonised or infected with MRSA. This form of transmission is known as cross-transmission and mathematical models with this form of transmission have the structure shown in Figure 2.2.

Most mathematical models describe the colonisation of patients with MDRO rather than infections. Colonised patients are detected through screening tests as part of a hospital’s surveillance system. Once detected as colonised, interventions will be put in place for the patient to prevent further transmission of the pathogen from the patient. This means models that describe change in the colonisation status of patient would more readily mimic hospital intervention policies for MDRO. In addition, colonisation counts typically outnumber infection counts (since infections are preceded by

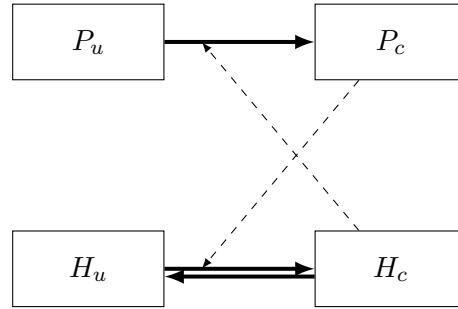


Figure 2.2: Compartmental diagram for a cross-transmission model adapted from Austin et al. (1999) where P_u denotes uncolonised patients, P_c colonised patients, H_u uncontaminated healthcare workers (HCWs) and H_c temporarily contaminated HCWs. The solid lines represent transitions between states while the dashed lines represent the influence of states on different transitions.

colonisations) so model parameters associated with colonisation data can often be better estimated compared with infection data. A common practice is to aggregate both colonised and infected patients into a MRSA-positive group (Raboud et al., 2005).

The first MRSA transmission model was proposed by Sébille et al. (1997). The model investigated if hand hygiene interventions, antimicrobial policies and a strict policy of not allowing any colonised admissions individually decreased the proportion of colonised patients in a 10-bed ICU. The deterministic model of Sébille et al. (1997), similar to that shown in Figure 2.2 but with the colonised patient and HCW groups separated by the resistance status of the pathogen, showed only moderate success of implementing hand hygiene and antimicrobial strategies over a wide range of efficacies for each intervention in terms of patient prevalence, and that only the cessation of any colonised admissions (most likely through strict admission screening and isolation of patients) succeeded in reducing the proportion of colonised patients in the ward to 0.

Subsequent modelling studies focused on using the model formulation in Figure 2.2 and its extensions to evaluate the effects of a variety of interventions including

- increased hand hygiene (Grundmann et al., 2002, McBryde et al., 2007b, Raboud et al., 2005, Sébille and Valleron, 1997),
- staff cohorting i.e. reducing patient-to-staff ratio (Grundmann et al., 2002, McBryde et al., 2007b, Raboud et al., 2005),
- active or admission screening (Bootsma et al., 2006, Hall et al., 2012, McBryde et al., 2007b, Raboud et al., 2005),
- improved screening test either in terms of increased sensitivity or shorter turnaround time (Hall et al., 2012),
- patient isolation (Bootsma et al., 2006, Hall et al., 2012) and
- improved patient treatment or decolonisation options (McBryde et al., 2007b, Meng et al., 2010).

Hand hygiene improvements were frequently found to be a very efficacious intervention when comparing multiple interventions (McBryde et al., 2007b, Raboud et al., 2005, Sébille et al., 1997, Wang et al., 2011). However, the only intervention to eradicate MRSA from a ward is to restrict admissions into the ward through admission screening, preventing admission of colonised patients (Hall et al., 2012, McBryde et al., 2007b, Sébille et al., 1997). However, the strict admission screening intervention is rarely feasible in practice and is also associated with negative patient outcomes.

A challenge with the models described above is that HCW-related data are not routinely collected and the colonisation status of HCWs, transient or otherwise, is not usually observed unless there is a specific study in the hospital that included HCW screening. As such, HCW-related transmission parameters are more difficult to parametrise accurately compared with the patient-related parameters. Due to the unavailability of data on colonised HCWs, McBryde et al. (2007b) assumed that colonised HCWs are at quasi-equilibrium and solved the corresponding ODE for HCW to obtain an expression for the steady-state value of HCWs, given the other values of the model parameters and number of colonised patients. Other studies fit HCW parameters to obtain a close match between the model's realisation of the patient dynamics and observed patient data (Hall et al., 2012, Wang et al., 2012), or assume plausible values based on literature, expert opinion or both (Bootsma et al., 2006, Raboud et al., 2005).

Another possibility is to instead model only the status transitions of the patients in the ward, with the implicit assumption that colonisation is facilitated by a vector (e.g. HCWs, visitors) (Forrester et al., 2007, Forrester and Pettitt, 2005, Meng et al., 2010). A popular approach here is to model patient MRSA status transition as a non-homogeneous Poisson process (see Section 2.2.3 below).

Environmental contamination

The previously identified lack of advanced environmental surveillance in hospitals, in particular microbiological measurements, has resulted in little development of mathematical models that explicitly account for transmission through environmental contamination. As such, this section will also include modelling studies for other hospital MDROs. The first model was only proposed in 2006 for VRE (McBryde and McElwain, 2006) while later studies include Wolkewitz et al. (2008) (VRE), Wang et al. (2012, 2013) (MRSA), Hall et al. (2012) (MRSA) and Doan et al. (2015) (*Acinetobacter baumannii*).

While environmental contamination-related transmission may not be the dominant transmission route for these MDROs, omission of this transmission route was shown to provide substantially different model predictions on the effects of interventions. The model of McBryde and McElwain (2006) predicted that VRE will remain endemic due to environmental contamination even if no VRE colonised patients are allowed to be admitted. The corresponding model, without environmental contamination, predicted

VRE will be successfully eradicated with the same intervention. In light of the sustained persistence of MDROs in hospitals, it is likely that environmental contamination plays a minor yet influential role.

An alternative approach to incorporating environmental contamination is to include a background rate or importation rate which is independent of the number of colonised patients in a ward (Forrester et al., 2007). This approach however combines multiple potential transmission routes and is unable to provide a direct estimate of the contribution of environmental contamination to MDRO transmission, and as such complicates subsequent modelling efforts to quantify the impact of environmental cleaning interventions in the models. The modelling approach of Forrester et al. (2007) is discussed in more detail in Section 2.2.3.

None of the papers identified which explicitly modelled environmental contamination transmissions have used environmental contamination data to fit the model parameters associated with environmental contamination transmission. McBryde and McElwain (2006) assumed that the transmission rate via environmental contamination was 25% of patient or HCW contamination and Wolkewitz et al. (2008) subsequently used these parameter values in their VRE simulation study. In the other identified studies (Hall et al., 2012, Wang et al., 2012, 2013), the environmental contamination transmission parameters were estimated through comparison of the average simulated number of cross-transmissions obtained using candidate parameter values with the observed number of cross-transmissions. Doan et al. (2015) used the estimated parameter value from Wang et al. (2012).

An argument for improved surveillance and control of environmental contamination could be provided by a mathematical model which includes environmental contamination transmission fitted using environmental contamination data, in addition to patient data. The quantification of the effect of environmental contamination in MRSA transmission is the focus of Chapter 7, and a new mathematical model using the estimates found is proposed in Chapter 8.

2.2.3 Poisson processes

Poisson processes model the occurrences of an event over time and are fully characterised by their intensity $\lambda(t)$. The simplest form of a Poisson process is the homogeneous Poisson process (HPP) with a constant intensity λ . The HPP assumes that the events occur with a constant instantaneous rate λ . As a result, the number of events observed from the HPP in a particular time period, Δ_t , has a Poisson distribution with a mean $\lambda\Delta_t$ and the time between events is exponentially distributed (with mean $\frac{1}{\lambda}$). The assumption of homogeneity, or constant intensity, is frequently too simplistic to represent real-world applications.

Instead, non-homogeneous Poisson processes (NHPPs) are more commonly used. The intensity of a NHPP is allowed to vary in time, i.e. $\lambda(t)$, and could also incorporate covariate information, provided $\lambda(t)$ remains well-behaved and non-negative. Consider a generic Poisson process with intensity function $\lambda(t)$ observed in a finite time interval $[0, t_E]$ where n events were recorded at times t_1, t_2, \dots, t_n . It can be readily shown (Davison, 2003) that the Poisson process likelihood is given by

$$\prod_{i=1}^n \lambda(t_i) \exp \left\{ - \int_0^{t_E} \lambda(u) du \right\}, \quad 0 < t_1 < \dots < t_n < t_E. \quad (2.1)$$

As such, the Poisson process is fully specified once the intensity $\lambda(t)$ is known. In practice, the evaluation of the integral is done numerically. It is straightforward to extend the Poisson process definition to include a spatial component.

NHPPs are used in a wide variety of applications, for example seismic modelling (Ogata, 1999), ecology (Warton et al., 2010), traffic modelling (Frost and Melamed, 1994), software engineering (Kuo and Yang, 1996) and infection occurrences in hospital wards.

Forrester et al. (2007) developed a comprehensive NHPP model for describing patient MRSA acquisition in a hospital ward. The MRSA acquisition model accounts for imperfect sensitivity of the screening test and imperfect isolation of patients through modification of the Poisson process likelihood expression (2.1). The Poisson process rate or force of colonization for a susceptible patient, $\lambda(t)$, for the Forrester et al. (2007) model was

$$\lambda(t) = \beta_0 + \beta_1 C(t) + \beta_2 Q(t)$$

where $C(t)$ is the number of non-isolated colonised patients, $Q(t)$ the number of colonised patients in isolation rooms, and the β 's are the corresponding transmission rates. This model accounts for three possible colonisation sources: background contamination (β_0), colonised patients, and colonised patients who are isolated. In addition, the model also has explicit representations of the sensitivity of the screening test and the probability of being colonised upon admission.

Forrester et al. (2007) estimated the model parameters by first imputing the unknown colonisation time of patients using regular surveillance swab results, admission dates and discharge dates, then performing the parameter inference on the augmented data set comprised of observed and imputed patient data. This was achieved using a data-augmented MCMC algorithm. A similar parameter estimation scheme was used in McBryde et al. (2007b). Since its proposal, the Forrester et al. (2007) method has been subsequently used and extended by a number of other researchers (Cooper et al., 2008, Kypraios et al., 2010, Wei et al., 2016). Kypraios et al. (2010) and Wei et al. (2016) analysed MRSA and VRE colonisation data, respectively, collected from the same eight ICUs using the approach of Forrester et al. (2007). Pooled estimates of the parameters were also obtained from the individual ICU estimates using a random effects model.

Kypraios et al. (2010) and Wei et al. (2016) expanded the Forrester et al. (2007) method by considering alternative epidemic models, namely the non-linear transmission or Greenwood (Greenwood, 1931) model where the Poisson process rate is now $\lambda(t) = \beta_0 + \beta_1 \mathbb{1}(C(t) > 0) + \beta_2 \mathbb{1}(Q(t) > 0)$ (where $\mathbb{1}(x)$ is the indicator function which equals 1 if x is true and 0 otherwise) and no-background model where the prior for β_0 was chosen to be close to zero with high probability.

Results from the different models in the MRSA analysis were used for sensitivity analyses purposes but were not compared directly as in the VRE study (Wei et al., 2016). It was found that different models were selected for different wards, emphasising the heterogeneity of study wards.

Cooper et al. (2008) proposed a number of extensions to the model introduced in Forrester et al. (2007) to analyse VRE data collected during a multiple-phase study, where the different phases corresponded to changes in the antibiotic use policy and the incorporation of hand hygiene education programs. The extensions proposed by Cooper et al. (2008) included incorporation of other patient and ward level covariates multiplicatively to the intensity functions (i.e. Cooper et al. (2008) specifies a form for $\log(\lambda(t))$ rather than $\lambda(t)$), and the possibility of a time-varying probability of being colonised upon readmission for patients who are readmitted into the ward during the study period. Cooper et al. (2008) omitted the background source term in Forrester et al. (2007) which is used to account for other sources of acquisition not directly modelled (such as environmental contamination and colonised staff) as the authors claimed that it was not important in their context.

The work in Chapter 7 proposes an extension of the NHPP model formulation which separates the contribution of environmental contamination from the generic background source term in the model in order to quantify the relative contribution of environmental contamination explicitly. The model is fitted to patient MRSA data and microbiological environmental contamination data originally collected for a cleaning intervention study (Dancer et al., 2009).

2.2.4 Statistical models for extremes

The investigation of maximum temperature data was motivated by the climate change experienced in the recent decades and its potential implications for human health. Changing climate not only changes the mean climatic conditions but also increases the variability of climatic conditions, making extreme weather events, such as floods and heatwaves, more likely (IPCC, 2012). Such events are linked with outbreaks of infectious diseases (McMichael, 2015) as well as increased hospitalisations (Hajat et al., 2010) and deaths (Poumadère et al., 2005). Both climate change and extreme weather events increase the burden placed on healthcare systems (Costello et al., 2009). In addition, some common hospital infections caused by bacterial pathogens, including *S. aureus*, exhibit seasonality with warmer months typically associated with increased

incidence (Durkin et al., 2015, Richet, 2012, Schröder et al., 2015, Schwab et al., 2014), and is likely to be affected by climate change (Patrozou, 2015). A better understanding of the spatial distribution of maximum temperature could lead to improved models to investigate the association between maximum temperature and infection occurrences, which could assist healthcare systems better prepare for the potential impacts of extreme heat events.

Extreme data analysis offers a unique statistical challenge as it is concerned with the modelling of the tails of the observed data and beyond. As such, statistical models for extreme data rely on an assumption of max-stability, i.e. the maximum is distributionally invariant subject to location and scale shifts, to ensure that the tail distributions are nondegenerate, and the associated analysis has an inherent assumption that the (finite) extreme data can be represented sufficiently well by the asymptotic extreme distributions.

The extreme distribution in the univariate case is well-established. For a sequence of independent and identically distributed variables X_1, X_2, \dots, X_n , define $M_n = \max(X_1, \dots, X_n)$. If there exist sequences of constants $\{a_n > 0\}$ and $\{b_n\}$ such that

$$P\left(\frac{M_n - b_n}{a_n} < y\right) \rightarrow F(y) \quad \text{as } n \rightarrow \infty$$

then $F(y)$ is the distribution function of a generalised extreme value (GEV) distribution provided $F(y)$ is nondegenerate. The distribution function for the univariate GEV model is defined as

$$F(y) = \begin{cases} \exp\left\{-\left[1 + \xi\left(\frac{y - \mu}{\sigma}\right)\right]^{-\frac{1}{\xi}}\right\} & \xi \neq 0 \\ \exp\left\{-\exp\left[-\frac{y - \mu}{\sigma}\right]\right\} & \xi = 0 \end{cases}$$

where the parameters μ , σ and ξ are the location, scale and shape parameters. The derivation for the univariate GEV distribution is credited to two seminal papers in the area, namely Fisher and Tippet (1928) and Gnedenko (1943), and as such is also referred to as the Fisher-Tippet-Gnedenko theorem. The univariate GEV can be categorised into three families depending on the value of ξ , which are the Gumbel ($\xi = 0$), Fréchet ($\xi > 0$) and reversed Weibull ($\xi < 0$) families. The reversed Weibull family of distributions is the only one with a finite upper bound.

Extensions of the theory to finite higher dimensions follow the univariate case straightforwardly (Coles, 2001, de Haan and Ferreira, 2006) and is not covered here as it is not the focus of the related work in this thesis. However, some key points from the extension to higher dimensions, or variables, are that the marginal distributions for each dimension are still univariate GEV distributions, and that the multivariate models are less fully prescribed by the corresponding theory. The latter point allows greater flexibility in model specification of the dependence between variables

The focus here is on spatial applications where the goal is to ascertain the spatial dependence of the extremes over a region from a finite collection of spatial location data. A number of different approaches have been proposed to address spatial extreme problems (see review by Davison et al. (2012)). The focus here is on spatial max-stable models which can be considered as the continuous analogue (or infinite dimensional extension), of the univariate GEV distributions described previously.

Max-stable models are typically defined assuming a fixed marginal GEV distributions for the data, allowing the emphasis on the spatial dependence structure. A practical consequence of this assumption is that a transformation will have to be applied to the extreme data investigated before fitting a max-stable model. A common choice for the fixed marginal distribution is the unit Fréchet distribution (i.e., the GEV distribution with $\mu = 0$, $\sigma = 1$ and $\xi = 1$) and the associated transformation from the originally observed GEV data Y to have a unit Fréchet marginal distribution is

$$\left(1 + \xi \frac{Y - \mu}{\sigma}\right)^{\frac{1}{\xi}}.$$

The parameters can be estimated by fitting a univariate GEV distribution to data from each observed location separately.

A general definition of max-stable models can be written as

$$\max_{i \geq 1} \zeta_i Z_i(x), \quad x \in \mathcal{X} \subseteq \mathbb{R}^d,$$

where

- $\{\zeta_i^{-1} : i \in \mathbb{N}\}$ are realisations of a homogeneous Poisson process with unit intensity, or more formally, $\{\zeta_i : i \in \mathbb{N}\}$ are points of a Poisson process on $(0, \infty)$ with intensity measure $d\Lambda(\zeta) = \zeta^{-2}d\zeta$,
- $Z_i(x)$ are independent realisations of a non-negative stochastic process $Z(x)$ with $E[Z(x)] = 1 \forall x$, and
- x denotes the spatial location in \mathcal{X} .

The specifications for the intensity of $\{\zeta_i : i \in \mathbb{N}\}$ and the expectation of $Z(x)$ ensure that the marginal distributions are distributed as unit Fréchet (Smith, 1990). From the general definition, it is possible to derive specific forms of many max-stable models described in the literature (Ribatet, 2013). Relevant derivations are provided in Chapter 4.

Estimation for max-stable models is complicated by the unavailability of a closed form expression for the model likelihood. However, simulations from such models are more straightforward and can be readily done using the R package **SpatialExtremes** (Ribatet et al., 2013). Details on the simulation methods used are provided in the package's user guide (Ribatet, 2009). This makes max-stable models an ideal case study for the

approximate Bayesian computation (ABC) methods (Section 2.3.4) which circumvent the need for likelihood evaluations through repeated model simulations (Beaumont, 2010, Beaumont et al., 2002). The work presented in Chapter 4 extends the use of ABC methods in spatial extremes applications (Barthelmé and Chopin, 2014, Erhardt and Smith, 2012, Prangle, 2016) to cover model selection problems.

2.2.5 Proportional hazard survival models

This section provides an overview of the survival models used in the thesis (Chapters 5 and 6). The analyses in those chapters are straightforward applications of the survival models to MRSA data sets. As such, the development of survival models is not an original contribution of this thesis and the topic is only given a brief treatment here, acknowledging the expansive literature on survival models. There also exists many excellent texts on the matter (see for example Cox and Oakes (1984), Hosmer et al. (2008), Ibrahim et al. (2005), Klein and Moeschberger (2005), Klein et al. (2014)).

Survival models are used to model time-to-event data for a population of individuals or items. The time-to-event T is modelled through the specification of the instantaneous probability of observing the event of interest, i.e. the hazard function

$$h(t) = \lim_{\Delta \rightarrow 0} \frac{P(t < T < t + \Delta | T > t)}{\Delta},$$

from which the probability density function for T can be obtained as

$$f(t) = h(t) \exp \left\{ - \int_0^t h(u) du \right\}. \quad (2.2)$$

The integral in (2.2) is commonly referred to as the integrated hazard and the term multiplying the hazard is commonly referred to as the survival function $S(t)$.

A commonly used survival model is the proportional hazard (PH) model, introduced by Cox (1972) to model the effects of covariates C which are assumed to affect the hazard proportionately (hence the name). The hazard function for the PH model is specified as

$$h(t) = h_0(t) \exp \{ C^T \boldsymbol{\theta} \}$$

where $\boldsymbol{\theta}$ denote the associated coefficients for the covariates, and $h_0(t)$ is the baseline hazard, i.e. the hazard for individuals with $C = 0$.

Specification of a parametric form of the baseline hazard leads to a fully parametric PH model and parameter estimates can be obtained straightforwardly via standard likelihood maximisation techniques. Alternatively, the baseline hazard can be left unspecified and $\boldsymbol{\theta}$ estimated using the partial likelihood approach in Cox (1972). This is referred to as the semi-parametric PH model.

The choice between a fully parametric and semi-parametric PH model depends on the context of the investigation. Fully parametric models allow for straightforward comparisons of the hazard function across different models as well as extrapolation of the hazard function. It may also be desirable to use a fully parametric approach when the time scale of the data is relatively large compared with the time scale of the event of interest (as in the data set used in Chapter 5). Furthermore, use of a fully parametric model allows access to standard model selection tools as described in Section 2.3.3. The semi-parametric approach obviously offers greater flexibility by not having to assume a particular form of the baseline hazard and is suited for when it is unclear how the baseline hazard might behave from prior knowledge of the situation under study.

A key advantage of using such models to analyse HAI data is that the models can correctly account for the time dependence inherent in the system compared with standard regression approaches (Beyersmann et al., 2008). This is achieved through the use of time-dependent covariates $C(t)$ in the model specification above.

Fully parametric PH models are used to investigate the temporal dynamics of MRSA occurrences in different wards in Chapter 5, while semi-parametric PH models are used to investigate the factors influencing MRSA acquisition and length of stay of patients in a neonatal intensive care unit during an MRSA outbreak in Chapter 6. Time dependent covariates are used in both investigations as motivated by Beyersmann et al. (2008).

2.3 Inference methods

The models discussed thus far have associated parameter values which need to be fitted to data. The majority of this thesis uses a Bayesian framework for inference which is detailed below. The exceptions to this are studies presented in Chapter 5 and 6 where a Frequentist approach, i.e. likelihood maximisation, was used due to the relatively simple models and data set considered in those chapters.

Bayesian inferences are made using the posterior distribution of the parameters θ given the observed data \mathbf{y} . The posterior distribution is defined as

$$p(\theta|\mathbf{y}) = \frac{p(\mathbf{y}|\theta)p(\theta)}{p(\mathbf{y})}$$

where $p(\mathbf{y}|\theta)$ is the likelihood of the data given the model parameters, $p(\theta)$ is the prior distribution of the parameters and $p(\mathbf{y})$ is the marginal likelihood or ‘evidence’.

The posterior distribution is typically only defined up to a proportionality constant (i.e. $p(\theta|\mathbf{y}) \propto \eta(\theta) = p(\mathbf{y}|\theta)p(\theta)$) as there are various Monte Carlo computation methods in the literature used to determine the posterior using this form. The normalising constant or marginal likelihood of \mathbf{y} , $p(\mathbf{y})$, is defined as

$$p(\mathbf{y}) = \int p(\mathbf{y}|\theta)p(\theta) d\theta$$

and is of importance in model choice problems.

The prior can be specified either as a vague or non-informative prior sufficient to cover the support of the parameter, or it could be used to incorporate information from either previous similar analysis or expert knowledge.

The rise in popularity of Bayesian methods was greatly facilitated by the introduction of Markov chain Monte Carlo (MCMC) methods for estimation coupled with increasing computational power which made such computational methods more accessible to the research audience, for example, through the free software BUGS (Lunn et al., 2009, 2000).

The remainder of this section is devoted to introducing the statistical inference methods that will be used in this thesis. Green et al. (2015) provides a more comprehensive survey of the developments in Bayesian computational methods.

2.3.1 Markov chain Monte Carlo

Markov chain Monte Carlo (MCMC) methods sample directly from the target distribution, which is the posterior $p(\boldsymbol{\theta}|\mathbf{y})$ for the applications considered here, using an ergodic Markov chain with $p(\boldsymbol{\theta}|\mathbf{y})$ as its stationary distribution.

The Markov chain must satisfy the detailed balance condition (also known as microscopic reversibility or time reversibility)

$$p(\boldsymbol{\theta}^*|\mathbf{y})q(\boldsymbol{\theta}^{[t]}|\boldsymbol{\theta}^*) = p(\boldsymbol{\theta}^{[t]}|\mathbf{y})q(\boldsymbol{\theta}^*|\boldsymbol{\theta}^{[t]})$$

where proposals ($\boldsymbol{\theta}^*$) are drawn from an arbitrary proposal distribution $q(\boldsymbol{\theta}|\boldsymbol{\theta}^{[t]})$ (dependant on the current iteration value of the Markov chain, $\boldsymbol{\theta}^{[t]}$). This is achieved by only accepting proposals with probability

$$\begin{aligned} \alpha &= \min \left(1, \frac{p(\boldsymbol{\theta}^*|\mathbf{y})q(\boldsymbol{\theta}^{[t]}|\boldsymbol{\theta}^*)}{p(\boldsymbol{\theta}^{[t]}|\mathbf{y})q(\boldsymbol{\theta}^*|\boldsymbol{\theta}^{[t]})} \right) \\ &= \min \left(1, \frac{\eta(\boldsymbol{\theta}^*)q(\boldsymbol{\theta}^{[t]}|\boldsymbol{\theta}^*)}{\eta(\boldsymbol{\theta}^{[t]})q(\boldsymbol{\theta}^*|\boldsymbol{\theta}^{[t]})} \right), \end{aligned} \quad (2.3)$$

where the fraction in the parentheses is the Metropolis-Hastings (MH) ratio. Otherwise, the parameter values remain unchanged for the next iteration. The detailed balance condition guarantees that the Markov chain converges to the correct target distribution (Chib and Greenberg, 1995).

The Gibbs algorithm (Geman and Geman, 1984) is an MCMC method that updates $\boldsymbol{\theta} = (\theta_1, \dots, \theta_J)$ one component at a time using the full conditional distribution for an individual component $p(\theta_j|\boldsymbol{\theta}_{-j}, \mathbf{y})$ as the corresponding proposal distribution where $\boldsymbol{\theta}_{-j} = (\theta_1, \dots, \theta_{j-1}, \theta_{j+1}, \dots, \theta_J)$. This particular choice of the proposal distribution

leads to the proposals always being accepted as the target distribution for each. The Gibbs algorithm can be generalised to consider ‘blocks’ of variables as well.

The Metropolis–Hastings (MH) algorithm (Hastings, 1970, Metropolis et al., 1953) is another common MCMC method. A generic form of the algorithm is shown in Algorithm 2.1.

Algorithm 2.1 Metropolis-Hastings algorithm

- 1: Initialise $\boldsymbol{\theta}^{[1]}$ and set $t = 1$
- 2: Draw proposal $\boldsymbol{\theta}^*$ from $q(\cdot|\boldsymbol{\theta}^{[t]})$
- 3: Set

$$\boldsymbol{\theta}^{[t+1]} = \begin{cases} \boldsymbol{\theta}^* & \text{if } u < \min(1, \alpha) \\ \boldsymbol{\theta}^{[t]} & \text{otherwise} \end{cases}$$

where α is as specified in (2.3) and u is a random variate drawn from Uniform[0,1].

- 4: Set $t = t + 1$
 - 5: Repeat steps 2 to 4 until $t = N + 1$.
-

The choice of the proposal distribution $q(\cdot)$ is typically user and application dependent. A common option is the random walk proposal where $q(\boldsymbol{\theta}^*|\boldsymbol{\theta}^{[t]})$ is a multivariate normal distribution $N(\boldsymbol{\theta}^{[t]}, \sigma^2 \mathbf{I}_J)$ with \mathbf{I}_J being a J -dimensional identity matrix. The choice of σ dictates the efficiency of the algorithm. Too large a value of σ results in proposals being rejected most of the time whereas too small a value of σ results in slow convergence of the chain to the target distribution. Roberts et al. (1997) showed that under some restrictive assumptions, the asymptotic (as $J \rightarrow \infty$) optimal acceptance rate of random walk proposals is 0.234. Further work showed that this result still holds when some the assumptions were relaxed (Rosenthal, 2011) and that it applies sufficiently well to cases with finite J as small as 5 (Roberts et al., 2001). Gelman et al. (1996) showed that the optimal acceptance rate is larger for smaller values of J , and in particular the optimal acceptance rate for $J = 1$ is 0.44. In practice, acceptance rates between 0.1 and 0.6 would not result in substantial loss in efficiency (Roberts et al., 2001, Rosenthal, 2011).

When the proposal distribution is chosen to be symmetric ($q(\boldsymbol{\theta}^*|\boldsymbol{\theta}^{[t]}) = q(\boldsymbol{\theta}^{[t]}|\boldsymbol{\theta}^*)$), the acceptance probability simplifies to $\alpha = \min\left(1, \frac{\eta(\boldsymbol{\theta}^*)}{\eta(\boldsymbol{\theta}^{[t]})}\right)$. The algorithm in this case is referred to as the Metropolis algorithm.

For computational efficiency, it is common to update one parameter in $\boldsymbol{\theta} = (\theta_1, \dots, \theta_J)$ at a time, i.e. at iteration t , steps 2 and 3 are repeated J times (once for each θ_j , $j = 1, \dots, J$) before moving on to step 4 in Algorithm 2.1. As such, the MH ratio for the update of an individual θ_j in this case is

$$\frac{p(\theta_j^*|\boldsymbol{\theta}_{-j}^{[t]}, \mathbf{y})q(\theta_j^{[t]}|\theta_j^*, \boldsymbol{\theta}_{-j}^{[t]})}{p(\theta_j^{[t]}|\boldsymbol{\theta}_{-j}^{[t]}, \mathbf{y})q(\theta_j^*|\theta_j^{[t]}, \boldsymbol{\theta}_{-j}^{[t]})}. \quad (2.4)$$

As before, the full conditional terms $p(\theta_j | \boldsymbol{\theta}_{-j}, \mathbf{y})$ can be replaced with the corresponding unnormalised densities $\eta(\theta_j)$. This approach could also be applied to blocks of variables and as such has been referred to as ‘variable-at-a-time’ or ‘block-at-a-time’ approaches (Chib and Greenberg, 1995). In addition, for the ‘variable-at-a-time’ approach where the full conditionals of some of the variables can be directly sampled from, a Gibbs update scheme can be applied to those variables.

Data-augmented Markov chain Monte Carlo

The data-augmented Markov chain Monte Carlo (DA-MCMC) is an extended version of the straightforward MCMC methods to perform parameter inference in problems with missing or latent data \mathbf{z} . The motivation in using DA-MCMC is that the joint likelihood $p(\mathbf{y}, \mathbf{z} | \boldsymbol{\theta})$ has a much simpler form than the marginal likelihood for the observed data $p(\mathbf{y} | \boldsymbol{\theta}) = \int p(\mathbf{y}, \mathbf{z} | \boldsymbol{\theta}) d\mathbf{z}$.

The term ‘data augmentation’ was first used in Tanner and Wong (1987) where the authors showed the utility of data augmentation for the expectation-maximisation (EM) algorithm applied to problems with missing data. It is acknowledged that there is an extensive literature on modelling different mechanisms of missingness which is not explored here (see for example Little and Rubin (2002) and Molenberghs et al. (2014)).

Data augmentation also highlights an attractive feature of Bayesian inference as the missing data can be thought of as additional parameters in the model. As such, the Metropolis-Hastings algorithm can be extended quite straightforwardly to handle such problems by the inclusion of an additional parameter update step to impute the missing data. The use of data augmentation in the context of modelling infectious disease transmission is particularly relevant given that the pathogen transmission process is never completely observed, i.e. individuals are only known to be infected when they are symptomatic or have been screened and as such, the exact infection time is unknown. Gibson and Renshaw (1998) provides the first example of data augmentation under a Bayesian framework for stochastic epidemic models.

Use of data augmentation in modelling hospital MDRO with NHPP is motivated by the fact that the exact MDRO acquisition times are not directly observable. These acquisition times are required to compute the Poisson process likelihood. Instead, patient statuses are ascertained from regular screening tests. The acquisition time for a patient is imputed using a finite time interval between when the MDRO is first detected and the negative screening test immediately preceding it. The full conditional distribution for the imputed acquisition time can be straightforwardly derived from the full model likelihood assuming a piecewise constant intensity function (as shown in McBryde et al. (2007b) and the Supplementary materials for Chapter 7), as is the norm in such applications (Cooper et al., 2008, Forrester et al., 2007, McBryde et al., 2007a,b).

Chapter 7 uses a DA-MCMC algorithm to estimate the parameters in the proposed NHPP which incorporates the contribution of environmental contamination explicitly.

Reversible-jump Markov chain Monte Carlo

The reversible jump Markov chain Monte Carlo (RJ-MCMC) algorithm (Green, 1995) is an extension of the MCMC methods to multiple model spaces. As such, it is sometimes known as transdimensional Markov chain Monte Carlo. There exist a number of excellent reviews of RJ-MCMC developments in the literature (Fan and Sisson, 2011, Green, 2003, Hastie and Green, 2012, Sisson, 2005) and as such, the focus here is merely to introduce the basic concept of RJ-MCMC to facilitate its use in the ABC method developed for model selection in Chapter 3. The same method is also used in Chapter 4.

RJ-MCMC is commonly used for model selection where the candidate models form the model spaces that the Markov chain can traverse between. Define a countable set K where $k \in K$ denotes the different model indices, and θ_k to be the collection of parameters in model k with likelihood $p(\mathbf{y}|k, \theta_k)$. Let $p(k, \theta_k)$ denote the joint prior distribution for the model index and parameters. The joint posterior in this case is

$$p(k, \theta_k | \mathbf{y}) = \frac{p(\mathbf{y}|k, \theta_k)p(k, \theta_k)}{\sum_{i \in K} \int p(\mathbf{y}|i, \theta_i)p(i, \theta_i) d\theta_i}$$

and can be factorised as $p(k, \theta_k | \mathbf{y}) = p(k | \mathbf{y})p(\theta_k | k, \mathbf{y})$. The posterior model probability $p(k | \mathbf{y})$ is typically the quantity of interest in model selection problems.

As with standard MCMC methods, the RJ-MCMC scheme must satisfy a corresponding detailed balance condition to ensure that the Markov chain has the correct invariant distribution.

Define $\phi = (k, \theta_k)$ to be of dimension n_k and assume m indexes the possible move types from the current state ϕ in a countable set \mathcal{M} . Let the move type m comprise of both the forward move from ϕ to the proposed $\phi^* = (k^*, \theta_k^*)$ of dimension n_k^* , and the reverse move from ϕ^* to ϕ . Denote \mathbf{u} to be a random variate of dimension r drawn from a known density $g_m(\cdot)$. \mathbf{u} , along with the transition function $h_m(\cdot)$, allows the forward move to be defined as $(\phi^*, \mathbf{u}^*) = h_m(\phi, \mathbf{u})$. \mathbf{u}^* is another random variate of dimension r^* drawn from density $g_m^*(\cdot)$ and is required for the reverse move through the inverse of h_m , h_m^* (i.e. $(\phi, \mathbf{u}) = h_m^*(\phi^*, \mathbf{u}^*)$). As such, $h_m(\cdot)$ must be a differentiable, one-to-one function. It is also required that $n_k + r = n_k^* + r^*$.

The detailed balance condition can then be specified as

$$\int p(\phi | \mathbf{y})p_m(\phi)g_m(\mathbf{u})\alpha_m(\phi, \phi^*) d\phi d\mathbf{u} = \int p(\phi^* | \mathbf{y})p_m(\phi^*)g_m^*(\mathbf{u}^*)\alpha_m(\phi^*, \phi) d\phi^* d\mathbf{u}^*$$

where $p_m(\phi)$ denotes the probability that move m from state ϕ is attempted, and $\alpha_m(\phi, \phi^*)$ denotes the acceptance probability for a move m from ϕ to ϕ^* . In order to

ensure the detailed balance condition is satisfied, a sufficient choice for $\alpha(\phi, \phi^*)$ is

$$\alpha(\phi, \phi^*) = \min \left\{ 1, \frac{p(\phi^*|\mathbf{y})p_m(\phi^*)g_m^*(\mathbf{u}^*)}{p(\phi|\mathbf{y})p_m(\phi)g_m(\mathbf{u})} \left| \frac{\partial(\boldsymbol{\theta}_{k^*}^*, \mathbf{u}^*)}{\partial(\boldsymbol{\theta}_k, \mathbf{u})} \right| \right\} \quad (2.5)$$

where the last term is the determinant of the Jacobian matrix of the transformation, which is also dependent on the move type m (Hastie and Green, 2012).

The general construction of a RJ-MCMC algorithm follows Algorithm 2.1 but with the proposal step now involves proposing a move step m , $\mathbf{u} \sim g_m(\cdot)$ and $\boldsymbol{\theta}_{k^*}^*$. The acceptance probability is as defined in (2.5).

In the context of modelling MRSA incidences in a hospital ward as a NHPP, a RJ-MCMC scheme can be used, in conjunction with data augmentation, to account for the possibility of patients being colonised with MRSA in the ward without being detected throughout the patient's hospitalisation (Forrester et al., 2007). In this case, the true number of colonised patients in the ward is allowed to vary from one MCMC iteration to the next and RJ-MCMC provides a useful framework for handling the changing model dimensions (noting that the acquisition time for each patient is a model parameter as discussed earlier). This is likely to occur if the screening test sensitivity is low, there is no pre-admission screening for the study ward, or a colonised patient's experienced a short hospitalisation and was discharged prior to their MRSA status being confirmed.

The data set used to fit the NHPP model proposed in Chapter 7 was collected in a hospital ward with pre-admission screening and the screening test used had a high sensitivity (Dancer et al., 2009). It is highly unlikely that a colonised patient was not detected during his or her hospitalisation. As such, only a DA-MCMC algorithm was used.

2.3.2 Sequential Monte Carlo

Sequential Monte Carlo (SMC) methods are an extension of the importance sampling (IS) method, both used when it is not possible to sample directly from the target distribution $p(\boldsymbol{\theta}|\mathbf{y})$. IS draws N samples from an importance distribution $g(\boldsymbol{\theta})$ and assign weights to the samples such that the weighted sample approximates the target distribution. The unnormalised importance weights are calculated as

$$w^i \propto \frac{\eta(\boldsymbol{\theta}^i)}{g(\boldsymbol{\theta}^i)}, \quad i = 1, \dots, N$$

and then normalised to ensure that they sum to one. $\eta(\boldsymbol{\theta})$ is the unnormalised density of the target distribution. $g(\boldsymbol{\theta})$ has to be a distribution that is readily sampled from and whose support covers that of the target distribution. The collection of sampled parameter values and weights $\{\boldsymbol{\theta}^i, W^i\}_{i=1}^N$, where W^i is the normalised weight for $\boldsymbol{\theta}^i$, is

also commonly referred to as a particle set. The difficulty of choosing $g(\boldsymbol{\theta})$ for high-dimensional targets led to the development of SMC methods.

SMC methods extend the IS method by iterating the samples through a smooth sequence of target distributions $\{p_1(\boldsymbol{\theta}|\mathbf{y}), p_2(\boldsymbol{\theta}|\mathbf{y}), \dots, p_T(\boldsymbol{\theta}|\mathbf{y})\}$ which more closely approximates the target distribution $(p(\boldsymbol{\theta}|\mathbf{y}))$ at each subsequent iteration and such that $p_T(\boldsymbol{\theta}|\mathbf{y}) = p(\boldsymbol{\theta}|\mathbf{y})$. The corresponding unnormalised density for $p_t(\boldsymbol{\theta}|\mathbf{y})$ is denoted by $\eta_t(\boldsymbol{\theta})$.

Following the derivation detailed in Del Moral et al. (2006), construction of an SMC algorithm requires the specification of a forwards in time Markov kernel $K_t(\boldsymbol{\theta}_{[t]}|\boldsymbol{\theta}_{[t-1]})$ and backwards in time Markov kernel $L_t(\boldsymbol{\theta}_{[t]}|\boldsymbol{\theta}_{[t+1]})$ for moving across the sequence of distributions and calculation of the corresponding weights.

It should be noted that the target distribution in SMC methods at iteration t is the joint distribution $\tilde{p}_t(\boldsymbol{\theta}_{[1:t]}|\mathbf{y})$ where $\boldsymbol{\theta}_{[1:t]} = \{\boldsymbol{\theta}_{[1]}, \dots, \boldsymbol{\theta}_{[t]}\}$, $\boldsymbol{\theta}_{[t]}$ is the parameters of $p_t(\boldsymbol{\theta}|\mathbf{y})$ and

$$\tilde{p}_t(\boldsymbol{\theta}_{[1:t]}|\mathbf{y}) = \frac{1}{\tilde{p}_t(\mathbf{y})} \eta_t(\boldsymbol{\theta}_{[t]}) \prod_{j=1}^{t-1} L_t(\boldsymbol{\theta}_{[t]}|\boldsymbol{\theta}_{[t+1]}).$$

The posterior distribution of interest $(p(\boldsymbol{\theta}|\mathbf{y}) = p_T(\boldsymbol{\theta}_{[T]}|\mathbf{y}))$ is recovered as a marginal of $\tilde{p}_T(\boldsymbol{\theta}_{[1:T]}|\mathbf{y})$ (i.e., $p_T(\boldsymbol{\theta}_{[T]}|\mathbf{y}) = \int \tilde{p}_T(\boldsymbol{\theta}_{[1:T]}|\mathbf{y}) d\boldsymbol{\theta}_{[1:T-1]}$). As such, $\boldsymbol{\theta}_{[1:T-1]}$ can be considered auxiliary variables to facilitate the derivation of the posterior distribution of interest in SMC methods.

The joint importance distribution at iteration t is

$$\tilde{g}_t(\boldsymbol{\theta}_{[1:t]}) = g_1(\boldsymbol{\theta}_{[1]}) \prod_{t=2}^T K_t(\boldsymbol{\theta}_{[t]}|\boldsymbol{\theta}_{[t-1]})$$

and the unnormalised weights given by

$$w_t(\boldsymbol{\theta}_{[1:t]}) = \frac{\tilde{\eta}_t(\boldsymbol{\theta}_{[1:t]})}{\tilde{g}_t(\boldsymbol{\theta}_{[1:t]})}$$

with $\tilde{\eta}_t(\boldsymbol{\theta}_{[1:t]})$ denoting the unnormalised target distribution, i.e.

$$\tilde{\eta}_t(\boldsymbol{\theta}_{[1:t]}) = \tilde{p}_t(\mathbf{y}) \tilde{p}_t(\boldsymbol{\theta}_{[1:t]}|\mathbf{y}).$$

Substituting the identities

$$\begin{aligned} \tilde{\eta}_t(\boldsymbol{\theta}_{[1:t]}) &= \tilde{\eta}_{t-1}(\boldsymbol{\theta}_{[1:t-1]}) \frac{\eta_t(\boldsymbol{\theta}_{[t]})}{\eta_{t-1}(\boldsymbol{\theta}_{[t-1]})} L_{t-1}(\boldsymbol{\theta}_{[t-1]}|\boldsymbol{\theta}_{[t]}), \text{ and} \\ \tilde{g}_t(\boldsymbol{\theta}_{[1:t]}) &= \tilde{g}_{t-1}(\boldsymbol{\theta}_{[1:t-1]}) K_t(\boldsymbol{\theta}_{[t]}|\boldsymbol{\theta}_{[t-1]}) \end{aligned}$$

into the expression for $w_t(\boldsymbol{\theta}_{[1:t]})$ provides the following recursive formula for calculating the weights:

$$\begin{aligned} w_t(\boldsymbol{\theta}_{[1:t]}) &= \left[\frac{\tilde{\eta}_{t-1}(\boldsymbol{\theta}_{[1:t-1]})}{\tilde{g}_{t-1}(\boldsymbol{\theta}_{[1:t-1]})} \right] \left(\frac{\eta_t(\boldsymbol{\theta}_{[t]}) L_{t-1}(\boldsymbol{\theta}_{[t-1]} | \boldsymbol{\theta}_{[t]})}{\eta_{t-1}(\boldsymbol{\theta}_{[t-1]}) K_t(\boldsymbol{\theta}_{[t]} | \boldsymbol{\theta}_{[t-1]})} \right) \\ &= w_{t-1}(\boldsymbol{\theta}_{[1:t-1]}) \tilde{w}(\boldsymbol{\theta}_{[t]}, \boldsymbol{\theta}_{[t-1]}) \end{aligned} \quad (2.6)$$

with the (unnormalised) incremental weight $\tilde{w}(\boldsymbol{\theta}_{[t]}, \boldsymbol{\theta}_{[t-1]})$ defined as the parenthesised expression in (2.6).

Del Moral et al. (2006) showed that the optimal choice of the backward kernel $L_t(\boldsymbol{\theta}_{[t]} | \boldsymbol{\theta}_{[t+1]})$ (in terms of minimising the variance of the w_t^i 's) is

$$L_{t-1}(\boldsymbol{\theta}_{[t-1]} | \boldsymbol{\theta}_{[t]}) = \frac{g_{t-1}(\boldsymbol{\theta}_{[t-1]}) K_t(\boldsymbol{\theta}_{[t]} | \boldsymbol{\theta}_{[t-1]})}{g_t(\boldsymbol{\theta}_{[t]})}$$

resulting in the simplification of the expression for the unnormalised weights

$$w_t(\boldsymbol{\theta}_{[1:t]}) = w_t(\boldsymbol{\theta}_{[t]}) = \frac{\eta_t(\boldsymbol{\theta}_{[t]})}{g_t(\boldsymbol{\theta}_{[t]})}$$

i.e., each SMC iteration is simply an importance sampling scheme on the respective marginal target $p_t(\boldsymbol{\theta}_t | \mathbf{y})$. However, the marginal importance distribution $g_t(\boldsymbol{\theta}_{[t]})$ can be difficult to compute in practice. This motivated Del Moral et al. (2006) to consider ‘suboptimal’ backward kernels which attempt to approximate the optimal backward kernel. One suboptimal backward kernel considered was obtained by replacing the $g_t(\cdot)$ terms with $p_t(\cdot | \mathbf{y})$

$$\begin{aligned} L_{t-1}(\boldsymbol{\theta}_{[t-1]} | \boldsymbol{\theta}_{[t]}) &= \frac{p_{t-1}(\boldsymbol{\theta}_{[t-1]}) K_t(\boldsymbol{\theta}_{[t]} | \boldsymbol{\theta}_{[t-1]})}{p_t(\boldsymbol{\theta}_t | \mathbf{y})} \\ &= \frac{p_{t-1}(\boldsymbol{\theta}_{[t-1]}) K_t(\boldsymbol{\theta}_{[t]} | \boldsymbol{\theta}_{[t-1]})}{\int p_{t-1}(\boldsymbol{\theta}_{[t-1]}) K_t(\boldsymbol{\theta}_{[t]} | \boldsymbol{\theta}_{[t-1]}) d\boldsymbol{\theta}_{[t-1]}} \end{aligned} \quad (2.7)$$

which results in the expression for the incremental weights

$$\tilde{w}(\boldsymbol{\theta}_{[t]}, \boldsymbol{\theta}_{[t-1]}) = \frac{\eta_t(\boldsymbol{\theta}_{[t]})}{\int p_{t-1}(\boldsymbol{\theta}_{[t-1]}) K_t(\boldsymbol{\theta}_{[t]} | \boldsymbol{\theta}_{[t-1]}) d\boldsymbol{\theta}_{[t-1]}}.$$

The integral can be approximated using the particle set as

$$\int p_{t-1}(\boldsymbol{\theta}_{[t-1]}) K_t(\boldsymbol{\theta}_{[t]} | \boldsymbol{\theta}_{[t-1]}) d\boldsymbol{\theta}_{[t-1]} \approx \sum_{i=1}^N W_{t-1}^i K_t(\boldsymbol{\theta}_{[t]} | \boldsymbol{\theta}_{[t-1]}^i).$$

An alternative to the above suboptimal backward kernel is to use an MCMC kernel for K_t with invariant distribution $p_t(\boldsymbol{\theta}_{[t]} | \mathbf{y})$. This results in a backward kernel specification of

$$L_{t-1}(\boldsymbol{\theta}_{[t-1]} | \boldsymbol{\theta}_{[t]}) = \frac{p_t(\boldsymbol{\theta}_{[t-1]} | \mathbf{y}) K_t(\boldsymbol{\theta}_{[t]} | \boldsymbol{\theta}_{[t-1]})}{p_t(\boldsymbol{\theta}_{[t]} | \mathbf{y})} \quad (2.8)$$

and associated incremental weight of

$$\tilde{w}(\boldsymbol{\theta}_{[t]}, \boldsymbol{\theta}_{[t-1]}) = \frac{\eta_t(\boldsymbol{\theta}_{[t-1]})}{\eta_{t-1}(\boldsymbol{\theta}_{[t-1]})}.$$

SMC is coupled with the approximate Bayesian computation (discussed in Section 2.3.4) methods to provide a more computationally efficient algorithm, commonly referred to as SMC ABC. Chapters 3 and 4 use an SMC ABC algorithm.

2.3.3 Model selection

In addition to developing improved models for describing the transmission of MDROs in hospitals, it would also be of interest to select between candidate models representing different transmission modes (and their various combinations) to ascertain which transmission mode(s) interventions should focus on. This is referred to as model choice or model selection problems in the statistics literature.

This comparison can be done for nested models in a Frequentist setting by comparing the likelihoods of a pair of nested models. The likelihood ratio (LR) is distributed as a χ_d^2 distribution with the degree of freedom d being the difference in the number of parameters estimated in the two models under comparison. The LR test is limited to only comparing two nested models at a time.

In a Bayesian setting, model comparison can be performed by evaluating the posterior model probability $p(k|\mathbf{y})$ for the K candidate models ($k = 1, \dots, K$). One way to compute these $p(k|\mathbf{y})$ is by using the RJ-MCMC algorithm as explained in Section 2.3.1. However, in practice, it can be quite difficult to construct an appropriate transition function $h_m(\cdot)$ connecting parameters between different models (Fan and Sisson, 2011), except in special cases e.g., nested models. Neal and Roberts (2004) is a rare example of the use of RJ-MCMC to perform model selection for nested disease transmission models fitted to a historic measles data set. The measles data set was also analysed in the model selection work presented in Chapter 3 however the work compared non-nested models using an ABC algorithm instead.

It is often easier to fit the candidate models separately and compare the marginal likelihood $p(\mathbf{y}|k)$ between pairs of candidate models. This ratio of marginal likelihoods is referred to as the Bayes factor

$$BF_{k_1, k_2} = \frac{p(\mathbf{y}|k = k_1)}{p(\mathbf{y}|k = k_2)} = \frac{\int p(\mathbf{y}|\boldsymbol{\theta}_{k_1}, k = k_1)p(\boldsymbol{\theta}_{k_1}|k = k_1) d\boldsymbol{\theta}_{k_1}}{\int p(\mathbf{y}|\boldsymbol{\theta}_{k_2}, k = k_2)p(\boldsymbol{\theta}_{k_2}|k = k_2) d\boldsymbol{\theta}_{k_2}}.$$

Robert and Wraith (2009) provides an overview of methods that can be used to compute the Bayes factor.

More general statistical model comparisons, particularly for non-nested models, have been proposed. The Bayesian information criterion (BIC) (Schwarz, 1978) is an approximation to the $\log(p(\mathbf{y}|k))$ (Kass and Wasserman, 1995) defined as

$$BIC = -2\log p(\mathbf{y}|\hat{\boldsymbol{\theta}}) + p\log n = D(\mathbf{y}, \hat{\boldsymbol{\theta}}) + p\log n$$

where p is the number of model parameters, n is the number of observations, $\hat{\boldsymbol{\theta}}$ is typically the maximum likelihood estimate for $\boldsymbol{\theta}$, and $D(\mathbf{y}, \boldsymbol{\theta}) = -2\log p(\mathbf{y}|\boldsymbol{\theta})$ is commonly referred to as the model deviance. The BIC allows for comparisons of non-nested models as well as straightforward comparisons between more than two models. The candidate model with a smaller BIC value is generally preferred.

The Akaike information criterion (AIC) (Akaike, 1974) is another commonly used measure for model comparisons. The AIC is defined as

$$AIC = D(\mathbf{y}, \hat{\boldsymbol{\theta}}) + 2p$$

and was formulated to favour the model with the stronger predictive power.

Both the AIC and BIC can be thought of as measures of model fit (as assessed by the deviance term $D(\mathbf{y}, \hat{\boldsymbol{\theta}})$), penalised by model complexity. The BIC has a larger penalty compared with the AIC in general (when $\log n > 2$, i.e., $n > 7$).

The deviance information criterion (DIC) (Spiegelhalter et al., 2002, 2014) was proposed as a measure of model fit that could be easily calculated from MCMC outputs. The DIC can be defined as

$$DIC = \bar{D} + p_D$$

with $\bar{D} = E_{\boldsymbol{\theta}|\mathbf{y}}(D(\mathbf{y}, \boldsymbol{\theta}))$ (i.e. the posterior expectation of the model deviance) and the effective number of parameters p_D given by

$$p_D = E_{\boldsymbol{\theta}|\mathbf{y}}[-2\log p(\mathbf{y}|\boldsymbol{\theta})] + 2\log p(\mathbf{y}|\tilde{\boldsymbol{\theta}})$$

where $\tilde{\boldsymbol{\theta}}$ is an estimator of $\boldsymbol{\theta}$ and typically taken to be the posterior mean $E(\boldsymbol{\theta}|\mathbf{y})$ (the posterior mode or median are also viable alternatives that are readily computed).

Substituting the forms of \bar{D} and p_D into the expression of DIC gives

$$DIC = -4E_{\boldsymbol{\theta}|\mathbf{y}}[\log p(\mathbf{y}|\boldsymbol{\theta})] + 2\log p(\mathbf{y}|\tilde{\boldsymbol{\theta}}). \quad (2.9)$$

The DIC has grown in popularity with the rise of MCMC methods despite some of its known limitations (Spiegelhalter et al., 2014). One possible explanation of its popularity is that it is easily available from the free software for MCMC sampling BUGS (Lunn et al., 2009).

A key limitation of the standard DIC definition for the work presented in this thesis is that the effective number of parameters is not well-defined for models with missing or latent data. Celeux et al. (2006) provided extensions of the standard DIC to models with latent variables, or accounting for missing data. Out of the eight DIC variants proposed by Celeux et al. (2006), DIC_6 has been used for the NHPP models applied to HAI data (Wei et al., 2016, Worby, 2013) and is also used in the work presented in Chapter 7.

The DIC_6 is defined as by taking the expectation of (2.9) over the posterior of \mathbf{z} after replacing the observed data likelihood $p(\mathbf{y}|\boldsymbol{\theta})$ with the complete data likelihood $p(\mathbf{y}, \mathbf{z}|\boldsymbol{\theta})$, i.e.

$$\begin{aligned} DIC_6 &= E_{\mathbf{z}} \left\{ -4E_{\boldsymbol{\theta}|\mathbf{z}, \mathbf{y}} [\log p(\mathbf{y}, \mathbf{z}|\boldsymbol{\theta})] + 2 \log p(\mathbf{y}, \mathbf{z}|\tilde{\boldsymbol{\theta}}) \right\} \\ &= -4E_{\mathbf{z}, \boldsymbol{\theta}|\mathbf{y}} [\log p(\mathbf{y}, \mathbf{z}|\boldsymbol{\theta})] + 2E_{\mathbf{z}|\mathbf{y}} [\log p(\mathbf{y}, \mathbf{z}|\tilde{\boldsymbol{\theta}})] \end{aligned}$$

where $\tilde{\boldsymbol{\theta}} = E(\boldsymbol{\theta}|\mathbf{y})$. The DIC_6 is appropriate in settings where the missing data assist in forming tractable likelihood evaluations but are not the focus of the analysis, as is the setting here with modelling MDRO transmission in a hospital ward.

There are also alternative forms of information criteria for particular settings which are not considered here. Examples include the Takeuchi information criterion (TIC) for composite likelihoods, Hannan-Quinn information criterion (HQC) which is primarily used in autoregressive time series models (Hannan and Quinn, 1979) and the more recently proposed widely applicable information criteria (WAIC and WBIC) for singular statistical models (Friel et al., 2016, Watanabe, 2010, 2013). A statistical model is singular if there is no uniquely defined mode in its likelihoods, i.e. there is no one-to-one mapping from the model parameters to a probability distribution and the corresponding Fisher information matrix is not always positive definite.

2.3.4 Approximate Bayesian Computation

Approximate Bayesian computation (ABC) methods can be used for problems where direct evaluation of the likelihood $p(\mathbf{y}|\boldsymbol{\theta})$ is prohibitively expensive, or the likelihood is analytically intractable. ABC methods replace the likelihood evaluations with simulations from the model likelihood (denoted $\mathbf{x} \sim p(\mathbf{x}|\boldsymbol{\theta})$) instead. These simulations are generated using parameter values sampled from a proposal distribution. The proposed parameter values are only accepted as a sample from the correct posterior distribution if the discrepancy measure $\rho(\mathbf{x}, \mathbf{y})$ between the observed data and simulated data generated using the proposal was less than a pre-specified tolerance, ϵ . The discrepancy measure is typically a normed distance of the difference between summary statistics $s(\cdot)$ of the observed and simulated data. The choice of summary statistics used is typically specified by the user as summary statistics believed to be informative about the parameter of interest $\boldsymbol{\theta}$. A trade-off of its simplicity is that ABC methods only produce approximate posterior distributions $p(\boldsymbol{\theta}|\mathbf{y}, \epsilon)$.

The target distribution for ABC methods is the joint posterior of the parameters θ and simulated data \mathbf{x}

$$p(\mathbf{x}, \theta | \mathbf{y}, \epsilon) \propto p(\mathbf{x} | \theta) p(\theta) \psi(\mathbf{y} | \mathbf{x}, \theta, \epsilon)$$

where $\psi(\mathbf{y} | \mathbf{x}, \theta, \epsilon)$ is the weighting function measuring the similarity between the observed data \mathbf{y} and simulated data \mathbf{x} . In this thesis, $\psi(\mathbf{y} | \mathbf{x}, \theta, \epsilon)$ is taken to be an indicator function $\psi(\mathbf{y} | \mathbf{x}, \theta, \epsilon) = \mathbb{1}(\rho(\mathbf{x}, \mathbf{y}) < \epsilon)$.

The approximate posterior distribution of the parameters can then be obtained by marginalizing over the simulated data

$$\begin{aligned} p(\theta | \mathbf{y}, \epsilon) &= E_{\mathbf{x} \sim p(\mathbf{x} | \theta)} [p(\mathbf{x}, \theta | \mathbf{y}, \epsilon)] \\ &\propto \int_{\mathbf{x}} p(\mathbf{x} | \theta) p(\theta) \psi(\mathbf{y} | \mathbf{x}, \theta, \epsilon) d\mathbf{x} \\ &= \int_{\mathbf{x}} p(\mathbf{x} | \theta) p(\theta) \mathbb{1}(\rho(\mathbf{x}, \mathbf{y}) < \epsilon) d\mathbf{x}. \end{aligned}$$

While initially proposed for genetic applications where the models had intractable likelihood but were readily simulated from (Beaumont et al., 2002, Fu and Li, 1997, Pritchard et al., 1999, Weiss and von Haeseler, 1998), the application areas for ABC algorithms have grown considerably since its introduction because of its intuitive premise and relative ease in implementation compared with some of the other Bayesian computation methods (Beaumont, 2010, Csilléry et al., 2010, Marin et al., 2012). Of particular interest here are the application of ABC methods to models of infectious disease transmission (Blum and Tran, 2010, Brooks-Pollock et al., 2014, Drovandi and Pettitt, 2011b, McKinley et al., 2009, Prangle, 2016, Ratmann et al., 2014, Tanaka et al., 2006, Toni and Stumpf, 2010, Toni et al., 2009).

ABC methods were originally proposed using a rejection sampling scheme, as such is referred to as RS ABC, where parameter proposals are always drawn from the prior distribution and the tolerance value remains unchanged throughout the algorithm (Fu and Li, 1997). A typical schematic of RS ABC is shown in Algorithm 2.2.

Algorithm 2.2 Rejection sampling ABC algorithm

- 1: Draw θ^* from the prior.
 - 2: Simulate \mathbf{x} using θ^* , i.e. $\mathbf{x} \sim p(\mathbf{x} | \theta^*)$.
 - 3: Accept θ^* if $\rho(\mathbf{x}, \mathbf{y}) \leq \epsilon$.
 - 4: Repeat steps 1 to 3 until N draws of θ^* are accepted.
-

An alternative to running Algorithm 2.2 until N accepted proposals are obtained is to instead draw and simulate a substantially larger number of (θ^*, \mathbf{x}) , say $100N$, and consider the 1% of the samples (i.e. yielding N draws) with the smallest discrepancy values as draws from the approximate posterior. The tolerance value is then set to be the largest discrepancy value in the N samples from the approximate posterior. An

advantage to this adaptation is that it is easier to anticipate the expected run time compared with the approach in Algorithm 2.2.

However, the RS ABC scheme can be highly inefficient particularly when the prior distribution is substantially more diffuse than the target posterior distribution. In this case, the RS ABC method wastes substantial computational effort and time in drawing from regions of the parameter prior space which have little support in the targeted posterior. Subsequent ABC methods, such as the Markov chain Monte Carlo ABC (MCMC ABC) and sequential Monte Carlo ABC (SMC ABC) were proposed to provide more efficient methods of exploring the parameter space.

As its name suggest, MCMC ABC algorithms draw strengths from both the ABC and MCMC methods. An MCMC ABC algorithm is initiated as with the RS ABC by drawing candidate values from the prior, and model simulations from the likelihood until a proposal is accepted. After the initial proposal has been accepted, the subsequent candidate values and model simulations are then generated from a proposal distribution $Q(\cdot|\mathbf{x}^{[t-1]}, \boldsymbol{\theta}^{[t-1]})$ which depends on the last accepted value, where t indexes the MCMC iteration. Candidate values which satisfy the tolerance criterion (after the initial accepted proposal) are only accepted with a probability α , calculated from a MH ratio similar to that used in standard MCMC algorithms.

The form of the acceptance probability α for an MCMC ABC algorithm is:

$$\begin{aligned} \alpha &= \min \left\{ 1, \frac{p(\mathbf{x}^*|\boldsymbol{\theta}^*)p(\boldsymbol{\theta}^*)\mathbb{1}(\rho(\mathbf{x}^*, \mathbf{y}) < \epsilon)}{p(\mathbf{x}^{[t-1]}|\boldsymbol{\theta}^{[t-1]})p(\boldsymbol{\theta}^{[t-1]})\mathbb{1}(\rho(\mathbf{x}^{[t-1]}, \mathbf{y}) < \epsilon)} \frac{Q(\mathbf{x}^{[t-1]}, \boldsymbol{\theta}^{[t-1]}|\mathbf{x}^*, \boldsymbol{\theta}^*)}{Q(\mathbf{x}^*, \boldsymbol{\theta}^*|\mathbf{x}^{[t-1]}, \boldsymbol{\theta}^{[t-1]})} \right\} \\ &= \min \left\{ 1, \frac{p(\mathbf{x}^*|\boldsymbol{\theta}^*)p(\boldsymbol{\theta}^*)\mathbb{1}(\rho(\mathbf{x}^*, \mathbf{y}) < \epsilon)}{p(\mathbf{x}^{[t-1]}|\boldsymbol{\theta}^{[t-1]})p(\boldsymbol{\theta}^{[t-1]})\mathbb{1}(\rho(\mathbf{x}^{[t-1]}, \mathbf{y}) < \epsilon)} \frac{p(\mathbf{x}^{[t-1]}|\boldsymbol{\theta}^{[t-1]})q(\boldsymbol{\theta}^{[t-1]}|\boldsymbol{\theta}^*)}{p(\mathbf{x}^*|\boldsymbol{\theta}^*)q(\boldsymbol{\theta}^*|\boldsymbol{\theta}^{[t-1]})} \right\} \end{aligned} \quad (2.10)$$

$$= \min \left\{ 1, \frac{p(\boldsymbol{\theta}^*)\mathbb{1}(\rho(\mathbf{x}^*, \mathbf{y}) < \epsilon)q(\boldsymbol{\theta}^{[t-1]}|\boldsymbol{\theta}^*)}{p(\boldsymbol{\theta}^{[t-1]})q(\boldsymbol{\theta}^*|\boldsymbol{\theta}^{[t-1]})} \right\} \quad (2.11)$$

where $\mathbb{1}(\rho(\mathbf{x}^{[t-1]}, \mathbf{y}) < \epsilon) = 1$ as it has been accepted.

The choice of the model likelihood as the proposal distribution for \mathbf{x} allows for the cancellation of the likelihood terms in (2.10) (since $Q(\mathbf{x}^*, \boldsymbol{\theta}^*|\mathbf{x}^{[t-1]}, \boldsymbol{\theta}^{[t-1]}) = q(\mathbf{x}^*|\boldsymbol{\theta}^*)q(\boldsymbol{\theta}^*|\boldsymbol{\theta}^{[t-1]}) = p(\mathbf{x}^*|\boldsymbol{\theta}^*)q(\boldsymbol{\theta}^*|\boldsymbol{\theta}^{[t-1]})$), resulting in the simplified form shown in (2.11).

A full schematic of an MCMC ABC algorithm is provided in Algorithm 2.3.

The SMC ABC algorithms, also referred to as population Monte Carlo ABC in Beaumont et al. (2009), improve on the MCMC ABC by proposing a series of target distributions which more closely resemble the actual posterior distribution of interest as

Algorithm 2.3 MCMC ABC algorithm adapted by Marjoram *et al.* (2003)

- 1: Initialise the chain by obtaining a single accepted draw $\boldsymbol{\theta}^{[0]}$ from the rejection sampling algorithm.
 - 2: For $t = 1$ to N :
 - i. Draw a proposal $\boldsymbol{\theta}^*$ from the proposal distribution $q(\cdot|\boldsymbol{\theta}^{[t-1]})$.
 - ii. Simulate data using the proposed value $\boldsymbol{\theta}^*$, i.e $\mathbf{x} \sim p(\mathbf{x}|\boldsymbol{\theta}^*)$.
 - iii. If $\rho(\mathbf{x}, \mathbf{y}) \leq \epsilon$
 - Compute the MH ratio $\alpha = \min \left\{ 1, \frac{p(\boldsymbol{\theta}^*)q(\boldsymbol{\theta}^{[t-1]}|\boldsymbol{\theta}^*)}{p(\boldsymbol{\theta}^{[t-1]})q(\boldsymbol{\theta}^*|\boldsymbol{\theta}^{[t-1]})} \right\}$
 - If a random draw from $U(0, 1) < \alpha$ then accept proposed value $\boldsymbol{\theta}^{[t]} = \boldsymbol{\theta}^*$.
 - Otherwise $\boldsymbol{\theta}^{[t]} = \boldsymbol{\theta}^{[t-1]}$.
 - end
 - end
-

the algorithm progresses along the SMC iterations (Drovandi and Pettitt, 2011a, Sisson et al., 2009, Toni et al., 2009). The joint target distribution at iteration t is

$$p_t(\boldsymbol{\theta}, \mathbf{x}|\mathbf{y}, \epsilon_t) \propto p(\mathbf{x}|\boldsymbol{\theta})p(\boldsymbol{\theta})\mathbb{1}(\rho(\mathbf{x}, \mathbf{y}) \leq \epsilon_t)$$

At each iteration, the tolerance value (ϵ_t) is decreased and as such, more closely approximates the true posterior.

The sequence of tolerance values could be pre-specified (as in Beaumont et al. (2009), Sisson et al. (2009), Toni et al. (2009)), or determined dynamically by setting tuning parameters in the SMC ABC algorithm related to the proportion of particles dropped at each SMC iteration (α) and the theoretical probability of a particle not moving at each proposal step (c) (as in Drovandi and Pettitt (2011a)). The dynamic determination of the tolerance sequence provides a more generalisable way of obtaining the tolerance sequences rather than having to propose new tolerance sequences for each new application.

In addition to the choice of the tolerance sequence, the forward and backward (in time) Markov kernels also need to be specified for the SMC ABC algorithms. Beaumont et al. (2009) used the suboptimal backward kernel specified in (2.7) to construct their SMC ABC algorithm and componentwise, independent normal random walk proposals for $K_t(\cdot)$ with the variance set to be twice the sample variance of the current particle set's $\boldsymbol{\theta}$ values. The forward kernel is used to perturb sampled particles from the current particle set to ensure particle diversity. The perturbed value is then used to simulate from the model. The parameter proposal and model simulation is repeated until $\rho(\mathbf{x}, \mathbf{y} \leq \epsilon_t)$ is satisfied. The importance weight for this algorithm is then

$$\begin{aligned} W_{[t]}^i &\propto \frac{p_t(\boldsymbol{\theta}_{[t]}^i|\mathbf{y})}{\sum_{j=1}^N W_{[t-1]}^j K_t(\boldsymbol{\theta}_{[t]}^i|\boldsymbol{\theta}^*, \boldsymbol{\theta}_{[t-1]})} \\ &= \frac{p(\boldsymbol{\theta}_{[t]}^i)}{\sum_{j=1}^N W_{[t-1]}^j K_t(\boldsymbol{\theta}_{[t]}^i|\boldsymbol{\theta}^*, \boldsymbol{\theta}_{[t-1]})} \end{aligned}$$

where the simplification in the numerator is a result of $\theta_{[t]}^i$ being associated with a model simulation that satisfies the current tolerance value ϵ_t . The SMC ABC algorithm of Beaumont et al. (2009) is shown in Algorithm 2.4.

The SMC ABC replenishment algorithm of Drovandi and Pettitt (2011a) used an MCMC kernel rather than a forward kernel and the resulting backward kernel form specified by (2.8). As such, the incremental weight for particle i (at SMC iteration t) in this case simplifies to

$$\tilde{w}_t^i = \frac{\mathbb{1}(\rho(\mathbf{x}^i, \mathbf{y}) \leq \epsilon_t)}{\mathbb{1}(\rho(\mathbf{x}^i, \mathbf{y}) \leq \epsilon_{t-1})}.$$

Since $W_t^i \propto \tilde{w}_t^i W_{t-1}^i$, the particles that are dropped at each SMC iteration in this SMC ABC replenishment algorithm are those with zero weights. The remaining $(1 - \alpha)N$ particles are then used to ‘replenish’ the particle set to recover a particle set of size N using repeated MCMC steps. The full algorithm is specified in Algorithm 2.5.

Algorithm 2.4 Population Monte Carlo ABC (PMC ABC) proposed by Beaumont et al. (2009)

- 1: Specify the sequences of tolerances $\epsilon_1, \dots, \epsilon_T$ and the initial importance sampling distribution $g_1(\theta)$.
- 2: In the first iteration ($t = 1$),
 - For $i = 1, \dots, N$:
 - Simulate $\theta_{[1]}^i$ from $g_1(\theta)$ and $\mathbf{x} \sim p(\mathbf{x}|\theta_{[1]}^i)$ until $\rho(\mathbf{x}, \mathbf{y}) < \epsilon_1$
 - Set $W_{[1]}^i = \frac{p_1(\theta_{[1]}^i|\mathbf{y})}{g_1(\theta_{[1]}^i)}$
 - end
 - Update the tuning parameter for K_t based on the obtained set of $\{\theta_{[1]}^i, W_{[1]}^i\}_{i=1}^N$.
- 3: For $t = 2, \dots, T$:
 - i. For $i = 1, \dots, N$:
 - Sample a proposal $\theta^{*,i}$ from the previous sample $\{\theta_{[t-1]}^j, W_{[t-1]}^j\}_{j=1}^N$. Perturb the particle $\theta^{*,i}|\theta^{*,i}, \theta_{[t-1]} \sim K_t(\theta^{**}|\theta^{*,i}, \theta_{[t-1]})$ and simulate $\mathbf{x}^i \sim p(\mathbf{x}|\theta^{*,i})$. Repeat this step until $\rho(\mathbf{x}^i, \mathbf{y}) < \epsilon_t$. The accepted $\theta^{*,i}$ is denoted $\theta_{[t]}^i$.
 - end
 - ii. Set

$$W_{[t]}^i \propto \frac{p(\theta_{[t]}^i)}{\sum_{j=1}^N W_{[t-1]}^j K_t(\theta_{[t]}^i|\theta^*, \theta_{[t-1]})}.$$

Update the tuning parameter for the K_t based on the obtained set of $\{\theta_{[t]}^i, W_{[t]}^i\}$.

end

Throughout the descriptions of the various ABC methods above, it was assumed that the form of the discrepancy measure $\rho(\cdot)$ is known. However, specifying the discrepancy measure can be quite challenging. When ABC methods were first proposed, the selection of summary statistics is typically specific to the particular application at hand, i.e. the practitioner has to determine which summary features of the data will be most informative about the model parameters to be estimated and/or if there are particular

Algorithm 2.5 SMC ABC replenishment algorithm (Drovandi and Pettitt, 2011)

-
- 1: Initiate the algorithm by running the rejection sampling algorithm with ϵ_1 to produce a set of N particles $\{\boldsymbol{\theta}_{[1]}^i, \rho_{[1]}^i\}_{i=1}^N$. Set p_{acc_1} as the proportion of accepted draws in the rejection sampling algorithm, $R_2 = \lceil \frac{\log(c)}{\log(1-p_{acc_1})} \rceil$ and $t = 2$.
 - 2: Sort the particle set by their discrepancy values $\rho_{[t-1]}$ and set $\epsilon_t = \rho_{[t-1]}^{N-N_\alpha}$ ($N_\alpha = \lceil \alpha N \rceil$) and $\epsilon_{MAX} = \rho_{[t-1]}^N$. If $\epsilon_{MAX} < \epsilon_T$, the algorithm is finished. Otherwise proceed to the next step.
 - 3: Compute the tuning parameters of the MCMC kernel $q_t(\cdot|\cdot)$ using the particle set $\{\boldsymbol{\theta}_{[t-1]}^i, \rho_{[t-1]}^i\}_{i=1}^{N-N_\alpha}$. Set $\{\boldsymbol{\theta}_{[t]}^i, \rho_{[t]}^i\}_{i=1}^{N-N_\alpha} = \{\boldsymbol{\theta}_{[t-1]}^i, \rho_{[t-1]}^i\}_{i=1}^{N-N_\alpha}$ and $i_{acc} = 0$.
 - 4: For $j = N - N_\alpha + 1$ to N :

Sample $\boldsymbol{\theta}^{*,j}$ from $\{\boldsymbol{\theta}_{[t-1]}^i\}_{i=1}^{N-N_\alpha}$.
 For $k = 1$ to R_t :
 Propose move $\boldsymbol{\theta}^{*,j} \sim q(\cdot|\boldsymbol{\theta}^{*,j})$ and simulate data $\mathbf{x}^j \sim p(\mathbf{x}|\boldsymbol{\theta}^{*,j})$.
 Compute MH ratio $r = \min\left(1, \frac{p(\boldsymbol{\theta}^{*,j})q(\boldsymbol{\theta}^{*,j}|\boldsymbol{\theta}^{*,j})}{p(\boldsymbol{\theta}^{*,j})q(\boldsymbol{\theta}^{*,j}|\boldsymbol{\theta}^{*,j})}\mathbb{1}(\rho(\mathbf{x}^j, \mathbf{y}) \leq \epsilon_t)\right)$.
 If $U(0, 1) < r$
 Set $\boldsymbol{\theta}_{[t]}^j = \boldsymbol{\theta}^{*,j}$ and $\rho_{[t]}^j = \rho(\mathbf{x}^j, \mathbf{y})$. Also, $i_{acc} = i_{acc} + 1$.
 end
 end
 - 5: end
 - 6: Compute the acceptance probability $p_{acc_t} = \frac{i_{acc}}{R_t N_\alpha}$.
 - 7: Compute $R_{t+1} = \lceil \frac{\log(c)}{\log(1-p_{acc_t})} \rceil$, increase t by 1, and return to 2:
-

features that the simulated data should be able to match well to the observed data. It is also necessary to be prudent with the number of summaries to include in the discrepancy measure as it gets progressively more difficult to generate samples from the approximate posterior with larger numbers of summary statistics in the discrepancy measure. This is commonly referred to as the curse of dimensionality in ABC applications.

Fearnhead and Prangle (2012) proposed a semi-automatic approach to the summary statistics selection process for parameter inference. The authors showed that the choice of the posterior mean of the parameters as summary statistics minimises the quadratic error loss in the estimation. As such, they proposed the use of the posterior mean as the summary statistic in an ABC algorithm for parameter inference. The posterior mean is estimated from a large pool of candidate summary statistics using a linear regression approach. A large number of prior draws and corresponding model simulations is used to fit the linear regression model prior to the implementation of an ABC algorithm. The estimated regression coefficients are then used to construct the estimated posterior means of the parameters in the ABC algorithm. The authors also trialled alternative approaches such as the lasso and canonical correlation analysis, but found that the simpler linear regression approach performed just as well. This approach also alleviates some of the issues associated with the curse of dimensionality in ABC applications as there is now only one summary statistic per parameter in the ABC scheme, while still

having the flexibility of specifying a large number of candidate summary statistics in the regression model.

ABC is still a relatively new area of research and there still exists plenty of room for development, particularly for model selection problems. A more flexible framework for estimating posterior model probabilities of models in general could also be achieved using approximate Bayesian computation (ABC) methods (Prangle et al., 2014, Toni and Stumpf, 2010). In particular, Prangle et al. (2014) extends the approach in Fearnhead and Prangle (2012) by using binomial logistic regression to estimate the posterior model probabilities as summary statistics for model selection problems. The posterior model probabilities satisfy the criteria set out in Marin et al. (2014) for summary statistics that are relevant for model selection using ABC. The development of an ABC method for model selection problems along with validation and application of the method to infectious disease application is the focus of Chapter 3. Chapter 4 extends the application of the method to model selection among spatial extremes models.

Part 1

Approximate Bayesian model choice

3 Model choice problems using approximate Bayesian computation with applications to pathogen transmission data

Abstract

Analytically or computationally intractable likelihood functions can arise in complex statistical inferential problems making them inaccessible to standard Bayesian inferential methods. Approximate Bayesian computation (ABC) methods address such inferential problems by replacing direct likelihood evaluations with repeated sampling from the model. ABC methods have been predominantly applied to parameter estimation problems and less to model choice problems due to the added difficulty of handling multiple model spaces. The ABC algorithm proposed here addresses model choice problems by extending Fearnhead and Prangle (2012) where the posterior mean of the model parameters estimated through regression formed the summary statistics used in the discrepancy measure. An additional stepwise multinomial logistic regression is performed on the model indicator variable in the regression step and the estimated model probabilities are incorporated into the set of summary statistics for model choice purposes. A reversible jump Markov chain Monte Carlo step is also included in the algorithm to increase model diversity for thorough exploration of the model space. This algorithm was applied to a validating example to demonstrate the robustness of the algorithm across a wide range of true model probabilities. Its subsequent use in three pathogen transmission examples of varying complexity illustrates the utility of the algorithm in inferring preference of particular transmission models for the pathogens.

Statement of Authorship for Chapter 3

This chapter has been written as a journal article. The authors listed below have certified that:

1. they meet the criteria for authorship in that they have participated in the conception, execution, or interpretation, of at least that part of the publication in their field of expertise;
2. they take public responsibility for their part of the publication, except for the responsible author who accepts overall responsibility for the publication;
3. there are no other authors of the publication according to these criteria;
4. potential conflicts of interest have been disclosed to (a) granting bodies, (b) the editor or publisher of journals or other publications, and (c) the head of the responsible academic unit, and
5. they agree to the use of the publication in the students thesis and its publication on the Australasian Research Online database consistent with any limitations set by publisher requirements.


In the case of this chapter, the reference for the associated publication is:

Lee, X. J., Drovandi, C. C., and Pettitt, A. N. (2015). Model choice problems using approximate Bayesian computation with applications to pathogen transmission data sets. *Biometrics*, 71(1):198–207

Contributor	Statement of contribution
X.J. Lee	developed methods, conducted analysis, wrote manuscript
Signature & Date:	
C.C. Drovandi	developed methods, discussed methods and results, reviewed manuscript
A.N. Pettitt	conceived study, developed methods, supervised research, discussed methods and results, reviewed manuscript

Principal Supervisor Confirmation

I have sighted email or other correspondence from all Co-authors confirming their certifying authorship.

<u>A N PETTITT</u>	<u></u>	<u>13/2/17</u>
Name	Signature	Date

3.1 Introduction

The genesis of mathematical models to describe pathogen transmission data is usually attributed to the susceptible-infectious-recovered (SIR) model proposed by Kermack and McKendrick (1927). There have since been various modifications to the basic SIR model form to account for the inclusion of an exposed class (SEIR model), re-introduction of the removed or infectious class back into the susceptible class (SIRS or SIS models), lagged infections and more complex contact processes, such as network models, to account for inhomogeneous mixing (Diekmann et al., 2012). For the applications considered here, the models involve discrete event Markov processes, which can be simulated exactly using the Gillespie algorithm (Gillespie, 1977), to account for the effect of variability due to small population sizes.

There is often uncertainty about the most appropriate model out of a selection of competing models to best describe the pathogen transmission data and the dynamics of the disease. In a Bayesian context, there are several approaches to address this issue: calculation of a comparison measure (e.g. Bayes factor (Kass and Raftery, 1995), DIC (Spiegelhalter et al., 2002) and marginal likelihood or ‘evidence’ (Friel and Pettitt, 2008)) and model jumping algorithms such as the reversible jump Markov chain Monte Carlo (RJ-MCMC) algorithm (Green, 1995) are the most commonly used. This paper explores the use of a novel approximate Bayesian computation (ABC) model choice algorithm based on posterior model probabilities to address model choice problems for pathogen transmission data sets. The use of posterior model probabilities for model choice corresponds to the ‘M-closed’ perspective (Bernardo and Smith, 2000) where it is assumed that the true model is among the selection of competing models considered.

ABC is a relatively new field of study developed for problems where the likelihood function is intractable, either computationally or analytically (Beaumont et al., 2002). ABC algorithms rely on repeated simulation from the model to overcome this intractability.

McKinley et al. (2009) applied ABC using pre-specified summary statistics to epidemic data and compared the ABC algorithms used with data-augmented MCMC which is considered the gold standard for likelihood-based inference methodologies. O’Neill (2010) and Jewell et al. (2009) provided summaries of Bayesian methodologies for pathogen transmission data. Also, McKinley et al. (2014) proposed an alternative simulation-based Bayesian inference method using a pseudo-marginal MCMC approach (Andrieu and Roberts, 2009).

Exploration of model choice problems using ABC however has remained relatively limited due to the added complexity of handling multiple model spaces. Criticism of the ability of ABC algorithms to handle model choice problems was noted by Robert et al. (2011). Marin et al. (2014) proposed theoretical properties of summary statistics that would allow for appropriate discrimination between models when ABC is used with

those summary statistics. Grelaud et al. (2009) and Didelot et al. (2011) explored the use of ABC for model choice problems involving models from the exponential family, where low dimensional sufficient statistics exist for both parameter estimation and model choice. Toni et al. (2009) and Toni and Stumpf (2010) investigated the use of their sequential Monte Carlo ABC (SMC ABC) algorithm for both parameter estimation and model choice purposes.

This paper explores the use of a multinomial logistic regression for the model indicator variable to extend the Fearnhead and Prangle (2012) method for model choice problems using ABC algorithms with applications to various pathogen transmission data sets. This differs from the approach in Prangle et al. (2014) where multiple binomial logistic regressions were used instead for applications involving more than two models.

Section 3.2 presents and validates the introduced ABC model choice algorithm that extends Drovandi and Pettitt (2011a) and Fearnhead and Prangle (2012). Section 3.3 applies the method to pathogen transmission data sets of varying levels of detail. Section 3.4 presents a discussion of the proposed method and potential further directions. Additional details and results for the applications considered are provided in the chapter's Supplementary Materials¹ (Section A.1 for the validating example, Section A.2 and Section A.3 for the hospital MRSA example, Section A.4 for the Tristan da Cunha example and Section A.5 for the Hagelloch measles example).

3.2 Methodology

3.2.1 Overview of ABC algorithms

ABC algorithms originated with the rejection sampling ABC algorithm (RS ABC) (Beaumont et al., 2002, Fu and Li, 1997, Pritchard et al., 1999, Weiss and von Haeseler, 1998) to analyse statistical inferential problems with intractable likelihoods. RS ABC proposes parameter values from the prior distribution, generates simulations using the proposed parameters and rejects the proposed parameter set unless some chosen discrepancy measure denoted by $\rho(\cdot)$, typically the (normed) differences of user-specified summary statistics between the observed and simulated data, is less than a pre-specified tolerance ϵ . The algorithm terminates when a fixed number of proposals has been accepted at the specified tolerance.

While straightforward to implement, RS ABC produces a large amount of computational wastage as each parameter proposal is drawn from the prior distribution which may be very diffuse compared with the posterior distribution of interest. This issue was alleviated substantially through the development of Markov chain Monte Carlo ABC (MCMC ABC) (Marjoram et al., 2003) where, after an initial rejection sampling step, parameter values are drawn from a tuned proposal distribution that is dependent

¹Supplementary Materials for Chapters 3 to 8 are placed at the end of the thesis.

on the values at the previous iteration. Simulated data are generated using the proposed parameter values and the proposals are only accepted with a certain probability according to the Metropolis-Hastings ratio and provided the discrepancy between the simulated and observed data is within the pre-specified tolerance similar to RS ABC.

The development of SMC ABC algorithms further improved the computational efficiency of ABC algorithms (Beaumont et al., 2009, Sisson et al., 2009, Toni et al., 2009). SMC ABC algorithms propagate a set of ‘particles’ or parameter values through a sequence of non-increasing tolerances and the particle set corresponding to the final tolerance is the approximate posterior distribution of interest.

3.2.2 Approximate Bayesian Model Choice Algorithm

There has been limited research on ABC algorithms for model choice problems in comparison with problems solely involving parameter estimation. Grelaud et al. (2009) showed how the addition of a model indicator variable into the parameter set could be used to handle model choice problems for competing models from the exponential family while Beaumont (2008) illustrated a post-simulation regression adjustment for the model indicator variable using logistic regression. Toni et al. (2009) and Toni and Stumpf (2010) extended their variant of the basic SMC ABC algorithm to incorporate model choice problems in a similar fashion as Grelaud et al. (2009) and applied it to various biological examples.

This section introduces a new variant of the adaptive SMC ABC algorithm with replenishment (Algorithm 3.2) of Drovandi and Pettitt (2011a) for model choice problems. The full algorithm is referred to as the ‘approximate Bayesian model choice’ (ABMC) algorithm to distinguish it from the ABC model choice algorithm (Grelaud et al., 2009). The algorithm comprises of two parts: the Fearnhead and Prangle (FP) step (Algorithm 3.1) estimates the regression coefficients used to calculate the summary statistics in the discrepancy measure extending Fearnhead and Prangle (2012), and the SMC step (Algorithm 3.2) is the SMC ABC replenishment algorithm (Drovandi and Pettitt, 2011a) with an RJ-MCMC kernel for jumping between models.

The first modification undertaken is the inclusion of the model indicator ($\mathcal{M} \in \{1, 2, \dots, K\}$ where K is the total number of candidate models) in the set of parameters $\boldsymbol{\theta}$. The vector of parameters in model k is denoted $\boldsymbol{\theta}_k$. The target (posterior) density is then

$$\pi_{\epsilon}(\boldsymbol{\theta}_k, k | \mathbf{y}) \propto P(\mathcal{M} = k) \pi(\boldsymbol{\theta}_k | \mathcal{M} = k) \int_{\mathbf{x}} f_k(\mathbf{x} | \boldsymbol{\theta}_k) \mathbb{1}(\rho(\mathbf{x}, \mathbf{y}) < \epsilon) d\mathbf{x}$$

where \mathbf{y} denotes the observed data, \mathbf{x} is the data simulated from the likelihood for model k , $f_k(\cdot | \cdot)$, $P(\mathcal{M} = k)$ is the prior probability for the model indicator \mathcal{M} , $\pi(\boldsymbol{\theta}_k | \mathcal{M} = k)$ is the prior density for the parameters in model k conditional on the

model indicator and $\mathbb{1}(\rho(\mathbf{x}, \mathbf{y}) < \epsilon)$ is the indicator function which equals to 1 when $\rho(\mathbf{x}, \mathbf{y}) < \epsilon$ and 0 otherwise.

Fearnhead and Prangle (2012) proposed the use of posterior mean estimates of the model parameters obtained through stepwise linear regressions as the summary statistics for the ABC discrepancy measure. The method estimates the regression coefficients from a large simulation study prior to executing the main ABC algorithm.

The FP step (Algorithm 3.1) extends the Fearnhead and Prangle (2012) method to include a stepwise multinomial (or binomial for cases with two candidate models) logistic regression to estimate the summary statistics related to model choice. The forward stepwise algorithm used here terminates when the decrease in BIC (Schwarz, 1978) from its current value to the next is less than 0.5% of its current value. The logistic regression is performed on the model indicator variable to obtain the regression coefficients to estimate the posterior model probabilities. The estimated posterior model probabilities will then be used as the summary statistics in the ABC discrepancy measure for model choice. The stepwise linear regressions for the model parameters (conditional on the model indicator) then estimate regression coefficients for the posterior means as in Fearnhead and Prangle (2012).

For notational convenience, $h(\mathbf{x})$ denotes the regression summary statistics or covariates for the logistic and linear regressions as a multivariate function of simulated data from the candidate models. However, different functions can be used for the different regressions.

The SMC step (Algorithm 3.2) implements the SMC ABC replenishment algorithm (Drovandi and Pettitt, 2011a) using the Euclidean distance between the estimated model probabilities and posterior means of the parameters (using the coefficients of the regressions) obtained from the observed and simulated data sets as the discrepancy measure. Prangle et al. (2014) proved that the posterior model probabilities are Bayes sufficient for the model indicator, i.e. the posterior distribution is dependent on the data (\mathbf{y}) only through the Bayes sufficient statistics for any prior distribution and almost all \mathbf{y} (Kolmogorov, 1942).

The SMC step is initialised using rejection sampling with a user-specified initial tolerance ϵ_1 to produce a set of N particles $\{\boldsymbol{\theta}^i, \rho^i\}_{i=1}^N$, where ρ^i denotes the discrepancy calculated for $\boldsymbol{\theta}^i$. The particle set is then sorted by the discrepancy values and a proportion ($\alpha \in (0, 1)$) of the particles with the largest discrepancies are dropped from the particle set. The tolerance value for the next iteration t (ϵ_t) is the value of the largest ρ^i in the remaining particle set.

The remaining particles are then used to resample (with replacement) the particle set until there are N particles in the set again. Specifically, a new particle value is drawn by sampling from the current set and perturbed using an MCMC kernel R_t times to help ensure diversity in the particle set. The MCMC kernel used here was an independent

proposal from model to model using RJ-MCMC to allow for a particle to swap models during a move step with probabilities $\pi_{k_{old}, k_{prop}}$ where k_{old} is the current model indicator and k_{prop} is the value of the new model indicator. The model move step is similar to that of Toni and Stumpf (2010).

The model parameter values θ_k^* are then drawn from a user-specified proposal distribution $q_k(\cdot)$. The proposal distributions used here were multivariate normal (Beaumont et al., 2009, Filippi et al., 2013) with the mean and covariance structure computed from the remaining particle set for continuous parameters in each model (Drovandi and Pettitt, 2011a). Moves for discrete parameters in a model are proposed using the relative frequencies of the particles in the corresponding model's remaining particle set.

After the $N_\alpha = \alpha N$ particles are resampled, the acceptance probability p_t^{acc} and R_t values are calculated as $p_t^{acc} = \frac{i_{acc}}{R_{t-1}N_\alpha}$ and $R_t = \lceil \frac{\log(c)}{\log(1-p_t^{acc})} \rceil$ where i_{acc} is the number of accepted proposals in iteration t and c is the theoretical non-move probability for a resampled particle (Drovandi and Pettitt, 2011a). The process is then repeated until the tolerance is below some user-specified final tolerance ϵ_T or the acceptance probability becomes too small.

The algorithm introduced here differs from the approach described in Prangle et al. (2014) where only binomial logistic regressions were used in the FP step. Pairwise estimation of the model probabilities was implemented for the case with three models in Prangle et al. (2014) whereas we utilise the multinomial logistic regression instead. The truncation correction factor proposed by Prangle et al. (2014) was also omitted as the same priors were used for both the FP step and SMC step, but should be included otherwise.

In order to assess the performance of the (multinomial) logistic regression in distinguishing between competing models, the misclassification matrix is presented in the applications considered here. The (i, j) -th entry in a misclassification matrix is the proportion of simulations generated from model i that is classified as model j . The classification rule used here is to select the model corresponding to the largest posterior model probability estimated from additional simulated data generated using random draws from the priors and the estimated logistic regression coefficients. The number of simulations used to calculate the misclassification matrix is the same as the number of simulations used in the FP step for simplicity, but need not be the same.

Histograms and cumulative distribution function (cdf) plots of the probabilities of correct model allocation (i.e. probability of being allocated to model k given the simulation was generated from model k) calculated from the additional simulated data are also produced and presented in the corresponding Supplementary Material sections (Appendix A.3, Appendix A.4 and Appendix A.5) for the pathogen transmission examples. As these diagnostics are computed in the FP step, the set of regression

summary statistics can be modified and the FP step repeated until sufficiently good diagnostics are obtained prior to commencing with the SMC step.

Algorithm 3.1 FP Step

- 1: Given that there are K candidate models, draw M/K sets of parameters from each of the candidate model's prior distribution where M is large.
 - 2: For each set of parameter values, simulate a data set from the corresponding model and compute the regression summary statistics of the simulated data sets $h(\mathbf{x})$.
 - 3: Perform a stepwise multinomial logistic regression on the model indicator variable using $h(\mathbf{x})$ as the covariates. Then, for each candidate model, perform a stepwise linear regression on each of the model's parameters with the corresponding subset of $h(\mathbf{x})$.
-

For the applications considered here, it was assumed that all models were equally likely a priori, and probabilities of transitioning from one model to another (itself included) in the RJ-MCMC move ($\pi_{k_{old}, k_{prop}}$) were also equal. The ABMC algorithm was run with 50,000 simulations for each model in the FP step, 2,000 particles in the SMC step, half the particles being dropped from one iteration to the next ($\alpha = 0.5$) and a value of 0.01 for the theoretical non-move probability c in the formula for R_t . The algorithm was terminated when the final tolerance (ϵ_T) of 1 was reached or when the acceptance probability dropped below the pre-specified threshold (p_T^{acc}) of 1% (unless otherwise specified).

3.2.3 Validating Example

To validate the ABMC algorithm, we trialled the method on a relatively simple model choice problem involving three discrete distributions. The 1,000 observed data sets (each of size 100) used in this example were generated from a Poisson distribution with a mean of 0.5, referred to below as the generated data sets. The competing models considered are the Poisson distribution with mean λ , the geometric distribution with probability of 'success' p_{geo} (and support including 0) and the negative binomial distribution with parameters r and p_{nb} . The priors for the parameters were $Exp(1)$ for λ and r , and $U[0, 1]$ for p_{geo} and p_{nb} .

The posterior model probabilities were also derived numerically (Appendix A.1) for the specification of the models and priors above, and compared with the ABMC estimates (see Didelot et al. (2011) for the model comparison example with just the Poisson and geometric distributions). To investigate the performance of the algorithm across a spectrum of model probability values, 1,000 data sets were generated such that the model probabilities of the correct model (Poisson) for the collection of generated data sets were approximately uniformly distributed between 0.01 and 0.99.

The set of regression summary statistics considered comprised of the mean, variance, median absolute deviation, number of zeros, maximum value, interquartile range, skewness, kurtosis, and mean-variance ratio.

Algorithm 3.2 SMC step

- 4: Run a rejection sampling algorithm with the initial tolerance ϵ_1 to produce a set of N particles $\{\boldsymbol{\theta}^i, \rho^i\}_{i=1}^N$ using the difference between the observed and simulated estimates of model probabilities and posterior means (using the regression coefficients) as the discrepancy measure. Compute also the acceptance probability p_1^{acc} and R_1 . Set $t = 1$.
 - 5: Sort the particle set by their discrepancy values ρ and set $\epsilon_t = \rho^{(N-N_\alpha)}$ (where $\rho^{(\cdot)}$ denotes the ordered values of ρ) and $\epsilon_{MAX} = \rho^{(N)}$. If $\epsilon_{MAX} < \epsilon_T$ or $p_t^{acc} < p_T^{acc}$, then the algorithm is terminated.
 - 6: Compute the parameters of the K separate MCMC kernels $q_k(\cdot)$ using the particle set $\{\boldsymbol{\theta}^i, \rho^i\}_{i=1}^{N-N_\alpha}$. Set $i_{acc} = 0$.
 - 7: **for** $j = N - N_\alpha + 1$ to N **do**
 - 8: Resample $\boldsymbol{\theta}^j$ from $\{\boldsymbol{\theta}^i\}_{i=1}^{N-N_\alpha}$.
 - 9: **for** $l = 1$ to R_t **do**
 - 10: Denote the current model indicator as k_{old} .
 - 11: Draw a new model indicator $k_{prop} \sim \text{Multinomial}(1; \pi_{k_{old},1}, \dots, \pi_{k_{old},K})$.
 - 12: Propose move $\boldsymbol{\theta}_{k_{prop}}^* \sim q_{k_{prop}}(\cdot)$ then simulate data $\mathbf{x}_{k_{prop}}^* \sim f_{k_{prop}}(\cdot | \boldsymbol{\theta}_{k_{prop}}^*)$.
 - 13: Compute the Metropolis-Hastings ratio $r = \min(1, MH_{k_{old},k_{prop}})$ where

$$MH_{k_{old},k_{prop}} = \frac{P(\mathcal{M} = k_{prop})}{P(\mathcal{M} = k_{old})} \frac{\pi(\boldsymbol{\theta}_{k_{prop}}^* | \mathcal{M} = k_{prop})}{\pi(\boldsymbol{\theta}_{k_{old}} | \mathcal{M} = k_{old})} \mathbb{1}(\rho(\mathbf{x}_{k_{prop}}^*, \mathbf{y}) < \epsilon_t)$$

$$\frac{q_{k_{old}}(\boldsymbol{\theta}_{k_{old}})}{q_{k_{prop}}(\boldsymbol{\theta}_{k_{prop}}^*)} \frac{\pi_{k_{prop},k_{old}}}{\pi_{k_{old},k_{prop}}}.$$
 - 14: **if** $U(0,1) < r$ **then**
 - 15: Set $\boldsymbol{\theta}^j = \{k_{prop}, \boldsymbol{\theta}_{k_{prop}}^*\}$, $\rho^j = \rho(\mathbf{x}_{k_{prop}}^*, \mathbf{y})$ and $i_{acc} = i_{acc} + 1$.
 - 16: **end if**
 - 17: **end for**
 - 18: **end for**
 - 19: Set $t = t + 1$.
 - 20: Compute the acceptance probability $p_t^{acc} = \frac{i_{acc}}{R_t - 1 - N_\alpha}$ and $R_t = \lceil \frac{\log(c)}{\log(1 - p_t^{acc})} \rceil$. Return to 5:
-

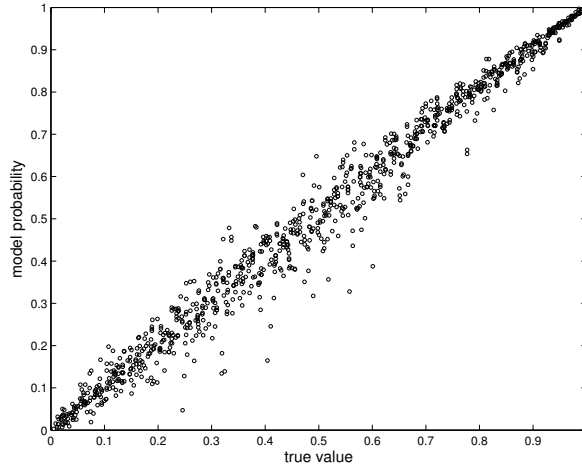


Figure 3.1: Validating example: plot of the estimated posterior model probabilities for the Poisson model obtained using the ABMC algorithm against the true model probabilities for the Poisson model.

For the collection of 1,000 generated data sets, the average misclassification matrix was calculated instead. It was obtained by taking the element-wise average of each misclassification matrix obtained from the 1,000 generated data sets in the validating example. The standard deviations were obtained similarly. The average misclassification matrix from the 1,000 generated data sets with standard deviations in parentheses is given below.

	$p(\text{geometric})$	$p(\text{Poisson})$	$p(\text{negative binomial})$
geometric	0.689 (0.007)	0.109 (0.003)	0.202 (0.005)
Poisson	0.067 (0.004)	0.866 (0.004)	0.066 (0.002)
negative binomial	0.408 (0.004)	0.114 (0.002)	0.478 (0.004)

The average misclassification matrix suggests good identification for the Poisson model using the set of regression summary statistics specified however the discrimination between the geometric and negative binomial models is less evident. This result is consistent with the facts that non-informative priors were chosen for the parameters in the models and the geometric distribution is a special case of the negative binomial distribution (with $r = 1$). Hence it is possible to simulate data from the negative binomial distribution with characteristics of the geometric model and vice versa.

The model choice results obtained from the 1,000 generated data sets are illustrated in Figure 3.1 with the estimated model probabilities obtained using the ABMC algorithm plotted against the true posterior model probabilities of the Poisson model. It is clear that there is a strong agreement between the analytical and ABC results for this simple example.

3.3 Application to Pathogen Transmission Data Sets

It may not always be clear what transmission model best represents the underlying transmission process of reported infection data, particularly for a new strain of pathogen or a pathogen that exhibits long term persistence despite control measures. A better understanding of the transmission process could improve control measures for the pathogen. One possible avenue of investigation is to compare different transmission models, proposed either through expert clinical opinions or transmission models of similar diseases, which translates into a model choice problem thus facilitating the use of the ABMC algorithm proposed.

3.3.1 Pathogen Transmission in a Hospital Ward

Antibiotic-resistant nosocomial infections such as methicillin-resistant *Staphylococcus aureus* (MRSA) is an issue that affects most hospitals around the world (Bonten and Bootsma, 2010) despite continual control efforts. The analysis here used observed weekly patient MRSA incidence data collected for 134 weeks from 2001 to 2004 in an ICU ward at the Princess Alexandra Hospital (Brisbane, Australia) (McBryde et al., 2007b) as shown in Figure A.3.

The two models compared here comprised of the original model proposed by McBryde et al. (2007b) (herein referred to as the standard model)

$$\frac{dY_p}{dt} = \phi_p Y_h (N_p - Y_p) - \mu'(1 - \sigma)Y_p + \mu\sigma(N_p - Y_p) \quad (3.1a)$$

$$\frac{dY_h}{dt} = \phi_h Y_p (N_h - Y_h) - \kappa Y_h \quad (3.1b)$$

and an alternative model based on the transmission dynamic of Greenwood (1931) which we refer to as the Greenwood model (whereby provided that at least one person is colonised, there is a constant colonisation pressure for the corresponding susceptible group)

$$\frac{dY_p}{dt} = \phi'_p \mathbf{1}(Y_h > 0) (N_p - Y_p) - \mu'(1 - \sigma)Y_p + \mu\sigma(N_p - Y_p) \quad (3.2a)$$

$$\frac{dY_h}{dt} = \phi_h \mathbf{1}(Y_p > 0) (N_h - Y_h) - \kappa Y_h. \quad (3.2b)$$

Here, Y_p and Y_h represent the number of colonised patients and health-care workers (HCWs) respectively, and N_p and N_h the total number of patients and HCWs in the ward (see Appendix A.2 and McBryde et al. (2007b) for more details). The only model parameters to be estimated are ϕ_p and ϕ'_p . All other parameters are fixed and summarised in Table A.2.

Due to the small population sizes in the ICU, purely deterministic models as described by (3.1) and (3.2) will not accurately represent the system as they do not capture the stochasticity inherent in such systems. Hence, stochastic variants of the models were

implemented as discrete Markov processes using the rates specified in (3.1) and (3.2) as the relative probabilities with the initial population sizes for the simulations sampled from the stationary distribution of the corresponding Markov process assuming MRSA is endemic in the study ward (McBryde et al., 2007b). A new variable $I(t)$ measuring the incidence was also introduced into the system in order to compare the simulations with the observed data (Drovandi and Pettitt, 2008).

As Y_h is not directly observed in the data, we utilised a pseudo-equilibrium approximation in which the number of colonised HCWs (Y_h) is eliminated from the system by approximating it with the steady-state value (\bar{Y}_h) obtained by setting $\frac{dY_h}{dt}$ ((3.1b) and (3.2b)) to zero (see Appendix A.2 and Drovandi and Pettitt (2008) for further details).

For this comparatively small scale problem, the ABMC algorithm was run with the final tolerance set to 0 thus the SMC step only terminates when the acceptance probability is below the set threshold of 1%. The priors for the parameters were $U[0, 0.5]$ for both ϕ_p and ϕ'_p (Appendix A.2). The regression summary statistics for this example comprised of the mean, variance, median absolute deviation, autocovariances and autocorrelations up to lag 5, counts of zeros, ones and twos in the data, AR(1) coefficient, maximum value and coefficients of the categorical regression of data on indicators of previous time step data

$$\mathbf{x}_t = \beta_0 + \beta_1 \mathbf{1}(\mathbf{x}_{t-1} = 0) + \beta_2 \mathbf{1}(\mathbf{x}_{t-1} = 1) + \beta_3 \mathbf{1}(\mathbf{x}_{t-1} = 2) + \beta_4 \mathbf{1}(\mathbf{x}_{t-1} > 2)$$

where \mathbf{x}_t is the incidence at time t .

The misclassification matrix was

$$\begin{array}{cc} & \begin{array}{cc} p(\text{standard}) & p(\text{Greenwood}) \end{array} \\ \begin{array}{c} \text{standard} \\ \text{Greenwood} \end{array} & \begin{pmatrix} 0.527 & 0.473 \\ 0.256 & 0.745 \end{pmatrix} \end{array}.$$

The misclassification matrix showed a lack of discrimination between the two models for simulations from the standard model, but identified Greenwood model simulations well. It was suspected that this was because the standard model simulations over the prior range chosen exhibited a wide range of behaviour, some of which resemble simulations from the Greenwood model. The corresponding histograms and cdf plots of the probabilities of correct model allocation are provided in Figure A.5 and Figure A.6.

The final estimated model probability obtained was 0.979 in favour of the standard model (Figure 3.2). The estimates of the transmission parameters for the standard and Greenwood models were 0.0429 (95% CI:[0.0319,0.0554]) and 0.00867 (95% CI: [0.00629, 0.0123]) respectively (Figure A.7).

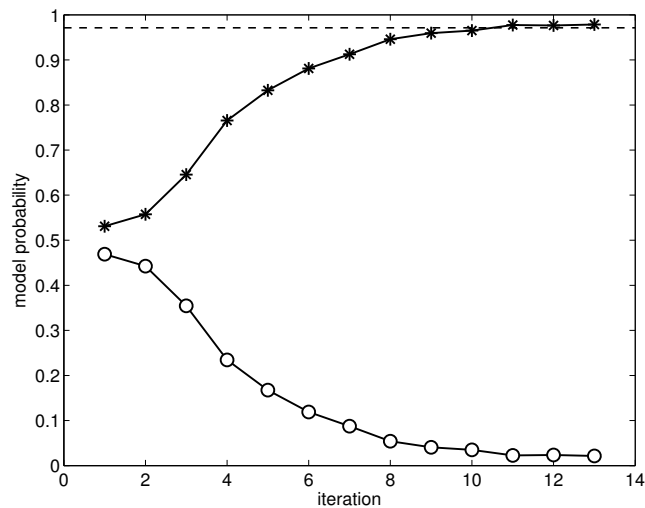


Figure 3.2: Hospital MRSA example: estimated model probabilities for the standard model (asterisks) and Greenwood model (circles) across the SMC iterations. The model probability for the standard model estimated using numerical integration is indicated by the dashed horizontal line.

The ABMC algorithm inferred a strong preference towards the standard model over the Greenwood model for the observed MRSA data set as measured by the empirical estimate of the model probabilities. For this example, it was also possible to calculate the evidence for each of the models (using the likelihood evaluation described in Drovandi and Pettitt (2008) and numerical integration) and arrive at an estimated posterior probability of 0.966 for the standard model, similar to the estimate obtained by the ABMC algorithm.

While the results provided strong evidence for the standard model compared with the Greenwood model for the spread of MRSA in the ICU, consistent with previous studies (McDonald, 1997), caution should be used in generalising the results due to the simplifications made in the models. It may also be desirable to include effects of environmental contamination directly as well as community-acquired MRSA acquisitions (van Kleef et al., 2013).

3.3.2 Tristan da Cunha Cold Outbreak

We now consider a more involved example where there are more than two competing models and there is more than one parameter per model which could be continuous or discrete valued. Specifically, we revisit the Tristan da Cunha October-November 1967 common cold outbreak example analysed as a model choice problem using SMC ABC (Toni et al., 2009).

The data used in the analysis to follow were the number of infectious and recovered individuals collected over a period of 21 days between October 1967 and November 1967 (as shown in Table 3 in Toni et al. (2009)). The four candidate models considered in Toni et al. (2009), as summarised in Table 3.1, were used.

	Model 1	Model 2	Model 3	Model 4
$\frac{dS}{dt}$	$-\gamma_1 S(t)I(t)$	$-\gamma_2 S(t)I(t - \tau)$	$-\gamma_3 S(t)I(t)$	$-\gamma_4 S(t)I(t) + eR(t)$
$\frac{dI}{dt}$	$\gamma_1 S(t)I(t) - \nu_1 I(t)$	$\gamma_2 S(t)I(t - \tau) - \nu_2 I(t)$	$\delta E(t) - \nu_3 I(t)$	$\gamma_4 S(t)I(t) - \nu_4 I(t)$
$\frac{dR}{dt}$	$\nu_1 I(t)$	$\nu_2 I(t)$	$\nu_3 I(t)$	$\nu_4 I(t) - eR(t)$
$\frac{dE}{dt}$	—	—	$\gamma_3 S(t)I(t) - \delta E(t)$	—

Table 3.1: Tristan da Cunha cold outbreak example: model descriptions for the four candidate models where S , E , I and R represent the susceptible, exposed, infectious and recovered populations respectively, γ_k ($k = 1, 2, 3, 4$) is the transmission rate in Model k , ν_k is the recovery rate, τ is the time delay between being infected and infectious in Model 2, δ is the rate of progression from exposed to infectious in Model 3 and e is the rate immunity diminishes in Model 4.

Stochastic variants of these deterministic models were used to generate the simulated data for the ABMC algorithm. The initial number of susceptibles (S_0) is unknown and was estimated as a separate discrete valued parameter in each model. It was assumed that there were no initially recovered individuals in the population and the outbreak was triggered by one initial infectious individual. The priors used are listed in Appendix A.4.

The set of regression summary statistics used here comprised of the mean, variance, median absolute deviation, autocovariances and autocorrelations up to lag 5, number of zeros observed, AR(5) coefficients, maximum value and time point at which it was recorded, 10th, 15th, ..., 90th percentiles of the time-ordered data points for both the infectious and recovered individual numbers, time at which the last infectious individual recovers and cross-covariances up to lag ± 10 between the infectious and recovered individual numbers.

The misclassification matrix obtained for this example was

$$\begin{matrix} & p(\text{Model 1}) & p(\text{Model 2}) & p(\text{Model 3}) & p(\text{Model 4}) \\ \begin{matrix} \text{Model 1} \\ \text{Model 2} \\ \text{Model 3} \\ \text{Model 4} \end{matrix} & \left(\begin{matrix} 0.929 & 0.012 & 0.056 & 0.002 \\ 0.228 & 0.704 & 0.067 & 0.001 \\ 0.189 & 0.050 & 0.761 & 0.001 \\ 0.007 & 0.003 & 0.001 & 0.990 \end{matrix} \right)
 \end{matrix}$$

The histograms and cdf plots of the probabilities of the correct model allocation are shown in Figure A.17 and Figure A.18 respectively.

For this example, the final estimated model probabilities obtained from the ABMC algorithm were $[0.064, 0.664, 0.272, 0]$ giving stronger support for Model 2 and Model 3 out of the four competing models (Figure 3.3). The algorithm was unable to select the most dominant model as was also reported by Toni et al. (2009). This is not surprising as the transmission mechanisms of Model 2 and Model 3 are similar with the lagged infectious individuals in Model 2 essentially playing the role of the exposed class in Model 3. The main inference that can be drawn is that a latent period is a key component of the cold outbreak observed.

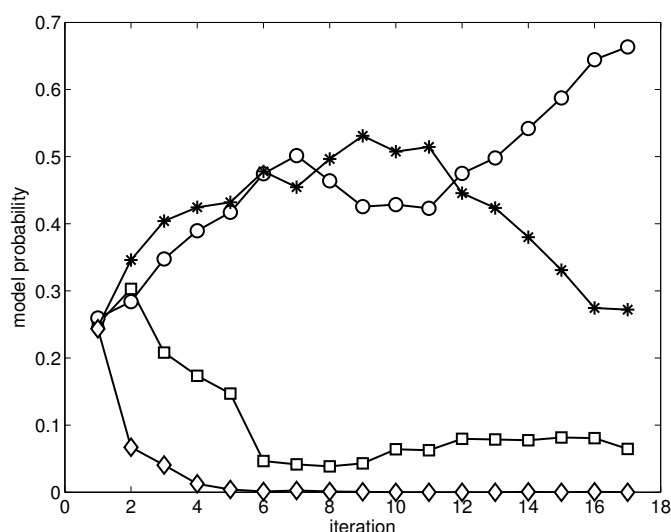


Figure 3.3: Tristan da Cunha cold outbreak example: estimated model probabilities for Model 1 (squares), Model 2 (circles), Model 3 (asterisks) and Model 4 (diamonds) across the SMC iterations.

model	parameter	mean	95% CI
Model 2	S_0	40.3	[37.0, 48.0]
	γ_2	0.103	[0.0256, 0.320]
	ν_2	0.387	[0.198, 0.631]
	τ	3.61	[1.24, 4.95]
Model 3	S_0	40.7	[37.0, 49.0]
	γ_3	0.531	[0.0965, 2.94]
	ν_3	0.290	[0.142, 0.902]
	δ	1.22	[0.105, 3.89]

Table 3.2: Tristan da Cunha cold outbreak example: parameter estimation results for the two most preferred models using the ABMC algorithm.

The parameter estimates for the two most preferred models are summarised in Table 3.2 as well as Figure A.19 and Figure A.20.

It should be noted that the data used for this analysis only covered one of the outbreaks recorded in the 1964-1968 period (Shibli et al., 1971). A clearer picture of the outbreaks may possibly be obtained by incorporating the other outbreaks provided they are of the same strain. Another improvement to the transmission models considered here might be to incorporate covariates such as the household, gender, age, and social structure (school or workplace) of the individuals (Becker and Hopper, 1983).

3.3.3 Hagelloch Measles Outbreak 1861

A detailed epidemic data set is available for a measles outbreak in the German village Hagelloch in 1861 (Oesterle, 1992, Pfeilsticker, 1863). The data set has been recently analysed by Britton et al. (2011) using a three-level mixing multitype epidemic model and by Groendyke et al. (2012) using an exponential-family random graph model

(ERGM) contact network approach. In both cases, an SEIR epidemic model was used to model the observed measles outbreak. Neal and Roberts (2004) considered the data set in a model choice context with competing nested contact network models using an RJ-MCMC algorithm.

Britton et al. (2011) assumed the spread of the measles outbreak was propagated by a three-level mixing multitype epidemic model. Transmissions could occur either through household contacts, classroom contacts (for two separate classes) or contacts with community members at large with different transmission rates (λ_H , λ_{G1} , λ_{G2} and λ_C respectively). The exposure and infectious periods were assumed to be fixed.

For the network model of Groendyke et al. (2012), the disease was assumed to spread with transmission rate λ through a contact network generated using an ERGM where the probability of contact between individuals i and j (p_{ij}) was given by

$$\log \left(\frac{p_{ij}}{1 - p_{ij}} \right) = \mathbf{X}_{ij} \boldsymbol{\eta}$$

and \mathbf{X}_{ij} is the set of pairwise covariates for individual i and individual j which includes a constant term, binary (whether the pair share a household, class, or gender) and continuous covariates (age difference and Euclidean distance between house locations). The contact network parameters $\boldsymbol{\eta} = (\eta_1, \eta_2, \eta_3, \eta_4, \eta_5, \eta_6, \eta_7, \eta_8)$ are defined as in Groendyke et al. (2012) where η_1 is the household effect, η_2 is the Class 1 effect, η_3 is the intercept, η_4 is the Class 2 effect, η_5 is the female effect, η_6 is the male effect, η_7 is the age difference effect and η_8 is the house location distance effect.

For our analysis, it was assumed that the exposure and infectious periods in both models follow gamma distributions (see Appendix A.5 for a justification). For notation purposes, let k_E and θ_E denote the shape and scale parameters for the gamma distribution describing the exposure period, and similarly k_I and θ_I for the infectious period. The modified multitype epidemic (MME) model and contact network (CN) model described were then compared using the ABMC algorithm. The priors used are listed in Appendix A.5.

The regression summary statistics used were the mean, variance, number of zero counts, median absolute deviation, autocovariances and autocorrelations up to lag 5, maximum value and time at which the maximum value occurred (for the exposed and infectious classes only) and AR(5) coefficients for the four different epidemic groups (S, E, I, R) as well as the cross-covariances up to lag ± 5 between different epidemic group pairs, aggregated separately by school class, house, gender and age.

The misclassification matrix was

$$\begin{array}{cc} & p(\text{MME}) & p(\text{CN}) \\ \begin{array}{c} \text{MME} \\ \text{CN} \end{array} & \begin{pmatrix} 0.997 & 0.003 \\ 0.004 & 0.996 \end{pmatrix} \end{array}.$$

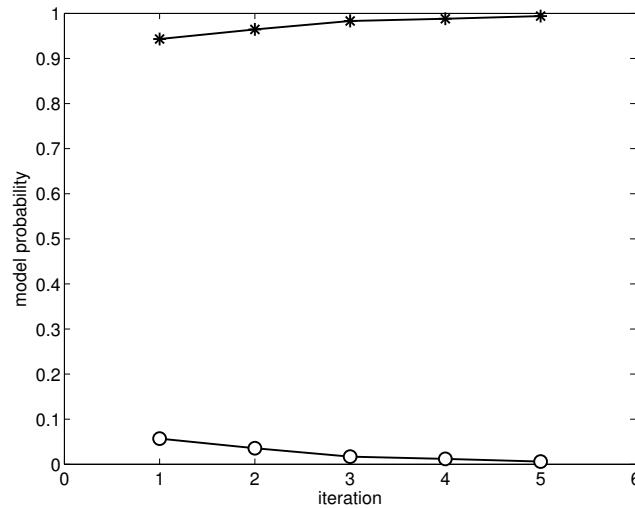


Figure 3.4: Hagelloch measles example: estimated model probabilities for the multitype epidemic model (asterisks) and contact network model (circles) across the SMC iterations.

parameter	mean	95% CI
λ_h	2.01	[0.11, 3.87]
λ_{g1}	2.62	[0.59, 3.96]
λ_{g2}	2.07	[0.17, 3.92]
λ_c	0.31	[0.10, 0.94]
k_E	15.9	[9.44, 19.9]
θ_E	0.80	[0.43, 0.99]
k_I	20.3	[15.1, 24.8]
θ_I	0.53	[0.27, 0.74]

Table 3.3: Hagelloch measles example: parameter estimation results for the MME model using the ABMC algorithm.

The histogram and cdf plots of the probabilities of the correct model allocation are provided in Figure A.24 and Figure A.25.

The final estimated model probability from the ABMC algorithm was 0.994 for the MME model (Figure 3.4). The parameter estimates for the MME model are summarised in Table 3.3 with associated histograms provided in Figure A.26 and Figure A.27.

Based on the observed data, there is strong support for the MME model over the CN model for the observed measles data set of the 1861 outbreak in Hagelloch. The model choice result implies that after accounting for the difference in the households and school classes of the individuals, the effects of age, gender and house location differences between individuals were of secondary importance to the transmission process as these variables were explicitly accounted for in the CN model but not in the MME model.

While the models considered in this analysis were fairly detailed, there exists additional information from the data set not considered in the models which could potentially provide a more comprehensive understanding of this particular outbreak. For instance,

both models used in this example did not factor in the recorded deaths or maximum fever temperatures which may act as proxies for the severity of the measles infection for each individual.

3.4 Discussion

An inferential method for model choice problems based on ABC has been presented here. The approach of Fearnhead and Prangle (2012) was extended with a stepwise multinomial logistic regression to estimate the summary statistics for model choice purposes, namely the posterior model probabilities estimated from the regression coefficients. The algorithm then proceeds with a standard ABC algorithm to obtain the approximate posteriors of interest. For our purposes, we have used the SMC ABC replenishment algorithm (Drovandi and Pettitt, 2011a). The method was validated using a simple example where the posterior model probabilities can be obtained directly through numerical integration. The algorithm was then applied to pathogen transmission data sets with varying levels of detail.

A potential improvement to the algorithm would be to incorporate bias-reduction (Firth, 1993) when performing the logistic regression in the FP step as its maximum likelihood estimates are known to be biased, and there is a non-zero probability that the estimates are unbounded, affecting the comparison between different subsets in the stepwise regression. The impact of bias-reduction was briefly investigated for the hospital MRSA example in Appendix A.3 which showed good agreement with the results in Section 3.3.1. This provides some degree of confidence in the inferences drawn here. Implementation of the bias-reduced multinomial logistic regression (Bull et al., 2002, Kosmidis and Firth, 2011) cannot be readily applied to large data sets as is required by the FP step due to the matrix operations involved.

Similar to Fearnhead and Prangle (2012), the examples above have used forward stepwise regressions in the FP step as it is easily implemented, straightforwardly handles large sets of summary statistics and increases computational efficiency by setting non-significant regression coefficients to 0. There are however certain contexts or selections of summary statistics where other variable subset selection or shrinkage methods, such as ridge regression or lasso, may perform better, such as for sets of highly correlated summary statistics. Another alternative to these methods is the SMC algorithm on a binary space proposed in Schäfer and Chopin (2013) for variable selection which could potentially be more robust. Explorations and comparisons of these variable selection methods would improve the algorithm performance and applicability, and could be investigated in future work.

Further computational savings could also be achieved if the user-specified parameters for the ABC algorithm (e.g. the proportion of particles dropped at each iteration (α) and theoretical non-move probability (c) for the SMC ABC replenishment algorithm) were

tuned to their optimal values. While there has been some recent research into the fine-tuning of ABC algorithms (Sedki et al., 2012, Silk et al., 2013), there still exists plenty of opportunities to expand and improve on the current literature.

Practitioners should also be cautious about the potentially strong dependence on the priors used for the parameters. If it was deemed appropriate to truncate the priors after the FP step, the truncation correction proposed in Prangle et al. (2014) must be incorporated to account for this modification. As with any Bayesian analysis, the sensitivity of the inference to prior choice used should be thoroughly investigated, particularly in model choice problems where the priors can have a substantial influence. This could be done through repetition of the analysis using alternative priors, or even a family of priors (Doss, 2010). However, this was not investigated here as the main focus was to illustrate the application of the ABMC algorithm on a variety of pathogen transmission model choice problems rather than in-depth analyses of the examples. The inferences drawn here are still valid for the choice of priors used, and showed strong agreement with the model probabilities calculated without the use of ABC for examples in Section 3.2.3 and Section 3.3.1.

Acknowledgements

The authors acknowledge the use of Dr Kevin Sheppard’s MFE Toolbox, the modified Mersenne Twister pseudorandom number generator C code by Takuji Nishumura and Makoto Matsumoto, and the computational resources and support provided by the HPC and Research Support Group at QUT. We thank Dr Emma McBryde for the MRSA data, and Dr Theodore Kypraios and Professor Klaus Dietz for the Hagelloch measles outbreak data. This research is supported by the Australian Research Council through a Discovery project (DP110100159). The first author receives PhD scholarship funding from the Centre of Research Excellence in Reducing Healthcare Associated Infections (NHMRC Grant 1030103). The authors are affiliated with the ARC Centre of Excellence for Mathematical & Statistical Frontiers (ACEMS) where CCD is an Associate Research Fellow and ANP is a chief investigator.

We thank the two referees and associate editor for their helpful inputs which led to substantial improvements in the paper.

4 ABC model selection for spatial max-stable models applied to South Australian maximum temperature data

Abstract

Max-stable models are a common choice for spatial extreme data as they arise naturally as the infinite dimensional generalisation of multivariate extreme value theory. Statistical inference for such models is complicated by the intractability of the multivariate density function. Nonparametric and composite likelihood based approaches have been proposed to address this difficulty. More recently, a simulation-based approach using approximate Bayesian computation (ABC) has been proposed for estimating parameters of max-stable models. ABC algorithms rely on evaluation of discrepancies between model simulations and the observed data rather than explicit evaluations of computationally expensive or intractable likelihood functions, as is the case for max-stable models. Use of an ABC method to perform model selection for max-stable models is explored. Six max-stable models were considered: the Smith model, the Schlather model with either a Whittle–Matérn, Cauchy, powered exponential or Bessel covariance function, and the Brown–Resnick model. The method was applied to annual maximal temperature data from 26 weather stations dispersed around South Australia.

Statement of Authorship for Chapter 4

This chapter has been written as a journal article. The authors listed below have certified that:

1. they meet the criteria for authorship in that they have participated in the conception, execution, or interpretation, of at least that part of the publication in their field of expertise;
2. they take public responsibility for their part of the publication, except for the responsible author who accepts overall responsibility for the publication;
3. there are no other authors of the publication according to these criteria;
4. potential conflicts of interest have been disclosed to (a) granting bodies, (b) the editor or publisher of journals or other publications, and (c) the head of the responsible academic unit, and
5. they agree to the use of the publication in the students thesis and its publication on the Australasian Research Online database consistent with any limitations set by publisher requirements.

In the case of this chapter, the reference for the associated publication is:

Lee, X. J., McKeone, J.P., Drovandi, C. C., and Pettitt, A. N. (2016). ABC model selection for spatial max-stable models applied to South Australian maximum temperature data *Computational Statistics & Data Analysis*, under review.

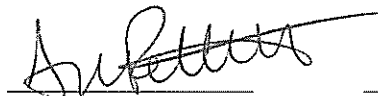
Contributor	Statement of contribution
X.J. Lee	developed methods, conducted analysis, wrote manuscript
Signature & Date:	
J.P. McKeone	developed methods, conducted initial analysis, wrote preliminary manuscript
C.C. Drovandi	developed methods, discussed methods and results, reviewed manuscript
A.N. Pettitt	conceived study, developed methods, supervised research, discussed methods and results, reviewed manuscript

Principal Supervisor Confirmation

I have sighted email or other correspondence from all Co-authors confirming their certifying authorship.

AN PETTITT

Name



Signature

13/2/17

Date

4.1 Introduction

The statistical analysis of extreme data offers a unique challenge as the interest lies in the tails of the distribution and is of importance in a wide range of application fields, e.g., finance (Embrechts et al., 1997), hydrology (Katz et al., 2002), engineering and meteorology (Castillo et al., 2005). Special consideration was given to develop statistical models particular to univariate extreme data which have now been generalised into a family of distributions known as the generalised extreme value (GEV) distribution with three subfamilies (Fréchet, Gumbel and Weibull) following the Fisher-Tippett-Gnedenko theorem (Section 2.2.4). Coles (2001) provides an excellent introductory treatment of the topic. A particular feature of the GEV distribution is its max-stable property which will be used in the following exposition. The max-stable property implies that the maximum (or minimum) is distributionally invariant up to location and scaling parameters.

Extensions to multivariate extreme data and models have been limited initially by the intractability of the model likelihood except for some lower dimensional cases. These special cases are of limited use in most applications where typical multivariate extreme applications arise from spatial data with a large number of spatial locations. Even current approaches to parameter estimation for spatial extremes models avoid the computation of the likelihood, relying instead on nonparametric (de Haan and Ferreira, 2006), composite likelihood (Padoan et al., 2010) and more recently, approximate Bayesian computation (ABC) (Erhardt and Smith, 2012) methods to estimate model parameters.

The research presented here investigates the use of a simulation-based ABC approach to address model selection problems involving a general group of spatial extreme models known as max-stable models. The aim here is to use ABC to determine the most preferred model to describe the spatial dependence of the annual maximum temperature data collected from weather stations located around the state of South Australia. An accurate representation of the spatial dependence of the spatial maxima would also allow for a more accurate depiction of the spatial distribution of the maximum temperature across the region. This is useful in estimating the maxima at locations with no observations, as well as areas where the largest maximum is likely to be observed.

The remainder of the paper is structured as follows. The data set used is described in Section 4.2. The max-stable models considered are introduced in Section 4.3 with the ABC method elaborated in Section 4.4. Implementation details specific to the data set and the corresponding results obtained are presented in Sections 4.5.1 and 4.5.2 respectively. A discussion of the results along with limitations and further extensions are provided in Section 4.6. Additional parameter inference results for the South Australia data set and simulation examples are provided in Section B.2 and Section B.3, respectively.

4.2 South Australian annual maximum temperature data

South Australia experiences a dry and hot Mediterranean climate. Extreme high temperatures can cause public health and safety concerns, for example heatwaves and bushfires. Understanding the spatial distribution of maximum temperature around the state is a vital component in planning for future adverse events related to extreme high temperatures.

The data considered in this paper contains annual maxima temperature values for the 18 year period spanning from 1979 to 1996 at 26 weather stations around Adelaide, the capital of South Australia. The particular time period (1979 – 1996) is the longest uninterrupted period of temperature recordings for the largest collection of weather stations reasonably close to Adelaide. The publicly available data were sourced from the Australian Bureau of Meteorology website. These maximum temperatures were originally recorded in monthly observation blocks and converted to yearly maximum temperature values. The autocorrelation plots of the yearly maxima for each observed location did not show any statistically significant temporal dependence in the data.

The locations of these 26 weather stations are shown in Figure 4.1. While the weather stations might seem far away from each other, the spatial scale is not unreasonable given the maxima temperature data analysis in Erhardt and Smith (2012). The marginal GEV parameter estimates plotted in Figure 4.1 also suggest that there is some degree of spatial dependence in the data, particularly from the location and scale parameter plots. These estimates are used to transform the data to have unit Fréchet margins as described in Section 4.5.1.

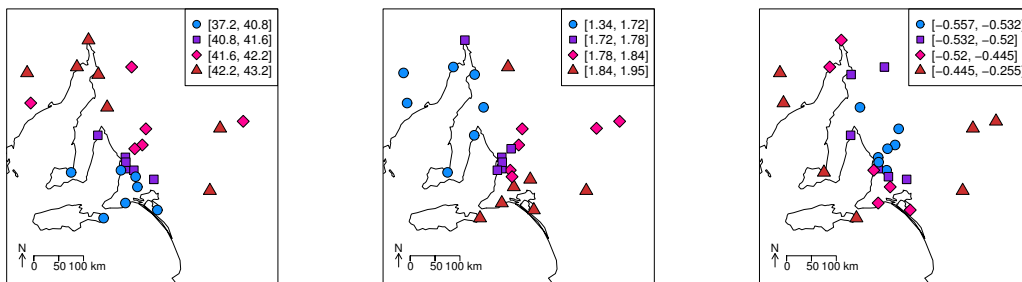


Figure 4.1: Colour-coded quartile sets of the three GEV parameter estimates (location μ [left], scale σ [middle], and shape ξ [right]) for the 26 land based weather stations around South Australia where data were collected. The quartile set with the smallest values is denoted by the blue filled circles. Sets with progressively larger values are denoted by coloured purple squares, pink diamonds and red triangles, respectively. The ranges for the quartiles are provided in the legends.

4.3 Max-stable models

As stated in Section 4.1, statistical analysis of extrema data uses specialised models developed for such data. Here, we consider the use of spatial max-stable models to describe the spatial dependence of the South Australian maximum temperature data. Specifically, we investigate the following six max-stable models: the Smith model (Smith, 1990), the Schlather models (Schlather, 2002) with either a Whittle–Matérn, Cauchy, powered exponential or Bessel correlation function, and the Brown–Resnick model (Brown and Resnick, 1977, Kabluchko et al., 2009).

The Smith model is specified as

$$\max_{i \geq 1} \zeta_i \varphi(x - U_i; \Sigma),$$

where $\varphi(\cdot; \Sigma)$ is the d -variate probability density function of a centred Gaussian random vector with covariance matrix Σ . $\{(\zeta_i, U_i) : i \in \mathbb{N}\}$ are points of a Poisson process on $(0, \infty) \times \mathbb{R}^d$ with intensity $d\Lambda(\zeta, u) = \zeta^{-2} d\zeta du$.

Following the notation in Ribatet (2013), the other five max-stable models considered here are defined as

$$\max_{i \geq 1} \zeta_i Y_i(x), \quad x \in \mathcal{X} \subseteq \mathbb{R}^d,$$

where $\{\zeta_i : i \in \mathbb{N}\}$ are Poisson process points on $(0, \infty)$ with intensity $d\Lambda(\zeta) = \zeta^{-2} d\zeta$, and $Y_i(x)$ are independent realisations of a non-negative stochastic process $Y(x)$ with $E[Y(x)] = 1 \forall x$. The different max-stable models differ primarily in their specification of $Y(x)$.

The Schlather models are specified as

$$Y_i(x) = \sqrt{2\pi} \max\{0, \epsilon_i(x)\},$$

where ϵ_i are independent copies of a standard Gaussian process with correlation function $\rho(h)$ as defined in Table 4.1 for the four particular Schlather models considered. We defined h to be the two-norm distance measure between locations in \mathcal{X} .

	$\rho(h)$
Whittle–Matérn	$\frac{2^{1-\nu}}{\Gamma(\nu)} \left(\frac{h}{c_2}\right)^\nu K_\nu\left(\frac{h}{c_2}\right), \nu > 0$
Cauchy	$\left[1 + \left(\frac{h}{c_2}\right)^2\right]^{-\nu}, \nu > 0$
Powered-exponential	$\exp\left[-\left(\frac{h}{c_2}\right)^\nu\right], 0 < \nu \leq 2$
Bessel	$\left(\frac{2c_2}{h}\right)^\nu \Gamma(\nu + 1) J_\nu\left(\frac{h}{c_2}\right), \nu \geq \frac{d-2}{2}$

Table 4.1: Correlation function $\rho(h)$ specification for the four Schlather models considered here. $K_\nu(\cdot)$ is the modified Bessel function of order ν , $\Gamma(\cdot)$ is the gamma function and $J_\nu(\cdot)$ is the Bessel function of order ν . All c_2 parameters are positive.

The Brown–Resnick model has

$$Y_i(x) = \exp \left(\epsilon_i(x) - \frac{\sigma^2(x)}{2} \right), \quad (4.1)$$

where ϵ_i are independent copies of a centred Gaussian process with stationary increments and $\text{Var}[\epsilon_i(x)] = \sigma^2(x) \quad \forall x \in \mathcal{X}$, with semivariogram $\gamma(h) = \left(\frac{h}{c_2}\right)^\nu$ (h being the distance between two locations in \mathcal{X} , $c_2 > 0$ and $0 < \nu \leq 2$).

The Schlather models and Brown–Resnick model contain two parameters in their respective correlation functions and semivariogram; the range (c_2) and smoothness (ν) parameters. The Smith model is parametrised by the unique entries of the covariance matrix Σ . The work presented here assumed there was no nugget effect, i.e. no discontinuity in the correlation or semivariogram at $h = 0$. As such, the nugget parameter c_0 was set to 0 (and conversely, the sill parameter c_1 was set to 1 as the sill and nugget parameters have to sum to 1 to ensure that the correlation at the origin, as defined in (4.2), is 1). If a nugget effect is thought to be appropriate, then the correlation functions are straightforwardly modified as follows:

$$\rho_{mod}(h) = \begin{cases} c_0 + c_1, & h = 0 \\ c_1 \rho(h), & h > 0 \end{cases} \quad (4.2)$$

where c_0 and c_1 are positive-valued parameters between 0 and 1 such that $c_0 + c_1 = 1$.

Semi-parametric estimators for simple max-stable models in \mathbb{R} and \mathbb{R}^2 were proposed by de Haan and Ferreira (2006). An alternative estimation method was provided by Padoan et al. (2010) using the well established result that while for $H > 2$, the H dimensional distribution of a max-stable process,

$$p(Z(x_1) \leq z_1, Z(x_2) \leq z_2, \dots, Z(x_H) \leq z_H),$$

often is not available analytically, a class of bivariate spatial models is available under certain reasonable conditions. The composite likelihood, formed from the second-order partial derivatives of the bivariate cumulative distribution function of the spatial model, can then be maximised to obtain the maximum composite likelihood estimates (Padoan et al., 2010).

For the Schlather models, the bivariate cumulative distribution function is given by

$$p(Z(x_1) \leq z_1, Z(x_2) \leq z_2) = \exp \left[-\frac{1}{2} \left(\frac{1}{z_1} + \frac{1}{z_2} \right) \left(1 + \sqrt{1 - \frac{2[1 + \rho(x_1 - x_2)]z_1 z_2}{(z_1 + z_2)^2}} \right) \right].$$

Under the Smith and Brown–Resnick models, the bivariate cumulative distribution function is given by

$$p(Z(x_1) \leq z_1, Z(x_2) \leq z_2) = \exp \left[-\frac{1}{z_1} \Phi \left(\frac{a}{2} + \frac{1}{a} \log \left(\frac{z_2}{z_1} \right) \right) - \frac{1}{z_2} \Phi \left(\frac{a}{2} + \frac{1}{a} \log \left(\frac{z_1}{z_2} \right) \right) \right],$$

where $\Phi(\cdot)$ is the standard normal cumulative distribution function, and $a = (x_1 - x_2)' \Sigma^{-1} (x_1 - x_2)$ for the Smith model and $a = \sqrt{\text{Var}[\epsilon(x_1 - x_2)]}$ with $\epsilon(x)$ as in equation (4.1) for the Brown–Resnick model.

More recently, approximate Bayesian computation (ABC) methods have been proposed as an alternative approach to obtain approximate estimates of the parameter posterior distributions (Erhardt and Smith, 2012). The ABC methods rely on simulations from the max-stable models rather than approximations to the model likelihood in order to perform the required statistical inference. The above max-stable models are readily simulated using the R package **SpatialExtremes** (Ribatet et al., 2013). Only model simulations which are ‘similar’ to the observed data are used in the inference and this measure of similarity is typically a function of informative summary statistics. Empirical estimates of the madogram, pairwise extremal coefficients and tripletwise extremal coefficients were used here along with the composite likelihood estimates of the model parameters.

The madogram is an analogue of the variogram, popular in geostatistics, and one of the summary statistics considered. The theoretical variogram is not always defined for a max-stable process (due to the possibility of non-finite mean and variance), instead the madogram, which is based on the mean absolute difference, was used. Given a stationary, isotropic max-stable random field $Z(x)$ with GEV margins having a shape parameter $\xi < 1$, the madogram is defined as

$$m(h) = \frac{1}{2} E [|Z(x+h) - Z(x)|].$$

The pairwise extremal coefficient $\theta(x_1, x_2)$ (Schlather and Tawn, 2003) is another measure of spatial dependence between pairs of observations (assumed observed at locations x_1 and x_2) and another summary statistic considered. An extremal coefficient value of 1 indicates complete dependence between the observations, and 2 for complete independence. The pairwise extremal coefficient is defined generally by the equality

$$p(Z(x_1) \leq z, Z(x_2) \leq z) = \exp \left(-\frac{\theta(x_1, x_2)}{z} \right).$$

The tripletwise extremal coefficient $\theta(x_1, x_2, x_3)$ for an observation triplet (observed at x_1, x_2 and x_3) is similarly defined from the relationship

$$p(Z(x_1) \leq z, Z(x_2) \leq z, Z(x_3) \leq z) = \exp \left(-\frac{\theta(x_1, x_2, x_3)}{z} \right).$$

Note that the unit Fréchet margins do not have a finite mean, precluding the computation of the madogram. Instead, following Cooley et al. (2006), the madogram and pairwise extremal coefficients are estimated for a transformation of $Z(x)$ with unit Fréchet margins, denoted by $\tilde{Z}(x)$ with identical GEV margins. Denoting the parameters for these GEV margins by $(\bar{\mu}, \bar{\sigma}, \bar{\xi})$, provided $\bar{\xi} < 1$, it is then possible to estimate the madogram and pairwise extremal coefficients. For this application, $\bar{\mu}$, $\bar{\sigma}$ and $\bar{\xi}$ are computed as the average of the respective GEV parameters estimated at the 26 different locations.

For $\tilde{z}_i(x)$ the i th realisation of $\tilde{Z}(x)$ at location x , an empirical estimate of the madogram is given by

$$\hat{m}(h) = \frac{1}{2n} \sum_{i=1}^n |\tilde{z}_i(x+h) - \tilde{z}_i(x)|.$$

An empirical estimate for the pairwise extremal coefficients can then be calculated as

$$\hat{\theta}(x_1, x_2) = u \left(\bar{\mu} + \frac{\hat{m}(h)}{\Gamma(1 - \bar{\xi})} \right),$$

where $u(x) = (1 + \bar{\xi} \frac{x - \bar{\mu}}{\bar{\sigma}})_+^{\frac{1}{\bar{\xi}}}$ and a_+ is equal to a if $a > 0$ and 0 otherwise (Cooley et al., 2006).

An empirical estimate for the tripletwise extremal coefficients is given by

$$\hat{\theta}(x_1, x_2, x_3) = \frac{n}{\sum_{i=1}^n 1 / \max\{z_i(x_1), z_i(x_2), z_i(x_3)\}}.$$

In contrast with the other empirical estimates considered here, this empirical estimate for the tripletwise extremal coefficients is defined for $Z(x)$ with unit Fréchet margins with the corresponding i th realisation at location x denoted by $z_i(x)$ (Erhardt and Smith, 2012).

4.4 Approximate Bayesian computation for model selection

Approximate Bayesian computation (ABC) methods rely on model simulation to obtain approximate Bayesian inference and are particularly useful in circumventing analytically or computationally intractable likelihood evaluations. ABC methods were originally developed for statistical inference of genetic data where algorithms and software for model simulation were readily available. The methods have since been expanded to various other application areas, including spatial extremes analysis (Erhardt and Sisson, 2016), because of their intuitive premise and flexible framework (Beaumont, 2010).

ABC methods generate model simulations using parameter draws from a distribution (or sequence of distributions) and compare the discrepancies between the simulated and

observed data through a selection of summary statistics as direct comparison would be computationally exhaustive. Only parameter draws which produce simulations sufficiently similar to the observed data would be accepted as being draws from the desired (approximate) posterior distribution. The initial ABC algorithm proposed uses a rejection sampling scheme where the parameters are always drawn from the prior distribution. This method is known as rejection ABC (Beaumont et al., 2002, Pritchard et al., 1999). Markov chain Monte Carlo ABC (MCMC ABC) (Marjoram et al., 2003) and, later, sequential Monte Carlo ABC (SMC ABC) (Beaumont et al., 2009, Drovandi and Pettitt, 2011a, Sisson et al., 2007, 2009, Toni et al., 2009) were proposed to alleviate the computational burden of rejection ABC using more efficient parameter proposal distributions to explore the parameter space.

The selection of summary statistics was typically user-specified based on what was believed to be most informative about the model. Fearnhead and Prangle (2012) proposed a ‘semi-automatic’ version of this summary statistic selection process by applying a dimension reduction method (the simplest being stepwise regression) on a larger pool of candidate (or regression) summary statistics to estimate the optimal ABC summary statistics for specific loss functions. In particular, Fearnhead and Prangle (2012) showed that the choice of the quadratic error loss function yields the posterior mean as the optimal ABC summary statistic for parameter estimation. Thus, the dimension reduction method is then used to provide a way of approximating the posterior mean such that it could be used in the ABC algorithm. They later expanded the approach to model selection (Prangle et al., 2014) after it was shown that the posterior model probabilities form sufficient statistics for model selection (Marin et al., 2014).

There have been few applications of ABC methods involving extreme data models. Erhardt and Sisson (2016) provided an introduction to the use of ABC methods in modelling extremes. The first application of ABC methods to extremes applications was by Bortot et al. (2007) where an MCMC ABC algorithm was used for a stereological extremes application. Subsequent ABC work has focused on spatial extremes applications (Barthelmé et al., 2015, Erhardt and Smith, 2012, Hainy et al., 2016, Prangle, 2016, Ruli et al., 2016). Prangle (2016), Barthelmé et al. (2015) and Ruli et al. (2016) used spatial extremes applications to illustrate the performance of their proposed ABC methods (Lazy ABC, parallel EP-ABC, ABC-CS) for parameter estimation acknowledging that spatial extremes applications of ABC methods are computationally demanding. A different perspective of using ABC methods for spatial extremes applications was provided by Hainy et al. (2016) where the optimal design for estimating the spatial dependence structure of extremes. None of the previous work mentioned investigated model selection for spatial extremes applications using ABC. This is the focus of the work presented here.

The full generic algorithm specification for the ABC method used here for model selection is detailed in Lee et al. (2015). Briefly, the method has two steps: the

Fearnhead-Prangle (FP) step and the ABC step (referred to as the SMC step in Lee et al. (2015)) and is outlined as follows:

1. FP step

Inputs: number of model simulations M , K candidate models, parameter prior distributions $\pi_k(\theta)$ ($k = 1, \dots, K$), choice of regression summary statistics

- (a) Assuming uniform prior for the model indicator k , draw $\frac{M}{K}$ parameter sets from each candidate model's prior distribution.
- (b) Simulate from the respective candidate models using each of the M parameter sets drawn from the K candidate models, and compute the regression summary statistics for each simulated data set.
- (c) Perform a stepwise multinomial logistic regression using all M model simulations using the model indicator as the outcome variable and the regression summary statistics as covariates. Compute the misclassification matrix using the estimated logistic regression coefficients and a new collection of M simulated data sets generated using a different set of parameter draws from the priors.
- (d) Perform stepwise linear regressions for each model parameter using the respective $\frac{M}{K}$ parameter draws as the outcome variable and the regression summary statistics as covariates.

Outputs: regression coefficient estimates from the logistic and linear regressions, misclassification matrix

2. ABC step

Inputs: regression coefficient estimates from FP step, initial tolerance ϵ_1 , number of particles N , SMC replenishment tuning parameters α and c , observed data \mathbf{y} , discrepancy function $\rho(\cdot, \cdot)$, MCMC kernels for model k 's parameters $q_k(\cdot)$

($k = 1, \dots, K$), stopping criterion (either final tolerance ϵ_T or final acceptance probability in MCMC move step p_T)

- (a) Perform rejection ABC to get the initial particle set $\{k_i, \theta_i, \rho_i = \rho(\tilde{\mathbf{y}}_i, \mathbf{y}); \rho_i \leq \epsilon_1\}_{i=1}^N$ where $\tilde{\mathbf{y}}_i$ is the simulated data generated from θ_i . Compute the acceptance probability p_1 (as the proportion of simulations accepted) and $R_1 = \lceil \frac{\log(c)}{\log(1-p_1)} \rceil$. Set $t = 1$.
- (b) Denote ϵ_M to be the largest discrepancy value in the current particle set. If $\epsilon_M \leq \epsilon_T$ or $p_t \leq p_T$, terminate algorithm.
- (c) Drop the $N_\alpha = \alpha N$ particles with the largest discrepancy values from the particle set. Set ϵ_t to be the largest discrepancy value of the remaining $N - N_\alpha$ particles.
- (d) Compute the parameters in $q_k(\cdot)$ using the remaining particles from model k .
- (e) Resample from the particle set until a full set of N particles is recovered with the new tolerance value ϵ_t . Each newly resampled particle is perturbed R_t

times where the Metropolis-Hastings (MH) ratio for acceptance of a move from (k, θ) to (k^*, θ^*) is

$$\frac{p(k^*)}{p(k)} \frac{\pi_{k^*}(\theta^*)}{\pi_k(\theta)} \mathbb{1}(\rho(\tilde{\mathbf{y}}^*, \mathbf{y}) \leq \epsilon_t) \frac{q_k(\theta)}{q_{k^*}(\theta^*)} \frac{\pi_{k^*,k}}{\pi_{k,k^*}}$$

where $\mathbb{1}(\cdot)$ is the indicator function. The model prior and model proposal ratios simplify to one as the model prior is assumed to be uniform ($p(k) = \frac{1}{K}$ for $k = 1, \dots, K$) and the model move probabilities (π_{k_1, k_2} is the probability of moving from model k_1 to k_2) are assumed to be equally likely for all model pair combinations here.

- (f) Increase t by 1, compute the acceptance probability $p_t = \frac{a_t}{R_{t-1} N_\alpha}$ (where a_t is the number of accepted proposals in the t -th iteration) and $R_t = \lceil \frac{\log(c)}{\log(1-p_t)} \rceil$. Return to step 2(b).

Outputs: final particle set $\{k_i, \theta_i, \rho_i; \rho_i \leq \epsilon_T\}_{i=1}^N$ or $\{k_i, \theta_i, \rho_i; p_t \leq p_T\}_{i=1}^N$

The FP step performs the summary statistic automatic process introduced by Fearnhead and Prangle (2012) for both model selection (using stepwise logistic regression to estimate the posterior model probabilities) and parameter estimation (using stepwise linear regression to estimate the parameters' posterior means from a large number (M) of model simulations from the priors).

The performance of the final summary statistic set selected in the FP step for model selection was summarised using a misclassification matrix (Lee et al., 2015). The (J, K) -th element of the misclassification matrix corresponds to the proportion of model K simulations classified as model J using the largest estimated posterior model probability obtained from the logistic regression coefficient estimates as the classification rule. For the six max-stable models considered here, model 1 refers to the Whittle-Matérn model, model 2 to the Cauchy model, model 3 to the powered exponential model, model 4 to the Bessel model, model 5 to the Smith model and model 6 to the Brown-Resnick model.

The ABC step carries out ABC model selection and estimation using the regression summary statistics and coefficients estimated in the FP step to form the ABC summary statistics. The specific ABC algorithm used for the application here was the SMC ABC replenishment algorithm (Drovandi and Pettitt, 2011a). This SMC ABC algorithm dynamically determines the non-increasing sequence of tolerances given the specification of two tuning parameters: the proportion of particles to be dropped at each SMC iteration (α), and the theoretical probability of moving a particle during the resampling step ($1 - c$). The choice of α values is a balance between the quality of the SMC approximations and how rapidly the algorithm moves towards the target distribution. A large α value will generate an ϵ sequence that decreases quickly but the SMC approximations would be poor as it is only based on a small proportion of particles at each iteration, and conversely with a small α value. Small values of c is preferred as it encourages diversity in the particle set. Choice of these tuning parameters are generally

considered to be problem-specific although Drovandi and Pettitt (2011a) suggested values of 0.5 and 0.01 for α and c , respectively, to be sensible general choices.

The performance of the specified ABC algorithm (referred to as ABMC in Lee et al. (2015)) in identifying the correct model from the six candidate max-stable models was assessed through simulated examples. The model selection result obtained using the South Australian data set was also validated by running the ABMC algorithm on a posterior simulation from the most preferred max-stable model. In both cases, the algorithm performed well in recovering the model used to generate the ‘observed’ data. The details and results of these simulated examples are provided in the Supplementary Materials (Section B.3).

4.5 Application

4.5.1 Implementation details

The max-stable models defined in Section 4.3 are conditional on fixed margins. A common choice is to set the margins to be unit Fréchet margins. So, for real data, the marginal GEV parameters at each location are first estimated in order to transform the data to have unit Fréchet margins using the fact that if $Y(x) \sim \text{GEV}(\mu, \sigma, \xi)$, i.e. $p(Y(x) \leq y) = \exp \left\{ - \left[1 + \xi \frac{y - \mu}{\sigma} \right]^{\frac{1}{\xi}} \right\}$, then

$$Z(x) = \left(1 + \xi \frac{Y(x) - \mu}{\sigma} \right)^{\frac{1}{\xi}},$$

is unit Fréchet, i.e. $p(Z(x) \leq z) = \exp \left\{ -\frac{1}{z} \right\}$, $z > 0$. These marginal GEV parameter estimates were obtained from maximum likelihood estimation.

There is an abundance of summary statistics available for ABC inference for models of spatial extremes. The advantage of using the FP step described in Section 4.4 is that summary statistics that best explain a model or its parameters are weighted by the coefficients at the logistic and linear regression stages of the algorithm and, conveniently, superfluous summary statistics are eliminated through the stepwise procedure. The summary statistics considered here were the madogram, pairwise and tripletwise extremal coefficient and maximum composite likelihood estimates of model parameters as defined in Section 4.3. Other candidates, such as the F-madogram, λ -madogram or other metrics to capture the spatial structure can easily be incorporated but were not considered further for this analysis.

As an aim of the present analysis is to include as little pre-data analysis as possible when selecting the summary statistics, we therefore do not consider theoretical representations of the madogram or extremal coefficients. Instead, the empirical estimates of these summary statistics are computed and binned into sections from small

to large spatial lags. The mean and standard deviation for each bin are used as regression summary statistics.

A practical issue in computing the tripletwise extremal coefficients is determining how similar one location triple is to another among the $\binom{D}{3}$ triples (where D is the number of locations). Erhardt and Smith (2012) proposed clustering the $\binom{D}{3}$ triples into G groups or clusters (with $G \ll \binom{D}{3}$) based on the geometry of the location triples rather than the estimates of the tripletwise extremal coefficients as the candidate models assume that the field is isotropic and stationary. This also allows the same clustering to be used for all candidate models.

For the particular application presented here, we found that $G = 100$ groups suggested by Erhardt and Smith (2012) to be too large as there was great similarity among the 100 clusters suggested by the algorithm (noting that it was difficult to get reproducible cluster membership with 100 clusters). Instead, smaller values of G were tested and a G value of 10 was chosen for our investigation as the automatic clustering algorithm (k -means++) tended to have little variation in the assignment of members for repeated runs for this smaller value of G . The tripletwise extremal coefficient summary statistics are then taken to be the average $\hat{\theta}(x_1, x_2, x_3)$ for each group.

The vague priors used were $U(0, 5)$ for all the range parameters of the Schlather and Brown–Resnick models, $U(0, 5)$ for the smoothness parameters of the Cauchy and Bessel models, $U(0, 10)$ for the Whittle–Matérn model, $U(0, 2)$ for the powered exponential smoothness parameter, and $U(0.05, 2)$ for the smoothness parameter in the Brown–Resnick model. The smaller upper bounds for the smoothness parameter priors of the powered exponential and Brown–Resnick models are required as the parameter is only defined for values less than 2 in these two models. Each of the Smith model parameters was assigned a $U(0, 5)$ prior. These priors are flat, vague priors which produced prior predictive model simulations with spatial dependence structures similar to the observed data (Section B.1) as there is no additional information known about likely parameter values for this particular setting prior to the analysis.

The SMC ABC replenishment algorithm was implemented with $N = 2,000$ particles and stopped when the particle acceptance probability was less than 10^{-3} , i.e. $p_T = 10^{-3}$. The tuning parameters were set to 0.5 for α and 0.01 for c (as in Drovandi and Pettitt (2011a) and Lee et al. (2015)).

4.5.2 Results

The misclassification matrix (as defined in Section 4.4) obtained for the South Australian weather station spatial locations using the ABC method and priors as specified in the previous section is

	$K=1$	$K=2$	$K=3$	$K=4$	$K=5$	$K=6$
$P(\text{Whittle-Matérn} K)$	0.29	0.06	0.02	0.24	0.005	0.02
$P(\text{Cauchy} K)$	0.16	0.63	0.18	0.15	0.03	0.02
$P(\text{Powered Exponential} K)$	0.09	0.13	0.63	0.02	0.001	0.06
$P(\text{Bessel} K)$	0.39	0.06	0.02	0.50	0.03	0.04
$P(\text{Smith} K)$	0.03	0.07	0.02	0.07	0.90	0.06
$P(\text{Brown-Resnick} K)$	0.04	0.05	0.12	0.02	0.03	0.79

The misclassification matrix shows good identification for the Smith (column $K = 5$) and Brown-Resnick (column $K = 6$) models with the corresponding diagonal entries (0.90 and 0.79) dominating the off-diagonal column entries. Identification of the Schlather models ($K \in \{1, 2, 3, 4\}$) is adequate but weaker than the non-Schlather models ($K \in \{5, 6\}$). The diagonal entries of the Schlather models are still the largest entries in the respective columns except for the Whittle-Matérn model simulations (column $K = 1$). In fact, there is some lack of identification between Whittle-Matérn model simulations and Bessel model simulations for the set of vague priors used.

For the actual South Australian data, the progression of model probabilities across the SMC iterations is shown in Figure 4.2. Simultaneous 95% intervals for the model probability estimates were obtained from the fact that the model indicator is a multinomial variable (Sison and Glaz, 1995). While there is an initial preference for the powered exponential model, the Brown-Resnick model was more strongly preferred for smaller discrepancy values (i.e. later SMC iterations), followed closely by the Whittle-Matérn and powered exponential models, as the particle set preference stabilised. The other three max-stable models considered (Cauchy, Bessel and Smith models) did not have any posterior support in the final particle set.

The estimated approximate posterior distribution for the best-fitting model's parameters are in Figure 4.3 and Table 4.2. Both model parameters appear well identified with a unimodal posterior well within the original prior ranges ($(0, 5)$ for c_2 and $(0.05, 2)$ for ν). The estimated posterior mean for the range parameter (c_2) was 3.77 (95% credible interval (CrI): $[3.20, 4.28]$) and 0.855 (95% CrI: $[0.753, 0.947]$) for the smoothness parameter (ν). The parameter inference for the other two candidate models with non-negligible support from the final particle set (the powered exponential and Whittle-Matérn models) are in Appendix B.2.

<i>Parameter</i>	<i>Mean</i>	<i>SD</i>	<i>2.5% quantile</i>	<i>Median</i>	<i>97.5% quantile</i>
c_2	3.77	0.266	3.20	3.76	4.28
ν	0.855	0.0499	0.753	0.856	0.947

Table 4.2: Parameter estimates of the fitted Brown-Resnick model for the South Australian data set.

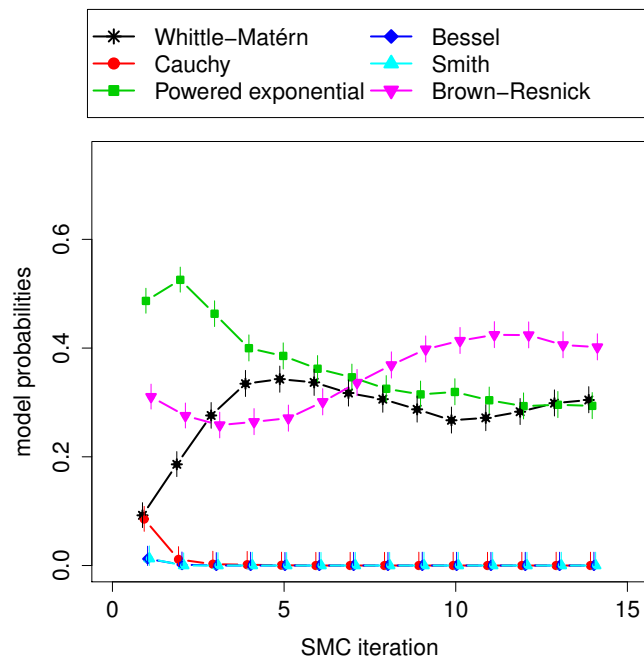


Figure 4.2: Progression of estimated model probabilities across SMC iterations.

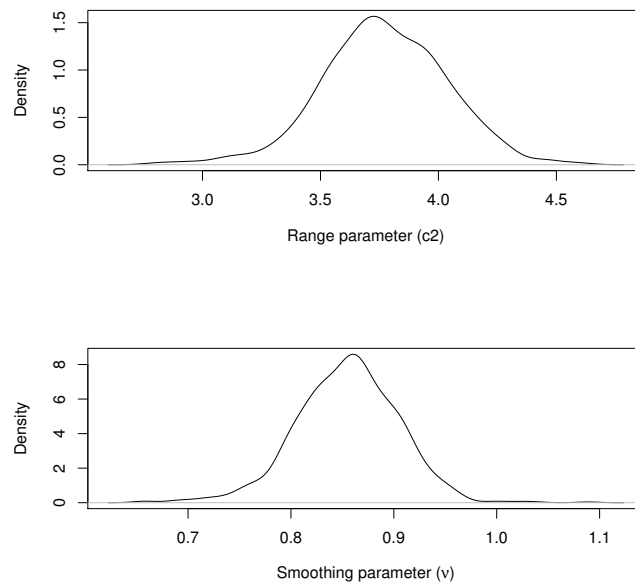


Figure 4.3: Posterior parameter estimates for the fitted Brown-Resnick model.

The pairwise extremal coefficients estimated from Brown-Resnick model simulations using parameter draws from the estimated posterior distributions are shown in Figure 4.4 along with the corresponding empirical estimates from the observed data. Model simulations obtained using the estimated posteriors were able to capture the spatial dependence of the observed data well.

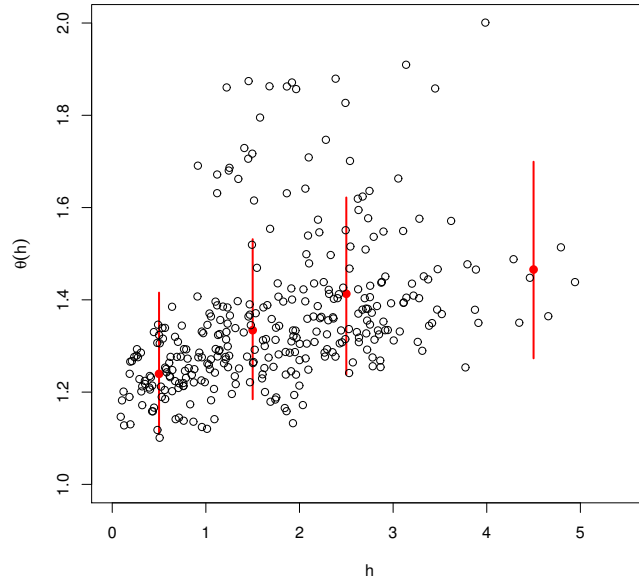


Figure 4.4: Empirical pairwise extremal coefficient estimates using ABC posterior simulations from the fitted Brown–Resnick model (binned means and 95% credible intervals in red), and observed data (black \circ).

4.6 Discussion

The research presented here expanded the use of ABC for spatial extremes applications to include model selection problems. Specifically, it was shown that the spatial dependence structure of the maximum temperature data collected around the state of South Australia is best captured by a Brown–Resnick model out of a selection of six max-stable models. It should be emphasised that the South Australian result presented here is merely a case study of the application of ABC to model selection problems for spatial extremes and is not meant to be directly used to inform decision-making. As such, the max-stable models used are relatively simple and do not capture the intricacies of the particular application. However, it could be argued that such results, along with the simulated examples in the Supplementary Materials (Section B.3), confirm that the method is a viable research avenue.

We would like to highlight some extensions to the straightforward max-stable models used that would provide a more realistic representation of the spatial structure of the maximum temperature for further research. As the temperature recordings were of air temperature, the work here has ignored any effect that might be attributable to the fact that part of the region in Figure 4.1 is actually a large body of water that would affect the local temperature near the coast. As such, it might be more appropriate to analyse just the land mass of the region either through determining a transformation of the land mass to a regular geometry (while keeping the distance measure used positive-definite) using complex spatial smoothers (Sangalli et al., 2013, Wood et al., 2008), or a form of

spatially sparse autoregressive lattice model (Pettitt et al., 2002) to block out the regions of water.

Additional max-stable models (the extremal- t models (Opitz, 2013) in particular as generalisations of the Schlather models) could be considered in the future provided the chosen set of regression summary statistics is able to distinguish between the models sufficiently well. This could be a challenge given that the Schlather models are special cases of the extremal- t models and it could prove difficult to distinguish between model simulations from these two model groups.

There is recent work on efficient exact simulation methods for max-stable models (Dieker and Mikosch, 2015, Dombry et al., 2016) which would also be of interest to consider in place of the approximate simulation methods for max-stable models used here (Ribatet et al., 2013) in order to minimise one source of approximation in the method. Preliminary comparisons of the two simulation methods did not yield substantial differences in the spatial dependence generated under the same model and parameter sets (as measured by the pairwise extremal coefficient estimates). However, there appears to be some difficulty in recovering the correct theoretical marginal distributions under both simulation methods (Section B.4). This issue should be investigated further in subsequent work.

The max-stable formulation used here relies on the assumption of stationary, unit Fréchet marginal distributions, which necessitates either the appropriate transformation of the data prior to model fitting or increasing the number of parameters to be estimated drastically (an addition of 3 times the number of observed locations). Further, additional modelling of the marginal GEV parameters is required if the fitted max-stable model is used to interpolate to unobserved locations in order to recover values on the original measurement scale. This is typically done by smoothing the GEV parameters over the spatial region of interest. For example, Erhardt and Smith (2012) applied Kriging and Ribatet et al. (2013) facilitates the use of p-splines and GEV response surface modelling. The shape parameter ξ is generally too complex and variable to be smoothed, and is instead set to a constant value (Erhardt and Smith, 2012, Ribatet, 2013). Investigations of the appropriate modelling of the marginal GEV parameters and quantification of the corresponding uncertainty on model results are beyond the scope of this study but would be of interest in further work.

The stationarity assumption of the marginal distributions for max-stable models could be relaxed through more sophisticated functional specification of the marginal model than the unit Fréchet margins used here (Sang and Gelfand, 2010). This would naturally involve a more sophisticated simulation process and substantially more parameters to be estimated for each candidate model. There are also other models for spatial extremes that could be considered, such as those based on latent variable models or copulas (Davison et al., 2012), using the method presented here but were not considered in this first instance.

In addition, there are still numerous improvement opportunities for the ABC model selection algorithm and ABC algorithms in general. Use of more sophisticated classification methods such as random forests (Pudlo et al., 2016) in the FP step could potentially provide improved performance at the expense of increased computation and less straightforward interpretations of the classification method’s direct outputs. Optimising the efficiency of the ABC algorithm is also an active research area. Such optimisations are particularly vital for applications involving computationally intensive model simulation such as some of the max-stable models considered here which could preclude more widespread adoption of the method. Alleviating the computational burden in both complex model simulation and the ABC algorithm would make ABC methods a more attractive alternative for such applications. Research which incorporates additional approximation to the standard ABC method, such as Lazy ABC (Prangle, 2016) and EP ABC (Barthelmé et al., 2015), to decrease the computational time required to obtain the approximate posterior for computationally expensive models, such as max-stable models, appear promising for model selection problems as well, as noted in Barthelmé et al. (2015) (where the approximate model evidence can be directly obtained from the EP ABC output and used for model selection).

Acknowledgements

The authors would like to acknowledge the instrumental role of Mathieu Ribatet’s Spatial Extremes R package (Ribatet et al., 2013) which was used to generate the max-stable model simulations required for the method. XJL, CCD and ANP are affiliated with the ARC Centre of Excellence for Mathematical & Statistical Frontiers (ACEMS) where CCD is an Associate Research Fellow and ANP is a chief investigator. XJL receives PhD scholarship funding from the Centre of Research Excellence in Reducing Healthcare Associated Infections (NHMRC Grant 1030103). CCD was supported by an Australian Research Council’s Discovery Early Career Researcher Award funding scheme DE160100741. ANP was supported by an Australian Research Council Discovery Project DP 110100159.

Part 2

Case studies in biostatistics

5 Parametric survival analysis of hospital ward MRSA incidence allowing for carryover effects from previous cases

Abstract

Objective: To investigate the temporal dependence of new multiresistant methicillin-resistant *Staphylococcus aureus* (mrMRSA) occurrences on prior cases in the same bed and mrMRSA cases detected within the beds ward-cubicle, i.e. a carryover effect, up to four weeks prior.

Design: New analysis of an existing data set (Kong et al., 2012) collected in a one year retrospective cohort study in a single tertiary hospital using data from the seven wards with the most new mrMRSA cases

Methods: Parametric survival models with multiplicative lagged covariates, ranging from none up to four weeks lag, were fitted to data from each ward-cubicle separately. The final model for each combination was selected based on AIC, BIC and likelihood-ratio tests. The parametric baseline hazards considered were the exponential and power law distributions.

Results: None of the twelve ward-cubicles considered was estimated to have a power law baseline hazard. Three ward-cubicles were estimated to have constant hazard of acquiring a new mrMRSA case over the study period. Four of the nine ward-cubicles were estimated to have carryover effects up to two weeks prior, two had carryover effects up three weeks prior, two had carryover effects up four weeks prior, and the remaining ward-cubicle had a carryover effect of up to one week prior.

Conclusions: There was notable heterogeneity in the temporal dependence estimated for the ward-cubicles investigated. This has potential implications for targeted infection control practices or interventions in ward-cubicles with a strong carryover effect.

Statement of Authorship for Chapter 5

This chapter has been written as a journal article. The authors listed below have certified that:

1. they meet the criteria for authorship in that they have participated in the conception, execution, or interpretation, of at least that part of the publication in their field of expertise;
2. they take public responsibility for their part of the publication, except for the responsible author who accepts overall responsibility for the publication;
3. there are no other authors of the publication according to these criteria;
4. potential conflicts of interest have been disclosed to (a) granting bodies, (b) the editor or publisher of journals or other publications, and (c) the head of the responsible academic unit, and
5. they agree to the use of the publication in the students thesis and its publication on the Australasian Research Online database consistent with any limitations set by publisher requirements.

In the case of this chapter, the reference for the associated publication is:

Lee, X. J., Ruggeri, F. and Pettitt, A. N. (2016). Parametric survival analysis of hospital ward MRSA incidence allowing for carryover effects from previous cases *BMJ Open*, under review.

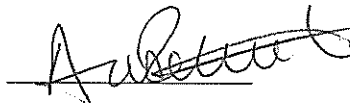
Contributor	Statement of contribution
X.J. Lee	developed methods, conducted analysis, wrote manuscript
Signature & Date:	
F. Ruggeri	developed methods, discussed results, reviewed manuscript
A.N. Pettitt	conceived study, developed methods, supervised research, discussed results, reviewed manuscript

Principal Supervisor Confirmation

I have sighted email or other correspondence from all Co-authors confirming their certifying authorship.

AN PETTITT

Name



Signature

13/2/17

Date

5.1 Introduction

Methicillin-resistant *Staphylococcus aureus* (MRSA) infections are a persistent challenge in hospitals worldwide. (Stefani et al., 2012) These infections are typically preceded by MRSA colonisation which can be detected through routine patient screening. Treatment options for both MRSA infections and colonisations are at risk of becoming ineffective with increasing resistance to commonly used treatments. (Edwards et al., 2014, Poovelikunnel et al., 2015) Combined with the typical paucity of healthcare resources, it is important to better understand the dynamics of MRSA occurrences in hospitals to be able to refine existing MRSA control strategies.

MRSA occurrences were found to exhibit heterogeneity across different wards within a hospital. (Kong et al., 2013, 2012) This heterogeneity also extends to smaller structural scales, specifically to the cubicle structures which are walled partitions within a hospital ward. (Kong et al., 2012) Each cubicle is comprised of a small number of beds. This study expands on the spatial heterogeneity finding (Kong et al., 2012) by analysing the difference in temporal behaviours of cubicle-level MRSA occurrences for the same data set.

Parametric survival models were used here due to the relatively coarse time scale of the data (weeks rather than days) and fitted separately to data from cubicles of the same size in a hospital ward (herein referred to as ward-cubicle). The parametric survival function provides a straightforward means of interpolating and extrapolating the underlying hazard, if needed. The relative sparsity of the cases observed at the individual cubicles coupled with the coarse time scale would likely yield results which are more difficult to interpret from the more commonly used non-parametric or semi-parametric survival models.

This study is also relevant to research identifying increased transmission risk for patients in beds with known prior MRSA patient occupancy (Mitchell et al., 2014) as we also investigate if there is a dependence between the previous occurrences of MRSA in a cubicle with new cases detected in a bed within the cubicle.

5.2 Method

5.2.1 Data

Weekly indicator data were collected for individual hospital beds on whether the bed was occupied by MRSA-positive patients over a 52 weeks period beginning from 1 January 2007. These patients MRSA categories are based on the broad classification of the MRSA strain they carry which is a non-multiresistant, multiresistant or epidemic (UK eMRSA-15) variant, and whether or not they were old or newly colonised patients for the particular MRSA strain. A patient is classified as new if the patient had no

previous clinical history of MRSA. An MRSA sample is denoted to be multiresistant MRSA (mrMRSA) if it exhibited resistance to methicillin and 3 or more non β -lactam antimicrobials. (Kong et al., 2012)

The study hospital is a tertiary hospital with 25 acute care wards. For this study where the data were analysed separately for each ward-cubicle combination, the analysis was restricted to the seven wards with the most new mrMRSA cases as this MRSA categorisation has the most clinical concern due to the limited treatment options. The covariates used aggregated new and old cases of mrMRSA as it is assumed that both groups could contribute to occurrences of new cases. The epidemic MRSA data were not analysed here. These seven wards accounted for 65.6% of new mrMRSA cases and 70.7% of all old mrMRSA cases observed in the hospital over the study period.

Figure 5.1 plots the mrMRSA cases over time for the beds in Ward A (the ward with the most mrMRSA cases). Corresponding plots for the other six wards are in the supplementary material (Section C.2). Further details about the data collection and hospital have been described elsewhere. (Kong, 2014)

5.2.2 Parametric survival models

Parametric survival models with covariates for recurrent events, assuming perfect recovery after an event, were used here due to the relatively coarse time scale of the data (weeks rather than days) and fitted separately to data from cubicles of the same size within a hospital ward (herein referred to as ward-cubicle). Technical details of the model are provided in the supplementary material (Section C.1).

The model likelihood is fully defined once the hazard function is specified in the form of a baseline hazard and covariates. For this study, the baseline hazard function was assumed to be either an exponential or power law hazard defined as:

$$h_0(t_a, t_b) = \begin{cases} M & \text{exponential} \\ M\beta(t_b - t_a)^{\beta-1} & \text{power law.} \end{cases}$$

where t_a and t_b are the start and end time (in weeks) of a particular recurrence respectively.

The exponential baseline hazard implies a fixed instantaneous chance, or hazard, of event occurrence over time excluding any covariate effect. The power law baseline hazard offers a more flexible behaviour with potentially increasing, decreasing or constant baseline hazard over time depending on β .

Four covariates were used which were (i) the proportion of beds in the same cubicle with an mrMRSA patient in the previous week, (ii) two weeks prior, (iii) three weeks prior and (iv) four weeks prior. The four week limit on the covariates was also used in previous analysis of the data set.(Kong et al., 2012) Each covariate has an associated

coefficient γ_i ($i = 1, 2, 3, 4$) where γ_i is associated with the i weeks prior covariate. These covariates represent the carryover effect of past mrMRSA patients in the cubicle on the hazard of a new mrMRSA case in a bed within the cubicle, arising from either direct or indirect contact, facilitated by vectors such as shared hospital equipment, staff or environmental contamination, between the patients in the same cubicle.

Shorthand for the models is used with either ‘e’ or ‘pl’ denoting the use of the exponential or power law baseline hazard form, respectively, followed by an integer between 0 and 4 to denote the maximum number of past weeks used as covariates. AIC, BIC and likelihood ratio tests were evaluated to select the statistically best-fitting model out of the ten candidate models for each ward-cubicle.

5.3 Results

The parameter estimates obtained for the best-fitting models for each of the ward-cubicle combinations are in Table 5.1. The model selection outputs are provided in the supplementary material (Section C.3).

Ward-cubicle (selected model)	Parameter	MLE	SE	p-value ¹
Ward A 2bed (e3)	M	0.0187	0.0062	–
	γ_1	−0.1208	0.7444	0.8711
	γ_2	0.4810	0.6040	0.4258
	γ_3	2.7201	0.7343	0.0002
Ward A 4bed (e2)	M	0.0070	0.0046	–
	γ_1	1.8002	1.1365	0.1132
	γ_2	5.2087	1.1117	2.8×10^{-3}
Ward B ² (e4)	M	0.0040	0.0027	–
	γ_1	−1.8949	3.9981	0.6355
	γ_2	5.5685	3.8201	0.1449
	γ_3	5.6879	3.0962	0.0662
Ward C 2bed (e3)	M	0.0212	0.0122	–
	γ_1	0.5396	1.3502	0.6894
	γ_2	1.8177	0.7470	0.0150
	γ_3	2.3743	0.7366	0.0013
Ward C 4bed (e2)	M	0.0110	0.0038	–
	γ_1	−3.8747	1.7919	0.0306
	γ_2	4.7616	1.1670	4.5×10^{-5}

Continued on next page

¹p-values for the M parameters were omitted as the hazard has to be positive.

²Ward B is an open plan ward with no cubicle structure

Table 5.1 – *Continued from previous page*

Ward-cubicle (selected model)	Parameter	MLE	SE	p-value
Ward D 2bed (e2)	M	0.0053	0.0057	–
	γ_1	10.4835	2.9340	0.0004
	γ_2	9.0972	2.9341	0.0019
Ward D 4bed (e4)	M	0.0033	0.0022	–
	γ_1	1.1732	2.9961	0.6954
	γ_2	14.4756	3.2234	7.1×10^{-6}
	γ_3	–8.1178	3.7252	0.0293
	γ_4	20.5886	4.9535	3.2×10^{-5}
Ward E 2bed (e0)	M	0.0243	0.0092	–
Ward E 4bed (e2)	M	0.0043	0.0022	–
	γ_1	11.2066	4.4984	0.0127
	γ_2	7.9611	2.2158	0.0003
Ward F 4bed (e1)	M	0.0030	0.0019	–
	γ_1	9.6865	2.4856	0.0001
Ward G 2bed (e0)	M	0.0087	0.0039	–
Ward G 4bed (e0)	M	0.0013	0.0014	–

Table 5.1: Parameter estimates for the best-fitting parametric survival model of the weekly MRSA data in the different ward-cubicles investigated.

Notes: (i) Hazard forms: e0 $h(t_a, t_b) = M$; e1 $h(t_a, t_b) = M \exp \{\gamma_1 X_1(t_a, t_b)\}$; e2 $h(t_a, t_b) = M \exp \{\gamma_1 X_1(t_a, t_b) + \gamma_2 X_2(t_a, t_b)\}$;

e3 $h(t_a, t_b) = M \exp \{\gamma_1 X_1(t_a, t_b) + \gamma_2 X_2(t_a, t_b) + \gamma_3 X_3(t_a, t_b)\}$;

e4 $h(t_a, t_b) = M \exp \{\gamma_1 X_1(t_a, t_b) + \gamma_2 X_2(t_a, t_b) + \gamma_3 X_3(t_a, t_b) + \gamma_4 X_4(t_a, t_b)\}$;

pl0 $h(t_a, t_b) = M\beta(t_b - t_a)^{\beta - 1}$.

(ii) MLE, maximum likelihood estimate; SE, standard error.

All 12 different ward-cubicle combinations investigated were estimated to have exponential baseline hazards. Hence, barring the effects of the covariates, the hazard of a new case occurring was constant over the data collection period. Three of these (Ward E 2-bed cubicles, Ward G 2-bed cubicles, and Ward G 4-bed cubicles) have no covariates inferring that the hazard of a new mrMRSA case occurring in these ward-cubicles was indeed constant over the study period, regardless of the presence of other mrMRSA patients in these ward-cubicles.

Of the remaining 9 ward-cubicle models with an exponential baseline hazard and statistically significant covariates, four (Ward A 4-bed cubicles, Ward C 4-bed cubicles, Ward D 2-bed cubicles, Ward E 4-bed cubicles) had covariates up to two weeks prior, two (Ward A 2-bed cubicles and Ward C 2-bed cubicles) with covariates up to three

weeks prior, two (Ward B and Ward D 4-bed cubicles) with the full four weeks of covariates, and one (Ward F 4-bed cubicles) with one week prior.

For the four fitted models with covariates up to two weeks prior, the estimated coefficients for the covariates were positive in three of these four models implying a synergistic effect between past mrMRSA patients from one week and two weeks prior in these ward-cubicles. The remaining fitted model with two weeks of covariates (Ward C 4-bed cubicles) had a negative effect (3.88 [1.79]) for mrMRSA patients one week prior but a positive effect (4.76 [1.17]) for mrMRSA patients two weeks prior.

The fitted model for Ward C 2-bed cubicles with three weeks of covariates estimated positive, statistically significant coefficients for the two week and three week coefficients (1.82 [0.75] and 2.37 [0.74] respectively). The other fitted model with three weeks of covariates (for Ward A 2-bed cubicles) only estimated a positive, statistically significant coefficient for the three week coefficient (2.72[0.73]).

A large, positive, statistically significant coefficient was estimated for the fourth week covariate in both models with four weeks of covariates (16.57 [4.90] for Ward B and 20.59 [4.95] for Ward D 4-bed cubicles). In the fitted model for Ward D 4-bed cubicles, the coefficients for the two and three week covariates were also statistically significant (14.48 [3.22] for the two week covariate and a -8.12 [3.73] for the three week covariate).

The fitted model for Ward F 4-bed cubicles had a statistically significant positive coefficient estimate (9.69 [2.22]) for the one week covariate effect.

5.4 Discussion

Overall, we see a heterogeneous pattern to the occurrences of new mrMRSA cases over time as well as in their dependence on previous mrMRSA cases in the same ward-cubicles in both duration and magnitude. Nine of the 12 final fitted models had statistically significant carryover effects although the inferred duration of this effect differs for the different ward-cubicles. The weekly time resolution of the data here might not be very informative about the MRSA acquisition process, however the use of parametric survival models provides some ability to interpolate the hazard between weeks, if needed, as opposed to the piecewise constant structure of Kaplan–Meier estimates.

The results obtained were broadly consistent with the earlier findings (Kong et al., 2012) which showed the most significant variation was detected at ward-cubicle level as well as identification of two weeks as the critical time period after a case detection for increased likelihood of a new case. The work presented here extends these findings by providing estimates of the period which which past mrMRSA cases might influence occurrences of new mrMRSA specific to the particular ward cubicles. This study provides a more targeted estimate of the carryover effect than earlier work (Kong et al.,

2013, 2012) where time dependency was determined assuming the temporal dynamics were identical for all ward-cubicles in the hospital. This work also provides a means of evaluating the efficacy of infection control policies for particular ward (and/or ward cubicles) in order to determine more specific areas for improvement rather than instigating a hospital-wide effort to improve infection control which is a costly endeavour with potentially a large wastage.

The method here provides an alternative view from the more commonly used statistical process control charts (Morton et al., 2013) (e.g. CUSUM, EWMA or Shewhart charts) which focus on detecting anomalous behaviour or outbreaks from a pre-defined baseline period. The work here instead focuses on ascertaining the potential permanence of MRSA acquisition in hospital wards and the effect of other MRSA-positive patients in the same cubicle under routine settings. The model described could also be used to evaluate other intervention strategies or changes in infection control policies which typically have fixed start and end dates. More generally, the parametric form of the survival model can be used in applications with a certain level of prior knowledge (in order to specify reasonable parametric forms) and where data collected are typically sparse. In contrast with previous analyses of the data set, (Kong et al., 2013, 2012) the ward-cubicle data were analysed separately for each ward cubicle rather than pooling observations together. While this decision precluded more sophisticated analysis, it is also practically motivated as most interventions do not apply to the entire hospitals, and if they do, heterogeneity in implementation between wards also typically exists.

The particular survival models considered here are relatively simple and this choice was motivated by the coarse time scale for which the data were collected. The two distributional forms of the baseline hazard used here were thought to be sufficiently flexible for the application, i.e., baseline hazards are assumed to be either constant, monotonically decreasing, or monotonically increasing. Extensions to the model structure are well-documented in the literature and should be considered if deemed necessary to the particular application. Examples of such extensions include consideration of other possible forms for the baseline hazard (e.g. log-Normal, Gompertz, and log-logistic distributions), imposition of additional grouping structure (e.g. adding a frailty term), and generalisation of the covariate parameters γ_i to be time-dependent.

Acknowledgements

The authors would like to thank Fiona Kong, PhD, for providing the de-identified data set which was aggregated with GIS (2014). XJL and ANP are affiliated with the ARC Centre of Excellence for Mathematical & Statistical Frontiers (ACEMS) where ANP is a chief investigator.

Competing interest

All authors report no conflicts of interest relevant to this article

Financial support

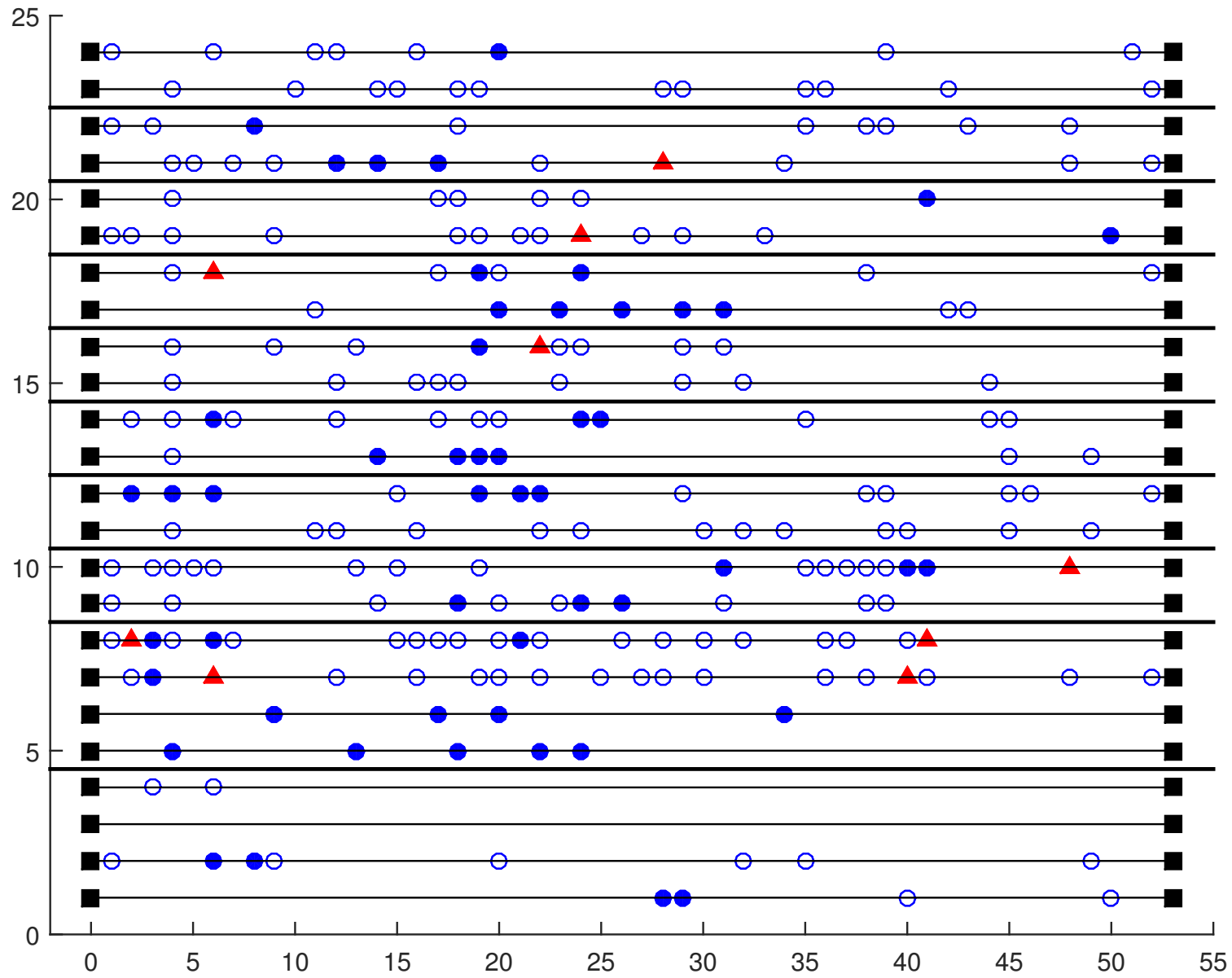
XJL receives PhD scholarship funding from the Centre of Research Excellence in Reducing Healthcare Associated Infections (NHMRC Grant 1030103). FR acknowledges the support obtained as Adjunct Professor from the Institute for Future Environments, Queensland University of Technology. ANP acknowledges the support obtained from the Australian Research Council through a Discovery Grant DP110100159.

Contributorship statement

All authors jointly developed the methods. XJL conducted the analysis and wrote the manuscript. FR provided feedback on the results and critically reviewed the manuscript. ANP conceived the study design, provided feedback on the results and critically reviewed the manuscript.

Data sharing statement

The data set used in this study was originally collected by Fiona Kong and first reported elsewhere (Kong et al., 2012). Data request should be directed to the corresponding author in Kong et al. (2012). The statistical codes used for the analysis presented are available from the corresponding author upon request (xj.lee@qut.edu.au).



6 Quantifying the impact of an MRSA outbreak on patient outcomes in a NICU

Abstract

Neonatal intensive care unit (NICU) patients are particularly susceptible to methicillin-resistant *Staphylococcus aureus* (MRSA) colonisation and infection due to their under-developed immune system. MRSA acquisition in NICU patients has been associated with adverse outcomes. As such, it is important to investigate factors facilitating MRSA transmission in a NICU, particularly during an outbreak. This study used a Cox proportional hazards model with time-dependent covariates to investigate the potential effects of patient bed movement, colonisation pressure (CP), and an out-of-ward indicator on MRSA acquisition during an outbreak. A separate Cox proportional hazards model was used to investigate the effects of these three covariates along with MRSA status on patients' length-of-stay (LOS). The out-of-ward indicator (hazard ratio [95% confidence interval]: 26.8 [5.2, 138.4]) and CP (1.11 [1.00, 1.22]) were associated with increased hazards of MRSA acquisition, although the out-of-ward indicator effect is most likely due to patient management rather than a risk factor. CP (0.97 [0.94, 1.00]) and MRSA acquisition (0.37 [0.16, 0.83]) were both associated with increased LOS. The study showed the importance of CP during an MRSA outbreak in a NICU, and supports findings from adult ICUs where MRSA acquisition is associated with increased LOS.

Statement of Authorship for Chapter 6

This chapter has been written as a journal article. The authors listed below have certified that:

1. they meet the criteria for authorship in that they have participated in the conception, execution, or interpretation, of at least that part of the publication in their field of expertise;
2. they take public responsibility for their part of the publication, except for the responsible author who accepts overall responsibility for the publication;
3. there are no other authors of the publication according to these criteria;
4. potential conflicts of interest have been disclosed to (a) granting bodies, (b) the editor or publisher of journals or other publications, and (c) the head of the responsible academic unit, and
5. they agree to the use of the publication in the students thesis and its publication on the Australasian Research Online database consistent with any limitations set by publisher requirements.

In the case of this chapter, the reference for the associated publication is:


Lee, X. J., Pettitt, A. N. and Givney, R. (2016). Quantifying impact of an MRSA outbreak in a NICU, in preparation.

Contributor	Statement of contribution
X.J. Lee	developed method, conducted analysis, wrote manuscript
Signature & Date:	
A.N. Pettitt	developed methods, supervised research, discussed methods and results, reviewed manuscript
R. Givney	conceived study, provided clinical feedback, discussed results, reviewed manuscript

Principal Supervisor Confirmation

I have sighted email or other correspondence from all Co-authors confirming their certifying authorship.

AN PETTITT
Name


Signature

13/2/17
Date

6.1 Introduction

Patients admitted to neonatal intensive care units (NICUs) are typically premature and critically ill neonates who are very vulnerable to infections. These infants are particularly susceptible to colonisation and infection by MRSA (Giuffré et al., 2013). MRSA acquisition (either colonisation or infection) is typically opportunistic, facilitated by the immunocompromised status of hospitalised patients, and have been associated with increased mortality, length-of-stay (LOS) and financial burden in infants (Song et al., 2010). Treatment options for MRSA are becoming increasingly limited with the rise of antibiotic resistance and there have also been reports of decolonisation failures for common treatments (Gould et al., 2012).

The data set used in the analysis presented here were collected in a two month period where a NICU experienced an MRSA outbreak. Ten patients were detected with MRSA during the outbreak. None of these patients died during the hospitalisation.

We were interested in determining if bed movement, LOS and colonisation pressure (Ajao et al., 2011, Bonten et al., 1998) are associated with the MRSA acquisition observed in the outbreak. It is also of interest to estimate the effect of MRSA acquisition and colonisation pressure on LOS, if any. We also note that due to the setting, the number of cases (MRSA patients) is small and any analysis should be interpreted with caution.

6.2 Data

The data set is the de-identified bed movements for the 164 patients admitted to the 41-bed neonatal intensive care unit (NICU) over the two month duration (61 days) where an MRSA outbreak was reported in the ward. Ten of the 164 patients were detected with MRSA (MRSA-positive) during this two months.

Four patients had a re-admission into the NICU, where two of the four patients were identified to be MRSA-positive upon re-admission. The other patients only had one admission. This information was used to form the out-of-ward indicator covariate.

The colonisation pressure covariate was defined to be the daily proportion of MRSA patients in the ward (expressed as a percentage of total patients in the NICU) (Bonten et al., 1998).

Some additional patient information for MRSA-positive patients was also provided. Specifically, the MRSA genetic cluster, patient sibling ID, and durations the patients were known to be MRSA-negative, MRSA status unclear and MRSA-positive were specified.

There were two MRSA clusters detected with nine out of the ten MRSA-positive patients assigned to Cluster 1 based on the multi-locus sequence typing carried out. Seven of the ten MRSA-positive patients had siblings who were also MRSA-positive in the NICU.

6.3 Method

Given the small sample size, an exploratory data analysis was first performed to assess if the data set is sufficiently informative for a more thorough analysis.

For the exploratory analysis, we focused on investigating if there were differences in the MRSA and MRSA-negative (control) patient data in terms of bed allocations and LOS. The number of bed allocations and LOS for MRSA-positive patients were measured up to the date of MRSA-positive status confirmation for the exploratory analysis as a crude approach to remove the potential effect of MRSA acquisition on these two measures. The effect of MRSA acquisition on LOS was quantified in the subsequent analysis presented. Poisson distributions were fitted to either the full data set, or separately for the MRSA and control patients for both variables separately. A likelihood ratio test was used to assess if the distributions were statistically different between the MRSA and control patients.

Following the findings of the exploratory analysis, separate Cox proportional hazard (PH) models with time-dependent covariates were used to model the two outcomes of interest (MRSA acquisition and LOS). Statistical analysis involving patient hospitalisation episodes should be aware of the potential for time-dependent bias. For example, in investigating the impact of hospital infection on patient survival, it is critical to account for the timing of events as patients who died shortly after admission are less likely to have acquired and been diagnosed with a hospital infection. Treating infection acquisition to be known on admission artificially creates a positive association between acquiring hospital infection and improved survival. The Cox PH model with time-dependent covariates provides an appropriate approach for analysis of such data.

The Cox PH model is characterised by its hazard function, which can be denoted mathematically as

$$\lambda(t) = \lambda_0(t) \exp \{ \beta^T Z(t) \}$$

where $\lambda_0(t)$ is the baseline hazard function, β is coefficient vector of length p and $Z(t)$ is the p covariates at time t . The Cox PH model estimation focuses on β using the partial likelihood approach in Cox (1972) and the baseline hazard $\lambda_0(t)$ is typically left unspecified as the interest is on the effects of the covariates on the hazard.

The key model assumption here is the proportionality hazards assumption. One approach to assess this assumption is to test if β is time-dependent (hence in violation of the proportional hazards assumption) using the scaled Schoenfeld residuals s^* as

$E(s_k^* + \hat{\beta}) \approx \beta(t_k)$ where $\hat{\beta}$ is the estimated time-static coefficients values using the partial likelihood approach and k is the the observed event index (Grambsch and Therneau, 1994). As such, a plot of $s_k^* + \hat{\beta}$ against the event times t_k provides a visual assessment of any potential violation of the proportional hazards assumption.

The scaled Schoenfeld residual for an observed event k (s_k^*) is the product of the Schoenfeld residual (s_k) and inverse of the covariance matrix of $Z(t)$ ($V(\beta, t)$), i.e., $s_k^* = V^{-1}(\beta, t_k)s_k$. The Schoenfeld residual and covariance matrix is calculated as

$$s_k = Z(t_k) - \frac{\sum_{i=1}^n Y_i(t) Z_i(t_k) \exp \{ \beta^T Z_i(t_k) \}}{\sum_{i=1}^n Y_i(t) Z_i(t_k) \exp \{ \beta^T Z_i(t_k) \}}$$

and

$$V_{j,l}(\beta, t) = \frac{\sum_{i=1}^n Y_i(t) r_i(t) [Z_{ij}(t) - \bar{Z}_j(t)] [Z_{il}(t) - \bar{Z}_l(t)]}{\sum_{i=1}^n Y_i(t) r_i(t)}$$

where i is the observation index (including censored observations), $Y_i(t)$ is the risk indicator for patient i at time t , $r_i(t) = \exp \{ \beta^T Z_i(t) \}$, $Z_{ij}(t)$ is the j -th covariate for patient i at time t and $\bar{Z}_j(t)$ is the running mean of the j -th covariate at time t .

A formal statistical test was also derived by assuming that the time-varying coefficient $\beta(t)$ will be of the form $\beta(t) = \beta + \theta g(t)$ where $g(t)$ is a predictable process and testing if $\theta = 0$ (Grambsch and Therneau, 1994). The asymptotic χ_p^2 test statistic was shown to be of the form

$$\left(\sum_k G_k \hat{s}_k \right)^T D^{-1} \left(\sum_k G_k \hat{s}_k \right)$$

where G_k is a diagonal matrix with $g_j(t_k)$ as the (j, j) -th diagonal entry, $\hat{s}_k = s_k(\hat{\beta})$ and

$$D = \sum_k G_k V(\hat{\beta}, t_k) G_k^T - \left(\sum_k G_k V(\hat{\beta}, t_k) \right) \left(\sum_k V(\hat{\beta}, t_k) \right)^{-1} \left(\sum_k G_k V(\hat{\beta}, t_k) \right)^T.$$

For each outcome, we first fitted the Cox PH model with all time-dependent covariates of interest. For both the MRSA acquisition and LOS outcomes, the following covariates were considered: (i) number of bed movements, (ii) colonisation pressure, and (iii) indicator if the patient was re-admitted into the NICU within the hospital stay (outward). The LOS analysis included an additional covariate of patient MRSA status indicator (MRSA). For the bed movement covariate, values greater than 5 were recoded to 5 as only two patients had more than 5 bed movements. The proportionality hazards assumption was assessed for the fitted models to ensure that this assumption was not violated.

The analysis was carried out using the R package `survival` (Therneau, 2015). Both the visual assessment and χ^2 test for testing the proportional hazards assumption are readily computed using `cox.zph()` function in the R package `survival`.

6.4 Results

The average number of bed allocations for MRSA-positive patients prior to their MRSA-positive status confirmation was 3.2 (standard deviation [SD]: 0.6; range: 2 - 5), while the average for the control patients was 2.5 allocations (SD: 0.1; range: 1 - 12). The likelihood ratio test provided no statistical evidence ($p = 0.19$) to prefer having two separate Poisson distributions to describe the number of bed allocations for MRSA and control patients over having a common Poisson distribution (with mean 2.5 and standard error [SE]: 0.1).

The average LOS was 26.0 [SD: 1.6] days for MRSA patients prior to their status confirmation and 11.8 [SD: 0.3] for the control patients. The two separate Poisson distributions for LOS was strongly preferred by likelihood ratio test ($p < 10^{-16}$) over a common Poisson distribution for the LOS (with mean 12.6 [SE: 0.3]).

However, results from the exploratory data analysis suffer from time-dependent bias (Beyersmann et al., 2009, van Walraven et al., 2004) as we used future information (MRSA status) to group the patients (as discussed in the Methods section). That said, the statistically significant finding for the LOS does motivate more thorough analysis in light of the small sample size. For our purpose, the Cox proportional hazard (PH) model with time-dependent covariates provides a more suitable method to avoid the time-dependent bias.

6.4.1 MRSA acquisition

The fitted model coefficients and hazard ratios (HRs) for the MRSA acquisition outcome are summarised in Table D.1. There were no issues with violations of proportionality hazard assumption in the model (see Table D.1 and Figure D.1).

	coefficient (robust SE)	HR [95% CI]	p-value
bed movement	0.04 (0.24)	1.04 [0.65, 1.67]	0.86
outward	3.29 (0.84)	26.84 [5.20, 138.37]	8.46×10^{-5}
colonisation pressure	0.10 (0.05)	1.11 [1.00, 1.22]	0.042

Table 6.1: Estimated coefficients, standard errors, hazard ratios (HRs) and p-values for the covariates of the Cox PH model fitted to the MRSA acquisition outcome.

There was a very strong effect of being transferred back to the NICU on increasing the hazard of the patient acquiring MRSA (HR: 26.84 [5.20, 138.37]). This estimated effect was also highly variable as only four patients were transferred back into the ward and two of these four patients acquired MRSA. Colonisation pressure also had a weak effect on increasing the patient MRSA acquisition hazard (HR: 1.11 [1.00, 1.22]). While the estimated HR for colonisation pressure is considerably smaller than that of the outward variable, it should also be noted that the outward indicator is binary whereas the observed colonisation pressure ranged from 0 to 22.6 during the study period. As such,

the actual estimated multiplicative effect of colonisation pressure on the MRSA acquisition hazard varies between 1 (no effect when colonisation pressure is 0) and 10.03 for the range of values observed in the study period.

The effect of bed movement on the hazard of MRSA acquisition was comparatively smaller and not statistically significant. In fact, the overall model fit (as measured by the fitted model likelihood) of simplified model which omitted the bed movement covariate was not significantly different from the full model. The corresponding likelihood-ratio χ^2_1 test statistic was 0.012 with a p-value of 0.91, i.e. the bed movement model coefficient could be effectively treated as zero. The fitted coefficient values for the outward and colonisation pressure covariates from the simplified model was similar to those obtained from the full model (3.30[0.82] and 0.10[0.05]).

Given the small number of cases observed, it might also be of interest to investigate each of the covariates separately. These fitted models are presented in the supplementary material and the estimates were in agreement with the full model shown here. The separate models still estimated statistically significant effects for the outward and colonisation pressure with comparable magnitudes to the estimates obtained in the full model. The bed movement coefficient remained not statistically significant.

6.4.2 Length of stay

The fitted model coefficients are summarised in Table 6.2. There was no evidence to support violation of the proportional hazards assumption for the LOS outcome fitted model (see Table D.8 and Figure D.6). As the outcome for this analysis is the patient discharge indicator, a HR of less than 1 (i.e. negative coefficient estimate) indicates that the corresponding covariate extends a patient's LOS (by decreasing the hazard of the patient being discharged).

	coefficient (robust SE)	HR [95% CI]	p-value
MRSA	-1.01 (0.42)	0.37 [0.16, 0.83]	0.017
colonisation pressure	-0.031 (0.017)	0.97 [0.94, 1.00]	0.067
bed movement	0.23 (0.085)	1.26 [1.07, 1.49]	0.006
outward	-0.10 (0.57)	0.90 [0.30, 2.74]	0.86

Table 6.2: Estimated coefficients, standard errors, hazard ratios (HRs) and p-values for the covariates of the Cox PH model fitted to the LOS acquisition outcome.

The bed movement covariate appears to have a strong effect on increasing the patient discharge hazard (HR: 1.26 [1.07, 1.49]). This is broadly in agreement with the data (Figure D.5). Inclusion of this covariate was to adjust for the plausible effect of bed movement on LOS. The effect itself was not of primary interest for this study.

The acquisition of MRSA was associated with a decreased hazard of discharge (HR: 0.37 [0.16, 0.83]). There also appears to be a weak effect of colonisation pressure in

reducing the discharge hazard in the study period (HR: 0.97 [0.94, 1.00]). Similar to the analysis for the MRSA acquisition outcome above, the MRSA covariate is a binary variable whereas colonisation pressure varies between 0 and 22.6 during the study period. As such, the multiplicative effect of colonisation pressure on the discharge hazard actually ranges from 1 to 0.52.

The outward indicator did not have a statistically significant effect on the discharge hazard. A simplified model fitted with only the MRSA, colonisation pressure and bed movement yielded similar estimates as those shown in Table 6.2 (results for the simpler model provided in the supplementary material). The likelihood ratio test comparing the overall goodness-of-fit of the simplified model against the full model shown here suggest that it is possible to omit the outward indicator without a significant decrease in the model likelihood ($\chi^2_1 = 9.5 \times 10^{-3}; p = 0.92$).

6.5 Discussion

This study showed that colonisation pressure was associated with increased hazard of MRSA acquisition and prolonged LOS for patients in the study NICU during an MRSA outbreak. However, interpretation of the results should be done with caution, particularly for the MRSA acquisition model, due to the statistically small number of MRSA cases. There was no statistically significant effect of patient bed movements on their MRSA acquisition hazard. MRSA acquisition was also shown to prolong a patient's LOS, consistent with findings from adult ICU data (Barnett et al., 2009, De Angelis et al., 2011), as well as other NICUs (Schultz et al., 2009, Song et al., 2010).

The readmission of a patient into the NICU strongly increased the MRSA acquisition hazard. This effect is most likely due to patients being transferred back into the NICU as they were detected with MRSA. However, the two patients who were detected with MRSA after readmission were also in the NICU when other MRSA-positive patients were present and it is possible that they could have acquired MRSA as a result of indirect contact with these MRSA patients. Omission of these two cases would also not be preferable as it would have distorted the risk set for when they were first admitted to the NICU.

An analysis excluding the outward variable provided similar effect estimates for the colonisation pressure variable on the MRSA acquisition hazard and a substantially smaller effect of bed movement which remained not statistically significant (Table D.2).

There was additional information from the data set which could not be incorporated in the current analysis. For example, siblings with MRSA have been associated with increased likelihood of acquiring MRSA (Khoury et al., 2005, Maraqa et al., 2011). However sibling information had only been collected for MRSA-positive patients in this data set and therefore could not be compared with the control patients who have siblings.

The model used here is a relatively simple model that appropriately accounts for time-dependent bias, and the dependence between individuals in the transmission of communicable diseases. The choice of the model was motivated by the small sample size and available information about the outbreak.

Some potential extensions include attempting to model the proportion of undetected colonised patients in the ward and allowing for increased uncertainty about the exact acquisition date using a non-homogeneous Poisson process model (NHPP) (Forrester et al., 2007) or a hidden Markov model (McBryde et al., 2007a). The NHPP can be considered an extension of the Cox proportional hazards model used here. Other extensions of the Cox model include the multistate model which could be used to handle competing risks, which is likely to be relevant to the NICU cohort, and the hidden Markov model structure (Jackson et al., 2003).

Additionally, there is emerging work using whole genome sequencing data, which is becoming increasingly common data collected for NICU outbreak investigations (Giuffr  et al., 2013, Lindsay, 2014, Ugolotti et al., 2016), to construct a probabilistic transmission network using an extended NHPP (Worby et al., 2016).

Acknowledgements

XJL would like to thank Professor Adrian Barnett for his helpful suggestions on the analysis performed here. XJL and ANP are affiliated with the ARC Centre of Excellence for Mathematical & Statistical Frontiers (ACEMS) where ANP is a chief investigator. XJL receives PhD scholarship funding from the Centre of Research Excellence in Reducing Healthcare Associated Infections (NHMRC Grant 1030103). ANP acknowledges the support obtained from the Australian Research Council through a Discovery Grant DP110100159.

Part 3

Transmission contribution of environmental contamination

7 Quantifying the relative effect of environmental contamination on surgical ward MRSA incidence

Abstract

Background: Healthcare associated infections, particularly those involving multidrug-resistant organisms (MROs) such as methicillin-resistant *Staphylococcus aureus* (MRSA), are associated with increased mortality, morbidity, and cost to healthcare services. Stochastic models provide insight into MRO transmission mechanisms in a hospital ward, supplementing more conventional statistical analyses and adding value to existing data.

Methods: A non-homogeneous Poisson process model was developed to explicitly represent the relationship between environmental contamination and MRSA incidence in a UK surgical ward during a cleaning intervention study. The fractional risks (FRs) from colonised patients, environmental contamination and a generic background source in describing the observed MRSA incidence were quantified using the model.

Results: The estimated environmental contamination FR was 0.22 (95% CrI: [0.01, 0.62]) and 0.32 (95% CrI: [0.01, 0.76]) (out of a maximum value of 1) in the enhanced and normal cleaning periods respectively showing a notable albeit variable contribution. This contribution would have been amalgamated into the background source term in a corresponding model without an environmental contamination term.

Conclusions: Accounting for environmental contamination in stochastic modelling of MRSA transmission within a hospital ward provides a richer interpretation of the FRs, and is particularly pertinent in quantitative investigations of hospital cleaning interventions to reduce MRO acquisition.

Statement of Authorship for Chapter 7

This chapter has been written as a journal article. The authors listed below have certified that:

1. they meet the criteria for authorship in that they have participated in the conception, execution, or interpretation, of at least that part of the publication in their field of expertise;
2. they take public responsibility for their part of the publication, except for the responsible author who accepts overall responsibility for the publication;
3. there are no other authors of the publication according to these criteria;
4. potential conflicts of interest have been disclosed to (a) granting bodies, (b) the editor or publisher of journals or other publications, and (c) the head of the responsible academic unit, and
5. they agree to the use of the publication in the students thesis and its publication on the Australasian Research Online database consistent with any limitations set by publisher requirements.

In the case of this chapter, the reference for the associated publication is:

Lee, X. J., Pettitt, A. N., and Dancer, S.J. (2016). Quantifying the relative effect of environmental contamination on surgical ward MRSA incidence. *BMC Infectious Diseases*, under review.

Contributor	Statement of contribution
X.J. Lee	conceived study, developed methods, conducted analysis, wrote manuscript
Signature & Date:	
A.N. Pettitt	conceived study, developed methods, supervised research, discussed methods and results, reviewed manuscript
S.J. Dancer	provided data and clinical feedback, discussed results, reviewed manuscript

Principal Supervisor Confirmation

I have sighted email or other correspondence from all Co-authors confirming their certifying authorship.

AN PETTITT

Name



Signature

13/2/17

Date

7.1 Introduction

Antimicrobial resistance is a serious global health issue that is becoming increasingly difficult to manage. This issue is particularly pertinent in the healthcare setting where vulnerable patients are more likely to develop infections, which in turn have increasingly limited treatment options. One way to mitigate this is to reduce or prevent such healthcare associated infections from occurring in the first place. For hospital multidrug-resistant organisms (MROs) such as methicillin-resistant *Staphylococcus aureus* (MRSA), where colonisation typically precedes infection, this involves preventing MRSA colonisation of susceptible patients from sources such as previously colonised patients (Tong et al., 2015), MRSA-positive healthcare workers (Albrich and Harbarth, 2008) and contaminated environmental sources (Boyce et al., 1997, Dancer, 2014).

While previous research has associated environmental reservoirs with MRO incidence in hospital wards (Weber and Rutala, 2013), only a small proportion of the mathematical modelling literature has explicitly included environmental contamination as a transmission source (Hall et al., 2012, McBryde and McElwain, 2006, Wang et al., 2012, 2013, Wolkewitz et al., 2008). None of these papers however, have used environmental surveillance data to estimate the parameters associated with transmission via environmental contamination due to difficulties in using such microbiological data. Rather, environmental contamination transmission parameter estimates were obtained by fitting simulations from models to observed MRSA patient data.

A non-homogeneous Poisson process (NHPP) is presented to model MRSA incidence in a UK surgical ward over one year. Patient and environmental data were collected for an earlier prospective cross-over cleaning study where a dedicated cleaner was introduced into the ward (Dancer et al., 2009). The incorporation of an explicit environmental contamination term in the model is a novel extension of previous NHPP applications for hospital MRO (Cooper et al., 2008, Forrester et al., 2007, Kypraios et al., 2010, Wei et al., 2016, Worby et al., 2013).

7.2 Methods

NHPPs are stochastic models used to describe the number of events occurring over time, and are characterized by the instantaneous rate of event occurrences, the intensity function ($\lambda(t)$), which varies with time (t). They can be used to model observed MRO incidence in hospital wards (Forrester et al., 2007).

For modelling MRSA incidence, the basic form of the model first assumes that at any time t , the ward comprises $S(t)$ susceptible patients and $C(t)$ patients colonised with MRSA. Susceptible patients are at risk of instantaneous colonisation at a rate given by $\lambda(t)$ which is typically a function of $C(t)$ and a background term β_0 to represent other sources of colonisations not explicitly accounted for in the model. This means, over a

small time period from t to $t + \Delta$, the probability of a susceptible patient being colonised is $\lambda(t)\Delta$.

Denoting the transmission coefficient of colonised patients by β_1 , this basic intensity function is $\lambda(t) = \beta_0 + \beta_1 C(t)$ which can be modified to more closely represent features of the ward under study, provided that the intensity function remains positive.

Examples of such modifications are the addition of a term to represent patients in isolation rooms (Forrester et al., 2007) and step functions to represent different study phases (Cooper et al., 2008). Similar work analysing more than one ward (Kypraios et al., 2010, Wei et al., 2016, Worby et al., 2013) pooled estimates across wards using random-effects meta-analysis to give a summary estimate of overall efficacy of patient isolation.

A common finding of previous work is that the estimated generic background parameter β_0 forms a substantial proportion of $\lambda(t)$ for most of the wards investigated. However, this finding does not lead to clear, practical recommendations as this term encompasses any, and all other, transmission sources not explicitly accounted for in the intensity function, e.g. contributions from environmental contamination.

An issue common to the applications of such models to hospital infection data (or any epidemic surveillance data in general) is that the transmission process is imperfectly observed, i.e. it is not possible to pinpoint the exact time a susceptible patient becomes colonised. To address this issue, the model fitting procedure involves the imputation of these unobserved colonisation times along with parameter estimation. This is typically done using a data-augmented Markov chain Monte Carlo (MCMC) algorithm (Gibson and Renshaw, 1998). In particular, the imputed colonisation time for a patient is estimated from the intensity function values over the possible range of colonisation times for the patient. This range is determined by study features, such as how often patients are screened in the wards, previous (negative) screening dates of the patients and isolation of pathogen of interest (MRSA).

Details about the data set used in this paper, including its limitations, are discussed in the following subsection before describing the specific NHPP developed for this application. Additional details about the model can be found in the Supplementary Materials.

7.2.1 Data

The data were collected as part of a prospective cross-over study evaluating the impacts of an additional, dedicated cleaner on ward cleanliness and MRSA incidence across two surgical wards in a UK hospital (Dancer et al., 2009). Each ward was assigned the same cleaner for separate six month durations and the number of new patient MRSA acquisitions with and without the extra cleaner were compared. Colonised patients were initiated on a topical clearance regimen (antiseptic nasal cream and body wash) on the

date of first laboratory confirmation of MRSA positivity at any site, and remained so until discharge, or after three negative screens had been obtained one week apart. The data were collected over 59 weeks.

The NHPP model presented below used the dates of the first and last positive screening of all patients detected with MRSA within the data collection period, and the weekly aggregate environmental contamination data in the form of aerobic colony counts (ACC). The ACC data were measured in colony forming units (cfu) per cm^2 and aggregated from 10 sampling sites per ward each week. Patient admission and discharge dates were not available.

All patients with a positive MRSA screen were included as colonised cases and cases were not distinguished between new acquisitions or otherwise as the model formulation was unable provide this distinction given the available information. There were 28 patients detected with MRSA in Ward A during the first six months of the study when the ward received enhanced cleaning and a subsequent 15 colonised patients detected in the remainder of the study period when the ward received normal cleaning practices. In comparison, there were 8 colonised patients detected in the enhanced cleaning period for Ward B and 7 during the normal cleaning period. This research therefore focused on only one of the wards (Ward A) for the analysis presented, as the second ward (Ward B) had substantially fewer MRSA acquisitions, further complicating the estimation and potential inference in the presence of limited data. Results for Ward B are described in the supplementary material (Section E.4).

The difference in case numbers between Ward A and Ward B could be suggestive of unmeasured effects that differentiate the MRSA acquisition process in the two wards despite the wards having been matched for ward, staff and patient cohort characteristics (Dancer et al., 2009). Examples of such unmeasured effects include specific patient risk factors, potential staff MRSA carriers and staff compliance levels on routine infection control practices (such as hand hygiene).

Additionally, the counter-intuitive observations of increased MRSA cases in the enhanced cleaning period compared with the normal cleaning period (where the reverse might be expected) in both wards highlight the strong stochastic nature of hospital ward population dynamics and the need for appropriate stochastic models, such as NHPPs, to represent such data.

7.2.2 Non-homogeneous Poisson process formulation

The intensity function used here is a function of a background source, colonised patients, and environmental contamination. A distinction is made between undetected colonised patients (C_{xt}) and detected colonised patients (C_t) with the assumption that the contribution of a C_{xt} patient is greater than a C_t patient by an amount of α_1 , as detected colonised patients were given decolonisation treatment.

The mathematical expression for the intensity function is

$$\begin{aligned}\lambda(t) &= \beta_0 + (\beta_1 + \alpha_1) C_{xt}(t) + \beta_1 C_t(t) + \beta_2 E(t) \\ &= \beta_0 + \beta_1 C(t) + \alpha_1 C_{xt}(t) + \beta_2 E(t)\end{aligned}\tag{7.1}$$

where $C(t) = C_{xt}(t) + C_t(t)$ and $E(t)$ is the environmental contamination measurement (ACC) in the ward at time t (in days) with the corresponding transmission coefficient β_2 .

The likelihood for the model $L(\boldsymbol{\theta})$ follows the general NHPP likelihood form for such systems

$$\exp \left\{ \sum_{i:\text{all patients}} \left[\mathbb{1}(\text{patient } i \text{ becomes colonised}) \log \left(\lambda(t_{C_i}^-) \right) - \int_{u \in T_{S_i}} \lambda(u) du \right] \right\}$$

where $t_{C_i}^-$ is the time point immediately preceding the colonisation of patient i , $\mathbb{1}(x)$ the indicator function for x which equals 1 if x is true and 0 if x is false, and T_{S_i} is the time period that patient i is susceptible. The four parameters to be estimated from the intensity function (7.1) are denoted $\boldsymbol{\theta} = (\beta_0, \beta_1, \beta_2, \alpha_1)$.

For this particular model, a more directly interpretable comparison measure between the different components can instead be obtained by considering the separate components of the intensity function (7.1) rather than the straightforward parameter estimates which have different units (apart from β_1 and α_1). To facilitate this comparison, the intensity function was rewritten as

$$\lambda(t) = \lambda_{bg}(t) + \lambda_{cxt}(t) + \lambda_{ct}(t) + \lambda_{env}(t)$$

where $\lambda_{bg}(t) = \beta_0$, $\lambda_{cxt}(t) = (\beta_1 + \alpha_1) C_{xt}(t)$, $\lambda_{ct}(t) = \beta_1 C_t(t)$ and $\lambda_{env}(t) = \beta_2 E(t)$. The four components in the intensity function now represent the four different potential MRSA acquisition pathways considered: the generic background source (bg), undetected colonised patients (cxt), detected colonised patients (ct) and environmental contamination (env).

The fractional risk (FR) measure (originally termed relative risk in (Forrester, 2006)) was used to quantify the relative importance of the different components in the intensity function for the observed patient MRSA acquisition. The FRs are defined as

$$FR_j = \frac{1}{N_C} \sum_{i=1}^{N_C} \frac{\lambda_j(t_{C_i}^-)}{\lambda(t_{C_i}^-)} \quad j \in \{bg, cxt, ct, env\}$$

where N_C is the total number of colonised patients recorded in the ward for the particular time period, and t_{C_i} is the time point immediately preceding the colonisation time of patient i , i.e. the FRs estimate the average relative magnitude of the components in the intensity function immediately prior to a patient being colonised.

While the NHPP could be extended to include the possibility of a proportion of patients being undetected colonised on admission (Forrester et al., 2007), this was not considered here as most patients admitted to the study ward were screened pre-admission. Only patients admitted directly from the Accident & Emergency department were not screened pre-admission. These admissions form a small proportion of all admissions to the ward (Dancer et al., 2009).

Using piecewise-constant $\lambda(t)$ means the integral in the likelihood can be simplified thus circumventing the requirement of the patient admission dates (McBryde et al., 2007a) as follows:

$$\begin{aligned} L(\boldsymbol{\theta}) &= \exp \left\{ \sum_{\text{col. patients}} \log \left(\lambda(t_{C_i}^-) \right) - \sum_{\text{all patients}} \int_{T_{S_i}} \lambda(u) du \right\} \\ &= \exp \left\{ \sum_{\text{col. patients}} \log \left(\lambda(t_{C_i}^-) \right) - \sum_{l=1}^{L-1} \lambda(t_l) S(t_l) (t_{l+1} - t_l) \right\} \end{aligned}$$

where ‘col. patients’ refers to the set of patients who were colonised, t_l the time points where the intensity function value changes and t_L is the final time point for a period.

The colonisation times and discharge dates of MRSA-positive patients remain to be imputed in order to evaluate $\lambda(t)$ and estimate $\boldsymbol{\theta}$ and the FRs.

7.2.3 Patient time imputation

The number of patients with different MRSA status $X(t) = [S(t), C_{xt}(t), C_t(t)]$ at time t is used to evaluate $\lambda(t)$ in the model. However, computing $X(t)$ requires the admission dates, exact colonisation times and discharge dates (in days) for each MRSA-positive patient which were not available. These three quantities were instead imputed using the model and local knowledge of the ward’s infection control practices.

All patients were assumed to have been screened during the regular Monday weekly screenings. The colonisation time for a patient was then imputed between the patient’s first positive screen date and the immediately preceding Monday with relative weights for each day given by the unknown parameter full conditional posterior distributions evaluated for the day (with numerical derivation provided in Appendix E.1). Similarly, the patient’s discharge date was randomly sampled between the patient’s last positive screen date and the following Monday.

The ward was assumed to be fully occupied throughout the study since exact patient admission dates were not available for this data set. This means that a colonised patient’s discharge was immediately followed by the admission of a susceptible patient. A similar assumption was made in a previous MRO modelling study (McBryde et al., 2007a).

7.2.4 Smoothing of environmental contamination data

In order to obtain daily estimates of environmental contamination, the weekly environmental contamination data were smoothed using a robust lowess smoother with a span of 0.3 (Gijbels and Prosdocimi, 2010) for each time period. These smoothed daily estimates ($E(t)$) are used as inputs to the intensity function.

These daily estimates exhibited only small variations over time within each period compared with the weekly measurements (Figure 7.1). The small variations are consistent with findings from a study which used an identical measurement protocol for environmental contamination but with repeat measurements taken from between 0 to 48 hours of the cleaning procedure at the same site (Stewart et al., 2014). That study found a substantial drop in ACC levels immediately following cleaning, though the change observed 24 hours after cleaning was less dramatic. It would then be expected that a daily time series would not vary very much. If a finer time scale was used in the model instead, then it would be more appropriate to use a smoother which allowed for greater variations in the smoothed values. This is subject to the availability of appropriately informative data on both patients and environment.

The choice of the span parameter of 0.3 was within the recommended range (Gijbels and Prosdocimi, 2010) and corresponds to 8 weeks for the enhanced cleaning period and 10 weeks for the normal cleaning period. These durations were within the time range (7 days to 7 months) for MRSA persistence on dry inanimate surfaces (Kramer et al., 2006). Other spans and simple smoothers (loess smoothers and linear interpolation) were also investigated, though the differences estimated between the enhanced and normal cleaning periods were less evident due to the substantial increase in variability of the estimates.

The particular smoother used reflected the uncertainty surrounding two factors in the use of ACC for this application. The first was the utility of the measurement type (ACC) as a reflection of environmental contamination attributable to specific transmission events (MRSA colonisations) in a hospital ward. The second was the measurement accuracy due to the aggregation of categorical classifications (converted to a numerical value per category of an originally continuous measurement due to the heavy time and resource burden required to obtain the actual continuous measurements) (Dancer et al., 2009).

7.2.5 Estimation procedure

The model parameters were estimated using a data-augmented MCMC algorithm (Forrester et al., 2007, McBryde et al., 2007a) where the MRSA patient unobserved colonisation times and discharge dates were imputed at each MCMC iteration, as described above. Uniform priors ($U(0, 1)$) were assigned to the model parameters θ .

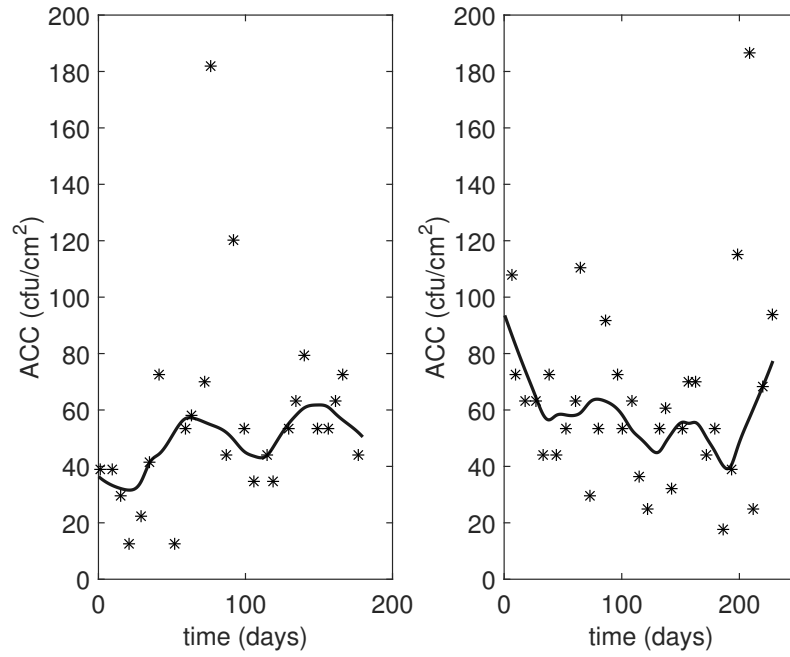


Figure 7.1: Smoothed time series of the environmental contamination measure (ACC) for the enhanced cleaning period (left) and normal cleaning period (right). Black asterisks denote the raw weekly data. Aerobic colony count (ACC) is measured in colony forming units per cm^2 (cfu/cm^2).

At each MCMC iteration, each parameter in the intensity function is independently updated using a Metropolis-Hastings step with the parameters' full conditional forms derived from the likelihood (Appendix E.1). Independent multiplicative random walk proposals (Sherlock et al., 2010) were specified for each parameter with the variances tuned to achieve acceptance rates between 0.1 and 0.6 (Brooks et al., 2011).

A posterior predictive test was used to assess the model adequacy in representing the data (Gelman et al., 2013). The posterior predictive test quantity for this application was the total number of MRSA patients as it was the only directly observed quantity in the data. Hence, in each posterior predictive test, the probability of a posterior predictive simulation generating more MRSA-positive patients than observed in the same period, or posterior predictive probability, was estimated from 10,000 posterior predictive simulations. Extreme values of this probability (close to 0 or 1) would indicate the estimated posterior provides a poor fit to the data.

Appendix E.1 expands on the data-augmented MCMC algorithm used while Appendix E.1.1 details the simulation method for the proposed NHPP. The estimation procedure was shown to be able to recover parameter values well from a simulation study (detailed in Appendix E.2).

7.3 Results

The estimated posterior distributions for the four parameters in the intensity function (7.1) are summarised in Table 7.1.

Parameter ($\times 10^5$)	Enhanced cleaning				Normal cleaning			
	β_0	β_1	β_2	α_1	β_0	β_1	β_2	α_1
Mean	539	84.2	5.07	494	192	48.3	2.69	614
MCSE	0.5	0.1	0.009	0.6	0.2	0.07	0.004	0.7
SD	241	72.6	4.05	367	121	44.1	1.97	462
2.5% quantile	118	2.55	0.171	22.3	10.6	1.39	0.103	29.9
Median	526	65.0	4.12	423	179	35.7	2.33	520
97.5% quantile	1043	269	15.0	1381	457	164	7.27	1747

Table 7.1: Summary of parameter estimates from the combined sample of 2,400,000 iterations from three converged and well-mixed MCMC chains. MCSE denotes the Monte Carlo standard error and SD the posterior standard deviation. β_0 , β_1 , β_2 and α_1 are the coefficients in the intensity function associated with the background source, colonised patients, environmental contamination and additional contribution from being undetected while colonised, respectively.

The posterior predictive distribution of the total number of colonised patients in each time period was used to assess the model adequacy in describing the observed data (Figure 7.2). The distributions were consistent with the observed numbers of MRSA patients in both periods with the estimated posterior predictive probabilities (as defined in Section 7.2.5) of 0.494 in the enhanced cleaning period and 0.556 in the normal cleaning period. This indicates that the estimated posterior distributions, along with the proposed NHPP, provide adequate representations of the patient MRSA acquisition process in the ward for both the enhanced and normal cleaning periods.

As the model parameters for the enhanced cleaning and normal cleaning periods were estimated independently, we can directly compare the difference of each estimate in the two periods. This provides a ‘Bayesian hypothesis test’ with the particular null hypothesis of interest here being if the parameter values in the two periods are equal.

Based on the posterior samples, there was statistical evidence for the value of the β_0 parameter to be substantially different between the two periods. The estimated posterior probability of β_0 in the enhanced cleaning period being larger than the β_0 value in the normal cleaning period was 0.904. Conversely, there was no evidence of a difference between the values in both periods for the other three parameters ($\beta_1, \beta_2, \alpha_1$) with posterior probabilities of the parameter values in the enhanced cleaning period being larger than the normal cleaning period estimated to be 0.654, 0.674 and 0.429, respectively. The histograms of these differences are in Figure 7.3 with each of the histograms centred on 0 except β_0 .

The stochastically larger β_0 estimate in the enhanced cleaning period is due to the larger number of colonised patients detected in the enhanced cleaning period, having accounted

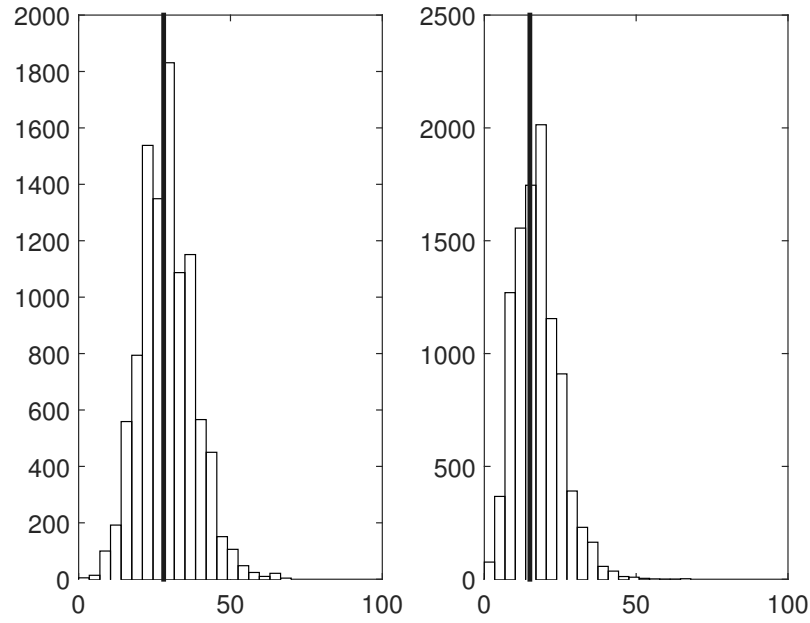


Figure 7.2: Histograms of number of colonised patients from 10,000 simulations using parameters sampled from the estimated posterior distributions obtained from the enhanced cleaning period data (left) and normal cleaning period data (right). The thick vertical black lines represent the observed value in each period (28 for the enhanced cleaning period and 15 for the normal cleaning period).

for the influences of the other colonised patients in the ward and the environmental contamination $E(t)$, noting that although variable, $E(t)$ is still lower, on average, in the enhanced cleaning period (49.2 compared with 57.9 in the normal cleaning period).

In both time periods, the additional contribution of a colonised patient being undetected (α_1) is substantially larger than the general contribution of a (detected) colonised patient (β_1) to subsequent MRSA acquisitions. In fact, the estimated posterior probability of α_1 being greater than β_1 was 0.888 in the enhanced cleaning period and 0.951 in the normal cleaning period.

The FRs estimated from the enhanced and normal cleaning periods are summarised in Table 7.2 and Figure 7.4. In both periods, the background source had the largest mean FR of the four components which form the intensity function $\lambda(t)$ (0.50 and 0.41 in the enhanced and normal cleaning periods respectively). The second largest mean FR was for the environmental contamination component (0.22 and 0.32) followed by the undetected and detected colonised patients (0.16 and 0.18 for undetected and 0.12 and 0.085 for detected) (Table 7.2).

There were two notable differences between the FR distributions in the enhanced and normal cleaning periods. Firstly, the FR_{bg} distribution in the enhanced cleaning period had a clearly defined mode just larger than 0.5 whereas the corresponding distribution in the normal cleaning period is more dispersed with a smaller mean (0.41 compared with 0.50 in the enhanced cleaning period). Secondly, the FR_{env} distribution in the enhanced cleaning period was more concentrated around smaller values with a right

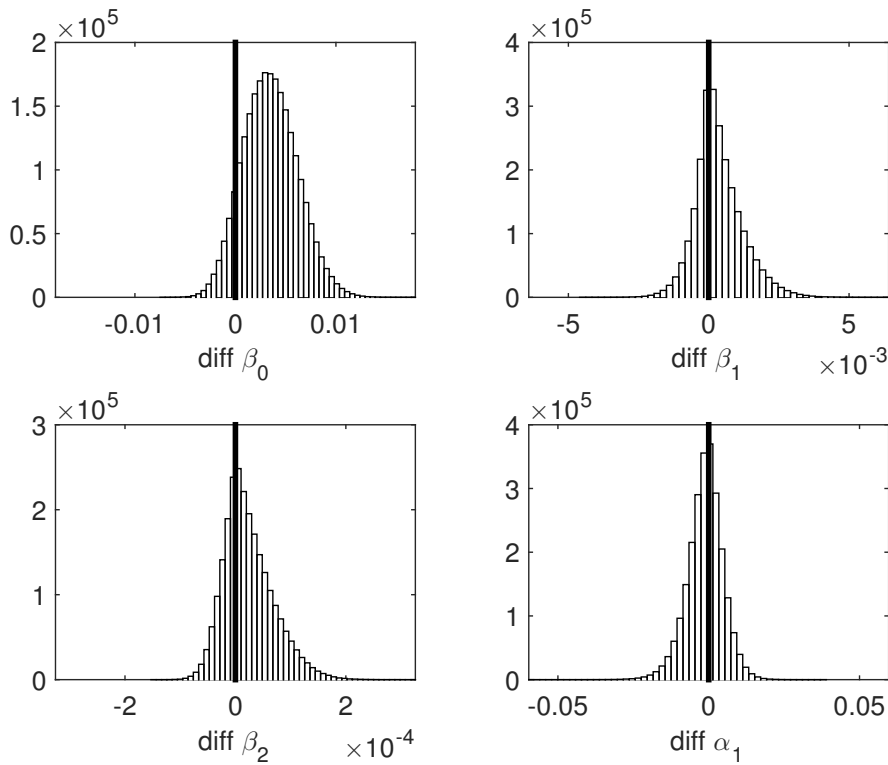


Figure 7.3: Histogram of the differences (diff) in parameter values between the enhanced cleaning period and normal cleaning period from the combined sample of 2,400,000 iterations from three converged and well-mixed MCMC chains. The parameters β_0 , β_1 , β_2 and α_1 are the coefficients in the intensity function associated with the background source, colonised patients, environmental contamination and additional contribution from being undetected while colonised, respectively.

	Enhanced cleaning				Normal cleaning			
	<i>bg</i>	<i>cxt</i>	<i>ct</i>	<i>env</i>	<i>bg</i>	<i>cxt</i>	<i>ct</i>	<i>env</i>
Mean	0.50	0.16	0.12	0.22	0.41	0.18	0.085	0.32
SD	0.19	0.079	0.097	0.17	0.22	0.088	0.072	0.22
2.5% quantile	0.12	0.030	0.0038	0.0080	0.026	0.025	0.0026	0.013
Median	0.51	0.16	0.094	0.19	0.42	0.18	0.066	0.30
97.5% quantile	0.83	0.33	0.36	0.62	0.81	0.35	0.27	0.76

Table 7.2: Summary of mean fractional risks (FR) for the four different components of the intensity function for the enhanced and normal cleaning period. SD refers to the standard deviation. The background source is denoted by *bg*, undetected colonised patient by *cxt*, detected colonised patient by *ct* and environmental contamination by *env*.

skew and had a more dispersed distribution with a larger mean in the normal cleaning period (0.32 compared with 0.22). In contrast, the FR_{cxt} and FR_{ct} distributions were similar between the two periods.

The estimated posterior distributions of FR ranking for both periods are in Figure 7.5 with rank 1 denoting the largest component (highest rank) and rank 4 the smallest component (lowest rank). While there was considerable uncertainty surrounding the

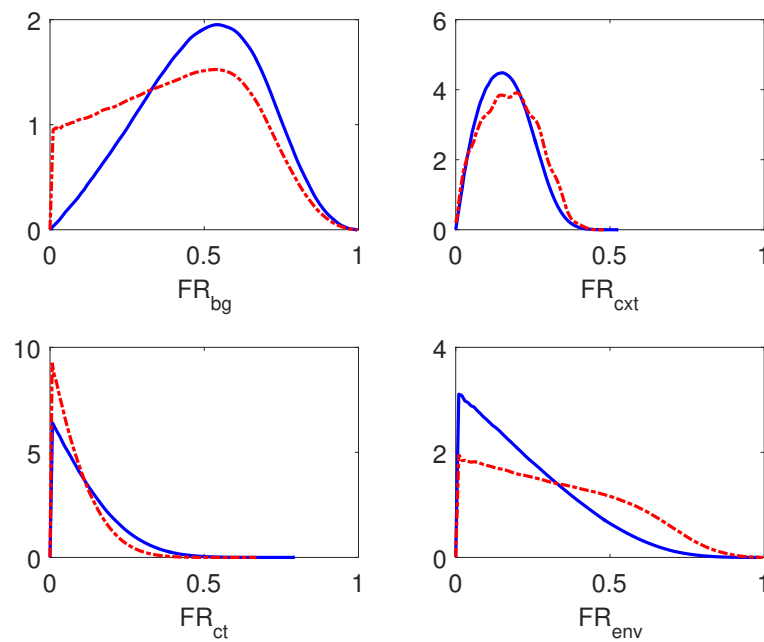


Figure 7.4: Kernel density estimates of mean fractional risks (FR). The blue and red outlines correspond to the enhanced cleaning period and normal cleaning period, respectively. The background source is denoted by *bg*, undetected colonised patient by *cxt*, detected colonised patient by *ct*, and environmental contamination by *env*.

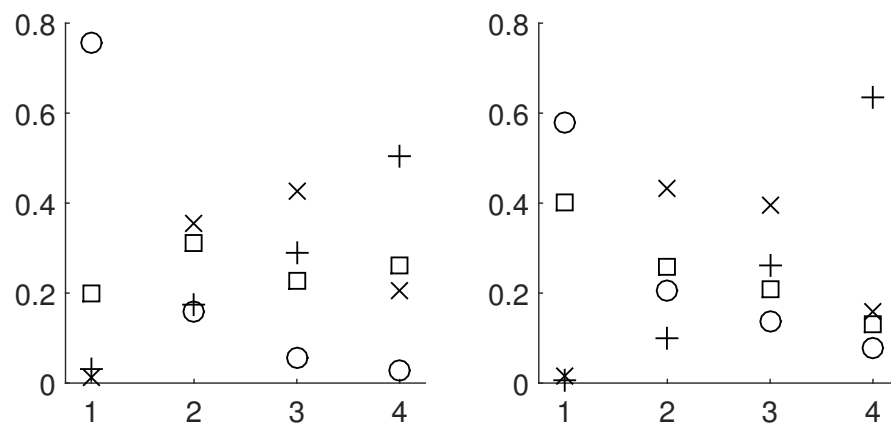


Figure 7.5: Posterior probabilities of the ranks for the four components of the intensity function in the enhanced cleaning period (left), and normal cleaning period (right). The \circ denotes the background source component, \square for environmental contamination, \times for undetected MRSA patient, and $+$ for detected MRSA patients. The rank order is in descending order along the horizontal axis (with rank 1 being the highest and rank 4 the lowest).

‘true’ rank of each component, there were also notable trends across the rank orders for the four components.

There was substantial posterior probability for the background source to be the largest FR component in the enhanced cleaning period (0.76) with decreasing probabilities of being associated with lower ranks. Both these features diminished in the normal cleaning period (with a posterior probability of being assigned to rank 1 of 0.58).

In contrast, there was no obvious preferred rank for the environmental contamination component in the enhanced cleaning period with fairly similar posterior probabilities of being assigned to any rank. In the normal cleaning period however, there was a gradual posterior preference for the environmental contamination to be assigned to higher ranks. The posterior probability of environmental contamination being assigned to rank 1 increased from 0.20 in the enhanced cleaning period to 0.40 in the normal cleaning period.

The posterior distributions for the ranks of undetected and detected colonised patient components were similar across periods. The posterior probabilities for either component being assigned to rank 1 were very small (0.01 and 0.03 in the normal cleaning period, and 0.01 and 0.00 in the enhanced cleaning period). There was considerable posterior support for the *cxt* component to be of either rank 2 or 3, followed by rank 4, and lastly rank 1 in both periods. The *ct* component instead had the largest posterior probability of being assigned to rank 4 with decreasing probabilities associated with higher ranks. This trend was more marked in the normal cleaning period.

The results obtained from the full model described in the Methods section were compared with a simplified model without the environmental contamination component in order to investigate how the estimates differ for the various components (see Appendix E.3 for corresponding results and graphical outputs). Very similar results were obtained for the patient-related parameters β_1 and α_1 , as well as their FR distributions, indicating that the environmental contamination component actually explains a portion of the general ‘background’ term in other similar models.

From the MCMC outputs, it is also possible to evaluate and compare a measure of statistical fit for both models. The comparison assesses if there is a statistical preference for one of the models. Due to the fact that both models involve missing data (in the form of unobserved colonisation times), the DIC_6 model comparison measure (Celeux et al., 2006) was used.

The full model with environmental contamination obtained similar DIC_6 values in both periods compared with the model without environmental contamination, specifically 317.75 (standard error (SE): 0.01) and 317.10 (SE: 0.009) respectively in the enhanced cleaning period, and 198.40 (SE: 0.01) and 198.13 (SE: 0.01) in the normal cleaning period (with the standard errors in parentheses). These results indicate that the requirement of estimating an additional parameter in the full model did not disadvantage the model’s performance (in terms of DIC_6) compared with the model without environmental contamination. The full model is thus a viable alternative to the model without environmental contamination when environmental contamination data are available. Similar inferences were obtained with the other environmental data smoothers.

The numerical evidence above shows that environmental contamination does contribute to MRSA incidence in a hospital ward. This contribution would have been amalgamated with the generic ‘background source’ in the absence of an environmental contamination term in the intensity function and so inflate the importance of the background source.

The identification of a relatively large background source term however is of limited practical use due to the difficulty in proposing an intervention to target the various unaccounted for transmission sources that form the term (aside from the costly ‘search-and-destroy’ and isolation upon admission policies). Hence, the inclusion of an environmental contamination term provides a more readily targeted transmission source for infection control interventions.

For this particular study ward, the environmental contamination was identified to have the second largest FR contribution (behind the generic background source) in the MRSA acquisition process in both the normal and enhanced cleaning period with a slightly increased contribution in the normal cleaning period (Figure 7.4 and Table 7.2). The environmental contamination contribution is greater than those from undetected and detected colonised patients, suggesting that it might be more beneficial to target improvements in cleaning practices rather than interventions solely targeting MRSA patients for this ward. The MRSA patient management practices currently in place appear efficacious noting the relatively smaller contributions from *cxt* and *ct*.

7.4 Discussion

The NHPP model presented here is the first to incorporate environmental contamination into the intensity function and use environmental contamination data to estimate model parameters. The model was able to obtain good parameter estimates with limited data using specific simplifications that draw upon properties of the proposed model, specifically the piecewise constant intensity and the assumption of full ward capacity, along with local knowledge of ward-specific practices and clinical expertise.

The fitted model was able to identify clinically sensible differences, or lack thereof, between the time period with the enhanced cleaning intervention and the one without. The first is the larger background source parameter in the enhanced cleaning period accounting for the fact that there were more MRSA colonisations reported in the enhanced cleaning period. Secondly, the model showed very similar results for patient-related parameters and inferences across the periods, reflecting the fact that the cleaning intervention was unlikely to have affected the transmission intensity from direct contact with colonised patients.

While the NHPP model also estimated a larger relative colonisation risk from environmental contamination in the normal cleaning period compared with the enhanced cleaning period, this effect is dependent on the choice of smoother used for $E(t)$ where the choice of the more variable smoother might not provide as clear a

separation between the results obtained for the different periods. Despite this uncertainty in the environmental contamination result, the model with the environmental contamination component provided similar DIC_6 estimates compared with the model without environmental contamination for both periods. Furthermore, a larger weight, as measured by the FRs, was merely assigned to the generic background source in the absence of an environmental contamination term in the intensity function. This particular inference does not provide a readily targeted transmission source and is of limited value to clinical decision makers.

The DIC_6 was used for model comparison here as the quantity can be readily computed from standard MCMC output. More sophisticated and computationally demanding model comparison methods could be considered in future work, including model comparison based on latent residual tests (Lau et al., 2014, Streftaris and Gibson, 2012), power posterior estimate of the marginal likelihood (Friel and Pettitt, 2008) and Bayes factor estimation using a mixture model formulation for partially observed stochastic processes (O'Neill and Kypraios, 2016).

The use of ACC as an indicator of environmental contamination contributing to MRSA transmission in a hospital ward is a proxy measure; there is a statistically significant positive association between ACC levels and detection of *S. aureus* in environmental samples (Dancer et al., 2008). While a more direct measure would be ideal, it is difficult to detect MRSA from a randomly sampled environmental site, and more sophisticated data collection methods are generally too costly. Use of high resolution genetic data, such as whole genome sequencing data, of the pathogen to infer a detailed transmission network (Worby et al., 2016) also has its own set of difficulties (Worby et al., 2014) and could further complicate the modelling process.

The environmental contamination data smoother used here provided a conservative assumption on how closely ACC reflected the actual MRSA pressure from environmental contamination. The smoother could be extended to further scrutinize the role of environmental contamination in the MRSA colonisation process. Two noteworthy extensions are the use of more sophisticated smoothers such as generalized additive models (Wood, 2006) or Gaussian processes (Lloyd et al., 2015, Rasmussen and Williams, 2006), and the addition of colonised patient covariates into the smoothing procedure to more realistically capture the interlinkage of MRSA-positive patients, environmental contamination and patient colonisation. The main challenge here would be to formulate a smoother that could handle the relative sparsity of the environmental contamination data in obtaining daily estimates (or finer) from weekly data as required by the NHPP model.

The NHPP patient model used here could also be extended subject to the availability of additional data. Extensions such as the inclusion of screening test sensitivity, and probabilistic colonisation upon admission have been proposed and implemented (Forrester et al., 2007), but rely on data structures not available with this data set.

Patient heterogeneity could be incorporated by including patient-specific covariates (for example, antibiotic use) into the intensity function, or extending the NHPP model to have a non-exponential tolerance level before developing an MRSA colonisation (Streftaris and Gibson, 2012). Such extensions however would result in the intensity function no longer being piecewise constant, complicating the inference procedure for this particular data set with limited information.

Recent research using whole genome sequencing inferred that colonised patients may not make as strong a contribution to the risk of colonisation in non-outbreak scenarios (Long et al., 2014, Price et al., 2014). This inference is supported by findings from the NHPP model in this study. Therefore, increasing model complexity in terms of patient heterogeneity might not yield substantially different findings at the cost of complicating the inference procedure further, particularly for limited-information data sets such as the one used here. A more fruitful avenue of investigation might be to quantify the influx of community-associated MRSA (DeLeo et al., 2010) instead, as it may form a more substantial part of the background source term. The FR measure used here is readily adapted to handle this inclusion of another source term with a different unit.

7.5 Conclusions

The NHPP model presented here was able to infer that environmental contamination does play a contributory role toward MRSA incidence observed in the study ward despite limitations in the data set. It also showed that the environmental contamination component accounts for what would have been included in the background source in the absence of the component. A larger relative contribution and fractional colonisation risk from the environmental contamination was also inferred by the model during the normal cleaning period compared with the enhanced cleaning period. However, this inference should be interpreted with caution as it is sensitive to the choice of smoother used and requires further investigation with a larger, more detailed data set than currently available. This might potentially require a more complex model, as described above.

8 A stochastic model for MRSA transmission within a hospital ward incorporating environmental contamination

Abstract

Methicillin-resistant *Staphylococcus aureus* (MRSA) transmission in hospital wards is associated with adverse outcomes for patients and increased costs for hospitals. The transmission process is inherently stochastic and the randomness emphasised by the small population sizes involved. As such, a stochastic model was proposed to describe the MRSA transmission process, taking into account the related contribution and modelling of the associated microbiological environmental contamination. The model was used to evaluate the performance of five common interventions and their combinations on six potential outcomes of interest under two hypothetical disease burden settings. The model showed that the optimal intervention combination varied depending on the outcome measure and burden setting. Some outcomes only needed a small subset of targeted interventions to control the outcome measure, while other outcomes still had reduction in the outcome distribution with all five interventions included. This study described a new stochastic model for MRSA transmission in a ward and highlighted the use of the generalised Mann–Whitney statistic to compare the distribution of outcomes under different intervention combinations to assist in planning future interventions in hospital wards under different potential outcome measures and disease burden.

Statement of Authorship for Chapter 8

This chapter has been written as a journal article. The authors listed below have certified that:

1. they meet the criteria for authorship in that they have participated in the conception, execution, or interpretation, of at least that part of the publication in their field of expertise;
2. they take public responsibility for their part of the publication, except for the responsible author who accepts overall responsibility for the publication;
3. there are no other authors of the publication according to these criteria;
4. potential conflicts of interest have been disclosed to (a) granting bodies, (b) the editor or publisher of journals or other publications, and (c) the head of the responsible academic unit, and
5. they agree to the use of the publication in the students thesis and its publication on the Australasian Research Online database consistent with any limitations set by publisher requirements.

In the case of this chapter, the reference for the associated publication is:

Lee, X. J., Fulford, G.R., Pettitt, A. N., and Ruggeri, F. (2016). A stochastic model for MRSA transmission within a hospital ward incorporating environmental contamination *Epidemiology & Infection*, doi:10.1017/S0950268816002880s

Contributor	Statement of contribution
X.J. Lee	developed methods, conducted analysis, wrote manuscript
Signature & Date:	
G.R. Fulford	developed methods, discussed methods and results, reviewed manuscript
A.N. Pettitt	developed methods, supervised research, discussed methods and results, reviewed manuscript
F. Ruggeri	conceived study, developed methods, discussed methods and results, reviewed manuscript

Principal Supervisor Confirmation

I have sighted email or other correspondence from all Co-authors confirming their certifying authorship.

AN PETTITT

Name



Signature

13/2/17

Date

8.1 Introduction

Healthcare associated infections (HAIs) are adverse events that can arise during hospitalisation. Multidrug-resistant organisms (MDROs), for example methicillin resistant *Staphylococcus aureus* (MRSA), are common causes of these HAIs with patients typically becoming colonized with the organism prior to developing an infection. Treatment options for MDROs are becoming increasingly limited due to the relative sparsity in development of new treatments compared with the rate of resistance acquisition (Gould et al., 2012). As such, the role of routine infection control and prevention (ICP) practices are of great importance in reducing the occurrence of HAIs.

Intervention studies which typically investigate the effects of one or a combination of interventions in reducing HAIs provide a good first line of evidence for particular interventions to be incorporated into routine ICP practices. These studies also assist in building mathematical model representations of the healthcare setting. Such models then allow for further probing of the effects of the interventions which may not have been feasible or potentially ethical to investigate in a clinical setting but could prove useful in assisting decision-making, particularly when hospital resources are limited. The model findings could also provide recommendations for future intervention studies.

Susceptible patients are typically modelled to be colonized (a state which precedes an infection) through a forcing term (referred to as the force of infection) which is a function of the number of colonized patients currently present in the ward as well as the colonized hospital staff in the ward at the time. As hospital staff are not routinely screened for pathogen colonization, obtaining quality data on hospital staff has proven difficult.

That said, the vast majority of mathematical models consider vector based cross-transmission between patients and transiently contaminated healthcare workers (HCWs) to be the dominant transmission mechanism for MDROs such as MRSA (Doan et al., 2014). Only a small number of papers have considered alternative transmission routes typically by incorporating a constant source (such as in Forrester et al. (2007)). Even fewer explicitly modelled environmental contamination as an alternative transmission route (Doan et al., 2015, Hall et al., 2012, McBryde and McElwain, 2006, Wang et al., 2012, 2013, Wolkewitz et al., 2008).

This paper presents a stochastic model for ward MDRO transmission based on patient dynamics (as patient data are typically more readily available compared with hospital staff) coupled with environmental contamination. The model was run under two settings; the first is based on MRSA dynamics in a developed country (UK and Switzerland) where MRSA data and parameters are more easily readily sourced, and the second is for a hypothetical scenario where the pathogen is more readily transmitted and not as easy to detect. The second setting could be representative of: a novel pathogen in the healthcare setting, a new strain of MRSA that is more virulent than

existing strains or a resource-poor setting such as in low-income countries (Christopher et al., 2011) where such modelling studies have great benefit. The impact of five common healthcare interventions (Doan et al., 2014) and their various combinations were investigated for six potential outcomes under both settings separately. Limitations and future directions in model development are discussed in Section 8.4.

8.2 Methods

8.2.1 Model formulation

The model proposed is for a single ward and comprises: (i) a ward-level patient arrival process; (ii) an individual-based model for patient transitions in the ward; and (iii) a time series for the level of environmental contamination.

At any time t , patients in the ward are categorized based on their MRSA status where they can be in either: the susceptible group ($S(t)$); undetected MRSA colonized ($C_{xd}(t)$); detected with MRSA colonization and undergoing appropriate treatment ($C_d(t)$); undetected MRSA infected ($I_{xd}(t)$); and detected with MRSA infection and undergoing appropriate treatment ($I_d(t)$). A schematic illustration of the model is provided in Figure 8.1 with $E(t)$ representing the ward environmental contamination levels.

The model is an example of Discrete Event Simulation (DES) widely used in the health care sector (Fone et al., 2003, Mielczarek and Uziółko-Mydlikowska, 2012, Pitt et al., 2016). While perhaps more commonly used in scheduling problems, DES has also been applied to investigate pathogen transmission (Mielczarek and Uziółko-Mydlikowska, 2012). DES provides a flexible modelling approach to represent individual patient transitions during their hospitalisation episode, allowing for the inclusion of stochastic variability (important for small population studies such as in a hospital ward) and effects of individual patient information.

Patient admissions into the ward are modelled as a right-censored (at ward capacity M) Poisson process ($A(t) \sim \text{Po}(\lambda)$) with a Binomial variable to separate arrivals to either susceptibles ($AS(t)$) or colonized (but not detected, C_{xd}) ($AC(t)$). It is assumed that patients cannot be infected on admission (as infected patients are typically isolated or cohorted to reduce transmission risk to other patients). Excess arrivals, beyond the ward capacity M , are assumed to be allocated to a separate ward thus creating the right censoring in the arrival process.

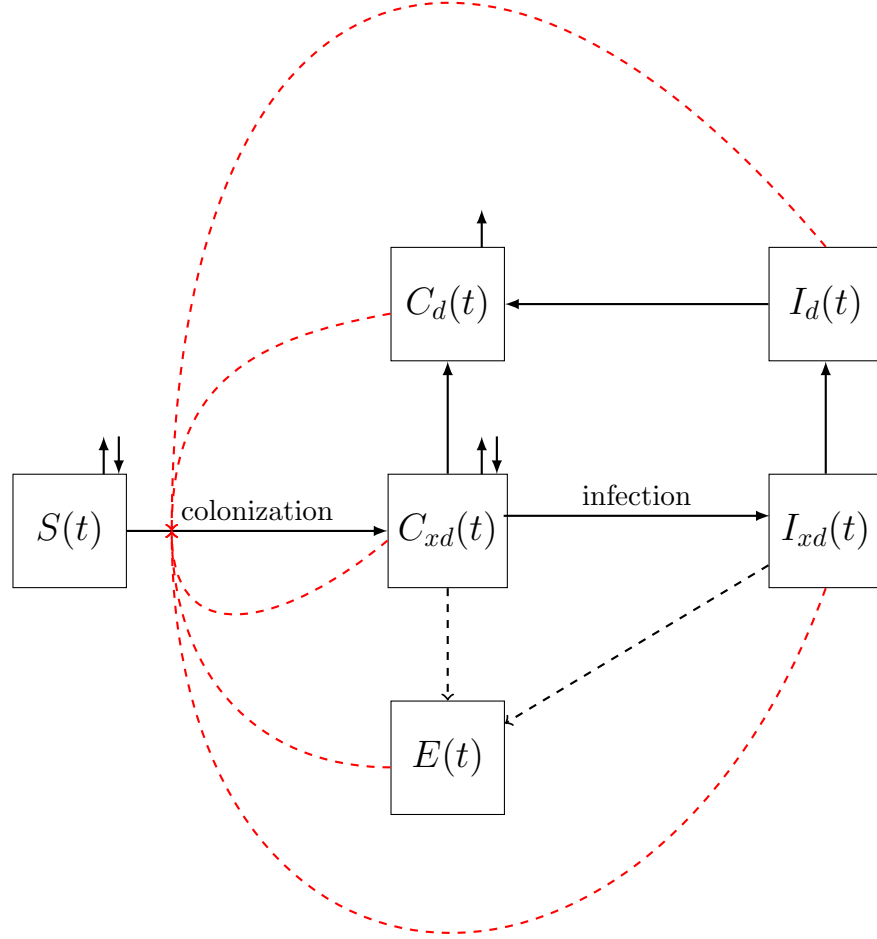


Figure 8.1: Compartmental diagram for the MRSA transmission model incorporating environmental contamination. The solid black lines are patient transitions between the different states as well as admissions and discharges (only for the $S(t)$ and $C_{xd}(t)$ compartments). The red dashed lines represent the contribution from the various compartments to the colonization process while the black dashed lines represent the compartments contributing to the evolution of the $E(t)$ compartment.

The likelihood for the admissions at time t can therefore be written as:

$$\begin{aligned}
 P(A(t) = k, AS(t) = j, AC(t) = k - j | Y(t-1)) \\
 = \begin{cases} \frac{\lambda^k}{k!} e^{-\lambda} \binom{k}{j} \vartheta^j (1 - \vartheta)^{k-j} & 0 \leq k < Y(t-1) \\ \sum_{i=Y(t-1)}^{\infty} \frac{\lambda^i}{i!} e^{-\lambda} \binom{i}{j} \vartheta^j (1 - \vartheta)^{i-j} & k = Y(t-1) \end{cases}
 \end{aligned}$$

where $Y(t)$ is the number of empty beds in the ward at time t and ϑ is the proportion of admissions that arrive susceptible.

The admissions at time t will then be assigned to the empty beds in the ward but will not undergo the individual patient transitions until the next time point.

The individual-based model, which is for patient transitions in the ward, processes each patient present in the ward at each time point based on the patients current MRSA status. The following assumptions were used to formulate the individual-based model patient transitions:

1. each patient can only undergo one transition (discharge, colonization, infection, recovery, detection) per time period
2. susceptible patients have to be colonized before developing an infection
3. patient colonization will always be undetected when first colonized
4. colonized patients will not return to susceptible state
5. undetected colonized patients cannot transition directly to detected infected as it counts as two transitions (detection and infection)
6. detected colonized and infected patients cannot return to undetected state
7. detected colonized patients are placed under treatment and will not develop an infection
8. infected patients only recover to the colonized state, and not the susceptible state
9. detected infected patients are placed under appropriate treatment which increases their probability of recovery over their infection duration
10. undetected infected patients will not recover as they have not yet received appropriate treatment

At each time point t , each susceptible patient S can either leave the ward as susceptible with probability p_L , become colonized (but not detected) with probability p_C , or remain susceptible with probability p_S such that $p_L + p_C + p_S = 1$.

The probability of being colonized is modelled as $p_C = f_E(1 - p_L)$ where f_E is an increasing function of $E(t)$, $C_{xd}(t - 1)$, $C_d(t - 1)$, $I_{xd}(t - 1)$ and $I_d(t - 1)$. Specifically, the following form for f_E was used

$$f_E(t) = 1 - \exp \{-\nu(t)\Delta t\}$$

where $\nu(t) = \beta_0 + \beta_1 C_{xd}(t - 1) + \beta_2 C_d(t - 1) + \beta_3 I_{xd}(t - 1) + \beta_4 I_d(t - 1) + \beta_5 E(t)$ is the instantaneous hazard of being colonized or also known as the force of infection for this model, and $0 < f_E(t) < 1 \forall t$. Lastly, $p_S = (1 - f_E)(1 - p_L)$.

Each undetected colonized patient C_{xd} is detected with probability ρ (assumed to be the screening test sensitivity). Otherwise, the undetected colonized patient can either leave the ward with probability q_L , develop an infection with probability q_I , or remain colonized in ward with probability q_C such that $q_L + q_I + q_C = 1$. No additional structure is imposed on these probabilities values as it is assumed that each colonized patient will have the same probabilities.

Each detected colonized patient C_d can either leave the ward with probability q_L or remain colonized and detected with probability $1 - q_L$. Due to a lack of information to differentiate the probability of leaving for undetected and detected colonized patients, these were assumed to be same. One of the interventions considered (DECOL) increases the probability of leaving for just the detected colonized patients.

Each undetected infected patient I_{xd} can either be detected with probability ρ or remain undetected with probability $1 - \rho$.

Each detected infected patient I_d will have a probability r_C of recovering (transitioning to C_d) where

$$r_C(t|\psi, ti_k) = 1 - \exp\{-\psi(t - ti_k)\} \quad (8.1)$$

is an increasing function of the difference of the current time (t) and the time the individual became infected (ti_k). In other words, it is assumed that the longer a patient is infected, the more likely the patient will recover at the next time point. An infected patient remains infected with probability $1 - r_C$.

By definition, only the (approximate) date that a patient is detected to be colonized or infected is available from hospital surveillance databases. The transition times from susceptible to undetected with MRSA colonization, and subsequently undetected infection (ti_k) are typically imputed from a range of plausible values depending on the patient's admission date and screening test dates (Forrester et al., 2007).

An autoregressive-moving average time series model with exogenous covariates (ARMAX) (Hyndman and Athanasopoulos, 2013) is used to describe the environmental contamination levels $E(t)$. The exogenous covariates assumed to be contributing to the levels of environmental contamination at time t are the C_{xd} and I_{xd} patients in the ward at time $t - 1$. It is assumed that detected (colonized and infected) MRSA patients undergo decolonization treatments which halts shedding from patient to environment. The orders of the ARMAX model are determined using the `auto.arima()` function in the R package `forecast` (Hyndman and Khandakar, 2007).

8.2.2 Parameter values

The model parameter values used for the normal burden setting simulations (Section 8.3.1) are summarized in Table 8.1. Additional details of the parametrisation are provided in the supplementary material. The normal burden setting is reflective of MRSA burden in a typical hospital ward in a developed country. These parameters values are also used in the high burden setting simulations with the following modifications:

1. there is an additional factor of two multiplying $\nu(t)$
2. the probability of a colonized patient developing an infection q_I is doubled and q_C is reduced accordingly to ensure $q_L + q_I + q_C = 1$

3. there is decreased sensitivity in screening test $\rho = 0.6$

i.e. we assumed that in this setting, the hypothetical pathogen is more likely to colonize susceptible patients, colonized patients more readily develop an infection and it is harder to detect the presence of the pathogen. The high burden setting attempts to mimic either the MRSA dynamics in a developing country (Allegranzi et al., 2011) or a novel strain of pathogen that is more virulent and less readily detected by routine surveillance.

There were no available sources to estimate the parameter ω which represents the difference between colonized and infected patients on the force of infection. The ω value used to obtain the results in Sections 8.3.1 and 8.3.2 was 1 as a reflection of the lack of information on the parameter. alternative values of 0.5 and 2 were also investigated in the parameter sensitivity analysis (provided in the supplementary material). We found that the AR, C_{xd} and C_d outcomes (defined in Section 8.2.3) were particularly sensitive to a low value of ω (giving a stronger influence to colonized patients) in both normal and high burden settings. Distributions of AR outcome for the different values of ω are provided in Figure 8.2. Similar plots for the other outcomes and parameters are provided in the supplementary material.

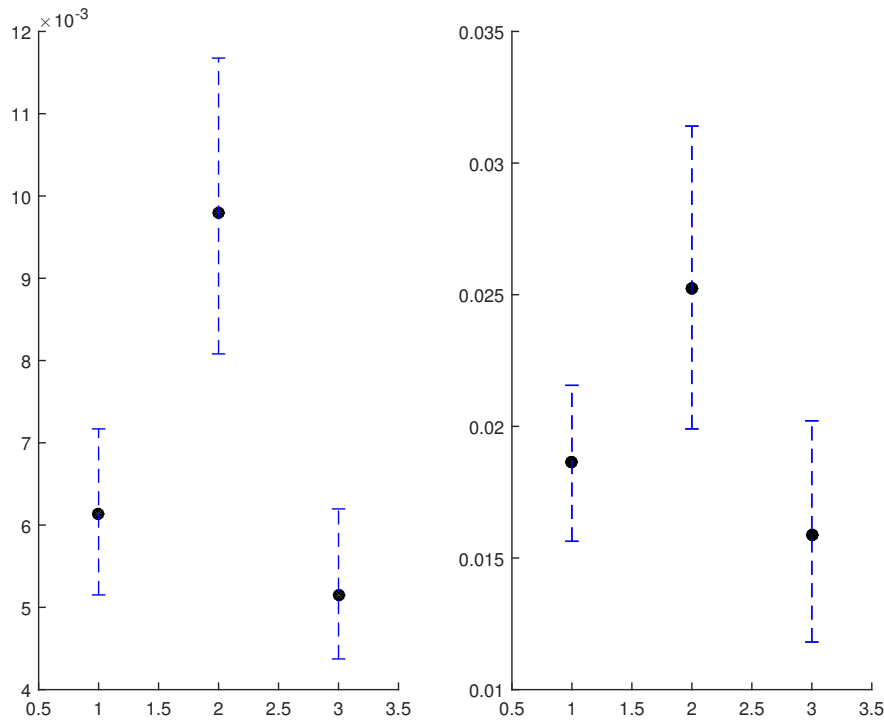


Figure 8.2: AR outcome for normal burden (left plot) and high burden (right plot) settings. The scenarios represented are the baseline, low ω value and high ω value moving from left to right along the x-axis.

8.2.3 Interventions

Five common intervention strategies were considered in the model investigation below:

1. no colonized on admission (COA) ($\vartheta = 1$) where all patients who are colonized on admission are assumed to be detected on admission and isolated elsewhere, i.e. universal screening (Harbarth et al., 2008).
2. improved environmental cleaning (ENV) which halved the intercept term in the environmental time series model (α_1) (Dancer et al., 2009).
3. improved contact precaution practices (CP) which decreases ν by a factor of ξ where ξ was set to 0.75 (Kypraios et al., 2010).
4. perfect screening test sensitivity (SENS) where test sensitivity ρ was set to 1 (McBryde et al., 2007b).
5. improved decolonization treatment for colonized patients (DECOL) where the probability for a C_d patient leaving the ward is now $q_L + \Delta$ (with the probability of staying adjusted accordingly) (McBryde et al., 2007b).

We considered six outcome measures for the investigations. They are the attack rate (AR) defined as the average force of infection (McBryde et al., 2007b)

$$\nu(t) = \beta_0 + \beta_1 C_{xd} + \beta_2 C_d + \beta_3 I_{xd} + \beta_4 I_d + \beta_5 E$$

as well as the cumulative numbers of

- patients who were colonized on admission (AC),
- patients who were colonized but not detected (C_{xd})
- detected, colonized patients (C_d)
- patients who were infected but not detected (I_{xd}), and
- detected, infected patients (I_d).

Note that there is a slight abuse of notations where C_{xd} , C_d , I_{xd} and I_d refer to the cumulative number of patients in each group for the outcome measures, but the time-varying prevalence of the groups in the model.

Due to the stochastic model formulation, each intervention setting was simulated 1000 times and we compared the distributional differences of the outcomes rather than just point estimates.

A natural choice for comparing samples from two distributions (denoted generally by X and Y here) is the generalized Mann–Whitney statistic ($\theta = Pr(Y > X) + \frac{1}{2}Pr(Y = X)$) which is estimated by $\hat{\theta} = \frac{U}{mn}$ where $U = \sum_{i=1}^m \sum_{j=1}^n \mathbf{1}(Y_j > X_i) + \frac{1}{2} \sum_{j=1}^n \mathbf{1}(Y_j = X_i)$ with $\{Y_j; j = 1, \dots, n\}$ and $\{X_i; i = 1, \dots, m\}$ being samples from the Y and X distributions respectively. The generalized MannWhitney statistic was used as it is a general measure of the distributional difference between two distributions which does not require parametric assumptions and accounts for ties in the data. Confidence intervals for $\hat{\theta}$ were computed based on Method 5 of Newcombe (2006).

Following the definition above, values of θ larger than 0.5 indicate that the Y distribution is larger than X and conversely, values of θ less than 0.5 indicate X is

larger than Y . For the results below, θ values between 0 and 0.2 (and similarly between 0.8 and 1) are considered strong evidence that the two distributions are substantially different. Intermediate θ values between 0.2 to 0.4 (or 0.6 to 0.8) are assumed to provide weak evidence of a difference between the distributions. Values of θ close to 0.5 (between 0.4 and 0.6) indicate that there is no evidence that the two distributions being compared are dissimilar.

8.3 Results

The results for the normal burden setting and high burden setting are summarized below. More detailed comparisons of the interventions combinations for all outcome measures using the generalized Mann–Whitney statistic are provided in the supplementary material.

The results for the AC, I_{xd} and I_d outcomes were similar for both the normal and high burden settings, and discussed together here. Results for the AR, C_{xd} and C_d outcomes are discussed separately for the normal burden setting (Section 8.3.1) and high burden setting (Section 8.3.2).

The most important intervention for the AC outcome was the COA intervention which eliminates the possibility of colonized patients being admitted. As such, the COA intervention (and any other intervention combinations which include COA) greatly outperforms interventions of any size which do not include the COA intervention in both settings. Any intervention combination which includes the COA intervention achieved 0 AC, whereas intervention combinations without the COA intervention produced AC distributions with 95% intervals that do not include 0.

The performance of the interventions on the I_d outcome was very similar to that for the I_{xd} since the only transition to I_d is through I_{xd} , i.e. eliminating the I_{xd} would also eliminate the I_d population. As such, only the results for the I_{xd} results are discussed for brevity as identical inferences apply to the I_d outcome. The SENS intervention was the most important intervention for the I_{xd} outcome as having perfect sensitivity would allow detection of all colonized patients prior to infection developing. As such, the best performing intervention of any size will include the SENS intervention.

However, it should also be noted that the I_{xd} outcome is generally small for the normal burden setting with even the baseline I_{xd} having a 95% interval of $[0, 2]$ (see Table 8.2).

In contrast with the normal burden setting, the SENS intervention (or any combination which includes the SENS intervention) was more favourable in the high burden setting. The SENS intervention substantially outperformed all intervention combinations which excluded the SENS intervention (Table 8.5).

8.3.1 Normal burden setting

Table 8.2 provides the numerical summary of the six outcomes under the baseline, and the various combinations of the five interventions investigated. The baseline scenario refers to the case without any interventions.

There were great improvements in reducing AR when increasing the number of interventions by up to three with the optimal triplet being {COA, ENV, CP} (mean (95% interval): $2.66 (2.20, 3.31) \times 10^{-3}$). This triplet outperformed the best single intervention (CP with AR of $4.32(3.69, 5.05) \times 10^{-3}$) and intervention pair ({COA, CP} with AR of $3.35(2.88, 4.01) \times 10^{-3}$). The addition of one extra intervention (either DECOL or SENS) to four in total did not improve the AR distribution ($2.50(2.13, 3.02) \times 10^{-3}$ and $2.53(2.19, 2.92) \times 10^{-3}$ respectively). However, there is a benefit in implementing all five interventions ($AR = 2.39(2.11, 2.71) \times 10^{-3}$) compared with just the best three interventions.

For the C_{xd} outcome, the two best performing pairs ({COA, CP} and {ENV, CP} with C_{xd} of 17.59 (10, 27) and 17.60 (9, 28) respectively) performed slightly better compared with the best single intervention (CP with C_{xd} of 20.78 (12, 31)). A similar performance gain was noted when comparing the best intervention triplet ({COA, ENV, CP} with $C_{xd} = 14.29$ (6, 24)) to both the best performing pairs. There was no substantial changes in the C_{xd} difference when comparing across the best performing triplet, quartets ({COA, ENV, CP, DECOL} and {COA, ENV, CP, SENS} with C_{xd} of 13.65 (6, 23) and 13.94 (6, 23) respectively) and the combination of all interventions (13.44 (6, 22)), indicating that there is little gain from considering anything beyond the best performing triplet in reducing the distributional outcome of C_{xd} for this scenario.

Comparing across different intervention sizes, there are notable reductions in support of considering additional number of interventions up to the best performing intervention triplet ({COA, ENV, CP} with C_d of 13.96 (6, 24)) for the C_d outcome. The best performing single intervention for the C_d outcome was COA (24.22 (14, 36)) and the best performing intervention pair was {COA, CP} (17.21 (9.5, 27)). There are no discernible difference in the C_d outcome distributions in implementing all five interventions ($C_d = 13.43(6, 22)$) or either of the two best performing quartets identified ({COA, ENV, CP, DECOL} and {COA, ENV, CP, SENS} with C_d of 13.32 (6, 22) and 13.95 (6, 23) respectively) compared with having just the best performing intervention triplet (with θ estimates ranging from 0.46 to 0.50).

8.3.2 High burden setting

The mean and 95% intervals for the six outcome measures across the different intervention combinations considered are in Table 8.4.

Compared with the baseline scenario in the normal burden setting (Table 8.2), we see notable increases in the average AR, C_{xd} , C_d , I_{xd} and I_d outcomes but a slight reduction in the AC outcome likely due to the decreased number of admissions overall as colonized and infected patients stay in the ward longer.

For the AR outcome in the high burden setting, there is evidence to consider implementing the maximum number of interventions possible (subject to resource constraint) beginning with the CP intervention ($12.44 (10.14, 14.83) \times 10^{-3}$), followed by the SENS intervention ($\{CP, SENS\}$ with AR of $9.50 (8.35, 10.79) \times 10^{-3}$), either the COA or ENV intervention ($\{COA, CP, SENS\}$ with AR of $7.88 (6.77, 9.14) \times 10^{-3}$ or $\{ENV, CP, SENS\}$ with AR $7.97 (6.71, 9.24) \times 10^{-3}$) or both ($\{COA, ENV, CP, SENS\}$ with AR $6.26 (5.10, 7.53) \times 10^{-3}$), up to all five interventions ($5.55 (4.73, 6.46) \times 10^{-3}$). The reduction in the AR distribution when moving from the best performing quartet to all intervention was not as great as the other increases in intervention sizes.

Only small gains were obtained from increasing the size of the intervention combinations sequentially for the C_{xd} outcome. More notable reductions were obtained by moving from the best performing single intervention (CP with C_{xd} of $45.46 (30, 61)$) to at least one of the best performing triplets ($\{ENV, CP, SENS\}$, $\{COA, ENV, CP\}$ or $\{COA, CP, SENS\}$ with C_{xd} 's of $36.57 (23, 50)$, $37.24 (22, 53)$ and $39.21 (26, 55)$ respectively), and similarly from one of the best performing intervention pairs ($\{ENV, CP\}$, $\{CP, SENS\}$ or $\{COA, CP\}$ with C_{xd} 's of $40.95 (28, 55.5)$, $42.70 (29.5, 58)$ and $43.56 (28, 60)$ respectively) to either the $\{COA, ENV, CP, SENS\}$ quartet ($32.02 (19, 46)$) or all five interventions ($29.95 (17, 45)$).

For the C_d outcome measure, the results obtained suggest it would be beneficial to consider up to the best performing triplet of interventions ($\{COA, ENV, CP\}$ with C_d $33.85 (20, 49)$) subject to resource constraints. The best performing single interventions were COA ($53.96 (39, 72.5)$) and CP ($55.58 (39, 74)$), and the best performing intervention pair was $\{COA, CP\}$ ($39.72 (26, 55)$). There was only a slight gain in moving from the best performing triplet to the combination of all interventions ($29.95 (17, 45)$). The two best performing intervention quartets ($\{COA, ENV, CP, SENS\}$ and $\{COA, ENV, CP, DECOL\}$) (with C_d 's of $32.02 (19, 46)$ and $32.80 (19, 49)$ respectively) did not yield C_d distributions substantially different from the best performing triplet.

8.4 Discussion

The results from the proposed stochastic model showed that there are differences in the optimal set of interventions depending on the outcome measure of interest as well as the burden setting of the pathogen (as summarized in Table 8.6).

For the AC outcome, I_{xd} and I_d outcome measures where one of the interventions considered eradicated the respective outcome measure (COA for the AC outcome and SENS for both I_{xd} and I_d), only that particular intervention was required. This finding,

particular for the I_{xd} and I_d outcome measures, may not be terribly realistic given that there is always some amount of delay between sample collection and the corresponding action based on the screening results. However, the θ performance measure still showed that in the normal burden setting, eradication of I_{xd} and I_d was only a slight improvement compared with the other intervention combinations and the baseline because of the already low baseline I_{xd} and I_d prevalence. This is not the case in the high burden setting where eradication of the I_{xd} and I_d outcomes with the SENS intervention was drastically different from the other intervention combinations which exclude SENS and the baseline scenario. The addition of the aforementioned small delay would have affected all scenarios considered equally and would unlikely have changed the finding in the normal burden setting. It is also unlikely to change the findings in the high burden setting unless the delay was substantive (in the order of days).

The model presented used parameter estimates combined from multiple sources (see Table 8.1). While it would be ideal if the model parameters were all obtained from one source, this is frequently not the case in such modelling studies where the hypothetical investigations considered typically require some form of data collation from multiple sources in order to fully parametrize the model (Doan et al., 2015, Hall et al., 2012, McBryde et al., 2007b, Wang et al., 2012, 2013, Wolkewitz et al., 2008). It could also be argued that this provides such modelling studies with a level of flexibility that could not be obtained from clinical intervention studies.

The lack of additional individual patient data for this study also precluded demonstration of the full utility of the individual-based patient transition component in the model. For this application, only the patient transition from I_d to C_d was based on their individual infection times (as measured in (8.1)). However, the model can readily include individual-specific covariates into other transition probabilities in the model as well.

There are a number of extensions to our stochastic model that were not considered here. Most of these extensions also involve additional data structures that are not readily available.

One extension is to generalize the force of infection term such that the colonization threshold is no longer constant (Streftaris and Gibson, 2012). Under the current model formulation, the probability of a patient being colonized is only a function of the current force of infection. However, the generalization proposed in Streftaris and Gibson (2012) allows for this transition to also depend on the accumulation of the force of infection terms from a patient's admission date to their colonization date. This quantity is known as the colonization threshold and requires prior knowledge or imputation of the colonization date to compute. This extension is another approach to incorporate patient heterogeneity into the model, specifically related to patient susceptibility.

Another potential extension is to build up the one ward model into a multi-ward model using one of the meta-population models (Riley, 2007, Rock et al., 2014) such as the multi-patch models (where each patch represents a ward) or more generally, temporal network models taking into account the fact that the edges between nodes change quite frequently with staff shift changes, and patient admissions and discharges, making the temporal element of the network more important (Holme, 2015, Pastor-Satorras et al., 2015). The high-frequency contact data required for such models have only recently been collected (Obadia et al., 2015) and could prove to be a promising research avenue in providing a realistic, detailed representation of hospital pathogen transmission in a ward.

Supplementary Materials

Supplementary materials are provided in Section F.

Acknowledgements:

X.J.L. receives PhD scholarship funding from the Centre of Research Excellence in Reducing Healthcare Associated Infections (NHMRC Grant 1030103). A.N.P.

acknowledges the financial support obtained from the Australian Research Council

through a Discovery Grant DP110100159. F.R. acknowledges the financial support

obtained as Adjunct Professor from the Institute for Future Environments, Queensland University of Technology.

Declaration of interest:

None.

Symbol	Definition ^a	Value	Source ^b
M	Maximum ward capacity ($S(t) + C(t) + I(t) + A(t) = M$)	20	data
λ	weekly admission rate to ward	5	data
ϑ	probability of being susceptible on admission	0.95	(Robotham et al., 2011)
p_L	probability of leaving the ward as a susceptible patient	0.1155	(De Angelis et al., 2011)
q_L	probability of leaving the ward as a colonized patient	0.053	(De Angelis et al., 2011)
q_I	probability of a colonized patient developing an infection	0.047	(Robotham et al., 2011)
q_C	probability of a colonized patient remaining colonized	$1 - q_L - q_I \approx 0.900$	
ψ	functional form parameter for probability of recovering from infection to colonized state	0.029	(De Angelis et al., 2011)
ρ	screening test sensitivity	0.8	assumption
β_0	intercept term associated with f_E ($\times 10^5$)	190	data
β_1	undetected colonized patients related parameter in expression for f_E ($\times 10^5$)	$660 \times \frac{2}{\omega+1}$	unpublished observations
β_2	detected colonized patients related parameter in expression for f_E ($\times 10^5$)	$48 \times \frac{2}{\omega+1}$	unpublished observations
β_3	undetected infected patients related parameter in expression for f_E	$\omega\beta_1$	unpublished observations
β_4	detected infected patients related parameter in expression for f_E	$\omega\beta_2$	unpublished observations
β_5	environmental contamination related parameter in expression for f_E ($\times 10^5$)	2.7	unpublished observations
ω	ratio difference between effects of colonized and infected patients in f_E	1	assumption
a_1	AR(1) coefficient	1.40(0.08)	data
a_2	AR(2) coefficient	-0.48(0.08)	data
b_1	MA(1) coefficient	0.34(0.09)	data
b_0	MA(2) coefficient	0.30(0.06)	data
α_1	time series time-constant mean parameter	60(5)	data
α_2	time series coefficient for C at previous time period	-0.07(0.4)	data
α_3	time series coefficient for I at previous time period	0.06(0.3)	data
α_4	time series coefficient for intervention	-0.10(3.7)	data
σ^2	white noise variance	24.5	data

Table 8.1: Parameter estimates for the stochastic model describing MDRO transmission in a hospital ward.

^aAR, autoregressive; MA, moving average.

^bUnpublished observations are estimates obtained from fitting a non-homogeneous Poisson process to the data. More details provided in the supplementary material.

	AR $\times 10^3$	AC	C_{xd}	C_d	I_{xd}	I_d
baseline	6.14 (5.15, 7.17)	20.91 (12.5, 30)	28.53 (17, 41.5)	48.24 (34, 63)	0.56 (0, 2)	0.56 (0, 2)
COA	4.82 (4.04, 5.71)	0	24.79 (14, 37)	24.22 (14, 36)	0.27 (0, 2)	0.27 (0, 2)
ENV	5.14 (4.30, 6.22)	21.22 (13, 30)	24.10 (13, 35)	44.26 (31, 58)	0.51 (0, 2)	0.5 (0, 2)
CP	4.32 (3.69, 5.05)	21.52 (13, 30)	20.78 (12, 31)	41.29 (30, 55)	0.47 (0, 2)	0.47 (0, 2)
SENS	5.69 (4.98, 6.43)	22.07 (14, 31)	27.13 (17, 40)	49.20 (36, 64)	0	0
DECOL	5.57 (4.79, 6.61)	23.57 (15, 34)	27.57 (16, 41)	49.91 (36, 66)	0.59 (0, 2)	0.58 (0, 2)
COA, ENV	3.84 (3.13, 4.76)	0	19.94 (10, 32)	19.44 (10, 30)	0.23 (0, 1)	0.23 (0, 1)
COA, CP	3.35 (2.88, 4.01)	0	17.59 (10, 27)	17.21 (9.5, 27)	0.18 (0, 1)	0.18 (0, 1)
COA, SENS	4.58 (3.95, 5.35)	0	23.98 (13, 37)	23.98 (13, 37)	0	0
COA, DECOL	4.5 (3.88, 5.32)	0	24.26 (13.5, 36)	23.70 (13, 35)	0.27 (0, 2)	0.27 (0, 2)
ENV, CP	3.64 (3.00, 4.37)	21.76 (13.5, 31)	17.60 (9, 28)	38.37 (26, 51)	0.47 (0, 2)	0.46 (0, 2)
ENV, SENS	4.77 (4.08, 5.52)	22.43 (14, 31)	23.33 (13, 35)	45.76 (32, 61)	0	0
ENV, DECOL	4.65 (3.84, 5.55)	23.74 (15, 33)	23.37 (13, 35)	45.98 (32, 61)	0.55 (0, 2)	0.55 (0, 2)
CP, SENS	4.05 (3.56, 4.57)	22.80 (14, 32)	19.83 (11, 30)	42.63 (30, 57)	0	0
CP, DECOL	3.98 (3.42, 4.67)	23.97 (14.5, 33.5)	20.37 (11, 31)	43.25 (30, 58)	0.58 (0, 2)	0.58 (0, 2)
SENS, DECOL	5.12 (4.55, 5.72)	24.77 (16, 35)	26.34 (16, 38)	51.11 (36, 66)	0	0
COA, ENV, CP	2.66 (2.20, 3.31)	0	14.29 (6, 24)	13.96 (6, 24)	0.15 (0, 1)	0.16 (0, 1)
COA, ENV, SENS	3.59 (3.04, 4.25)	0	18.91 (10, 30)	18.91 (10, 30)	0	0
COA, ENV, DECOL	3.54 (2.98, 4.35)	0	19.02 (10, 29)	18.57 (10, 28)	0.20 (0, 1)	0.20 (0, 1)
COA, CP, SENS	3.22 (2.82, 3.67)	0	17.47 (9, 28)	17.48 (9, 28)	0	0
COA, CP, DECOL	3.18 (2.77, 3.79)	0	17.33 (8, 28)	16.90 (8, 27)	0.19 (0, 1)	0.19 (0, 1)
COA, SENS, DECOL	4.24 (3.81, 4.71)	0	23.12 (13, 34)	23.14 (13, 34)	0	0
ENV, CP, SENS	3.38 (2.88, 3.92)	22.62 (14, 31.5)	16.82 (8, 27)	39.45 (26.5, 53)	0	0
ENV, CP, DECOL	3.30 (2.80, 3.95)	23.76 (15, 33)	16.96 (8, 27)	39.72 (27, 54)	0.48 (0, 2)	0.48 (0, 2)
ENV, SENS, DECOL	4.21 (3.65, 4.79)	24.70 (15, 35)	21.71 (12, 33)	46.38 (31, 63.5)	0	0
CP, SENS, DECOL	3.67 (3.26, 4.08)	24.58 (16, 34)	19.12 (10, 29)	43.70 (31, 59)	0	0
COA, ENV, CP, SENS	2.53 (2.19, 2.92)	0	13.94 (6, 23)	13.95 (6, 23)	0	0
COA, ENV, CP, DECOL	2.5 (2.13, 3.02)	0	13.65 (6, 23)	13.32 (6, 22)	0.15 (0, 1)	0.14 (0, 1)
COA, ENV, SENS, DECOL	3.34 (2.91, 3.81)	0	18.57 (9, 29.5)	18.57 (9, 29.5)	0	0
COA, CP, SENS, DECOL	3.04 (2.73, 3.38)	0	16.88 (9, 27)	16.87 (9, 27)	0	0
ENV, CP, SENS, DECOL	3.02 (2.66, 3.41)	24.96 (16, 35.5)	15.88 (9, 25)	40.84 (28, 56)	0	0
all	2.39 (2.11, 2.71)	0	13.44 (6, 22)	13.43 (6, 22)	0	0

Table 8.2: Numerical summaries of output measures for normal burden setting.

outcome	comparison	$\hat{\theta}$ (95% CI)
AR	CP v baseline	0.00 (0.00, 0.00)
	{COA, CP} v CP	0.02 (0.01, 0.03)
	{COA, ENV, CP} v {COA, CP}	0.04 (0.04, 0.06)
	{COA, ENV, CP, DECOL} v {COA, ENV, CP}	0.33 (0.30, 0.35)
	{COA, ENV, CP, SENS} v {COA, ENV, CP}	0.38 (0.35, 0.40)
	all v {COA, ENV, CP}	0.20 (0.18, 0.22)
	all v {COA, ENV, CP, DECOL}	0.35 (0.33, 0.38)
	all v {COA, ENV, CP, SENS}	0.28 (0.26, 0.30)
C_{xd}	CP v baseline	0.17 (0.15, 0.19)
	{COA, CP} v CP	0.32 (0.30, 0.35)
	{ENV, CP} v CP	0.33 (0.30, 0.35)
	{COA, ENV, CP} v {COA, CP}	0.30 (0.28, 0.33)
	{COA, ENV, CP} v {ENV, CP}	0.31 (0.29, 0.33)
	{COA, ENV, CP, DECOL} v {COA, ENV, CP}	0.46 (0.44, 0.49)
	{COA, ENV, CP, SENS} v {COA, ENV, CP}	0.48 (0.46, 0.51)
	all v {COA, ENV, CP}	0.45 (0.42, 0.47)
	all v {COA, ENV, CP, DECOL}	0.49 (0.46, 0.51)
	all v {COA, ENV, CP, SENS}	0.47 (0.44, 0.49)
C_d	COA v baseline	0.01 (0.00, 0.01)
	{COA, CP} v COA	0.17 (0.15, 0.19)
	{COA, ENV, CP} v {COA, CP}	0.31 (0.28, 0.33)
	{COA, ENV, CP, DECOL} v {COA, ENV, CP}	0.46 (0.44, 0.49)
	{COA, ENV, CP, SENS} v {COA, ENV, CP}	0.50 (0.48, 0.53)
	all v {COA, ENV, CP}	0.47 (0.44, 0.49)
	all v {COA, ENV, CP, DECOL}	0.51 (0.48, 0.53)
	all v {COA, ENV, CP, SENS}	0.47 (0.44, 0.49)

Table 8.3: Summary of intervention combination comparisons for the normal burden setting.

	AR $\times 10^3$	AC	C_{xd}	C_d	I_{xd}	I_d
baseline	18.63 (15.63, 21.56)	13.83 (6, 23)	60.73 (45, 78)	68.07 (49, 88)	4.20 (1, 8)	4.20 (1, 8)
COA	16.22 (12.55, 19.76)	0	59.22 (43.5, 78)	53.96 (39, 72.5)	3.41 (0, 8)	3.41 (0, 8)
ENV	16.42 (13.16, 19.59)	14.32 (6, 24)	55.39 (39.5, 72)	63.52 (47, 82)	3.97 (1, 8)	3.97 (1, 8)
CP	12.44 (10.14, 14.83)	15.57 (7, 25)	45.46 (30, 61)	55.58 (39, 74)	3.52 (0, 7)	3.52 (0, 7)
SENS	14.00 (12.17, 15.92)	20.20 (13, 29)	58.57 (42, 75)	78.79 (61, 98)	0	0
DECOL	17.61 (14.26, 20.91)	16.44 (7, 27)	63.51 (45, 82)	72.99 (52, 96)	4.52 (1, 9)	4.51 (1, 9)
COA, ENV	13.70 (9.91, 17.42)	0	52.63 (34, 70.5)	47.98 (31.5, 65)	3.04 (0, 7)	3.05 (0, 7)
COA, CP	10.33 (7.94, 13.11)	0	43.56 (28, 60)	39.72 (26, 55)	2.45 (0, 6)	2.44 (0, 6)
COA, SENS	11.85 (10.13, 13.83)	0	54.80 (37, 73.5)	54.81 (37, 73)	0	0
COA, DECOL	14.85 (11.32, 18.85)	0	61.01 (43, 80.5)	55.65 (38, 74)	3.33 (0, 7.5)	3.33 (0, 8)
ENV, CP	10.82 (8.63, 13.19)	16.12 (8, 25)	40.95 (28, 55.5)	52.04 (37, 68)	3.26 (0, 7)	3.26 (0, 7)
ENV, SENS	11.90 (10.05, 13.81)	20.70 (12, 30)	51.55 (36, 69)	72.25 (54, 93)	0	0
ENV, DECOL	15.33 (11.98, 18.64)	17.20 (8, 27)	57.71 (41, 77)	68.36 (49.5, 88)	4.22 (1, 8)	4.23 (1, 8)
CP, SENS	9.5 (8.35, 10.79)	21.33 (13, 30)	42.70 (29.5, 58)	64.05 (48, 81)	0	0
CP, DECOL	11.66 (9.34, 14.13)	18.35 (9, 28)	46.70 (32.5, 63)	59.37 (43, 79)	3.65 (1, 8)	3.66 (1, 8)
SENS, DECOL	12.22 (10.71, 13.81)	24.48 (16, 34)	58.48 (41.5, 79)	82.98 (63, 105)	0	0
COA, ENV, CP	8.51 (6.09, 11.46)	0	37.24 (22, 53)	33.85 (20, 49)	2.23 (0, 6)	2.23 (0, 6)
COA, ENV, SENS	9.56 (7.72, 11.62)	0	45.56 (27.5, 63)	45.53 (27.5, 63)	0	0
COA, ENV, DECOL	12.44 (8.80, 16.63)	0	52.54 (35, 72)	47.73 (32, 66.5)	3.10 (0, 7)	3.08 (0, 7)
COA, CP, SENS	7.88 (6.77, 9.14)	0	39.21 (26, 55)	39.22 (26, 55)	0	0
COA, CP, DECOL	9.55 (7.30, 12.11)	0	43.19 (28, 59)	39.34 (26, 54.5)	2.47 (0, 6)	2.48 (0, 6)
COA, SENS, DECOL	10.33 (8.89, 11.77)	0	52.55 (34, 71)	52.52 (34, 71.5)	0	0
ENV, CP, SENS	7.97 (6.71, 9.24)	21.55 (14, 30)	36.57 (23, 50)	58.10 (42, 74)	0	0
ENV, CP, DECOL	10.11 (7.72, 12.68)	18.54 (9, 29)	41.32 (27, 57)	54.60 (39, 72.5)	3.43 (0, 7)	3.42 (0, 7)
ENV, SENS, DECOL	10.14 (8.65, 11.60)	24.76 (15, 35)	49.23 (33, 66.5)	73.98 (53, 94)	0	0
CP, SENS, DECOL	8.38 (7.40, 9.38)	24.59 (15, 34)	41.43 (28, 56)	65.97 (49, 84)	0	0
COA, ENV, CP, SENS	6.26 (5.10, 7.53)	0	32.02 (19, 46)	32.02 (19, 46)	0	0
COA, ENV, CP, DECOL	7.71 (5.51, 10.51)	0	36.02 (20, 53)	32.80 (19, 49)	2.08 (0, 5.5)	2.08 (0, 5.5)
COA, ENV, SENS, DECOL	8.18 (6.90, 9.61)	0	42.35 (25.5, 60.5)	42.37 (26, 60.5)	0	0
COA, CP, SENS, DECOL	7.03 (6.26, 7.93)	0	37.21 (24, 53)	37.22 (24, 53)	0	0
ENV, CP, SENS, DECOL	6.92 (5.96, 7.96)	24.59 (15, 35)	34.80 (22, 50)	59.40 (41, 78.5)	0	0
all	5.55 (4.73, 6.46)	0	29.95 (17, 45)	29.95 (17, 45)	0	0

Table 8.4: Numerical summaries of output measures for high burden setting.

outcome	comparison	$\hat{\theta}$ (95% CI)
AR	CP v baseline	0.00 (0.00, 0.00)
	{CP, SENS} v CP	0.01 (0.01, 0.02)
	{COA, CP, SENS} v {CP, SENS}	0.03 (0.02, 0.04)
	{ENV, CP, SENS} v {CP, SENS}	0.04 (0.04, 0.05)
	{COA, ENV, CP, SENS} v {COA, CP, SENS}	0.03 (0.02, 0.04)
	{COA, ENV, CP, SENS} v {ENV, CP, SENS}	0.03 (0.02, 0.04)
	all v {COA, ENV, CP, SENS}	0.16 (0.15, 0.18)
C_{xd}	CP v baseline	0.09 (0.08, 0.10)
	{ENV, CP} v CP	0.33 (0.31, 0.36)
	{CP, SENS} v CP	0.39 (0.37, 0.42)
	{COA, CP} v CP	0.43 (0.40, 0.45)
	{ENV, CP, SENS} v CP	0.19 (0.18, 0.21)
	{COA, ENV, CP} v CP	0.22 (0.20, 0.24)
	{COA, CP, SENS} v CP	0.27 (0.25, 0.30)
	{ENV, CP, SENS} v {ENV, CP}	0.33 (0.31, 0.36)
	{COA, ENV, CP} v {ENV, CP}	0.36 (0.34, 0.38)
	{COA, CP, SENS} v {ENV, CP}	0.43 (0.40, 0.45)
	{ENV, CP, SENS} v {CP, SENS}	0.27 (0.25, 0.30)
	{COA, ENV, CP} v {CP, SENS}	0.30 (0.28, 0.33)
	{COA, CP, SENS} v {CP, SENS}	0.37 (0.34, 0.39)
	{ENV, CP, SENS} v {COA, CP}	0.25 (0.23, 0.27)
	{COA, ENV, CP} v {COA, CP}	0.28 (0.26, 0.30)
	{COA, CP, SENS} v {COA, CP}	0.34 (0.32, 0.36)
	{COA, ENV, CP, SENS} v {ENV, CP}	0.19 (0.17, 0.21)
	{COA, ENV, CP, SENS} v {CP, SENS}	0.15 (0.13, 0.17)
	{COA, ENV, CP, SENS} v {COA, CP}	0.14 (0.12, 0.16)
	{COA, ENV, CP, SENS} v {ENV, CP, SENS}	0.33 (0.30, 0.35)
	{COA, ENV, CP, SENS} v {COA, ENV, CP}	0.32 (0.29, 0.34)
	{COA, ENV, CP, SENS} v {COA, CP, SENS}	0.25 (0.23, 0.27)
	all v {ENV, CP}	0.13 (0.12, 0.15)
	all v {CP, SENS}	0.10 (0.09, 0.12)
	all v {COA, CP}	0.10 (0.08, 0.11)
	all v {ENV, CP, SENS}	0.25 (0.23, 0.27)
	all v {COA, ENV, CP}	0.24 (0.22, 0.26)
	all v {COA, CP, SENS}	0.18 (0.16, 0.20)
	all v {COA, ENV, CP, SENS}	0.42 (0.39, 0.44)
C_d	COA v baseline	0.14 (0.12, 0.15)
	{COA, CP} v COA	0.10 (0.09, 0.11)
	{COA, ENV, CP} v COA	0.03 (0.03, 0.04)
	{COA, ENV, CP} v {COA, CP}	0.28 (0.26, 0.30)
	{COA, ENV, CP, SENS} v {COA, CP}	0.23 (0.21, 0.25)
	{COA, ENV, CP, DECOL} v {COA, CP}	0.25 (0.23, 0.27)
	{COA, ENV, CP, SENS} v {COA, ENV, CP}	0.43 (0.41, 0.46)
	{COA, ENV, CP, DECOL} v {COA, ENV, CP}	0.46 (0.43, 0.48)
	all v {COA, CP}	0.16 (0.15, 0.18)
	all v {COA, ENV, CP}	0.35 (0.32, 0.37)
	all v {COA, ENV, CP, SENS}	0.42 (0.39, 0.44)
	all v {COA, ENV, CP, DECOL}	0.39 (0.37, 0.41)

Table 8.5: Summary of intervention combination comparisons for the high burden setting.

Outcome measure	normal burden setting	high burden setting
AR	CP, COA, ENV, DECOL // SENS	CP, SENS, COA // ENV, DECOL
AC	COA .	COA .
C_{xd}	CP, COA // ENV DECOL // SENS	CP, ENV // COA // SENS DECOL
C_d	COA, CP, ENV DECOL // SENS	COA // CP, ENV SENS // DECOL
I_{xd}	SENS .	SENS .
I_d	SENS .	SENS .

Table 8.6: Overall order of importance for the five interventions considered under the normal and high burden setting. // denotes exchangeability in the order of the interventions and || denotes the optimal sized interventions i.e. addition of interventions to the right of the || symbol would not affect the associated outcome measure.

9 Conclusions

9.1 Summary

The investigations on the use of the ABMC model selection method developed in Chapter 3 showed that it can be successfully applied to model selection problems for a wide variety of pathogen transmission models (Chapter 3) as well as computationally intensive models for spatial extremes (Chapter 4). For the pathogen transmission data sets investigated in Chapter 3, it was shown that:

- MRSA transmission in an ICU is more likely facilitated by pseudo-mass action transmission (facilitated by contact between individuals) rather than Greenwood based transmission (which is more indicative of airborne transmission)
- the latent period is an important part of the transmission of influenza in an historical outbreak data set collected from the remote island of Tristan da Cunha
- the multitype epidemic model was strongly preferred in explaining an historical measles outbreak in the German village Hagelloch, suggesting that the additional complexity of a network model was not necessary to describe the outbreak.

The ABMC algorithm also inferred that the Brown–Resnick model was the most preferred spatial max-stable models to describe the South Australia maximum temperature, out of the six competing max-stable models (Chapter 4). The powered exponential and Whittle–Matérn models also have notable posterior support in the final SMC iteration. The Smith, Cauchy and Bessel models were unlikely candidate max-stable models to explain the spatial dependence present in the data set.

In Chapter 5, the temporal heterogeneity of MRSA occurrences in hospital beds within wards of a hospital was highlighted despite the coarse time scale of the data (weekly), extending the spatial heterogeneity finding of Kong et al. (2012) for the same data set. Knowledge on the temporal dynamics of these MRSA occurrences could provide a useful measure to quantify efficacy of changes in terminal cleaning practices (cleaning performed on the patient’s bed and surrounding area after patient discharge). It is also useful in identifying ward-cubicles which require more stringent infection control policies

to control the carryover effect from previous MRSA-positive patients in the same bed or ward-cubicle.

The factors driving an MRSA outbreak in a neonatal intensive care unit were investigated in Chapter 6. The analysis showed that colonisation pressure had a statistically significant effect in increasing the hazard of acquiring MRSA during the outbreak and it should be further investigated if improved infection control and prevention practices could ameliorate this effect (thus potentially minimising the size of the outbreak). It was also found that MRSA acquisition was associated with a longer length of stay, consistent with adult ICU findings.

Chapter 7 focused on a single ward to avoid the potential heterogeneity arising from including more than one ward given the limited information available from the data set (see also heterogeneity finding from Chapter 5). The results in Chapter 7 provided a quantification of relative contribution of the microbiological environmental contamination to MRSA incidence in a hospital ward. While the model used in Chapter 7 is relatively simplistic, it is the first quantification of environmental contamination based on actual environmental contamination data. These results do support an increased focus on appropriate hospital cleaning as well as encourage the collection of microbiological surveillance data of hospital cleanliness.

The parameter estimates from Chapter 7 were then used in Chapter 8 to parametrise the stochastic hospital ward MRSA transmission simulation model developed. Such simulation models are useful tools to explore the impacts of intervention combinations which may not be possible to evaluate in a clinical setting due to cost or ethical constraints, to add value to existing clinical intervention data, and to determine intervention combinations for future investigation in a clinical setting. The novelty of this particular model is that it coupled the temporal evolution of the environmental contamination with the patient MRSA acquisition. The modelling of environmental contamination is important to accurately capture the effect of cleaning interventions which directly affects environmental contamination rather than the patients. The model was used to investigate the impact of five common interventions, including a cleaning intervention, and their various combinations on six outcome measures. We also used the Mann–Whitney statistic to compare the distributions of the indicators under pairs of different intervention combinations to assess if one of the distributions under comparison can be considered to be stochastically dominating the other. We are not aware of the use of the Mann–Whitney statistic in this capacity in the literature.

9.2 Future work

The main focus of this thesis was on furthering our understanding of MRSA transmission in a hospital setting, with a particular focus on the role of environmental contamination. An obvious next step is to use the findings to inform MRSA

transmission models used to investigate impacts of different interventions, particularly if the interventions include environmental cleaning. It was achieved to some degree with the work presented in Chapter 8. However, there still exists room for improvement. A vital extension to the work would be to also incorporate economic modelling in order to assess the cost-effectiveness of the interventions (see for example Robotham et al. (2016, 2011)). The added cost-effectiveness dimension to such modelling work would provide compelling evidence for implementing or disinvesting from particular interventions given the constantly increasing healthcare demand and limited health budget.

The NHPP model used in quantifying the relative contribution of microbiological environmental contamination to MRSA incidence in Chapter 7 has a relatively simple structure as motivated by the available information in the data set and knowledge that both measures of interest, MRSA incidence and microbiological environmental contamination, are highly variable. A few potential extensions to the model are presented below provided appropriately informative data are available.

Community associated (CA) MRSA incidences in hospital settings have been on the rise (Nimmo et al., 2013) and future work should incorporate the influences of CA MRSA. If it is possible to quantify the burden of CA MRSA for a particular hospital, which is likely to be a function of the hospital catchment area, it is straightforward then to include this quantity as an additional input into the intensity function similar to how the environmental contamination was incorporated in Chapter 7. In addition, the relative colonisation risk measure used in Forrester (2006) and Chapter 7 can be readily adapted to quantify the relative contribution from CA MRSA.

Heterogeneity in patient susceptibility can be addressed within the NHPP model framework. Incorporation of patient-specific susceptibility can be straightforwardly done through addition of patient-specific covariates into the hazard function as illustrated in Cooper et al. (2008). Some known patient risk factors that affect a patient's MRSA susceptibility include antibiotic exposure (Catry et al., 2014, Tacconelli et al., 2008), use of invasive medical devices (Oztoprak et al., 2006), presence of skin lesions (Lucet et al., 2003) and age (Catry et al., 2014, Lucet et al., 2003). An alternative way of incorporating heterogeneous susceptibility without specification of individual patient covariates is described in Streftaris and Gibson (2012). The authors proposed the use of a Weibull distribution to model the infection threshold of patients. In a typical NHPP formulation, the infection threshold is exponentially distributed.

Incorporating heterogeneity in infectivity is more challenging and requires additional information on the patients, specifically knowledge on the potential contacts each patient has, directly or indirectly. Such data are expensive and challenging to collect, and have only recently been investigated. Obadia et al. (2015) collected these contact data from wireless sensors provided to both patients and HCWs. The multitype epidemic and contact network models used in the Hagelloch measles example in Chapter 3 are ideal transmission models to use with such data.

The inclusion of genome data, in particular whole genome sequencing (WGS) data, would be of great interest to further the knowledge of transmission pathways of MRSA. WGS data are beginning to be collected more frequently, particularly in MRSA outbreaks in NICUs. The NHPP model used in Chapter 7 can be extended to incorporate this genetic information in an attempt to construct a probabilistic transmission networks (Worby et al., 2016) and could form an alternative way of parametrising models with heterogeneous infectivity, as discussed previously. However, there still exist some issues that need to be resolved (Didelot et al., 2014, Worby et al., 2014). In particular, the bacterial diversity of the pathogen has to be appropriately quantified prior to being able to accurately infer the transmission network. Additionally, the reconstructed transmission networks from WGS data are typically associated with high uncertainty (Didelot et al., 2014). As such, the current method proposed requires high frequency sampling which is not currently part of routine data collection in the clinical setting. However, with decreasing cost of genome sequencing and improvements in analytical tools for such data (Price et al., 2013), it is likely that WGS could be adopted into routine surveillance practices in the healthcare setting (Aanensen et al., 2016, Ugolotti et al., 2016).

Another potential research area in the modelling of MDRO is the evolution, spread and competition between different strains of the pathogen, with particular focus on the competition between susceptible and resistant strains of a pathogen, and the potential impact of antimicrobial use on prevalence of either strain. Recent reviews on the topic are provided in Opatowski et al. (2011) and Spicknall et al. (2013). Such models could provide interesting insights into the competitive dynamics between strains and could possibly be applied to model the competition between HA and CA MRSA (D'Agata et al., 2010, Kouyos et al., 2013). This is also another research area that would likely benefit from the increasingly detailed genomic data to better distinguish between different strains.

The stochastic simulation model investigation presented in Chapter 8 could be extended in a number of ways. A more systematic investigation of the interventions and their combinations could be undertaken using a factorial experimental design instead, particularly if there is interest in considering more than two levels, in factorial experiment design terminology, for each intervention (i.e. beyond the absence or presence of an intervention). For example, the separate investigations of varying individual intervention effects in Section F.3 and the investigations of different intervention combinations presented in Section 8.3 could potentially be combined in a factorial experiment setup. The stochastic model itself could also be extended to include the healthcare workers as separate entities in the models with their own states provided the associated parameters can be sourced. Extensions to multiple wards, and potentially the entire hospital (or multiple neighbouring hospitals for a regional perspective), could also be considered at the expense of a substantial increase in computational effort and storage required to track each individual's progression in the simulations.

The relatively straightforward model structures used here allows them to be easily adapted to other potential hospital pathogens of concern, subject to availability of appropriate data. In particular, there is a rising concern for highly resistant gram-negative organisms such as extended-spectrum β -lactamase producing enterobacteriaceae and carbapenem-resistant enterobacteriaceae (Huttner et al., 2013, Peleg and Hooper, 2010). Environmental contamination is likely to be a viable transmission pathway from these gram-negative organisms, possibly even more so compared with MRSA, as they have been shown to persist longer on inanimate surfaces (Kramer et al., 2006). It could also be of interest in modelling other infectious diseases that can be spread via an environmental contamination reservoir, e.g. Ebola, cholera.

The work presented in this thesis has focused on the transmission of MRSA in individual hospital wards. A different perspective that was not investigated here is the regional or spatial spread of MRSA between hospitals. Network models have been used to investigate the spread of MRSA through patient transfers between hospitals. In such investigations, each hospital is a node in the network and is connected to other hospitals through patient transfers, i.e., MRSA is “transmitted” between hospitals through the transfer on MRSA-positive patients (Ciccolini et al., 2014, Donker et al., 2012, Lee et al., 2011). Network models are one example of spatial extensions to the models investigated here for disease transmission. Caprarelli and Fletcher (2014) and Rock et al. (2014) are recent reviews on relevant spatial statistical and mathematical models respectively. The max-stable models in Chapter 4 could be used in such spatial investigations to interpolate spatial (extreme) covariates to or near hospital locations in order to investigate the potential association between maximum temperature and hospital admissions (Hajat et al., 2010) or infections (Schwab et al., 2014), for example.

The max-stable models considered in Chapter 4 have an in-built assumption that the marginal distributions are unit Fréchet. As such, observed extreme data have to be transformed prior to being fitted to the max-stable models. A more involved version of these models could also include the estimation of the marginal GEV parameter surface over the entire region of interest (rather than just having pointwise estimates) into the max-stable model formulation. This would provide a straightforward means of backtransforming the model’s predictions over the entire region (including areas which have no observed data) to the original measurement scale. However, it is foreseen that the use of ABC methods for model selection on extensions to the already computationally expensive max-stable model would require improvements in the computational efficiency of ABC algorithms to obtain model inference in a sensible time frame.

The development of more computationally efficient ABC algorithms is a very active area of research due to the wide applicability of the ABC methods. Some recent examples of novel ABC algorithms which aim to improve the algorithm’s efficiency are Prangle (2016) and Barthelmé and Chopin (2014). It would be of interest to investigate the improvements in computational efficiency gained from using such algorithms in the

model selection problems investigated, particularly with the computationally intensive spatial extremes model application in Chapter 4.

9.3 Concluding remarks

Data collection of pathogen occurrence or transmission in hospitals remains a challenging issue, particularly when it competes with the healthcare workers' primary duty of patient care. That being said, such data are useful to obtain a better understanding of the pathogen, and to build a quantitative evidence base related to the pathogen transmission and efficacy of infection control practices for a specific hospital, or even hospital ward. This is particularly so, given the variation inherent in both clinical care and heterogeneity of pathogen dynamics in small population sizes associated with hospital wards.

This thesis showed that it is still possible to obtain informative inference despite 'scrappy' data sets, or data sets not designed for research and analysis, using appropriate statistical methods. In particular, the work presented in this thesis highlighted the structural heterogeneity in MRSA occurrences within a hospital despite having coarse time series data, identified colonisation pressure as a statistically significant predictor of MRSA acquisition during a two-month outbreak period in a NICU, and quantified the relative importance of environmental contamination in hospital ward MRSA transmission using a combination of microbiological environmental contamination data and limited patient information. A general simulation-based method for Bayesian model selection was also developed as part of this thesis and shown to perform well across a variety of pathogen transmission models with imperfectly observed data sets as well as for more statistically challenging spatial extreme models.

Success of the work presented in this thesis is facilitated by strong collaborations between the clinical partners and statisticians, bringing together their expertise to overcome the limitations and scrappiness of the data sets. The work here serves to encourage more data collection, reporting and analysis of hospital pathogen data despite shortcomings of the data provided they are appropriately accounted for, as well as to encourage further collaboration between clinicians and statisticians.

Appendices

A Supplementary Material for Chapter 3: ‘Model choice problems using approximate Bayesian computation with applications to pathogen transmission data’

A.1 Additional details for the validating example

This section contains the additional details and results for the validating example in Section 3.2.3.

A.1.1 Direct evaluation of the posterior model probabilities

The marginal likelihoods or evidences for the Poisson model (M_1) and geometric model (M_2) considered in the validating example are given by:

$$p(\mathbf{y}|M_1) = \frac{s_1!}{\exp(t_1)(n+1)^{s_1+1}} \quad \text{and} \quad p(\mathbf{y}|M_2) = \frac{n!s_1!}{(n+s_1+1)!}$$

where $s_1 = \sum y_j$ and $t_1 = \sum \ln(y_j!)$. The statistics s_1 and t_1 are hence sufficient for model choice problems with these two models (as investigated in Didelot et al. (2011)).

However there is no closed form expression for the evidence of the negative binomial model (M_3):

$$p(\mathbf{y}|M_3) = \int_0^\infty \int_0^1 \prod_{j=1}^n \frac{(r+y_j-1)!}{y_j!(r-1)!} p^r (1-p)^{y_j} e^{-r} dp dr.$$

Instead, the evidence for the negative binomial model was calculated using numerical integration.

Regression summary statistic	Set A	Set B	Set C	Set D
mean	0	0	0	0
variance	0	0	0	0
median absolute deviation	0	0	0	0
count of zeros	1000	1000	1000	1000
maximum value	0	0	0	0
interquartile range	0	0	0	0
skewness	306	321	1000	1000
kurtosis	694	679	1000	1000
$t_1 = \sum_{j=1}^{100} \ln(y_j!)$	0	–	0	–
mean-variance ratio	1000	1000	–	–

Table A.1: Validating example: frequency of regression summary statistics selected in the multinomial logistic regression step for each subset of regression summary statistics considered for the 1,000 generated data sets.

The posterior model probabilities can then be straightforwardly computed from the following relations:

$$\frac{p(M_i|\mathbf{y})}{p(M_j|\mathbf{y})} = \frac{p(\mathbf{y}|M_i) p(M_i)}{p(\mathbf{y}|M_j) p(M_j)}, \quad i, j \in \{1, 2, 3; i \neq j\} \quad (\text{A.1})$$

$$p(M_1|\mathbf{y}) + p(M_2|\mathbf{y}) + p(M_3|\mathbf{y}) = 1.$$

For this example where the model priors were assumed to be uniform, (A.1) can be further simplified as $p(M_i|\mathbf{y})$ are the normalized $p(\mathbf{y}|M_i)$, i.e. $p(M_i|\mathbf{y}) \propto p(\mathbf{y}|M_i)$.

A.1.2 Validating example with different sets of regression summary statistics

Table A.1 summarises the regression summary statistics selected in the stepwise multinomial logistic regression for the 1,000 generated data sets considered in the validating example in Section 3.2.3 using different subsets of regression summary statistics. The results presented in Section 3.2.3 correspond to Set B.

The final estimated posterior model probabilities for the 1,000 generated data sets using the ABMC algorithm and each of the four sets of regression summary statistics are shown in Figure A.1. It is evident that the mean-variance ratio was the most vital statistic for model choice between the candidate models considered in this example as model choice results from Sets C and D perform poorly compared with Sets A and B.

There were no discernible differences in the parameter estimation results of the correct (Poisson) model for the four different sets of regression summary statistics considered (as shown in Figure A.2).

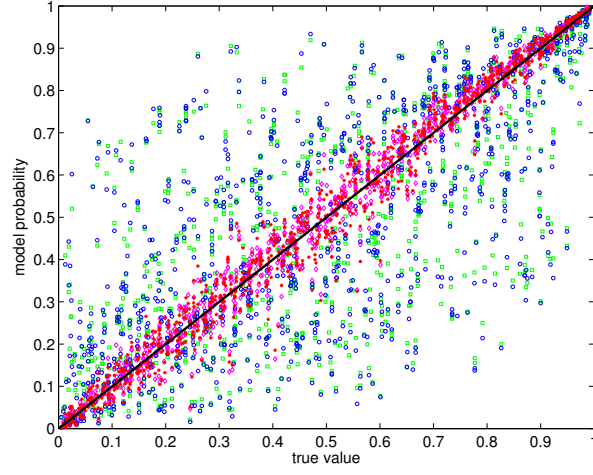


Figure A.1: Validating example: estimated model probabilities for the Poisson model obtained from the ABMC algorithm plotted against the true model probability calculated from the marginal likelihoods for Set A (red asterisks), Set B (pink diamonds), Set C (blue circles) and Set D (green squares).

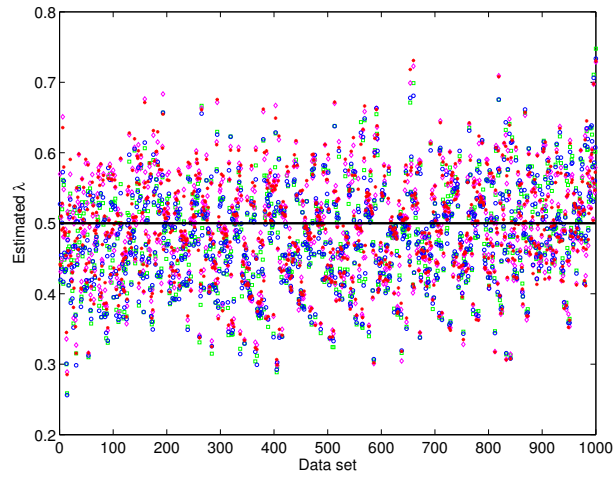


Figure A.2: Validating example: plot of the estimated mean of the Poisson parameter from the ABMC algorithm using Set A (red asterisks), Set B (pink diamonds), Set C (blue circles) and Set D (green squares). The true value of the parameter is 0.5 as indicated by the horizontal line.

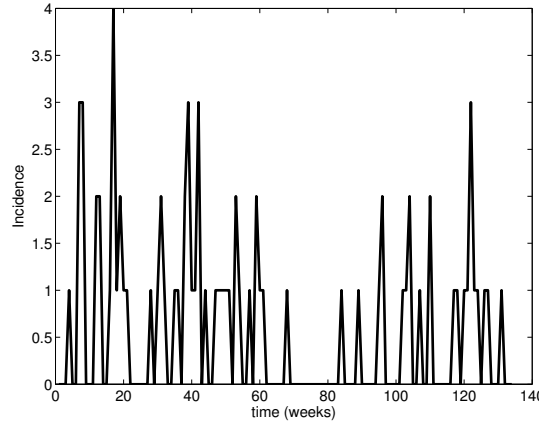


Figure A.3: Hospital MRSA example: weekly incidence data of MRSA colonisation obtained from the ICU at Princess Alexandra Hospital, Brisbane, Australia (McBryde *et al.*, 2007).

A.2 Additional details for the hospital MRSA example

The following are the additional details and results for the example of MRSA transmission within an ICU discussed in Section 3.3.1.

The observed weekly incidences of MRSA in the ICU ward are plotted in Figure A.3.

A.2.1 Pseudo-equilibrium approximation

The models considered in Section 3.3.1 to describe the transmission dynamics of MRSA within an ICU ward can be written in a general form:

$$\frac{dY_p}{dt} = \lambda_{hp} (N_p - Y_p) - \mu'(1 - \sigma)Y_p + \mu\sigma(N_p - Y_p) \quad (\text{A.2})$$

$$\frac{dY_h}{dt} = \lambda_{ph} (N_h - Y_h) - \kappa Y_h \quad (\text{A.3})$$

where Y_p and Y_h represent the number of colonised patients and health-care workers (HCWs) respectively. N_p and N_h are the total number of patients and HCWS in the ward.

For the analysis in Section 3.3.1, it is assumed that the number of patients and HCWs in the ward are constant and equal throughout the study duration (i.e. $N_p = N_h = N$) and their colonisations are detected perfectly. Forrester et al. (2007) provided a method for incorporating imperfect sensitivity if it is believed to be an important feature of the hospital system under study.

The value of the hand hygiene rate parameter κ can be determined from the relation $h = \frac{\kappa}{\kappa + cN}$ (see Drovandi and Pettitt (2008) for derivation and justification). The fixed parameter values used in the example are listed in Table A.2.

Parameter	Description	Value	Units
N	ward size	15	persons
σ	probability of colonisation upon entry	0.03	-
μ'	discharge rate of colonised patients	1/10.6	day ⁻¹
μ	discharge rate of uncolonised patients	1/4	day ⁻¹
p_{ph}	probability of pathogen transmission from a colonised patient to a HCW	0.13	-
h	hand hygiene compliance rate	0.59	-

Table A.2: Hospital MRSA example: fixed parameter values for both the candidate models proposed for modelling MRSA transmission (McBryde *et al.* (2007)).

The λ_{ij} terms represent the ‘force of colonisation’ for patients and HCWs, and can be written as the product of a function $g(\cdot)$ of the transmission parameter ϕ_j (defined to be the product of the contact rate c and probability of transmission per contact p_{ij} , i.e. $\phi_j = cp_{ij}$ as in McBryde *et al.* (2007b)) and a function $h(\cdot)$ of the corresponding colonised population, i.e.

$$\lambda_{ij} = g(\phi_j) h(Y_i), \quad i, j \in \{h, p; i \neq j\}.$$

Furthermore, if $g(\cdot)$ is linear in terms of ϕ_j , λ_{ij} can be rewritten as $\lambda_{ij} = cg(p_{ij}) h(Y_i)$ using the fact that $\phi_j = cp_{ij}$. The two models considered in this example assumed $g(p_{ij}) = p_{ij}$.

For the model introduced in McBryde *et al.* (2007b), $h(\cdot)$ is linear, i.e. $h(Y_i) = Y_i$, which gives rise to the standard mass-action transmission susceptible-infectious (SI) model.

For the Greenwood model (Greenwood, 1931), $h(Y_i) = \mathbb{1}(Y_i > 0)$ where $\mathbb{1}(Y_i > 0)$ is equal to 1 when $Y_i > 0$ and 0 otherwise. In other words, provided that at least one person is colonised, there is a constant colonisation pressure (ϕ_j) for the corresponding susceptible group. Other models may take $h(Y) = Y^\alpha$ or some non-linear function of Y .

The pseudo-equilibrium approximation used, in which the number of colonised HCWs is eliminated from the system by approximating it with the steady-state value (\bar{Y}_h) obtained by setting $\frac{dY_h}{dt}$ to zero, yields the following general expression for \bar{Y}_h :

$$\bar{Y}_h = \frac{\lambda_{ph}^* N}{\lambda_{ph}^* + \left(\frac{hN}{1-h}\right)}$$

where $\lambda_{ph} = c\lambda_{ph}^*$, assuming $g(\cdot)$ is linear in terms of ϕ_j .

This approximation reduces the system down from a trivariate Markov process (of (Y_p, Y_h, I) where I is the weekly incidence of patient MRSA cases) to a bivariate Markov process (of (Y_p, I)). Drovandi and Pettitt (2011b) showed that the pseudo-equilibrium approximation above still performs favourably when compared with the full trivariate Markov process and was used in the example to reduce the computational burden required for the simulations.

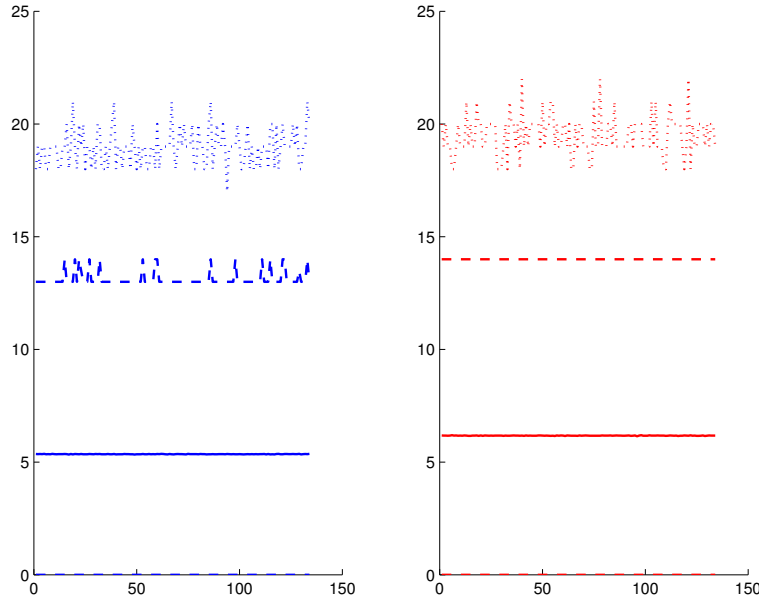


Figure A.4: Hospital MRSA example: simulations from the standard model (blue lines) and Greenwood model (red lines) using the prior distributions specified. The full lines are the mean of the 100,000 simulations for each model at each time point. The dashed lines are the 99% intervals (with the lower bound on the zero line) and the dotted lines are the maximums at each time point.

A.2.2 Priors used

The priors used for the parameters were based on historical data (Ismail et al., 2003) from the same hospital ward as used in the example here. The priors are independent $U[0, 0.5]$ for both ϕ_p and ϕ'_p . These priors generated model simulations with 99% probability intervals for both models which contain the number of weekly MRSA cases reported in Ismail et al. (2003).

A.2.3 Additional output from ABMC algorithm

The histograms and cumulative distribution function (cdf) plots of the probabilities of correct model allocation (i.e. probability of being allocated to model k given the simulation was generated from model k) for the MRSA example are shown in Figure A.5 and Figure A.6 respectively.

The histograms for the parameter estimation results for the two models are provided in Figure A.7.

One of the benefits of the ABC procedure in terms of model choice is the ability to obtain an estimate of the distribution for the model probabilities directly from the simulated data of the particle set and the estimated logistic regression coefficients (Figure A.8). There were no particles with an estimated model probability for the standard model of less than 0.9.

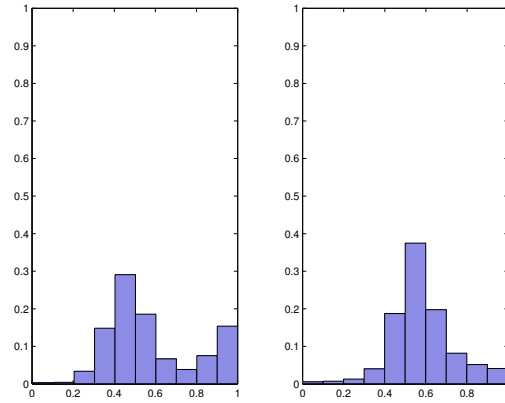


Figure A.5: Hospital MRSA example: histograms of the probability of correct model allocation for the standard model (left) and Greenwood model (right). The x-axes denote the probability of correct model allocation defined to be the estimated probability of being in model k using the logistic regression coefficient estimates and simulated data, given that the simulation used was generated from model k .

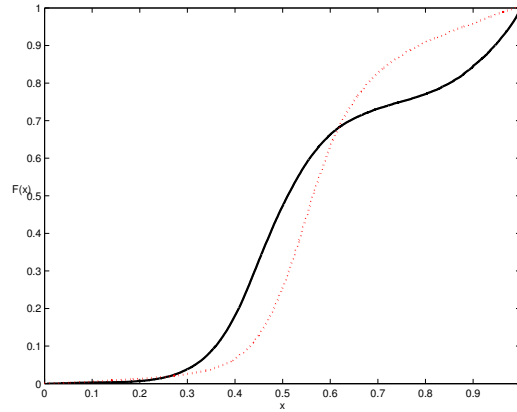


Figure A.6: Hospital MRSA example: cdf plots of the probability of correct model allocation for the two candidate models. The solid black line corresponds to the standard model and the dotted red line corresponds to the Greenwood model. The x-axis denotes the probability of correct model allocation defined to be the estimated probability of being in model k using the logistic regression coefficient estimates and simulated data, given that the simulation used was generated from model k .

Figure A.9 shows the distribution of estimated model probabilities for the standard model obtained from the final particle set, aggregated by the model indicator variable.

A.3 Investigation of the use of bias-reduced logistic regression for the hospital MRSA example

The following results were obtained using the bias-reduced binomial logistic regression estimation (Kosmidis, 2007) on the model indicators in the FP step for the hospital MRSA example (Section 3.3.1) with the original set of priors. Other details of implementations are as described previously.

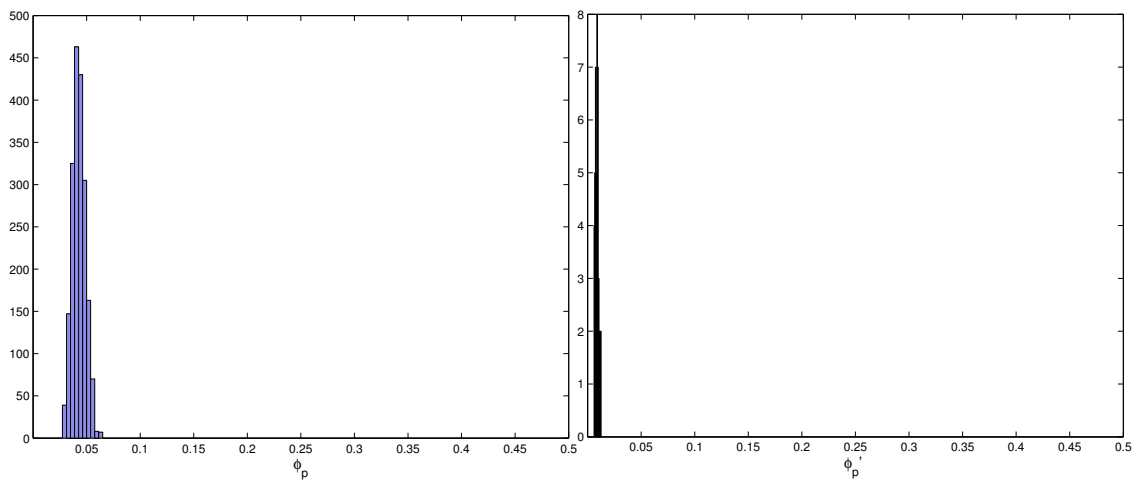


Figure A.7: Hospital MRSA example: histograms of the parameters for the standard model (left) and the Greenwood model (right) obtained using the ABMC algorithm. The x-axes were adjusted to the width of the uniform priors used.

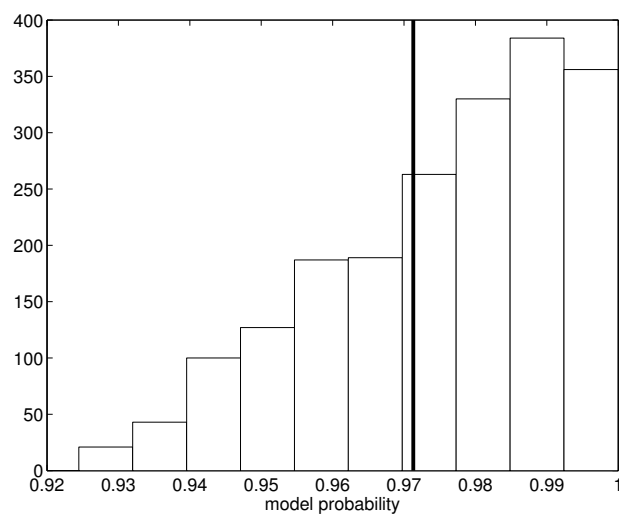


Figure A.8: Hospital MRSA example: histogram of the model probabilities for the standard model estimated using the logistic regression coefficients and the final particle set. The vertical line corresponds to the value obtained using numerical integration.

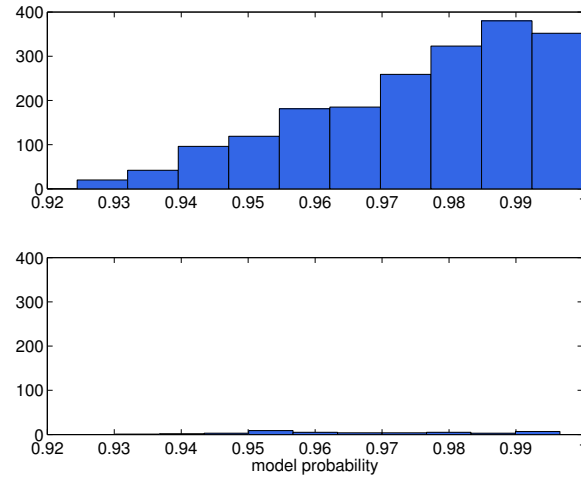


Figure A.9: Hospital MRSA example: histograms of the model probabilities for the standard model estimated using the logistic regression coefficients and the final particle set, aggregated by the model indicator (where the top figure is for particles ‘belonging to’ the standard model and the bottom figure corresponds to those from the Greenwood model) with axes scaled so both histograms are on the same axes.

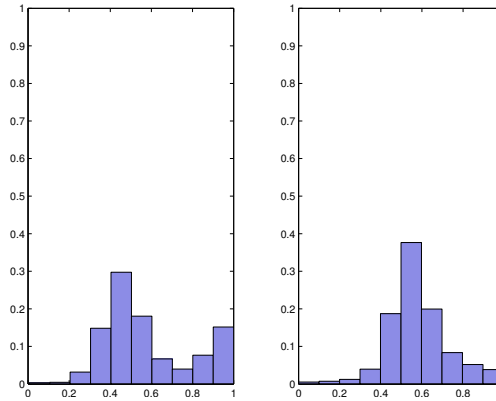


Figure A.10: Hospital MRSA example: histograms of the probability of correct model allocation for the standard model (left) and Greenwood model (right) using bias-reduced logistic regression. The x-axes denote the probability of correct model allocation defined to be the estimated probability of being in model k using the bias-reduced logistic regression coefficient estimates and simulated data, given that the simulation used was generated from model k .

The misclassification matrix obtained was

$$\begin{array}{cc} & p(\text{standard}) & p(\text{Greenwood}) \\ \text{standard} & 0.523 & 0.477 \\ \text{Greenwood} & 0.257 & 0.743 \end{array} \left(\begin{array}{cc} & \\ & \end{array} \right).$$

The corresponding histograms and cdf plots of the probabilities of correct model allocation are provided in Figure A.10 and Figure A.11 respectively.

The final estimated model probability obtained was 0.972 in favour of the standard model for the implementation using bias-reduced logistic regression and the plot of model probabilities across the 13 SMC iterations is provided in Figure A.12.

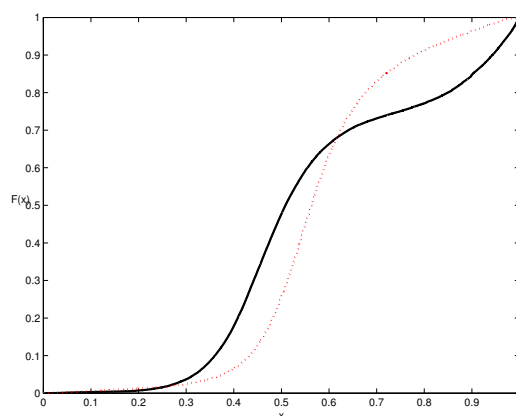


Figure A.11: Hospital MRSA example: cdf plots of the probability of correct model allocation for the two candidate models using bias-reduced logistic regression. The solid black line corresponds to the standard model and the dotted red line corresponds to the Greenwood model. The x-axis denotes the probability of correct model allocation defined to be the estimated probability of being in model k using the bias-reduced logistic regression coefficient estimates and simulated data, given that the simulation used was generated from model k .

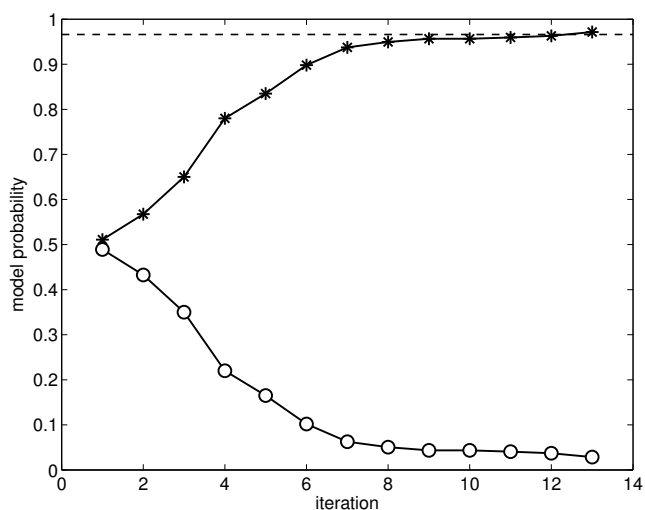


Figure A.12: Hospital MRSA example: estimated model probabilities for the standard model (asterisks) and Greenwood model (circles) across the SMC iterations for the ABMC algorithm with bias-reduced binomial logistic regression. The model probability for the standard model estimated using numerical integration is indicated by the dashed horizontal line.

model	parameter	mean	95% CI
standard	ϕ_p	0.043	[0.031, 0.056]
Greenwood	ϕ'_p	0.0085	[0.0058, 0.011]

Table A.3: Hospital MRSA example: parameter estimation results using the ABMC algorithm with bias-reduced logistic regression.

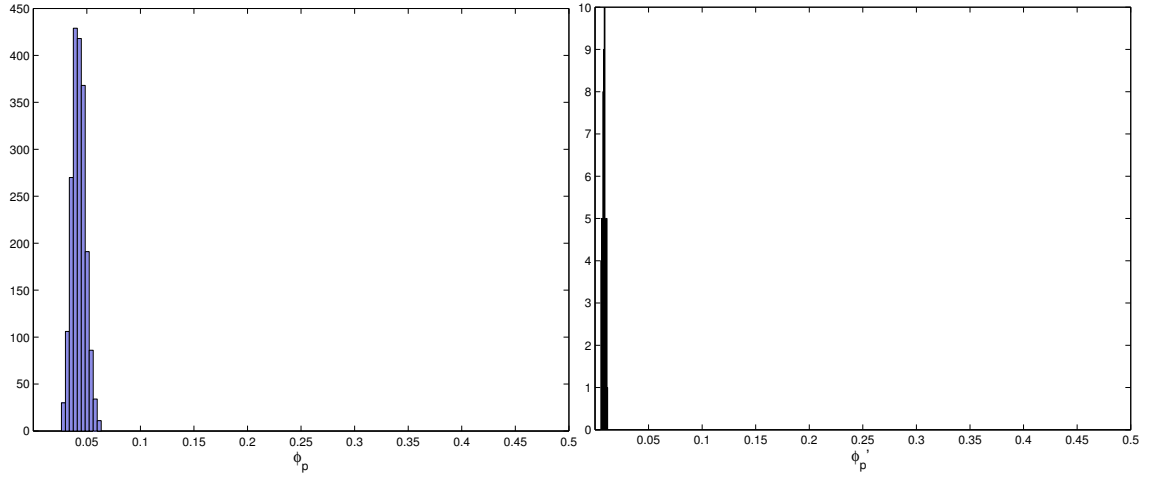


Figure A.13: Hospital MRSA example: histograms of the parameters for the standard model (left) and the Greenwood model (right) obtained using the ABC model choice algorithm with bias-reduced binomial logistic regression. The x-axes were adjusted to the width of the uniform priors used.

The parameter estimation results obtained are summarised in Table A.3 and Figure A.13.

The histogram of model probabilities for the standard model estimated using the logistic regression coefficients and the final SMC particle set are shown in Figure A.14, and Figure A.15 where the results were aggregated by their model indicator.

The results with and without the bias reduction logistic regression are similar for the hospital MRSA example when the acceptance probability limit was 1% (the default value used throughout the paper) as well as 0.1%.

A.4 Additional details for the Tristan da Cunha cold outbreak example

For the Tristan da Cunha Oct-Nov 1967 cold outbreak example in Section 3.3.2, there were three parameters in Model 1 (S_0, γ_1, ν_1), and four in each of the other three models ($S_0, \gamma_2, \nu_2, \tau$ for Model 2, $S_0, \gamma_3, \nu_3, \delta$ for Model 3, and S_0, γ_4, ν_4, e for Model 4).

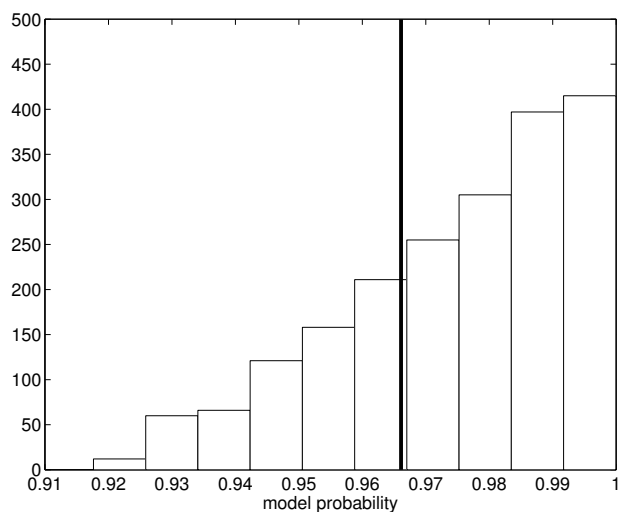


Figure A.14: Hospital MRSA example: histogram of the model probabilities for the standard model estimated using the bias-reduced binomial logistic regression coefficients and the final particle set. The vertical line corresponds to the value obtained using numerical integration.

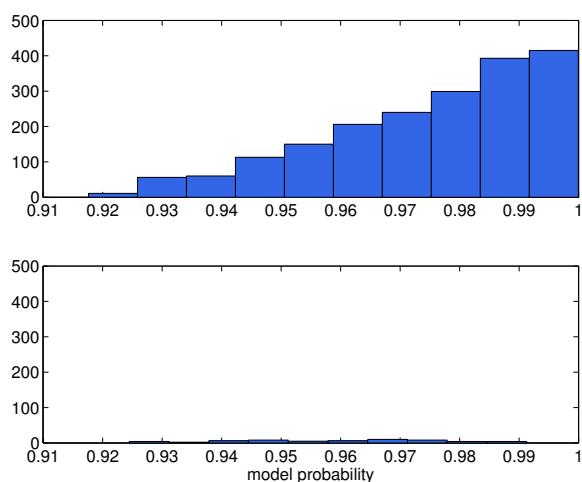


Figure A.15: Hospital MRSA example: histograms of the model probabilities for the standard model using the bias-reduced binomial logistic regression coefficients and the final particle set, aggregated by the model indicator (where the top figure is for particles from the standard model and the bottom figure corresponds to those from the Greenwood model) with axes scaled so both histograms have the same axes.

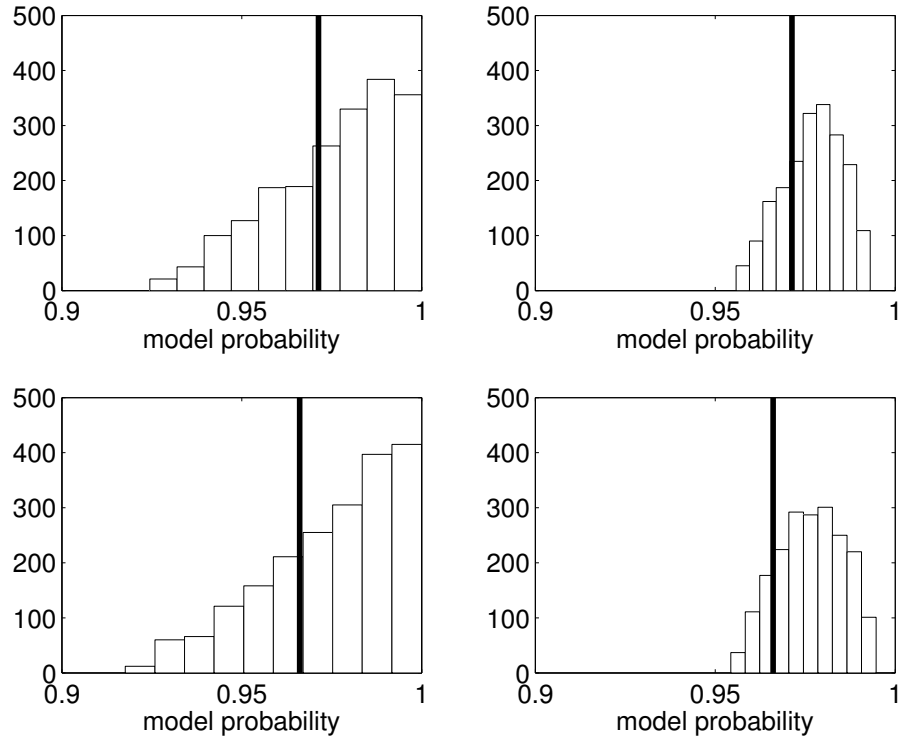


Figure A.16: Hospital MRSA example: histograms of the model probabilities for the standard model from the final SMC particle sets without and with bias-reduction in the binomial logistic regression (top and bottom rows respectively). The left column corresponds to when the acceptance probability limit was set to 1% (default used) and the right column was 0.1%. The vertical lines correspond to the value obtained using numerical integration. The axes were scaled so all histograms have the same axes.

A.4.1 Priors used

The set of priors used are as follows: $U[37, 100]$ for S_0 , $U[0, 3]$ for γ_1 and $U[0, 3]$ for ν_1 in Model 1; $U[37, 100]$ for S_0 , $U[0, 3]$ for γ_2 , $U[0, 3]$ for ν_2 , and $U[0, 5]$ for τ in Model 2; $U[37, 100]$ for S_0 , $U[0, 3]$ for γ_3 , $U[0, 3]$ for ν_3 , $U[0, 5]$ for δ in Model 3; and $U[37, 100]$ for S_0 , $U[0, 3]$ for γ_4 , $U[0, 3]$ for ν_4 and $U[0, 5]$ for e in Model 4.

These priors were identical to those used by Toni et al. (2009) except the lower bounds of the priors for τ , σ and e were set to 0 instead of -0.5 for more sensible interpretations of the parameters.

A.4.2 Additional output from ABMC algorithm

The histograms and cdf plots of the probabilities of the correct model allocation for the Tristan da Cunha cold outbreak example are shown in Figure A.17 and Figure A.18 respectively.

The histograms for the parameter estimation results for the two most likely models in the Tristan da Cunha cold outbreak example are provided in Figure A.19 for Model 2 and Figure A.20 for Model 3.

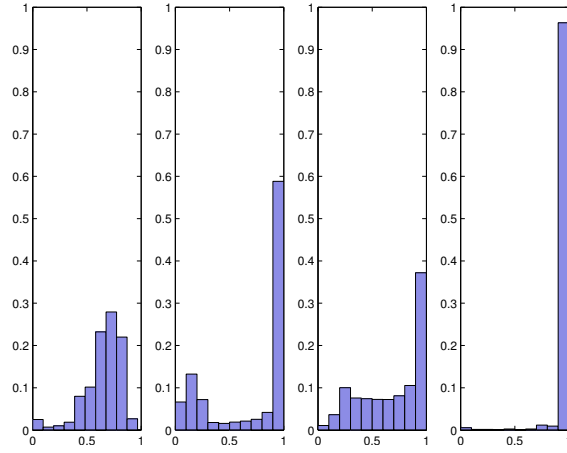


Figure A.17: Tristan da Cunha cold outbreak example: histograms of the probability of correct model allocation for the candidate models corresponding to Models 1, 2, 3 and 4 moving from left to right. The x-axes denote the probability of correct model allocation defined to be the estimated probability of being in model k using the logistic regression coefficient estimates and simulated data, given that the simulation used was generated from model k .

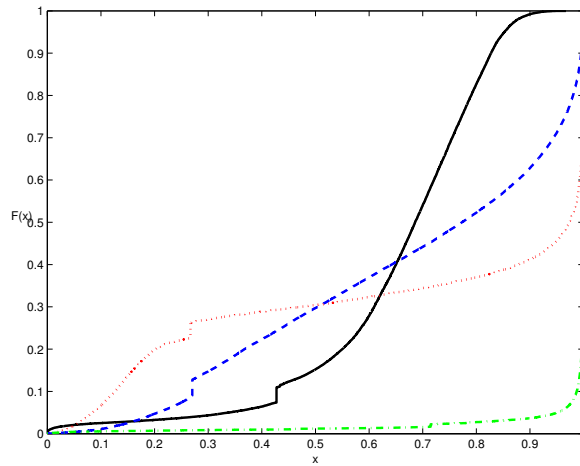


Figure A.18: Tristan da Cunha cold outbreak example: cdf plots of the probability of correct model allocation for the candidate models. The solid black line corresponds to Model 1, the dotted red line corresponds to Model 2, the dashed blue line corresponds to Model 3 and the dot-dashed green line corresponds to Model 4. The x-axis denotes the probability of correct model allocation defined to be the estimated probability of being in model k using the logistic regression coefficient estimates and simulated data, given that the simulation used was generated from model k .

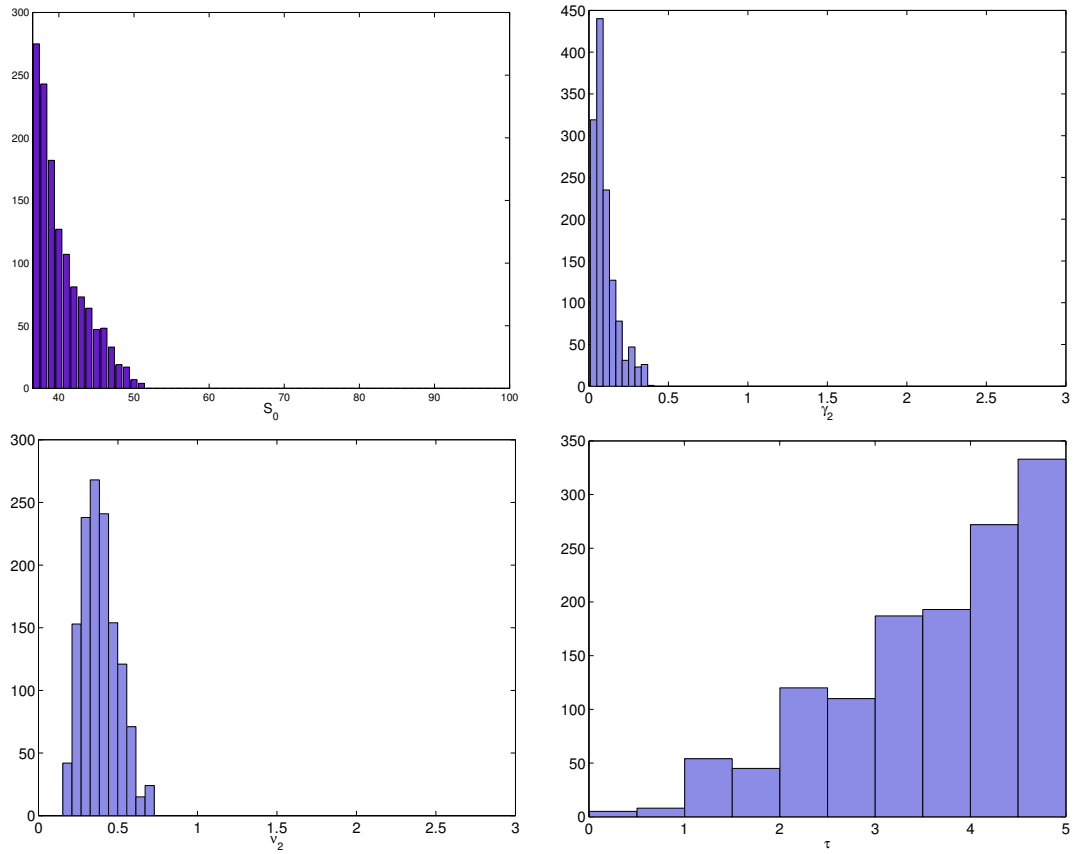


Figure A.19: Tristan da Cunha cold outbreak example: histograms and frequency plot of the continuous parameters (γ_2 , ν_2 and τ) and discrete parameter (S_0) respectively for Model 2. The x-axes were adjusted to the width of the uniform priors used.

The histogram of model probabilities estimated using the logistic regression coefficients and the final particle set are shown in Figure A.21, and Figure A.22 where the results were aggregated by their model indicator.

A.5 Additional details for the Hagelloch measles example

The following are additional details and results for the Hagelloch measles example in Section 3.3.3.

A.5.1 Derivation of observed data set

As only the dates which the individuals exhibit symptoms (or the start of the prodromal period) and the dates on which rashes begin to appear are recorded, the following assumptions were made to convert the recorded data into SEIR data: it was assumed that individuals become infectious one day before the onset of the prodromal period and that the infectious period ends three days after the onset of rashes for the observed data set. Furthermore, it was also assumed that each individual remains in the exposed class for 9 days before becoming infectious (see Britton et al. (2011) for a justification of

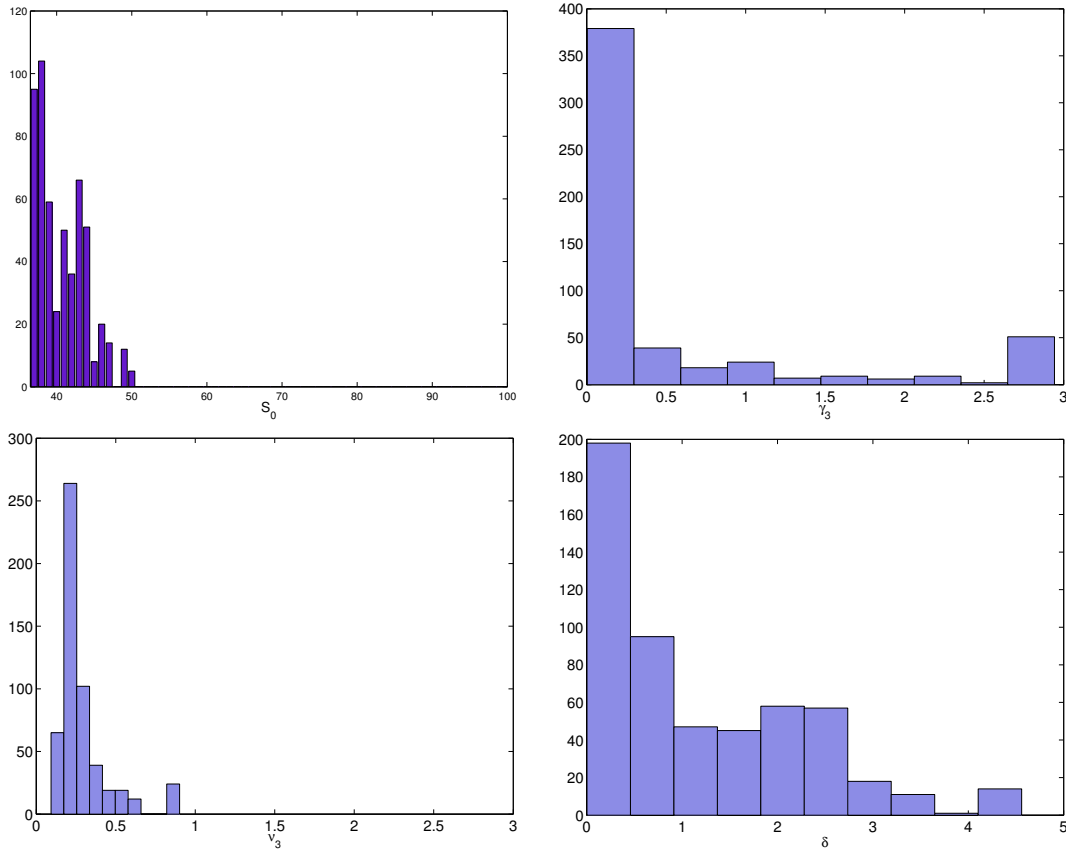


Figure A.20: Tristan da Cunha cold outbreak example: histograms and frequency plot of the continuous parameters (γ_3 , ν_3 and δ) and discrete parameter (S_0) respectively for Model 3. The x-axes were adjusted to the width of the uniform priors used.

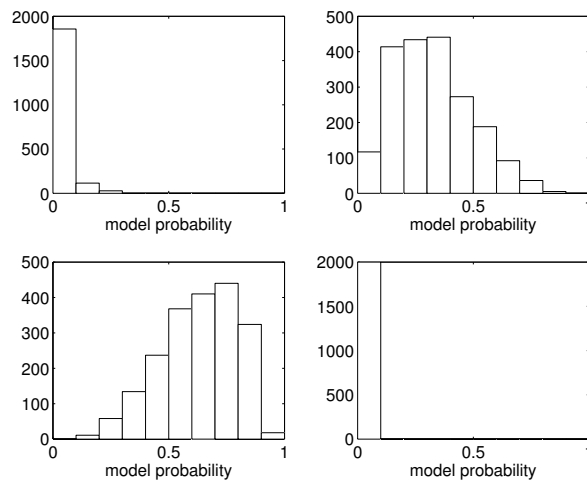


Figure A.21: Tristan da Cunha cold outbreak example: histograms of the model probabilities for the candidate models estimated using the logistic regression coefficients and the final particle set, where the top left figure corresponds to Model 1, top right Model 2, bottom left Model 3 and bottom right Model 4.

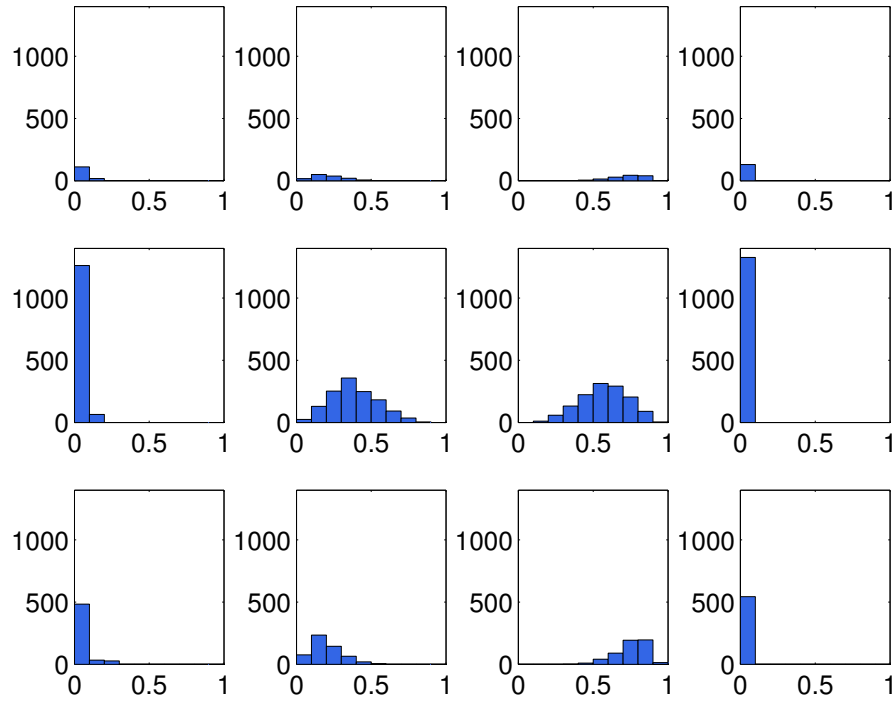


Figure A.22: Tristan da Cunha cold outbreak example: histograms of model probabilities for the four models (by column, with the leftmost corresponding to Model 1, then Model 2, Model 3 and the rightmost column to Model 4) estimated using the logistic regression coefficients and the final particle set for particles from Model 1 (top row), Model 2 (middle row) and Model 3 (bottom row). There were no particles assigned to Model 4 in the final particle set. The axes were scaled so all histograms have the same axes.

these assumptions). Using these assumptions, the observed data set can be represented as SEIR data as shown in Figure A.23.

A.5.2 Exposure and infectious periods distributions

The multitype epidemic model described in Britton et al. (2011) assumed fixed exposure and infectious periods (of 9 and 3 days respectively) and the outbreak was initially triggered by one lone infectious individual. However there were four individuals who became infectious in less than 9 days after the first infectious individual was recorded, which implies that these individuals were either not infected by the initial infectious individual or that the exposure period is not necessarily fixed at 9 days. Furthermore, there was also one individual who only became infectious a long period of time after the other individuals in the data set were no longer infectious.

In light of these points, it would appear more sensible to assume a variable exposure and infectious time periods for the models as was done in Groendyke et al. (2012) and our analysis. The exposure and infectious periods in both models were assumed to follow gamma distributions with k_E and θ_E denote the shape and scale parameters for the gamma distribution describing the exposure period, and similarly k_I and θ_I for the infectious period.

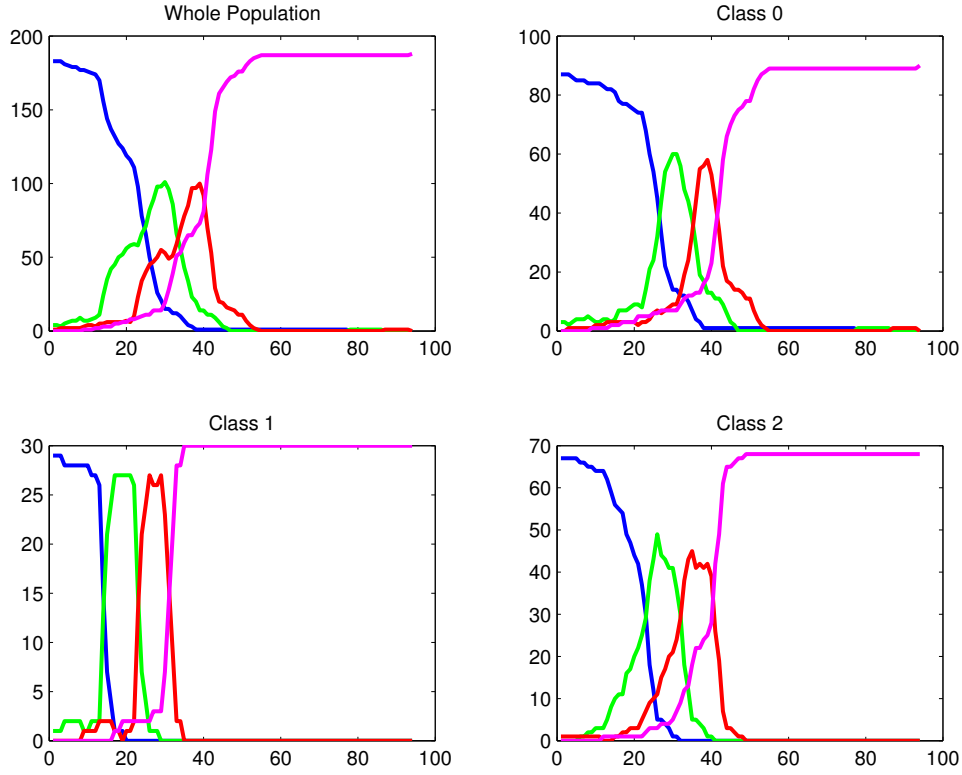


Figure A.23: Hagelloch measles example: observed SEIR numbers over time for the Hagelloch measles outbreak in 1861 for the entire community (top left), and separated by classrooms where Class 0 refers to those who were not part of the Class 1 or Class 2. The dark blue lines refer to the number of susceptible children, the green lines represent the exposed children, the red lines indicate the number of infectious children and the pink lines denote the number of recovered children.

A.5.3 Priors used

There were eight parameters to be estimated in the MME model

$(\lambda_H, \lambda_{G1}, \lambda_{G2}, \lambda_C, k_E, \theta_E, k_I, \theta_I)$ and 13 in the CN model

$(\lambda, \eta_1, \eta_2, \eta_3, \eta_4, \eta_5, \eta_6, \eta_7, \eta_8, k_E, \theta_E, k_I, \theta_I)$.

A vague $U[0, 4]$ prior was chosen for each of the transmission rate parameters

$(\lambda_H, \lambda_{G1}, \lambda_{G2}$ and λ_C in the MME model and λ in the CN model) as in Groendyke et al. (2012).

For both models, the same priors were used for the gamma distributions' parameters namely $U[8, 20]$ for k_E , $U[0.25, 1]$ for θ_E , $U[15, 25]$ for k_I and $U[0.25, 0.75]$ for θ_I . These prior ranges cover exposure and infectious periods consistent with the epidemiology of measles (Groendyke et al., 2012).

The priors for the network parameters $\boldsymbol{\eta} = (\eta_1, \eta_2, \eta_3, \eta_4, \eta_5, \eta_6, \eta_7, \eta_8)$ in the CN model were motivated by Gelman et al. (2008). Specifically, Gelman et al. (2008) recommended the use of a Cauchy distribution prior with centre 0 and scale 10 for the intercept parameter (η_3) and a Cauchy distribution prior with centre 0 and scale 2.5 for the other η_i for weakly informative priors. We used uniform prior distributions based on

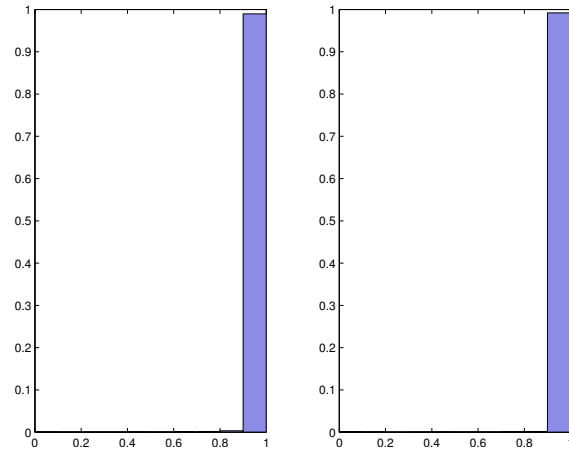


Figure A.24: Hagelloch measles example: histograms of the probability of correct model allocation for the MME model (left) and CN model (right). The x-axes denote the probability of correct model allocation defined to be the estimated probability of being in model k using the logistic regression coefficient estimates and simulated data, given that the simulation used was generated from model k .

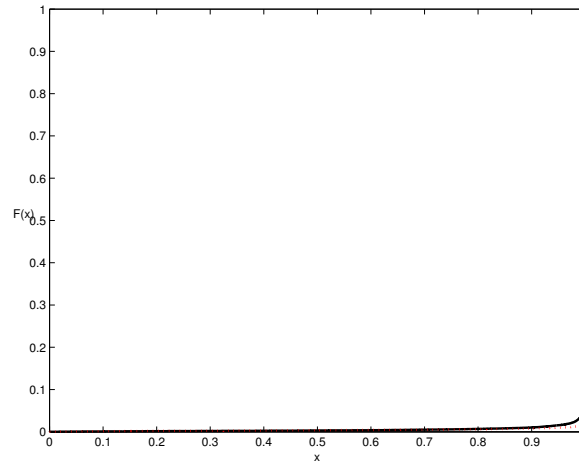


Figure A.25: Hagelloch measles example: cdf plots of the probability of correct model allocation for two candidate models. The solid black line corresponds to the MME model and the dotted red line corresponds to the CN model. The x-axis denotes the probability of correct model allocation defined to be the estimated probability of being in model k using the logistic regression coefficient estimates and simulated data, given that the simulation used was generated from model k .

the 2.5% and 97.5% percentiles of the Cauchy distributions, giving $U[-128, 128]$ for the intercept η_3 and $U[-32, 32]$ for the other η_i 's ($i = 1, 2, \dots, 8; i \neq 3$).

A.5.4 Additional output from ABMC algorithm

The histogram and cdf plots of the probabilities of the correct model allocation for the Hagelloch measles example are shown in Figure A.24 and Figure A.25 respectively.

Figure A.26 and Figure A.27 provide the histograms of the MME model parameters estimated in the final SMC particle set.

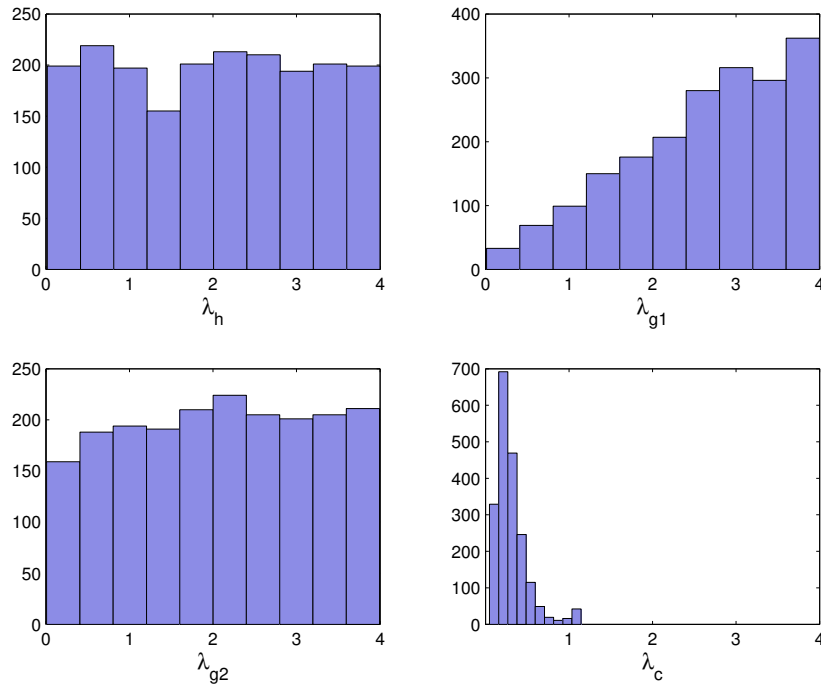


Figure A.26: Hagelloch measles example: histograms of the various transmission parameters (λ_h , λ_{g1} , λ_{g2} and λ_c) in the MME model. The x-axes were adjusted to the width of the uniform priors used.

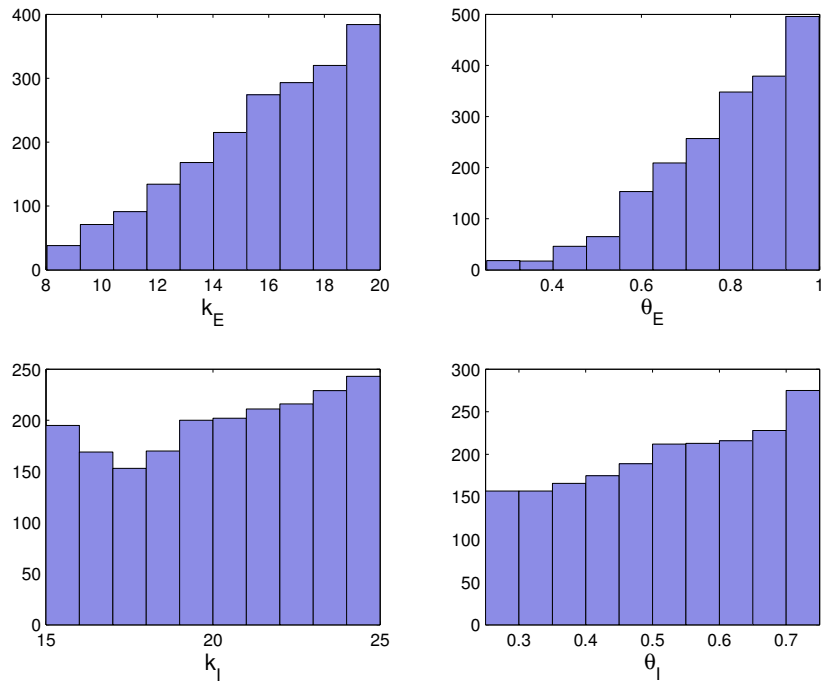


Figure A.27: Hagelloch measles example: histograms of the Gamma distribution parameters for the exposed (k_E and θ_E) and infectious periods (k_I and θ_I) in the MME model. The x-axes were adjusted to the width of the uniform priors used.

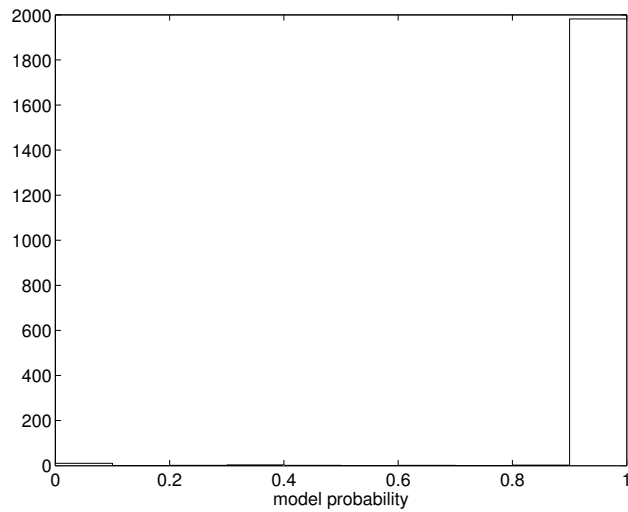


Figure A.28: Hagelloch measles example: histogram of the model probabilities for the MME model obtained estimated using the logistic regression coefficients and the final particle set.

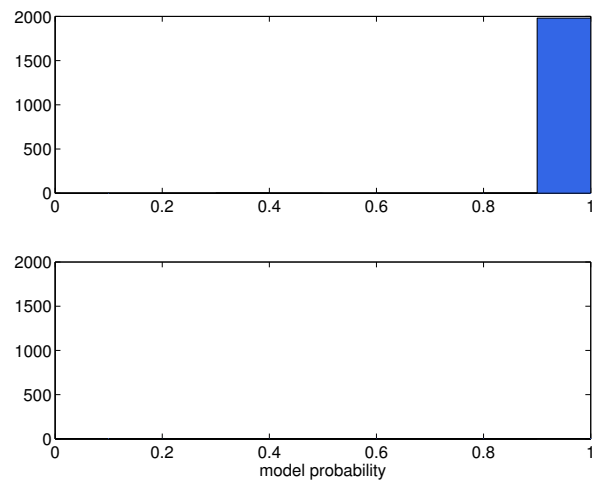


Figure A.29: Hagelloch measles example: histograms of the model probabilities for the MME model estimated using the logistic regression coefficients and the final particle set, aggregated by the model indicator (where the top figure is for particles from the MME model and the bottom figure corresponds to those from the CN model) with axes scaled so both histograms have the same axes.

The histogram of model probabilities for the MME model estimated using the logistic regression coefficients and the final SMC particle set are shown in Figure A.28, and Figure A.29 where the results were aggregated by their model indicator.

B Supplementary Material for Chapter 4: ‘ABC model selection for spatial max-stable models applied to South Australian maximum temperature data’

B.1 Prior predictive checks

The prior distributions used for the model parameters were chosen to be flat, vague priors. Specifically, the prior distributions are

- $U(0, 5)$ for c_2 and $U(0, 10)$ for ν in the Whittle–Matérn model
- $U(0, 5)$ for c_2 and $U(0, 5)$ for ν in the Cauchy model
- $U(0, 5)$ for c_2 and $U(0, 2)$ for ν in the powered exponential model
- $U(0, 5)$ for c_2 and $U(0, 5)$ for ν in the Bessel model
- $U(0, 5)$ for each of the Smith model parameters
- $U(0, 5)$ for c_2 and $U(0.05, 2)$ for ν in the Brown–Resnick model

The smaller upper bounds for the smoothness parameter (ν) priors of the powered exponential and Brown–Resnick models are required as the parameter is only defined for values less than 2 in these two models.

For each of the six models, 10,000 model simulations were generated using the prior distributions specified above. The spatial dependence structure generated from the simulated data, as measured by the madogram and pairwise extremal coefficient estimates used in the main text (Section 3), are shown in Figures B.1 and B.2, respectively. These figures show that the prior distributions specified for the six models were able to generate model simulations that produce spatial dependence structures similar to the observed data and are reasonable prior choices.

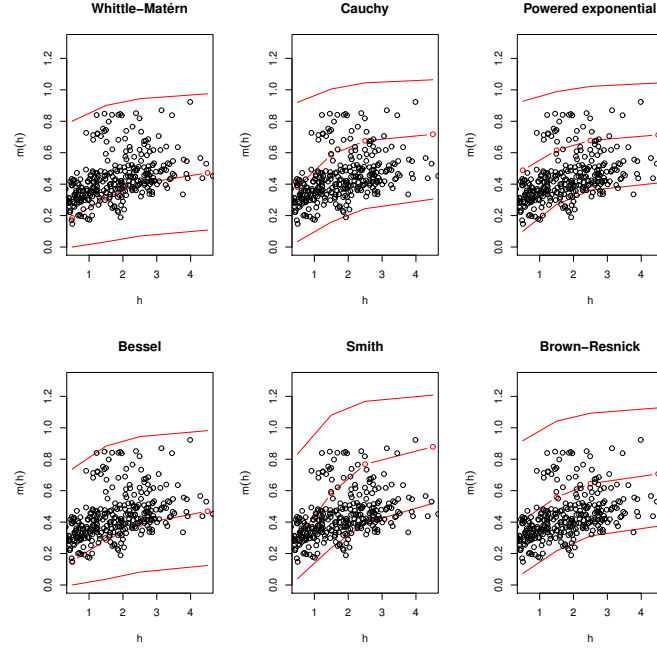


Figure B.1: Comparison of empirical madogram estimates (calculated using $GEV(\bar{\mu}, \bar{\sigma}, \bar{\xi})$ margins where $\bar{\mu}$, $\bar{\sigma}$ and $\bar{\xi}$ are the average of the GEV estimates from the 26 observed locations) using prior simulations from the six candidate models (the red lines denote the mean and 95% intervals) with observed data estimates (black circles).

B.2 Posterior distributions

There was considerable support for the powered exponential and Whittle-Matérn models in the final SMC particle set after the Brown-Resnick model. There were no particles from the other three candidate models (Cauchy, Bessel and Smith) in the final SMC particle set.

The posterior distributions for the powered exponential and Whittle-Matérn model parameters are shown in Figure B.3 and Figure B.4, respectively, with numerical summaries given in Table B.1 and Table B.2. The estimated posteriors were well within the prior ranges specified for the parameters in Section 4.5.1.

<i>Parameter</i>	<i>Mean</i>	<i>SD</i>	<i>2.5% quantile</i>	<i>Median</i>	<i>97.5% quantile</i>
c_2	3.90	0.297	3.30	3.91	4.46
ν	0.998	0.0590	0.873	0.997	1.10

Table B.1: Parameter estimates of the fitted powered exponential model for the South Australian data set.

<i>Parameter</i>	<i>Mean</i>	<i>SD</i>	<i>2.5% quantile</i>	<i>Median</i>	<i>97.5% quantile</i>
c_2	3.85	0.250	3.36	3.86	4.30
ν	0.517	0.0293	0.460	0.515	0.575

Table B.2: Parameter estimates of the fitted Whittle-Matérn model for the South Australian data set.

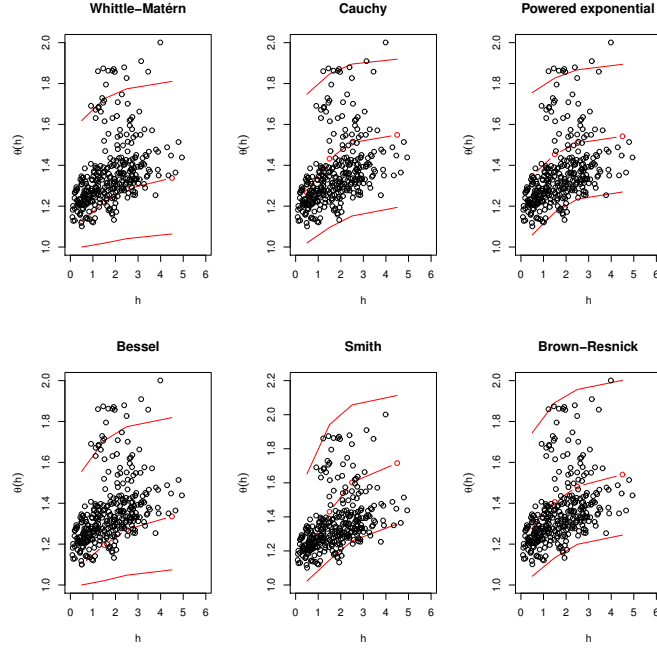


Figure B.2: Comparison of empirical pairwise extremal coefficient estimates (calculated using $\text{GEV}(\bar{\mu}, \bar{\sigma}, \bar{\xi})$ margins) using prior simulations (the red lines denote the mean and 95% intervals) with observed data estimates (black circles).

As with the fitted Brown–Resnick model in the main text, the fitted powered exponential and Whittle–Matérn models from the final particle set were also able to capture the spatial dependence of the observed data well in terms of the pairwise extremal coefficients (Figure B.5 for the fitted powered exponential model and Figure B.6 for the fitted Whittle–Matérn model).

In addition, the ABC posterior simulations at each observed location were compared with the corresponding observed data to assess if the posteriors obtained are adequate representations of the observed data at the 26 locations. This assessment was performed using the bootstrapped Kolmogorov–Smirnov test (Abadie, 2002) which allows for ties in the data (as implemented by the `ks.boot` function from the R package `Matching` (Sekhon, 2011)).

There was no evidence to suggest the fitted Brown–Resnick model is a poor fit to the data at the observed locations with p-values obtained ranging from 0.22 to 0.98 (Table B.3) and the corresponding quantile-quantile plots shown in Figure B.8. There were no obvious deviations in these plots that indicated misfit between the observed data and posterior simulations at the observed locations.

Similar inferences were obtained from the fitted posteriors of the other two candidate model with posterior support in the final particle set (quantile-quantile plots for the fitted powered exponential model shown in Figure B.9 and Figure B.10 for the fitted Whittle–Matérn model, and corresponding Kolmogorov–Smirnov test p-values in Table B.3).

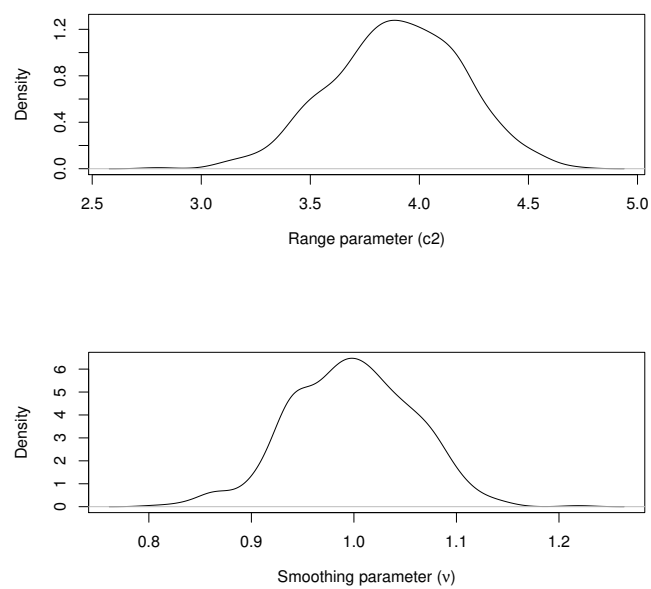


Figure B.3: Posterior parameter estimates for the powered exponential model.

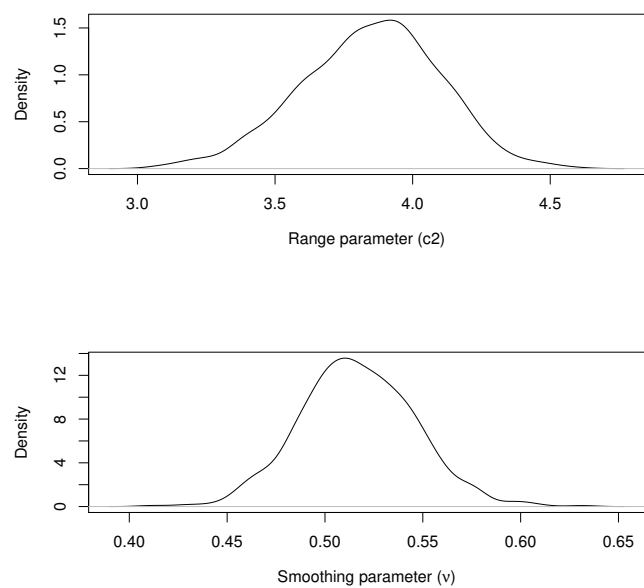


Figure B.4: Posterior parameter estimates for the Whittle-Matérn model.

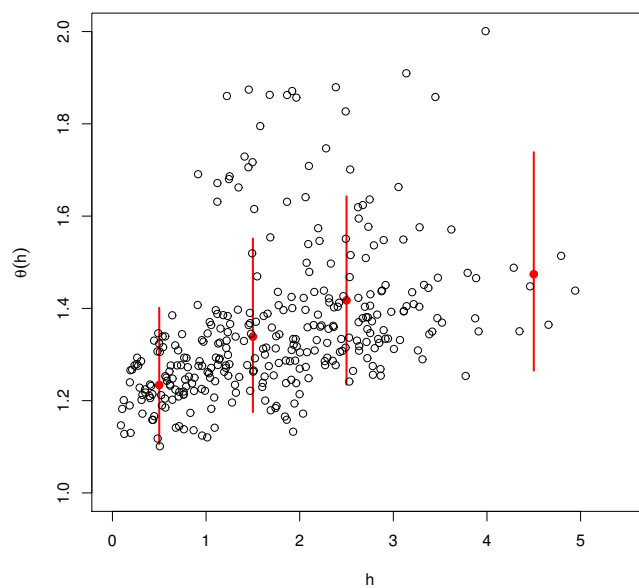


Figure B.5: Empirical pairwise extremal coefficient estimates using ABC posterior simulations from the fitted powered exponential model (binned means and 95% credible intervals in red), and observed data (black o).

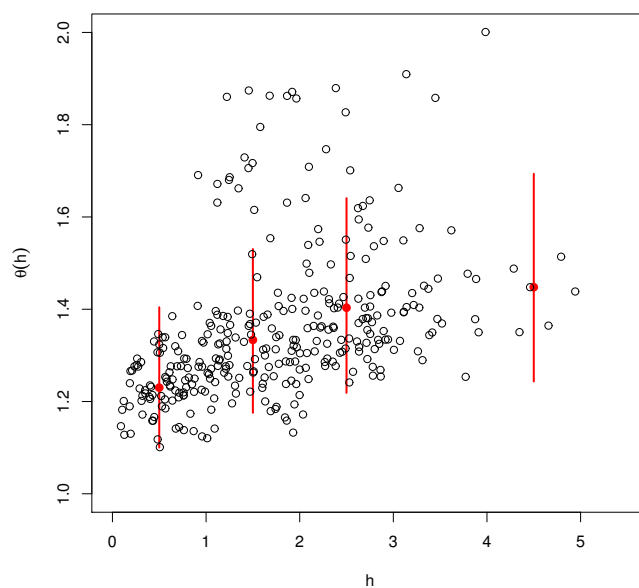


Figure B.6: Empirical pairwise extremal coefficient estimates using ABC posterior simulations from the fitted Whittle–Matérn model (binned means and 95% credible intervals in red), and observed data (black o).

<i>Station index</i>	<i>Station name</i>	<i>Brown–Resnick</i>	<i>powered exponential</i>	<i>Whittle–Matérn</i>
1	Lake Victoria Storage	0.98	0.48	0.80
2	Port Augusta Power Station	0.85	0.77	0.71
3	Cleve	0.54	0.56	0.38
4	Lenswood Research Centre	0.36	0.19	0.26
5	Nuriootpa	0.55	0.43	0.36
6	Snowtown	0.65	0.85	0.70
7	Whyalla	0.69	0.95	0.71
8	Strathalbyn	0.82	0.55	0.63
9	Renmark	0.72	0.74	0.72
10	Victor Harbor Comparison	0.39	0.31	0.24
11	Warooka	0.85	0.74	0.68
12	Adelaide (Kent Town)	0.51	0.34	0.45
13	Price	0.31	0.69	0.53
14	Edinburgh	0.22	0.45	0.36
15	Parafield Airport	0.31	0.44	0.46
16	Rosedale	0.68	0.60	0.52
17	Lameroo Comparison	0.82	0.79	0.83
18	Port Pirie Nyrstar Comparison	0.72	0.83	0.76
19	Kimba	0.45	0.70	0.72
20	Murray Bridge Comparison	0.33	0.22	0.33
21	Cape Willoughby	0.55	0.64	0.65
22	Meningie	0.48	0.30	0.42
23	Eudunda	0.58	0.54	0.40
24	Mount Barker	0.72	0.55	0.55
25	Yongala	0.68	0.66	0.40
26	Adelaide Airport	0.72	0.73	0.73

Table B.3: The bootstrapped Kolmogorov-Smirnov test p-values assessing goodness-of-fit of each of the fitted candidate models from the final SMC particle set to the observed data by location. Station indices are mapped in Figure B.7.

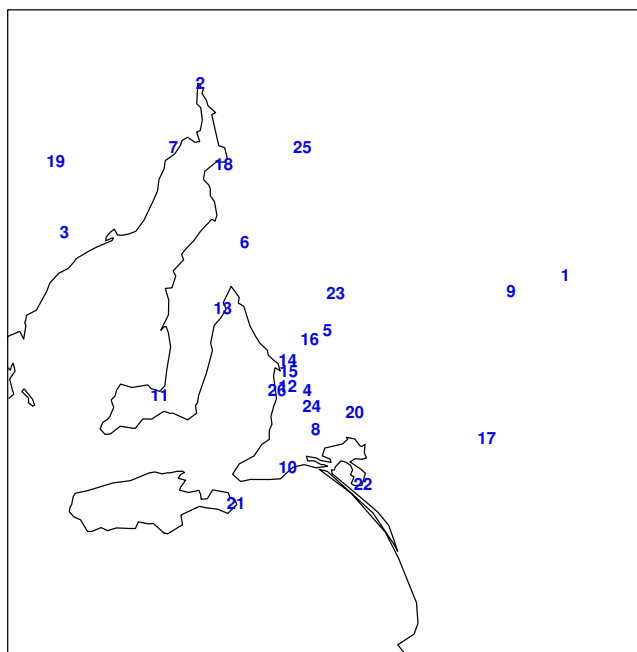


Figure B.7: Station index for the 26 weather stations where data were collected.

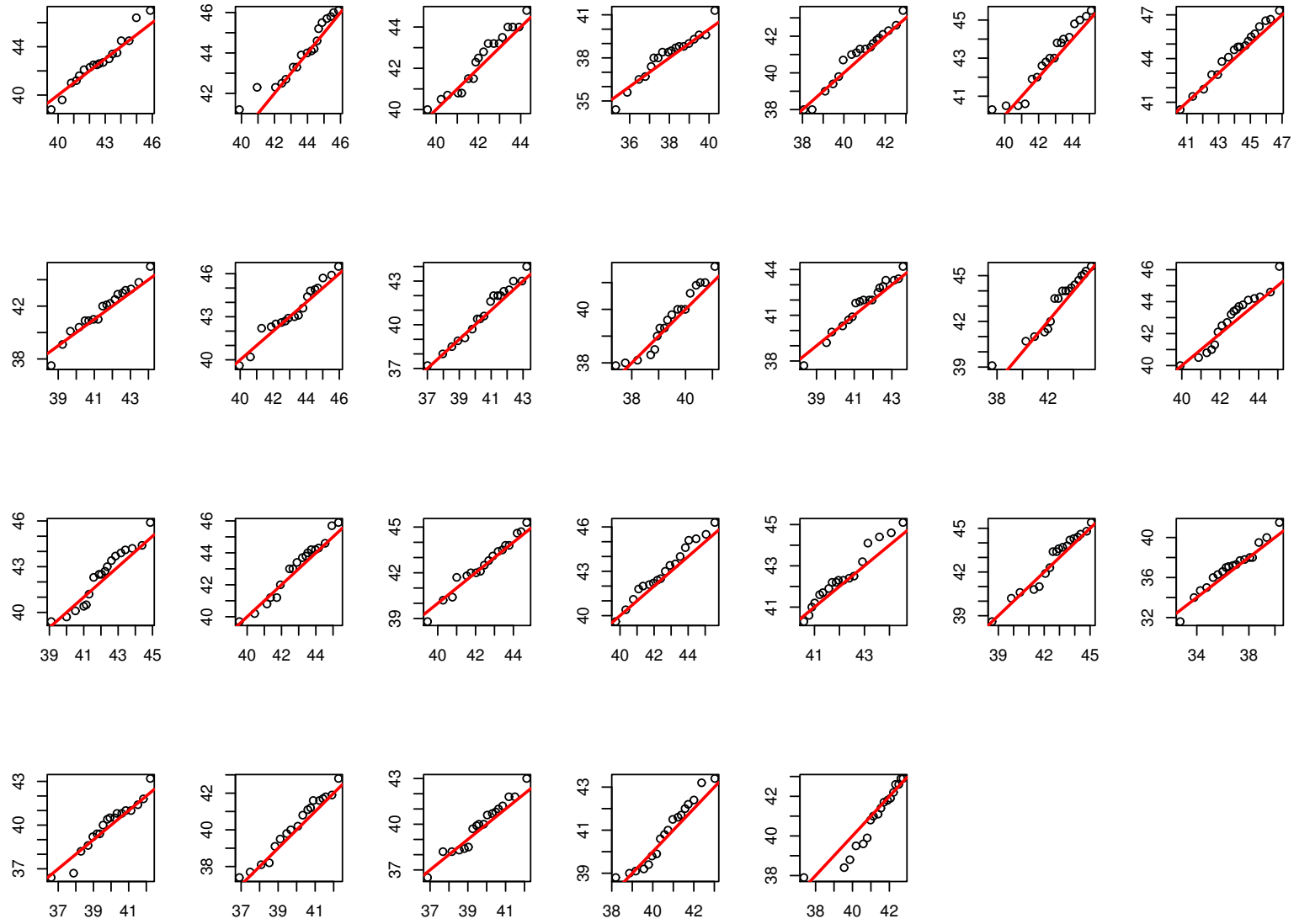


Figure B.8: Quantile-quantile plots of observed versus simulated data at each observed location using posterior simulations from the fitted Brown-Resnick model.

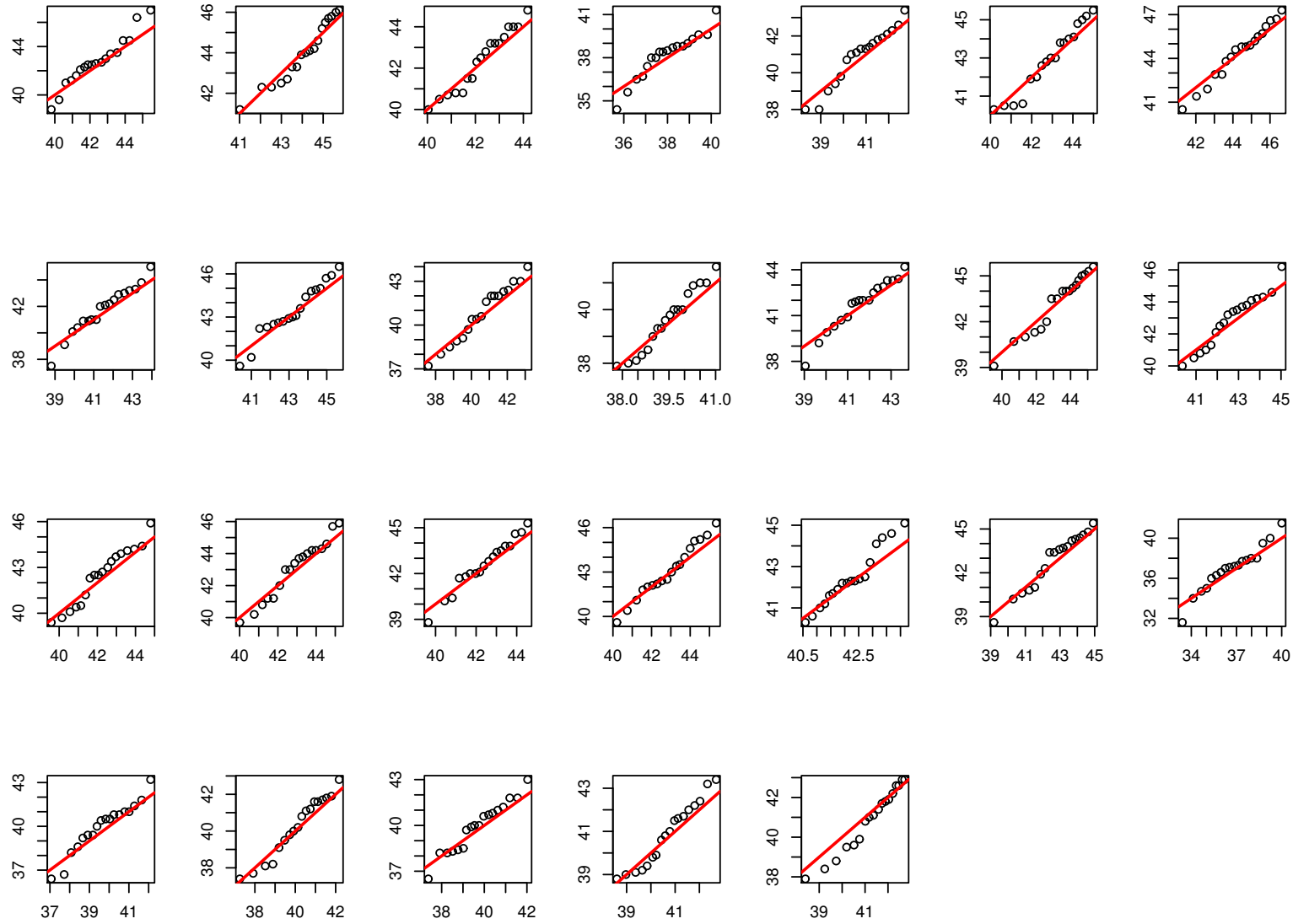


Figure B.9: Quantile-quantile plots of observed versus simulated data at each observed location using posterior simulations from the fitted powered exponential model.

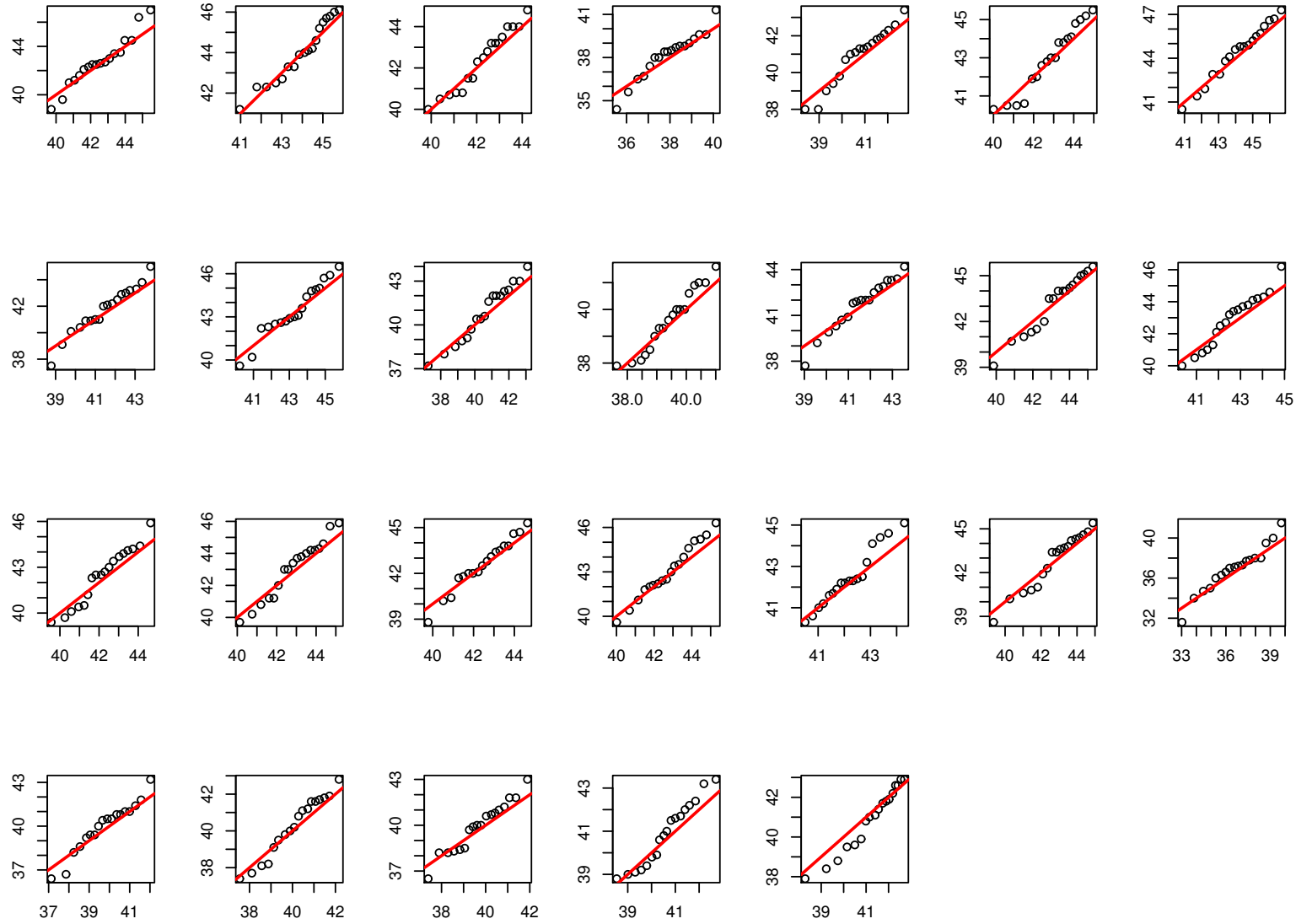


Figure B.10: Quantile-quantile plots of observed versus simulated data at each observed location using posterior simulations from the fitted Whittle-Matérn model.

B.3 Simulation examples

The capability of the ABMC method in identifying the correct max-stable models for model selections problems involving spatial extreme data was assessed through simulated examples. Specifically, three such simulated examples were performed where the three observed data sets were generated from the Whittle-Matérn, powered exponential and Brown-Resnick models with all model parameters set to 1.

For each of the three models, forty observations were generated at each of the thirty locations on an arbitrary 10-by-10 (degree latitude and longitude) grid with the parameter priors previously defined in Section 4.5.1. The spatial locations of the generated observations were drawn from a $U(0, 10) \times U(0, 10)$ distribution and the same thirty locations were used in all three examples. A minor computational benefit of using the same set of locations and priors in these examples is that the FP step is independent of the observed extrema data (unless one implements the optional ‘pilot ABC’ step in Fearnhead and Prangle (2012)), allowing the same set of regression coefficient estimates to be used in all three examples.

The misclassification matrix generated in the FP step for this setup is

$$\begin{array}{l}
 P(\text{Whittle-Matérn}|K=\dots) \\
 P(\text{Cauchy}|K=\dots) \\
 P(\text{Powered Exponential}|K=\dots) \\
 P(\text{Bessel}|K=\dots) \\
 P(\text{Smith}|K=\dots) \\
 P(\text{Brown-Resnick}|K=\dots)
 \end{array}
 \begin{bmatrix}
 K=1 & K=2 & K=3 & K=4 & K=5 & K=6 \\
 0.43 & 0.10 & 0.03 & 0.27 & 0.000 & 0.02 \\
 0.16 & 0.73 & 0.20 & 0.15 & 0.000 & 0.001 \\
 0.10 & 0.12 & 0.70 & 0.02 & 0.001 & 0.04 \\
 0.29 & 0.04 & 0.03 & 0.53 & 0.004 & 0.02 \\
 0.004 & 0.008 & 0.005 & 0.009 & 0.98 & 0.01 \\
 0.02 & 0.007 & 0.05 & 0.01 & 0.01 & 0.90
 \end{bmatrix}.$$

The misclassification matrix obtained was similar to the one obtained from the South Australian specifications particularly in terms of correct model identification probabilities, i.e. the diagonal entries. Of the six max-stable models, the Smith ($K = 5$) and Brown-Resnick ($K = 6$) models appear to be very well-identified. The Schlather models ($K \in \{1, 2, 3, 4\}$) performed adequately with better model identification for the Cauchy ($K = 2$) and powered exponential models ($K = 3$) compared with the Whittle-Matérn ($K = 1$) and Bessel models ($K = 4$). The only difference between the two misclassification matrices is for the identification of the Whittle-Matérn model ($K = 1$) where the diagonal entry of the corresponding column is now the largest entry in the column - an improvement from the South Australian case based purely on the different spatial grid used.

The three max-stable models chosen are representatives of the three different general trends in the misclassification matrix columns. The Whittle-Matérn model represents the two models (Whittle-Matérn and Bessel) where the model identification is less

evident for the particular regression summary statistics and prior specifications. The powered exponential model is representative of the two models (powered exponential and Cauchy) where the model identification strength is intermediate. Lastly, the Brown-Resnick model is representative of the two models (Smith and Brown-Resnick) with strong model identification in the misclassification matrix. In each of the three pairs above, the chosen model was the one with the weaker model identifiability in their respective pairs.

The ABMC algorithm was then applied to each of these data sets using the specifications in the main text for the South Australian data set. Specifically,

- the number of particles in SMC sample was set to 2000
- the tuning parameters α and c were set to 0.5 and 0.01 respectively
- the SMC ABC was terminated when the final acceptance probability dropped below 10^{-3} .

The progression of the estimated posterior model probabilities are plotted in Figures B.11, B.13 and B.15 for the observed data sets generated from the Whittle-Matérn, powered exponential and Brown-Resnick models respectively. The corresponding parameter posterior distributions for the correct model are also summarised in Figures B.12, B.14 and B.16, and Tables B.4, B.5 and B.6.

In all three simulated examples, the powered exponential model was preferred initially followed by the preference of the correct model as the discrepancy values decreases (with increasing SMC iterations). The strengths of the preference to the correct model were, perhaps unsurprisingly, related to their model identification results from the misclassification matrix.

For the Brown-Resnick example, there was a very strong preference for the Brown-Resnick model in particle sets of the final few SMC iterations with the posterior model probabilities for the other candidate models estimated to be very small or 0 (Figure B.15).

In the powered exponential example, the initial strong preference for the powered exponential model was tempered by an increasing posterior model probability for the Whittle-Matérn model. However, the estimated posterior model probability for the powered exponential model was still the largest out of all six candidate models for all SMC iterations (Figure B.13).

With the Whittle-Matérn example, the estimated posterior model probability for the powered exponential distribution was still larger than that for the Whittle-Matérn model. However, there is an obvious decreasing trend in the estimated posterior probabilities for the powered exponential model beginning from SMC iteration 8 which was sustained until the algorithm terminated. This decreasing trend was also coupled with the steady increase in the estimated model probability for the Whittle-Matérn

model (Figure B.11). It is likely that the posterior probability estimate for the Whittle-Matérn model would increase past that of the powered exponential model if the algorithm was continued further (with a smaller final acceptance probability of $< 10^{-3}$).

Overall, it can be said that the ABMC algorithm performed sufficiently well in identifying the correct model in the simulated examples. There were no issues with identifying the correct model in the powered exponential and Brown-Resnick examples. However, it appears to require a more stringent stopping criterion when dealing with observed data generated from models with weak model identifiability based on the misclassification matrix in the FP step.

All estimated parameter posteriors contained the true value used to generate the observed data sets except for the estimated range parameter (c_2) posterior in the Brown-Resnick model where the algorithm overestimated the value of c_2 (with an estimated posterior mean and 95% credible interval of 1.51(1.31, 1.73)).

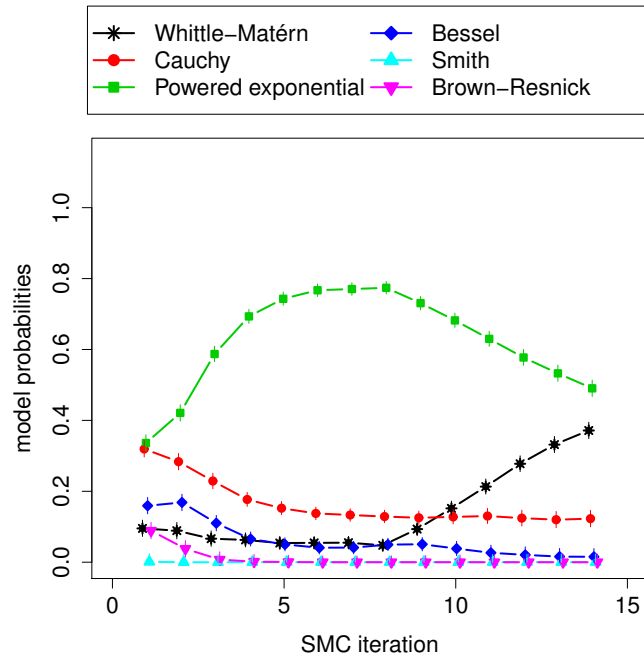


Figure B.11: Progression of estimated model probabilities across SMC iterations for the Whittle-Matérn simulation example.

<i>Parameter</i>	<i>Mean</i>	<i>SD</i>	<i>2.5% quantile</i>	<i>Median</i>	<i>97.5% quantile</i>
c_2	0.879	0.0836	0.710	0.881	1.04
ν	1.21	0.153	0.949	1.20	1.54

Table B.4: Parameter estimates of the correct fitted model for the Whittle-Matérn simulated data set.

A separate simulation example was also performed as a validation for the results obtained from the South Australian data set. The observed data set in this validation case study was generated from the posterior distribution of the most preferred model

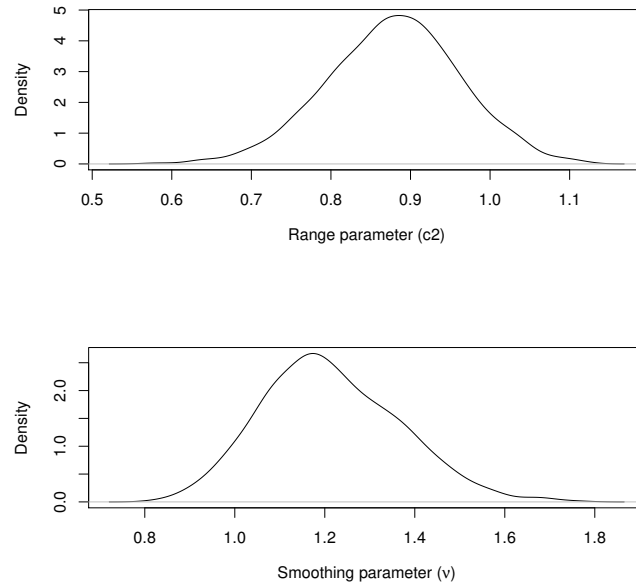


Figure B.12: Posterior parameter estimates for the Whittle-Matérn model.

<i>Parameter</i>	<i>Mean</i>	<i>SD</i>	<i>2.5% quantile</i>	<i>Median</i>	<i>97.5% quantile</i>
c_2	1.08	0.0762	0.925	1.09	1.23
ν	0.876	0.0749	0.749	0.878	1.01

Table B.5: Parameter estimates of the correct fitted model for the powered exponential simulated data set.

<i>Parameter</i>	<i>Mean</i>	<i>SD</i>	<i>2.5% quantile</i>	<i>Median</i>	<i>97.5% quantile</i>
c_2	1.51	0.104	1.31	1.51	1.73
ν	0.980	0.0327	0.914	0.981	1.04

Table B.6: Parameter estimates of the correct fitted model for the Brown-Resnick simulated data set.

inferred by the ABMC algorithm in Section 4.5.2, i.e. the Brown-Resnick model. Specifically, the particular parameter values used to generate the validation simulated example data set were 3.9 and 0.9 for c_2 and ν respectively.

The posterior model probabilities for this validation case is shown in Figure B.17 with a rapidly increasing estimated posterior model probability for the Brown-Resnick model following the initial preference for the powered exponential model (as observed in the other simulation examples). The estimated model probability for the Brown-Resnick model was substantially larger than all other candidate models at the termination of the algorithm.

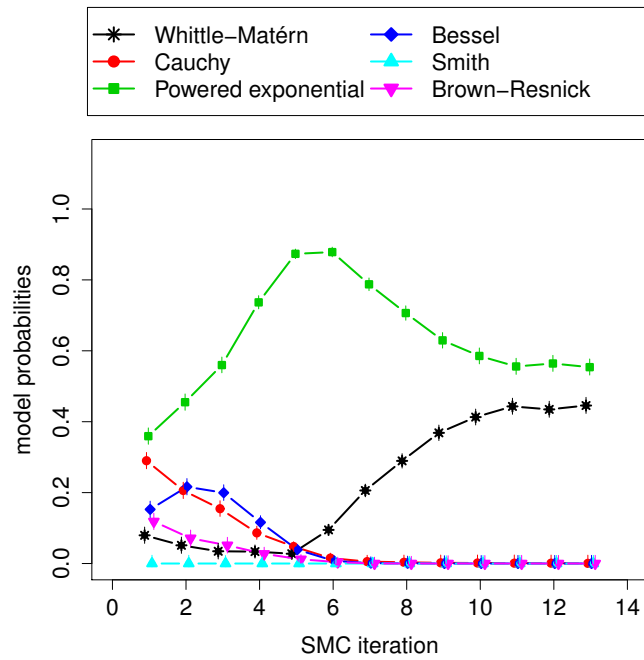


Figure B.13: Progression of estimated model probabilities across SMC iterations for the powered exponential simulation example.

The corresponding posterior distribution estimates for the Brown-Resnick model parameters are summarised in Figure B.18 and Table B.7. The estimated posterior distributions covered the true values of the parameters used to generate the data set.

<i>Parameter</i>	<i>Mean</i>	<i>SD</i>	<i>2.5% quantile</i>	<i>Median</i>	<i>97.5% quantile</i>
c_2	4.2	0.177	3.88	4.22	4.57
ν	0.99	0.0296	0.931	0.987	1.04

Table B.7: Parameter estimates of the fitted Brown-Resnick model for the South Australian validation simulated data set.

B.4 Preliminary comparison of characteristics of exact and approximate simulation from max-stable processes

This section briefly investigates the properties of max-stable model simulations generated using the approximate methods as implemented in the R package **SpatialExtremes** (Ribatet et al., 2013) and the exact method based on the extremal functions for a finite set of locations (Dombry et al., 2016).

Specifically, we compared the pairwise extremal coefficient empirical estimates, as defined in the main text (Section 3), generated from the three max-stable models with posterior support in the final particle set (Whittle-Matérn, powered exponential and Brown-Resnick). The parameter values used to generate the simulated data were the respective model's parameter posterior mean estimates and 10,000 model simulations

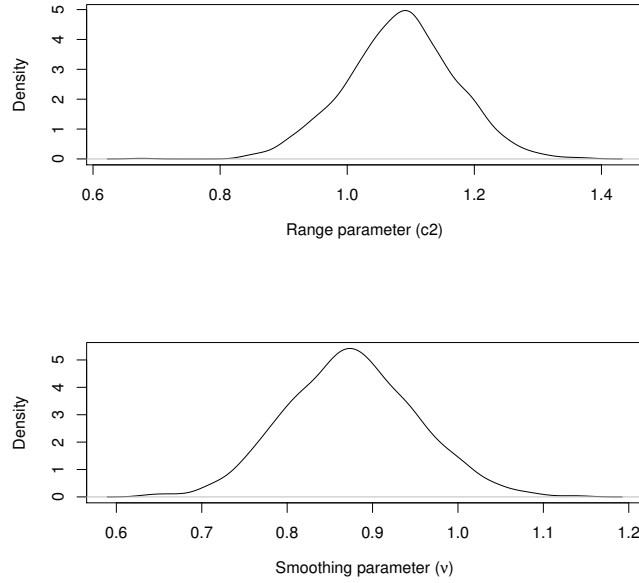


Figure B.14: Posterior parameter estimates for the powered exponential model.

were generated for each model. In addition, we also checked how well the model simulations generated using the two different simulation methods recover the theoretical marginal distributions (unit Fréchet i.e. $\text{GEV}(1, 1, 1)$) by comparing the maximum likelihood estimates of the margins with their theoretical values (of 1).

For the same model and parameter values, both approximate and exact simulation methods produced similar spatial dependence structures as measured by the empirical estimates of the pairwise extremal coefficients (Figures B.20, B.22 and B.24). This provides confidence that the results obtained in the main text (Section 4.5.2) would be relatively similar if the exact simulation method was used in place of the approximate method.

The marginal distribution parameter estimates in the Whittle–Matérn case, as shown in Figure B.19, were broadly in agreement with the theoretical distribution except for a few locations (location index 10, 15, and 26 for the exact simulation method and location index 19 for the approximate method).

Both simulation methods were able to produce model simulations with marginal distributions in agreement with the theoretical unit Fréchet distribution for the powered exponential case (Figure B.21).

In the Brown–Resnick case, the exact simulation method performed notably better than the approximate simulation method in recovering the theoretical marginal distributions (Figure B.23). The location and scale parameter estimates from the approximate simulation method were consistently below the theoretical value of 1 across all locations.

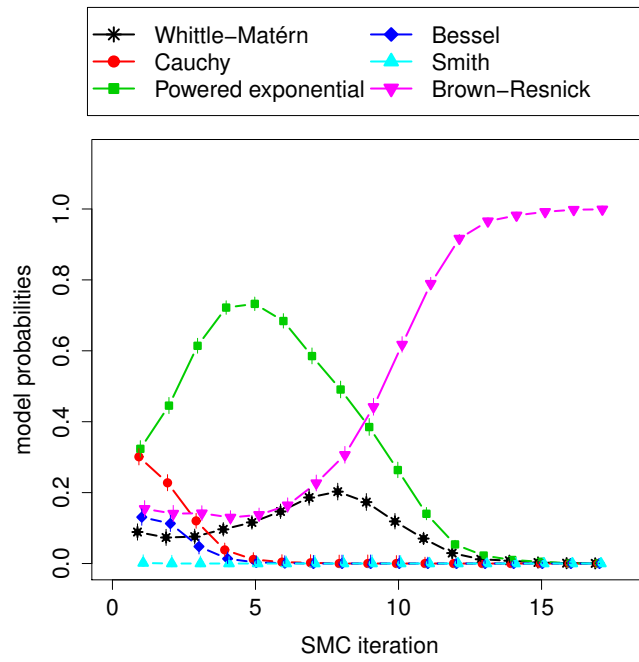


Figure B.15: Progression of estimated model probabilities across SMC iterations for the Brown-Resnick simulation example.

While this discrepancy would not likely impact the results in the main text (Section 4.5.2) considering the spatial dependence structure generated with the two methods are still very similar to one another (Figure B.24), it is worthy of further investigation in subsequent work. It would also be of interest to investigate the potential similarities and discrepancies of the two simulation methods for the other max-stable models and other parameter configurations.

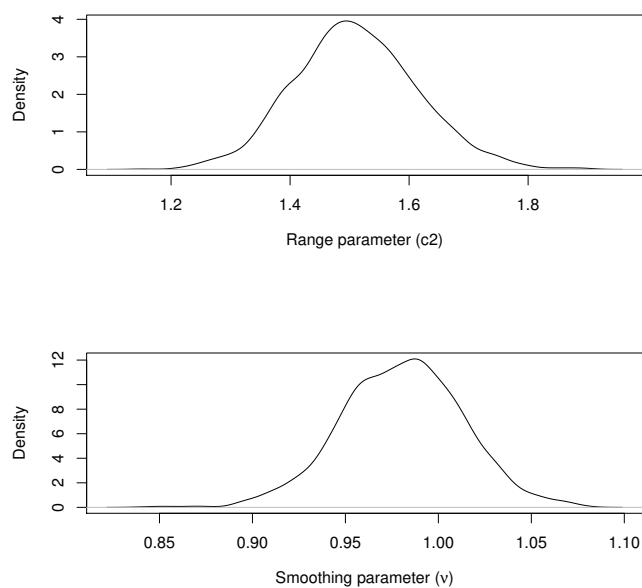


Figure B.16: Posterior parameter estimates for the Brown-Resnick model.

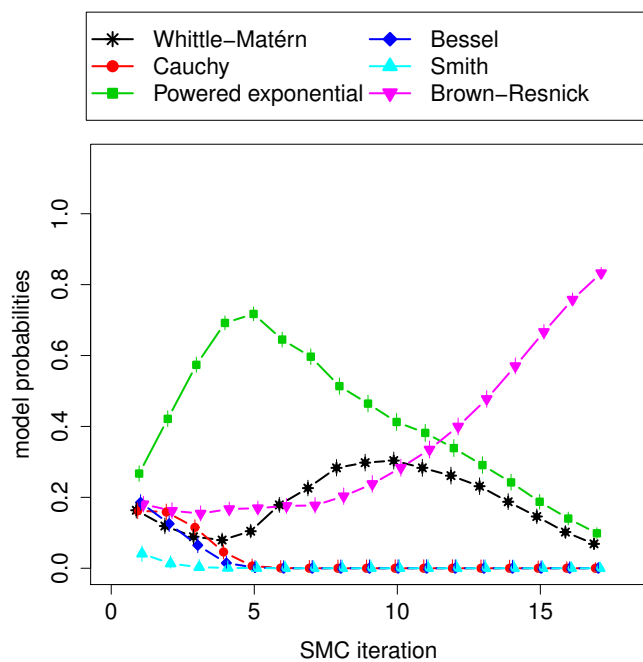


Figure B.17: Progression of estimated model probabilities across SMC iterations for the validation simulated example.

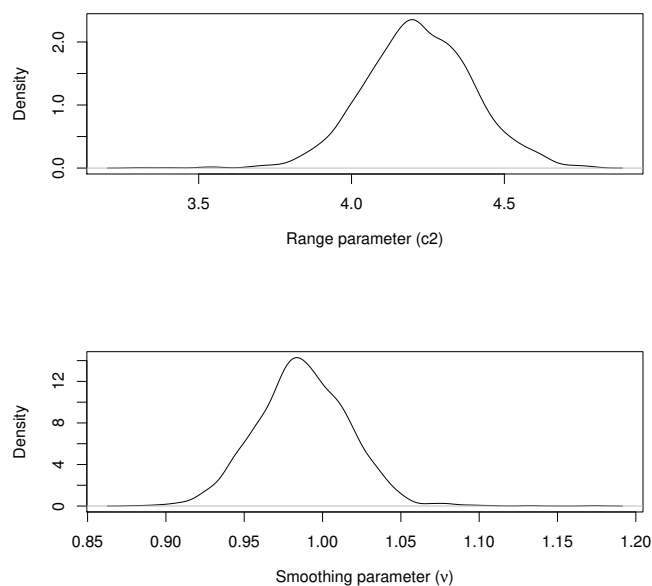


Figure B.18: Posterior parameter estimates for the correct model in the validation simulated example. The true parameter values were 3.9 for c_2 and 0.9 for ν .

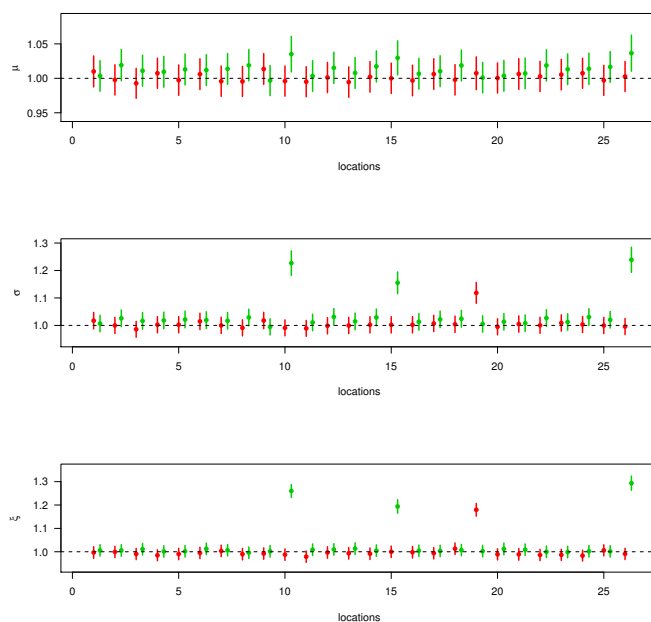


Figure B.19: Comparison of maximum likelihood estimates for the GEV margins using Whittle–Matérn model simulations from the R package `SpatialExtremes` (red) and exact simulation method based on extremal functions (green). Estimates obtained from 10000 simulations.

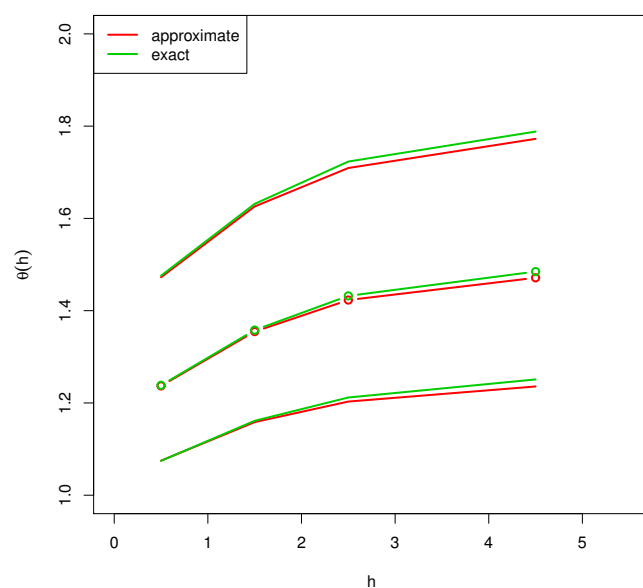


Figure B.20: Comparison of the empirical pairwise extremal coefficient estimates of Whittle–Matérn model simulations from the R package `SpatialExtremes` (red) and exact simulation method based on extremal functions (green).

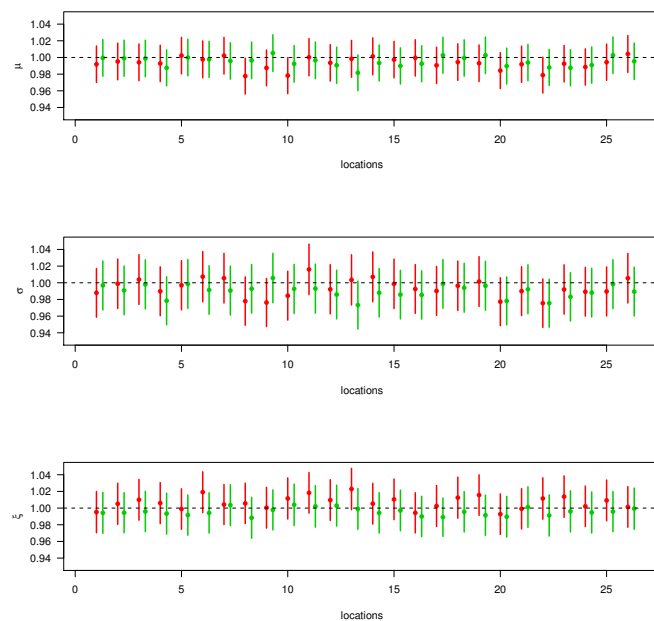


Figure B.21: Comparison of maximum likelihood estimates for the GEV margins using powered exponential model simulations from the R package `SpatialExtremes` (red) and exact simulation method based on extremal functions (green). Estimates obtained from 10000 simulations.

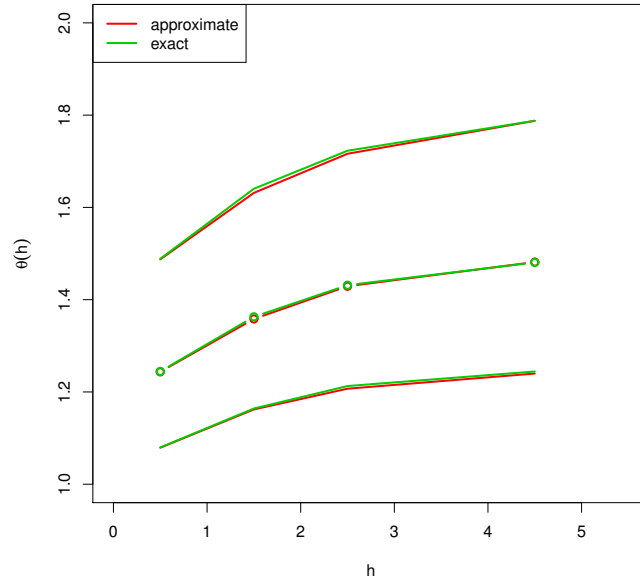


Figure B.22: Comparison of the empirical pairwise extremal coefficient estimates of powered exponential model simulations from the R package `SpatialExtremes` (red) and exact simulation method based on extremal functions (green).

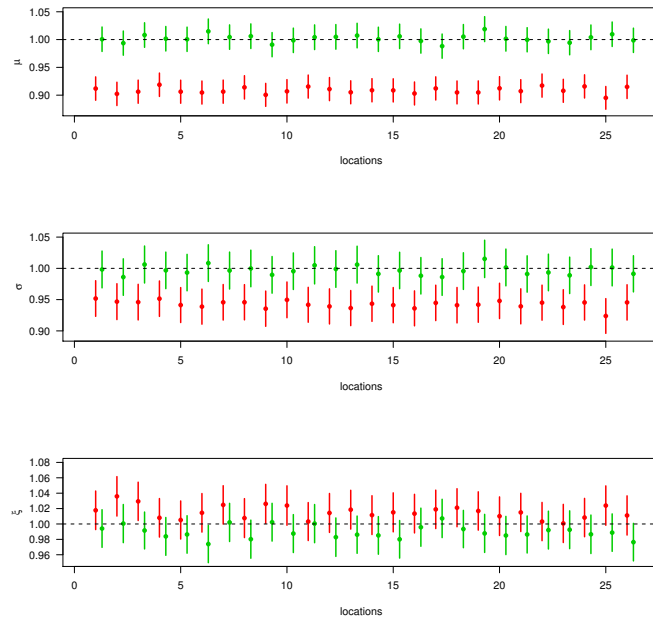


Figure B.23: Comparison of maximum likelihood estimates for the GEV margins using Brown-Resnick model simulations from the R package `SpatialExtremes` (red) and exact simulation method based on extremal functions (green). Estimates obtained from 10000 simulations.

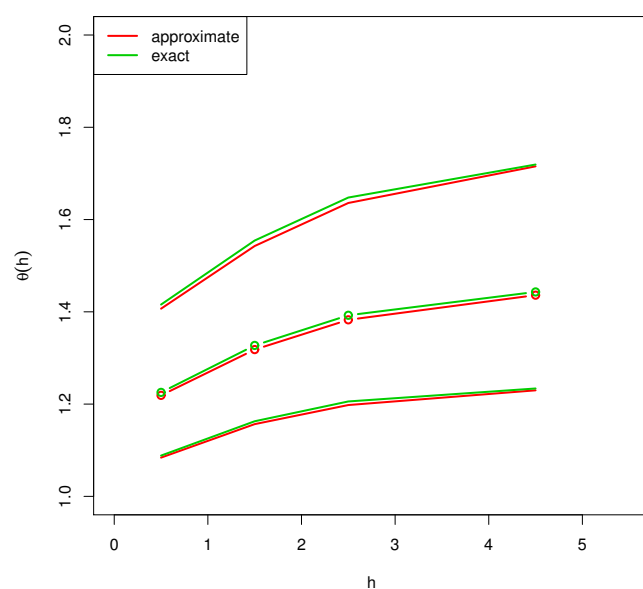


Figure B.24: Comparison of the empirical pairwise extremal coefficient estimates of powered exponential model simulations from the R package **SpatialExtremes** (red) and exact simulation method based on extremal functions (green).

C Supplementary Material for Chapter 5: ‘Parametric survival analysis of hospital ward MR-SA incidence allowing for carryover effects from previous cases’

C.1 Model details

This section provides additional details on the parametric survival model with covariates for recurrent events used in the main text.

The hazard function of the parametric survival model is denoted by $h(t_a, t_b)$ where t_a and t_b are the start and end time (in weeks) of a particular recurrence respectively. The hazard function is assumed to be a multiplicative function of a baseline hazard ($h_0(t_a, t_b)$) and covariates ($X_i(t_a, t_b)$) with coefficients γ_i as follows:

$$h(t_a, t_b) = h_0(t_a, t_b) \exp \left\{ \sum_{i=1}^W \gamma_i X_i(t_a, t_b) \right\} \quad t_a < t_b$$

where $W \in \{0, 1, 2, 3, 4\}$ and $X_i(t_a, t_b) = X(t_b - i)$ for the model used here. The survival and probability density functions are then derived from the standard survival model relationships $S(t_a, t_b) = \exp \left\{ - \int_{t_a}^{t_b} h(t_a, u) du \right\}$ and $f(t_a, t_b) = h(t_a, t_b)S(t_a, t_b)$.

The effects of left truncation and right censoring incurred by the fixed start and end date of the study design were accounted for in the model with the use of a survival function to denote the likelihood contribution of the time periods between the start of the study and the first observed case (left truncation), and the last observed case to the end of the study (right censoring). The likelihood contribution of a fully observed event is simply $f(t_a, t_b)$.

To construct the model likelihood, assume the data set (for a particular ward-cubicle combination) consists of N beds, with bed j having n_j events over the time period $[T_0, T]$ ($j = 1, \dots, N$). For beds with no events over the time period, the likelihood

contribution is merely $L_0 = S(T_0, T)$. For beds with exactly one event recorded at time $t_{j,1}$ in the time period, the likelihood contribution is $L_1 = S(T_0, t_{j,1})S(t_{j,1}, T)$. Note that this does not simplify to $S(T_0, T)$ from definition of $S(t_a, t_b)$ above (unless $h(t_a, t_b)$ is time-independent, i.e. exponential hazard). For other beds, the likelihood contribution is $L_* = S(T_0, t_{j,1}) \prod_{k=2}^{n_j} f(t_{j,k-1}, t_{j,k}) S(t_{j,n_j}, T)$. To illustrate, the likelihood contribution from a hypothetical bed shown in Figure C.1 with three observed cases (at times t_1 , t_2 and t_3) in the observation period ($[T_0, T]$) is $S(T_0, t_1)f(t_1, t_2)f(t_2, t_3)S(t_3, T)$.

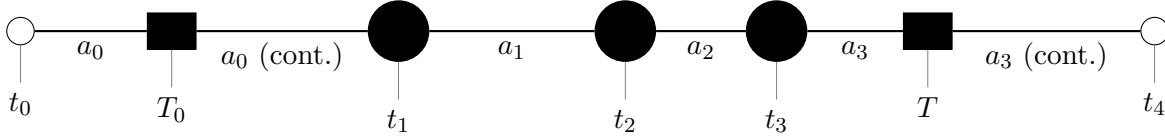


Figure C.1: Illustrative diagram of recurrent events for a particular bed in a ward. The filled squares mark the start (T_0) and end (T) points of the observation period. The filled circles represent observed events within the observation period. The hollow circles denote unobserved events immediately prior to the start (t_0) and end (t_4) of the observation period.

The full model likelihood is then

$$L = \prod_{j=1}^N L_0^{1(n_j=0)} L_1^{1(n_j=1)} L_*^{1(n_j>1)}$$

where $1(x)$ is an indicator function which equals 1 if x is true and 0 otherwise.

As mentioned in the main text, the baseline hazard function used in this study was assumed to be either an exponential or power law (or Weibull) hazard defined as:

$$h_0(t_a, t_b) = \begin{cases} M & \text{exponential} \\ M\beta(t_b - t_a)^{\beta-1} & \text{power law.} \end{cases}$$

The four covariates used were the proportion of beds in the same cubicle with a multiresistant methicillin-resistant *Staphylococcus aureus* (mrMRSA) patient in the previous week, two weeks prior, three weeks prior and four weeks prior (i.e. $W \in \{0, 1, 2, 3, 4\}$ where $W = 0$ is the case with no covariates). The four week limit on the covariates was also used in previous analysis of the data set. (Kong et al., 2012)

It was further assumed that models with a particular time lag covariates would also include all smaller time lags, e.g. a model with the proportion of mrMRSA patients three weeks prior as a covariate would also include the proportions two and one week prior. This results in five unique combinations of the four covariates: either no covariates, proportions one week prior only, proportions one and two weeks prior, proportions one to three weeks prior, and proportions from all four weeks prior.

The use of proportions as covariates was motivated as a way to capture the different intensities created by multiple mrMRSA patients in the same cubicle (compared with a

straightforward indicator covariate) standardising for ward occupancy. A consequence of using these covariates is the analysis had to be performed separately for the different cubicle sizes in each ward.

As there are two baseline hazards forms and five combinations of the covariates, data from each ward-cubicle were fitted to ten unique candidate parametric survival models. The simplest model considered was an exponential baseline hazard with no covariates (e0)

$$h(t_a, t_b) = M$$

and the most elaborate model considered was the power law baseline hazard with proportion of mrMRSA cases one to four weeks prior as covariates (pl4)

$$h(t_a, t_b) = M\beta(t_b - t_a)^{\beta-1} \exp \{ \gamma_1 X_1(t_a, t_b) + \gamma_2 X_2(t_a, t_b) + \gamma_3 X_3(t_a, t_b) + \gamma_4 X_4(t_a, t_b) \}$$

with $X_i(t_a, t_b)$ denoting the proportion of mrMRSA cases i weeks prior from t_b .

Shorthand for the other models is similarly constructed with either ‘e’ or ‘pl’ denoting the use of the exponential or power law baseline hazard form, respectively, followed by an integer between 0 and 4 to denote the maximum number of past weeks used as covariates.

Both the fitted AIC and BIC values were used to compare the statistical fit of the ten candidate models, and likelihood ratio tests were performed to compare specific nested pairs of candidate models in order to select a statistically ‘best-fitting’ model for each ward-cubicle (Section C.3).

C.2 Data plots

This section provides plots of the data from the other six wards used in the analysis presented in the main text. The plot for Ward A is in the main text. Additional ward classification information is also provided in Table C.1.

Ward	Type	Cubicles	Beds (cubicle partitioning)	new mrMRSA	old mrMRSA
A	Mixed	10	24 (2 2 2 2 2 2 2 2 4 4)	60	189
B	Mixed	1	30 (30)	53	58
C	Medical	7	24 (2 2 4 4 4 4 4)	46	73
D	Surgical	8	28 (2 2 4 4 4 4 4 4)	38	21
E	Surgical	8	26 (2 2 2 4 4 4 4 4)	35	29
F	Surgical	7	24 (2 2 4 4 4 4 4)	21	16
G	Medical	11	29 (1 2 2 2 2 2 2 4 4 4 4)	21	32

Table C.1: Brief description of the six wards used in the analysis.

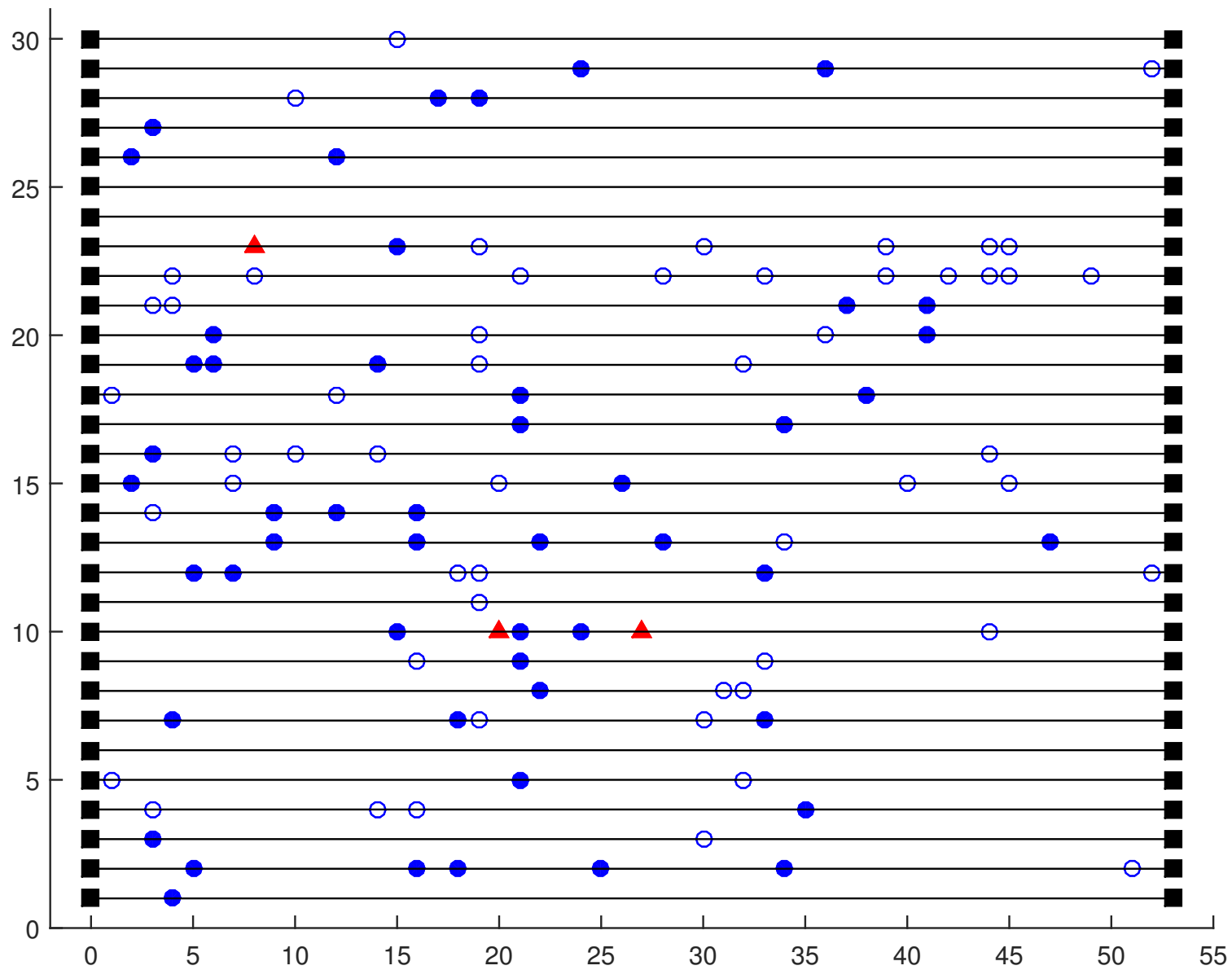


Figure C.2: Timeline of events in all beds located in Ward B. The empty circles are weeks where an old mrMRSA case was observed, filled circles for new mrMRSA, and filled triangles for both old and new cases of mrMRSA detected in the same week. Ward B is an open ward, i.e. no cubicles.

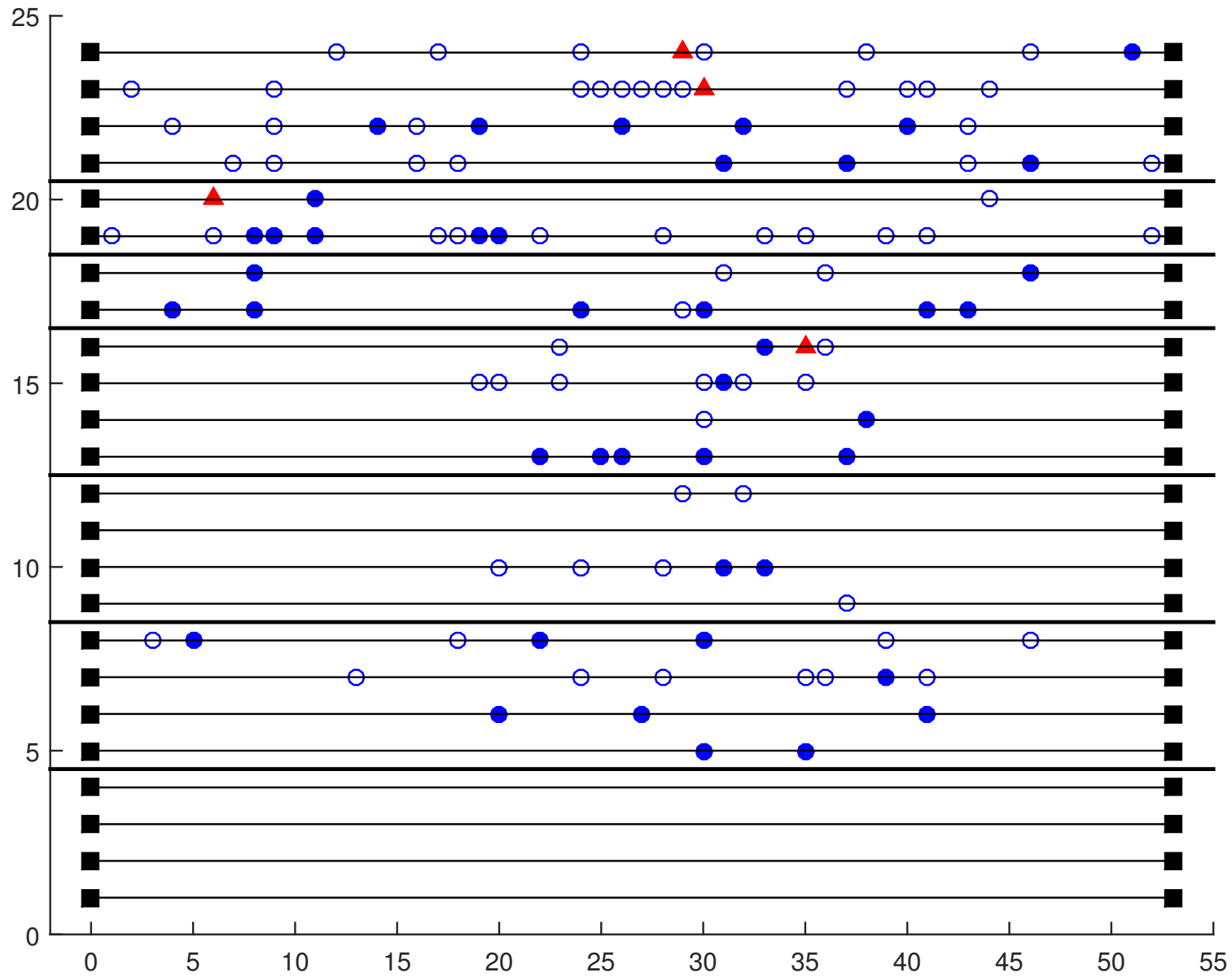
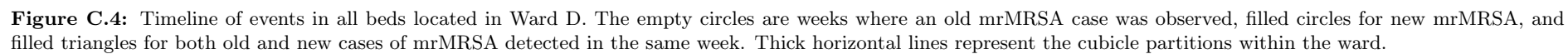


Figure C.3: Timeline of events in all beds located in Ward C. The empty circles are weeks where an old mrMRSA case was observed, filled circles for new mrMRSA, and filled triangles for both old and new cases of mrMRSA detected in the same week. Thick horizontal lines represent the cubicle partitions within the ward.



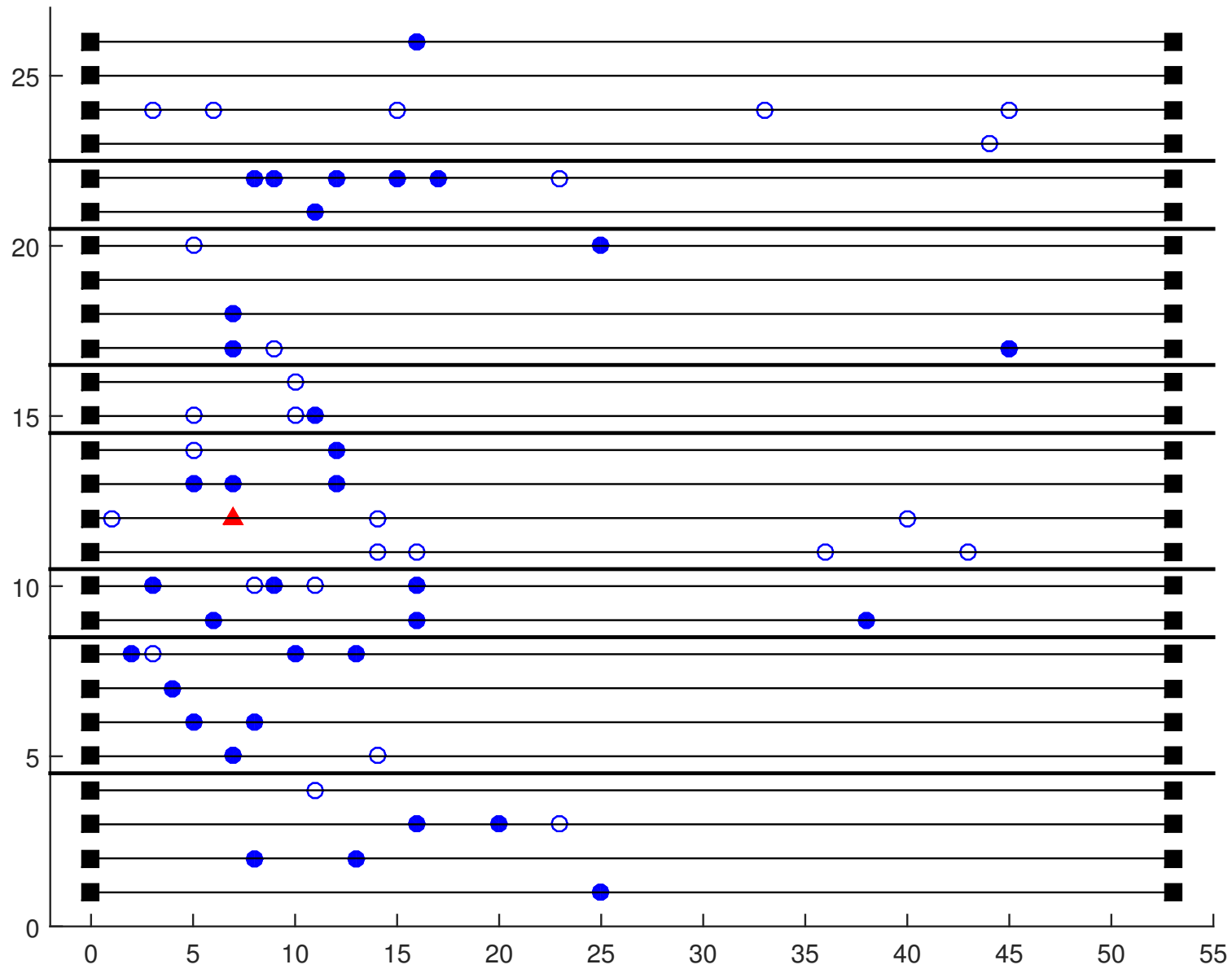
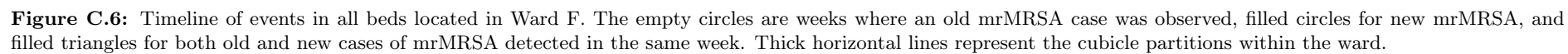


Figure C.5: Timeline of events in all beds located in Ward E. The empty circles are weeks where an old mrMRSA case was observed, filled circles for new mrMRSA, and filled triangles for both old and new cases of mrMRSA detected in the same week. Thick horizontal lines represent the cubicle partitions within the ward.



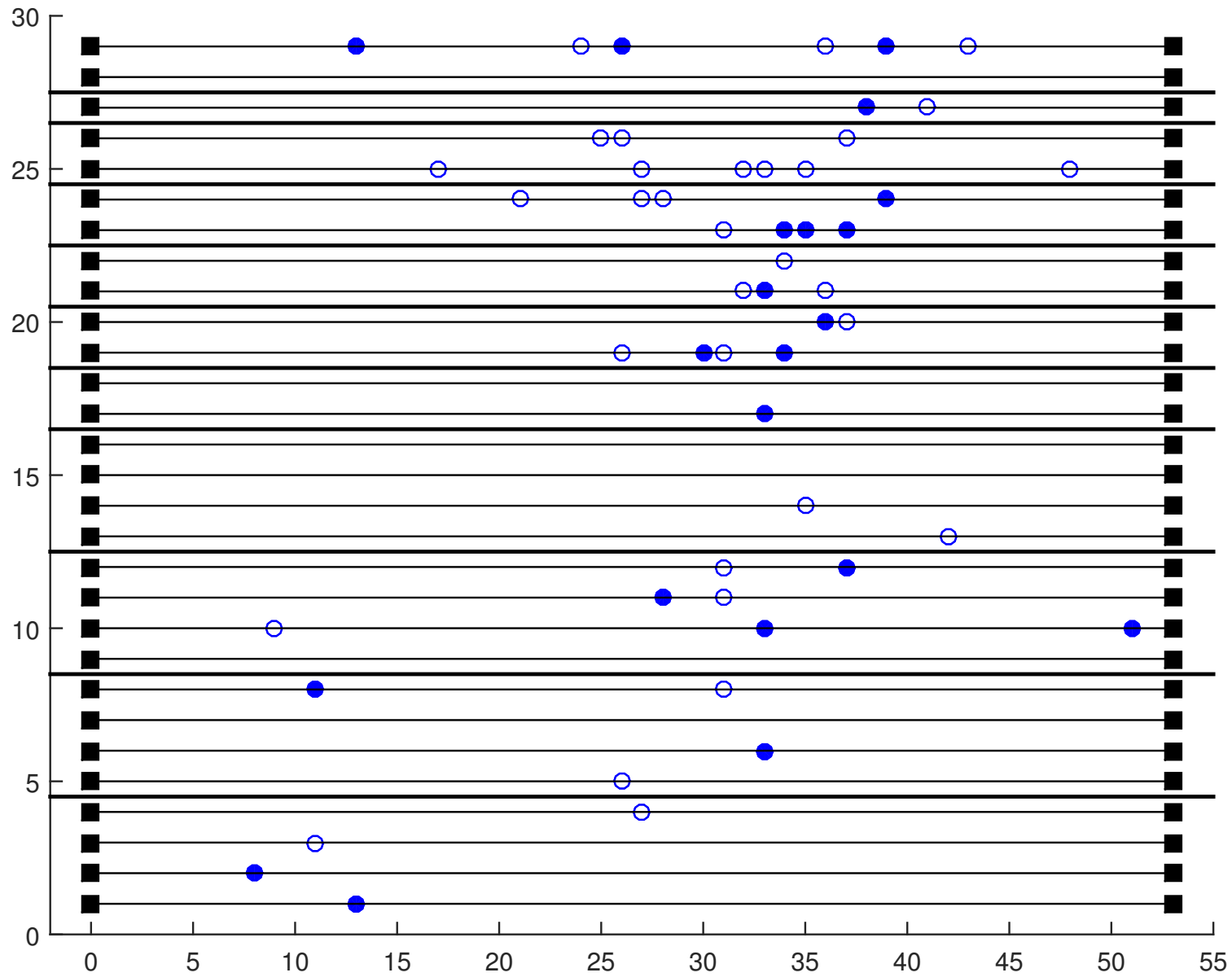


Figure C.7: Timeline of events in all beds located in Ward G. The empty circles are weeks where an old mrMRSA case was observed, filled circles for new mrMRSA, and filled triangles for both old and new cases of mrMRSA detected in the same week. Thick horizontal lines represent the cubicle partitions within the ward.

C.3 Model comparison outputs

This section collates the numerical outputs used to compare between the 10 candidate models for each ward-cubicle combination. Specifically, the AIC and BIC values were used to assess the relative goodness-of-fit of all models. Only models with an AIC or BIC difference of 6 (Kass and Raftery, 1995) compared with the model with the smallest AIC or BIC were given further consideration. The likelihood ratio tests were used to compare any pairs of nested candidate models in the smaller model pool.

There were convergence issues for some models with ward-cubicles with small numbers of new mrMRSA cases. These models were excluded from the outputs below for the particular ward-cubicles.

C.3.1 Output tables for Ward A 2-bed cubicles

Model	-log-likelihood	AIC	BIC
e0	107.18	216.36	218.33
e1	107.16	218.32	222.26
e2	105.14	216.28	222.20
e3	99.55	207.09	214.97
e4	99.23	208.45	218.30
pl0	102.98	209.95	213.89
pl1	102.98	211.95	217.86
pl2	101.73	211.45	219.33
pl3	98.10	206.19	216.04
pl4	97.87	207.75	219.57

Table C.2: Model negative log-likelihood, AIC and BIC values for different combinations of the 10 models fitted to data from beds in 2-bed cubicles in Ward A.

	LR TS	df	p-value
e1 v. e0	0.03	1	0.855
e2 v. e0	4.07	2	0.131
e3 v. e0	15.26	3	1.60×10^{-3}
e4 v. e0	15.90	4	3.15×10^{-3}
pl0 v. e0	8.40	1	3.75×10^{-3}
pl1 v. e0	8.40	2	1.50×10^{-2}
pl2 v. e0	10.90	3	1.23×10^{-2}
pl3 v. e0	18.16	4	1.15×10^{-3}
pl4 v. e0	18.61	5	2.27×10^{-3}
e2 v. e1	4.04	1	4.45×10^{-2}
e3 v. e1	15.23	2	4.93×10^{-4}
e4 v. e1	15.87	3	1.21×10^{-3}
pl1 v. e1	8.37	1	3.82×10^{-3}
pl2 v. e1	10.87	2	4.36×10^{-3}
pl3 v. e1	18.13	3	4.14×10^{-4}
pl4 v. e1	18.58	4	9.52×10^{-4}
e3 v. e2	11.19	1	8.21×10^{-4}
e4 v. e2	11.83	2	2.70×10^{-3}
pl2 v. e2	6.83	1	8.95×10^{-3}
pl3 v. e2	14.09	2	8.71×10^{-4}
pl4 v. e2	14.54	3	2.26×10^{-3}
e4 v. e3	0.64	1	0.424
pl3 v. e3	2.90	1	8.87×10^{-2}
pl4 v. e3	3.35	2	0.188
pl4 v. e4	2.71	1	1×10^{-1}
pl1 v. pl0	0	1	0.987
pl2 v. pl0	2.50	2	0.286
pl3 v. pl0	9.76	3	2.07×10^{-2}
pl4 v. pl0	10.21	4	3.71×10^{-2}
pl2 v. pl1	2.50	1	0.114
pl3 v. pl1	9.76	2	7.59×10^{-3}
pl4 v. pl1	10.21	3	1.69×10^{-2}
pl3 v. pl2	7.26	1	7.06×10^{-3}
pl4 v. pl2	7.70	2	2.12×10^{-2}
pl4 v. pl3	0.45	1	0.504

Table C.3: Likelihood-ratio test statistics (LR TS), degrees of freedom (df) and corresponding p-values for different combinations of the 10 models fitted to the 2-bed cubicles data in Ward A.

C.3.2 Output tables for Ward A 4-bed cubicles

Model	-log-likelihood	AIC	BIC
e0	50.08	102.16	103.38
e1	48.23	100.46	102.89
e2	38.86	83.72	87.38
e3	38.20	84.40	89.28
e4	38.13	86.27	92.36
pl0	49.54	103.09	105.53
pl1	48.00	101.99	105.65
pl2	37.19	82.38	87.26
pl3	35.94	81.88	87.97
pl4	35.92	83.85	91.16

Table C.4: Model negative log-likelihood, AIC and BIC values for different combinations of the 10 models fitted to data from beds in 4-bed cubicles in Ward A.

	LR TS	df	right-tail prob
e1 v. e0	3.70	1	5.43×10^{-2}
e2 v. e0	22.44	2	1.34×10^{-5}
e3 v. e0	23.76	3	2.81×10^{-5}
e4 v. e0	23.89	4	8.40×10^{-5}
pl0 v. e0	1.07	1	0.301
pl1 v. e0	4.17	2	0.124
pl2 v. e0	25.78	3	1.06×10^{-5}
pl3 v. e0	28.28	4	1.09×10^{-5}
pl4 v. e0	28.31	5	3.16×10^{-5}
e2 v. e1	18.73	1	1.50×10^{-5}
e3 v. e1	20.05	2	4.42×10^{-5}
e4 v. e1	20.19	3	1.55×10^{-4}
pl1 v. e1	0.46	1	0.496
pl2 v. e1	22.07	2	1.61×10^{-5}
pl3 v. e1	24.58	3	1.89×10^{-5}
pl4 v. e1	24.61	4	6.03×10^{-5}
e3 v. e2	1.32	1	0.251
e4 v. e2	1.45	2	0.484
pl2 v. e2	3.34	1	6.77×10^{-2}
pl3 v. e2	5.84	2	5.39×10^{-2}
pl4 v. e2	5.87	3	0.118
e4 v. e3	0.13	1	0.715
pl3 v. e3	4.52	1	3.34×10^{-2}
pl4 v. e3	4.55	2	0.103
pl4 v. e4	4.42	1	3.55×10^{-2}
pl1 v. pl0	3.10	1	7.85×10^{-2}
pl2 v. pl0	24.71	2	4.32×10^{-6}
pl3 v. pl0	27.21	3	5.32×10^{-6}
pl4 v. pl0	27.24	4	1.78×10^{-5}
pl2 v. pl1	21.61	1	3.34×10^{-6}
pl3 v. pl1	24.11	2	5.81×10^{-6}
pl4 v. pl1	24.14	3	2.33×10^{-5}
pl3 v. pl2	2.50	1	0.114
pl4 v. pl2	2.53	2	0.282
pl4 v. pl3	0.03	1	0.859

Table C.5: Likelihood-ratio test statistics (LR TS), degrees of freedom (df) and corresponding p-values for different combinations of the 10 models fitted to the 4-bed cubicles data in Ward A.

C.3.3 Output tables for Ward B

Model	-log-likelihood	AIC	BIC
e0	130.37	262.74	265.07
e1	129.84	263.69	268.35
e2	127.21	260.42	267.41
e3	121.12	250.25	259.57
e4	115.25	240.51	252.16
pl0	128.38	260.76	265.42
pl1	128.08	262.15	269.15
pl2	126.06	260.12	269.44
pl3	120.73	251.45	263.11
pl4	115.25	242.50	256.48

Table C.6: Model negative log-likelihood, AIC and BIC values for different combinations of the 10 models fitted to data from beds in Ward B.

	LR TS	df	right-tail prob
e1 v. e0	1.05	1	0.305
e2 v. e0	6.32	2	4.24×10^{-2}
e3 v. e0	18.49	3	3.48×10^{-4}
e4 v. e0	30.24	4	4.38×10^{-6}
pl0 v. e0	3.98	1	4.60×10^{-2}
pl1 v. e0	4.59	2	0.101
pl2 v. e0	8.63	3	3.47×10^{-2}
pl3 v. e0	19.29	4	6.89×10^{-4}
pl4 v. e0	30.25	5	1.32×10^{-5}
e2 v. e1	5.27	1	2.17×10^{-2}
e3 v. e1	17.44	2	1.63×10^{-4}
e4 v. e1	29.18	3	2.05×10^{-6}
pl1 v. e1	3.54	1	6.01×10^{-2}
pl2 v. e1	7.57	2	2.27×10^{-2}
pl3 v. e1	18.24	3	3.93×10^{-4}
pl4 v. e1	29.19	4	7.14×10^{-6}
e3 v. e2	12.17	1	4.85×10^{-4}
e4 v. e2	23.91	2	6.42×10^{-6}
pl2 v. e2	2.31	1	0.129
pl3 v. e2	12.97	2	1.53×10^{-3}
pl4 v. e2	23.93	3	2.59×10^{-5}
e4 v. e3	11.74	1	6.11×10^{-4}
pl3 v. e3	0.80	1	0.372
pl4 v. e3	11.75	2	2.80×10^{-3}
pl4 v. e4	0.01	1	0.910
pl1 v. pl0	0.61	1	0.435
pl2 v. pl0	4.65	2	9.79×10^{-2}
pl3 v. pl0	15.31	3	1.57×10^{-3}
pl4 v. pl0	26.27	4	2.79×10^{-5}
pl2 v. pl1	4.04	1	4.45×10^{-2}
pl3 v. pl1	14.70	2	6.42×10^{-4}
pl4 v. pl1	25.66	3	1.12×10^{-5}
pl3 v. pl2	10.66	1	1.09×10^{-3}
pl4 v. pl2	21.62	2	2.02×10^{-5}
pl4 v. pl3	10.96	1	9.32×10^{-4}

Table C.7: Likelihood-ratio test statistics (LR TS), degrees of freedom (df) and corresponding p-values for different combinations of the 10 models fitted to the data from beds in Ward B.

C.3.4 Output tables for Ward C 2-bed cubicles

Model	-log-likelihood	AIC	BIC
e0	39.55	81.10	81.99
e1	39.44	82.88	84.66
e2	37.91	81.82	84.49
e3	34.61	77.23	80.79
e4	34.48	78.97	83.42
pl0	39.20	82.40	84.18
pl1	39.16	84.32	86.99
pl2	37.90	83.79	87.36
pl3	34.50	79.00	83.45
pl4	34.41	80.81	86.15

Table C.8: Model negative log-likelihood, AIC and BIC values for different combinations of the 10 models fitted to data from beds in 2-bed cubicles in Ward C.

	LR TS	df	right-tail prob
e1 v. e0	0.22	1	0.638
e2 v. e0	3.28	2	0.194
e3 v. e0	9.87	3	1.97×10^{-2}
e4 v. e0	10.13	4	3.83×10^{-2}
pl0 v. e0	0.70	1	0.403
pl1 v. e0	0.78	2	0.676
pl2 v. e0	3.30	3	0.347
pl3 v. e0	10.10	4	3.88×10^{-2}
pl4 v. e0	10.29	5	6.75×10^{-2}
e2 v. e1	3.06	1	8.03×10^{-2}
e3 v. e1	9.65	2	8.03×10^{-3}
e4 v. e1	9.91	3	1.94×10^{-2}
pl1 v. e1	0.56	1	0.454
pl2 v. e1	3.08	2	0.214
pl3 v. e1	9.88	3	1.96×10^{-2}
pl4 v. e1	10.07	4	3.93×10^{-2}
e3 v. e2	6.59	1	1.03×10^{-2}
e4 v. e2	6.85	2	3.25×10^{-2}
pl2 v. e2	0.02	1	0.877
pl3 v. e2	6.82	2	3.31×10^{-2}
pl4 v. e2	7.01	3	7.17×10^{-2}
e4 v. e3	0.26	1	0.610
pl3 v. e3	0.23	1	0.634
pl4 v. e3	0.42	2	0.812
pl4 v. e4	0.16	1	0.692
pl1 v. pl0	0.08	1	0.771
pl2 v. pl0	2.61	2	0.272
pl3 v. pl0	9.40	3	2.44×10^{-2}
pl4 v. pl0	9.59	4	4.80×10^{-2}
pl2 v. pl1	2.52	1	0.112
pl3 v. pl1	9.32	2	9.49×10^{-3}
pl4 v. pl1	9.50	3	2.33×10^{-2}
pl3 v. pl2	6.79	1	9.15×10^{-3}
pl4 v. pl2	6.98	2	3.05×10^{-2}
pl4 v. pl3	0.19	1	0.664

Table C.9: Likelihood-ratio test statistics (LR TS), degrees of freedom (df) and corresponding p-values for different combinations of the 10 models fitted to the 2-bed cubicles data in Ward C.

C.3.5 Output tables for Ward C 4-bed cubicles

Model	-log-likelihood	AIC	BIC
e0	89.58	181.16	183.09
e1	89.51	183.02	186.88
e2	82.36	170.72	176.51
e3	81.94	171.88	179.61
e4	81.17	172.35	182.00
pl0	88.32	180.64	184.51
pl1	88.22	182.45	188.24
pl2	82.20	172.41	180.14
pl3	81.81	173.61	183.27
pl4	81.05	174.10	185.69

Table C.10: Model negative log-likelihood, AIC and BIC values for different combinations of the 10 models fitted to data from beds in 4-bed cubicles in Ward C.

	LR TS	df	right-tail prob
e1 v. e0	0.14	1	0.710
e2 v. e0	14.44	2	7.32×10^{-4}
e3 v. e0	15.27	3	1.60×10^{-3}
e4 v. e0	16.81	4	2.10×10^{-3}
pl0 v. e0	2.51	1	0.113
pl1 v. e0	2.71	2	0.258
pl2 v. e0	14.75	3	2.05×10^{-3}
pl3 v. e0	15.54	4	3.70×10^{-3}
pl4 v. e0	17.06	5	4.39×10^{-3}
e2 v. e1	14.30	1	1.56×10^{-4}
e3 v. e1	15.13	2	5.17×10^{-4}
e4 v. e1	16.67	3	8.25×10^{-4}
pl1 v. e1	2.57	1	0.109
pl2 v. e1	14.61	2	6.72×10^{-4}
pl3 v. e1	15.41	3	1.50×10^{-3}
pl4 v. e1	16.92	4	2×10^{-3}
e3 v. e2	0.83	1	0.362
e4 v. e2	2.37	2	0.306
pl2 v. e2	0.31	1	0.579
pl3 v. e2	1.10	2	0.576
pl4 v. e2	2.62	3	0.454
e4 v. e3	1.54	1	0.215
pl3 v. e3	0.27	1	0.602
pl4 v. e3	1.79	2	0.409
pl4 v. e4	0.25	1	0.619
pl1 v. pl0	0.20	1	0.658
pl2 v. pl0	12.24	2	2.20×10^{-3}
pl3 v. pl0	13.03	3	4.57×10^{-3}
pl4 v. pl0	14.55	4	5.74×10^{-3}
pl2 v. pl1	12.04	1	5.21×10^{-4}
pl3 v. pl1	12.83	2	1.63×10^{-3}
pl4 v. pl1	14.35	3	2.47×10^{-3}
pl3 v. pl2	0.80	1	0.372
pl4 v. pl2	2.31	2	0.315
pl4 v. pl3	1.51	1	0.218

Table C.11: Likelihood-ratio test statistics (LR TS), degrees of freedom (df) and corresponding p-values for different combinations of the 10 models fitted to the 4-bed cubicles data in Ward C.

C.3.6 Output tables for Ward D 2-bed cubicles

Model	-log-likelihood	AIC	BIC
e0	15.48	32.95	33.26
e1	12.12	28.24	28.84
e2	8.93	23.87	24.78
e3	8.93	25.87	27.08
e4	8.93	27.87	29.38
pl0	14.14	32.27	32.88
pl1	12.03	30.07	30.98
pl2	8.02	24.03	25.24
pl3	8.02	26.03	27.54
pl4	8.02	28.03	29.85

Table C.12: Model negative log-likelihood, AIC and BIC values for different combinations of the 10 models fitted to data from beds in 2-bed cubicles in Ward D.

	LR TS	df	right-tail prob
e1 v. e0	6.72	1	9.55×10^{-3}
e2 v. e0	13.08	2	1.44×10^{-3}
e3 v. e0	13.08	3	4.46×10^{-3}
e4 v. e0	13.08	4	1.09×10^{-2}
pl0 v. e0	2.68	1	0.102
pl1 v. e0	6.88	2	3.20×10^{-2}
pl2 v. e0	14.92	3	1.88×10^{-3}
pl3 v. e0	14.92	4	4.86×10^{-3}
pl4 v. e0	14.92	5	1.07×10^{-2}
e2 v. e1	6.37	1	1.16×10^{-2}
e3 v. e1	6.37	2	4.14×10^{-2}
e4 v. e1	6.37	3	9.51×10^{-2}
pl1 v. e1	0.17	1	0.683
pl2 v. e1	8.21	2	1.65×10^{-2}
pl3 v. e1	8.21	3	4.19×10^{-2}
pl4 v. e1	8.21	4	8.43×10^{-2}
e3 v. e2	0.00	1	1.00
e4 v. e2	0.00	2	1.00
pl2 v. e2	1.84	1	0.175
pl3 v. e2	1.84	2	0.399
pl4 v. e2	1.84	3	0.606
e4 v. e3	0.00	1	1.00
pl3 v. e3	1.84	1	0.175
pl4 v. e3	1.84	2	0.399
pl4 v. e4	1.84	1	0.175
pl1 v. pl0	4.20	1	4.03×10^{-2}
pl2 v. pl0	12.24	2	2.19×10^{-3}
pl3 v. pl0	12.24	3	6.59×10^{-3}
pl4 v. pl0	12.24	4	1.56×10^{-2}
pl2 v. pl1	8.04	1	4.58×10^{-3}
pl3 v. pl1	8.04	2	1.80×10^{-2}
pl4 v. pl1	8.04	3	4.52×10^{-2}
pl3 v. pl2	0.00	1	0.989
pl4 v. pl2	0.00	2	1.00
pl4 v. pl3	0.00	1	1.00

Table C.13: Likelihood-ratio test statistics (LR TS), degrees of freedom (df) and corresponding p-values for different combinations of the 10 models fitted to the 2-bed cubicles data in Ward D.

C.3.7 Output tables for Ward D 4-bed cubicles

Model	-log-likelihood	AIC	BIC
e0	47.76	97.52	99.35
e1	47.45	98.89	102.55
e2	42.99	91.98	97.47
e3	42.36	92.73	100.04
e4	38.53	87.06	96.20
pl0	47.23	98.47	102.13
pl1	46.97	99.95	105.43
pl2	42.98	93.96	101.28
pl3	42.36	94.71	103.86
pl4	38.07	88.13	99.10

Table C.14: Model negative log-likelihood, AIC and BIC values for different combinations of the 10 models fitted to data from beds in 4-bed cubicles in Ward D.

	LR TS	df	right-tail prob
e1 v. e0	0.63	1	0.429
e2 v. e0	9.54	2	8.49×10^{-3}
e3 v. e0	10.79	3	1.29×10^{-2}
e4 v. e0	18.46	4	1.01×10^{-3}
pl0 v. e0	1.05	1	0.306
pl1 v. e0	1.57	2	0.456
pl2 v. e0	9.56	3	2.27×10^{-2}
pl3 v. e0	10.80	4	2.88×10^{-2}
pl4 v. e0	19.38	5	1.63×10^{-3}
e2 v. e1	8.91	1	2.83×10^{-3}
e3 v. e1	10.16	2	6.21×10^{-3}
e4 v. e1	17.83	3	4.77×10^{-4}
pl1 v. e1	0.95	1	0.331
pl2 v. e1	8.93	2	1.15×10^{-2}
pl3 v. e1	10.18	3	1.71×10^{-2}
pl4 v. e1	18.76	4	8.77×10^{-4}
e3 v. e2	1.25	1	0.263
e4 v. e2	8.92	2	1.16×10^{-2}
pl2 v. e2	0.02	1	0.894
pl3 v. e2	1.27	2	0.531
pl4 v. e2	9.85	3	1.99×10^{-2}
e4 v. e3	7.67	1	5.63×10^{-3}
pl3 v. e3	0.02	1	0.90
pl4 v. e3	8.60	2	1.36×10^{-2}
pl4 v. e4	0.93	1	0.335
pl1 v. pl0	0.52	1	0.469
pl2 v. pl0	8.51	2	1.42×10^{-2}
pl3 v. pl0	9.76	3	2.07×10^{-2}
pl4 v. pl0	18.34	4	1.06×10^{-3}
pl2 v. pl1	7.98	1	4.72×10^{-3}
pl3 v. pl1	9.23	2	9.88×10^{-3}
pl4 v. pl1	17.81	3	4.81×10^{-4}
pl3 v. pl2	1.25	1	0.264
pl4 v. pl2	9.83	2	7.34×10^{-3}
pl4 v. pl3	8.58	1	3.40×10^{-3}

Table C.15: Likelihood-ratio test statistics (LR TS), degrees of freedom (df) and corresponding p-values for different combinations of the 10 models fitted to the 4-bed cubicles data in Ward D.

C.3.8 Output tables for Ward E 2-bed cubicles

Model	-log-likelihood	AIC	BIC
e0	33.02	68.04	68.93
e1	32.17	68.34	70.12
e2	31.16	68.32	70.99
e3	30.63	69.27	72.83
pl0	31.90	67.80	69.58
pl1	31.49	68.98	71.65
pl2	30.85	69.70	73.26
pl3	30.49	70.97	75.42

Table C.16: Model negative log-likelihood, AIC and BIC values for different combinations of the 8 models fitted to data from beds in 2-bed cubicles in Ward E.

	LR TS	df	right-tail prob
e1 v. e0	1.70	1	0.193
e2 v. e0	3.72	2	0.156
e3 v. e0	4.77	3	0.189
pl0 v. e0	2.24	1	0.135
pl1 v. e0	3.06	2	0.217
pl2 v. e0	4.34	3	0.227
pl3 v. e0	5.07	4	0.280
e2 v. e1	2.02	1	0.155
e3 v. e1	3.08	2	0.215
pl1 v. e1	1.36	1	0.244
pl2 v. e1	2.64	2	0.267
pl3 v. e1	3.37	3	0.338
e3 v. e2	1.06	1	0.304
pl2 v. e2	0.62	1	0.431
pl3 v. e2	1.35	2	0.509
pl3 v. e3	0.30	1	0.586
pl1 v. pl0	0.82	1	0.366
pl2 v. pl0	2.10	2	0.350
pl3 v. pl0	2.83	3	0.419
pl2 v. pl1	1.28	1	0.258
pl3 v. pl1	2.01	2	0.366
pl3 v. pl2	0.73	1	0.392

Table C.17: Likelihood-ratio test statistics (LR TS), degrees of freedom (df) and corresponding p-values for different combinations of the 8 models fitted to the 2-bed cubicles data in Ward E.

C.3.9 Output tables for Ward E 4-bed cubicles

Model	-log-likelihood	AIC	BIC
e0	41.45	84.89	86.58
e1	40.00	84.00	87.38
e2	36.31	78.62	83.69
e3	34.71	77.42	84.17
e4	33.27	76.55	84.99
pl0	39.74	83.48	86.86
pl1	38.80	83.60	88.66
pl2	36.19	80.39	87.14
pl3	34.71	79.41	87.86

Table C.18: Model negative log-likelihood, AIC and BIC values for different combinations of the 9 models fitted to data from beds in 4-bed cubicles in Ward E.

	LR TS	df	right-tail prob
e1 v. e0	2.89	1	8.91×10^{-2}
e2 v. e0	10.27	2	5.89×10^{-3}
e3 v. e0	13.48	3	3.71×10^{-3}
e4 v. e0	16.35	4	2.59×10^{-3}
pl0 v. e0	3.42	1	6.45×10^{-2}
pl1 v. e0	5.30	2	7.07×10^{-2}
pl2 v. e0	10.51	3	1.47×10^{-2}
pl3 v. e0	13.48	4	9.15×10^{-3}
e2 v. e1	7.38	1	6.60×10^{-3}
e3 v. e1	10.59	2	5.02×10^{-3}
e4 v. e1	13.46	3	3.74×10^{-3}
pl1 v. e1	2.41	1	0.121
pl2 v. e1	7.62	2	2.22×10^{-2}
pl3 v. e1	10.59	3	1.42×10^{-2}
e3 v. e2	3.21	1	7.32×10^{-2}
e4 v. e2	6.08	2	4.79×10^{-2}
pl2 v. e2	0.24	1	0.626
pl3 v. e2	3.21	2	0.201
e4 v. e3	2.87	1	9.03×10^{-2}
pl3 v. e3	0.00	1	0.954
pl1 v. pl0	1.88	1	0.170
pl2 v. pl0	7.09	2	2.89×10^{-2}
pl3 v. pl0	10.07	3	1.80×10^{-2}
pl2 v. pl1	5.21	1	2.25×10^{-2}
pl3 v. pl1	8.18	2	1.67×10^{-2}
pl3 v. pl2	2.98	1	8.45×10^{-2}

Table C.19: Likelihood-ratio test statistics (LR TS), degrees of freedom (df) and corresponding p-values for different combinations of the 9 models fitted to the 4-bed cubicles data in Ward E.

C.3.10 Output tables for Ward F 4-bed cubicles

Model	-log-likelihood	AIC	BIC
e0	31.29	64.57	66.13
e1	26.74	57.48	60.59
e2	26.66	59.31	63.98
e3	26.59	61.19	67.41
e4	22.93	55.86	63.64
pl0	29.76	63.52	66.63
pl1	26.35	58.70	63.37
pl2	26.23	60.46	66.69
pl3	26.21	62.43	70.21
pl4	22.93	57.86	67.19

Table C.20: Model negative log-likelihood, AIC and BIC values for different combinations of the 10 models fitted to data from beds in 4-bed cubicles in Ward F.

	LR TS	df	right-tail prob
e1 v. e0	9.09	1	2.56×10^{-3}
e2 v. e0	9.26	2	9.75×10^{-3}
e3 v. e0	9.39	3	2.46×10^{-2}
e4 v. e0	16.71	4	2.20×10^{-3}
pl0 v. e0	3.06	1	8.03×10^{-2}
pl1 v. e0	9.87	2	7.18×10^{-3}
pl2 v. e0	10.11	3	1.77×10^{-2}
pl3 v. e0	10.15	4	3.80×10^{-2}
pl4 v. e0	16.72	5	5.07×10^{-3}
e2 v. e1	0.17	1	0.683
e3 v. e1	0.29	2	0.864
e4 v. e1	7.62	3	5.46×10^{-2}
pl1 v. e1	0.78	1	0.377
pl2 v. e1	1.02	2	0.602
pl3 v. e1	1.05	3	0.789
pl4 v. e1	7.62	4	0.106
e3 v. e2	0.13	1	0.723
e4 v. e2	7.45	2	2.41×10^{-2}
pl2 v. e2	0.85	1	0.357
pl3 v. e2	0.88	2	0.642
pl4 v. e2	7.46	3	5.87×10^{-2}
e4 v. e3	7.33	1	6.80×10^{-3}
pl3 v. e3	0.76	1	0.383
pl4 v. e3	7.33	2	2.56×10^{-2}
pl4 v. e4	0.01	1	0.938
pl1 v. pl0	6.82	1	9.04×10^{-3}
pl2 v. pl0	7.05	2	2.94×10^{-2}
pl3 v. pl0	7.09	3	6.92×10^{-2}
pl4 v. pl0	13.66	4	8.46×10^{-3}
pl2 v. pl1	0.24	1	0.627
pl3 v. pl1	0.27	2	0.873
pl4 v. pl1	6.84	3	7.70×10^{-2}
pl3 v. pl2	0.04	1	0.850
pl4 v. pl2	6.61	2	3.67×10^{-2}
pl4 v. pl3	6.57	1	1.04×10^{-2}

Table C.21: Likelihood-ratio test statistics (LR TS), degrees of freedom (df) and corresponding p-values for different combinations of the 10 models fitted to the 4-bed cubicles data in Ward F.

C.3.11 Output tables for Ward G 2-bed cubicles

Model	-log-likelihood	AIC	BIC
e0	28.73	59.47	60.64
e1	28.04	60.08	62.44
e2	26.65	59.30	62.84
pl0	27.51	59.02	61.37
pl1	26.89	59.78	63.32
pl2	25.60	59.21	63.92

Table C.22: Model negative log-likelihood, AIC and BIC values for different combinations of the 6 models fitted to data from beds in 2-bed cubicles in Ward G.

	LR TS	df	right-tail prob
e1 v. e0	1.39	1	0.239
e2 v. e0	4.16	2	0.125
pl0 v. e0	2.45	1	0.118
pl1 v. e0	3.68	2	0.159
pl2 v. e0	6.26	3	9.97×10^{-2}
e2 v. e1	2.78	1	9.56×10^{-2}
pl1 v. e1	2.29	1	0.130
pl2 v. e1	4.87	2	8.76×10^{-2}
pl2 v. e2	2.09	1	0.148
pl1 v. pl0	1.23	1	0.267
pl2 v. pl0	3.81	2	0.149
pl2 v. pl1	2.58	1	0.109

Table C.23: Likelihood-ratio test statistics (LR TS), degrees of freedom (df) and corresponding p-values for different combinations of the 6 models fitted to the 2-bed cubicles data in Ward G.

C.3.12 Output tables for Ward G 4-bed cubicles

Model	-log-likelihood	AIC	BIC
e0	7.64	17.29	18.47
e1	7.64	19.29	21.64
e2	7.42	20.84	24.37
e3	7.42	22.84	27.55
e4	7.36	24.73	30.62
pl0	7.61	19.22	21.58
pl1	7.61	21.22	24.75
pl2	7.40	22.80	27.52
pl3	7.40	24.80	30.69
pl4	7.35	26.70	33.77

Table C.24: Model negative log-likelihood, AIC and BIC values for different combinations of the 10 models fitted to data from beds in 4-bed cubicles in Ward G.

	LR TS	df	right-tail prob
e1 v. e0	0.00	1	1.00
e2 v. e0	0.45	2	0.798
e3 v. e0	0.45	3	0.930
e4 v. e0	0.56	4	0.968
pl0 v. e0	0.07	1	0.796
pl1 v. e0	0.07	2	0.967
pl2 v. e0	0.48	3	0.922
pl3 v. e0	0.48	4	0.975
pl4 v. e0	0.59	5	0.989
e2 v. e1	0.45	1	0.502
e3 v. e1	0.45	2	0.798
e4 v. e1	0.56	3	0.906
pl1 v. e1	0.07	1	0.796
pl2 v. e1	0.48	2	0.785
pl3 v. e1	0.48	3	0.922
pl4 v. e1	0.59	4	0.965
e3 v. e2	0.00	1	1.00
e4 v. e2	0.11	2	0.948
pl2 v. e2	0.03	1	0.855
pl3 v. e2	0.03	2	0.983
pl4 v. e2	0.14	3	0.987
e4 v. e3	0.11	1	0.743
pl3 v. e3	0.03	1	0.855
pl4 v. e3	0.14	2	0.934
pl4 v. e4	0.03	1	0.866
pl1 v. pl0	0.00	1	1.00
pl2 v. pl0	0.42	2	0.812
pl3 v. pl0	0.42	3	0.937
pl4 v. pl0	0.52	4	0.972
pl2 v. pl1	0.42	1	0.518
pl3 v. pl1	0.42	2	0.812
pl4 v. pl1	0.52	3	0.915
pl3 v. pl2	0.00	1	1.00
pl4 v. pl2	0.10	2	0.950
pl4 v. pl3	0.10	1	0.749

Table C.25: Likelihood-ratio test statistics (LR TS), degrees of freedom (df) and corresponding p-values for different combinations of the 10 models fitted to the 4-bed cubicles data in Ward G.

D Supplementary Material for Chapter 6: ‘Quantifying the impact of an MRSA outbreak on patient outcome in a NICU’

D.1 MRSA outcome: Additional outputs

The outputs for assessing if the full Cox PH model for the MRSA outcome violated the proportional hazard model assumption are provided in Table D.1 and Figure D.1. There does not appear to be any violation of the proportional hazard assumption for this fitted model

It should be noted that there were only ten observed cases (MRSA acquisitions) for this data set. As such, it is difficult to ascertain if the proportional hazard assumption was satisfied or not. Any model interpretation should be done with caution.

	ρ	χ^2	p-value
bed movement number	-0.490	1.721	0.190
outward	0.623	0.284	0.594
colonisation pressure	-0.429	1.692	0.193
global	–	2.674	0.445

Table D.1: Proportional hazard assumption test results of the full Cox PH model for the MRSA outcome. ρ is the correlation coefficient between transformed survival time and the scaled Schoenfeld residuals, χ^2 is the χ^2 -distributed test statistic for testing $\theta = 0$, where θ is the coefficient for the time-varying covariate which forms $\beta(t)$, with associated p-value in the last column.

D.1.1 Simpler models for MRSA outcome

Given the smaller number of patients who were readmitted to the NICU during the study period, it was also of interest to investigate if a simpler model excluding the outward covariate. The qualitative effect of the covariates were similar to the full model (Table D.2). Corresponding outputs assessing the proportional hazards assumption are provided in Table D.3 and Figure D.2.

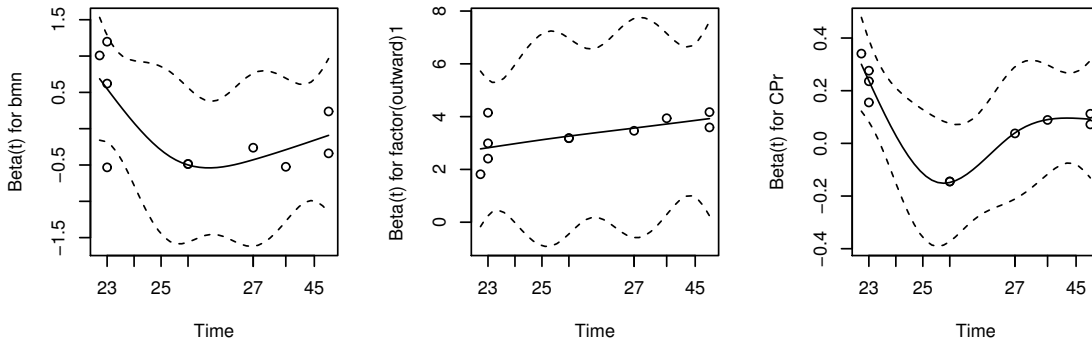


Figure D.1: Time-dependent coefficient estimates $\beta(t)$ of each of the covariates of the full Cox PH model for the MRSA outcome to assess the proportional hazards assumption. bmn refers to the bed movement number covariate, outward is the out-of-ward indicator and CPr is the colonisation pressure covariate.

	coefficient (robust SE)	HR [95% CI]	p-value
bed movement	0.004 (0.25)	1.00 [0.62, 1.63]	0.99
colonisation pressure	0.084 (0.05)	1.09 [0.99, 1.19]	0.075

Table D.2: Estimated coefficients, standard errors, hazard ratios (HRs) and p-values for the covariates of the simplified Cox PH model for MRSA outcome, omitting the outward covariate.

	ρ	χ^2	p-value
bed movement number	-0.603	2.96	0.085
colonisation pressure	-0.617	3.64	0.056
global	—	4.80	0.0906

Table D.3: Proportional hazard assumption test results of the simplified Cox PH model for MRSA outcome, omitting the outward covariate. ρ is the correlation coefficient between transformed survival time and the scaled Schoenfeld residuals, χ^2 is the χ^2 -distributed test statistic for testing $\theta = 0$, where θ is the coefficient for the time-varying covariate which forms $\beta(t)$, with associated p-value in the last column.

The estimated coefficients of a fitted Cox PH model for the MRSA outcome, omitting the bed movement covariate, are provided in Table D.4. There does not appear any violation of the proportional hazard assumption for this fitted model as well (Table D.5 and Figure D.3). The estimated coefficients for the outward and colonisation pressure covariate in this model were similar to the corresponding estimates from the full model. This confirms that the bed movement covariate was not informative about the MRSA acquisition hazard, at least for this data set.

The estimates for separate Cox PH models fitted to only a single covariate are provided in Table D.6. This was motivated by the small number of MRSA cases observed in the study period. The proportional hazard assumption for these models are assessed in

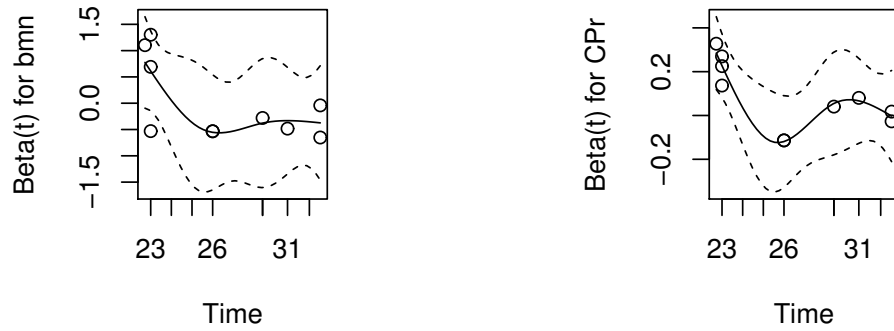


Figure D.2: Time-dependent coefficient estimates $\beta(t)$ of each of the covariates of the simplified Cox PH model for MRSA outcome, omitting the outward covariate, to assess the proportional hazards assumption. bm refers to the bed movement number covariate, outward is the out-of-ward indicator and CPr is the colonisation pressure covariate.

	coefficient (robust SE)	HR [95% CI]	p-value
outward	3.30 (0.82)	27.07 [5.40, 135.73]	6.06×10^{-5}
colonisation pressure	0.10 (0.05)	1.11 [1.01, 1.22]	0.039

Table D.4: Estimated coefficients, standard errors, hazard ratios (HRs) and p-values for the covariates of the simplified Cox PH model for MRSA outcome, omitting the bed movement covariate.

	ρ	χ^2	p-value
outward	0.489	0.053	0.818
colonisation pressure	-0.365	0.951	0.330
global	—	1.063	0.588

Table D.5: Proportional hazard assumption test results of the simplified Cox PH model for MRSA outcome, omitting the bed movement covariate. ρ is the correlation coefficient between transformed survival time and the scaled Schoenfeld residuals, χ^2 is the χ^2 -distributed test statistic for testing $\theta = 0$, where θ is the coefficient for the time-varying covariate which forms $\beta(t)$, with associated p-value in the last column.

Table D.7 and Figure D.4, and there does not appear to be any notable violations to the model assumption.

The estimates obtained from fitting each covariate separately were consistent with the estimates obtained with the full model. The estimates were slightly smaller in these models and associated with larger p-values compared with the full model outputs. The bed movement coefficient was estimated to be negative (with a relatively large standard error) when fitted singly to the MRSA outcome however this effect was not statistically significant in both the simple model here and the full model presented in the main text.

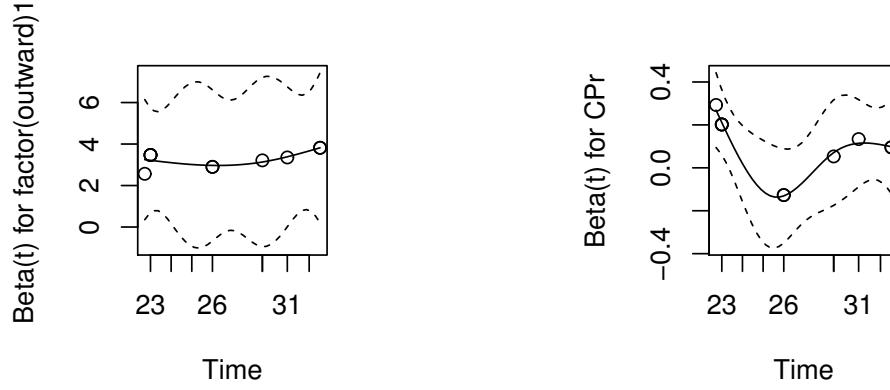


Figure D.3: Time-dependent coefficient estimates $\beta(t)$ of each of the covariates of the simplified Cox PH model for MRSA outcome, omitting the bed movement covariate, to assess the proportional hazards assumption. outward is the out-of-ward indicator and CPr is the colonisation pressure covariate.

	coefficient (robust SE)	HR [95% CI]	p-value
bed movement	-1.57×10^{-3} (0.240)	1.00 [0.62, 1.60]	1.00
outward	2.96 (0.83)	19.26 [3.80, 97.61]	3.54×10^{-4}
colonisation pressure	8.43×10^{-2} (0.047)	1.09 [0.99, 1.19]	0.07

Table D.6: Estimated coefficients, standard errors, hazard ratios (HRs) and p-values for three separate Cox PH models fitted to the MRSA outcome using each covariate individually.

	ρ	χ^2	p-value
bed movement number	-0.495	1.24	0.266
outward	0.663	0.093	0.76
colonisation pressure	-0.56	2.08	0.149

Table D.7: Proportional hazard assumption test results of the Cox PH models fitted to each covariate separately for the MRSA outcome. ρ is the correlation coefficient between transformed survival time and the scaled Schoenfeld residuals, χ^2 is the χ^2 -distributed test statistic for testing $\theta = 0$, where θ is the coefficient for the time-varying covariate which forms $\beta(t)$, with associated p-value in the last column.

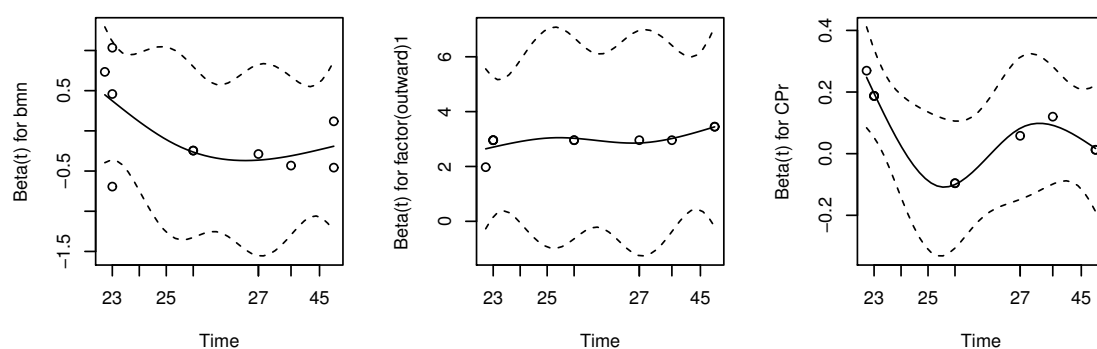


Figure D.4: Time-dependent coefficient estimates $\beta(t)$ for each of the Cox PH models fitted to a single covariate for the MRSA outcome. These plots are used to assess the proportional hazards assumption of the model. bmn refers to the bed movement covariate, outward is the out-of-ward indicator and CPr is the colonisation pressure covariate.

D.2 LOS outcome: Additional outputs

Figure D.5 plots the partial LOS (pLOS) associated with the different bed movement covariate values for all patients in the NICU over the study period. As mentioned in the main text, bed movement values of 6 or higher were recoded to 5. Only two patients had more than 5 bed movements. The spread of the pLOS values appears to be decreasing with increasing bed movement numbers.

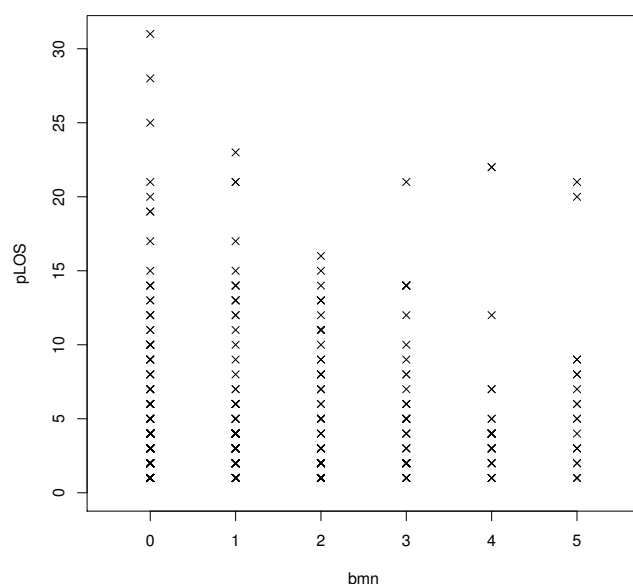


Figure D.5: Scatter plot of partial LOS (pLOS) against the corresponding bed movement number (bmnn). The partial LOS is calculated as the LOS associated with a particular bed movement number for each patient.

Table D.8 and Figure D.6 are the associated outputs for assessing the full Cox PH model for the LOS outcome satisfies the proportional hazard assumption of the model. The outputs do not provide any evidence that this assumption was violated for the fitted model.

	ρ	χ^2	p-value
MRSA	0.033	0.034	0.854
colonisation pressure	0.053	0.326	0.568
bed movement	-0.055	0.436	0.509
outward	0.026	0.063	0.803
global	—	0.775	0.942

Table D.8: Proportional hazard assumption test results of the full Cox PH model for the LOS outcome. ρ is the correlation coefficient between transformed survival time and the scaled Schoenfeld residuals, χ^2 is the χ^2 -distributed test statistic for testing $\theta = 0$, where θ is the coefficient for the time-varying covariate which forms $\beta(t)$, with associated p-value in the last column.

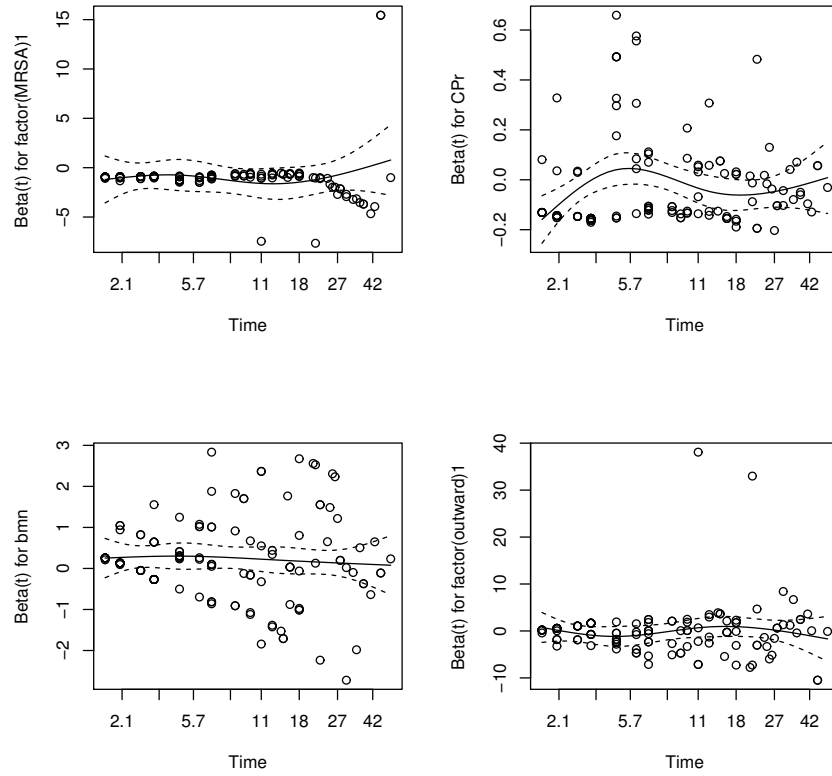


Figure D.6: Time-dependent coefficient estimates $\beta(t)$ of each of the covariates of the full Cox PH model for LOS outcome to assess the proportional hazards assumption. MRSA is the patient MRSA status indicator, bmn refers to the bed movement number covariate, outward is the out-of-ward indicator and CPr is the colonisation pressure covariate.

D.2.1 Simpler model for LOS outcome

A Cox PH model for the LOS outcome omitting the bed movement covariate was fitted to investigate if the potential association between pLOS and bed movement (Figure D.5) might have distorted the effects of the other covariates. The estimated coefficients and HRs for the remaining three covariates Table D.9 were similar to the corresponding estimates from the full model, and there were no violations of the proportionality hazards assumption with this simpler model (Table D.10 and Figure D.7). As such, the full model details were reported in the main text for completeness.

	coefficient (robust SE)	HR [95% CI]	p-value
MRSA	-1.13 (0.45)	0.32 [0.14, 0.78]	0.012
colonisation pressure	-0.029 (0.017)	0.97 [0.94, 1.00]	0.084
outward	0.336 (0.50)	1.40 [0.52, 3.76]	0.51

Table D.9: Estimated coefficients, standard errors, hazard ratios (HRs) and p-values for the covariates of the simplified Cox PH model fitted to the LOS outcome, omitting the bed movement covariate.

	ρ	χ^2	p-value
MRSA	0.030	0.029	0.864
colonisation pressure	0.037	0.162	0.688
outward	-0.0095	0.068	0.934
global	—	0.194	0.979

Table D.10: Proportional hazard assumption test results of the simplified Cox PH model fitted to the LOS outcome, omitting the bed movement covariate. ρ is the correlation coefficient between transformed survival time and the scaled Schoenfeld residuals, χ^2 is the χ^2 -distributed test statistic for testing $\theta = 0$, where θ is the coefficient for the time-varying covariate which forms $\beta(t)$, with associated p-value in the last column.

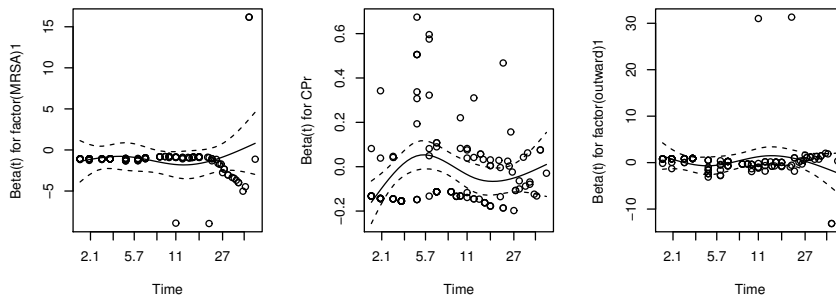


Figure D.7: Time-dependent coefficient estimates $\beta(t)$ of each of the covariates of the simplified Cox PH model fitted to the LOS acquisition outcome, omitting the bed movement covariate, to assess the proportional hazards assumption. MRSA is the patient MRSA status indicator, bmn refers to the bed movement number covariate, outward is the out-of-ward indicator and CPr is the colonisation pressure covariate.

Another simpler Cox PH model was also fitted for the LOS outcome using only the MRSA, colonisation pressure and bed movement covariates. The estimated coefficients for this simpler model are listed in Table D.11. The fitted model does not appear to violate the proportional hazards assumption of the model (Table D.12 and Figure D.8).

The estimated coefficients for this simpler model are similar to those obtained for the corresponding covariates in the full LOS model (Table 6.2) inferring that the outward covariate was indeed not informative about the LOS outcome for this data set.

	coefficient (robust SE)	HR [95% CI]	p-value
MRSA	-1.02 (0.41)	0.36 [0.16, 0.81]	0.013
colonisation pressure	-0.031 (0.017)	0.97 [0.94, 1.00]	0.067
bed movement	0.23 (0.081)	1.26 [1.08, 1.48]	0.004

Table D.11: Estimated coefficients, standard errors, hazard ratios (HRs) and p-values for the covariates of the simplified Cox PH model fitted to the LOS acquisition outcome, omitting the outward covariate.

	ρ	χ^2	p-value
MRSA	0.049	0.059	0.809
colonisation pressure	0.054	0.341	0.559
bed movement	-0.054	0.379	0.538
global	–	0.717	0.869

Table D.12: Proportional hazard assumption test results of the simplified Cox PH model fitted to the LOS outcome, omitting the outward covariate. ρ is the correlation coefficient between transformed survival time and the scaled Schoenfeld residuals, χ^2 is the χ^2 -distributed test statistic for testing $\theta = 0$, where θ is the coefficient for the time-varying covariate which forms $\beta(t)$, with associated p-value in the last column.

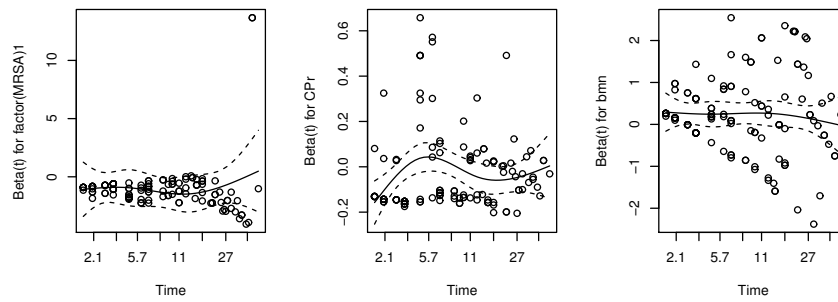


Figure D.8: Time-dependent coefficient estimates $\beta(t)$ of each of the covariates in the simplified Cox PH model for LOS outcome, omitting the outward covariate, to assess the proportional hazards assumption. MRSA is the patient MRSA status indicator, bmn refers to the bed movement number covariate, outward is the out-of-ward indicator and CPr is the colonisation pressure covariate.

E Supplementary material for Chapter 7: ‘Quantifying the relative effect of environmental contamination on surgical ward MRSA incidence’

E.1 MCMC specifications

Define $\boldsymbol{\theta} = (\beta_0, \beta_1, \alpha_1, \beta_2)$ to be the collection of parameters in the intensity function to be estimated. Independent, uniform vague priors were assigned to each of the parameters, i.e. $\pi(\boldsymbol{\theta}) = \pi(\beta_0) \pi(\beta_1) \pi(\alpha_1) \pi(\beta_2)$.

Previous parameters estimates in similar models for MRSA ranged between 10^{-5} and 10^{-2} (Forrester et al., 2007, Kypraios et al., 2010, Worby et al., 2013). As such, the model parameters here $(\beta_0, \beta_1, \beta_2, \alpha_1)$ were assigned vague uniform $U(0, 1)$ priors. Identical priors were assigned to the transmission parameters of a previous NHPP model for MRSA (Forrester et al., 2007).

Parameter proposals in the MCMC steps were made following a multiplicative random walk with a modification for parameters with substantial mass close to zero (Dellaportas and Roberts, 2003, Sherlock et al., 2010), i.e. a normal random walk proposal was used on $\psi_j = \log(\theta_j + a)$ (where a is a small positive constant which we have set to 1 in this case)

$$\psi_j^* = \psi_j + N(\mu_j, \sigma_j^2)$$

which, on the original θ scale, is equivalent to the proposal

$$\theta_j^* + a = (\theta_j + a) e^{N(\mu_j, \sigma_j^2)}. \quad (\text{E.1})$$

The corresponding Metropolis-Hastings (MH) ratio for this setup is

$$r_j = \frac{\pi(\theta_j^* | \boldsymbol{\theta}_{-j}) q(\psi(\theta_j) | \psi(\theta_j^*)) \theta_j^*}{\pi(\theta_j | \boldsymbol{\theta}_{-j}) q(\psi(\theta_j^*) | \psi(\theta_j)) \theta_j}$$

where $\pi(\theta_j^*|\boldsymbol{\theta}_{-j})$ is the full conditional for parameter θ_j , $q(\cdot)$ is the proposal distribution and the Jacobian of the transformation from ψ back to θ is $\frac{1}{\theta}$. As $q(\cdot)$ is symmetric, the MH ratio simplifies to

$$r_j = \frac{\pi(\theta_j^*|\boldsymbol{\theta}_{-j}) \theta_j^* + a}{\pi(\theta_j|\boldsymbol{\theta}_{-j}) \theta_j + a}$$

The normal proposal (on the log scales) means were set to $-\frac{1}{2}\sigma_j^2$ such that from (E.1)

$$\begin{aligned} E[(\theta_j^* + a)] &= (\theta_j + a) E[e^{N(\mu_j, \sigma_j^2)}] \\ &= (\theta_j + a) e^{-\frac{1}{2}\sigma_j^2 + \frac{1}{2}\sigma_j^2} = (\theta_j + a). \end{aligned}$$

and the variance terms σ_j^2 were tuned to achieve acceptance rates between 0.1 and 0.6 (Brooks et al., 2011).

The full conditionals for the four parameters in the intensity function can be obtained straightforwardly from the likelihood expression for piecewise-constant $\lambda(t)$ in the Methods section of the main document

$$L(\boldsymbol{\theta}) = \exp \left\{ \sum_i \log \left(\lambda(t_{C_i}^-) \right) - \sum_{l=1}^{L-1} \lambda(t_l) S(t_l) (t_{l+1} - t_l) \right\}$$

where $\lambda(t) = \beta_0 + \beta_1 C(t) + \alpha_1 C_{xt}(t) + \beta_2 E(t)$, i indexes the colonised patients and t_{C_i} is the imputed colonisation time for patient i .

The full conditional forms for the parameters can be expressed as

$$\begin{aligned} p(\beta_0|rest) &\propto \exp \left\{ \sum_i \log \left[\beta_0 + \beta_1 C(t_{C_i}^-) + \alpha_1 C_{xt}(t_{C_i}^-) + \beta_2 E(t_{C_i}^-) \right] - \beta_0 \sum_{l=1}^{L-1} S(t_l) \right\} \pi(\beta_0) \\ p(\beta_1|rest) &\propto \exp \left\{ \sum_i \log \left[\beta_0 + \beta_1 C(t_{C_i}^-) + \alpha_1 C_{xt}(t_{C_i}^-) + \beta_2 E(t_{C_i}^-) \right] - \beta_1 \sum_l C(t_l) S(t_l) \right\} \pi(\beta_1) \\ p(\alpha_1|rest) &\propto \exp \left\{ \sum_i \log \left[\beta_0 + \beta_1 C(t_{C_i}^-) + \alpha_1 C_{xt}(t_{C_i}^-) + \beta_2 E(t_{C_i}^-) \right] - \alpha_1 \sum_l C_{xt}(t_l) S(t_l) \right\} \pi(\alpha_1) \\ p(\beta_2|rest) &\propto \exp \left\{ \sum_i \log \left[\beta_0 + \beta_1 C(t_{C_i}^-) + \alpha_1 C_{xt}(t_{C_i}^-) + \beta_2 E(t_{C_i}^-) \right] - \beta_2 \sum_l E(t_l) S(t_l) \right\} \pi(\beta_2) \end{aligned}$$

with $\pi(\cdot)$ s as the vague uniform priors for the parameters as defined earlier. It was assumed $(t_{l+1} - t_l) = 1$ for all potential values of l , as is the case with the model formulation where data were assumed to be daily. The assumption also implies that $t_l^- \equiv t_{l-1}$ for all valid values of l .

To derive the full conditional used in imputing the colonisation time (in days), first define $Z(t)$ to be the incidence (number of new colonisations) recorded at time t . Using

$Z(t)$, the piecewise-constant $\lambda(t)$ likelihood expression is further simplified to a single summation over time, rather than separate summations over colonised patients and time:

$$\begin{aligned} L(\theta) &= \exp \left\{ \sum_i \log \left(\lambda(t_{C_i}^-) \right) - \sum_{l=1}^{L-1} \lambda(t_l) S(t_l) (t_{l+1} - t_l) \right\} \\ &= \exp \left\{ \sum_{l=1}^L Z(t_l) \log [\lambda(t_{l-1})] - \sum_{l=1}^{L-1} \lambda(t_l) S(t_l) \right\} \\ &= \exp \left\{ Z(t_L) \log [\lambda(t_{L-1})] + \sum_{l=1}^{L-1} \{ Z(t_l) \log [\lambda(t_{l-1})] - \lambda(t_l) S(t_l) \} \right\}. \end{aligned}$$

The full conditional for colonisation time k for patient i is then:

$$\begin{aligned} p(T_{ik}|rest) &\propto \exp \left\{ \sum_{t=t_{min}}^{t_{max}} \{ Z(t) \log [\lambda(t)] - \lambda(t) S(t) \} \right\} \\ &= \prod_{t=t_{min}}^{t_{max}} \exp \{ Z_{ik}(t) \log [\beta_0 + \beta_1 C_{ik}(t) + \alpha_1 C_{xt,ik}(t) + \beta_2 E(t)] \\ &\quad - S_{ik}(t) [\beta_0 + \beta_1 C_{ik}(t) + \alpha_1 C_{xt,ik}(t) + \beta_2 E(t)] \} \\ &= \prod_{t=t_{min}}^{t_{max}} \exp \left\{ \sum_{j=1}^{Z_{ik}(t)} \log \left[\beta_0 + \beta_1 C_{ik} \left(t_{C_j}^- \right) + \alpha_1 C_{xt,ik} \left(t_{C_j}^- \right) + \beta_2 E \left(t_{C_j}^- \right) \right] \right. \\ &\quad \left. - S_{ik}(t) [\beta_0 + \beta_1 C_{ik}(t) + \alpha_1 C_{xt,ik}(t) + \beta_2 E(t)] \right\} \end{aligned}$$

where $k \in \{t_{min}, \dots, t_{max}\}$.

The imputed colonisation time for patient i (t_{C_i}) can then be drawn from the full conditional $p(T_{ik}|rest)$. $S_{ik}(t)$, $C_{ik}(t)$, $C_{xt,ik}(t)$ and $Z_{ik}(t)$ are the number of susceptibles, all colonised patients, undetected colonised patients and incidence at time t if patient i 's colonisation time was equal to k .

Imputation of patient i 's discharge day (t_{R_i}) is more straightforward as it was assumed to be uniformly distributed between the patient's last positive screen date and the following Monday (when the patient would have been screened again if he or she was still in the ward). Once both colonisation and discharge days have been imputed, $X(t) = [S(t), C_{xt}(t), C_t(t)]$ can be constructed $\forall t$ which allows for the computation of $\lambda(t)$.

Using the full conditionals derived above, the model parameters can then be estimated using a data-augmented MCMC algorithm as outlined in Algorithm E.1.

Three separate MCMC chains were run for 1,000,000 iterations in each estimation with different initial conditions. The chains were assessed for convergence and mixing before combining the last 800,000 iterations (i.e. removing the first 200,000 iterations as

Algorithm E.1 MCMC scheme for the NHPP model

-
- 1: Initiate MCMC by drawing $\theta \sim \pi(\theta)$.
 - 2: Using the prior draw for θ , impute t_C and t_R to construct $X(t)$ and $Z(t)$.
 - 3: **for** $j = 1 : 4$ **do**
 - a. Draw proposal θ_j^* as defined in (E.1).
 - b. Calculate MH ratio
$$r_j = \frac{\pi(\theta_j^*|\theta_{-j}) \theta_j^* + a}{\pi(\theta_j|\theta_{-j}) \theta_j + a}$$
and accept θ_j^* with probability r_j .
 - 4: **end for**
 - 5: Using the latest θ value, impute t_C and t_R and reconstruct $X(t)$ and $Z(t)$.
 - 6: Repeat steps 3: to 5: until convergence in distribution is achieved for θ .
-

burn-in) of the chains to obtain a final MCMC sample of 2,400,000. The assessment was performed using the R package `coda` (Plummer et al., 2006).

E.1.1 Simulation method

From the model formulation and definition of the piecewise constant intensity function, given that we are currently at time t , the time until the next colonisation event is exponentially distributed with parameter $\lambda(t)S(t)$. Hence, a simulation algorithm for the model proceeds as follows:

1. Initialize algorithm with parameters $\theta = (\beta_0, \beta_1, \beta_2, \alpha_1)$, initial condition $X(0) = [S(0), C_{xt}(0), C_t(0)]$ and end time for simulation, T . For simplicity, we set $X(0) = [18, 0, 0]$, i.e. a fully susceptible ward. Set $t = 0$ and $t_n = 1$.
 2. If $S(t) > 0$, generate a colonised proposal time c_p for a randomly selected $S(t)$.
 3. If $c_p < t_n$, the colonisation proposal time is accepted. The following information about the newly colonised patients are then generated:
 - (a) day of first positive
 - To replicate the effect that a patient can be screened either on ad-hoc basis or during regular screenings on Mondays:
 - if $r < p_M$ (where r is a uniform random number and p_M the proportions of observed first positive days which are Mondays), the day of first positive is assigned to the Monday immediately following $\lceil c_p \rceil$.
 - else, the day of first positive is set to $\lceil c_p \rceil$.
 - (b) day of last positive
 - Duration between first and last positive sampled from observed data.
 - (c) removal day
 - Removal day randomly sampled between day of last positive to the following Monday.
- Update $X(t)$ and set $t = t + c_p$.

4. If $c_p \geq t_n$, colonisation proposal time is rejected as the intensity function is no longer constant in $[t, cp)$.
 - (a) Set $t = t_n$ and $t_n = t_n + 1$.
 - (b) Update queued events that occur at time t , in particular patient transitions from undetected to detected, and detected to removal (i.e. susceptible).
5. If $t < T$, return to step 2. Otherwise, terminate simulation.

The model simulation algorithm above was used to generate the posterior predictive distribution plots (Figure 7.2 for the full model, Figure E.9 for the model without $E(t)$ and Figure E.14 for the Ward B analysis) as well as the simulated data for the simulated study in Appendix E.2.

E.2 Simulation study

A simulation study was conducted to evaluate if the MCMC estimation procedure described was able to recover parameter values from simulated data for this particular non-homogeneous Poisson process (NHPP) when the true parameter values were known (and used to simulate the data sets).

In particular, ten data sets were simulated for each of the two sets of posterior mean estimates obtained from the observed data (Table 7.1) as we were interested in determining if these posterior estimates were well identified. The estimation procedure was then used to obtain posterior estimates for these simulated data sets.

Each data set was simulated for a period of six months and the number of MRSA-positive patients simulated were consistent with the observed data. The range of total MRSA-positive patients simulated in the ten data sets using the enhanced cleaning parameter estimates was $[24, 36]$ and $[12, 25]$ using the normal cleaning estimates (noting that 28 MRSA-positive patients were observed in the enhanced cleaning period and 15 in the normal cleaning period). This was to be expected given the posterior predictive check plots in Figure 7.2.

The estimated posterior mean, median and 95% interval estimates from the simulated data sets were compared with the observed data estimates for both parameter sets. Figures E.1, E.2, E.3 and E.4 plot these estimates for the simulated data sets from the enhanced cleaning period posterior mean estimates alongside the observed data estimates. The corresponding plots for simulated data from the normal cleaning period estimates are shown in Figures E.5, E.6, E.7 and E.8.

There was good agreement overall between the simulated data estimates compared with the corresponding observed data estimates. The posterior mean and median estimates from the simulated data sets were consistent with their corresponding true values (the blue and black squares for median estimates along with the green asterisks and red

horizontal line for mean estimates). The 95% intervals were also similar between simulated and observed data.

There were two estimates for β_1 which deviated slightly from the observed estimates (simulated data set 8 from the enhanced cleaning estimates and simulated data set 5 from the normal cleaning estimates) noting that vague $U[0, 1]$ priors were used. Given the comparatively smaller role of the MRSA-positive patients (which the β_1 parameter quantifies) relative to the background and environmental contamination, the slight lack in identifiability of parameter β_1 would unlikely have a significant impact on the general inferences made.

The simulation study thus provides confidence in the ability of the estimation procedure to correctly identify parameter values of the NHPP and in particular the estimated values obtained from the observed data (Table 7.1).

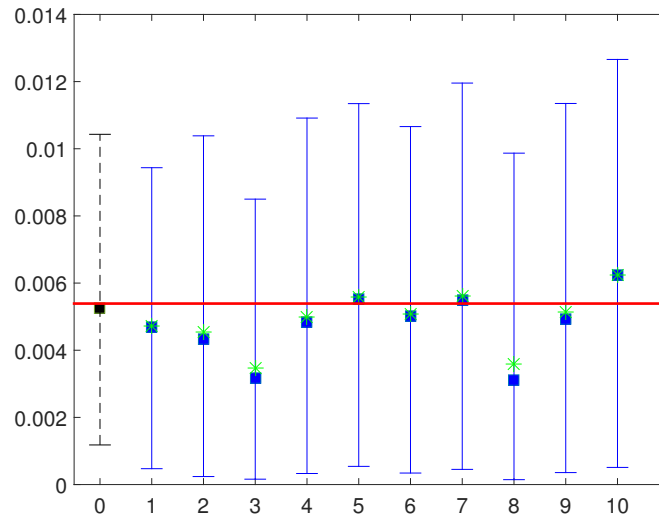


Figure E.1: Estimation for β_0 from 10 simulated data sets (in blue and green) compared with estimation results from observed data (in black and red). The squares are the median estimates, with whiskers corresponding to the 95% posterior interval. The red line denotes the estimated posterior mean from the observed data in the enhanced cleaning period and the value for β_0 used to generate the simulated data. The green asterisks are the estimated posterior means from the simulated data.

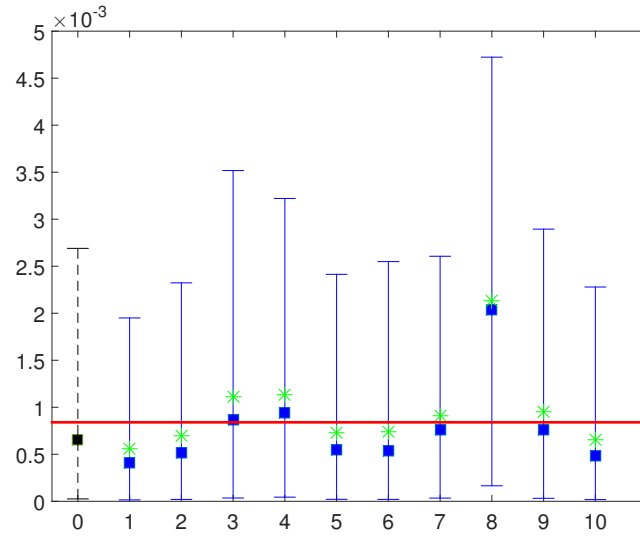


Figure E.2: Estimation for β_1 from 10 simulated data sets (in blue and green) compared with original estimation results from observed data (in black and red). The squares are the median estimates, with whiskers corresponding to the 95% posterior interval. The red line denotes the estimated posterior mean from the observed data in the enhanced cleaning period and the value for β_1 used to generate the simulated data. The green asterisks are the estimated posterior means from the simulated data.

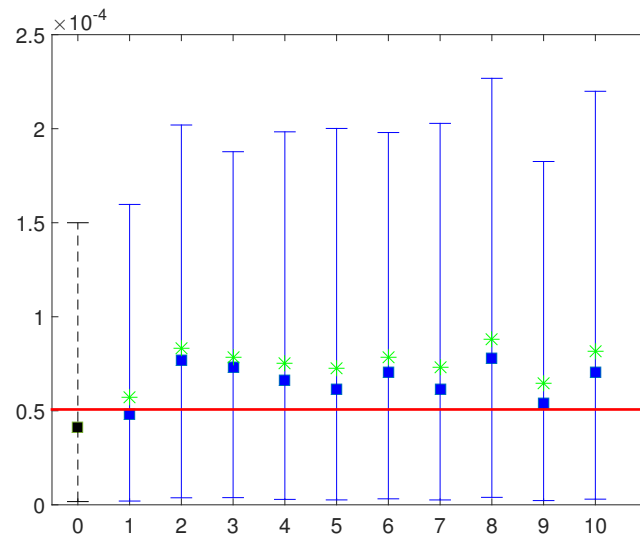


Figure E.3: Estimation for β_2 from 10 simulated data sets (in blue and green) compared with original estimation results from observed data (in black and red). The squares are the median estimates, with whiskers corresponding to the 95% posterior interval. The red line denotes the estimated posterior mean from the observed data in the enhanced cleaning period and the value for β_2 used to generate the simulated data. The green asterisks are the estimated posterior means from the simulated data.

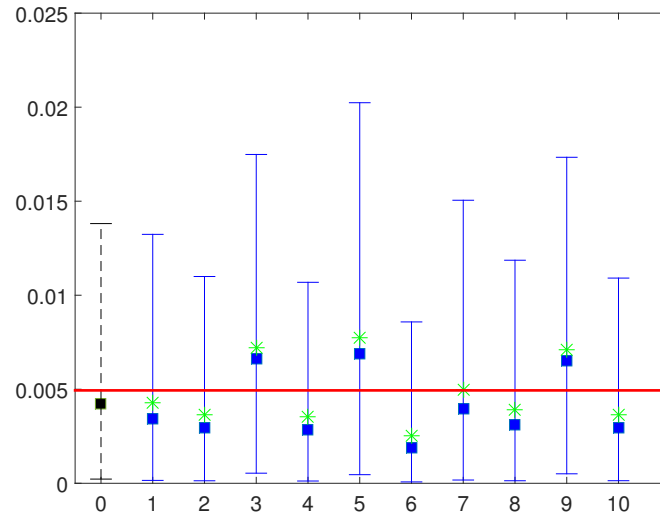


Figure E.4: Estimation for α_1 from 10 simulated data sets (in blue and green) compared with original estimation results from observed data (in black and red). The squares are the median estimates, with whiskers corresponding to the 95% posterior interval. The red line denotes the estimated posterior mean from the observed data in the enhanced cleaning period and the value for α_1 used to generate the simulated data. The green asterisks are the estimated posterior means from the simulated data.

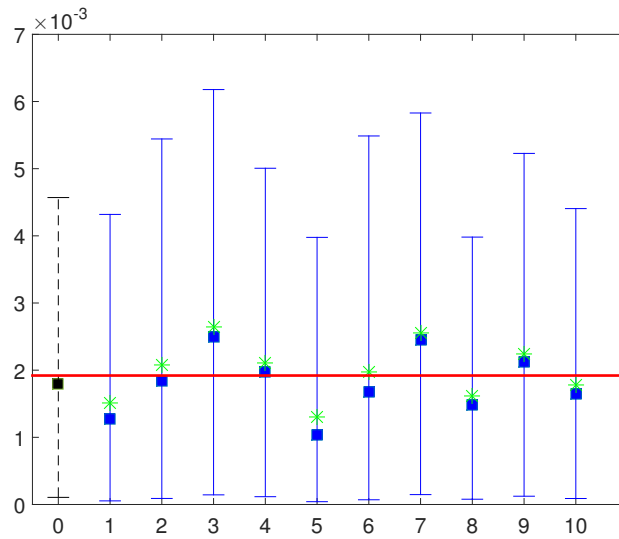


Figure E.5: Estimation for β_0 from 10 simulated data sets (in blue and green) compared with original estimation results from observed data (in black and red). The squares are the median estimates, with whiskers corresponding to the 95% posterior interval. The red line denotes the estimated posterior mean from the observed data in the normal cleaning period and the value for β_0 used to generate the simulated data. The green asterisks are the estimated posterior means from the simulated data.

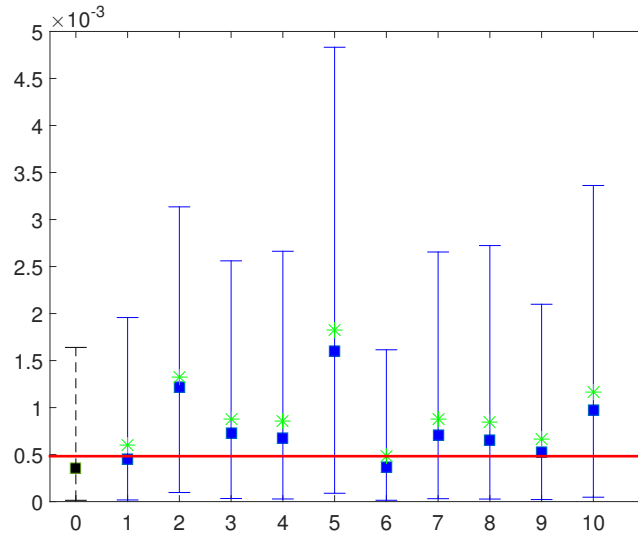


Figure E.6: Estimation for β_1 from 10 simulated data sets (in blue and green) compared with original estimation results from observed data (in black and red). The squares are the median estimates, with whiskers corresponding to the 95% posterior interval. The red line denotes the estimated posterior mean from the observed data in the normal cleaning period and the value for β_1 used to generate the simulated data. The green asterisks are the estimated posterior means from the simulated data.

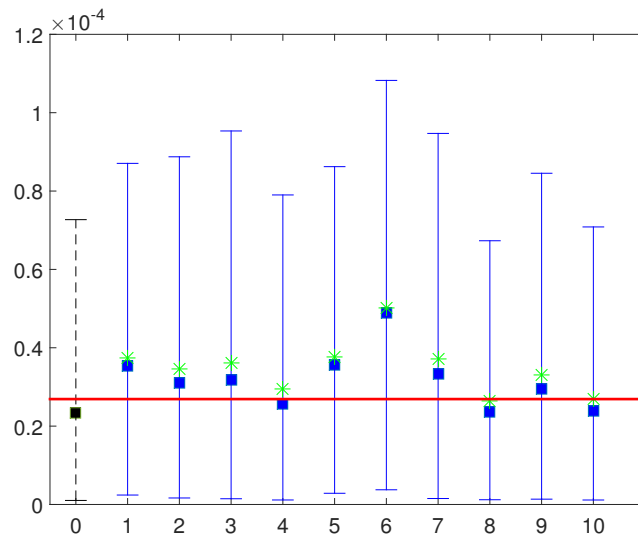


Figure E.7: Estimation for β_2 from 10 simulated data sets (in blue and green) compared with original estimation results from observed data (in black and red). The squares are the median estimates, with whiskers corresponding to the 95% posterior interval. The red line denotes the estimated posterior mean from the observed data in the normal cleaning period and the value for β_2 used to generate the simulated data. The green asterisks are the estimated posterior means from the simulated data.

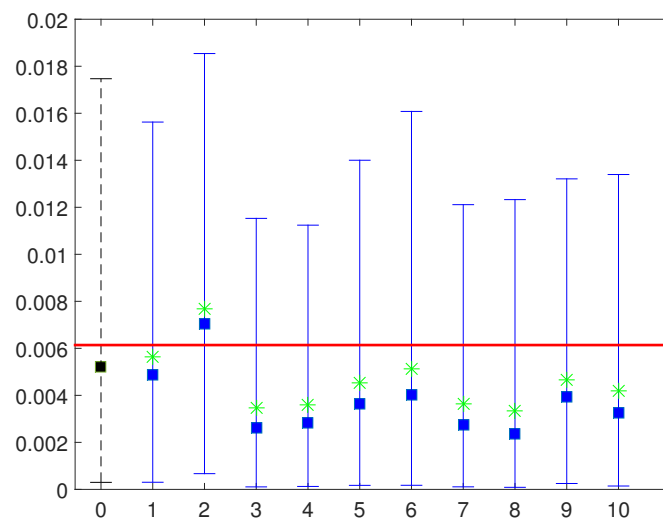


Figure E.8: Estimation for α_1 from 10 simulated data sets (in blue and green) compared with original estimation results from observed data (in black and red). The squares are the median estimates, with whiskers corresponding to the 95% posterior interval. The red line denotes the estimated posterior mean from the observed data in the normal cleaning period and the value for α_1 used to generate the simulated data. The green asterisks are the estimated posterior means from the simulated data.

E.3 Results without environmental contamination component

This section replicated the analysis done in the main text with the environmental contamination component omitted from the intensity function, i.e.

$$\lambda(t) = \beta_0 + \beta_1 C(t) + \alpha_1 C_{xt}(t).$$

This helps identify the impact of not having accounted for the environmental contamination on the model inferences and allows for a model comparison with the full model (as discussed in the main text). The model estimates are summarised in Table E.1.

The posterior predictive distributions obtained were consistent with the observed number of MRSA colonised patient in both the enhanced cleaning and normal cleaning periods (Figure E.9).

The background rate β_0 was larger in the enhanced cleaning period as before due to the larger number of colonisations detected in that period but the estimates for the other two model parameters were similar (Figure E.10).

Parameter ($\times 10^5$)	Enhanced cleaning			Normal cleaning		
	β_0	β_1	α_1	β_0	β_1	α_1
Mean	719	95	525	312	51	649
MCSE	0.5	0.2	0.7	0.6	0.2	3
SD	223	79.7	378	106	46.0	474
2.5% quantile	307	3.04	25.5	133	1.5	35
Median	710	74.8	455	303	38.1	555
97.5% quantile	1182	295	1426	548	171	1789

Table E.1: Summary of parameter estimates for the model without environmental contamination using the combined sample of 2,400,000 iterations from three converged and well-mixed MCMC chains. MCSE denotes the Monte Carlo standard error and SD the posterior standard deviation. β_0 , β_1 and α_1 are the coefficients in the intensity function associated with the background source, colonised patients and additional contribution from being undetected while colonised, respectively.

The estimated fractional risks (FRs) from the three different transmission sources in this model were similar between periods (Figure E.11 and Table E.2).

The rank orders for the three components of the mode were the same across periods (Figure E.12). The background source component was assigned the highest rank (rank 1) with posterior probabilities close to 1 (0.971 in the enhanced cleaning period and 0.999 in the normal cleaning period). The undetected MRSA patients component was most likely to be assigned to rank 2 followed by rank 3 and rank 1. The detected MRSA patients component had the largest posterior probability of being assigned to rank 3,

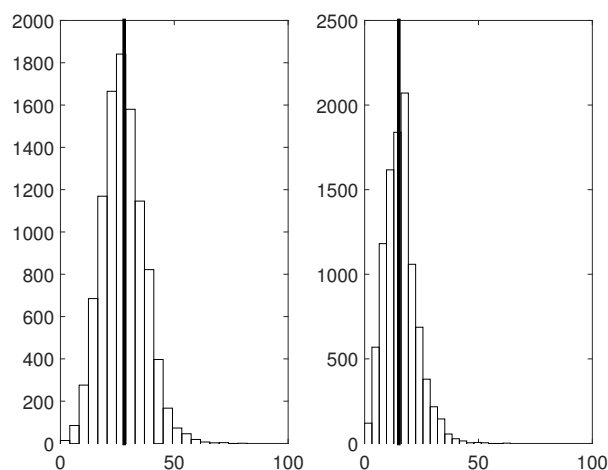


Figure E.9: Histograms of number of colonised patients from 10,000 simulations using parameters sampled from the estimated posterior distributions obtained from the enhanced cleaning period data (left) and normal cleaning period data (right). The thick vertical black lines represent the observed value in each period (28 for the enhanced cleaning period and 15 for the normal cleaning period).

	Enhanced cleaning			Normal cleaning		
	<i>bg</i>	<i>cxt</i>	<i>ct</i>	<i>bg</i>	<i>cxt</i>	<i>ct</i>
Mean	0.687	0.177	0.137	0.718	0.189	0.0925
SD	0.140	0.0786	0.109	0.109	0.0874	0.0773
2.5% quantile	0.378	0.0371	0.0465	0.499	0.0311	0.00291
Median	0.700	0.174	0.111	0.719	0.190	0.0730
97.5% quantile	0.923	0.333	0.404	0.925	0.352	0.286

Table E.2: Summary of mean fractional risks (FR) for the three different components of the intensity function for the enhanced and normal cleaning period. The background source is denoted by *bg*, undetected colonised patient by *cxt*, detected colonised patient by *ct* and environmental contamination by *env*.

followed by rank 2 and rank 1. These rankings were more distinct in the normal cleaning period compared with the enhanced cleaning period.

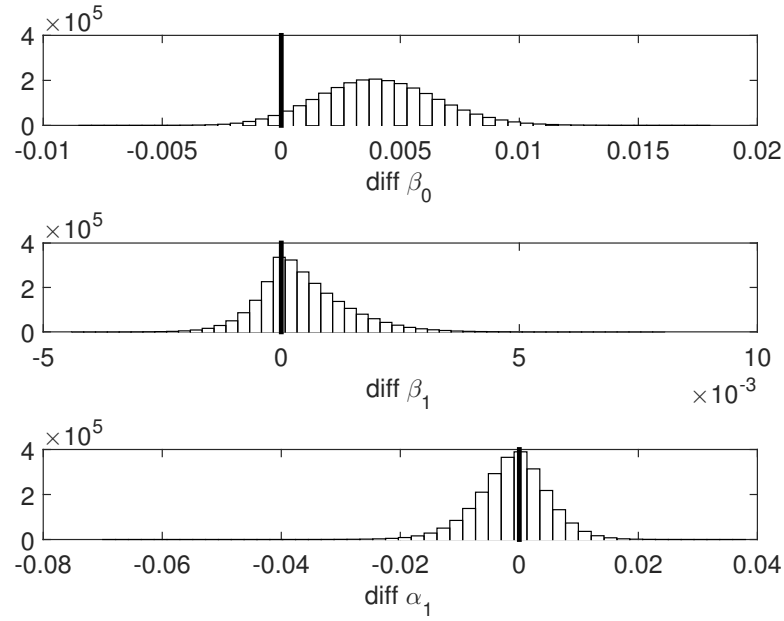


Figure E.10: Histogram of the differences (diff) in parameter values between the enhanced cleaning period and normal cleaning period from the combined sample of 2,400,000 iterations from three converged and well-mixed MCMC chains. 95.4% of the difference in sampled β_0 using the enhanced cleaning period data was greater than when using the normal cleaning period data. Similarly, 67.4% for β_1 and 42.9% for α_1 . The parameters β_0 , β_1 and α_1 are the coefficients in the intensity function associated with the background source, colonised patients and additional contribution from being undetected while colonised, respectively.

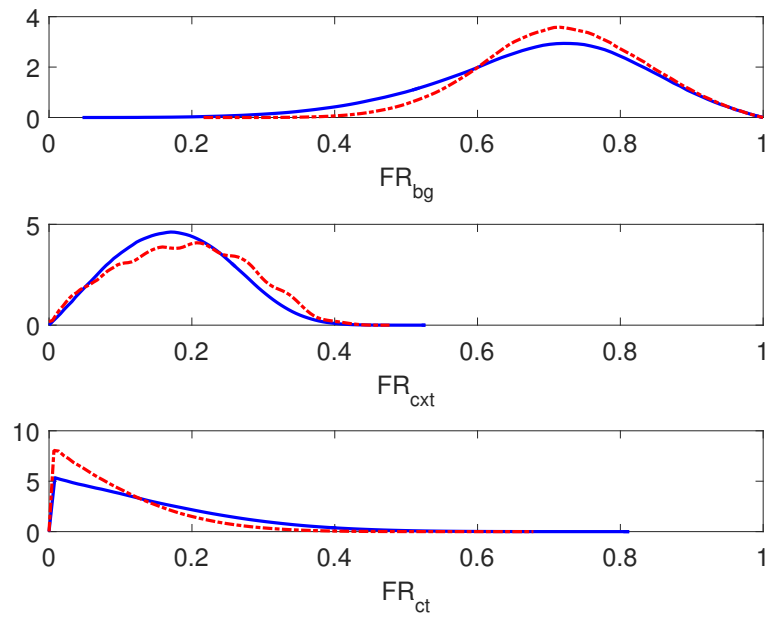


Figure E.11: Kernel density estimates of mean fractional risks (FR) for the model without environmental contamination. The blue and red outlines correspond to the enhanced cleaning period and normal cleaning period, respectively. The background source is denoted by bg , undetected colonised patient by cxt , and detected colonised patient by ct .

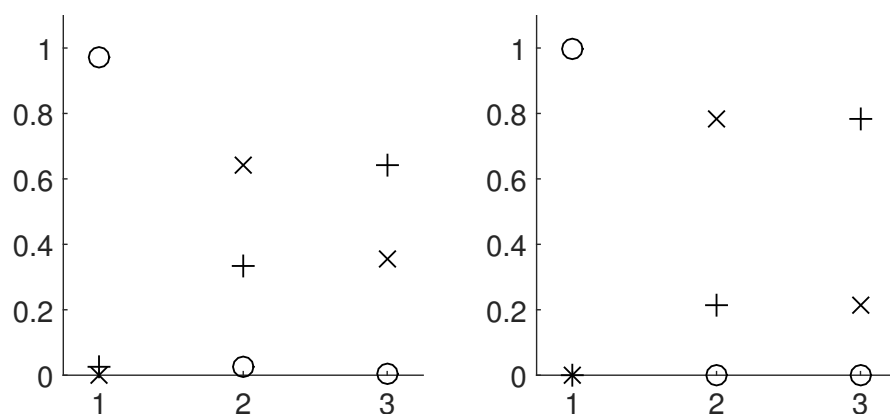


Figure E.12: Posterior probabilities of the ranks for the three components of the intensity function in the enhanced cleaning period (left), and normal cleaning period (right). The \circ denotes the background source component, \times for undetected MRSA patient, and $+$ for detected MRSA patients. The rank order is in descending order along the horizontal axis (with rank 1 being the highest and rank 3 the lowest).

E.4 Ward B Results

This section describes the results obtained and limitations of using data from the other ward (Ward B) of the original study (Dancer et al., 2009). Ward B received normal cleaning practices for the first six months of the observation period, followed by six months with the extra cleaner. There were substantially fewer MRSA-positive patients detected in Ward B compared with Ward A in both the enhanced and normal cleaning periods (8 and 7 respectively in Ward B compared with 28 and 15 in Ward A).

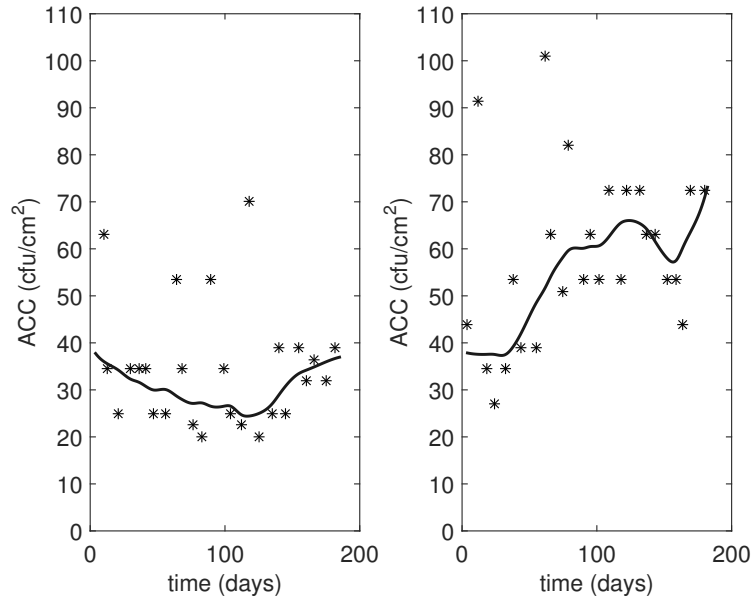


Figure E.13: Smoothed time series of the environmental contamination measure (ACC) for the enhanced cleaning period (left) and normal cleaning period (right) for Ward B. The black asterisks denote the raw weekly data. Aerobic colony count (ACC) is measured in colony forming units per cm^2 (cfu/cm^2).

The posterior estimates for Ward B are summarised in Table E.3. While it was still possible to estimate the posterior distributions of the four parameters relatively well, caution should be placed on any further inference made given the small number of MRSA-positive patients.

This caution is particularly pertinent for the α_1 estimates which represent the additional effect of a colonised patient being undetected on subsequent MRSA acquisition which relies on the imputation of the unobservable colonisation times (t_C). Only one out of the eight MRSA-positive patients in the enhanced cleaning period and three out of the seven patients in the normal cleaning period were detected sufficiently close in time to another MRSA-positive patient such that it is possible that the number of (imputed) undetected MRSA-positive patients (C_{xt}) is non-zero in the time period when the patient's colonisation time was imputed from (between the date of the first positive screen for the patient and the Monday immediately preceding the first positive date). This was not an issue with the Ward A data as 21 of the 28 MRSA-positive patients in

the enhanced cleaning period, and 12 of the 17 patients in the normal cleaning period had non-zero C_{xt} in their respective colonisation time ranges.

The posterior predictive distributions of the number of simulated MRSA-positive patients (Figure E.14) were centred around the observed value indicating that the estimated posterior distributions were still able to replicate the observed system reasonably well. However, there was considerably more variability in the distributions with a small proportion of simulations with a substantially larger number of MRSA-positive patients, particularly for the normal cleaning period estimates. This discrepancy was likely due to the small number of cases actually observed in the ward.

Still, it was promising that the order of magnitude of these estimates matches those obtained from Ward A as this provides some degree of confidence as to the consistency of the parameter estimates expected in hospital wards of similar configuration.

The FR distributions estimated for Ward B were less informative than those of Ward A due to the comparatively smaller number of MRSA-positive patients observed in Ward B. This was evident from the relatively flat shape of the FR distributions of the background and environmental contamination components (compared with Figure 7.4) with the FR distributions for the colonised patients again having only very small relative contributions.

Note also that the FR distribution for the undetected MRSA-positive patients (FR_{cxt}) in the enhanced cleaning period was strongly centred on zero. This was again due to spread (in time) of the small number of occurrences of MRSA-positive patients in Ward B.

Despite the increased uncertainty, it was still evident that the background, followed closely by the environmental contamination, accounted for the vast majority of the FR. Both detected and undetected colonised patients had small FRs, although this could have been exaggerated by the small numbers of observed cases.

Parameter ($\times 10^5$)	Enhanced cleaning				Normal cleaning			
	β_0	β_1	β_2	α_1	β_0	β_1	β_2	α_1
Mean	158	52.4	4.43	564	155	51.9	4.85	564
MCSE	0.2	0.1	0.007	2.8	0.2	0.09	0.007	2.5
SD	107	49.6	3.21	829	107	49.4	3.47	809
2.5% quantile	7.8	1.4	0.18	12.8	7.06	1.4	0.206	12.5
Median	143	37.7	3.87	353	140	37.3	4.27	352
97.5% quantile	402	184	11.9	2253.3	399	183	12.9	2259.0

Table E.3: Summary of parameter estimates for Ward B from the combined sample of 2,400,000 iterations from three converged and well-mixed MCMC chains. MCSE denotes the Monte Carlo standard error and SD the posterior standard deviation. β_0 , β_1 , β_2 and α_1 are the coefficients in the intensity function associated with the background source, colonised patients, environmental contamination and additional contribution from being undetected while colonised, respectively.

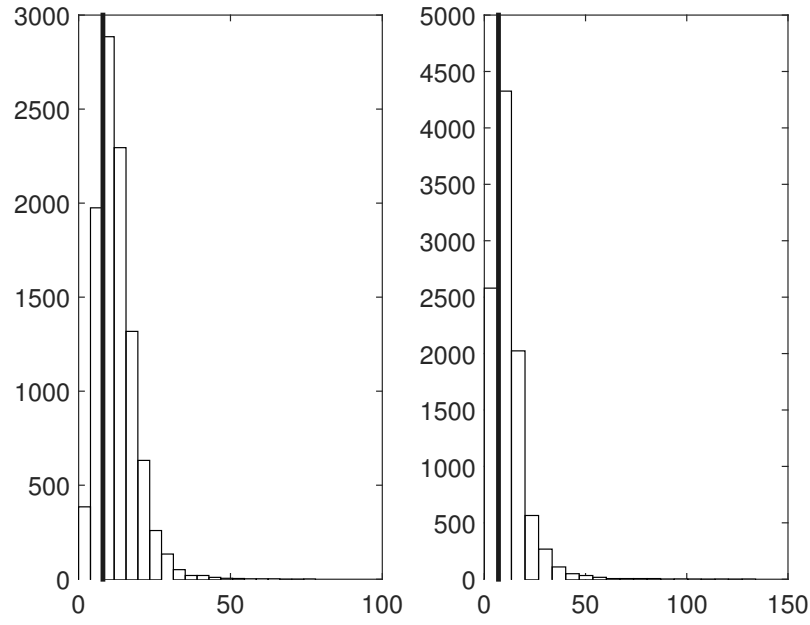


Figure E.14: Histograms of number of colonised patients from 10,000 simulations using parameters sampled from the estimated posterior distributions obtained from the enhanced cleaning period data (left) and normal cleaning period data (right) for Ward B. The thick vertical black lines represent the observed value in each period (8 for the enhanced cleaning period and 7 for the normal cleaning period).

	Enhanced cleaning				Normal cleaning			
	<i>bg</i>	<i>cxt</i>	<i>ct</i>	<i>env</i>	<i>bg</i>	<i>cxt</i>	<i>ct</i>	<i>env</i>
Mean	0.471	0.0118	0.0804	0.437	0.421	0.166	0.0492	0.364
SD	0.267	0.0290	0.0718	0.264	0.229	0.0728	0.0425	0.227
2.5% quantile	0.0247	0	0.00230	0.0207	0.0251	0.0148	0.00166	0.0168
Median	0.474	0	0.0601	0.427	0.429	0.173	0.0387	0.348
97.5% quantile	0.924	0.1009	0.267	0.912	0.821	0.269	0.163	0.794

Table E.4: Summary of mean fractional risks (FRs) for the four different components of the intensity function for the enhanced and normal cleaning period estimated using Ward B data. The background source is denoted by *bg*, undetected colonised patient by *cxt*, detected colonised patient by *ct* and environmental contamination by *env*.

The rank ordering for the background source and environmental contamination were similar across periods for Ward B (Figure E.16). Both components have the largest posterior probability of being assigned to rank 1 with decreasing probabilities associated with lower ranks.

The undetected MRSA patient component had a large posterior probability (0.890) of being assigned to rank 4 in the enhanced cleaning period whereas the detected MRSA patient component was most likely to be assigned to rank 3. This odd result was again caused by the small number of MRSA-positive patients being detected far apart in time in that period for Ward B.

The rank orders of the undetected and detected MRSA patient components in the normal cleaning period were consistent with the Ward A. The detected MRSA patient

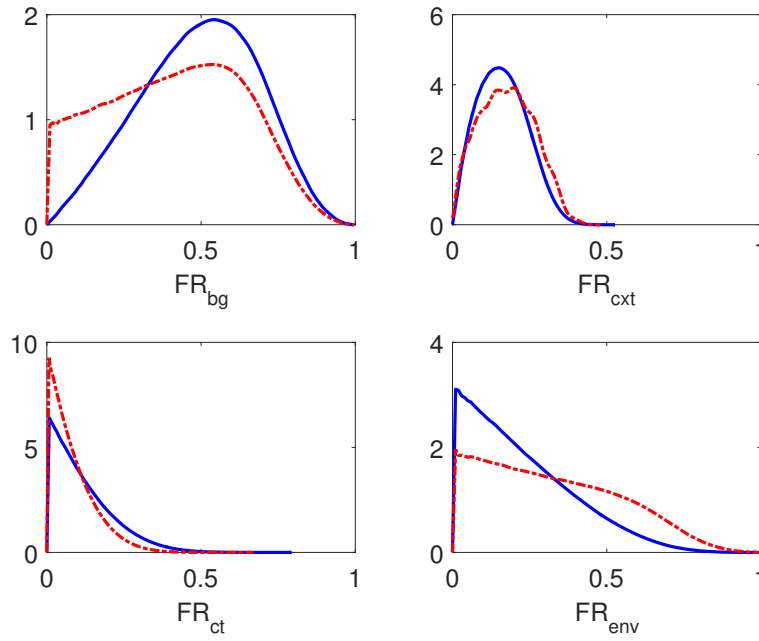


Figure E.15: Kernel density estimates of mean fractional risks (FR) for Ward B. The blue and red outlines correspond to the enhanced cleaning period and normal cleaning period, respectively. The background source is denoted by *bg*, undetected colonised patient by *cxt*, detected colonised patient by *ct*, and environmental contamination by *env*.

component had a large posterior probability of being assigned to rank 4 (0.799) and the undetected MRSA component had largest posterior probabilities of being assigned to either rank 2 or 3 (0.421 and 0.493 respectively).

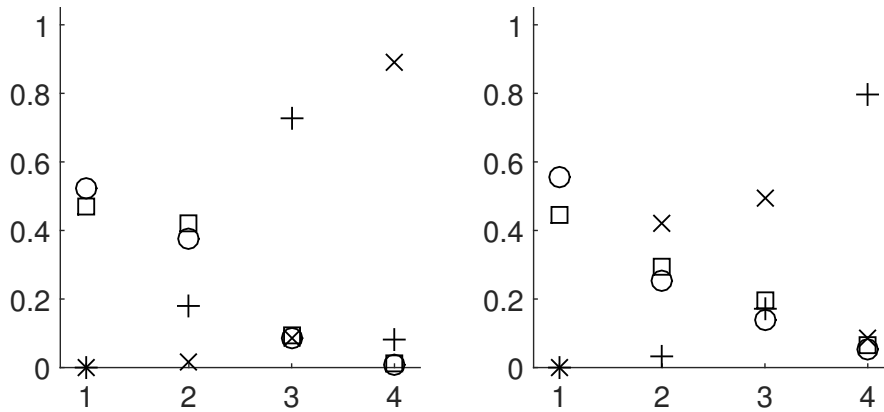


Figure E.16: Posterior probabilities of the ranks for the four components of the intensity function in the enhanced cleaning period (left), and normal cleaning period (right) for Ward B. The \circ denotes the background source component, \square for environmental contamination, \times for undetected MRSA patient, and $+$ for detected MRSA patients. The rank order is in descending order along the horizontal axis (with rank 1 being the highest and rank 4 the lowest).

F Supplementary Material for Chapter 8: ‘A stochastic model for MRSA transmission within a hospital ward incorporating environmental contamination’

F.1 Additional model details

For all model simulations, the model was initialised with 10 S patients, 5 C_{xd} patients, 5 empty beds and $E(0) = 3.5$. The simulations were ran for 460 days and the simulation of first 100 days were omitted to remove any transient effect of the initial condition. Model inference were made using the latter 360 days (approximately 12 months).

F.1.1 Parameter estimation for fixed parameters

The ward capacity M and daily admission rate λ were based on the ward from where data used to estimate the individual model force of infection parameters and environmental time series model parameters were collected from (Dancer et al., 2009). Specifically, the ward capacity was set to 20 (rounded down from 21 in Dancer et al. (2009)) and λ was set to 5 which achieved a weekly ward occupancy of approximately 94.4% from repeated model simulations (close to the reported rates between 89.7% and 91.8% in Dancer et al. (2009)). Unfortunately, this data set did not have sufficient information to estimate the other parameters in the model (namely, the probability transitions aside from the probability of being colonised). As such, these parameter estimates were sourced from the literature in similar settings, noting that the data were collected in a UK surgical ward between 2006 and 2007 (Dancer et al., 2009).

The probability of a colonised patient developing an infection used here was originally estimated using ICU data in a UK hospital between 2002 and 2006 (Robotham et al., 2011).

The probabilities of leaving the ward as a susceptible patient (p_L) or colonised patient (q_L) were estimated from the corresponding median length of stay (LOS) durations

reported for surgical unit patients in Switzerland between 2004 and 2006 (De Angelis et al., 2011). It was assumed that the p_L and q_L parameters corresponded to the rate parameters of exponential distributions whose medians are as reported in De Angelis et al. (2011) (6 days for susceptible patients and 13 days for patients who were colonised but not infected).

The infection recovery parameter (ψ) was also estimated from the same Swiss data set (De Angelis et al., 2011) by fitting the r_C functional form

$$r_C(t|\psi, ti_k) = 1 - \exp\{-\psi(t - ti_k)\}$$

such that $r_C(t) = 0.5$ for when t is equal to the difference in median LOS reported for infected and colonised-only MRSA patients reported in De Angelis et al. (2011), i.e. $r_C(48 - 13|\psi) = 0.5$ where 48 was the median LOS reported for infected patients.

F.1.2 Parameter estimation for individual model's force of infection

The β parameters were estimated by fitting a non-homogeneous Poisson process (NHPP) to the Dancer et al. (2009) data set. The force of infection (FoI) term from NHPP aggregated MRSA-positive patients (T_{xd} and T_d for undetected and detected MRSA-positive patients respectively) as there were insufficient patients to obtain reliable estimates separately for the colonised and infected patients, i.e.

$$FoI_T(t) = \gamma_0 + \gamma_1 T_{xd}(t) + \gamma_2 T_d(t) + \gamma_3 E(t).$$

The γ parameters were estimated using a data-augmented Markov chain Monte Carlo algorithm to impute the unobserved colonisation times (similar to the approach in McBryde et al. (2007b)). The full details and outputs of the NHPP model are available upon request.

However, the FoI used in the individual model proposed here distinguished between patients with MRSA colonisation from those with an MRSA infection, i.e.

$$FoI_{IM}(t) = \beta_0 + \beta_1 C_{xd}(t) + \beta_2 C_d(t) + \beta_3 I_{xd}(t) + \beta_4 I_d(t) + \beta_5 E(t).$$

In order to use the NHPP parameter estimates to derive estimates for the β terms here, we assume

1. There is a simple relationship between the parameters associated with C and I terms in FoI_{IM} , namely there exists a non-negative parameter ω such that $\beta_3 = \omega\beta_1$ and $\beta_4 = \omega\beta_2$.
2. The background and environmental contamination parameters in FoI_{IM} and FoI_T are identical, i.e. $\beta_0 = \gamma_0$ and $\beta_5 = \gamma_3$.

3. The T terms in FoI_T implicitly averages the ‘true’ parameters from the C and I patients to arrive at ‘homogeneous’ γ parameters for the homogeneous MRSA-positive patient cohorts T_{xd} and T_d , e.g.

$\gamma_1 T_{xd} = \gamma_1 [(1 - p)C_{xd} + (1 + p)I_{xd}]$. The parameter p adjusts the ‘homogeneous’ γ parameter when splitting the T cohort into C and I and is related to the ω parameter in the FoI_{IM} formulation (as shown below).

- when $p = 0$, the parameters for C and I are the same
- when $p < 0$, the parameter for C is larger than the corresponding parameter for I
- when $p > 0$, the parameter for I is larger than the corresponding parameter for C

For the undetected group, we can then relate the FoI components from the two models as follows

$$\gamma_1 [(1 - p)C + (1 + p)I] = \beta_1 C + \omega \beta_1 I \quad (\text{F.1})$$

where we have dropped the ‘xd’ subscripts and time dependence for notational convenience. An identical relationship holds for the detected groups with the appropriate parameters.

To obtain the estimate for β_1 required for the individual model, we solve the simultaneous equation system obtained from matching the coefficients for C and I on the left- and right-hand side of the equality in (F.1).

$$\begin{aligned} \gamma_1(1 - p) &= \beta_1 & \gamma_1(1 + p) &= \omega \beta_1 \\ \gamma_1(1 + p) &= \omega \gamma_1(1 - p) \\ \Rightarrow \omega &= \frac{1 + p}{1 - p} & i.e. \quad p &= \frac{\omega - 1}{\omega + 1}. \end{aligned}$$

Substituting the expression for p back into the expression for β_1 ,

$$\beta_1 = \gamma_1 \left(1 - \frac{\omega - 1}{\omega + 1} \right) = \gamma_1 \frac{2}{\omega + 1}$$

such that if $\omega > 1$, then $\beta_1 < \gamma_1$ and $\beta_3 > \gamma_1$ as required from formulation.

F.1.3 Parameter estimation for time series component

The Dancer et al. (2009) data set was also used to fit the time series component of the proposed stochastic model. As the data were originally collected to investigate the effect of a cleaning intervention, the ward received enhanced cleaning for the first half of the study period and normal cleaning for the second half. Of interest here are the estimates associated with the normal cleaning. However given the small number of patients associated with the two time periods, the time series model was fitting using the full

data set with the inclusion of an indicator covariate for the intervention $U(t)$ in the ARMAX model where

$$U(t) = \begin{cases} 1 & \text{enhanced cleaning} \\ 0 & \text{normal cleaning.} \end{cases}$$

The other exogenous covariates were the number of undetected colonised and infected patients in the ward. The time a colonised or infected patient is categorised as undetected is assumed to 5 days prior to the day of first positive. The duration of 5 days was the average time between the first positives and first preceding Monday for MRSA patients in the ward (where routine weekly screening would have taken place). This is a simplifying approximation to circumvent the need for data imputation of the undetected duration for all patients on top of the model selection procedure of the appropriate time series model.

The ARMAX(p, q) model for $E(t)$ in this case is then

$$\begin{aligned} E(t) &= \alpha_1 + \alpha_2 C_{xd}(t-1) + \alpha_3 I_{xd}(t-1) + \alpha_4 U(t) + n(t) \\ (1 - a_1 B - \dots - a_q B^q) n(t) &= (1 + b_1 B + \dots + b_q B^q) z(t) \quad z(t) \sim WN(0, \sigma^2) \end{aligned}$$

i.e. we assumed that the enhanced cleaning intervention only affected the levels of environmental contamination directly rather than contributions from MRSA patients.

The parameter estimates were obtained using the `auto.arima()` function from the `forecast` package in R. The order selection procedure is a stepwise model selection procedure based on AIC particular to time series models as each model fit is also checked to ensure the fitted model isn't too close to being non-invertible or non-causal (Hyndman and Khandakar, 2007). The selected time series model was an ARMAX(2,2) model.

F.1.4 Additional details on interventions

The five intervention strategies considered in the model investigation are:

1. no colonised on admission (COA) where all patients who are colonised on admission are assumed to be detected on admission and isolated elsewhere, i.e. $\vartheta = 1$ (Harbarth et al., 2008).
2. improved environmental cleaning (ENV) which halved the intercept term in the environmental time series model (α_1). Dancer et al. (2009) found a 32.5%(95%CI : 20.2 – 42.9) reduction in mean levels of ward environmental contamination from just the addition of one additional cleaner on weekdays. Therefore, a reduction of 50% should be quite readily achievable from larger scale cleaning interventions which are more typical.

3. improved contact precaution practices (CP) which decreases ν by a factor of ξ where ξ was set to 0.75 based on estimated efficacy of barrier precautions in Kypraios et al. (2010).
4. perfect screening test sensitivity (SENS) where test sensitivity ρ was set to 1 (McBryde et al., 2007b).
5. improved decolonisation treatment for colonised patients (DECOL) where the probability for a C_d patient leaving the ward is now $q_L + \Delta$ (with the probability of staying adjusted accordingly). For the simulation results shown, Δ was set to q_L , i.e. colonised patients are twice as likely to leave the ward due to the improved treatment received. In a systematic review on mupirocin (used together with chlorohexadine bathes and throat sprays as decolonisation treatments in Dancer et al. (2009)) resistance and alternative decolonisation treatment for MRSA (Poovelikunnel et al., 2015), it was shown that there was a lack of studies investigating alternative decolonisation options for MRSA despite reports of high levels of mupirocin resistance which could lead to decolonisation failure. As such, the effects of the improvement decolonisation treatment was assumed to be a halving of the expected LOS for colonised patients. Alternative efficacies were also investigated but were not shown to have substantial difference from the chosen value except for alternative values which lead to an increased LOS instead which would unlikely be considered.

A sixth intervention representing improved treatment for infected patients (INF) was initially considered where the infection recovery parameter (ψ) was doubled. This reflected the alternative treatment options to vancomycin to treat MRSA infections such as linezolid (Tsoulas and Nathwani (2015) conducted a meta-analysis review on the efficacy of these alternative treatments for MRSA skin and soft-tissue infections). However, direct evidence for the efficacy of alternative treatment options over vancomycin was found to be lacking (and was also shown in an earlier Cochrane review (Gurusamy et al., 2013) for MRSA surgical site infections). As such, the intervention effect for an infected patient was assumed to be as a result of novel antibacterial treatment which doubles ψ and as such, reduces the period of time an infected patient remains infected notably. While doubling the estimate is potentially overly optimistic, sensitivity analysis on the effect of this intervention (where the intervention effect varied from 0.25 to 3) showed that there was no evident differences in any of the outcome measures when varying the effect size of this intervention singly for both the normal and high burden setting. Thus, this intervention was not considered further here.

The interventions were compared using the generalised Mann–Whitney statistics

$$\theta = Pr(Y > X) + \frac{1}{2}Pr(Y = X)$$

which is approximated by $\hat{\theta} = \frac{U}{mn}$ where

$$U = \sum_{i=1}^m \sum_{j=1}^n \mathbb{1}(Y_j > X_i) + \frac{1}{2} \mathbb{1}(Y_j = X_i)$$

with $\{Y_j; j = 1, \dots, n\}$ and $\{X_i; i = 1, \dots, m\}$ being samples from the Y and X distributions respectively, as defined in the main text.

The confidence intervals for $\hat{\theta}$ were computed based on Method 5 of Newcombe (2006). Specifically, the following equation was solved for θ

$$|\theta - \hat{\theta}| = z \sqrt{\frac{\theta(1-\theta)}{mn} \left[1 + \frac{m_s(1-\theta)}{2-\theta} + \frac{m_s\theta}{1+\theta} \right]}$$

where z is the appropriate standard normal quantile and $m_s = \frac{1}{2}(m+n) - 1$. Both m and n are equal to 1000 for the investigations here. Alternatively, the confidence intervals could be approximated assuming a normal distribution for the test statistic using a central limit theorem argument.

F.2 Parameter sensitivity analysis

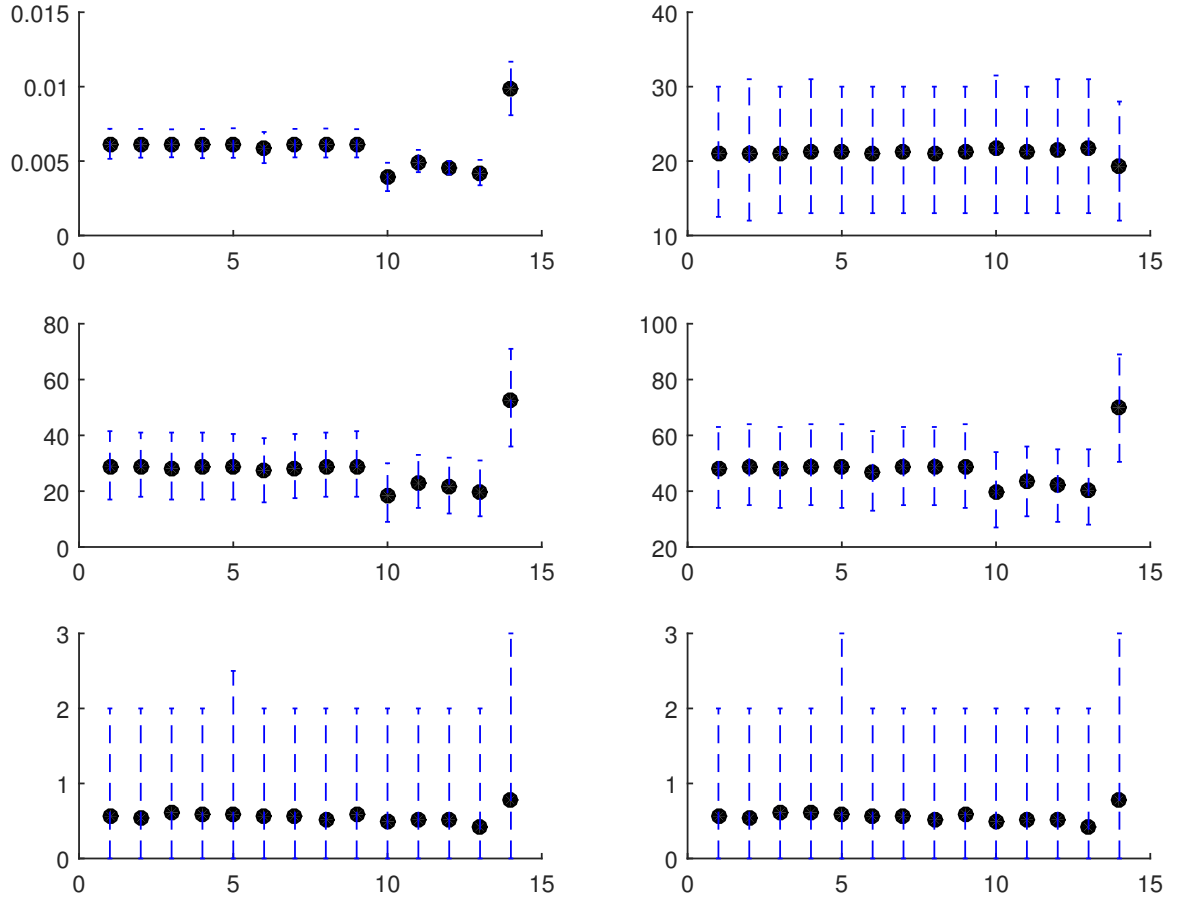
To test the sensitivity of the outcome measures to the individual parameters, the simulations were repeated with modified parameter sets. Each modified parameter set had one of the parameters altered from its original value to either a ‘high’ or ‘low’ value for that parameter. The high and low values were chosen such that they are symmetric about the mean as specified in Table F.1.

- low values for the transmission parameters were set to their respective 2.5% quantile estimated previously. The high values were constructed by adding the difference between the low value and mean to the mean.
- the high and low values for the time series parameters were set to be two times the standard error of estimates away from the mean, except for the AR coefficients and noise variance term
 - The high values for the AR coefficients were set to ensure the roots of the AR polynomial are outside the unit circle, i.e. the time series model remains stationary. The low values were then taken to be the mean, less the difference between the mean and high value
 - The high and low values for the noise variance were set to be 1.5 and 0.5 times the mean respectively.

F.2.1 Normal burden setting

There is little change in the distribution of outcome measures AC, I_{xd} and I_d for both the low and high values of all parameters tested in the normal burden setting.

Parameter	γ_0 ($\times 10^5$)	γ_1 ($\times 10^5$)	γ_2 ($\times 10^5$)	γ_3 ($\times 10^5$)	ω	a_1	a_2	b_1	b_2	α_1	α_2	α_3	σ^2
Low value	11	31.4	1.4	0.1	0.1	1.33	-0.55	0.16	0.18	50	-0.87	0.54	12.25
High value	370	1295	95	5.3	1.9	1.47	-0.41	0.52	0.42	70	0.73	0.66	36.75

Table F.1: High and low values for the parameters**Figure F.1:** Output measures (AR, AC, C_{xd} , C_d , I_{xd} , I_d) for low values of the parameters. The x-axis denotes the different scenarios: baseline, low time series parameters (a_1 , a_2 , b_1 , b_2 , α_1 , α_2 , α_3 , σ^2), low transmission parameters (β_0 , β_1 , β_2 , β_5) and low ω .

The other three outcomes (AR, C_{xd} and C_d) were most sensitive to changes in the ω parameter, more so for the low ω value tested due to the larger number of colonised patient compared with infected patients in this setting. To a lesser extent, these outcomes were also sensitive to changes in the transmission parameters considered. The outcomes do not appear sensitive to changes in the time series parameters.

There were also notable increases in the spread of the AR outcome associated with the high values tested for a_1 and a_2 . These are most likely caused by increasing fluctuations in the time series for $E(t)$ as the parameter values are close to the non-stationary regime for the autoregressive component in the ARMAX model.

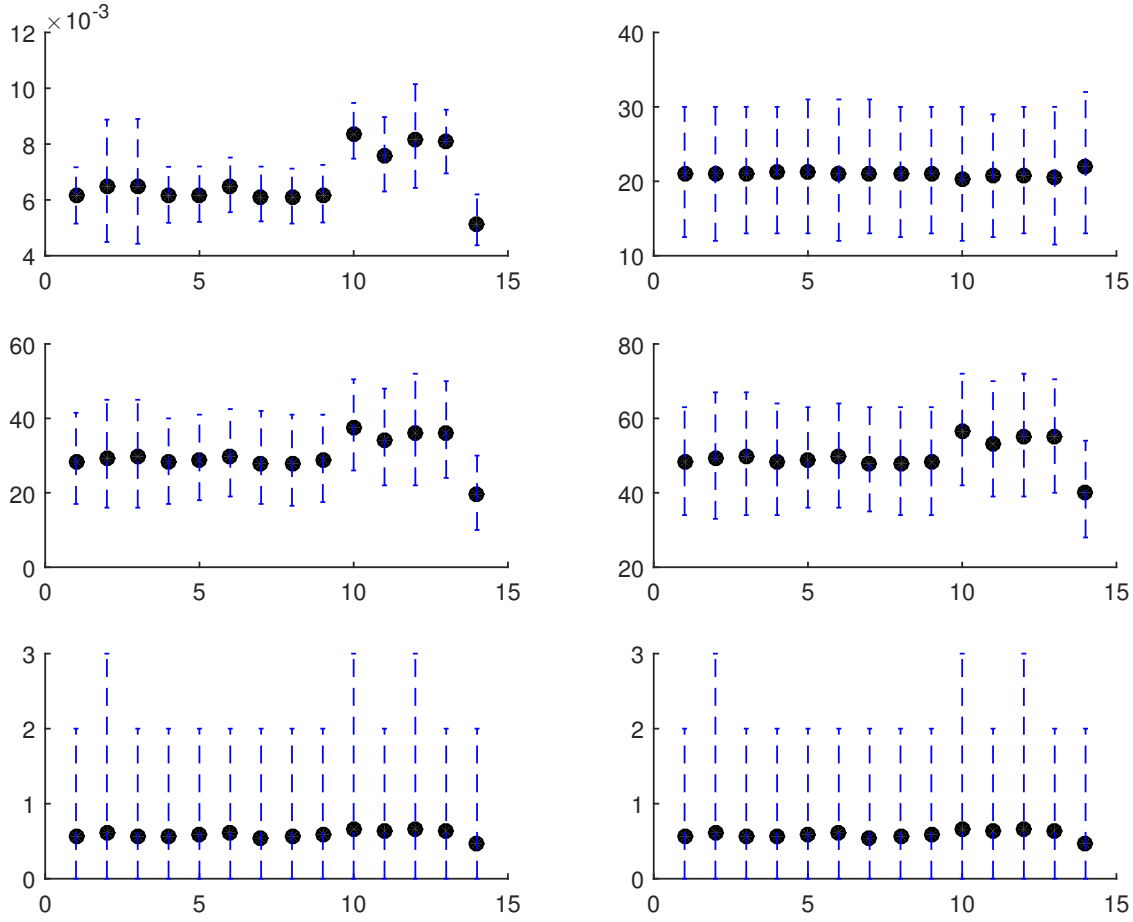


Figure F.2: Output measures (AR, AC, C_{xd} , C_d , I_{xd} , I_d) for high values of the parameters. The x-axis denotes the different scenarios: baseline, high time series parameters (a_1 , a_2 , b_1 , b_2 , α_1, α_2 , α_3 , σ^2), high transmission parameters (β_0 , β_1 , β_2 , β_5) and high ω .

F.2.2 High burden setting

For the high burden setting, the AC, I_{xd} and I_d outcomes remain relatively insensitive to changes in the parameter values considered. However, there are now slight deviations associated with changes in the ω parameters and the transmission parameters.

The AR, C_{xd} and C_d outcomes still exhibit notable sensitivity to the changes in the ω parameter value. Changes to the transmission parameters now also notably affect these outcomes, particularly the AR outcome due to the larger number of colonised and infected patients in the high burden setting. These outcomes still appear insensitive to changes in the time series parameters, except for the high a_1 and a_2 parameter values, similar to the normal burden setting.

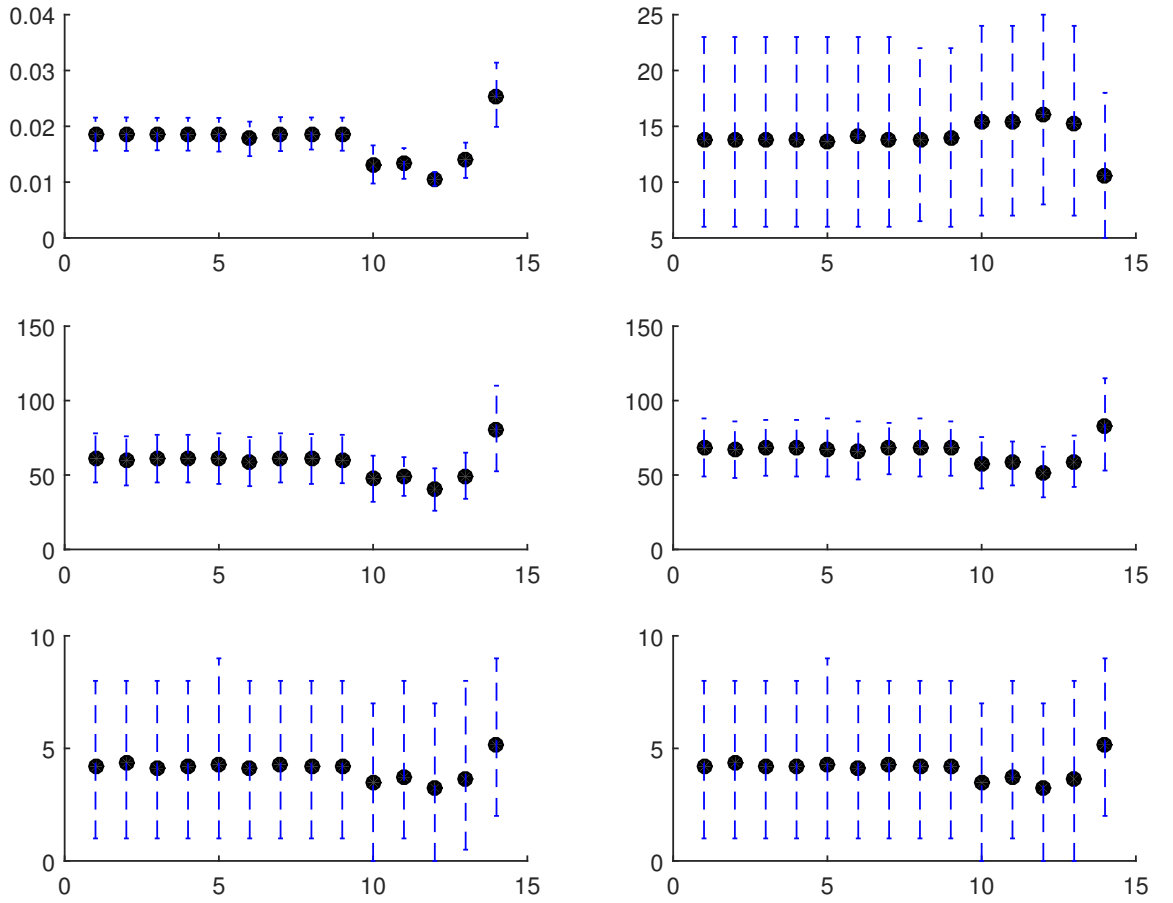


Figure F.3: Output measures (AR, AC, C_{xd} , C_d , I_{xd} , I_d) for low values of the parameters in the high burden setting. The x-axis denotes the different scenarios: baseline, low time series parameters (a_1 , a_2 , b_1 , b_2 , α_1 , α_2 , α_3 , σ^2), low transmission parameters (β_0 , β_1 , β_2 , β_5) and low ω .

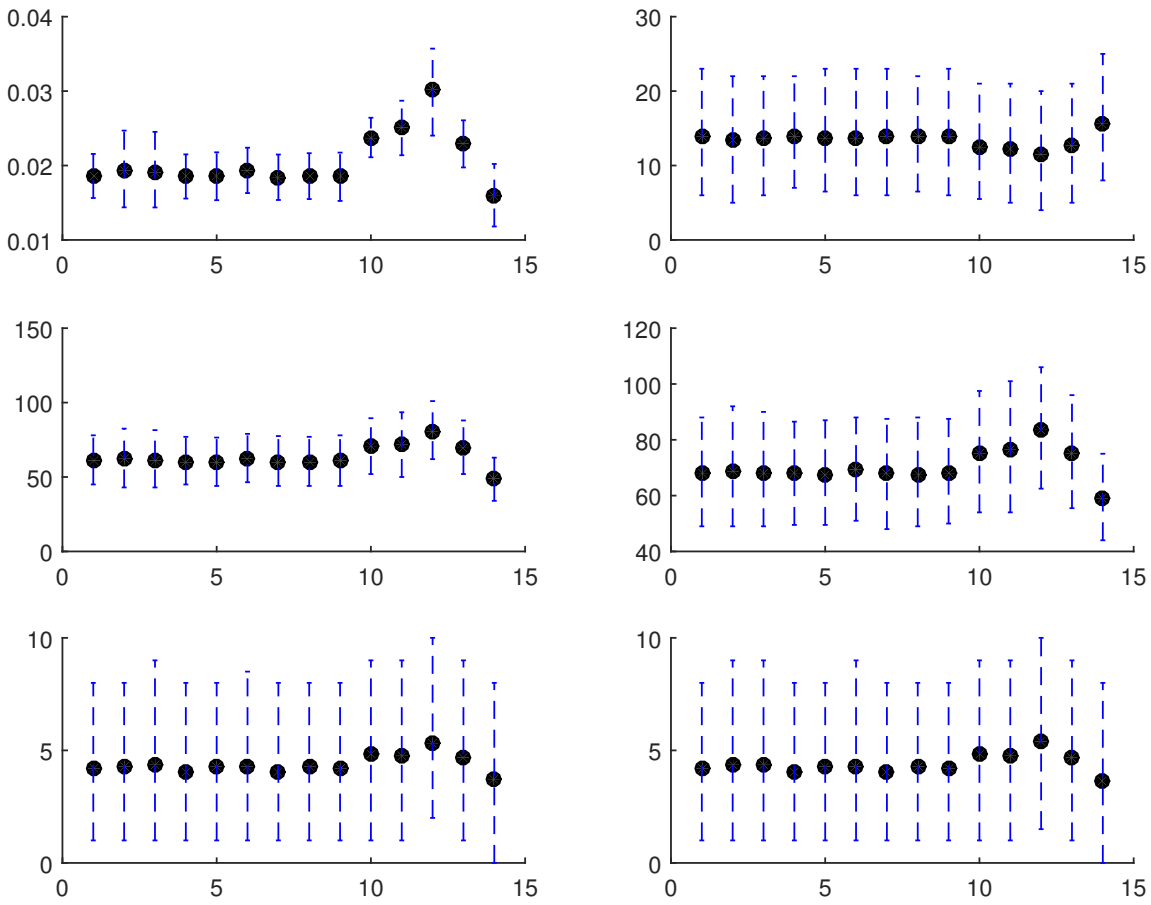


Figure F.4: Output measures (AR, AC, C_{xd} , C_d , I_{xd} , I_d) for high values of the parameters in the high burden setting. The x-axis denotes the different scenarios: baseline, high time series parameters (a_1 , a_2 , b_1 , b_2 , α_1, α_2 , α_3 , σ^2), high transmission parameters (β_0 , β_1 , β_2 , β_5) and high ω .

F.3 Varying strength of single interventions

This section presents the six outcome measures (AR, AC, C_{xd} , C_d , I_{xd} , I_d) obtained when varying the magnitude of the six interventions defined in Section F.1.4 for the normal burden setting (Section F.3.1) and high burden setting (Section F.3.2).

There were no notable difference in the infection treatment (INF) intervention (which modifies ψ) across the range of values tested (Figure F.10 for the normal burden setting and Figure F.16 for the high burden setting). As such, this intervention was not considered further in the results presented in the main text.

F.3.1 Normal burden setting

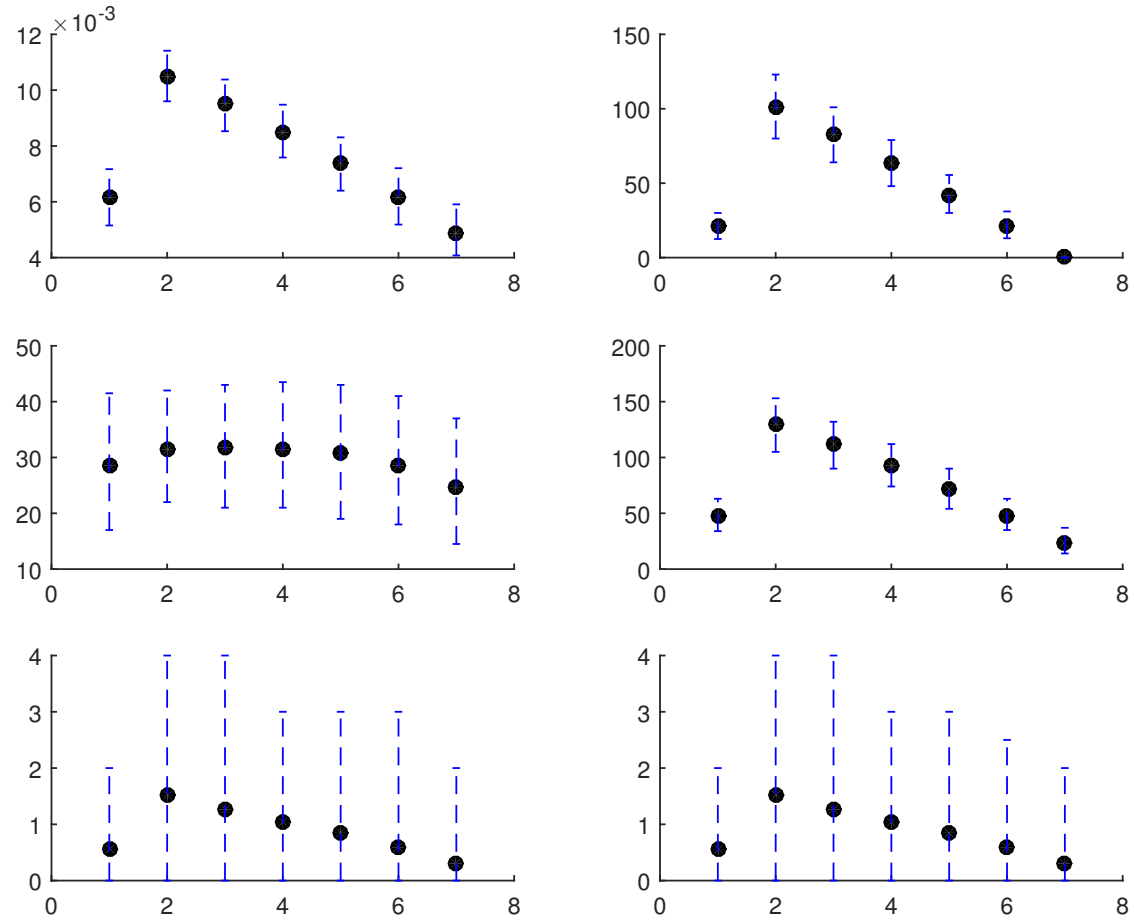


Figure F.5: Output measures (AR, AC, C_{xd} , C_d , I_{xd} , I_d) for a range of colonised on admission (COA) interventions. The x-axis denotes the different scenarios: baseline, $\vartheta \in \{0.75, 0.8, 0.85, 0.9, 0.95, 1\}$. Baseline value is 0.95.

F.3.2 High burden setting

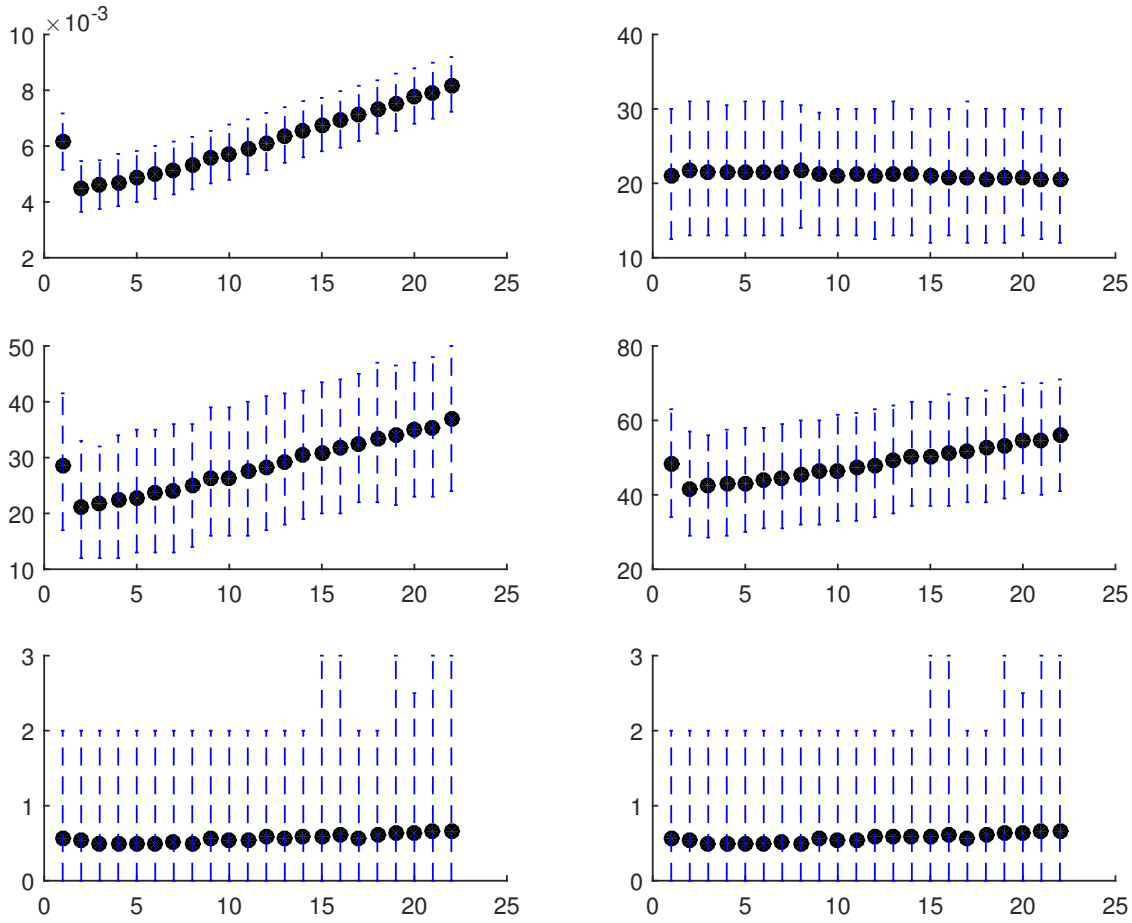


Figure F.6: Output measures (AR, AC, C_{xd} , C_d , I_{xd} , I_d) for a range of improved environmental contamination (ENV) interventions. The x-axis denotes the different scenarios: baseline, $\alpha_1 \in \{[0, 0.1, \dots, 2]\alpha_1\}$. Baseline value is α_1 .

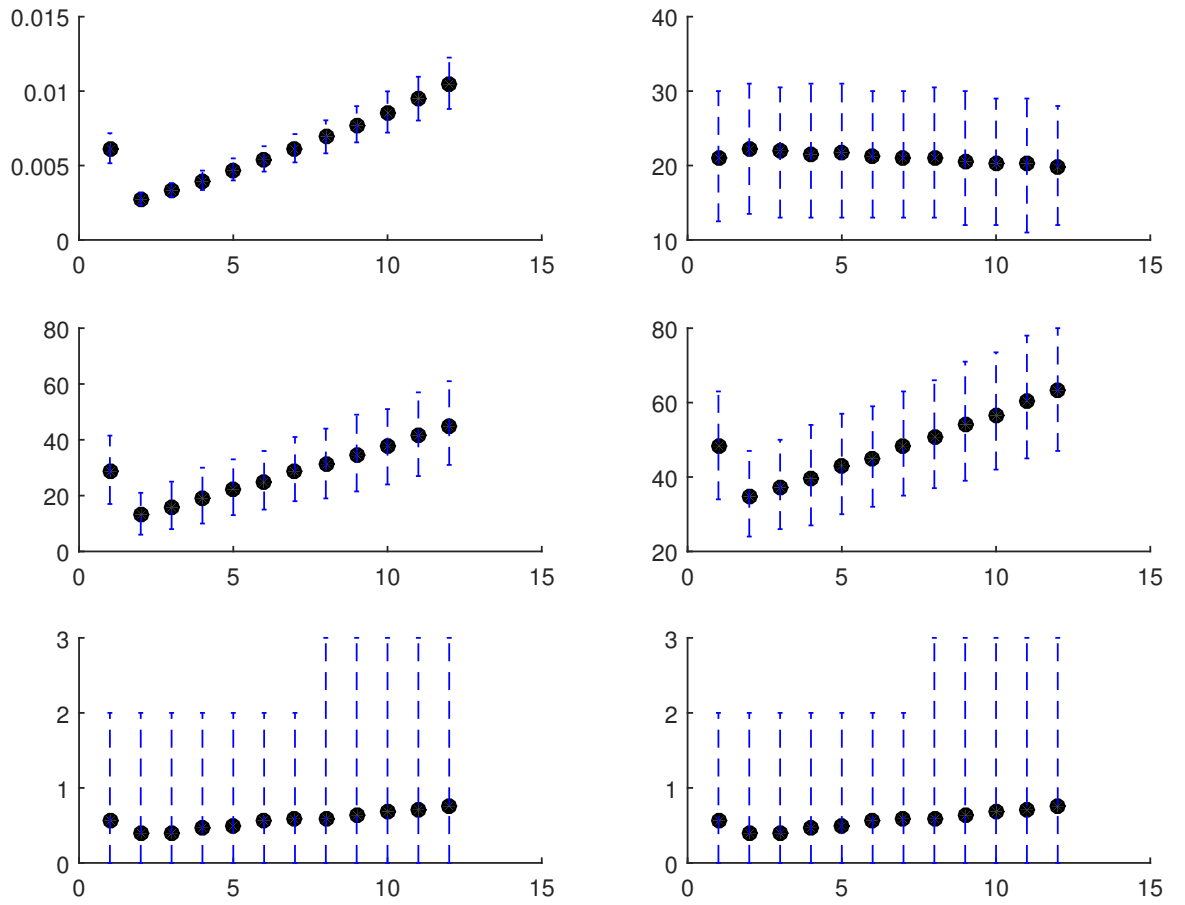


Figure F.7: Output measures (AR , AC , C_{xd} , C_d , I_{xd} , I_d) for a range of improved contact precaution (CP) interventions. The x-axis denotes the different scenarios: baseline, $\xi \in \{0.5, 0.6, \dots, 1.5\}$. Baseline value is 1.

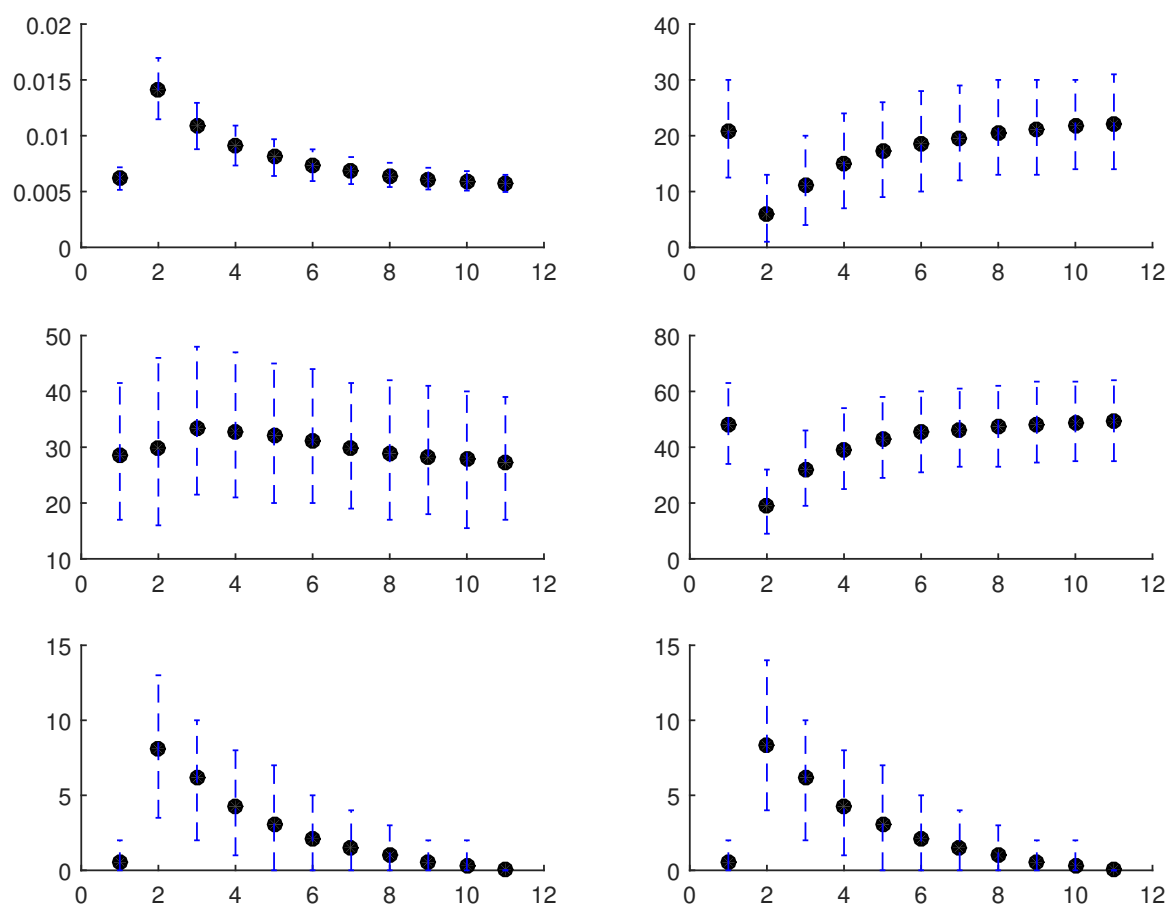


Figure F.8: Output measures (AR , AC , C_{xd} , C_d , I_{xd} , I_d) for a range of test sensitivity (SENS) interventions. The x-axis denotes the different scenarios: baseline, $\rho \in \{[0.1, 0.2, \dots, 1]\}$. Baseline value is 0.8.

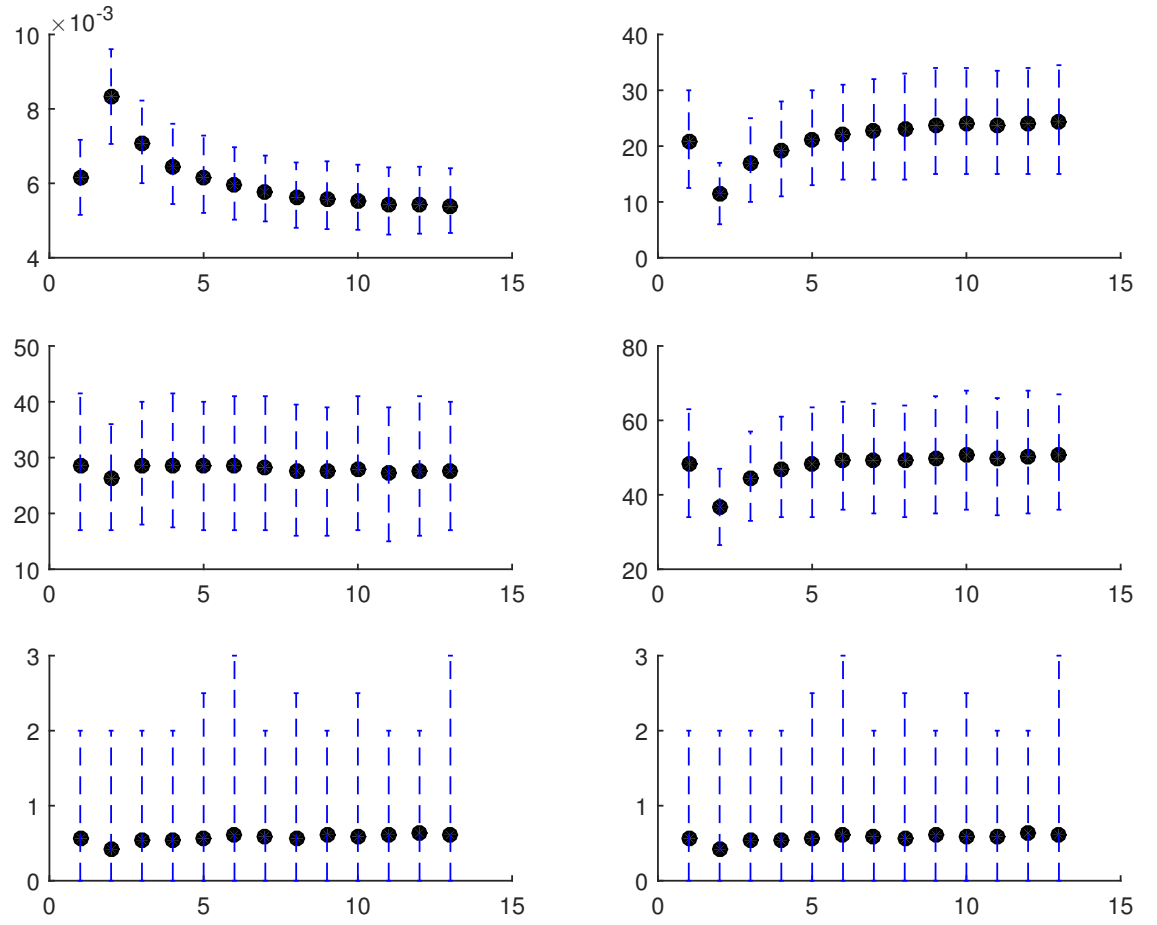


Figure F.9: Output measures (AR, AC, C_{xd} , C_d , I_{xd} , I_d) for a range of improved decolonisation treatment (DECOL) interventions. The x-axis denotes the different scenarios: baseline, $\Delta \in \{-0.75, -0.5, \dots, 2]q_L\}$. Baseline value is 0.

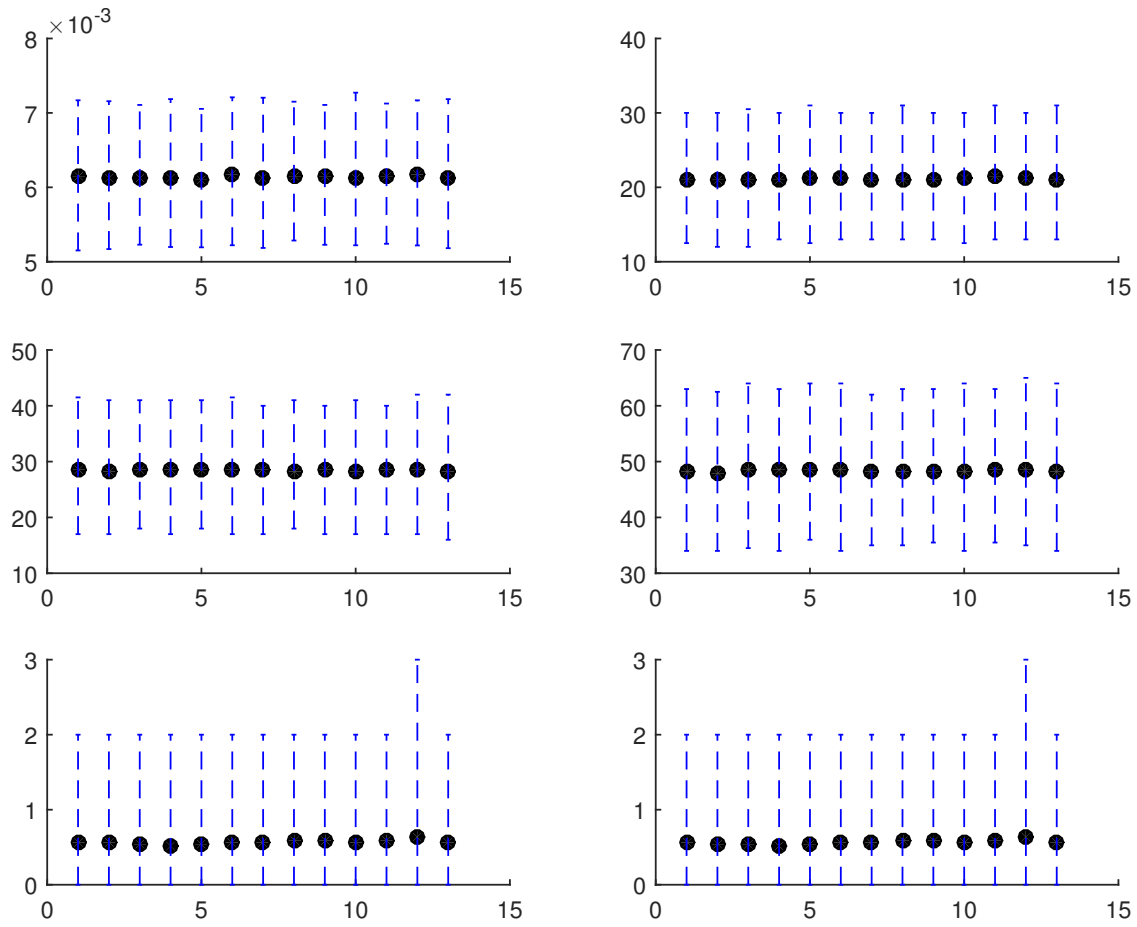


Figure F.10: Output measures (AR, AC, C_{xd} , C_d , I_{xd} , I_d) for a range of improved infection treatment (INF) interventions. The x-axis denotes the different scenarios: baseline, $\psi \in \{[0.25, 0.5, \dots, 3]\psi\}$. Baseline value is ψ .

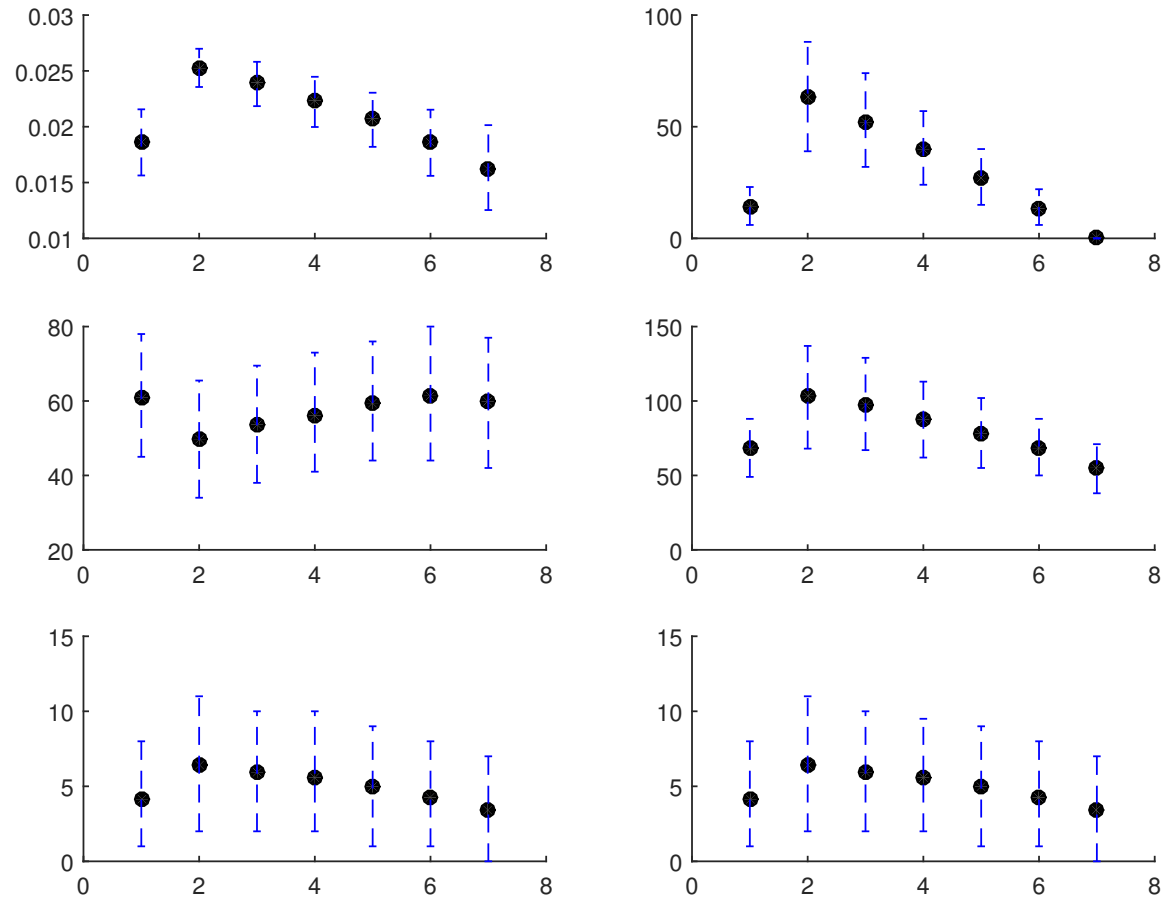


Figure F.11: Output measures (AR, AC, C_{xd} , C_d , I_{xd} , I_d) for a range of colonised on admission (COA) interventions in the high burden setting. The x-axis denotes the different scenarios: baseline, $\vartheta \in \{0.75, 0.8, 0.85, 0.9, 0.95, 1\}$. Baseline value is 0.95.

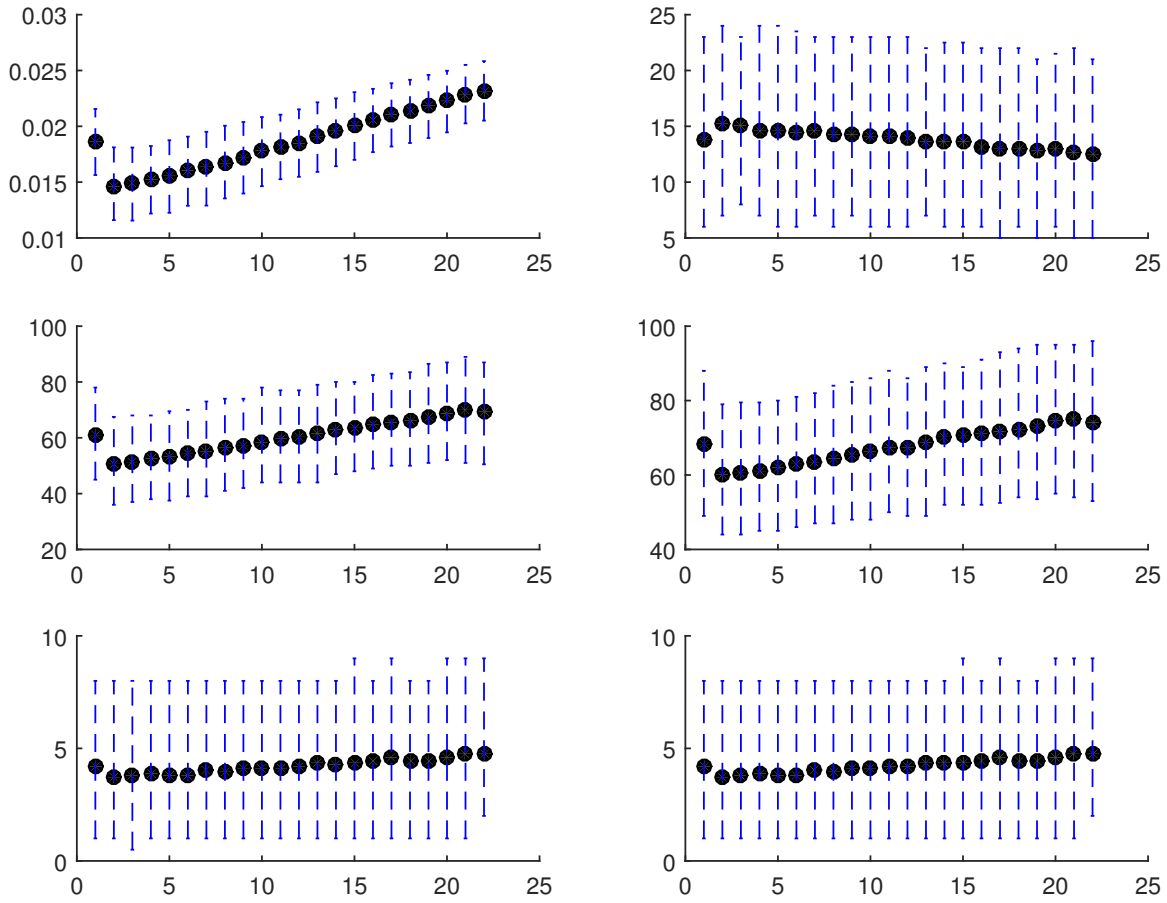


Figure F.12: Output measures (AR, AC, C_{xd} , C_d , I_{xd} , I_d) for a range of improved environmental contamination (ENV) interventions in the high burden setting. The x-axis denotes the different scenarios: baseline, $\alpha_1 \in \{[0, 0.1, \dots, 2]\alpha_1\}$. Baseline value is α_1 .

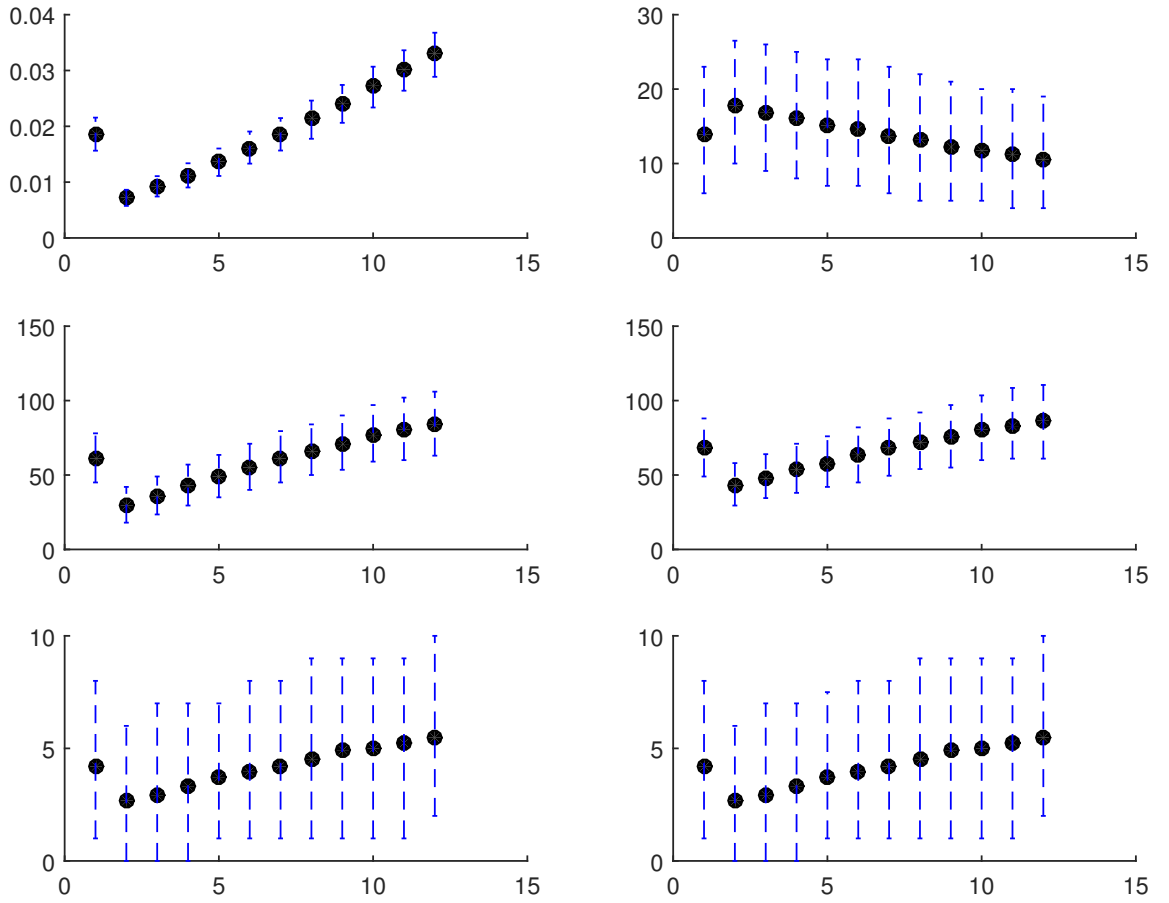


Figure F.13: Output measures (AR , AC , C_{xd} , C_d , I_{xd} , I_d) for a range of improved contact precaution (CP) interventions in the high burden setting. The x-axis denotes the different scenarios: baseline, $\xi \in \{0.5, 0.6, \dots, 1.5\}$. Baseline value is 1.

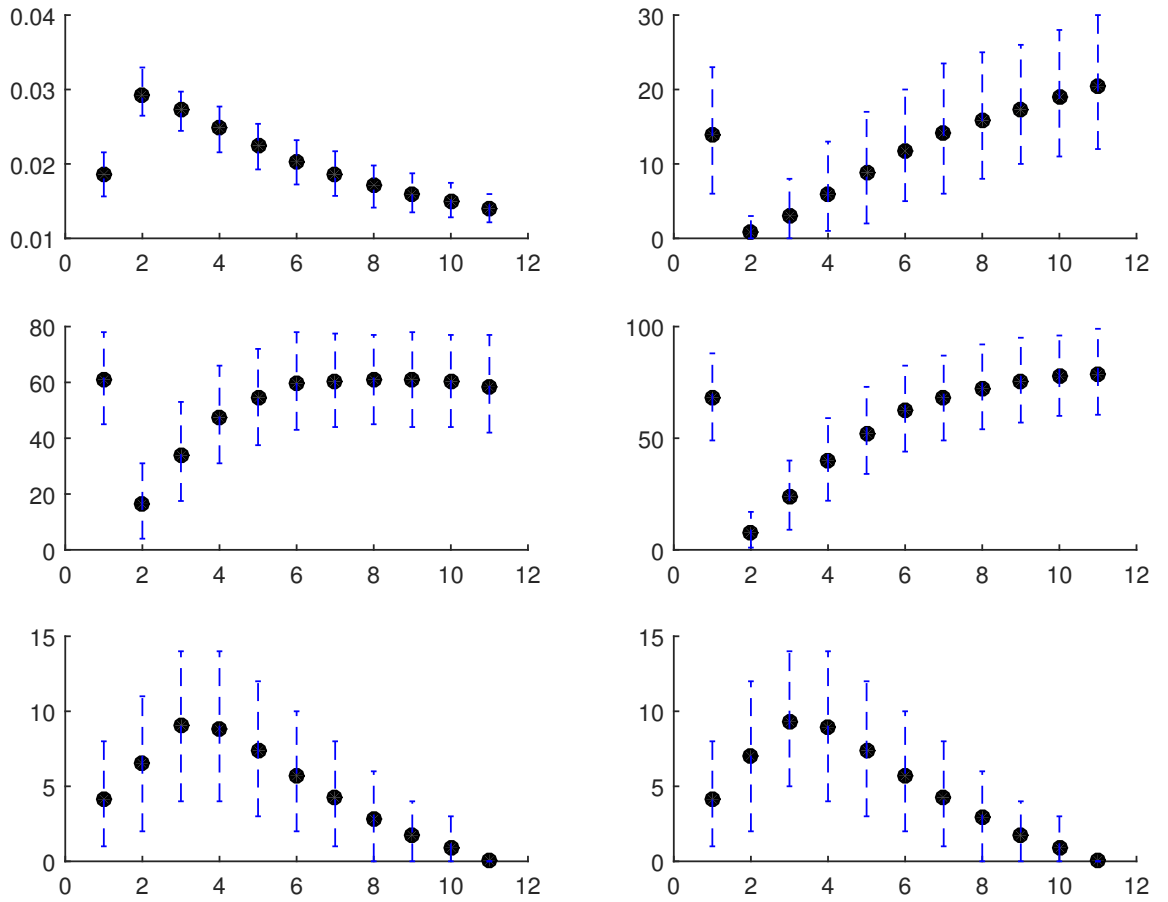


Figure F.14: Output measures (AR , AC , C_{xd} , C_d , I_{xd} , I_d) for a range of test sensitivity (SENS) interventions in the high burden setting. The x-axis denotes the different scenarios: baseline, $\rho \in \{[0.1, 0.2, \dots, 1]\}$. Baseline value is 0.8.

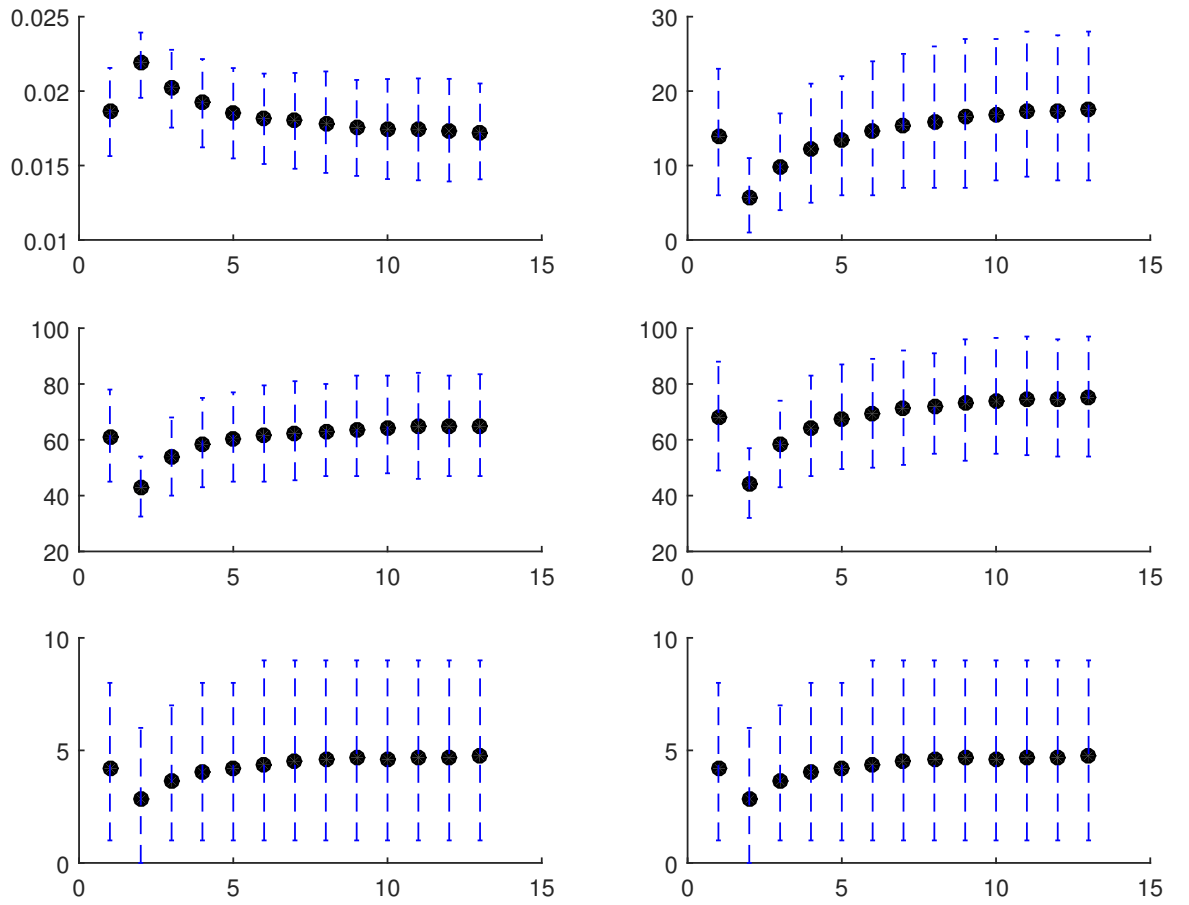


Figure F.15: Output measures (AR , AC , C_{xd} , C_d , I_{xd} , I_d) for a range of improved decolonisation treatment (DECOL) interventions in the high burden setting. The x-axis denotes the different scenarios: baseline, $\Delta \in \{-0.75, -0.5, \dots, 2]q_L\}$. Baseline value is 0.

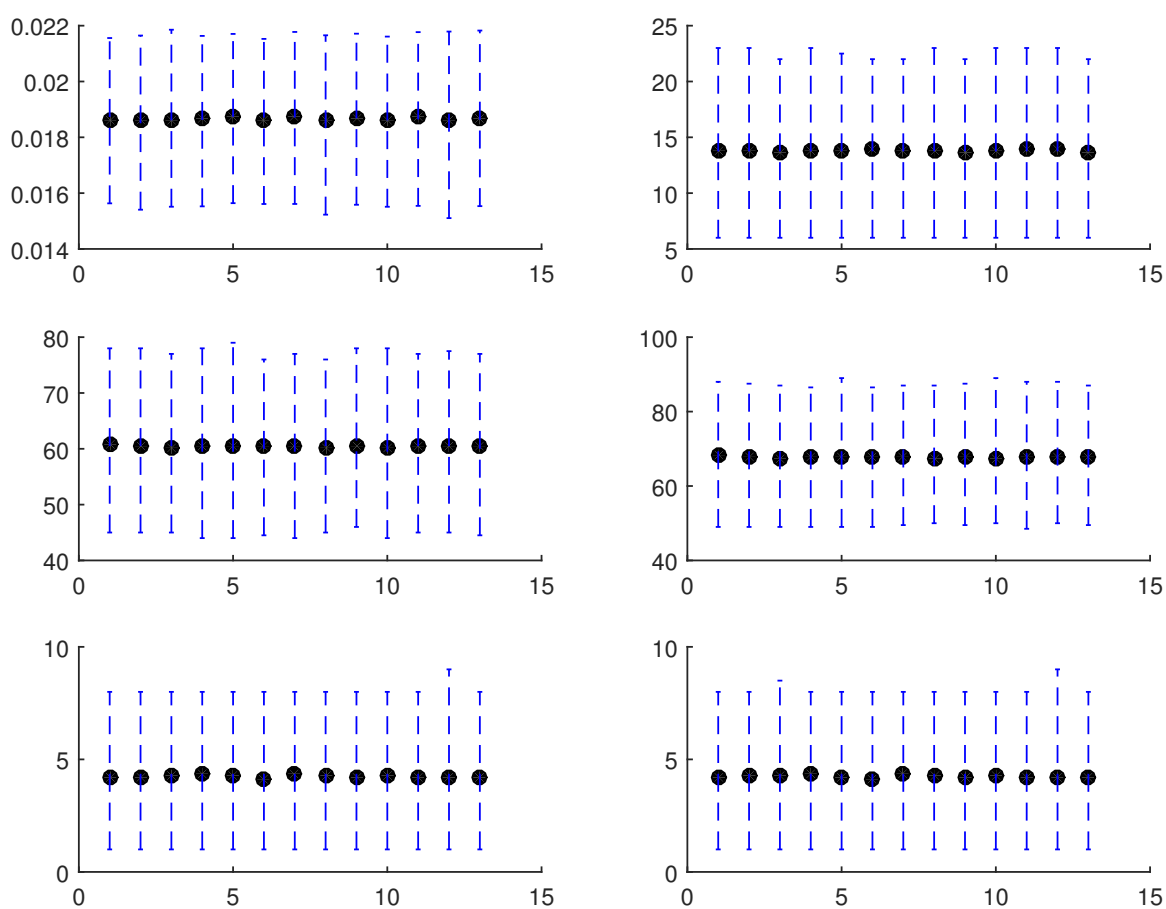


Figure F.16: Output measures (AR, AC, C_{xd} , C_d , I_{xd} , I_d) for a range of improved infection treatment (INF) interventions in the high burden setting. The x-axis denotes the different scenarios: baseline, $\psi \in \{[0.25, 0.5, \dots, 3]\psi\}$. Baseline value is ψ .

F.4 Additional results for normal burden setting

The plots of the average and 95% intervals of the different outcome measures (Supplementary Figures F.17, F.18, F.19, F.20, F.21 and F.22) share the same x-axis label ordering which denotes the different intervention combinations. The x-axis label ordering, moving from left to right, is

- the baseline scenario,
- single interventions (COA, ENV, CP, SENS, DECOL),
- two interventions ($\{\text{COA, ENV}\}$, $\{\text{COA, CP}\}$, $\{\text{COA, SENS}\}$, $\{\text{COA, DECOL}\}$, $\{\text{ENV, CP}\}$, $\{\text{ENV, SENS}\}$, $\{\text{ENV, DECOL}\}$, $\{\text{CP, SENS}\}$, $\{\text{CP, DECOL}\}$, and $\{\text{SENS, DECOL}\}$),
- three interventions ($\{\text{COA, ENV, CP}\}$, $\{\text{COA, ENV, SENS}\}$, $\{\text{COA, ENV, DECOL}\}$, $\{\text{COA, CP, SENS}\}$, $\{\text{COA, CP, DECOL}\}$, $\{\text{COA, SENS, DECOL}\}$, $\{\text{ENV, CP, SENS}\}$, $\{\text{ENV, CP, DECOL}\}$, $\{\text{ENV, SENS, DECOL}\}$, and $\{\text{CP, SENS, DECOL}\}$),
- four interventions ($\{\text{COA, ENV, CP, SENS}\}$, $\{\text{COA, ENV, CP, DECOL}\}$, $\{\text{COA, ENV, SENS, DECOL}\}$, $\{\text{COA, CP, SENS, DECOL}\}$ and $\{\text{ENV, CP, SENS, DECOL}\}$), and
- all five interventions combined.

The same ordering is also used in the corresponding plots for the high burden setting (Supplementary Figures F.23, F.24, F.25, F.26, F.27 and F.28).

F.4.1 AR outcome

All single interventions decreased the AR outcome measure, with the largest improvement obtained for the CP intervention out of all five interventions singly. The CP intervention also produced an AR distribution which is distributionally smaller than the other single interventions. This result was perhaps unsurprising as the CP intervention directly affects the AR outcome measure.

The best performing intervention pair in reducing the AR outcome was the $\{\text{COA, CP}\}$ pair. While there was only weak evidence that the AR distribution associated with this pair was smaller than that of the second best performing pair ($\{\text{ENV, CP}\}$ with $\hat{\theta} = 0.25(0.23, 0.27)$), it was substantially smaller than the AR distributions of the next three best performing intervention pairs ($\{\text{COA, ENV}\}$, $\{\text{CP, DECOL}\}$ and $\{\text{CP, SENS}\}$).

The best performing intervention triplet was $\{\text{COA, ENV, CP}\}$ which had an AR distribution substantially smaller than the other nine triplets. θ estimates for the comparison of $\{\text{COA, ENV, CP}\}$ with the four next best performing intervention triplets are provided in Table F.3.

The best performing intervention quartet in terms of the AR outcome was $\{\text{COA}, \text{ENV}, \text{CP}, \text{DECOL}\}$. However, its associated AR distribution is similar to that of the $\{\text{COA}, \text{ENV}, \text{CP}, \text{SENS}\}$ with an estimated θ value of $0.43(0.41, 0.46)$. While the mean AR estimate for $\{\text{COA}, \text{ENV}, \text{CP}, \text{DECOL}\}$ was smaller than that for $\{\text{COA}, \text{ENV}, \text{CP}, \text{SENS}\}$, the latter had a narrower 95% interval compared with the former. These two quartets performed better than the remaining three quartets.

Comparing across the best performing intervention combinations for the AR outcome, the $\{\text{COA}, \text{CP}\}$ pair outperforms CP singly and $\{\text{COA}, \text{ENV}, \text{CP}\}$ triplet outperforms the $\{\text{COA}, \text{CP}\}$ pair. However, the reductions in the AR distribution moving from the best performing triplet to either of the two best performing quartets ($\{\text{COA}, \text{ENV}, \text{CP}, \text{DECOL}\}$ or $\{\text{COA}, \text{ENV}, \text{CP}, \text{SENS}\}$) are less pronounced (with associated $\hat{\theta}$ of $0.33(0.30, 0.35)$ and $0.38(0.35, 0.40)$ respectively). The AR distribution for the case with all interventions was slightly smaller compared with the best performing triplet ($\{\text{COA}, \text{ENV}, \text{CP}\}$) with an estimated θ of $0.20(0.18, 0.22)$ and a narrower 95% interval. While the case with all interventions also outperformed the two best performing intervention quartets, the difference in the AR distributions here was less pronounced compared with the triplet comparison with $\hat{\theta}$ of $0.35(0.33, 0.38)$ and $0.28(0.26, 0.30)$ for the best and second best performing intervention quartets respectively.

F.4.2 AC outcome

The most important intervention for the AC outcome was obviously the COA intervention which eliminates the possibility of colonised patients being admitted. As such, the COA intervention (and any other intervention combinations which include COA) greatly outperforms interventions of any size which do not include the COA intervention.

F.4.3 C_{xd} outcome

In terms of the C_{xd} outcome distribution, the most effective single intervention appears to be the CP intervention with an estimated θ value of $0.17(0.15, 0.19)$. The COA and ENV interventions performed similarly to one another and produced a slightly smaller C_{xd} distribution compared with the baseline. The SENS and DECOL interventions singly did not seem to have affected the C_{xd} distribution when compared with the baseline. As such, the CP intervention outperforms the COA and ENV interventions and is superior to that of SENS and DECOL interventions in producing a smaller C_{xd} distribution.

The most effective intervention pair in reducing the C_{xd} outcome average was the $\{\text{COA}, \text{CP}\}$ pair. However, the second best pairing $\{\text{ENV}, \text{CP}\}$ produced a similar outcome distribution ($\hat{\theta} = 0.50(0.47, 0.52)$). More notable reduction in the C_{xd}

distributions were observed when comparing {COA, CP} to subsequent best performing pairs.

The {COA, ENV, CP} triplet was the most effective triplet in producing a smaller C_{xd} distribution, slightly outperforming the next four most effective triplets with $\hat{\theta}$ values of 0.35 or 0.32. Improved performance was noted when comparing the {COA, ENV, CP} triplet with subsequent triplets.

The most effective quartet of interventions appear to be either {COA, ENV, CP, DECOL} or {COA, ENV, CP, SENS} with similar distributions ($\hat{\theta} = 0.48(0.46, 0.51)$). Both these intervention quartets performed better than the other three quartets considered for the C_{xd} outcome.

Comparing across the different intervention combination sizes, the two best performing pairs ({COA, CP} and {ENV, CP}) performed slightly better in reducing the C_{xd} distribution compared with CP singly. A similar performance gain was noted when comparing the best intervention triplet ({COA, ENV, CP}) to both the best performing pairs. There does not appear to be substantial difference in the C_{xd} difference when comparing across the best performing triplet, quartets and the combination of all interventions.

F.4.4 C_d outcome

Of the five single interventions, only the COA, ENV and CP interventions produced a smaller C_d distributional outcome. The SENS and DECOL interventions did not produce C_d distributions that were notably different from baseline. The best performing single intervention in terms of the C_d outcome measure was the COA intervention, which greatly outperformed all four other single interventions.

The importance of the COA intervention for the C_d outcome measure was also reflected in the drastically smaller C_d distributions obtained for interventions sets with COA included compared with those without the COA intervention included.

The best performing intervention pair for the C_d outcome was {COA, CP}. The associated C_d distribution for {COA, CP} was slightly smaller compared with the second best pair ({COA, ENV} with $\hat{\theta}$ of 0.38(0.35, 0.40)). Improved performance was noted when comparing {COA, CP} with the three next best performing intervention pairs for the C_d outcome ({COA, DECOL}, {COA, SENS}, and {ENV, CP} with θ values of 0.19(0.17, 0.21), 0.18(0.16, 0.20) and 0.00(0.00, 0.01) respectively).

The best performing triplet was {COA, ENV, CP} with slight evidence that the associated C_d distribution was smaller than those of the next four best performing triplets with $\hat{\theta}$ estimates between 0.24 and 0.33. There was stronger evidence that the {COA, ENV, CP} triplet outperformed the next {COA, SENS, DECOL} triplet (the sixth best performing triplet) with $\hat{\theta}$ of 0.10(0.08, 0.11).

The two best performing quartets were {COA, ENV, CP, DECOL} and {COA, ENV, CP, SENS}, outperforming the other three quartets, in particular the quartet without the COA intervention.

Comparing across different intervention sizes, there are notable reductions in support of considering additional number of interventions up to the best performing intervention triplet ({COA, ENV, CP}) for the C_d outcome. There are no discernible difference in the C_d outcome distributions in implementing all five interventions or either of the two best performing quartets identified compared with having just the best performing intervention triplet (with θ estimates ranging from 0.46 to 0.51).

F.4.5 I_{xd} outcome

The SENS intervention was the most effective intervention for the I_{xd} outcome measure as having perfect sensitivity in the screening test ensures detection of colonised patients prior to the colonisation developing into an infection. As such, the SENS intervention singly was sufficient to reduce the I_{xd} outcome to 0. Any other intervention combinations with SENS was also able to achieve the same outcome for I_{xd} . However, it should also be noted that the I_{xd} outcome is generally small for the particular ward setting considered with even the baseline I_{xd} having a 95% interval of $[0, 2]$ (see Figure F.21).

There appears to be little difference in the I_{xd} outcome of the other single interventions (apart from SENS with $\hat{\theta} = 0.28(0.26, 0.30)$) compared with the baseline distribution with θ estimates ranging from 0.39 to 0.51. The SENS intervention only slightly outperform the other single interventions with $\hat{\theta}$ values ranging from 0.28 to 0.38 when compared with the other four single interventions. There is little evidence that the second best intervention (COA) is different from the remaining three single interventions (CP, ENV, DECOL) with $\hat{\theta}$ between 0.39 to 0.42.

With the combinations of two interventions, we see that any intervention pairs including SENS would achieve I_{xd} of 0. Thus, the comparison of the intervention pairs which exclude SENS was done with a representative intervention pair {SENS, .} denoting an intervention pair including SENS (as there is no need to compare between intervention pairs including SENS). Similarly, denoting any intervention triplet which include SENS by {SENS, ., .} and any intervention quartet with SENS by {SENS, ., ., .}, the eradication of I_{xd} only slightly outperforms the other interventions of similar sizes with $\hat{\theta}$ ranging between 0.28 to 0.43. This marginal gain is, again, due to the small numbers of I_{xd} involved.

Lastly, comparing across the different intervention sizes including SENS, it is unsurprising that there is no difference between their I_{xd} distributions. In other words, if the focus was solely on minimising I_{xd} , there is no need to consider anything beyond the SENS intervention singly.

F.4.6 I_d outcome

The performance of the interventions on the I_d outcome was very similar to that for the I_{xd} since the only transition to I_d is through I_{xd} , i.e. eliminating the I_{xd} would also eliminate the I_d population. As such, we see again that the SENS intervention singly is sufficient to control the I_d outcome (Figure F.22). The intervention comparisons were similar to those for the I_{xd} outcome.

Outcome	Ranking
AR	CP, COA, ENV, DECOL, SENS
	{COA, CP}, {ENV, CP}, {COA, ENV}, {CP, DECOL}, {CP, SENS}, {COA, DECOL}, {COA, SENS}, {ENV, DECOL}, {ENV, SENS}, {SENS, DECOL}
	{COA, ENV, CP}, {COA, CP, DECOL}, {COA, CP, SENS}, {ENV, CP, DECOL}, {ENV, CP, SENS}, {COA, ENV, DECOL}, {COA, ENV, SENS}, {CP, SENS, DECOL}, {ENV, SENS, DECOL}, {COA, SENS, DECOL}
	{COA, ENV, CP, DECOL}, {COA, ENV, CP, SENS}, {ENV, CP, SENS, DECOL}, {COA, CP, SENS, DECOL}, {COA, ENV, SENS, DECOL}
AC	COA, ENV, CP, SENS, DECOL
	{COA, ENV}, {COA, CP}, {COA, SENS}, {COA, DECOL}, {ENV, CP}, {ENV, SENS}, {CP, SENS}, {ENV, DECOL}, {CP, DECOL}, {SENS, DECOL}
	{COA, ENV, CP}, {COA, ENV, SENS}, {COA, ENV, DECOL}, {COA, CP, SENS}, {COA, CP, DECOL}, {COA, SENS, DECOL}, {ENV, CP, SENS}, {ENV, CP, DECOL}, {CP, SENS, DECOL}, {ENV, SENS, DECOL}
	{COA, ENV, CP, SENS}, {COA, ENV, CP, DECOL}, {COA, ENV, SENS, DECOL}, {COA, CP, SENS, DECOL}, {ENV, CP, SENS, DECOL}
C_{xd}	CP, ENV, COA, SENS, DECOL
	{COA, CP}, {ENV, CP}, {CP, SENS}, {COA, ENV}, {CP, DECOL}, {ENV, SENS}, {ENV, DECOL}, {COA, SENS}, {COA, DECOL}, {SENS, DECOL}
	{COA, ENV, CP}, {ENV, CP, SENS}, {ENV, CP, DECOL}, {COA, CP, DECOL}, {COA, CP, SENS}, {COA, ENV, SENS}, {COA, ENV, DECOL}, {CP, SENS, DECOL}, {ENV, SENS, DECOL}, {COA, SENS, DECOL}
	{COA, ENV, CP, DECOL}, {COA, ENV, CP, SENS}, {ENV, CP, SENS, DECOL}, {COA, CP, SENS, DECOL}, {COA, ENV, SENS, DECOL}
C_d	COA, CP, ENV, SENS, DECOL
	{COA, CP}, {COA, ENV}, {COA, DECOL}, {COA, SENS}, {ENV, CP}, {CP, SENS}, {CP, DECOL}, {ENV, SENS}, {ENV, DECOL}, {SENS, DECOL}
	{COA, ENV, CP}, {COA, CP, DECOL}, {COA, CP, SENS}, {COA, ENV, DECOL}, {COA, ENV, SENS}, {COA, SENS, DECOL}, {ENV, CP, SENS}, {ENV, CP, DECOL}, {CP, SENS, DECOL}, {ENV, SENS, DECOL}
	{COA, ENV, CP, DECOL}, {COA, ENV, CP, SENS}, {COA, CP, SENS, DECOL}, {COA, ENV, SENS, DECOL}, {ENV, CP, SENS, DECOL}
I_{xd}	SENS, COA, CP, ENV, DECOL
	{COA, SENS}, {ENV, SENS}, {CP, SENS}, {SENS, DECOL}, {COA, CP}, {COA, ENV}, {COA, DECOL}, {ENV, CP}, {ENV, DECOL}, {CP, DECOL}
	{COA, ENV, SENS}, {COA, CP, SENS}, {COA, SENS, DECOL}, {ENV, CP, SENS}, {ENV, SENS, DECOL}, {CP, SENS, DECOL}, {COA, ENV, CP}, {COA, CP, DECOL}, {COA, ENV, DECOL}, {ENV, CP, DECOL}
	{COA, ENV, CP, SENS}, {COA, ENV, SENS, DECOL}, {COA, CP, SENS, DECOL}, {ENV, CP, SENS, DECOL}, {COA, ENV, CP, DECOL}
I_d	SENS, COA, CP, ENV, DECOL
	{COA, SENS}, {ENV, SENS}, {CP, SENS}, {SENS, DECOL}, {COA, CP}, {COA, ENV}, {COA, DECOL}, {ENV, CP}, {ENV, DECOL}, {CP, DECOL}
	{COA, ENV, SENS}, {COA, CP, SENS}, {COA, SENS, DECOL}, {ENV, CP, SENS}, {ENV, SENS, DECOL}, {CP, SENS, DECOL}, {COA, ENV, CP}, {COA, CP, DECOL}, {COA, ENV, DECOL}, {ENV, CP, DECOL}
	{COA, ENV, CP, SENS}, {COA, ENV, SENS, DECOL}, {COA, CP, SENS, DECOL}, {ENV, CP, SENS, DECOL}, {COA, ENV, CP, DECOL}

Table F.2: Ranking of the various intervention combinations by the output measure means and intervention sizes.

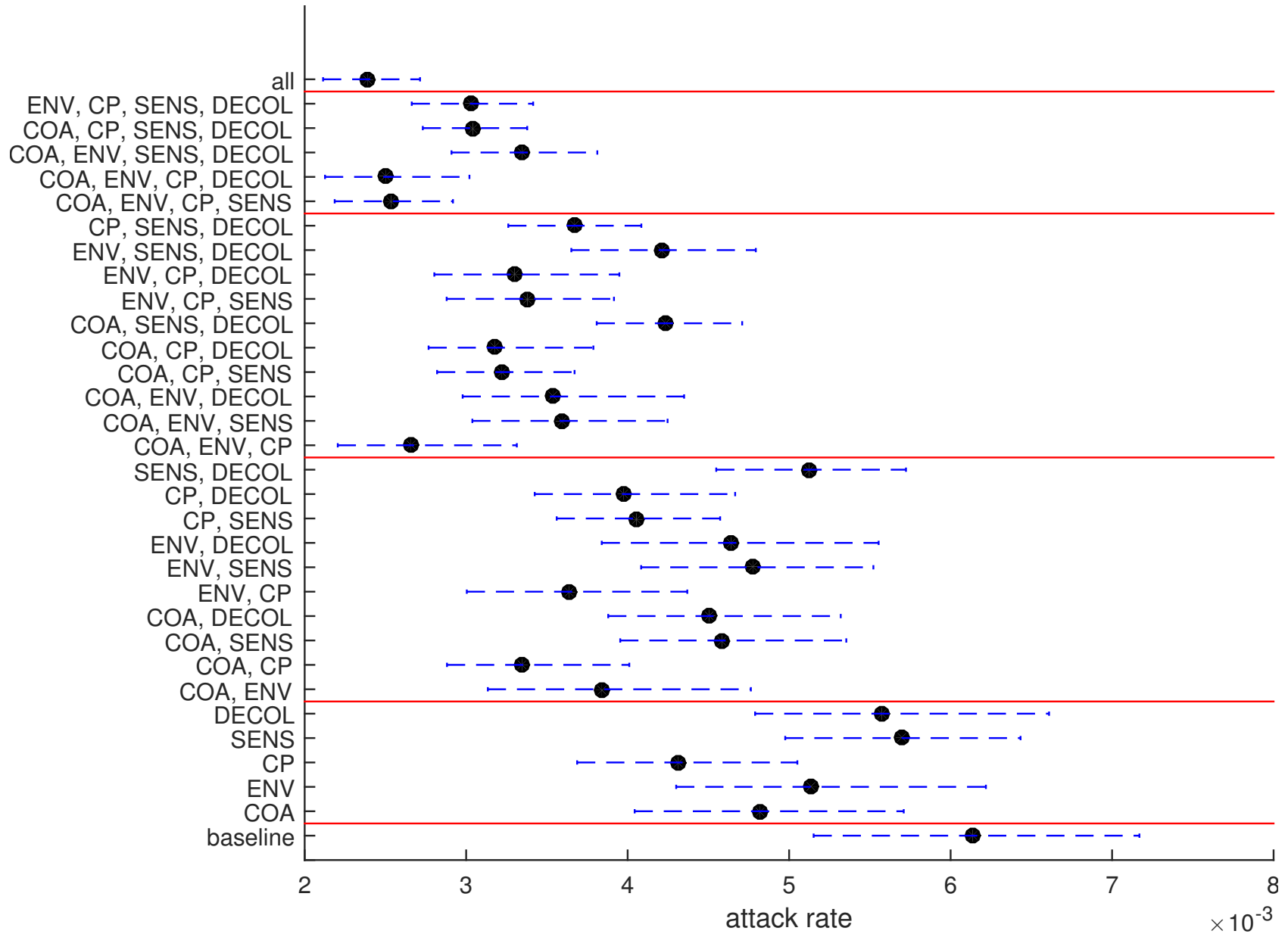


Figure F.17: Attack rate average and 95% intervals in the simulated ward.

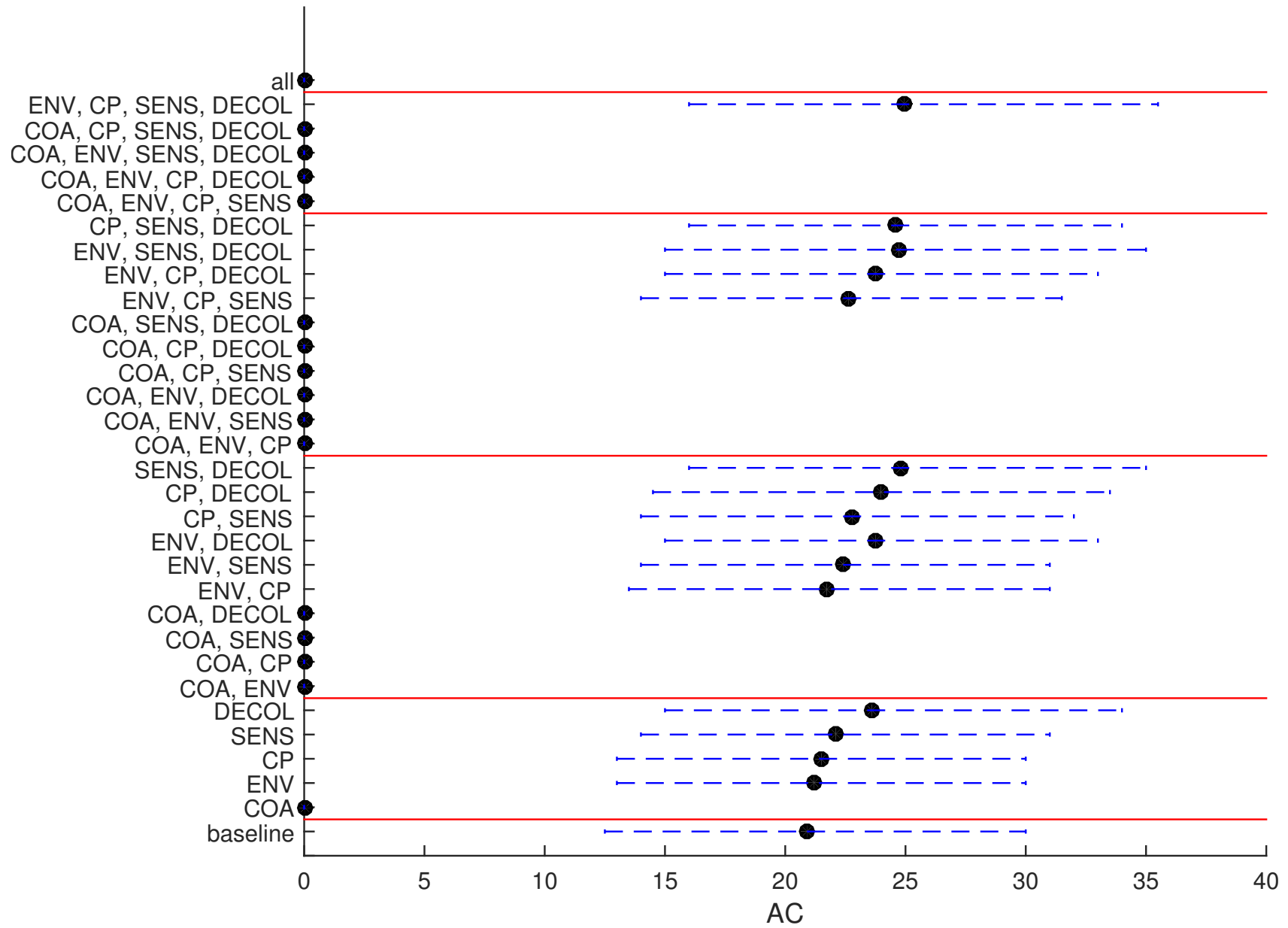
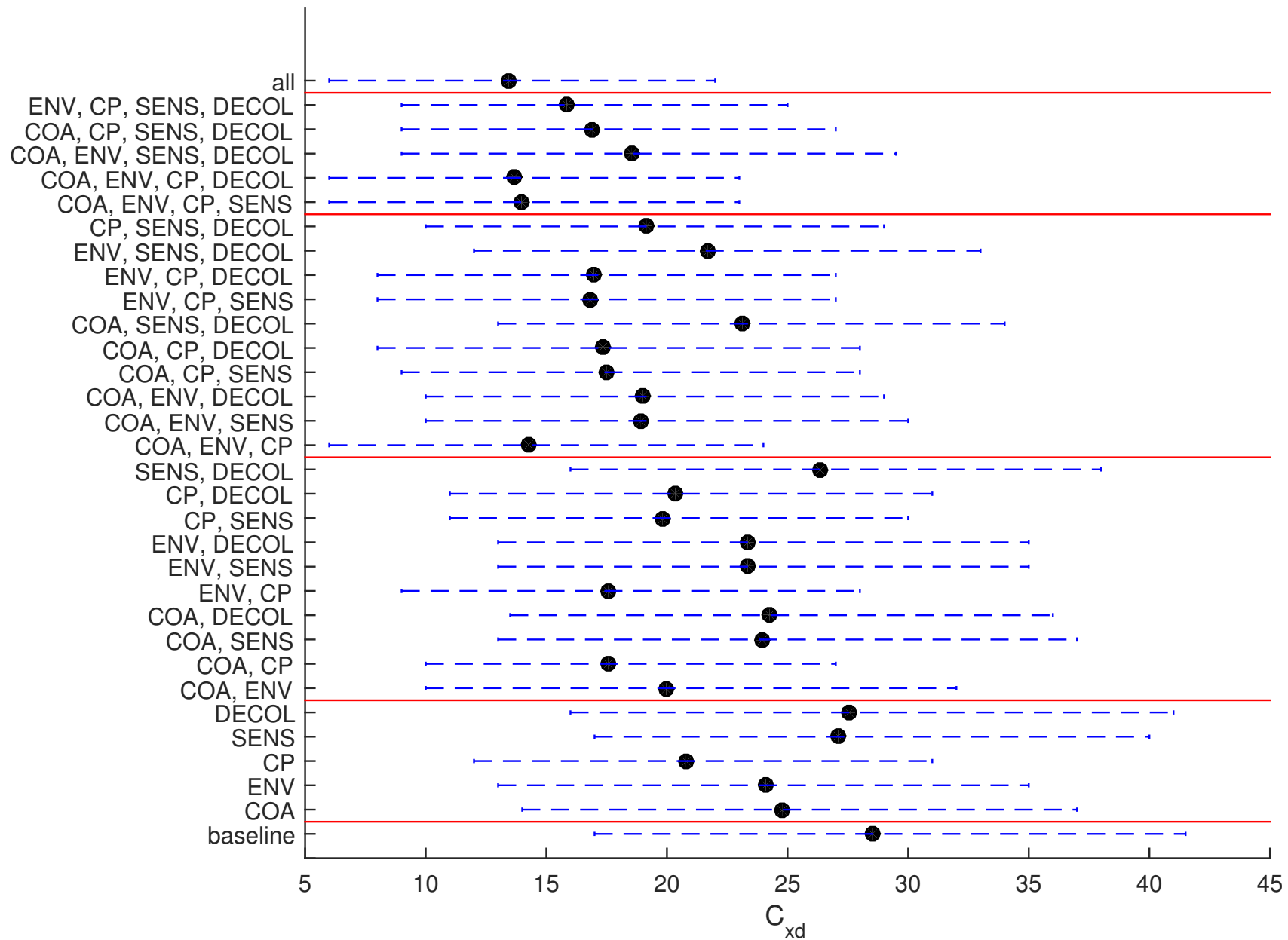
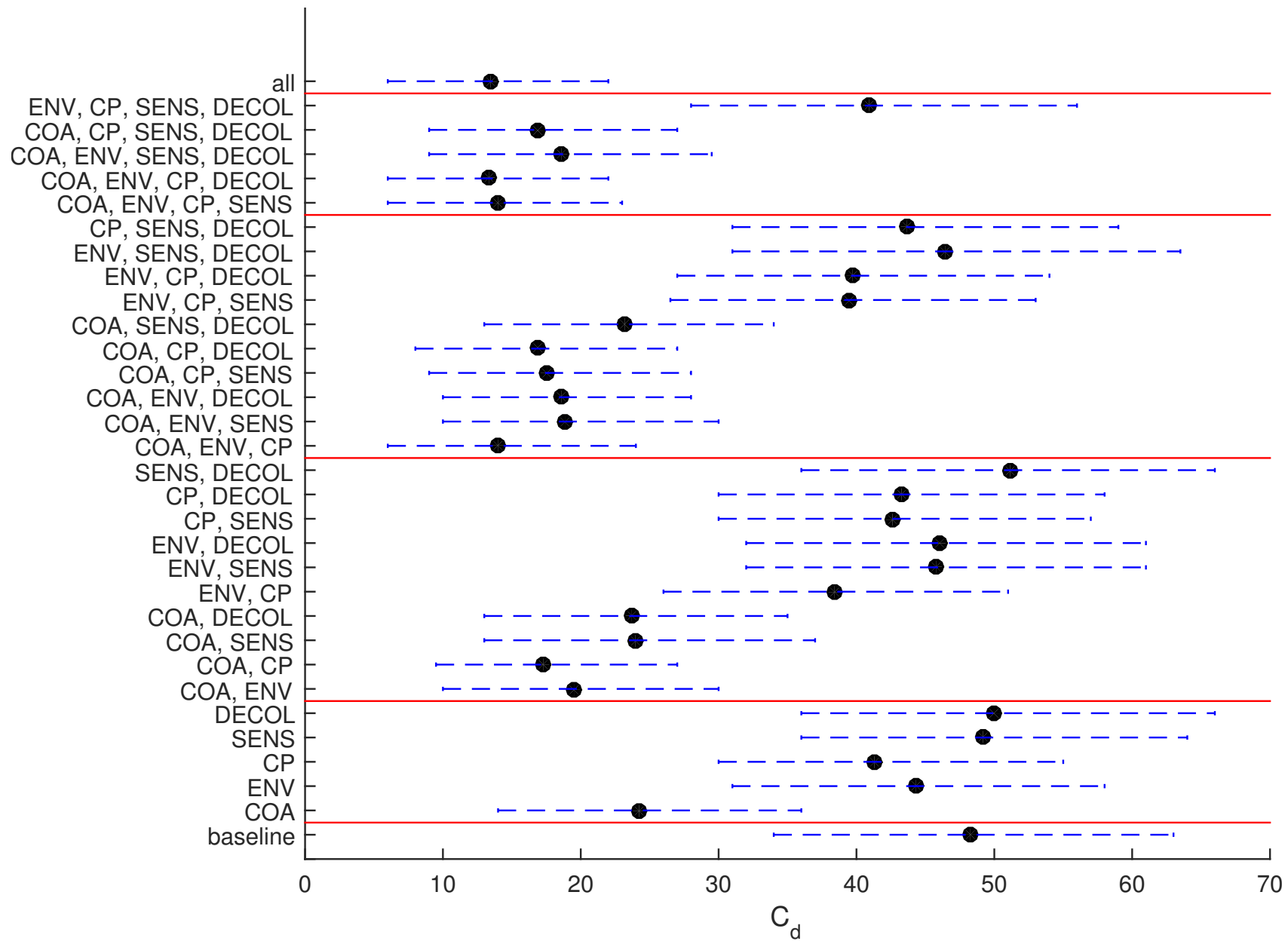


Figure F.18: AC average and 95% intervals in the simulated ward.

Figure F.19: C_{xd} average and 95% intervals in the simulated ward.

Figure F.20: C_d average and 95% intervals in the simulated ward.

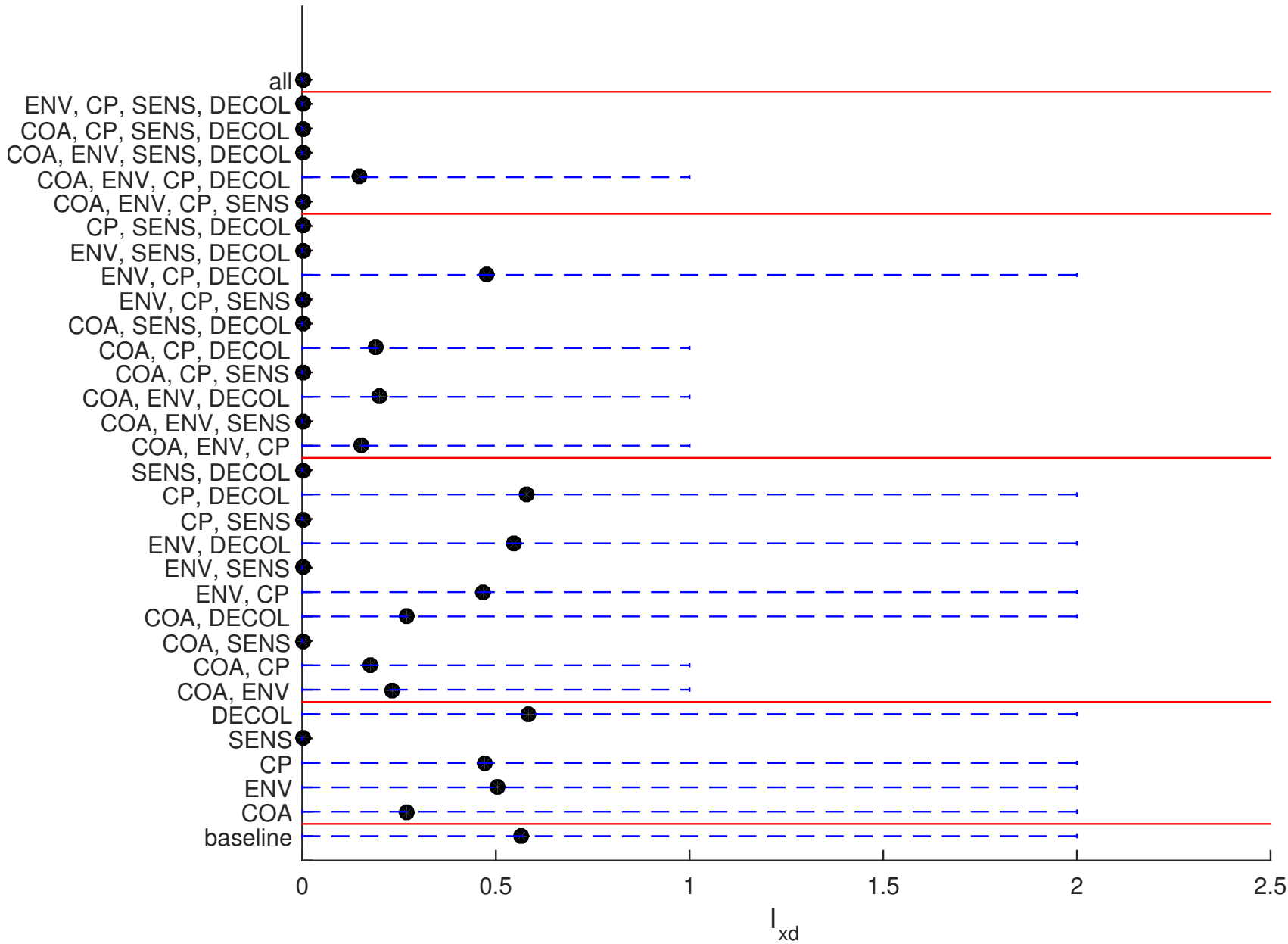
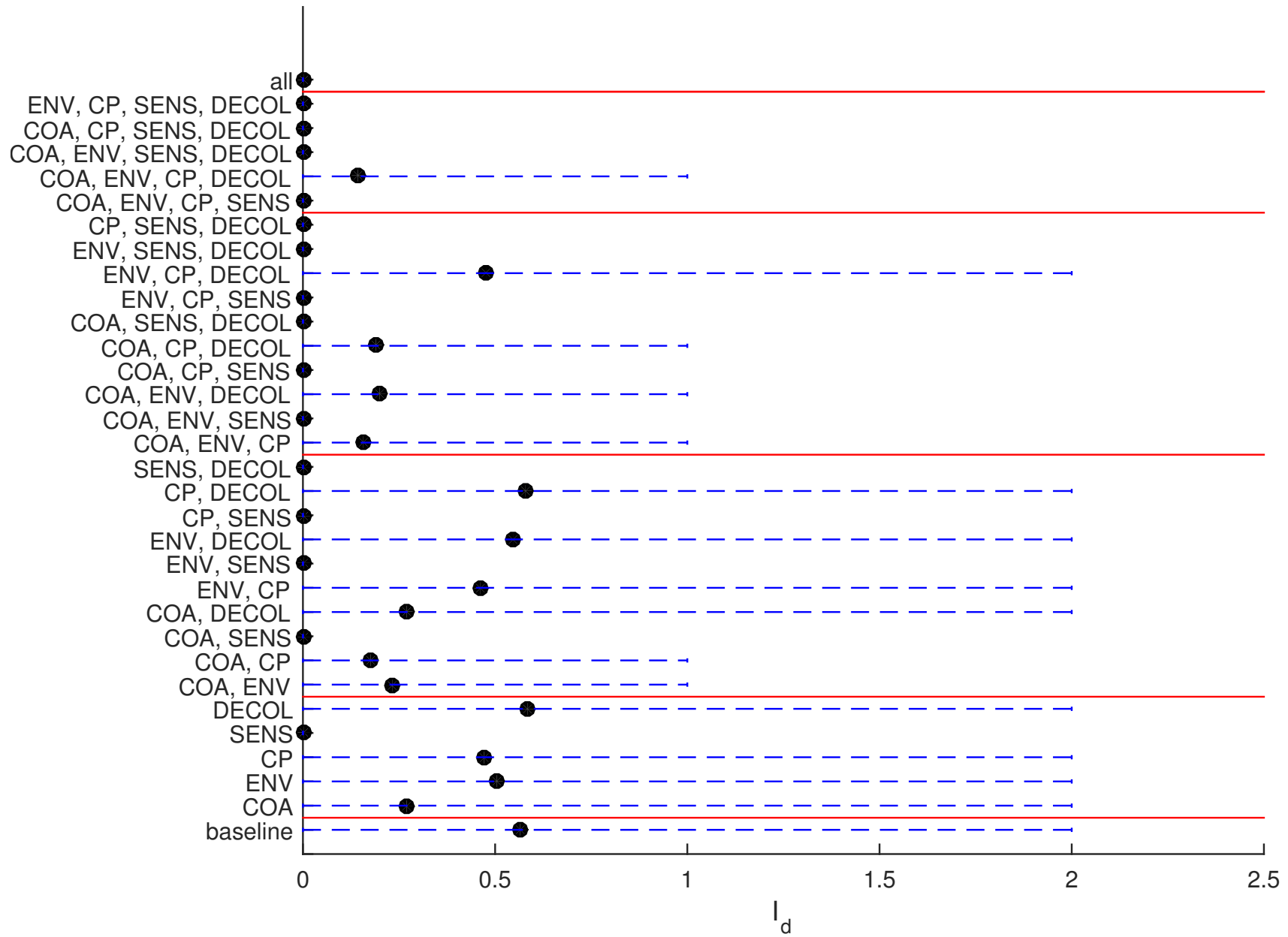


Figure F.21: I_{xd} average and 95% intervals in the simulated ward.

Figure F.22: I_d average and 95% intervals in the simulated ward.

Comparison	AR $\hat{\theta}$ (95% CI)
COA v baseline	0.03 (0.02 , 0.03)
ENV v baseline	0.08 (0.07 , 0.09)
CP v baseline	0.00 (0.00 , 0.00)
SENS v baseline	0.25 (0.23 , 0.27)
DECOL v baseline	0.20 (0.18 , 0.22)
CP v COA	0.18 (0.16 , 0.20)
CP v ENV	0.08 (0.07 , 0.09)
CP v SENS	0.00 (0.00 , 0.01)
CP v DECOL	0.01 (0.01 , 0.02)
{COA, CP} v {ENV, CP}	0.25 (0.23 , 0.27)
{COA, CP} v {COA, ENV}	0.16 (0.14 , 0.17)
{COA, CP} v {CP, DECOL}	0.07 (0.06 , 0.08)
{COA, CP} v {CP, SENS}	0.04 (0.04 , 0.05)
{COA, ENV, CP} v {COA, CP, DECOL}	0.09 (0.07 , 0.10)
{COA, ENV, CP} v {COA, CP, SENS}	0.07 (0.06 , 0.08)
{COA, ENV, CP} v {ENV, CP, DECOL}	0.06 (0.05 , 0.07)
{COA, ENV, CP} v {ENV, CP, SENS}	0.04 (0.03 , 0.05)
{COA, ENV, CP, DECOL} v {COA, ENV, CP, SENS}	0.43 (0.41 , 0.46)
{COA, ENV, CP, DECOL} v {COA, ENV, SENS, DECOL}	0.01 (0.01 , 0.01)
{COA, ENV, CP, DECOL} v {COA, CP, SENS, DECOL}	0.04 (0.03 , 0.05)
{COA, ENV, CP, DECOL} v {ENV, CP, SENS, DECOL}	0.04 (0.04 , 0.06)
{COA, CP} v CP	0.02 (0.01 , 0.03)
{COA, ENV, CP} v {COA, CP}	0.04 (0.04 , 0.06)
{COA, ENV, CP, DECOL} v {COA, ENV, CP}	0.33 (0.30 , 0.35)
{COA, ENV, CP, SENS} v {COA, ENV, CP}	0.38 (0.35 , 0.40)
all v {COA, ENV, CP}	0.20 (0.18 , 0.22)
all v {COA, ENV, CP, DECOL}	0.35 (0.33 , 0.38)
all v {COA, ENV, CP, SENS}	0.28 (0.26 , 0.30)

Table F.3: θ estimates for AR comparisons of intervention combinations.

Comparison	AC $\hat{\theta}$ (95% CI)
COA v baseline	0.00 (0.00 , 0.00)
ENV v baseline	0.52 (0.50 , 0.55)
CP v baseline	0.54 (0.51 , 0.57)
SENS v baseline	0.57 (0.54 , 0.59)
DECOL v baseline	0.65 (0.63 , 0.68)
COA v ENV	0.00 (0.00 , 0.00)
COA v CP	0.00 (0.00 , 0.00)
COA v SENS	0.00 (0.00 , 0.00)
COA v DECOL	0.00 (0.00 , 0.00)
{COA, .} v {ENV, CP}	0.00 (0.00 , 0.00)
{COA, .} v {ENV, SENS}	0.00 (0.00 , 0.00)
{COA, .} v {CP, SENS}	0.00 (0.00 , 0.00)
{COA, .} v {ENV, DECOL}	0.00 (0.00 , 0.00)
{COA, .} v {CP, DECOL}	0.00 (0.00 , 0.00)
{COA, .} v {SENS, DECOL}	0.00 (0.00 , 0.00)
{COA, ., .} v {ENV, CP, SENS}	0.00 (0.00 , 0.00)
{COA, ., .} v {ENV, CP, DECOL}	0.00 (0.00 , 0.00)
{COA, ., .} v {CP, SENS, DECOL}	0.00 (0.00 , 0.00)
{COA, ., .} v {ENV, SENS, DECOL}	0.00 (0.00 , 0.00)
{COA, ., ., .} v {ENV, CP, SENS, DECOL}	0.00 (0.00 , 0.00)

Table F.4: θ estimates for AC comparisons of intervention combinations.

Comparison	$C_{xd} \hat{\theta}$ (95% CI)
COA v baseline	0.33 (0.31 , 0.35)
ENV v baseline	0.30 (0.28 , 0.32)
CP v baseline	0.17 (0.15 , 0.19)
SENS v baseline	0.43 (0.41 , 0.46)
DECOL v baseline	0.45 (0.43 , 0.48)
CP v COA	0.30 (0.28 , 0.32)
CP v ENV	0.33 (0.31 , 0.35)
CP v SENS	0.20 (0.19 , 0.23)
CP v DECOL	0.20 (0.18 , 0.22)
{COA, CP} v {ENV, CP}	0.50 (0.47 , 0.52)
{COA, CP} v {CP, SENS}	0.37 (0.35 , 0.39)
{COA, CP} v {COA, ENV}	0.37 (0.35 , 0.40)
{COA, CP} v {CP, DECOL}	0.35 (0.32 , 0.37)
{COA, CP} v {ENV, SENS}	0.21 (0.20 , 0.24)
{COA, CP} v {ENV, DECOL}	0.22 (0.20 , 0.24)
{COA, CP} v {COA, SENS}	0.20 (0.18 , 0.22)
{COA, CP} v {COA, DECOL}	0.19 (0.17 , 0.21)
{COA, CP} v {SENS, DECOL}	0.12 (0.10 , 0.13)
{COA, ENV, CP} v {ENV, CP, SENS}	0.35 (0.32 , 0.37)
{COA, ENV, CP} v {ENV, CP, DECOL}	0.34 (0.32 , 0.36)
{COA, ENV, CP} v {COA, CP, DECOL}	0.32 (0.30 , 0.35)
{COA, ENV, CP} v {COA, CP, SENS}	0.32 (0.29 , 0.34)
{COA, ENV, CP} v {COA, ENV, SENS}	0.25 (0.23 , 0.27)
{COA, ENV, CP} v {COA, ENV, DECOL}	0.24 (0.22 , 0.26)
{COA, ENV, CP} v {CP, SENS, DECOL}	0.23 (0.21 , 0.25)
{COA, ENV, CP} v {ENV, SENS, DECOL}	0.15 (0.13 , 0.17)
{COA, ENV, CP} v {COA, SENS, DECOL}	0.11 (0.09 , 0.12)
{COA, ENV, CP, DECOL} v {COA, ENV, CP, SENS}	0.48 (0.46 , 0.51)
{COA, ENV, CP, DECOL} v {ENV, CP, SENS, DECOL}	0.36 (0.34 , 0.38)
{COA, ENV, CP, DECOL} v {COA, CP, SENS, DECOL}	0.30 (0.28 , 0.33)
{COA, ENV, CP, DECOL} v {COA, ENV, SENS, DECOL}	0.23 (0.21 , 0.25)
{COA, ENV, CP, SENS} v {ENV, CP, SENS, DECOL}	0.38 (0.36 , 0.40)
{COA, ENV, CP, SENS} v {COA, CP, SENS, DECOL}	0.32 (0.30 , 0.35)
{COA, ENV, CP, SENS} v {COA, ENV, SENS, DECOL}	0.24 (0.22 , 0.26)
{COA, CP} v CP	0.32 (0.30 , 0.35)
{ENV, CP} v CP	0.33 (0.30 , 0.35)
{COA, ENV, CP} v {COA, CP}	0.30 (0.28 , 0.33)
{COA, ENV, CP} v {ENV, CP}	0.31 (0.29 , 0.33)
{COA, ENV, CP, DECOL} v {COA, ENV, CP}	0.46 (0.44 , 0.49)
{COA, ENV, CP, SENS} v {COA, ENV, CP}	0.48 (0.46 , 0.51)
all v {COA, ENV, CP}	0.45 (0.42 , 0.47)
all v {COA, ENV, CP, DECOL}	0.49 (0.46 , 0.51)
all v {COA, ENV, CP, SENS}	0.47 (0.44 , 0.49)

Table F.5: θ estimates for C_{xd} comparisons of intervention combinations.

Comparison	$C_d \hat{\theta}$ (95% CI)
COA v baseline	0.01 (0.00 , 0.01)
ENV v baseline	0.35 (0.32 , 0.37)
CP v baseline	0.24 (0.22 , 0.26)
SENS v baseline	0.53 (0.51 , 0.56)
DECOL v baseline	0.56 (0.53 , 0.58)
COA v CP	0.02 (0.02 , 0.03)
COA v ENV	0.01 (0.01 , 0.02)
COA v SENS	0.00 (0.00 , 0.01)
COA v DECOL	0.00 (0.00 , 0.01)
{COA, CP} v {COA, ENV}	0.38 (0.35 , 0.40)
{COA, CP} v {COA, DECOL}	0.19 (0.17 , 0.21)
{COA, CP} v {COA, SENS}	0.18 (0.16 , 0.20)
{COA, CP} v {ENV, CP}	0.00 (0.00 , 0.01)
{COA, ENV, CP} v {COA, CP, DECOL}	0.33 (0.30 , 0.35)
{COA, ENV, CP} v {COA, CP, SENS}	0.30 (0.28 , 0.32)
{COA, ENV, CP} v {COA, ENV, DECOL}	0.24 (0.22 , 0.26)
{COA, ENV, CP} v {COA, ENV, SENS}	0.24 (0.22 , 0.26)
{COA, ENV, CP} v {COA, SENS, DECOL}	0.10 (0.08 , 0.11)
{COA, ENV, CP, DECOL} v {COA, ENV, CP, SENS}	0.46 (0.43 , 0.48)
{COA, ENV, CP, DECOL} v {COA, CP, SENS, DECOL}	0.29 (0.26 , 0.31)
{COA, ENV, CP, DECOL} v {COA, ENV, SENS, DECOL}	0.21 (0.19 , 0.23)
{COA, ENV, CP, DECOL} v {ENV, CP, SENS, DECOL}	0.00 (0.00 , 0.00)
{COA, ENV, CP, SENS} v {COA, CP, SENS, DECOL}	0.32 (0.30 , 0.35)
{COA, ENV, CP, SENS} v {COA, ENV, SENS, DECOL}	0.24 (0.22 , 0.26)
{COA, ENV, CP, SENS} v {ENV, CP, SENS, DECOL}	0.00 (0.00 , 0.00)
{COA, CP} v COA	0.17 (0.15 , 0.19)
{COA, ENV, CP} v {COA, CP}	0.31 (0.28 , 0.33)
{COA, ENV, CP, DECOL} v {COA, ENV, CP}	0.46 (0.44 , 0.49)
{COA, ENV, CP, SENS} v {COA, ENV, CP}	0.50 (0.48 , 0.53)
all v {COA, ENV, CP}	0.47 (0.44 , 0.49)
all v {COA, ENV, CP, DECOL}	0.51 (0.48 , 0.53)
all v {COA, ENV, CP, SENS}	0.47 (0.44 , 0.49)

Table F.6: θ estimates for C_d comparisons of intervention combinations.

Comparison	$I_{xd} \hat{\theta}$ (95% CI)
COA v baseline	0.39 (0.37 , 0.42)
ENV v baseline	0.48 (0.45 , 0.50)
CP v baseline	0.47 (0.44 , 0.49)
SENS v baseline	0.28 (0.26 , 0.30)
DECOL v baseline	0.51 (0.48 , 0.53)
SENS v COA	0.38 (0.36 , 0.40)
SENS v CP	0.31 (0.29 , 0.33)
SENS v ENV	0.30 (0.28 , 0.33)
SENS v DECOL	0.28 (0.25 , 0.30)
COA v CP	0.42 (0.40 , 0.45)
COA v ENV	0.42 (0.39 , 0.44)
COA v DECOL	0.39 (0.36 , 0.41)
{SENS, .} v {COA, CP}	0.42 (0.40 , 0.45)
{SENS, .} v {COA, ENV}	0.40 (0.37 , 0.42)
{SENS, .} v {COA, DECOL}	0.39 (0.36 , 0.41)
{SENS, .} v {ENV, CP}	0.31 (0.29 , 0.33)
{SENS, .} v {ENV, DECOL}	0.28 (0.26 , 0.31)
{SENS, .} v {CP, DECOL}	0.28 (0.26 , 0.31)
{SENS, ., .} v {COA, ENV, CP}	0.43 (0.40 , 0.45)
{SENS, ., .} v {COA, CP, DECOL}	0.41 (0.39 , 0.44)
{SENS, ., .} v {COA, ENV, DECOL}	0.41 (0.39 , 0.44)
{SENS, ., .} v {ENV, CP, DECOL}	0.31 (0.29 , 0.33)
{SENS, ., ., .} v {COA, ENV, CP, DECOL}	0.43 (0.41 , 0.46)
{SENS, .} v SENS	0.50 (0.47 , 0.53)
{SENS, ., .} v SENS	0.50 (0.47 , 0.53)
{SENS, ., ., .} v SENS	0.50 (0.47 , 0.53)
all v SENS	0.50 (0.47 , 0.53)

Table F.7: θ estimates for I_{xd} comparisons of intervention combinations.

Comparison	$I_d \hat{\theta}$ (95% CI)
COA v baseline	0.40 (0.37 , 0.42)
ENV v baseline	0.48 (0.45 , 0.50)
CP v baseline	0.47 (0.44 , 0.49)
SENS v baseline	0.28 (0.26 , 0.30)
DECOL v baseline	0.51 (0.48 , 0.53)
SENS v COA	0.38 (0.36 , 0.40)
SENS v CP	0.31 (0.29 , 0.33)
SENS v ENV	0.30 (0.28 , 0.33)
SENS v DECOL	0.28 (0.26 , 0.30)
COA v CP	0.42 (0.40 , 0.45)
COA v ENV	0.42 (0.39 , 0.44)
COA v DECOL	0.39 (0.36 , 0.41)
{SENS, .} v {COA, CP}	0.42 (0.40 , 0.45)
{SENS, .} v {COA, ENV}	0.40 (0.37 , 0.42)
{SENS, .} v {COA, DECOL}	0.39 (0.36 , 0.41)
{SENS, .} v {ENV, CP}	0.31 (0.29 , 0.33)
{SENS, .} v {ENV, DECOL}	0.28 (0.26 , 0.31)
{SENS, .} v {CP, DECOL}	0.28 (0.26 , 0.31)
{SENS, ., .} v {COA, ENV, CP}	0.43 (0.40 , 0.45)
{SENS, ., .} v {COA, CP, DECOL}	0.41 (0.39 , 0.44)
{SENS, ., .} v {COA, ENV, DECOL}	0.41 (0.39 , 0.44)
{SENS, ., .} v {ENV, CP, DECOL}	0.31 (0.29 , 0.33)
{SENS, ., ., .} v {COA, ENV, CP, DECOL}	0.44 (0.41 , 0.46)
{SENS, .} v SENS	0.50 (0.47 , 0.53)
{SENS, ., .} v SENS	0.50 (0.47 , 0.53)
{SENS, ., ., .} v SENS	0.50 (0.47 , 0.53)
all v SENS	0.50 (0.47 , 0.53)

Table F.8: θ estimates for I_d comparisons of intervention combinations.

F.5 Additional results for high burden setting

Supplementary Figures F.23, F.24, F.25, F.26, F.27 and F.28 have the same x-axis label ordering as the corresponding plots in the normal burden setting (see Section F.4).

F.5.1 AR outcome

For the AR outcome measure in the high burden setting, all single interventions produced a reduced AR distribution compared with the baseline. The CP intervention performed the best out of all five single interventions, followed by the SENS intervention. The COA and ENV interventions performed similarly and the DECOL intervention produced the smallest reduction in the AR outcome (with $\hat{\theta} = 0.33(0.30, 0.35)$ when compared with baseline). The best performing single intervention (CP) also substantially outperform the four other single interventions with $\hat{\theta}$ ranging from 0.01 (for DECOL) to 0.16 (for SENS).

The best performing intervention pair for the AR outcome was {CP, SENS} outperforming the second best intervention pair ({COA, CP}) with $\hat{\theta}$ of 0.29(0.27, 0.32) and greatly outperforming the other intervention pairs (with the θ estimates for the next five best pairs provided in Table F.10).

The {COA, CP, SENS} intervention triplet produced the smallest average AR mean (7.88×10^{-3}) out of all intervention triplets. However there is little evidence of a distributional difference in the AR outcome when compared with the second best performing intervention triplet ({ENV, CP, SENS}) an estimated θ of 0.45(0.43, 0.48). There is a slight improvement when comparing the {COA, CP, SENS} triplet with the triplets with the third and fourth smallest AR mean ({CP, SENS, DECOL} with $\hat{\theta} = 0.26(0.24, 0.28)$ and {COA, ENV, CP} with $\hat{\theta} = 0.35(0.33, 0.38)$). The wider 95% interval for the AR outcome associated with {COA, ENV, CP} produced a distribution that was more similar (i.e. larger $\hat{\theta}$) to the {COA, CP, SENS} triplet compared with the {CP, SENS, DECOL} triplet. The comparisons between the {ENV, CP, SENS} triplet with the other triplets with a larger AR mean was similar to those for {COA, CP, SENS} albeit with slightly larger θ estimates.

The best performing quartet for the AR outcome was {COA, ENV, CP, SENS} which produced a substantially smaller AR outcome distribution compared with the other four intervention quartets tested (with $\hat{\theta}$ values between 0.02 and 0.20).

There were substantial reductions in the AR outcome distribution when moving from the best performing single intervention to the best performing intervention pair ($\hat{\theta} = 0.01(0.01, 0.02)$), from the best pair to either of the best performing triplets ($\hat{\theta}$ of either 0.03(0.02, 0.04) or 0.04(0.04, 0.05)), and from either of the best performing triplets to the best performing quartet ($\hat{\theta}$ of 0.03(0.02, 0.04) in both comparisons). The reduction in the AR distribution when moving from the best performing quartet to all

intervention was also significant but not as drastic as the other increases in intervention sizes ($\hat{\theta} = 0.16(0.15, 0.18)$).

F.5.2 AC outcome

As with the normal setting, the COA intervention was the most important intervention for the AC outcome as it eliminates the possibility of colonised patients being admitted. Any intervention combination which include the COA intervention achieved 0 AC, whereas intervention combinations without the COA intervention produced AC distributions with 95% quantiles that do not include 0 (Figure F.24). This was also reflected in the θ estimates for the comparison of interventions combinations with the COA intervention against those without (Table F.11).

F.5.3 C_{xd} outcome

Comparison	$C_{xd} \hat{\theta}$ (95% CI)
COA v baseline	0.45 (0.42 , 0.47)
ENV v baseline	0.32 (0.30 , 0.35)
CP v baseline	0.09 (0.08 , 0.10)
SENS v baseline	0.43 (0.40 , 0.45)
DECOL v baseline	0.58 (0.56 , 0.61)
CP v ENV	0.18 (0.17 , 0.20)
CP v SENS	0.12 (0.11 , 0.14)
CP v COA	0.12 (0.10 , 0.13)
CP v DECOL	0.07 (0.06 , 0.08)
{ENV, CP} v {CP, SENS}	0.44 (0.41 , 0.46)
{ENV, CP} v {COA, CP}	0.40 (0.38 , 0.43)
{ENV, CP} v {CP, DECOL}	0.30 (0.27 , 0.32)
{ENV, CP} v {ENV, SENS}	0.17 (0.15 , 0.19)
{ENV, CP} v {COA, ENV}	0.16 (0.14 , 0.17)
{ENV, CP} v {COA, SENS}	0.12 (0.10 , 0.13)
{ENV, CP} v {ENV, DECOL}	0.07 (0.06 , 0.08)
{ENV, CP} v {SENS, DECOL}	0.06 (0.05 , 0.07)
{ENV, CP} v {COA, DECOL}	0.05 (0.04 , 0.06)
{ENV, CP, SENS} v {COA, ENV, CP}	0.48 (0.45 , 0.50)
{ENV, CP, SENS} v {COA, CP, SENS}	0.40 (0.38 , 0.43)
{ENV, CP, SENS} v {ENV, CP, DECOL}	0.32 (0.30 , 0.35)
{ENV, CP, SENS} v {CP, SENS, DECOL}	0.32 (0.29 , 0.34)
{ENV, CP, SENS} v {COA, CP, DECOL}	0.27 (0.25 , 0.29)
{ENV, CP, SENS} v {COA, ENV, SENS}	0.22 (0.20 , 0.24)
{ENV, CP, SENS} v {ENV, SENS, DECOL}	0.13 (0.11 , 0.15)
{ENV, CP, SENS} v {COA, ENV, DECOL}	0.09 (0.08 , 0.10)

Continued on next page

Table F.12 – *Continued from previous page*

Comparison	$C_{xd} \hat{\theta}$ (95% CI)
{ENV, CP, SENS} v {COA, SENS, DECOL}	0.09 (0.08 , 0.11)
{COA, ENV, CP, SENS} v {ENV, CP, SENS, DECOL}	0.39 (0.37 , 0.42)
{COA, ENV, CP, SENS} v {COA, ENV, CP, DECOL}	0.36 (0.34 , 0.39)
{COA, ENV, CP, SENS} v {COA, CP, SENS, DECOL}	0.31 (0.29 , 0.33)
{COA, ENV, CP, SENS} v {COA, ENV, SENS, DECOL}	0.18 (0.16 , 0.20)
{ENV, CP} v CP	0.33 (0.31 , 0.36)
{CP, SENS} v CP	0.39 (0.37 , 0.42)
{COA, CP} v CP	0.43 (0.40 , 0.45)
{ENV, CP, SENS} v CP	0.19 (0.18 , 0.21)
{COA, ENV, CP} v CP	0.22 (0.20 , 0.24)
{COA, CP, SENS} v CP	0.27 (0.25 , 0.30)
{ENV, CP, SENS} v {ENV, CP}	0.33 (0.31 , 0.36)
{COA, ENV, CP} v {ENV, CP}	0.36 (0.34 , 0.38)
{COA, CP, SENS} v {ENV, CP}	0.43 (0.40 , 0.45)
{ENV, CP, SENS} v {CP, SENS}	0.27 (0.25 , 0.30)
{COA, ENV, CP} v {CP, SENS}	0.30 (0.28 , 0.33)
{COA, CP, SENS} v {CP, SENS}	0.37 (0.34 , 0.39)
{ENV, CP, SENS} v {COA, CP}	0.25 (0.23 , 0.27)
{COA, ENV, CP} v {COA, CP}	0.28 (0.26 , 0.30)
{COA, CP, SENS} v {COA, CP}	0.34 (0.32 , 0.36)
{COA, ENV, CP, SENS} v {ENV, CP}	0.19 (0.17 , 0.21)
{COA, ENV, CP, SENS} v {CP, SENS}	0.15 (0.13 , 0.17)
{COA, ENV, CP, SENS} v {COA, CP}	0.14 (0.12 , 0.16)
{COA, ENV, CP, SENS} v {ENV, CP, SENS}	0.33 (0.30 , 0.35)
{COA, ENV, CP, SENS} v {COA, ENV, CP}	0.32 (0.29 , 0.34)
{COA, ENV, CP, SENS} v {COA, CP, SENS}	0.25 (0.23 , 0.27)
all v {ENV, CP}	0.13 (0.12 , 0.15)
all v {CP, SENS}	0.10 (0.09 , 0.12)
all v {COA, CP}	0.10 (0.08 , 0.11)
all v {ENV, CP, SENS}	0.25 (0.23 , 0.27)
all v {COA, ENV, CP}	0.24 (0.22 , 0.26)
all v {COA, CP, SENS}	0.18 (0.16 , 0.20)
all v {COA, ENV, CP, SENS}	0.42 (0.39 , 0.44)

Table F.12: θ estimates for C_{xd} comparisons of intervention combinations for high burden setting .

In the high burden setting, only the CP and ENV interventions singly produced C_{xd} outcome distributions which were smaller than the baseline scenario ($\hat{\theta}$ of

0.09(0.08, 0.10) for CP and 0.32(0.30, 0.35) for ENV). The other three interventions produced distributions which were similar to the baseline. The CP intervention also notably outperformed all other single interventions ($\hat{\theta}$ between 0.07 to 0.18).

The best performing intervention pair for this outcome is the {ENV, CP} pair. However, the {CP, SENS} and {COA, CP} intervention pairs have similar C_{xd} distributions as the {ENV, CP} pair (with $\hat{\theta}$ of 0.44(0.41, 0.46) and 0.40(0.38, 0.43) respectively). In short, the best performing duos comprise of the CP intervention with either the ENV, SENS or COA intervention.

Following the similarity of the top three intervention duos, the best performing triplet was found to be {ENV, CP, SENS} followed by the triplets {COA, ENV, CP} and {COA, CP, SENS}. All three interventions had similar distributions. Again, we note that these triplet combinations are of CP with two of the three interventions which formed the top three best performing pairs (ENV, SENS or COA).

The intervention quartet which produced the smallest C_{xd} outcome distribution was the combination of the four interventions previously identified, namely {COA, ENV, CP, SENS}. There was only slight evidence that this intervention quartet performed better than the next three best performing quartets ({ENV, CP, SENS, DECOL}, {COA, ENV, CP, DECOL} and {COA, CP, SENS, DECOL} with $\hat{\theta}$ ranging between 0.31 to 0.39. However, the {COA, ENV, CP, SENS} quartet performed noticeably better when compared with the remaining quartet under consideration ({COA, ENV, SENS, DECOL} with $\hat{\theta} = 0.18(0.16, 0.20)$).

Comparing the top three intervention pairs with the best performing single intervention, there are slight gains, in terms of C_{xd} distribution reduction, in considering the {ENV, CP} or {CP, SENS} pairs rather than just CP singly ($\hat{\theta}$ of 0.33(0.30, 0.35) and 0.39(0.36, 0.41) respectively). The improvement in moving from CP to {COA, CP} was less noticeable ($\hat{\theta} = 0.43(0.41, 0.46)$).

Notable improvements were observed when moving from the CP intervention singly to the top three performing triplets ({ENV, CP, SENS}, {COA, CP, SENS}, {COA, CP, SENS}) with θ estimates of between 0.19 to 0.27. However, the benefits from moving from one of the three intervention pairs identified to one of the three intervention triplets were less evident. There appears to be little gained in moving from the best performing pair ({ENV, CP}) to any of the triplets, particularly for {COA, CP, SENS} with $\hat{\theta} = 0.43(0.40, 0.45)$ (the other two triplets have $\hat{\theta}$ of 0.33(0.31, 0.36) and 0.36(0.34, 0.38)). Improved performance was noted when moving from either of the other two pairs ({CP, SENS} or {COA, CP}) to either {ENV, CP, SENS} or {COA, ENV, CP} ($\hat{\theta}$ ranging from 0.25 to 0.30) but less so for a move to the {COA, CP, SENS} triplet (with $\hat{\theta}$ of 0.37(0.34, 0.39) and 0.34(0.32, 0.36) respectively).

The best performing quartet outperforms the top three intervention pairs with $\hat{\theta}$ ranging from 0.14 to 0.19. Gains from moving from one of the three triplets identified to the best performing quartet were marginal with the best improvement obtained when moving from $\{\text{COA}, \text{CP}, \text{SENS}\}$ ($\hat{\theta} = 0.25(0.23, 0.27)$) and the least from $\{\text{ENV}, \text{CP}, \text{SENS}\}$ with $\hat{\theta} = 0.33(0.30, 0.35)$.

The combination of all interventions performed better than all three interventions pairs ($\hat{\theta}$ ranging from 0.10 to 0.13) and the $\{\text{COA}, \text{CP}, \text{SENS}\}$ triplet ($\hat{\theta} = 0.18(0.16, 0.20)$). It also outperformed the other two triplets ($\hat{\theta}$ of 0.2(0.23, 0.27) for $\{\text{ENV}, \text{CP}, \text{SENS}\}$ and 0.24(0.22, 0.26) for $\{\text{COA}, \text{ENV}, \text{CP}\}$) but not the best performing quartet (with $\hat{\theta} = 0.42(0.39, 0.44)$).

F.5.4 C_d outcome

Of the five single interventions, only the COA and CP interventions produced C_d distributions smaller than the baseline. In fact, both these single interventions performed similarly to one another (with $\hat{\theta} = 0.45(0.42, 0.47)$), and outperforms the other three single interventions.

The best performing intervention pair was $\{\text{COA}, \text{CP}\}$, outperforming the other nine intervention pairs with the closest competitor being $\{\text{COA}, \text{ENV}\}$ with $\hat{\theta} = 0.23(0.21, 0.25)$. The other pair comparisons with $\{\text{COA}, \text{CP}\}$ resulted in θ estimates of between 0.00 to 0.13.

The $\{\text{COA}, \text{ENV}, \text{CP}\}$ triplet produced the smallest C_d distribution of the intervention triplets, and was marginally better than the next two best performing triplets ($\{\text{COA}, \text{CP}, \text{SENS}\}$ with $\hat{\theta}$ of 0.30(0.28, 0.33) and $\{\text{COA}, \text{CP}, \text{DECOL}\}$ with $\hat{\theta}$ of 0.30 (0.27, 0.32)). The $\{\text{COA}, \text{ENV}, \text{CP}\}$ triplet performed more favourably when compared with the remaining triplets, yielding θ estimates between 0.00 and 0.16.

The two best performing quartets for the C_d outcome measure were $\{\text{COA}, \text{ENV}, \text{CP}, \text{SENS}\}$ and $\{\text{COA}, \text{ENV}, \text{CP}, \text{DECOL}\}$ ($\hat{\theta} = 0.47(0.45, 0.50)$), followed closely by $\{\text{COA}, \text{CP}, \text{SENS}, \text{DECOL}\}$ ($\hat{\theta}$ of 0.31(0.29, 0.33) for comparison with $\{\text{COA}, \text{ENV}, \text{CP}, \text{SENS}\}$ and 0.33(0.31, 0.36) for comparison with $\{\text{COA}, \text{ENV}, \text{CP}, \text{DECOL}\}$). The other two quartets were less effective than $\{\text{COA}, \text{ENV}, \text{CP}, \text{SENS}\}$ and $\{\text{COA}, \text{ENV}, \text{CP}, \text{DECOL}\}$ in reducing the C_d outcome ($\hat{\theta}$ ranging from 0.02 to 0.21).

Comparing across intervention sizes, the $\{\text{COA}, \text{CP}\}$ intervention pair was a drastic improvement from the COA intervention singly in terms of reduction in C_d distribution (with $\hat{\theta}$ of 0.08(0.07, 0.10)). The best performing triplet provided a slight improvement compared with the $\{\text{COA}, \text{CP}\}$ pair ($\hat{\theta} = 0.28(0.26, 0.30)$). The two best performing intervention quartets identified did not yield C_d distributions substantially different from that of the $\{\text{COA}, \text{ENV}, \text{CP}\}$ triplets ($\hat{\theta}$ values of 0.41(0.39, 0.44) and

0.49(0.46, 0.51)). These two quartets were still improvements over the best performing pair, but their comparative performance (with the pair) was similar to that of the best performing triplet (θ estimates of 0.21 and 0.27). While the combination of all five interventions provided a notable reduction in the C_d distribution from the best performing pair ($\hat{\theta} = 0.16(0.15, 0.18)$), it only performed marginally better than the {COA, ENV, CP} triplet and the {COA, ENV, CP, DECOL} quartet ($\hat{\theta}$ of 0.36(0.33, 0.38) and 0.37(0.35, 0.40) respectively) and offered a similar reduction in the C_d distribution as the {COA, ENV, CP, SENS} quartet $\hat{\theta} = 0.44(0.42, 0.47)$).

F.5.5 I_{xd} outcome

As with the normal burden setting, the SENS intervention was the most important intervention for the I_{xd} (and I_d) outcome(s) as having perfect sensitivity would allow detection of all colonised patients prior to infection developing. As such, the best performing intervention of any size will include the SENS intervention and are denoted by {SENS, .}, {SENS, ., .} and {SENS, ., ., .} to denote intervention pairs, triplets and quartets.

In contrast with the normal burden setting where the SENS intervention (of any size) only performed marginally better than the other intervention combinations despite completely removing any occurrence of I_{xd} patients as a result of the low baseline I_{xd} population, the SENS intervention (or any combination which includes the SENS intervention) was substantially more favourable in the high burden setting (Figure F.27). The SENS intervention substantially outperformed all intervention combinations which excluded the SENS intervention here (Table F.14).

F.5.6 I_d outcome

As with the I_{xd} outcome, the SENS intervention (or any intervention combination which included SENS) eradicated the I_d population and provided a drastic improvement from any intervention combinations which excluded the SENS intervention in the high burden setting (see Figure F.28 and Table F.15).

Outcome	Ranking
AR	CP, SENS, COA, ENV, DECOL
	{CP, SENS}, {COA, CP}, {ENV, CP}, {CP, DECOL}, {COA, SENS}, {ENV, SENS}, {SENS, DECOL}, {COA, ENV}, {COA, DECOL}, {ENV, DECOL}
	{COA, CP, SENS}, {ENV, CP, SENS}, {CP, SENS, DECOL}, {COA, ENV, CP}, {COA, CP, DECOL}, {COA, ENV, SENS}, {ENV, CP, DECOL}, {ENV, SENS, DECOL}, {COA, SENS, DECOL}, {COA, ENV, DECOL}
	{COA, ENV, CP, SENS}, {ENV, CP, SENS, DECOL}, {COA, CP, SENS, DECOL}, {COA, ENV, CP, DECOL}, {COA, ENV, SENS, DECOL}
AC	COA, ENV, CP, DECOL, SENS
	{COA, ENV}, {COA, CP}, {COA, SENS}, {COA, DECOL}, {ENV, CP}, {ENV, DECOL}, {CP, DECOL}, {ENV, SENS}, {CP, SENS}, {SENS, DECOL}
	{COA, ENV, CP}, {COA, ENV, SENS}, {COA, ENV, DECOL}, {COA, CP, SENS}, {COA, CP, DECOL}, {COA, SENS, DECOL}, {ENV, CP, DECOL}, {ENV, CP, SENS}, {CP, SENS, DECOL}, {ENV, SENS, DECOL}
	{COA, ENV, CP, SENS}, {COA, ENV, CP, DECOL}, {COA, ENV, SENS, DECOL}, {COA, CP, SENS, DECOL}, {ENV, CP, SENS, DECOL}
C_{xd}	CP, ENV, SENS, COA, DECOL
	{ENV, CP}, {CP, SENS}, {COA, CP}, {CP, DECOL}, {ENV, SENS}, {COA, ENV}, {COA, SENS}, {ENV, DECOL}, {SENS, DECOL}, {COA, DECOL}
	{ENV, CP, SENS}, {COA, ENV, CP}, {COA, CP, SENS}, {ENV, CP, DECOL}, {CP, SENS, DECOL}, {COA, CP, DECOL}, {COA, ENV, SENS}, {ENV, SENS, DECOL}, {COA, ENV, DECOL}, {COA, SENS, DECOL}
	{COA, ENV, CP, SENS}, {ENV, CP, SENS, DECOL}, {COA, ENV, CP, DECOL}, {COA, CP, SENS, DECOL}, {COA, ENV, SENS, DECOL}
C_d	COA, CP, ENV, DECOL, SENS
	{COA, CP}, {COA, ENV}, {ENV, CP}, {COA, SENS}, {COA, DECOL}, {CP, DECOL}, {CP, SENS}, {ENV, DECOL}, {ENV, SENS}, {SENS, DECOL}
	{COA, ENV, CP}, {COA, CP, SENS}, {COA, CP, DECOL}, {COA, ENV, SENS}, {COA, ENV, DECOL}, {COA, SENS, DECOL}, {ENV, CP, DECOL}, {ENV, CP, SENS}, {CP, SENS, DECOL}, {ENV, SENS, DECOL}
	{COA, ENV, CP, SENS}, {COA, ENV, CP, DECOL}, {COA, CP, SENS, DECOL}, {COA, ENV, SENS, DECOL}, {ENV, CP, SENS, DECOL}
I_{xd}	SENS, COA, CP, ENV, DECOL
	{COA, SENS}, {ENV, SENS}, {CP, SENS}, {SENS, DECOL}, {COA, CP}, {COA, ENV}, {ENV, CP}, {COA, DECOL}, {CP, DECOL}, {ENV, DECOL}
	{COA, ENV, SENS}, {COA, CP, SENS}, {COA, SENS, DECOL}, {ENV, CP, SENS}, {ENV, SENS, DECOL}, {CP, SENS, DECOL}, {COA, ENV, CP}, {COA, CP, DECOL}, {COA, ENV, DECOL}, {ENV, CP, DECOL}
	{COA, ENV, CP, SENS}, {COA, ENV, SENS, DECOL}, {COA, CP, SENS, DECOL}, {ENV, CP, SENS, DECOL}, {COA, ENV, CP, DECOL}
I_d	SENS, COA, CP, ENV, DECOL
	{COA, SENS}, {ENV, SENS}, {CP, SENS}, {SENS, DECOL}, {COA, CP}, {COA, ENV}, {ENV, CP}, {COA, DECOL}, {CP, DECOL}, {ENV, DECOL}
	{COA, ENV, SENS}, {COA, CP, SENS}, {COA, SENS, DECOL}, {ENV, CP, SENS}, {ENV, SENS, DECOL}, {CP, SENS, DECOL}, {COA, ENV, CP}, {COA, CP, DECOL}, {COA, ENV, DECOL}, {ENV, CP, DECOL}
	{COA, ENV, CP, SENS}, {COA, ENV, SENS, DECOL}, {COA, CP, SENS, DECOL}, {ENV, CP, SENS, DECOL}, {COA, ENV, CP, DECOL}

Table F.9: Ranking of the various intervention combinations by the output measure means and intervention sizes for the high burden setting.

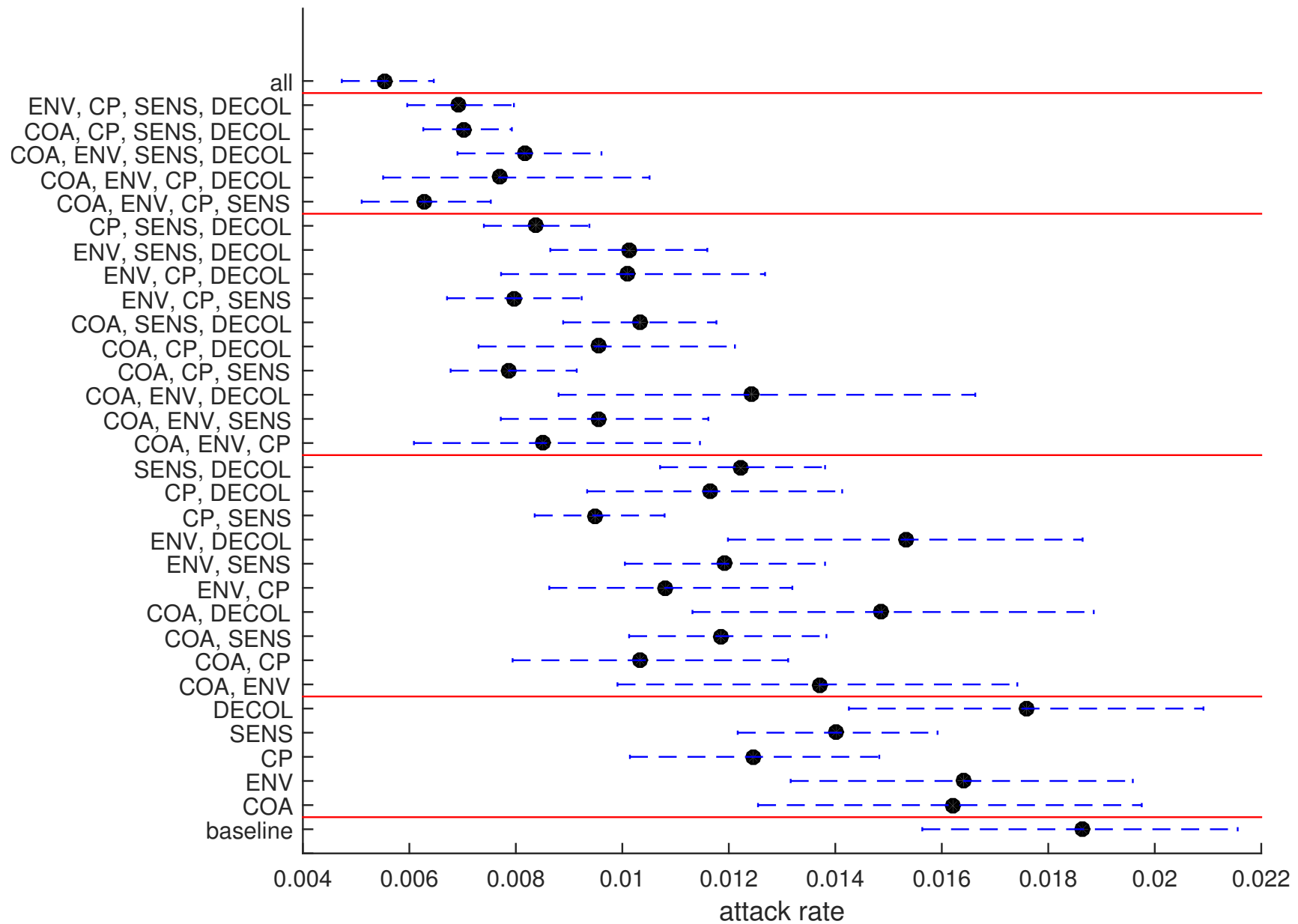


Figure F.23: Attack rate average and 95% intervals in the simulated ward for the high burden setting.

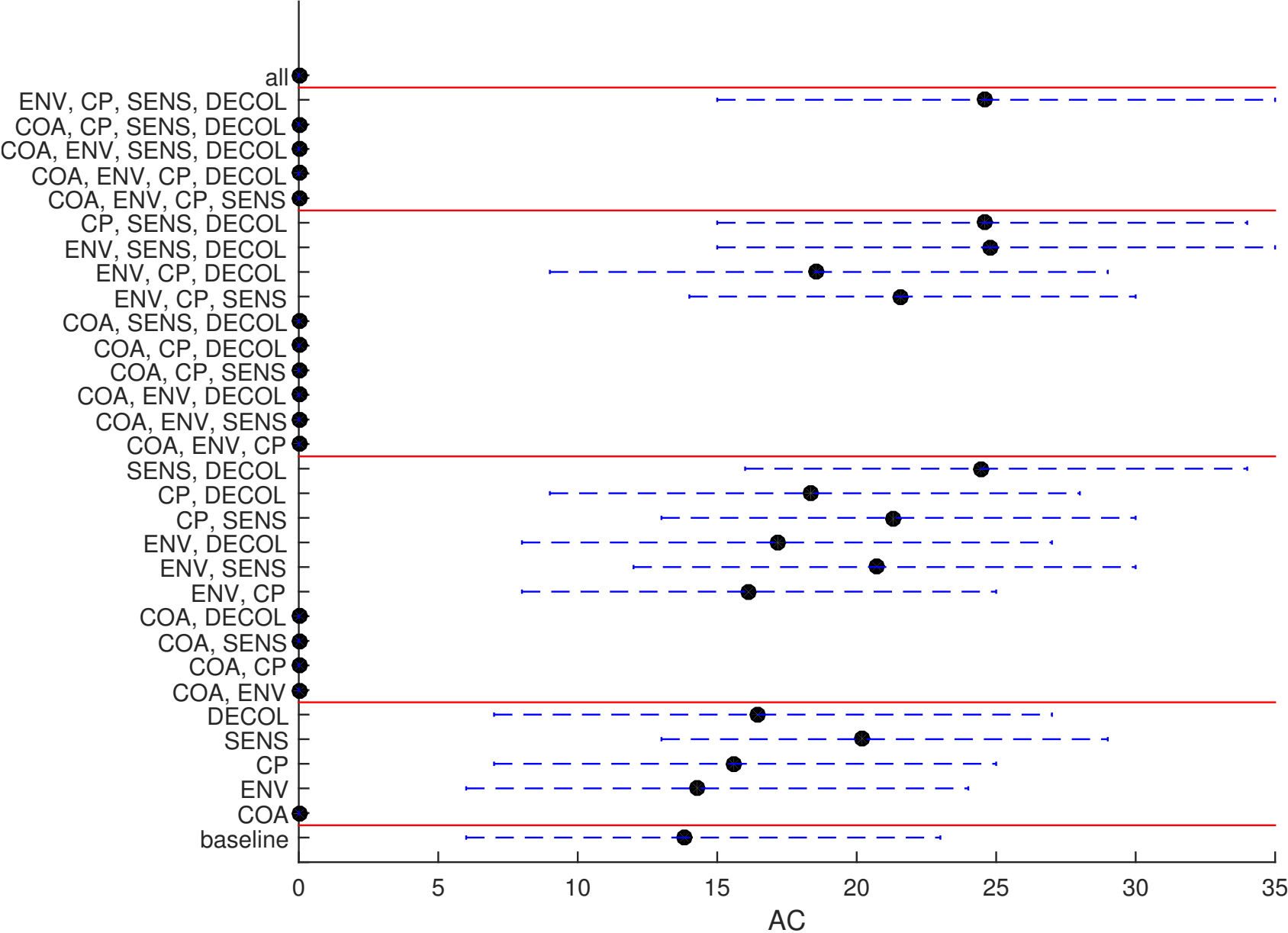


Figure F.24: AC average and 95% intervals in the simulated ward for the high burden setting.

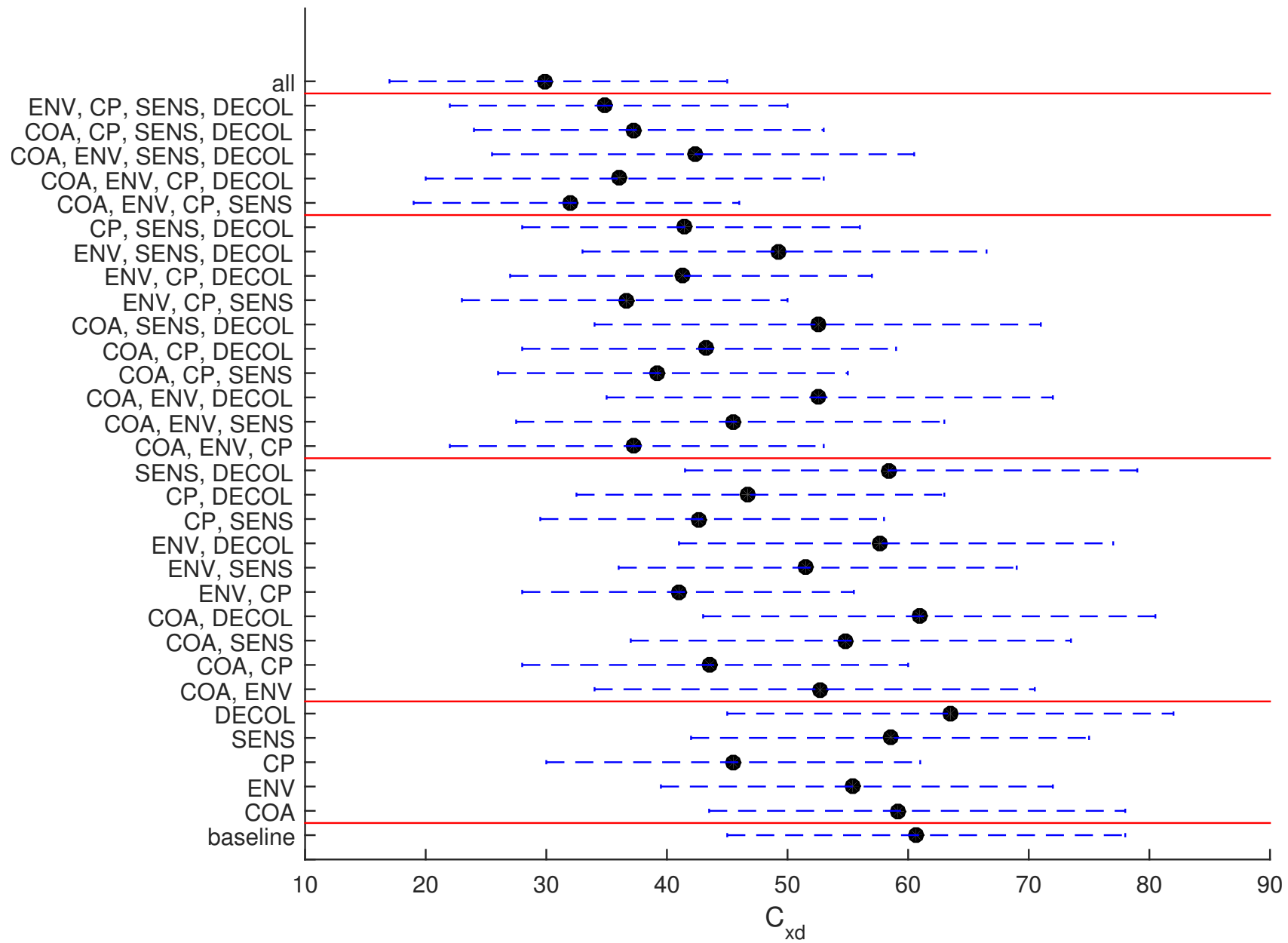


Figure F.25: C_{xd} average and 95% intervals in the simulated ward for the high burden setting.

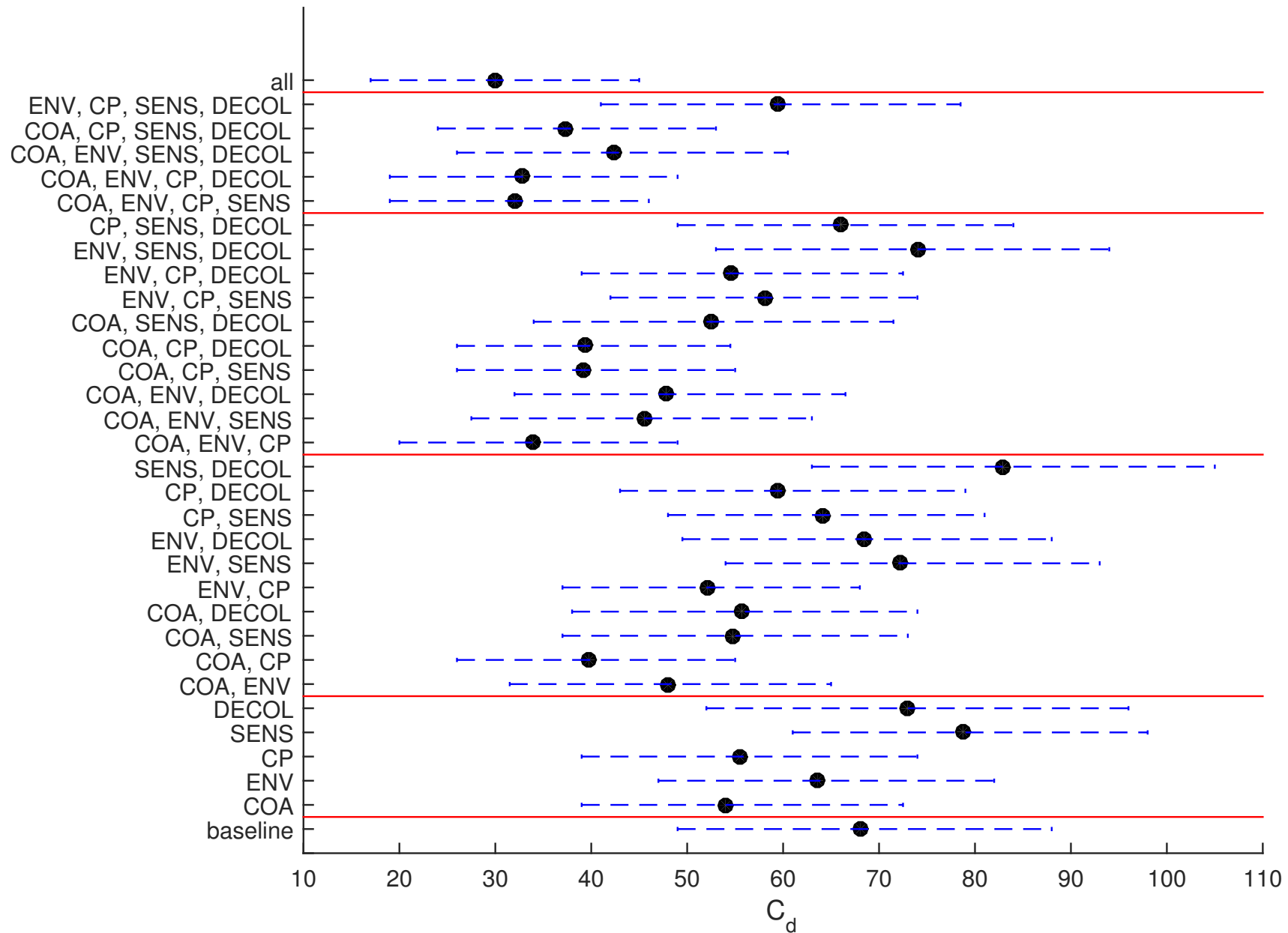


Figure F.26: C_d average and 95% intervals in the simulated ward for the high burden setting.

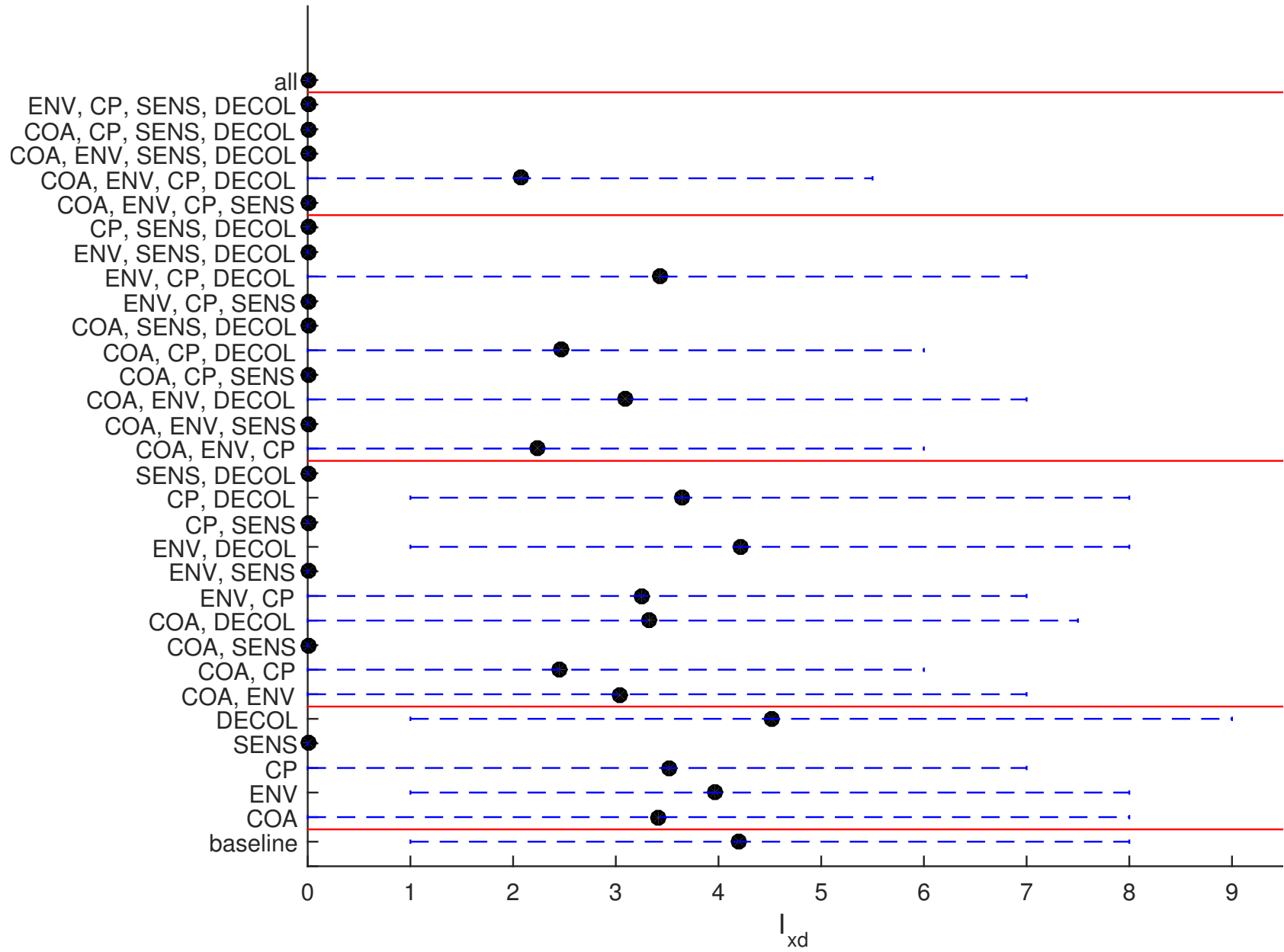


Figure F.27: I_{xd} average and 95% intervals in the simulated ward for the high burden setting.

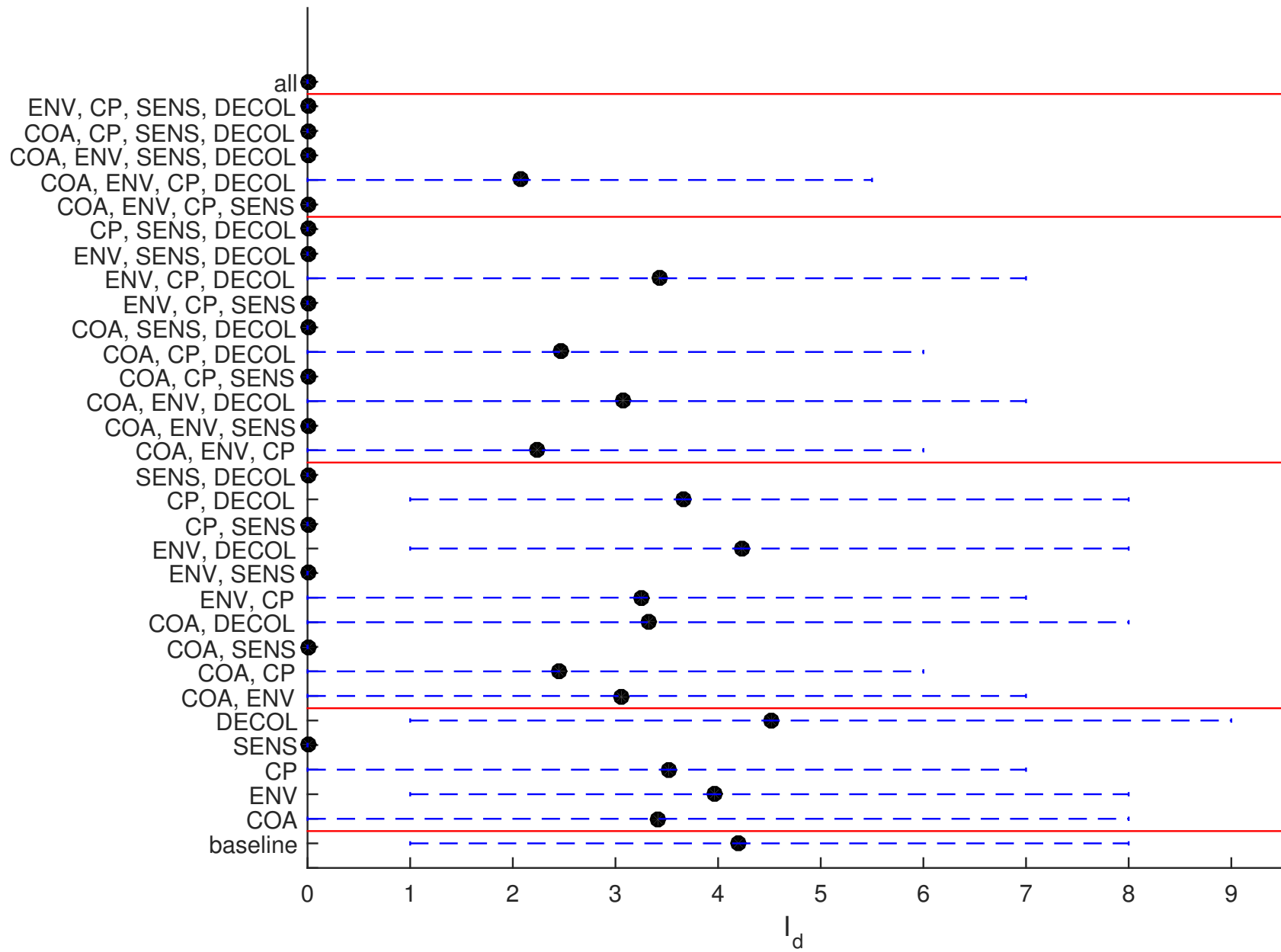


Figure F.28: I_d average and 95% intervals in the simulated ward for the high burden setting.

Comparison	AR $\hat{\theta}$ (95% CI)
COA v baseline	0.16 (0.15 , 0.18)
ENV v baseline	0.16 (0.15 , 0.18)
CP v baseline	0.00 (0.00 , 0.00)
SENS v baseline	0.00 (0.00 , 0.01)
DECOL v baseline	0.33 (0.30 , 0.35)
CP v SENS	0.16 (0.14 , 0.18)
CP v COA	0.05 (0.04 , 0.06)
CP v ENV	0.03 (0.02 , 0.04)
CP v DECOL	0.01 (0.00 , 0.01)
{CP, SENS} v {COA, CP}	0.29 (0.27 , 0.32)
{CP, SENS} v {ENV, CP}	0.17 (0.15 , 0.18)
{CP, SENS} v {CP, DECOL}	0.06 (0.05 , 0.07)
{CP, SENS} v {COA, SENS}	0.02 (0.01 , 0.02)
{CP, SENS} v {ENV, SENS}	0.02 (0.01 , 0.02)
{CP, SENS} v {SENS, DECOL}	0.00 (0.00 , 0.01)
{COA, CP, SENS} v {ENV, CP, SENS}	0.45 (0.43 , 0.48)
{COA, CP, SENS} v {CP, SENS, DECOL}	0.26 (0.24 , 0.28)
{COA, CP, SENS} v {COA, ENV, CP}	0.35 (0.33 , 0.38)
{COA, CP, SENS} v {COA, CP, DECOL}	0.12 (0.10 , 0.13)
{COA, CP, SENS} v {COA, ENV, SENS}	0.07 (0.06 , 0.08)
{COA, CP, SENS} v {ENV, CP, DECOL}	0.05 (0.04 , 0.06)
{COA, CP, SENS} v {ENV, SENS, DECOL}	0.01 (0.01 , 0.01)
{COA, CP, SENS} v {COA, SENS, DECOL}	0.01 (0.00 , 0.01)
{COA, CP, SENS} v {COA, ENV, DECOL}	0.01 (0.00 , 0.01)
{ENV, CP, SENS} v {CP, SENS, DECOL}	0.31 (0.29 , 0.34)
{ENV, CP, SENS} v {COA, ENV, CP}	0.38 (0.35 , 0.40)
{ENV, CP, SENS} v {COA, CP, DECOL}	0.14 (0.12 , 0.15)
{ENV, CP, SENS} v {COA, ENV, SENS}	0.09 (0.07 , 0.10)
{ENV, CP, SENS} v {ENV, CP, DECOL}	0.06 (0.05 , 0.07)
{ENV, CP, SENS} v {ENV, SENS, DECOL}	0.01 (0.01 , 0.02)
{ENV, CP, SENS} v {COA, SENS, DECOL}	0.01 (0.01 , 0.01)
{ENV, CP, SENS} v {COA, ENV, DECOL}	0.01 (0.01 , 0.01)
{COA, ENV, CP, SENS} v {ENV, CP, SENS, DECOL}	0.20 (0.18 , 0.22)
{COA, ENV, CP, SENS} v {COA, CP, SENS, DECOL}	0.15 (0.13 , 0.17)
{COA, ENV, CP, SENS} v {COA, ENV, CP, DECOL}	0.15 (0.13 , 0.17)
{COA, ENV, CP, SENS} v {COA, ENV, SENS, DECOL}	0.02 (0.01 , 0.02)
{CP, SENS} v CP	0.01 (0.01 , 0.02)
{COA, CP, SENS} v {CP, SENS}	0.03 (0.02 , 0.04)
{ENV, CP, SENS} v {CP, SENS}	0.04 (0.04 , 0.05)
{COA, ENV, CP, SENS} v {COA, CP, SENS}	0.03 (0.02 , 0.04)
{COA, ENV, CP, SENS} v {ENV, CP, SENS}	0.03 (0.02 , 0.04)
all v {COA, ENV, CP, SENS}	0.16 (0.15 , 0.18)

Table F.10: θ estimates for AR comparisons of intervention combinations for the high burden setting.

Comparison	AC $\hat{\theta}$ (95% CI)
COA v baseline	0.00 (0.00 , 0.00)
ENV v baseline	0.53 (0.51 , 0.56)
CP v baseline	0.61 (0.58 , 0.63)
SENS v baseline	0.86 (0.84 , 0.87)
DECOL v baseline	0.65 (0.63 , 0.67)
COA v ENV	0.00 (0.00 , 0.00)
COA v CP	0.00 (0.00 , 0.00)
COA v DECOL	0.00 (0.00 , 0.00)
COA v SENS	0.00 (0.00 , 0.00)
{COA, .} v {ENV, CP}	0.00 (0.00 , 0.00)
{COA, .} v {ENV, DECOL}	0.00 (0.00 , 0.00)
{COA, .} v {CP, DECOL}	0.00 (0.00 , 0.00)
{COA, .} v {ENV, SENS}	0.00 (0.00 , 0.00)
{COA, .} v {CP, SENS}	0.00 (0.00 , 0.00)
{COA, .} v {SENS, DECOL}	0.00 (0.00 , 0.00)
{COA, ., .} v {ENV, CP, DECOL}	0.00 (0.00 , 0.00)
{COA, ., .} v {ENV, CP, SENS}	0.00 (0.00 , 0.00)
{COA, ., .} v {ENV, SENS, DECOL}	0.00 (0.00 , 0.00)
{COA, ., .} v {CP, SENS, DECOL}	0.00 (0.00 , 0.00)
{COA, ., ., .} v {ENV, CP, SENS, DECOL}	0.00 (0.00 , 0.00)

Table F.11: θ estimates for AC comparisons of intervention combinations for high burden setting .

Comparison	$C_d \hat{\theta}$ (95% CI)
COA v baseline	0.14 (0.12 , 0.15)
ENV v baseline	0.36 (0.34 , 0.39)
CP v baseline	0.17 (0.15 , 0.19)
SENS v baseline	0.79 (0.76 , 0.80)
DECOL v baseline	0.62 (0.60 , 0.65)
COA v CP	0.45 (0.42 , 0.47)
COA v ENV	0.22 (0.20 , 0.24)
COA v DECOL	0.09 (0.08 , 0.10)
COA v SENS	0.03 (0.02 , 0.04)
CP v ENV	0.26 (0.24 , 0.28)
CP v DECOL	0.11 (0.10 , 0.13)
CP v SENS	0.04 (0.03 , 0.05)
{COA, CP} v {COA, ENV}	0.23 (0.21 , 0.25)
{COA, CP} v {ENV, CP}	0.13 (0.11 , 0.14)
{COA, CP} v {COA, SENS}	0.10 (0.09 , 0.12)
{COA, CP} v {COA, DECOL}	0.09 (0.08 , 0.10)
{COA, CP} v {CP, DECOL}	0.04 (0.04 , 0.05)
{COA, CP} v {CP, SENS}	0.01 (0.01 , 0.02)
{COA, CP} v {ENV, DECOL}	0.01 (0.01 , 0.02)
{COA, CP} v {ENV, SENS}	0.00 (0.00 , 0.01)
{COA, CP} v {SENS, DECOL}	0.00 (0.00 , 0.00)
{COA, ENV, CP} v {COA, CP, SENS}	0.30 (0.28 , 0.33)
{COA, ENV, CP} v {COA, CP, DECOL}	0.30 (0.27 , 0.32)
{COA, ENV, CP} v {COA, ENV, SENS}	0.16 (0.14 , 0.18)
{COA, ENV, CP} v {COA, ENV, DECOL}	0.11 (0.10 , 0.13)
{COA, ENV, CP} v {COA, SENS, DECOL}	0.06 (0.05 , 0.07)
{COA, ENV, CP} v {ENV, CP, DECOL}	0.03 (0.02 , 0.04)
{COA, ENV, CP} v {ENV, CP, SENS}	0.02 (0.01 , 0.02)
{COA, ENV, CP} v {CP, SENS, DECOL}	0.00 (0.00 , 0.01)
{COA, ENV, CP} v {ENV, SENS, DECOL}	0.00 (0.00 , 0.00)
{COA, ENV, CP, SENS} v {COA, ENV, CP, DECOL}	0.47 (0.45 , 0.50)
{COA, ENV, CP, SENS} v {COA, CP, SENS, DECOL}	0.31 (0.29 , 0.33)
{COA, ENV, CP, SENS} v {COA, ENV, SENS, DECOL}	0.18 (0.16 , 0.20)
{COA, ENV, CP, SENS} v {ENV, CP, SENS, DECOL}	0.01 (0.01 , 0.02)
{COA, ENV, CP, DECOL} v {COA, CP, SENS, DECOL}	0.33 (0.31 , 0.36)
{COA, ENV, CP, DECOL} v {COA, ENV, SENS, DECOL}	0.20 (0.18 , 0.22)
{COA, ENV, CP, DECOL} v {ENV, CP, SENS, DECOL}	0.01 (0.01 , 0.02)
{COA, CP} v COA	0.10 (0.09 , 0.11)
{COA, ENV, CP} v COA	0.03 (0.03 , 0.04)
{COA, ENV, CP} v {COA, CP}	0.28 (0.26 , 0.30)
{COA, ENV, CP, SENS} v {COA, CP}	0.23 (0.21 , 0.25)
{COA, ENV, CP, DECOL} v {COA, CP}	0.25 (0.23 , 0.27)
{COA, ENV, CP, SENS} v {COA, ENV, CP}	0.43 (0.41 , 0.46)
{COA, ENV, CP, DECOL} v {COA, ENV, CP}	0.46 (0.43 , 0.48)
all v {COA, CP}	0.16 (0.15 , 0.18)
all v {COA, ENV, CP}	0.35 (0.32 , 0.37)
all v {COA, ENV, CP, SENS}	0.42 (0.39 , 0.44)
all v {COA, ENV, CP, DECOL}	0.39 (0.37 , 0.41)

Table F.13: θ estimates for C_d comparisons of intervention combinations for high burden setting .

Comparison	$I_{xd} \hat{\theta}$ (95% CI)
COA v baseline	0.38 (0.36 , 0.41)
ENV v baseline	0.47 (0.44 , 0.49)
CP v baseline	0.40 (0.38 , 0.42)
SENS v baseline	0.00 (0.00 , 0.01)
DECOL v baseline	0.55 (0.52 , 0.57)
SENS v COA	0.02 (0.01 , 0.03)
SENS v CP	0.01 (0.01 , 0.02)
SENS v ENV	0.01 (0.00 , 0.01)
SENS v DECOL	0.00 (0.00 , 0.01)
{SENS, .} v {COA, CP}	0.04 (0.04 , 0.06)
{SENS, .} v {COA, ENV}	0.03 (0.02 , 0.03)
{SENS, .} v {ENV, CP}	0.02 (0.01 , 0.02)
{SENS, .} v {COA, DECOL}	0.02 (0.01 , 0.02)
{SENS, .} v {CP, DECOL}	0.01 (0.01 , 0.01)
{SENS, .} v {ENV, DECOL}	0.01 (0.00 , 0.01)
{SENS, ., .} v {COA, ENV, CP}	0.06 (0.05 , 0.08)
{SENS, ., .} v {COA, CP, DECOL}	0.05 (0.04 , 0.06)
{SENS, ., .} v {COA, ENV, DECOL}	0.03 (0.02 , 0.04)
{SENS, ., .} v {ENV, CP, DECOL}	0.01 (0.01 , 0.02)
{SENS, ., ., .} v {COA, ENV, CP, DECOL}	0.07 (0.06 , 0.08)

Table F.14: θ estimates for I_{xd} comparisons of intervention combinations for high burden setting .

Comparison	$I_d \hat{\theta}$ (95% CI)
COA v baseline	0.38 (0.36 , 0.41)
ENV v baseline	0.47 (0.44 , 0.49)
CP v baseline	0.40 (0.38 , 0.43)
SENS v baseline	0.00 (0.00 , 0.01)
DECOL v baseline	0.55 (0.52 , 0.57)
SENS v COA	0.02 (0.01 , 0.03)
SENS v CP	0.01 (0.01 , 0.02)
SENS v ENV	0.01 (0.00 , 0.01)
SENS v DECOL	0.00 (0.00 , 0.01)
{SENS, .} v {COA, CP}	0.05 (0.04 , 0.06)
{SENS, .} v {COA, ENV}	0.03 (0.02 , 0.03)
{SENS, .} v {ENV, CP}	0.01 (0.01 , 0.02)
{SENS, .} v {COA, DECOL}	0.02 (0.01 , 0.02)
{SENS, .} v {CP, DECOL}	0.01 (0.01 , 0.01)
{SENS, .} v {ENV, DECOL}	0.01 (0.00 , 0.01)
{SENS, ., .} v {COA, ENV, CP}	0.06 (0.05 , 0.08)
{SENS, ., .} v {COA, CP, DECOL}	0.05 (0.04 , 0.06)
{SENS, ., .} v {COA, ENV, DECOL}	0.03 (0.02 , 0.04)
{SENS, ., .} v {ENV, CP, DECOL}	0.01 (0.01 , 0.02)
{SENS, ., ., .} v {COA, ENV, CP, DECOL}	0.07 (0.06 , 0.08)

Table F.15: θ estimates for I_d comparisons of intervention combinations for high burden setting .

Bibliography

- Aanensen, D. M., Feil, E. J., Holden, M. T., Dordel, J., Yeats, C. A., Fedosejev, A., Goater, R., Castillo-Ramírez, S., Corander, J., Colijn, C., et al. (2016). Whole-genome sequencing for routine pathogen surveillance in public health: a population snapshot of invasive *Staphylococcus aureus* in Europe. *mBio*, 7(3):e00444–16.
- Abadie, A. (2002). Bootstrap tests for distributional treatment effects in instrumental variable models. *Journal of the American Statistical Association*, 97(457):284–292.
- Aboelela, S. W., Saiman, L., Stone, P., Lowy, F. D., Quiros, D., and Larson, E. (2006). Effectiveness of barrier precautions and surveillance cultures to control transmission of multidrug-resistant organisms: A systematic review of the literature. *American Journal of Infection Control*, 34(8):484 – 494.
- Ajao, A. O., Harris, A. D., Roghmann, M.-C., Johnson, J. K., Zhan, M., McGregor, J. C., and Furuno, J. P. (2011). Systematic review of measurement and adjustment for colonization pressure in studies of methicillin-resistant *Staphylococcus aureus*, vancomycin-resistant enterococci, and *Clostridium difficile* acquisition. *Infection Control & Hospital Epidemiology*, 32:481–489.
- Akaike, H. (1974). A new look at the statistical model identification. *The Transactions on Automatic Control*, 19(6):716–723.
- Albrich, W. C. and Harbarth, S. (2008). Health-care workers: source, vector, or victim of MRSA? *The Lancet Infectious Diseases*, 8(5):289 – 301.
- Allegranzi, B., Nejad, S. B., Combescure, C., Graafmans, W., Attar, H., Donaldson, L., and Pittet, D. (2011). Burden of endemic health-care-associated infection in developing countries: systematic review and meta-analysis. *The Lancet*, 377(9761):228 – 241.
- Allegranzi, B. and Pittet, D. (2009). Role of hand hygiene in healthcare-associated infection prevention. *Journal of Hospital Infection*, 73(4):305 – 315.
- Ammerlaan, H. S. M., Kluytmans, J. A. J. W., Wertheim, H. F. L., Nouwen, J. L., and Bonten, M. J. M. (2009). Eradication of methicillin-resistant *Staphylococcus aureus* carriage: A systematic review. *Clinical Infectious Diseases*, 48(7):922–930.
- Anderson, R. M. and Garnett, G. P. (2000). Mathematical models of the transmission and control of sexually transmitted diseases. *Sexually transmitted diseases*, 27(10):636–643.
- Andrieu, C. and Roberts, G. O. (2009). The pseudo-marginal approach for efficient Monte Carlo computations. *The Annals of Statistics*, 37(2):697–725.
- Austin, D. and Anderson, R. (1999). Transmission dynamics of epidemic methicillin-resistant *Staphylococcus aureus* and vancomycin-resistant enterococci in England and Wales. *The Journal of Infectious Diseases*, 179:883–891.
- Austin, D. J., Bonten, M. J. M., Weinstein, R. A., Slaughter, S., and Anderson, R. M. (1999). Vancomycin-resistant enterococci in intensive-care hospital settings: Transmission dynamics, persistence, and the impact of infection control programs. *Proceedings of the National Academy of Sciences*, 96(12):6908–6913.

- Barnett, A. G., Batra, R., Graves, N., Edgeworth, J., Robotham, J., and Cooper, B. (2009). Using a longitudinal model to estimate the effect of methicillin-resistant *Staphylococcus aureus* infection on length of stay in an intensive care unit. *American Journal of Epidemiology*, 170(9):1186–1194.
- Barthelmé, S. and Chopin, N. (2014). Expectation propagation for likelihood-free inference. *Journal of the American Statistical Association*, 109(505):315–333.
- Barthelmé, S., Chopin, N., and Cottet, V. (2015). Divide and conquer in ABC: Expectation-Propagation algorithms for likelihood-free inference. *ArXiv e-prints: 1512.00205v1*.
- Bauer, K. A., Perez, K. K., Forrest, G. N., and Goff, D. A. (2014). Review of rapid diagnostic tests used by antimicrobial stewardship programs. *Clinical Infectious Diseases*, 59(suppl 3):S134–S145.
- Beaumont, M. A. (2008). Joint determination of topology, divergence time, and immigration in population trees. In Renfrew, C., Matsumura, S., and Forster, P., editors, *Simulation, Genetics, and Human Prehistory*, McDonald Institute Monographs, pages 134–1541. McDonald Institute for Archaeological Research.
- Beaumont, M. A. (2010). Approximate Bayesian computation in evolution and ecology. *Annual Review of Ecology, Evolution and Systematics*, 41:379–406.
- Beaumont, M. A., Cornuet, J.-M., Marin, J.-M., and Robert, C. P. (2009). Adaptive approximate Bayesian computation. *Biometrika*, 96:983–990.
- Beaumont, M. A., Zhang, W., and Balding, D. J. (2002). Approximate Bayesian computation in population genetics. *Genetics*, 162:2025–2035.
- Becker, N. G. and Hopper, J. L. (1983). The heterogeneity of disease spread through a community. *American Journal of Epidemiology*, 117(3):362–374.
- Bernardo, J. M. and Smith, A. F., editors (2000). *Bayesian Theory*, chapter Remodelling, pages 377–426. John Wiley & Sons.
- Bernoulli, D. (1766). Essai d’une nouvelle analyse de la mortalité causée par la petite vérole. *Mémoires de Mathématiques et de Physique, Académie Royale des Sciences, Paris*.
- Beyersmann, J., Kneib, T., Schumacher, M., and Gastmeier, P. (2009). Nosocomial infection, length of stay, and time-dependent bias. *Infection Control & Hospital Epidemiology*, 30(3):273–276.
- Beyersmann, J., Wolkewitz, M., and Schumacher, M. (2008). The impact of time-dependent bias in proportional hazards modelling. *Statistics in Medicine*, 27(30):6439–6454.
- Blum, M. G. and Tran, V. C. (2010). HIV with contact tracing: a case study in approximate Bayesian computation. *Biostatistics*, 11(4):644–660.
- Bode, L., Wertheim, H., Kluytmans, J., Bogaers-Hofman, D., Vandenbroucke-Grauls, C., Roosendaal, R., Troelstra, A., Box, A., Voss, A., van Belkum, A., Verbrugh, H., and Vos, M. (2011). Sustained low prevalence of methicillin-resistant *Staphylococcus aureus* upon admission to hospital in The Netherlands. *Journal of Hospital Infection*, 79:198–201.
- Bonten, M. and Bootsma, M. (2010). Nosocomial transmission: Methicillin-resistant *Staphylococcus aureus* (MRSA). In Krämer, A., Kretzschmar, M., and Krickeberg, K., editors, *Modern Infectious Disease Epidemiology: Concepts, Methods, Mathematical Models, and Public Health (Statistics for Biology and Health)*, chapter 22, pages 395–407. Springer.
- Bonten, M. J., Slaughter, S., Ambergen, Anton, W., Hayden, M. K., van Voorhis, J., Nathan, C., and Weinstein, R. A. (1998). The role of “colonization pressure” in the spread of vancomycin-resistant enterococci: An important infection control variable. *Archives of Internal Medicine*, 158(10):1127–1132.

- Bootsma, M. C. J., Diekmann, O., and Bonten, M. J. M. (2006). Controlling methicillin-resistant *Staphylococcus aureus*: Quantifying the effects of interventions and rapid diagnostic testing. *Proceedings of the National Academy of Sciences*, 103(14):5620–5625.
- Bortot, P., Coles, S., and Sisson, S. (2007). Inference for stereological extremes. *Journal of the American Statistical Association*, 102:84–92.
- Boucher, H., Miller, L. G., and Razonable, R. R. (2010). Serious infections caused by methicillin-resistant *Staphylococcus aureus*. *Clinical Infectious Diseases*, 51(Supplement 2):S183–S197.
- Boyce, J. M., Potter-Bynoe, G., Chenevert, C., and King, T. (1997). Environmental contamination due to methicillin-resistant *Staphylococcus aureus*: Possible infection control implications. *Infection Control & Hospital Epidemiology*, 18(9):pp. 622–627.
- Breban, R., Drake, J. M., Stallknecht, D. E., and Rohani, P. (2009). The role of environmental transmission in recurrent avian influenza epidemics. *PLoS Computational Biology*, 5(4):e1000346.
- Britton, T., Kypraios, T., and O’Neill, P. D. (2011). Inference for epidemics with three levels of mixing: Methodology and application to a measles outbreak. *Scandinavian Journal of Statistics*, 38(3):578–599.
- Brooks, S., Gelman, A., Jones, G., and Meng, X.-L. (2011). *Handbook of Markov Chain Monte Carlo*. Chapman & Hall / CRC Press.
- Brooks-Pollock, E., Roberts, G. O., and Keeling, M. J. (2014). A dynamic model of bovine tuberculosis spread and control in Great Britain. *Nature*, 511:228–231.
- Brown, B. M. and Resnick, S. I. (1977). Extreme values of independent stochastic processes. *Journal of Applied Probability*, pages 732–739.
- Bull, S. B., Mak, C., and Greenwood, C. M. (2002). A modified score function estimator for multinomial logistic regression in small samples. *Computational Statistics & Data Analysis*, 39(1):57 – 74.
- Caprarello, G. and Fletcher, S. (2014). A brief review of spatial analysis concepts and tools used for mapping, containment and risk modelling of infectious diseases and other illnesses. *Parasitology*, 141(05):581–601.
- Carling, P. (2013). Methods for assessing the adequacy of practice and improving room disinfection. *American Journal of Infection Control*, 41(5, Supplement):S20 – S25.
- Castillo, E., Hadi, A. S., Balakrishnan, N., and Sarabia, J.-M. (2005). *Extreme Value and Related Models with Applications in Engineering and Science*. Wiley-Interscience, Hoboken, N.J.
- Catry, B., Latour, K., Jans, B., Vandendriessche, S., Preal, R., Mertens, K., and Denis, O. (2014). Risk factors for methicillin resistant *Staphylococcus aureus*: a multi-laboratory study. *PLoS ONE*, 9(2):e89579.
- Celeux, G., Forbes, F., Robert, C. P., Titterton, D. M., et al. (2006). Deviance information criteria for missing data models. *Bayesian Analysis*, 1(4):651–673.
- Cepeda, J. A., Whitehouse, T., Cooper, B., Hails, J., Jones, K., Kwaku, F., Taylor, L., Hayman, S., Cookson, B., Shaw, S., Kibbler, C., Singer, M., Bellingan, G., and Wilson, A. P. R. (2005). Isolation of patients in single rooms or cohorts to reduce spread of MRSA in intensive-care units: prospective two centre study. *The Lancet*, 365(9456):295 – 304.
- Chib, S. and Greenberg, E. (1995). Understanding the Metropolis-Hastings algorithm. *The American Statistician*, 49(4):327–335.
- Christiansen, K. J., Tibbett, P. A., Beresford, W., Pearman, J. W., Lee, R. C., Coombs, G. W., Kay, I. D., O’Brien, F. G., Palladino, S., Douglas, C. R., Montgomery, P. D., Orrell, T., Peterson, A. M., Kosaras, F. P., Flexman, J. P., Heath, C. H., and McCullough, C. A. (2004). Eradication of a large outbreak of a single strain of vanB vancomycin-resistant *Enterococcus faecium* at a major Australian teaching hospital. *Infection Control & Hospital Epidemiology*, 25(5):pp. 384–390.

- Christopher, S., Verghis, R. M., Antonisamy, B., Sowmyanarayanan, T. V., Brahma-dathan, K. N., Kang, G., and Cooper, B. S. (2011). Transmission dynamics of methicillin-resistant *Staphylococcus aureus* in a medical intensive care unit in India. *PLoS ONE*, 6(7):e20604.
- Ciccolini, M., Donker, T., Grundmann, H., Bonten, M. J., and Woolhouse, M. E. (2014). Efficient surveillance for healthcare-associated infections spreading between hospitals. *Proceedings of the National Academy of Sciences*, 111(6):2271–2276.
- Climo, M. W., Yokoe, D. S., Warren, D. K., Perl, T. M., Bolon, M., Herwaldt, L. A., Weinstein, R. A., Sepkowitz, K. A., Jernigan, J. A., Sanogo, K., and Wong, E. S. (2013). Effect of daily chlorhexidine bathing on hospital-acquired infection. *New England Journal of Medicine*, 368(6):533–542. PMID: 23388005.
- Coles, S. (2001). *An introduction to statistical modeling of extreme values*. Springer London.
- Cooley, D., Naveau, P., and Poncet, P. (2006). Variograms for spatial max-stable random fields. In *Dependence in Probability and Statistics*, pages 373–390. Springer.
- Cooper, B., Stone, S., Kibbler, C., Cookson, B., Roberts, J., Medley, G., Duckworth, G., Lai, R., and Ebrahim, S. (2004a). Isolation measures in the hospital management of methicillin resistant *Staphylococcus aureus* (MRSA): systematic review of the literature. *BMJ*, 329:533.
- Cooper, B. S., Medley, G. F., Bradley, S. J., and Scott, G. M. (2008). An augmented data method for the analysis of nosocomial infection data. *American Journal of Epidemiology*, 168(5):548–557.
- Cooper, B. S., Medley, G. F., Stone, S. P., Kibbler, C. C., Cookson, B. D., Roberts, J. A., Duckworth, G., Lai, R., and Ebrahim, S. (2004b). Methicillin-resistant *Staphylococcus aureus* in hospitals and the community: Stealth dynamics and control catastrophes. *Proceedings of the National Academy of Sciences*, 101(27):10223–10228.
- Cooper, R. A., Griffith, C. J., Malik, R. E., Obee, P., and Looker, N. (2007). Monitoring the effectiveness of cleaning in four British hospitals. *American Journal of Infection Control*, 35(5):338–341.
- Costello, A., Abbas, M., Allen, A., Ball, S., Bell, S., Bellamy, R., Friel, S., Groce, N., Johnson, A., Kett, M., et al. (2009). Managing the health effects of climate change. *The Lancet*, 373(9676):1693–1733.
- Coulter, S., Merollini, K., Roberts, J. A., Graves, N., and Halton, K. (2105). The need for cost-effectiveness analyses of antimicrobial stewardship programme: A structured review. *International Journal of Antimicrobial Agents*, 46:140–149.
- Cox, D. R. (1972). Regression models and life tables (with discussion). *Journal of the Royal Statistical Society. Series B*, 32:187–220.
- Cox, D. R. and Oakes, D. (1984). *Analysis of survival data*, volume 21. CRC Press.
- Csilléry, K., Blum, M. G., Gaggiotti, O. E., and François, O. (2010). Approximate Bayesian computation (ABC) in practice. *Trends in Ecology & Evolution*, 25(7):410–418.
- D’Agata, E. M., Webb, G. F., and Pressley, J. (2010). Rapid emergence of co-colonization with community-acquired and hospital-acquired methicillin-resistant *Staphylococcus aureus* strains in the hospital setting. *Mathematical Modelling of Natural Phenomena*, 5:76–93.
- Dancer, S., White, L., Lamb, J., Girvan, E. K., and Robertson, C. (2009). Measuring the effect of enhanced cleaning in a UK hospital: a prospective cross-over study. *BMC Medicine*, 7:28.
- Dancer, S. J. (2008). Importance of the environment in methicillin-resistant *Staphylococcus aureus* acquisition: the case for hospital cleaning. *The Lancet Infectious Diseases*, 8:101–113.

- Dancer, S. J. (2014). Controlling hospital-acquired infection: Focus on the role of the environment and new technologies for decontamination. *Clinical Microbiology Reviews*, 27(4):665–690.
- Dancer, S. J., White, L., and Robertson, C. (2008). Monitoring environmental cleanliness on two surgical wards. *International Journal of Environmental Health Research*, 18(5):357–364.
- Davison, A. (2003). *Statistical Models*, chapter 6: Stochastic Models, pages 274–291. Cambridge Series in Statistical and Probabilistic Mathematics. Cambridge University Press.
- Davison, A. C., Padoan, S. A., and Ribatet, M. (2012). Statistical modeling of spatial extremes. *Statistical Science*, 27(2):161–186.
- De Angelis, G., Allignol, A., Murthy, A., Wolkewitz, M., Beyersmann, J., Safran, E., Schrenzel, J., Pittet, D., and Harbarth, S. (2011). Multistate modelling to estimate the excess length of stay associated with meticillin-resistant *Staphylococcus aureus* colonisation and infection in surgical patients. *Journal of Hospital Infection*, 78(2):86 – 91.
- de Haan, L. and Ferreira, A. (2006). *Extreme Value Theory: An Introduction*. Springer.
- Del Moral, P., Doucet, A., and Jasra, A. (2006). Sequential Monte Carlo samplers. *Journal of the Royal Statistical Society: Series B (Statistical Methodology)*, 68:411–436.
- DeLeo, F. R., Otto, M., Kreiswirth, B. N., and Chambers, H. F. (2010). Community-associated meticillin-resistant *Staphylococcus aureus*. *The Lancet*, 375:1557 – 1568.
- Dellaportas, P. and Roberts, G. O. (2003). An introduction to MCMC. In Möller, J., editor, *Spatial Statistics and Computational Methods*, volume 173 of *Lecture Notes in Statistics*, chapter 1, pages 1–42. Springer.
- Didelot, X., Everitt, R. G., Johansen, A. M., and Lawson, D. J. (2011). Likelihood-free estimation of model evidence. *Bayesian Analysis*, 6(1):49–76.
- Didelot, X., Gardy, J., and Colijn, C. (2014). Bayesian inference of infectious disease transmission from whole-genome sequence data. *Molecular Biology and Evolution*, 31(7):169–1879.
- Dieker, A. and Mikosch, T. (2015). Exact simulation of Brown–Resnick random fields at a finite number of locations. *Extremes*, 18(2):301–314.
- Diekmann, O., Heesterbeek, H., and Britton, T. (2012). *Mathematical tools for understanding infectious disease dynamics*. Princeton University Press.
- Diekmann, O., Heesterbeek, J., and Roberts, M. (2009). The construction of next-generation matrices for compartmental epidemic models. *Journal of the Royal Society Interface*.
- Doan, T. N., Kong, D. C., Marshall, C., Kirkpatrick, C. M., and McBryde, E. S. (2015). Modeling the impact of interventions against *Acinetobacter baumannii* transmission in intensive care units. *Virulence*.
- Doan, T. N., Kong, D. C. M., Kirkpatrick, C. M. J., and McBryde, E. S. (2014). Optimizing hospital infection control: The role of mathematical modeling. *Infection Control & Hospital Epidemiology*, 35(12):1521–1530.
- Dombry, C., Engelke, S., and Oesting, M. (2016). Exact simulation of max-stable processes. *Biometrika*, 103(2):303–317.
- Donker, T., Wallinga, J., Slack, R., and Grundmann, H. (2012). Hospital networks and the dispersal of hospital-acquired pathogens by patient transfer. *PLoS ONE*, 7(4):e35002.
- Doss, H. (2010). Estimation of large families of Bayes factors from Markov chain output. *Statistica Sinica*, 20:537–560.
- Drovandi, C. C. and Pettitt, A. N. (2008). Multivariate Markov process models for the transmission of methicillin-resistant *Staphylococcus aureus* in a hospital ward. *Biometrics*, 64(3):851–859.

- Drovandi, C. C. and Pettitt, A. N. (2011a). Estimation of parameters for macroparasite population evolution using approximate Bayesian computation. *Biometrics*, 67(1):225–233.
- Drovandi, C. C. and Pettitt, A. N. (2011b). Using approximate Bayesian computation to estimate transmission rates of nosocomial pathogens. *Statistical Communications in Infectious Diseases*, 3:Iss. 1, Article 2.
- Duerden, B., Fry, C., Johnson, A. P., and Wilcox, M. H. (2015). The control of methicillin-resistant *Staphylococcus aureus* blood stream infections in England. *Open Forum Infectious Diseases*, 2(2).
- Durkin, M. J., Dicks, K. V., Baker, A. W., Lewis, S. S., Moehring, R. W., Chen, L. F., Sexton, D. J., and Anderson, D. J. (2015). Seasonal variation of common surgical site infections: does season matter? *Infection Control & Hospital Epidemiology*, 36(9):1011–1016.
- Edwards, B., Andini, R., Esposito, S., Grossi, P., Lew, D., Mazzei, T., Novelli, A., Soriano, A., and Gould, I. (2014). Treatment options for methicillin-resistant *Staphylococcus aureus* (MRSA) infection: Where are we now? *Journal of Global Antimicrobial Resistance*, 2(3):133 – 140.
- Eisenberg, M. C., Kujbida, G., Tuite, A. R., Fisman, D. N., and Tien, J. H. (2013). Examining rainfall and cholera dynamics in haiti using statistical and dynamic modeling approaches. *Epidemics*, 5(4):197 – 207.
- Embrechts, P., Klüppelberg, C., and Mikosch, T. (1997). *Modelling Extremal Events: for Insurance and Finance*, volume 33 of *Stochastic Modelling and Applied Probability*. Springer-Verlag, Berlin Heidelberg.
- Erhardt, R. and Sisson, S. A. (2016). Modelling extremes using approximate Bayesian computation. In *Extreme Value Modeling and Risk Analysis: Methods and Applications*, pages 281–306. CRC Press.
- Erhardt, R. J. and Smith, R. L. (2012). Approximate Bayesian computing for spatial extremes. *Computational Statistics & Data Analysis*, 56(6):1468–1481.
- Fan, Y. and Sisson, S. A. (2011). *Handbook of Markov chain Monte Carlo*, chapter 3: Reversible Jump MCMC, pages 67–91. Handbook of Modern Statistical Methods. Chapman & Hall / CRC Press.
- Fearnhead, P. and Prangle, D. (2012). Constructing summary statistics for approximate Bayesian computation: Semi-automatic approximate Bayesian computation. *Journal of the Royal Statistical Society: Series B (Statistical Methodology)*, 74(3):419–474.
- Filippi, S., Barnes, C., Cornebise, J., and Stumpf, M. P. (2013). On optimality of kernels for approximate Bayesian computation using sequential Monte Carlo. *Statistical Applications in Genetics and Molecular Biology*, 12(1):87–107.
- Firth, D. (1993). Bias reduction of maximum likelihood estimates. *Biometrika*, 80(1):27–38.
- Fisher, R. A. and Tippett, L. H. C. (1928). On the estimation of the frequency distributions of the largest or smallest member of a sample. *Proceedings of the Cambridge Philosophical Society*, 24:180–190.
- Fone, D., Hollinghurst, S., Temple, M., Round, A., Lester, N., Weightman, A., Roberts, K., Coyle, E., Bevan, G., and Palmer, S. (2003). Systematic review of the use and value of computer simulation modelling in population health and health care delivery. *Journal of Public Health*, 25(4):325–335.
- Forrester, M., Pettitt, A., and Gibson, G. (2007). Bayesian inference of hospital-acquired infectious diseases and control measures given imperfect surveillance data. *Biostatistics*, 8(2):383–401.
- Forrester, M. and Pettitt, A. N. (2005). Use of stochastic epidemic modeling to quantify transmission rates of colonization with methicillin-resistant *Staphylococcus aureus* in an intensive care unit. *Infection Control & Hospital Epidemiology*, 26(7):598–606.

- Forrester, M. L. (2006). *Epidemic models and inference for the transmission of hospital pathogens*. PhD thesis, School of Mathematical Sciences, Faculty of Science, Queensland University of Technology.
- Friel, N., McKeone, J. P., Oates, C. J., and Pettitt, A. N. (2016). Investigation of the widely applicable Bayesian information criterion. *Statistics and Computing*, in press.
- Friel, N. and Pettitt, A. N. (2008). Marginal likelihood estimation via power posteriors. *Journal of the Royal Statistical Society: Series B (Statistical Methodology)*, 70(3):589–607.
- Frost, V. S. and Melamed, B. (1994). Traffic modeling for telecommunications networks. *Communications Magazine, IEEE*, 32(3):70–81.
- Fu, Y.-X. and Li, W.-H. (1997). Estimating the age of the common ancestor of a sample of DNA sequences. *Molecular Biology and Evolution*, 14(2):195–199.
- Geiger, K. and Brown, J. (2013). Rapid testing for methicillin-resistant *Staphylococcus aureus*: Implications for antimicrobial stewardship. *American Journal of Health-System Pharmacy*, 70(4):335 – 342.
- Gelman, A., Carlin, J. B., Stern, H. S., and Rubin, D. B. (2013). *Bayesian data analysis*, volume 3. Chapman & Hall / CRC Press.
- Gelman, A., Jakulin, A., Pittau, M. G., and Su, Y.-S. (2008). A weakly informative default prior distribution for logistic and other regression models. *The Annals of Applied Statistics*, 2(4):pp. 1360–1383.
- Gelman, A., Roberts, G., and Gilks, W. (1996). Efficient Metropolis jumping rules. In Bernardo, J., Berger, J., Dawid, A., and Smith, A., editors, *Bayesian Statistics 5*, pages 599–608. Oxford University Press.
- Geman, S. and Geman, D. (1984). Stochastic relaxation, Gibbs distributions, and the Bayesian restoration of images. *IEEE Transactions on pattern analysis and machine intelligence*, (6):721–741.
- Gibson, G. J. and Renshaw, E. (1998). Estimating parameters in stochastic compartmental models using Markov chain methods. *Mathematical Medicine and Biology*, 15(1):19–40.
- Gijbels, I. and Prosdocimi, I. (2010). Loess. *Wiley Interdisciplinary Reviews: Computational Statistics*, 2(5):590–599.
- Gillespie, D. T. (1977). Exact stochastic simulation of coupled chemical reactions. *The Journal of Physical Chemistry*, 81(25):2340–2361.
- Gillespie, D. T. (2007). Stochastic simulation of chemical kinetics. *Annual Review of Physical Chemistry*, 58:35–55.
- Giuffré, M., Bonura, C., Cipolla, D., and Mammina, C. (2013). MRSA infection in the neonatal intensive care unit. *Expert Review of Anti-infective Therapy*, 11(5):499–509.
- Gnedenko, B. V. (1943). Sur la distribution limite du terme maximum d’une série aléatoire. *Annals of Mathematics*, 44:423–453.
- Gould, I. M., David, M. Z., Esposito, S., Garau, J., Lina, G., Mazzei, T., and Peters, G. (2012). New insights into meticillin-resistant *Staphylococcus aureus* (MRSA) pathogenesis, treatment and resistance. *International Journal of Antimicrobial Agents*, 39(2):96 – 104.
- Grambsch, P. M. and Therneau, T. M. (1994). Proportional hazards tests and diagnostics based on weighted residuals. *Biometrika*, 81(3):512–526.
- Green, P. J. (1995). Reversible jump Markov chain Monte Carlo computation and Bayesian model determination. *Biometrika*, 82(4):711–732.
- Green, P. J. (2003). Trans-dimensional Markov chain Monte Carlo. *Oxford Statistical Science Series*, pages 179–198.
- Green, P. J., Łatuszyński, K., Pereyra, M., and Robert, C. P. (2015). Bayesian computation: a summary of the current state, and samples backwards and forwards. *Statistics and Computing*, 25(4):835–862.

- Greenwood, M. (1931). On the statistical measure of infectiousness. *Journal of Hygiene*, 31(3):336–351.
- Grelaud, A., Robert, C. P., Marin, J.-M., Rodolphe, F., and Taly, J.-F. (2009). ABC likelihood-free methods for model choice in Gibbs random fields. *Bayesian Analysis*, 4(2):317–336.
- Groendyke, C., Welch, D., and Hunter, D. R. (2012). A network-based analysis of the 1861 Hagelloch measles data. *Biometrics*, 68(3):755–765.
- Grundmann, H., Hori, S., Winter, B., Tami, A., and Austin, D. J. (2002). Risk factors for the transmission of methicillin-resistant *Staphylococcus aureus* in an adult intensive care unit: fitting a model to the data. *Journal of Infectious Diseases*, 185(4):481–488.
- Gurusamy, K. S., Koti, R., Toon, C. D., Wilson, P., and Davidson, B. R. (2013). Antibiotic therapy for the treatment of methicillin-resistant *Staphylococcus aureus* (MRSA) infections in surgical wounds. *Cochrane Database of Systematic Reviews*, Issue 8:Art. No.: CD009726.
- Hainy, M., Müller, W. G., and Wagner, H. (2016). Likelihood-free simulation-based optimal design with an application to spatial extremes. *Stochastic Environmental Research and Risk Assessment*, 30(2):481–492.
- Hajat, S., O’Connor, M., and Kosatsky, T. (2010). Health effects of hot weather: from awareness of risk factors to effective health protection. *The Lancet*, 375(9717):856 – 863.
- Hall, I. M., Barrass, I., Leach, S., Pittet, D., and Hugonnet, S. (2012). Transmission dynamics of methicillin-resistant *Staphylococcus aureus* in a medical intensive care unit. *Journal of the Royal Society Interface*, 9(75):2639–2652.
- Hannan, E. J. and Quinn, B. G. (1979). The determination of the order of an autoregression. *Journal of the Royal Statistical Society. Series B (Methodological)*, 41(2):190–195.
- Harbarth, S., Fankhauser, C., Schrenzel, J., Christenson, J., Gervaz, P., Bandiera-Clerc, C., Renzi, G., Vernaz, N., Sax, H., and Pittet, D. (2008). Universal screening for methicillin-resistant *Staphylococcus aureus* at hospital admission and nosocomial infection in surgical patients. *JAMA*, 299(10):1149–1157.
- Harris, A. D., Bradham, D. D., Baumgarten, M., Zuckerman, I. H., Fink, J. C., and Perencevich, E. N. (2004). The use and interpretation of quasi-experimental studies in infectious diseases. *Clinical Infectious Diseases*, 38(11):1586–1591.
- Harris, A. D., Pineles, L., Belton, B., Johnson, J. K., Shardell, M., Loeb, M., Newhouse, R., Dembry, L., Braun, B., Perencevich, E. N., et al. (2013). Universal glove and gown use and acquisition of antibiotic-resistant bacteria in the ICU: A randomized trial. *JAMA*, 310(15):1571–1580.
- Hastie, D. I. and Green, P. J. (2012). Model choice using reversible jump Markov chain Monte Carlo. *Statistica Neerlandica*, 66(3):309–338.
- Hastings, W. K. (1970). Monte Carlo sampling methods using Markov chains and their applications. *Biometrika*, 57(1):97–109.
- Hayden, M. K., Bonten, M. J. M., Blom, D. W., Lyle, E. A., van de Vijver, D. A. M. C., and Weinstein, R. A. (2006). Reduction in acquisition of vancomycin-resistant enterococcus after enforcement of routine environmental cleaning measures. *Clinical Infectious Diseases*, 42(11):1552–1560.
- Hetem, D. J. and Bonten, M. J. (2013). Clinical relevance of mupirocin resistance in *Staphylococcus aureus*. *Journal of Hospital Infection*, 85(4):249–256.
- Hethcote, H. W. (2000). The mathematics of infectious diseases. *SIAM review*, 42(4):599–653.
- Holme, P. (2015). Information content of contact-pattern representations and predictability of epidemic outbreaks. *Scientific reports*, 5:14462.

- Horner, C., Mawer, D., and Wilcox, M. (2012). Reduced susceptibility to chlorhexidine in staphylococci: is it increasing and does it matter? *Journal of Antimicrobial Chemotherapy*, 67(11):2547–2559.
- Hosmer, D. W., Lemeshow, S., and May, S. (2008). *Applied Survival Analysis: Regression Modeling of Time-to-Event Data*. Wiley-Interscience, 2 edition.
- Huslage, K., Rutala, W. A., Sickbert-Bennett, E., and Weber, D. J. (2010). A quantitative approach to defining “high-touch” surfaces in hospitals. *Infection Control & Hospital Epidemiology*, 31(8):850–853.
- Huttner, A., Harbarth, S., Carlet, J., Cosgrove, S., Goossens, H., Holmes, A., Jarlier, V., Voss, A., and Pittet, D. (2013). Antimicrobial resistance: a global view from the 2013 World Healthcare-Associated Infections Forum. *Antimicrobial Resistance and Infection Control*, 2(31).
- Hyndman, R. and Athanasopoulos, G. (2013). *Forecasting: principles and practice*. O-Texts: Melbourne, Australia. <http://otexts.org/fpp/>.
- Hyndman, R. and Khandakar, Y. (2007). Automatic time series forecasting: the forecast package for R 7, 2008. URL <http://www.jstatsoft.org/v27/i03>.
- Ibrahim, J. G., Chen, M.-H., and Sinha, D. (2005). *Bayesian survival analysis*. Wiley Online Library.
- IPCC (2012). Summary for policymakers. In Field, C., Barros, V., Stocker, T., Qin, D., Dokken, D., Ebi, K., Mastrandrea, M., Mach, K., Plattner, G.-K., Allen, S., Tignor, M., and Midgley, P., editors, *Managing the Risks of Extreme Events and Disasters to Advance Climate Change Adaptation*. Cambridge University Press, Cambridge, UK, and New York, NY, USA.
- Ismail, N. A., Pettitt, A. N., and Webster, R. A. (2003). ‘Online’ monitoring and retrospective analysis of hospital outcomes based on a scan statistic. *Statistics in Medicine*, 22(18):2861–2876.
- Jackson, C. H., Sharples, L. D., Thompson, S. G., Duffy, S. W., and Couto, E. (2003). Multistate Markov models for disease progression with classification error. *Journal of the Royal Statistical Society. Series D (The Statistician)*, 52(2):193–209.
- Jevons, M. P. (1961). “Celbenin”-resistant staphylococci. *British Medical Journal*, 1:124–125.
- Jewell, C. P., Kypraios, T., Neal, P., and Roberts, G. O. (2009). Bayesian analysis for emerging infectious diseases. *Bayesian Analysis*, 4(3):465–496.
- Kabluchko, Z., Schlather, M., and de Haan, L. (2009). Stationary max-stable fields associated to negative definite functions. *The Annals of Probability*, 37(5):2042–2065.
- Kass, R. E. and Raftery, A. E. (1995). Bayes factors. *Journal of the American Statistical Association*, 90(430):773–795.
- Kass, R. E. and Wasserman, L. (1995). A reference Bayesian test for nested hypotheses and its relationship to the Schwarz criterion. *Journal of the American Statistical Association*, 90(431):928–934.
- Katz, R. W., Parlange, M. B., and Naveau, P. (2002). Statistics of extremes in hydrology. *Advances in Water Resources*, 25(8):1287–1304.
- Keeling, M. J. and Rohani, P. (2008). *Modeling infectious diseases in humans and animals*. Princeton University Press.
- Kermack, W. and McKendrick, A. (1927). A contribution to the mathematical theory of epidemics. *Proceedings of the Royal Society of London. Series A.*, 115(772):700–721.
- Khoury, J., Jones, M., Grim, A., Dunne, W. M., and Fraser, V. (2005). Eradication of methicillin-resistant *Staphylococcus aureus* from a neonatal intensive care unit by active surveillance and aggressive infection control measures. *Infection Control & Hospital Epidemiology*, 26(7):616–621.
- Klein, J. P. and Moeschberger, M. L. (2005). *Survival analysis: techniques for censored and truncated data*. Springer Science & Business Media.

- Klein, J. P., van Houwelingen, H. C., Ibrahim, J. G., and Scheike, Thomas, H. (2014). *Handbook of Survival Analysis*. Chapman & Hall / CRC Press.
- Knox, R. (1961). “Celbenin”-resistant staphylococci. *British Medical Journal*, 1:126.
- Kolmogorov, A. N. (1942). Definition of centre of dispersion and measure of accuracy to form a finite number of observations. *Izv. Akad. Nauk, USSR Ser. Mat*, 6:3–32.
- Kong, F., Paterson, D., Whitby, M., Coory, M., and Clements, A. (2013). A hierarchical spatial modelling approach to investigate MRSA transmission in a tertiary hospital. *BMC Infectious Diseases*, 13(1):449.
- Kong, F., Paterson, D. L., Coory, M., and Clements, A. C. (2012). A multilevel model of methicillin-resistant *Staphylococcus aureus* acquisition within the hierarchy of an Australian tertiary hospital. *American Journal of Infection Control*, 40(9):787 – 793.
- Kong, F. Y. M. (2014). *Novel Applications of Non-clinical Data to MRSA Surveillance in the Hospital*. PhD thesis, School of Population Health, The University of Queensland.
- Kosmidis, I. (2007). *brglm: Bias reduction in binary-response GLMs*. R package version 0.5-6.
- Kosmidis, I. and Firth, D. (2011). Multinomial logit bias reduction via the Poisson log-linear model. *Biometrika*, 98(3):755–759.
- Kouyos, R., Klein, E., and Grenfell, B. (2013). Hospital-community interactions foster coexistence between methicillin-resistant strains of *Staphylococcus aureus*. *PLoS Pathogens*, 9(2):e1003134.
- Kramer, A., Schwebke, I., and Kampf, G. (2006). How long do nosocomial pathogens persist on inanimate surfaces? A systematic review. *BMC Infectious Diseases*, 6(130).
- Kuo, L. and Yang, T. Y. (1996). Bayesian computation for nonhomogeneous Poisson processes in software reliability. *Journal of the American Statistical Association*, 91(434):763–773.
- Kypriaios, T., O’Neill, P. D., Huang, S. S., Rifas-Shiman, S. L., and Cooper, B. S. (2010). Assessing the role of undetected colonization and isolation precautions in reducing methicillin-resistant *Staphylococcus aureus* transmission in intensive care units. *BMC Infectious Diseases*, 10(29).
- Lau, M. S. Y., Marion, G., Streftaris, G., and Gibson, G. J. (2014). New model diagnostics for spatio-temporal systems in epidemiology and ecology. *Journal of the Royal Society Interface*, 11(93).
- Lee, B. Y., McGlone, S. M., Wong, K. F., Yilmaz, S. L., Avery, T. R., Song, Y., Christie, R., Eubank, S., Brown, S. T., Epstein, J. M., et al. (2011). Modeling the spread of methicillin-resistant *Staphylococcus aureus* (MRSA) outbreaks throughout the hospitals in Orange County, California. *Infection Control & Hospital Epidemiology*, 32(6):562.
- Lee, V. J., Lye, D. C., and Wilder-Smith, A. (2009). Combination strategies for pandemic influenza response - a systematic review of mathematical modeling studies. *BMC Medicine*, 7(1):76.
- Lee, X. J., Drovandi, C. C., and Pettitt, A. N. (2015). Model choice problems using approximate Bayesian computation with applications to pathogen transmission data sets. *Biometrics*, 71(1):198–207.
- Leekha, S., Diekema, D., and Perencevich, E. (2012). Seasonality of staphylococcal infections. *Clinical Microbiology and Infection*, 18:927–933.
- Lindsay, J. A. (2014). Evolution of *Staphylococcus aureus* and MRSA during outbreaks. *Infection, Genetics and Evolution*, 21:548 – 553.
- Little, R. J. and Rubin, D. B. (2002). *Statistical analysis with missing data*. John Wiley & Sons, 2 edition.
- Lloyd, C., Gunter, T., Osborne, M. A., and Roberts, S. J. (2015). Variational inference for Gaussian process modulated Poisson processes. In Bach, F. and Blei, D., editors, *The 32nd International Conference on Machine Learning*, volume 37, pages 1814–1822.

- Long, S. W., Beres, S. B., Olsen, R. J., and Musser, J. M. (2014). Absence of patient-to-patient intrahospital transmission of *Staphylococcus aureus* as determined by whole-genome sequencing. *mBio*, 5(5).
- Lucet, J.-C., Chevret, S., Durand-Zaleski, I., Chastang, C., and Regnier, B. (2003). Prevalence and risk factors for carriage of methicillin-resistant *Staphylococcus aureus* at admission to the intensive care unit: Results of a multicenter study. *Archives of Internal Medicine*, 163(2):181–188.
- Lunn, D., Spiegelhalter, D., Thomas, A., and Best, N. (2009). The BUGS project: Evolution, critique and future directions. *Statistics in medicine*, 28(25):3049–3067.
- Lunn, D., Thomas, A., Best, N., and Spiegelhalter, D. (2000). WinBUGS – a Bayesian modelling framework: concepts, structure, and extensibility. *Statistics and Computing*, 10:325–337.
- Maraqa, N. F., Aigbivbalu, L., Masnita-Iusan, C., Wludyka, P., Shareef, Z., Bailey, C., and Rathore, M. H. (2011). Prevalence of and risk factors for methicillin-resistant *Staphylococcus aureus* colonization and infection among infants at a level III neonatal intensive care unit. *American Journal of Infection Control*, 39(1):35–41.
- Marin, J.-M., Pillai, N. S., Robert, C. P., and Rousseau, J. (2014). Relevant statistics for Bayesian model choice. *Journal of the Royal Statistical Society: Series B (Statistical Methodology)*, 76(5):833–859.
- Marin, J.-M., Pudlo, P., Robert, C. P., and Ryder, R. J. (2012). Approximate Bayesian computational methods. *Statistics and Computing*, 22(6):1167–1180.
- Marjoram, P., Molitor, J., Plagnol, V., and Tavaré, S. (2003). Markov chain Monte Carlo without likelihoods. *Proceedings of the National Academy of Sciences*, 100(26):15324–15328.
- Massad, E., Lundberg, S., and Yang, H. M. (1993). Modeling and simulating the evolution of resistance against antibiotics. *International Journal of Bio-Medical Computing*, 33(1):65 – 81.
- McBryde, E. S. and McElwain, D. L. S. (2006). A mathematical model investigating the impact of an environmental reservoir on the prevalence and control of vancomycin-resistant enterococci. *Journal of Infectious Diseases*, 193(10):1473–1474.
- McBryde, E. S., Pettitt, A. N., Cooper, B. S., and McElwain, D. L. (2007a). Characterizing an outbreak of vancomycin-resistant enterococci using hidden Markov models. *Journal of the Royal Society Interface*, 4(15):745–754.
- McBryde, E. S., Pettitt, A. N., and McElwain, D. L. (2007b). A stochastic mathematical model of methicillin resistant *Staphylococcus aureus* transmission in an intensive care unit: Predicting the impact of interventions. *Journal of Theoretical Biology*, 245(3):470–481.
- McDonald, M. (1997). The epidemiology of methicillin-resistant *Staphylococcus aureus*: Surgical relevance 20 years on. *Australian and New Zealand Journal of Surgery*, 67(10):682–685.
- McKinley, T., Cook, A. R., and Deardon, R. (2009). Inference in epidemic models without likelihoods. *The International Journal of Biostatistics*, 5(1):24.
- McKinley, T. J., Ross, J. V., Deardon, R., and Cook, A. R. (2014). Simulation-based Bayesian inference for epidemic models. *Computational Statistics & Data Analysis*, 71:434 – 447.
- McMichael, A. J. (2015). Extreme weather events and infectious disease outbreaks. *Virulence*, 6(6):543–547.
- Meng, Y., Davies, R., Hardy, K., and Hawkey, P. (2010). An application of agent-based simulation to the management of hospital-acquired infection. *Journal of Simulation*, 4(1):60–67.

- Metropolis, N., Rosenbluth, A. W., Rosenbluth, M. N., Teller, A. H., and Teller, E. (1953). Equation of state calculations by fast computing machines. *The Journal of Chemical Physics*, 21(6):1087–1092.
- Mielczarek, B. and Uziako-Mydlikowska, J. (2012). Application of computer simulation modeling in the health care sector: a survey. *SIMULATION*, 88(2):197–216.
- Mitchell, B., Dancer, S., Anderson, M., and Dehn, E. (2015). Risk of organism acquisition from prior room occupants: a systematic review and meta-analysis. *Journal of Hospital Infection*, 91(3):211 – 217.
- Mitchell, B. G., Digney, W., and Ferguson, J. K. (2014). Prior room occupancy increases risk of methicillin-resistant *Staphylococcus aureus* acquisition. *Healthcare Infection*, 19:135–140.
- Molenberghs, G., Fitzmaurice, G., Kenward, M. G., Tsiatis, A., and Verbeke, G. (2014). *Handbook of Missing Data Methodology*. CRC Press.
- Morgan, D. J., Diekema, D. J., Sepkowitz, K., and Perencevich, E. N. (2009). Adverse outcomes associated with contact precautions: a review of the literature. *American Journal of Infection Control*, 37(2):85–93.
- Morton, A., Mengersen, K. L., Playford, G., and Whitby, M. (2013). *Statistical Methods for Hospital Monitoring with R*. John Wiley & Sons.
- Neal, P. J. and Roberts, G. O. (2004). Statistical inference and model selection for the 1861 Hagelloch measles epidemic. *Biostatistics*, 5(2):249–261.
- Newcombe, R. G. (2006). Confidence intervals for an effect size measure based on the Mann–Whitney statistic. Part 2: Asymptotic methods and evaluation. *Statistics in Medicine*, 25(4):559–573.
- Nightingale, F. (1863). *Notes on hospitals*. Longman, Green, Longman, Roberts, and Green, London.
- Nimmo, G. R., Bergh, H., Nakos, J., Whiley, D., Marquess, J., Huygens, F., and Paterson, D. L. (2013). Replacement of healthcare-associated MRSA by community-associated MRSA in Queensland: Confirmation by genotyping. *Journal of Infection*, 67(5):439 – 447.
- Obadia, T., Silhol, R., Opatowski, L., Temime, L., Legrand, J., Thibaut, A. C. M., Herrmann, J.-L., Fleury, r., Guillemot, D., Bolle, P.-Y., and on behalf of the I-Bird Study Group (2015). Detailed contact data and the dissemination of *Staphylococcus aureus* in hospitals. *PLoS Computational Biology*, 11(3):e1004170.
- Oesterle, H. (1992). Statistische reanalyse einer masernepidemie 1861 in Hagelloch. Master’s thesis, Eberhard-Karls Universität, Tübingen.
- Ogata, Y. (1999). Seismicity analysis through point-process modeling: A review. *Pure and Applied Geophysics*, 155(2):471–507.
- O’Neill, P. D. (2010). Introduction and snapshot review: Relating infectious disease transmission models to data. *Statistics in Medicine*, 29(20):2069–2077.
- O’Neill, P. D. and Kypraios, T. (2016). Bayesian model choice via mixture distributions with application to epidemics and population process models. *arXiv:1411.7888v2*.
- Opatowski, L., Guillemot, D., Boëlle, P.-Y., and Temime, L. (2011). Contribution of mathematical modeling to the fight against bacterial antibiotic resistance. *Current Opinion in Infectious Diseases*, 24(3):279–287.
- Opitz, T. (2013). Extremal t processes: Elliptical domain of attraction and a spectral representation. *Journal of Multivariate Analysis*, 122:409–413.
- Oztoprak, N., Cevik, M. A., Akinci, E., Korkmaz, M., Erbay, A., Eren, S. S., Balaban, N., and Bodur, H. (2006). Risk factors for ICU-acquired methicillin-resistant *Staphylococcus aureus* infections. *American Journal of Infection Control*, 34(1):1 – 5.
- Padoan, S. A., Ribatet, M., and Sisson, S. A. (2010). Likelihood-based inference for max-stable processes. *Journal of the American Statistical Association*, 105(489):263–277.

- Pastor-Satorras, R., Castellano, C., Van Mieghem, P., and Vespignani, A. (2015). Epidemic processes in complex networks. *Reviews of Modern Physics*, 87(3):925–979.
- Patrozou, E. (2015). Our changing world: Impacts on health and infectious diseases. *Virulence*, 6(6):533–534.
- Peacock, S. J. and Paterson, G. K. (2015). Mechanisms of methicillin resistance in *Staphylococcus aureus*. *Annual Review of Biochemistry*, 84:577–601.
- Peleg, A. Y. and Hooper, D. C. (2010). Hospital-acquired infections due to gram-negative bacteria. *New England Journal of Medicine*, 362(19):1804–1813. PMID: 20463340.
- Pettitt, A., Weir, I., and Hart, A. (2002). A conditional autoregressive Gaussian process for irregularly spaced multivariate data with application to modelling large sets of binary data. *Statistics and Computing*, 12(4):353–367.
- Pfeilsticker, A. (1863). Beiträge zur pathologie der masern mit besonderer berücksichtigung der statistischen verhältnisse. Master’s thesis, Eberhard-Karls Universität, Tübingen.
- Pitt, M., Monks, T., Crowe, S., and Vasilakis, C. (2016). Systems modelling and simulation in health service design, delivery and decision making. *BMJ Quality & Safety*, 25(1):38–45.
- Plummer, M., Best, N., Cowles, K., and Vines, K. (2006). CODA: Convergence Diagnosis and Output Analysis for MCMC. *R News*, 6(1):7–11.
- Poovelikunnel, T., Gethin, G., and Humphreys, H. (2015). Mupirocin resistance: clinical implications and potential alternatives for the eradication of MRSA. *Journal of Antimicrobial Chemotherapy*, 70(10):2681–2692.
- Poumadère, M., Mays, C., Le Mer, S., and Blong, R. (2005). The 2003 heat wave in France: Dangerous climate change here and now. *Risk Analysis*, 25(6):1483–1494.
- Prangle, D. (2016). Lazy ABC. *Statistics and Computing*, 26(1):171–185.
- Prangle, D., Fearnhead, P., Cox, M. P., Biggs, P. J., and French, N. P. (2014). Semi-automatic selection of summary statistics for ABC model choice. *Statistical Applications in Genetics and Molecular Biology*, 13(1):67–82.
- Price, J., Didelot, X., Crook, D., Llewelyn, M. J., and Paul, J. (2013). Whole genome sequencing in the prevention and control of *Staphylococcus aureus* infection. *Journal of Hospital Infection*, 83:14–21.
- Price, J. R., Golubchik, T., Cole, K., Wilson, D. J., Crook, D. W., Thwaites, G. E., Bowden, R., Walker, A. S., Peto, T. E. A., Paul, J., and Llewelyn, M. J. (2014). Whole-genome sequencing shows that patient-to-patient transmission rarely accounts for acquisition of *Staphylococcus aureus* in an intensive care unit. *Clinical Infectious Diseases*, 58(5):609–618.
- Pritchard, J. K., Seielstad, M. T., Perez-Lezaun, A., and Feldman, M. W. (1999). Population growth of human Y chromosomes: A study of Y chromosome microsatellites. *Molecular Biology and Evolution*, 16:1791–1798.
- Pudlo, P., Marin, J.-M., Estoup, A., Cornuet, J.-M., Gautier, M., and Robert, C. P. (2016). Reliable ABC model choice via random forests. *Bioinformatics*, 32(6):859–866.
- Raboud, J., Saskin, R., Simor, A., Loeb, M., Green, K., Low, D. E., and McGeer, A. (2005). Modeling transmission of methicillin-resistant *Staphylococcus aureus* among patients admitted to a hospital. *Infection Control & Hospital Epidemiology*, 26(07):607–615.
- Rai, S., Rani, M., Choudhury, D. D., Singh, N. P., Gupta, A., and Manchanda, V. (2016). Failure to decolonize mupirocin and linezolid resistant MRSA from a patient with necrotizing soft tissue infection. *Journal of Infection and Public Health*, in press.
- Rammelkamp, C. H. and Maxon, T. (1942). Resistance of *Staphylococcus aureus* to the action of penicillin. *Experimental Biology and Medicine*, 51(3):386–389.
- Rasmussen, C. E. and Williams, C. K. (2006). *Gaussian Processes for Machine Learning*. The MIT Press.

- Ratmann, O., Camacho, A., Meijer, A., and Donker, G. (2014). Statistical modelling of summary values leads to accurate approximate Bayesian computations. *ArXiv e-prints: 1305.4283v2*.
- Ribatet, M. (2009). A users guide to the SpatialExtremes package. *EPFL, Lausanne, Switzerland*.
- Ribatet, M. (2013). Spatial extremes: Max-stable processes at work. *Journal de la Société Française de Statistique*, 154(2):156–177.
- Ribatet, M., Singleton, R., and R Core team (2013). *SpatialExtremes: Modelling Spatial Extremes*. R package version 2.0-0.
- Richet, H. (2012). Seasonality in gram-negative and healthcare-associated infections. *Clinical Microbiology and Infection*, 18(10):934–940.
- Riley, S. (2007). Large-scale spatial-transmission models of infectious disease. *Science*, 316(5829):1298–1301.
- Robert, C. P., Cornuet, J.-M., Marin, J.-M., and Pillai, N. S. (2011). Lack of confidence in approximate Bayesian computation model choice. *Proceedings of the National Academy of Sciences*, 108(37):15112–15117.
- Robert, C. P. and Wraith, D. (2009). Computational methods for Bayesian model choice. *AIP Conference Proceedings*, 1193(1):251–262.
- Roberts, G. O., Gelman, A., and Gilks, W. R. (1997). Weak convergence and optimal scaling of random walk Metropolis algorithms. *The Annals of Applied Probability*, 7(1):110–120.
- Roberts, G. O., Rosenthal, J. S., et al. (2001). Optimal scaling for various Metropolis-Hastings algorithms. *Statistical Science*, 16(4):351–367.
- Robotham, J. V., Deeny, S. R., Fuller, C., Hopkins, S., Cookson, B., and Stone, S. (2016). Cost-effectiveness of national mandatory screening of all admissions to English National Health Service hospitals for meticillin-resistant *Staphylococcus aureus*: a mathematical modelling study. *The Lancet Infectious Diseases*, 16(3):348–356.
- Robotham, J. V., Graves, N., Cookson, B. D., Barnett, A. G., Wilson, J. A., Edgeworth, J. D., Batra, R., Cuthbertson, B. H., and Cooper, B. S. (2011). Screening, isolation, and decolonisation strategies in the control of meticillin resistant *Staphylococcus aureus* in intensive care units: cost effectiveness evaluation. *BMJ*, 343:d5694.
- Rock, K., Brand, S., Moir, J., and Keeling, M. J. (2014). Dynamics of infectious diseases. *Reports on Progress in Physics*, 77(2):026602.
- Rolinson, G. (1961). “Celbenin”-resistant staphylococci. *British Medical Journal*, 1:125.
- Rosenthal, J. S. (2011). *Handbook of Markov chain Monte Carlo*, chapter 4: Optimal proposal distributions and adaptive MCMC, pages 93–111. *Handbook of Modern Statistical Methods*. Chapman & Hall / CRC Press.
- Ruli, E., Sartori, N., and Ventura, L. (2016). Approximate Bayesian computation with composite score functions. *Statistics and Computing*, 26(3):679–692.
- Sang, H. and Gelfand, A. E. (2010). Continuous spatial process models for spatial extreme values. *Journal of Agricultural, Biological, and Environmental Statistics*, 15(1):49–65.
- Sangalli, L. M., Ramsay, J. O., and Ramsay, T. O. (2013). Spatial spline regression models. *Journal of the Royal Statistical Society: Series B (Statistical Methodology)*, 75(4):681–703.
- Saravolatz, L. D., Pawlak, J., and Johnson, L. B. (2012). In vitro susceptibilities and molecular analysis of vancomycin-intermediate and vancomycin-resistant *Staphylococcus aureus* isolates. *Clinical Infectious Diseases*, 55(4):582–586.
- Schäfer, C. and Chopin, N. (2013). Sequential Monte Carlo on large binary sampling spaces. *Statistics and Computing*, 23(2):163–184.
- Schlather, M. (2002). Models for stationary max-stable random fields. *Extremes*, 5(1):33–44.

- Schlather, M. and Tawn, J. A. (2003). A dependence measure for multivariate and spatial extreme values: Properties and inference. *Biometrika*, 90(1):139–156.
- Schröder, C., Schwab, F., Behnke, M., Breier, A.-C., Maechler, F., Piening, B., Dettenkofer, M., Geffers, C., and Gastmeier, P. (2015). Epidemiology of healthcare associated infections in Germany: Nearly 20 years of surveillance. *International Journal of Medical Microbiology*, 305(7):799–806.
- Schultz, E. D., Tanaka, D. T., Goldberg, R. N., Benjamin, D. K., and Smith, P. B. (2009). Effect of methicillin-resistant *Staphylococcus aureus* colonization in the neonatal intensive care unit on total hospital cost. *Infection Control & Hospital Epidemiology*, 30(0):383–385.
- Schwab, F., Gastmeier, P., and Meyer, E. (2014). The warmer the weather, the more gram-negative bacteria - impact of temperature on clinical isolates in intensive care units. *PLoS ONE*, 9(3):e91105.
- Schwarz, G. (1978). Estimating the dimension of a model. *The Annals of Statistics*, 6(2):461–472.
- Sébille, V., Chevret, S., and Valleron, A.-J. (1997). Modeling the spread of resistant nosocomial pathogens in an intensive-care unit. *Infection Control & Hospital Epidemiology*, 18:84–92.
- Sébille, V. and Valleron, A.-J. (1997). A computer simulation model for the spread of nosocomial infections caused by multidrug-resistant pathogens. *Computers and Biomedical Research*, 30(4):307–322.
- Sedki, M., Cornuet, J.-M., Marin, J.-M., Pudlo, P., and Robert, C. P. (2012). Efficient learning in ABC algorithms. *ArXiv e-prints: 1210.1388*.
- Sekhon, J. S. (2011). Multivariate and propensity score matching software with automated balance optimization: The Matching package for R. *Journal of Statistical Software*, 42(7):1–52.
- Sherertz, R. J., Bassetti, S., and Bassetti-Wyss, B. (2001). “Cloud” health-care workers. *Emerging Infectious Diseases*, 7(2):241.
- Sherlock, C., Fearnhead, P., and Roberts, G. O. (2010). The random walk Metropolis: Linking theory and practice through a case study. *Statistical Science*, 25(2):172–190.
- Shibli, M., Gooch, S., Lewis, H. E., and Tyrrell, D. A. J. (1971). Common colds on Tristan da Cunha. *Epidemiology & Infection*, 69(2):255–262.
- Silk, D., Filippi, S., and Stumpf, M. P. H. (2013). Optimizing threshold-schedules for sequential approximate Bayesian computation: applications to molecular systems. *Statistical Applications in Genetics and Molecular Biology*, 12(5):603–618.
- Sison, C. P. and Glaz, J. (1995). Simultaneous confidence intervals and sample size determination for multinomial proportions. *Journal of the American Statistical Association*, 90(429):366–369.
- Sisson, S., Fan, Y., and Tanaka, M. A. (2007). Sequential Monte Carlo without likelihoods. *Proceedings of the National Academy of Sciences*, 104:1760–1765.
- Sisson, S., Fan, Y., and Tanaka, M. A. (2009). Correction for Sisson et al., sequential Monte Carlo without likelihoods. *Proceedings of the National Academy of Sciences*, 106:16889–16890.
- Sisson, S. A. (2005). Transdimensional Markov chains: A decade of progress and future perspectives. *Journal of the American Statistical Association*, 100(471):1077–1089.
- Smith, D. L., Battle, K. E., Hay, S. I., Barker, C. M., Scott, T. W., and McKenzie, F. E. (2012). Ross, Macdonald, and a theory for the dynamics and control of mosquito-transmitted pathogens. *PLoS Pathogens*, 8(4):1–13.
- Smith, R. L. (1990). Max-stable processes and spatial extremes. *Unpublished manuscript*, pages 1–32.

- Song, X., Perencevich, E., Campos, J., Short, B., and Singh, N. (2010). Clinical and economic impact of methicillin-resistant *Staphylococcus aureus* colonization or infection on neonates in intensive care units. *Infection Control & Hospital Epidemiology*, 31(2):177–182.
- Spicknall, I. H., Foxman, B., Marrs, C. F., and Eisenberg, J. N. (2013). A modeling framework for the evolution and spread of antibiotic resistance: literature review and model categorization. *American Journal of Epidemiology*, 178(4):508–520.
- Spiegelhalter, D. J., Best, N. G., Carlin, B. P., and Van Der Linde, A. (2002). Bayesian measures of model complexity and fit. *Journal of the Royal Statistical Society: Series B (Statistical Methodology)*, 64(4):583–639.
- Spiegelhalter, D. J., Best, N. G., Carlin, B. P., and van der Linde, A. (2014). The deviance information criterion: 12 years on. *Journal of the Royal Statistical Society: Series B (Statistical Methodology)*, 76(3):485–493.
- Stefani, S., Chung, D. R., Lindsay, J. A., Friedrich, A. W., Kearns, A. M., Westh, H., and MacKenzie, F. M. (2012). Methicillin-resistant *Staphylococcus aureus* (MRSA): global epidemiology and harmonisation of typing methods. *International Journal of Antimicrobial Agents*, 39(4):273 – 282.
- Stelfox, H. T., Bates, D. W., and Redelmeier, D. A. (2003). Safety of patients isolated for infection control. *JAMA*, 290(14):1899–1905.
- Stewart, M., Bogusz, A., Hunter, J., Devanny, I., Yip, B., Reid, D., Robertson, C., and Dancer, S. J. (2014). Evaluating use of neutral electrolyzed water for cleaning near-patient surfaces. *Infection Control & Hospital Epidemiology*, 35(12):1505–1510.
- Streftaris, G. and Gibson, G. J. (2012). Non-exponential tolerance to infection in epidemic systems – modeling, inference, and assessment. *Biostatistics*, 13(4):580–593.
- Struelens, M. J. and Monnet, D. L. (2010). Prevention of methicillin-resistant *Staphylococcus aureus* infection: is Europe winning the fight? *Infection Control & Hospital Epidemiology*, 31(S1):S42–S44.
- Tacconelli, E., De Angelis, G., Cataldo, M. A., Pozzi, E., and Cauda, R. (2008). Does antibiotic exposure increase the risk of methicillin-resistant *Staphylococcus aureus* (MRSA) isolation? a systematic review and meta-analysis. *Journal of Antimicrobial Chemotherapy*, 61(1):26–38.
- Tacconelli, E. and Johnson, A. P. (2011). National guidelines for decolonization of methicillin-resistant *Staphylococcus aureus* carriers: the implications of recent experience in the Netherlands. *Journal of Antimicrobial Chemotherapy*, 66(10):2195–2198.
- Tanaka, M. M., Francis, A. R., Luciani, F., and Sisson, S. (2006). Using approximate Bayesian computation to estimate tuberculosis transmission parameters from genotype data. *Genetics*, 173:1511–1520.
- Tanner, M. A. and Wong, W. H. (1987). The calculation of posterior distributions by data augmentation. *Journal of the American Statistical Association*, 82(398):528–540.
- Therneau, T. M. (2015). *A Package for Survival Analysis in S*. version 2.38.
- Tong, S. Y., Holden, M. T., Nickerson, E. K., Cooper, B. S., Kser, C. U., Cori, A., Jombart, T., Cauchemez, S., Fraser, C., Wuthiekanun, V., Thaipadungpanit, J., Hongsuwan, M., Day, N. P., Limmathurotsakul, D., Parkhill, J., and Peacock, S. J. (2015). Genome sequencing defines phylogeny and spread of methicillin-resistant *Staphylococcus aureus* in a high transmission setting. *Genome Research*, 25(1):111–118.
- Toni, T. and Stumpf, M. P. (2010). Simulation-based model selection for dynamical systems in systems and population biology. *Bioinformatics*, 26(1):104–110.
- Toni, T., Welch, D., Strelkowa, N., Ipsen, A., and Stumpf, M. P. (2009). Approximate Bayesian computation scheme for parameter inference and model selection in dynamical systems. *Journal of the Royal Society Interface*, 6(31):187–202.

- Tsoulas, C. and Nathwani, D. (2015). Review of meta-analyses of vancomycin compared with new treatments for Gram-positive skin and soft-tissue infections: Are we any clearer? *International Journal of Antimicrobial Agents*, 46(1):1 – 7.
- Ugolotti, E., Larghero, P., Vanni, I., Bandettini, R., Tripodi, G., Melioli, G., Marco, E. D., Raso, A., and Biassoni, R. (2016). Whole genome sequence as standard practice for the analysis of clonality in methicillin-resistant *Staphylococcus aureus* paediatric outbreaks. *Journal of Hospital Infection*, in press.
- van den Driessche, P. and Watmough, J. (2002). Reproduction numbers and sub-threshold endemic equilibria for compartmental models of disease transmission. *Mathematical Biosciences*, 180(1):29–48.
- van Kleef, E., Robotham, J. V., Jit, M., Deeny, S. R., and Edmunds, W. J. (2013). Modelling the transmission of healthcare associated infections: a systematic review. *BMC Infectious Diseases*, 13(1):294.
- van Trijp, M. J. C. A., Melles, D. C., Hendriks, W. D. H., Parlevliet, G. A., Gommans, M., and Ott, A. (2007). Successful control of widespread methicillin-resistant *Staphylococcus aureus* colonization and infection in a large teaching hospital in The Netherlands. *Infection Control & Hospital Epidemiology*, 28(8):pp. 970–975.
- van Walraven, C., Davis, D., Forster, A. J., and Wells, G. A. (2004). Time-dependent bias was common in survival analyses published in leading clinical journals. *Journal of Clinical Epidemiology*, 57(7):672 – 682.
- Wang, J., Wang, L., Magal, P., Wang, Y., Zhuo, J., Lu, X., and Ruan, S. (2011). Modelling the transmission dynamics of methicillin-resistant *Staphylococcus aureus* in Beijing Tongren hospital. *Journal of Hospital Infection*, 79(4):302–308.
- Wang, X., Xiao, Y., Wang, J., and Lu, X. (2012). A mathematical model of effects of environmental contamination and presence of volunteers on hospital infections in China. *Journal of Theoretical Biology*, 293:161 – 173.
- Wang, X., Xiao, Y., Wang, J., and Lu, X. (2013). Stochastic disease dynamics of a hospital infection model. *Mathematical Biosciences*, 241(1):115 – 124.
- Warton, D. I., Shepherd, L. C., et al. (2010). Poisson point process models solve the pseudo-absence problem for presence-only data in ecology. *The Annals of Applied Statistics*, 4(3):1383–1402.
- Watanabe, S. (2010). Asymptotic equivalence of Bayes cross validation and widely applicable information criterion in singular learning theory. *The Journal of Machine Learning Research*, 11:3571–3594.
- Watanabe, S. (2013). A widely applicable Bayesian information criterion. *The Journal of Machine Learning Research*, 14(1):867–897.
- Weber, D. J. and Rutala, W. A. (2013). Introduction: Understanding and preventing transmission of healthcare-associated pathogens due to the contaminated hospital environment. *Infection Control & Hospital Epidemiology*, 34(5):pp. 449–452.
- Wei, Y., Kypraios, T., O'Neill, P. D., Huang, S. S., Rifas-Shiman, S. L., and Cooper, B. S. (2016). Evaluating hospital infection control measures for antimicrobial-resistant pathogens using stochastic transmission models: Application to vancomycin-resistant enterococci in intensive care units. *Statistical Methods in Medical Research*.
- Weiss, G. and von Haeseler, A. (1998). Inference of population history using a likelihood approach. *Genetics*, 149:1539–1546.
- Wertheim, H. F., Melles, D. C., Vos, M. C., van Leeuwen, W., van Belkum, A., Verbrugh, H. A., and Nouwen, J. L. (2005). The role of nasal carriage in *Staphylococcus aureus* infections. *The Lancet Infectious Diseases*, 5(12):751 – 762.
- Wilson, A. P. R., Smyth, D., Moore, G., Singleton, J., Jackson, R., Gant, V., Jeanes, A., Shaw, S., James, E., Cooper, B., et al. (2011). The impact of enhanced cleaning within the intensive care unit on contamination of the near-patient environment with hospital

- pathogens: A randomized crossover study in critical care units in two hospitals. *Critical Care Medicine*, 39(4):651–658.
- Wolkewitz, M., Dettenkofer, M., Bertz, H., Schumacher, M., and Huebner, J. (2008). Environmental contamination as an important route for the transmission of the hospital pathogen VRE: Modeling and prediction of classical interventions. *Infectious Diseases: Research and Treatment*, 1:3–11.
- Wood, S. (2006). *Generalized additive models: an introduction with R*. Chapman & Hall / CRC Press.
- Wood, S. N., Bravington, M. V., and Hedley, S. L. (2008). Soap film smoothing. *Journal of the Royal Statistical Society: Series B (Statistical Methodology)*, 70(5):931–955.
- Worby, C. J. (2013). *Statistical inference and modelling for nosocomial infections and the incorporation of whole genome sequence data*. PhD thesis, School of Mathematical Sciences, University of Nottingham.
- Worby, C. J., Jeyaratnam, D., Robotham, J. V., Kypraios, T., O’Neill, P. D., De Angelis, D., French, G., and Cooper, B. S. (2013). Estimating the effectiveness of isolation and decolonization measures in reducing transmission of methicillin-resistant *Staphylococcus aureus* in hospital general wards. *American Journal of Epidemiology*, 177(11):1306–1313.
- Worby, C. J., Lipsitch, M., and Hanage, W. P. (2014). Within-host bacterial diversity hinders accurate reconstruction of transmission networks from genomic distance data. *PLoS Computational Biology*, 10(3):e1003549.
- Worby, C. J., O’Neill, P. D., Kypraios, T., Robotham, J. V., De Angelis, D., Cartwright, E. J. P., Peacock, S. J., and Cooper, B. S. (2016). Reconstructing transmission networks for communicable diseases using densely sampled genomic data. *The Annals of Applied Statistics*, 10(1):395–417.
- World Health Organization (2009). *WHO guidelines on hand hygiene in health care: first global patient safety challenge. Clean care is safer care*. World Health Organization.
- World Health Organization (2014). Antimicrobial resistance: global report on surveillance.
- World Health Organization et al. (2011). Report on the burden of endemic health care-associated infection worldwide.
- Zaidi, A. K., Huskins, W. C., Thaver, D., Bhutta, Z. A., Abbas, Z., and Goldmann, D. A. (2005). Hospital-acquired neonatal infections in developing countries. *The Lancet*, 365(9465):1175–1188.